Copyright

by

Sarah Lynn Orton

2007

The Dissertation Committee for Sarah Lynn Orton Certifies that this is the approved version of the following dissertation:

Development of a CFRP System to Provide Continuity in Existing Reinforced Concrete Buildings Vulnerable to Progressive Collapse

Committee:

James O. Jirsa, Supervisor

Oguzhan Bayrak, Co-Supervisor

Sharon L. Wood

Eric B. Williamson

Kenneth M Liechti

Development of a CFRP System to Provide Continuity in Existing Reinforced Concrete Buildings Vulnerable to Progressive Collapse

by

Sarah Lynn Orton, BS; MS

Dissertation

Presented to the Faculty of the Graduate School of

The University of Texas at Austin

in Partial Fulfillment

of the Requirements

for the Degree of

Doctor of Philosophy

The University of Texas at Austin

August 2007

Dedication

To my family, who has unwaveringly supported, but may not have understood, my desire for higher education.

Acknowledgements

The research presented in this dissertation was supported by the National Science Foundation. The composite materials (carbon fiber, epoxy, and repair mortar) were donated by the Fyfe Co LLC. Special thanks go to Pete Milligan for his help in donating the materials and guidance in using the materials.

An industry advisory panel consisting of Loring Wyllie of Degenkolb, and Viral Patel and Dilip Choudhuri of Walter P. Moore provided useful insight for the project. Their advice and comments will hopefully make this research useful to practicing engineers and see implementation in the real world where it might be able to save lives.

The research was conducted under the supervision of Dr. James Jirsa and Dr. Oguzhan Bayrak. Their advice and comments were essential to the successful completion of my dissertation. I could not have asked for advisors more generous with their time and consideration. Thanks also go to the members of my dissertation committee, Dr. Sharon Wood, Dr. Eric Williamson, and Dr. Kenneth Leichti.

The personal at the Ferguson Structural Engineering Laboratory (FSEL) Blake Stasney, Dennis Fillip, Eric Schell, Mike Wason, and Greg Harris were instrumental in specimen construction, moving, and testing. I could not have completed this research without their assistance.

Finally, thanks go to all the students at FSEL who helped me in little ways here and there. Special thanks go to Insung Kim, my co-researcher on this project who helped in all phases of the project but most especially in numerous applications of CFRP.

Development of a CFRP System to Provide Continuity in Existing Reinforced Concrete Buildings Vulnerable to Progressive Collapse

Publication No.______________

Sarah Lynn Orton, Ph.D.
The University of Texas at Austin, 2007

Supervisor: James O. Jirsa
Co-Supervisor: Oguzhan Bayrak

Reinforced concrete buildings may be vulnerable to progressive collapse due to a lack of continuous reinforcement. Progressive collapse is an extreme form of collapse that is disproportionate to the originating cause. Such collapses cause not only significant damage to buildings, but also greater loss of life and injuries. Carbon fiber reinforced polymer (CFRP) may be used to retrofit existing reinforced concrete beams and provide the missing continuity needed to resist progressive collapse.

This research focuses on retrofitting the beams in a reinforced concrete building to provide sufficient continuity to reach catenary action. The catenary action may allow the beam to carry vertical loads at large displacements if a supporting column were removed. The CFRP can provide continuity through the negative moment reinforcement or through the positive moment reinforcement.

The research was broken into three major components. Anchorage tests form the design basis of the CFRP retrofit and ensure that the capacity of the retrofit can be accurately predicted. Continuity tests determine if the CFRP retrofit is capable of providing continuity and if the retrofit will allow the beam to reach catenary action and sustain a load representing resistance to progressive collapse. The analysis model forms a set of equations for catenary action so the results can be applied to reinforced concrete beams in general.

Forty anchorage tests, eight continuity tests, and one analysis model were constructed and evaluated. The anchorage tests found that carbon fiber anchors enabled improved utilization of the tensile capacity of a CFRP sheet and improved the efficiency of material usage in CFRP retrofits. The continuity tests found that beams without continuous reinforcement can reach catenary action (depending on design details) and a CFRP retrofit, if designed correctly (placed in locations that do not cause rebar fracture before catenary), may be able to reduce vulnerability to progressive collapse. The analysis model was able to accurately predict the load-deflection behavior of a reinforced concrete beam in catenary action. The overall conclusion is that a CFRP retrofit can reduce vulnerability to progressive collapse in reinforced concrete buildings.

Table of Contents

List of Tables xii

List of Figures xiii

Chapter 1 : Introduction 1

1.1 Objective and Scope 1

1.2 Research Components 5

1.2.1 Anchorage Tests 5

1.2.2 Continuity Tests 7

1.2.3 Catenary Model 8

Chapter 2 : Progressive Collapse Background 10

2.1 Progressive Collapse 10

2.1.1 Definition and Causes 10

2.1.2 Examples 11

2.1.2.1 Ronan Point 11

2.1.2.2 Murrah Building 12

2.1.2.3 L'Ambiance Plaza 15

2.1.2.4 Pentagon 16

2.1.2.5 Khobar Towers 18

2.1.3 Standards 19

2.2 Reinforced Concrete Structures and Progressive Collapse 22

2.3 Resistance to Progressive Collapse 25

2.3.1 Previous Research in Catenary Action 28

2.3.2 Previous mitigations for progressive collapse 31

2.4 Summary 34

Chapter 3 : CFRP Background 36

3.1 Material Characteristics of CFRP 36

3.1.1 CFRP History 36

3.1.2 Carbon Fiber Properties 38

3.1.3 Epoxy Matrix Properties 39

3.1.4 CFRP Composite Properties 41

3.1.5 Standard ASTM Test for CFRP 43

3.2 Structural Strengthening with CFRP 45

3.2.1 Structural Strengthening 45

3.2.2 CFRP Failure Modes...46

3.3 CFRP Debonding 47

3.4 Anchorage of CFRP 51

3.4.1 Carbon fiber anchors...53

3.4.2 Previous research 54

3.5 CFRP Application...61

3.6 Summary 65

Chapter 4 : Anchorage Tests..67

4.1 Introduction...67

4.2 Test Setup..68

4.2.1 CFRP layout...71

4.2.2 Instrumentation 74

4.2.3 Material Properties...75

4.3 Test Results..77

4.3.1 Tests With No Height Transition...77

4.3.1.1 No Anchorage 80

4.3.1.2 U-wraps...81

4.3.1.3 CFRP Anchors 83

4.3.1.4 Other Issues..87

4.3.2 Tests With Height Transition..89

4.3.2.1 Slope of Transition...89

4.3.2.2 Type of Fabric 93

4.3.2.3 Surface Preparation..94

4.3.2.4 Height Difference...96

4.3.2.5 Strains 98

4.3.2.6 Other Issues..101

4.4 Conclusions..102

Chapter 5 : Continuity Tests 104
5.1 Introduction..104
5.2 Specimen Design 107
5.3 Test Setup..109
5.4 Instrumentation 116
5.5 Test Results 117
5.5.1 NR-2 – No Retrofit 119
5.5.2 PM-1 – Positive Moment Retrofit...121
5.5.3 PM-2 – Positive Moment Retrofit...127
5.5.4 NM-1 – Negative Moment Retrofit 133
5.5.5 NM-2 – Negative Moment Retrofit 138
5.5.6 FR-1 – Flexural Retrofit...144
5.5.7 CR-1 Continuous Reinforcement...151
5.6 Test Comparisons...156
5.7 Conclusions...159

Chapter 6 : Catenary Model 163
6.1 Model Development..163
6.1.1 Case 1 (Retrofitted)..163
6.1.1.1 Equilibrium 164
6.1.1.2 Compatibility 166
6.1.1.3 Axial Extension..166
6.1.2 Case 2 (Un-retrofitted)...176
6.2 Comparison with Test Results 179
6.3 Parametric Study..185
6.4 Application to Prototype Structure 187
6.5 Conclusions...197

Chapter 7: Summary and Conclusions..199
7.1 Summary of Results..199
7.1.2 Anchorage Tests..199

7.1.2 Continuity Tests 201
7.1.3 Catenary Model..202
7.2 Conclusions..203
7.3 Future Research 205
Appendix A …………………………………………………………….….206
Appendix B…………………………………………………………….....288
Appendix C……………………………………………………………..…..311
Appendix D………………………………………………………….……..348
References …………………………………………………………………359
Vita………………………………………………………………………….…...364

List of Tables

Table 2-1 Static load combinations for alternate load path analysis 21
Table 3-1 Properties of commercially available carbon fibers 39
Table 3-2 Properties of commercially available epoxies 41
Table 3-3 Properties of CFRP composites 43
Table 4-1 Anchor sizes 74
Table 4-2 Specimen designation: ab-dce 74
Table 4-3 CFRP fabric properties (ASTM D-3039) 76
Table 4-4 Test results for no height transition 79
Table 5-1 Test specimen designation 117
Table 5-2 CFRP fabric properties 118
Table 5-3 Concrete compressive strength per specimen 118
Table 5-4 Results of continuity tests 160

List of Figures

Figure 1-1 Catenary action in a reinforced concrete frame 2
Figure 1-2 CFRP to provide continuity 3
Figure 1-3 CFRP retrofit to provide continuity through negative moment reinforcement 4
Figure 1-4 CFRP retrofit to provide continuity through positive moment reinforcement. 4
Figure 1-5 Division of research 5
Figure 1-6 Use of CFRP at height transitions.. 6
Figure 1-7 CFRP anchor 6
Figure 1-8 Relation of test specimen to prototype building (elevation view) 8
Figure 2-1 Ronan Point collapse [Nair, 2004] 12
Figure 2-2 Collapse of Murrah building [Crawford, 2002] 13
Figure 2-3 Collapsed area of Oklahoma City Murrah building [NIST, 2007] 14
Figure 2-4 North elevation of Murrah building [Sozen et al., 1998]............................... 14
Figure 2-5 Reinforcement diagram for 3rd floor transfer girder [Sozen et al., 1998] 15
Figure 2-6 L'Ambiance Plaza collapse [NIST, 2007] 16
Figure 2-7 Damage to first floor columns [Mlakar et al., 2003]..................................... 17
Figure 2-8 Rendering of damaged area of Pentagon before collapse [Mlakar et al., 2003] 18
Figure 2-9 Collapse of Pentagon building [Mlakar et al., 2003] 18
Figure 2-10 Khobar Towers bombing [NIST, 2007] 19
Figure 2-11 System of tie forces [DoD, 2003] 21
Figure 2-12 Forces on structure due to catenary loads [NIST, 2007]............................. 22
Figure 2-13 Lack of continuous reinforcement in RC buildings.................................... 23
Figure 2-14 Failed roof beam demonstrating continuity of bottom steel [Degenkolb, 1987] 24
Figure 2-15 Change in bending moment diagram due to loss of column........................ 25
Figure 2-16 Catenary tension forces 26
Figure 2-17 Transfer of catenary forces through stirrups 27
Figure 2-18 Catenary forces provided through the positive moment reinforcement....... 27
Figure 2-19 Catenary forces provided through the negative moment reinforcement...... 28
Figure 2-20 Catenary tests of precast floor strips [Regan, 1975] 29
Figure 2-21 Results of catenary tests of precast floor strips [Regan, 1975] 30
Figure 2-22 Catenary tests conducted by Wilford [Wong, 2002].................................... 31
Figure 2-23 Steel cable to develop catenary action [Astenah-Asl, 2003]........................ 33
Figure 2-24 SidePlate system for steel frames [Crawford, 2002]................................... 33
Figure 2-25 Steel retrofit to develop yield of bottom bars through a beam column joint [Estrada, 1990].. 34
Figure 3-1 Structure of graphite [Fitzer 1985].. 38
Figure 3-2 High resolution of highly aligned graphite chains in a carbon fiber [Fitzer 1985] 39
Figure 3-3 Reaction of epoxy components to form cross-linked solid [Mallick, 1993].. 40
Figure 3-4 Roll of prepeg carbon fiber composite [Lamanna, 2002] 42
Figure 3-5 Production of prepeg CFRP plates [Hollaway et al., 2000]........................... 42

Figure 3-6 Roll of CFRP fabric 43
Figure 3-7 CFRP coupon schematic 44
Figure 3-8 FRP coupons in hydraulic testing machine 44
Figure 3-9 Moment couple in RC beam [ACI 440, 2002] 45
Figure 3-10 Failure modes in FRP strengthened beams [Teng et al., 2001] 46
Figure 3-11 Types of debonding or loss of composite action [Teng et al., 2001] 47
Figure 3-12 Debonding in concrete [fib-14, 2001] 48
Figure 3-13 Normal and shear stresses at end of CFRP sheet [Teng et al., 2001] 48
Figure 3-14 Forces in crack initiated debonding [Lamanna, 2002] 49
Figure 3-15 Mechanical fastening of prepeg CFRP plate [Lamanna, 2002] 51
Figure 3-16 Splitting failure of prepeg plate with unidirectional fibers [Lamanna, 2002] 52
Figure 3-17 U-wrap anchorage on RC beam 53
Figure 3-18 U-anchor anchorage [Khalifa, 1999] 53
Figure 3-19 CFRP Anchor 54
Figure 3-20 Strips of CFRP used to form anchor and inserting anchor into predrilled hole 54
Figure 3-21 Pullout tests by Ozedemir [Ozedemir et al., 2005] 55
Figure 3-22 Bend in CFRP [Morphy 1999] 56
Figure 3-23 Fan opening angle studied by Koayashi and use of anchor fans [Kobayashi et al., 2001; Masuo et al., 2001] 57
Figure 3-24 Diverting forces due to unevenness of concrete surface [fib-14 2001] 57
Figure 3-25 GFRP anchor spikes [Ibell et al., 2003] 58
Figure 3-26 Shear test of carbon fiber anchor [Burr, 2004] 58
Figure 3-27 Use of FRP anchor on infill wall 59
Figure 3-28 Fracture of CFRP with anchors [Kim, 2006] 59
Figure 3-29 Fyfe anchors [Burr, 2004] 60
Figure 3-30 Sika anchors [Sika, 2005] 60
Figure 3-31 Grinding and sandblasting surface preparation 61
Figure 3-32 Drilling hole in concrete and rounding over edges (courtesy of Insung Kim) 62
Figure 3-33 Repair material components and painting of concrete with latex solution .. 62
Figure 3-34 Placing and leveling of ramp material 63
Figure 3-35 Mixing epoxy and saturating concrete surface 63
Figure 3-36 Rolling CFRP through PVC pipes and applying to concrete surface 64
Figure 3-37 Removing air bubbles from CFRP sheet and applying CFRP anchors 64
Figure 3-38 Strip of CFRP to make anchor and strip folded over steel wire 65
Figure 3-39 Saturating anchor and making hole in CFRP sheet to insert anchor 65
Figure 3-40 Inserting anchor and fanning ends of anchor over CFRP sheet 65
Figure 4-1 Use of CFRP at height transitions 68
Figure 4-2 CFRP anchor 68
Figure 4-3 Test setup 69
Figure 4-4 Free body diagram of half of test specimen 70
Figure 4-5 Concrete block formwork and rebar 71
Figure 4-6 CFRP application with no height transition 72

Figure 4-7 CFRP application with height transition 72
Figure 4-8 CFRP anchor depth 73
Figure 4-9 Measurement of vertical displacement and horizontal crack opening 75
Figure 4-10 FRP coupons tested in accordance with ASTM D-3039 76
Figure 4-11 Maximum tension and efficiency of CFRP 78
Figure 4-12 Debonding of CFRP 80
Figure 4-13 Strain distribution for test 00-ns1 81
Figure 4-14 Shear failure of U-wrap 82
Figure 4-15 Deformation capacity of various retrofits 82
Figure 4-16 Failure by FRP fracture of retrofit with double layer U-wraps (00-us2) 83
Figure 4-17 Failure by debonding and partial FRP fracture of retrofit with one anchor per row (00-2s2) 84
Figure 4-18 Failure by FRP fracture of retrofit with two anchors per row (00-4s2) 85
Figure 4-19 Failure by FRP fracture of retrofit with three anchors per row (00-6s1) 86
Figure 4-20 Strains in CFRP for test 00-6s1 86
Figure 4-21 Failure by CFRP fracture for retrofit with two larger anchors per row (00-4s3) 87
Figure 4-22 Failure by concrete fracture and debonding for retrofit with one row of two anchors (00-2s1) 88
Figure 4-23 Failure by shear in concrete block (00-4g1) 88
Figure 4-24 Effect of slope of transition 92
Figure 4-25 Fracture of CFRP at top of transition slope in test 22-6s1 92
Figure 4-26 Effect of type of CFRP fabric 94
Figure 4-27 Fracture of CFRP anchor 94
Figure 4-28 Effect of surface preparation 95
Figure 4-29 Failure of test 42-6n2 96
Figure 4-30 Effect of height difference 97
Figure 4-31 Failure of 41-6s1 with 1" height difference 97
Figure 4-32 Failure of 43-6s1 with 3" height difference 97
Figure 4-33 Example of strain gage locations on 22-2g1 98
Figure 4-34 Strain distribution across CFRP sheet in 22-2g1 98
Figure 4-35 Distribution of strains at CFRP fracture for tests with 6 anchors 99
Figure 4-36 Distribution of strains at CFRP fracture for tests with 1 to 2 transition slope 100
Figure 4-37 Forces in CFRP sheet 100
Figure 4-38 Cross fibers in column sheet 101
Figure 5-1 Use of CFRP to provide continuity through the positive moment reinforcement 105
Figure 5-2 CFRP to provide continuity 105
Figure 5-3 Relationship of test specimen to prototype building 106
Figure 5-4 Reinforcement design of test specimen (shown in test position) 108
Figure 5-5 Reinforcement cutoff locations 108
Figure 5-6 Schematic of test setup 109
Figure 5-7 Photo of test setup 109
Figure 5-8 Comparison of uniform and 3 point loads 110

Figure 5-9 Movable loading plates to allow for large deflections 111
Figure 5-10 Photo of loading point 112
Figure 5-11 Schematic of restraint at end of beam 113
Figure 5-12 Supports to provide moment resistance 113
Figure 5-13 Axial restraint and measurement 114
Figure 5-14 Spacers for compression restraint 114
Figure 5-15 Rollers to provide rotational restraint at column stub 115
Figure 5-16 Braces (green) to provide lateral restraint and support North and South blue columns 115
Figure 5-17 Instrumentation locations 116
Figure 5-18 Stress vs strain for reinforcing bar 118
Figure 5-19 Failure of specimen NR-2 120
Figure 5-20 Vertical and axial loads versus displacement for NR-2 121
Figure 5-21 Design of CFRP retrofit for PM-1 122
Figure 5-22 Drilling hole through column 123
Figure 5-23 Pulling CFRP through hole in column 123
Figure 5-24 CFRP retrofit for PM-1 124
Figure 5-25 Failure of PM-1 by fracture of rebar 125
Figure 5-26 Vertical and axial loads for PM-1 125
Figure 5-27 Strains in positive moment steel for PM-1 126
Figure 5-28 Strains in CFRP for PM-1 127
Figure 5-29 Design of CFRP retrofit for PM-2 128
Figure 5-30 CFRP retrofit for PM-2 128
Figure 5-31 Final state of PM-2 129
Figure 5-32 Vertical and axial load versus displacement for PM-2 129
Figure 5-33 Strain in CFRP prior to fracture for PM-2 130
Figure 5-34 Strains in positive moment steel in PM-2 131
Figure 5-35 Strains in negative moment reinforcement in PM-2 132
Figure 5-36 Design of CFRP retrofit for NM-1 133
Figure 5-37 Vertical and axial loads for NM-1 134
Figure 5-38 Final state of specimen NM-1 134
Figure 5-39 Fracture of threaded rod at 32 k axial tension 135
Figure 5-40 Wide crack and pulling out of #3 bars at column line 135
Figure 5-41 Hinging at support 136
Figure 5-42 Strains in positive moment rebar for NM-1 137
Figure 5-43 Strains in negative moment reinforcement for NM-1 137
Figure 5-44 Strains in CFRP for NM-1 138
Figure 5-45 Vertical and Axial loads for NM-2 139
Figure 5-46 Final state of specimen NM-2 139
Figure 5-47 Fracture of CFRP at 36 k axial tension in NM-2 140
Figure 5-48 Strains in positive moment reinforcement for NM-2 141
Figure 5-49 Strains in negative moment reinforcement for NM-2 141
Figure 5-50 Strains in CFRP for NM-2 142
Figure 5-51 Linear pots to measure hinge rotation 143
Figure 5-52 Distributed cracking in hinge region 144

Figure 5-53 Linear pot to measure crack opening 144
Figure 5-54 Design of CFRP retrofit for FR-1 145
Figure 5-55 Vertical and axial load versus displacement for FR-1 146
Figure 5-56 Fracture of anchors at end of positive moment reinforcement 147
Figure 5-57 Fracture of negative moment CFRP... 147
Figure 5-58 Fracture of rebar.. 147
Figure 5-59 Final state of FR-1.. 148
Figure 5-60 Strains in positive moment reinforcement for FR-1 149
Figure 5-61 Strains in negative moment reinforcement for FR-1................................. 149
Figure 5-62 Strains in CFRP over support region for FR-1.. 151
Figure 5-63 Strains in CFRP over column region for FR-1.. 151
Figure 5-64 Design of specimen CR-1 152
Figure 5-65 Vertical and axial load versus displacement for CR-1.............................. 153
Figure 5-66 Fracture of positive moment rebar... 154
Figure 5-67 Fracture of negative moment rebar 154
Figure 5-68 Final state of CR-1 154
Figure 5-69 Strains in positive moment reinforcement for CR-1................................. 155
Figure 5-70 Strains in negative moment reinforcement for CR-1 156
Figure 5-71 Vertical load versus displacement for all tests.. 157
Figure 5-72 Axial load versus displacement for all tests.. 157
Figure 5-73 Comparison of PM-1 and CR-1 158
Figure 5-74 Comparison of NM-1 and NM-2.. 159
Figure 6-1 Idealization of specimen NM-2 for case 1 164
Figure 6-2 Free body diagram of case 1 165
Figure 6-3 Deflection compatibility... 166
Figure 6-4 Extension due to geometry... 168
Figure 6-5 Axial extension measurement from brace.. 169
Figure 6-6 Axial extension measurement from floor.. 169
Figure 6-7 Measured axial displacements versus axial tension for specimens NM-2... 170
Figure 6-8 Division of beam for elongation analysis... 171
Figure 6-9 Determination of initial length of yielded reinforcement 173
Figure 6-10 Variation of yielding along beam (NM-2) 174
Figure 6-11 Comparison of Ramberg-Osgood and experimental stress strain curves for reinforcing bar.. 175
Figure 6-12 Idealization for case 2 177
Figure 6-13 Free body diagram of case 2 177
Figure 6-14 Division of beam for elongation analysis, case 2..................................... 179
Figure 6-15 Vertical load versus deflection for specimens NM-1 and NM-2 and analysis model.. 180
Figure 6-16 Axial tension versus deflection for specimens NM-1 and NM-2 and analysis model.. 180
Figure 6-17 Vertical load vs. displacement curves for spec NR-2 and PM-2 and analysis model.. 182
Figure 6-18 Axial tension vs. displacement curves for spec NR-2 and PM-2 and analysis model.. 182

Figure 6-19 Comparison of case 1 and case 2 vertical load vs displacement................ 184
Figure 6-20 Comparison of case 1 and case 2 axial load vs displacement.................... 184
Figure 6-21 Influence of parameter L_i on catenary response.. 186
Figure 6-22 Influence of parameter L_y on catenary response....................................... 186
Figure 6-23 Influence of parameter e_i on catenary response of beam 186
Figure 6-24 Influence of beam height on catenary response 187
Figure 6-25 Influence of beam length on catenary response 187
Figure 6-26 Determination of hinge locations for beam without retrofit 188
Figure 6-27 Determination of hinge locations for beam with CFRP retrofit................. 188
Figure 6-28 Application of representative axial loads.. 189
Figure 6-29 Prototype building with center column removed...................................... 190
Figure 6-30 Results of catenary analysis on prototype beam, uniform load vs displacement 192
Figure 6-31 Results of catenary analysis on prototype beam, axial load vs displacement 192
Figure 6-32 3D model of prototype building... 193
Figure 6-33 Application of axial loads representing catenary response of beams 193
Figure 6-34 Displacements in prototype building 194
Figure 6-35 Moment diagrams for columns 195
Figure 6-36 X direction stresses in first floor (ksi)... 195
Figure 6-37 Y direction stresses in first floor (ksi)... 196
Figure 6-38 Removal of column next to corner for progressive collapse analysis........ 197

Chapter 1: Introduction

Reinforced concrete buildings may be vulnerable to progressive collapse due to a lack of continuous reinforcement. Carbon fiber reinforced polymer (CFRP) may be used to retrofit existing reinforced concrete beams and provide the missing continuity needed to resist progressive collapse.

1.1 OBJECTIVE AND SCOPE

Progressive collapse is an extreme form of collapse that is disproportionate to the originating cause [NIST, 2007]. Examples of progressive collapse include the Ronan Point building in the U.K. and the Murrah building in the U.S. Progressive collapse is often caused by abnormal loads (loads not generally considered in building design) on a building, such as blast, vehicle impact, or faulty construction. Although the probability of such loads occurring is very low, the possible loss of life and injuries could be significant.

Because it is difficult to design for all possible loads on a building, many building codes have adopted requirements for general structural integrity that emphasize continuity, redundancy, and ductility. However, many of these requirements were not added until the 1980s and there is little experimental research to show that the integrity requirements are sufficient to limit progressive collapse. Reinforced concrete buildings often have discontinuity of both the positive and negative moment reinforcement. The lack of continuity may not allow for catenary tension ties to develop that could resist the progressive collapse loads on a beam. Therefore, many existing reinforced concrete buildings are vulnerable to progressive collapse, and a retrofit method to limit that vulnerability would be useful. Both Ronan Point and the Murrah building could have benefited from increased continuity and redundancy in the building [Breen, 1975; Corley, 2004]. Furthermore, carbon fiber reinforced polymers (CFRP) are an ideal retrofit material to provide continuity due to their high strength-to-weight ratio and moldability (before curing, CFRP is a flexible fabric that can conform to any surface). For more information about progressive collapse and the vulnerability of reinforced concrete buildings see Chapter 2.

The objective of this research is to develop strengthening procedures using CFRP materials to reduce vulnerability to progressive collapse in existing reinforced concrete buildings. If the column support between spans of a reinforced concrete frame is removed accidentally or by a blast, the lack of continuity of reinforcement may cause progressive collapse. While the CFRP retrofit may not be able to save the building from significant damage, it may be able to limit the progression of the collapse and save lives and reduce injuries. This research focuses on retrofitting the beams in a reinforced concrete building to provide sufficient continuity to reach catenary action. The catenary action may allow the beam to carry vertical loads at large displacements if a supporting column were removed, Figure 1-1.

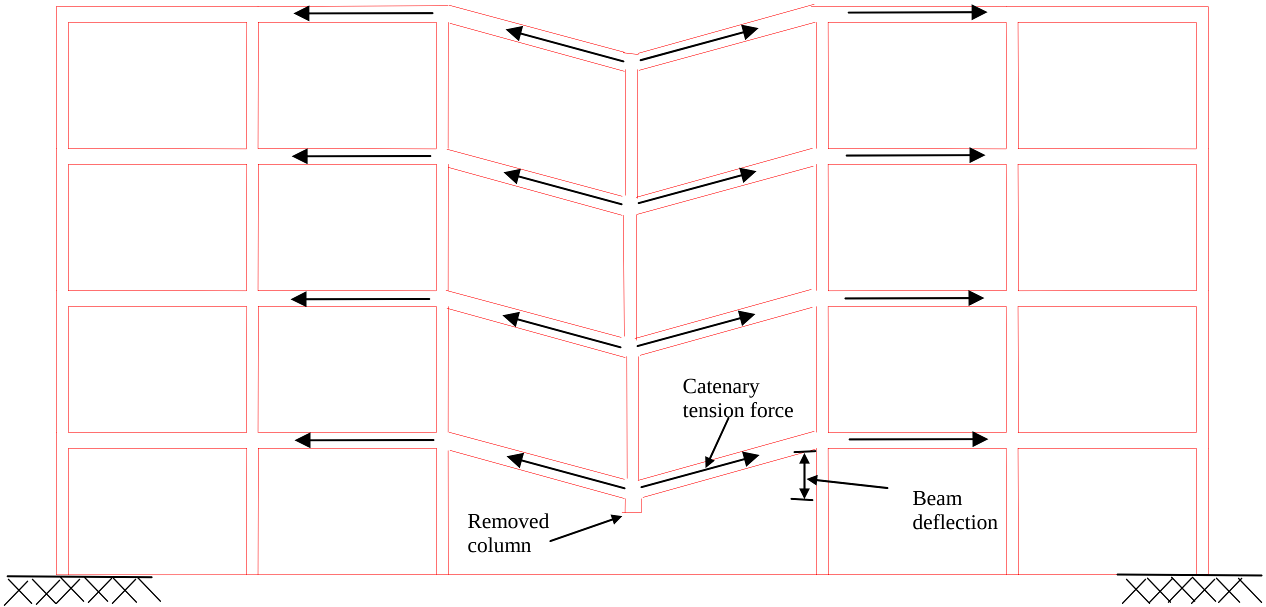

Figure 1-1 Catenary action in a reinforced concrete frame

The idea for the CFRP retrofit scheme is shown in Figure 1-2. The CFRP can provide continuity through the negative moment reinforcement by being means of a CFRP sheet applied to the top surface of the beam, Figure 1-3. Carbon fiber anchors at either end of the sheet aid in transferring the tension forces in the sheet to the negative moment reinforcement. Alternatively, the CFRP can provide continuity through the positive moment reinforcement by means of a CFRP sheet applied through a hole drilled in the column and attached to CFRP sheets applied on the bottom of the beams on either side of the column as shown in Figure 1-4. Because the hole through the column cannot be drilled flush with the bottom of the beam, a ramp of concrete can be applied to aid in transitioning the CFRP through the offset in surface level.

It is unknown which column may be removed and the CFRP retrofit is designed only to carry the loads on its floor (does not support floors above); therefore, the CFRP retrofit will need to be applied to all the perimeter beams. Some designers may consider the removal of an interior column in a progressive collapse analysis requiring the CFRP retrofit could be applied to all the beams in a building.

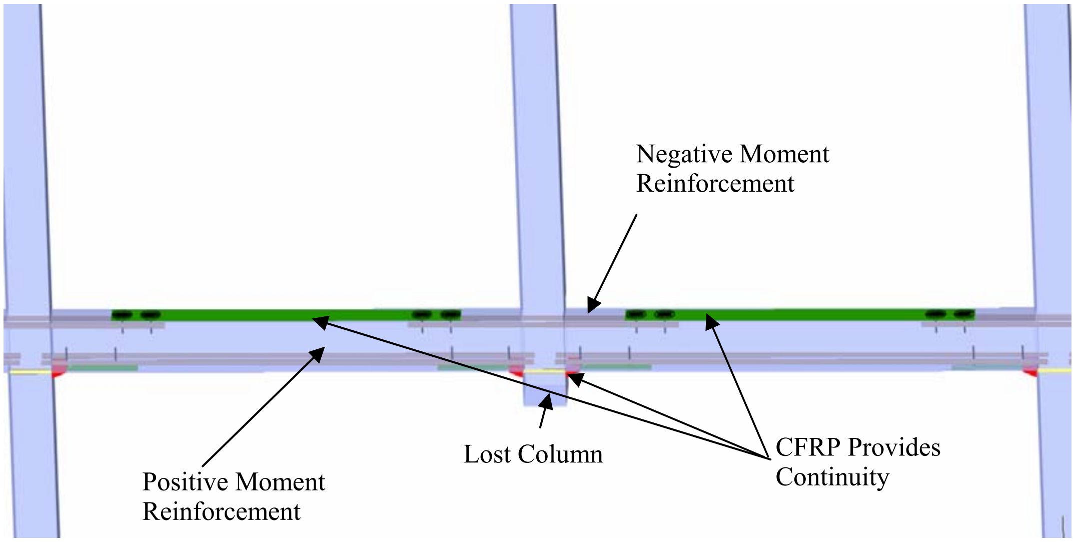

Figure 1-2 CFRP to provide continuity

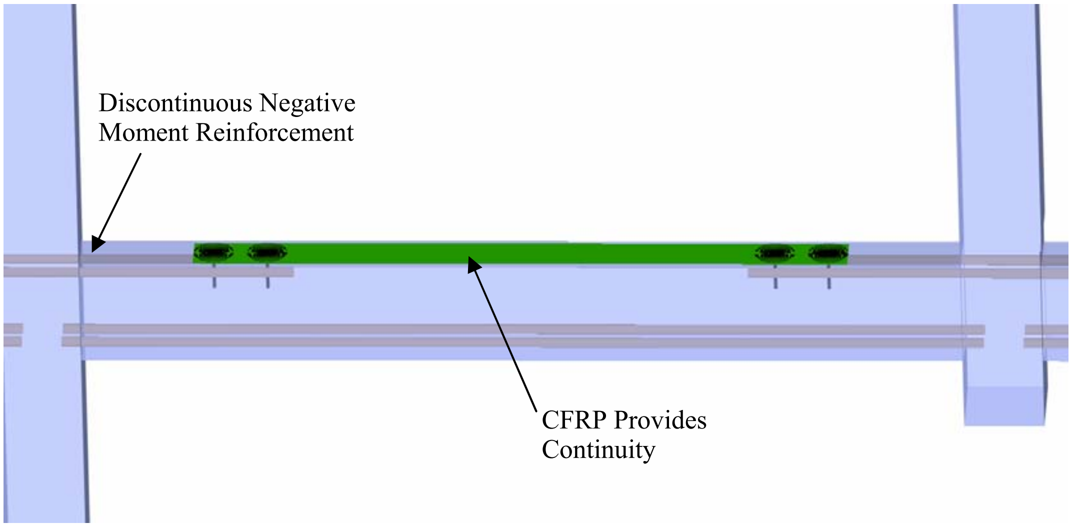
Discontinuous Negative
Moment Reinforcement
CFRP Provides
Continuity

Figure 1-3 CFRP retrofit to provide continuity through negative moment reinforcement

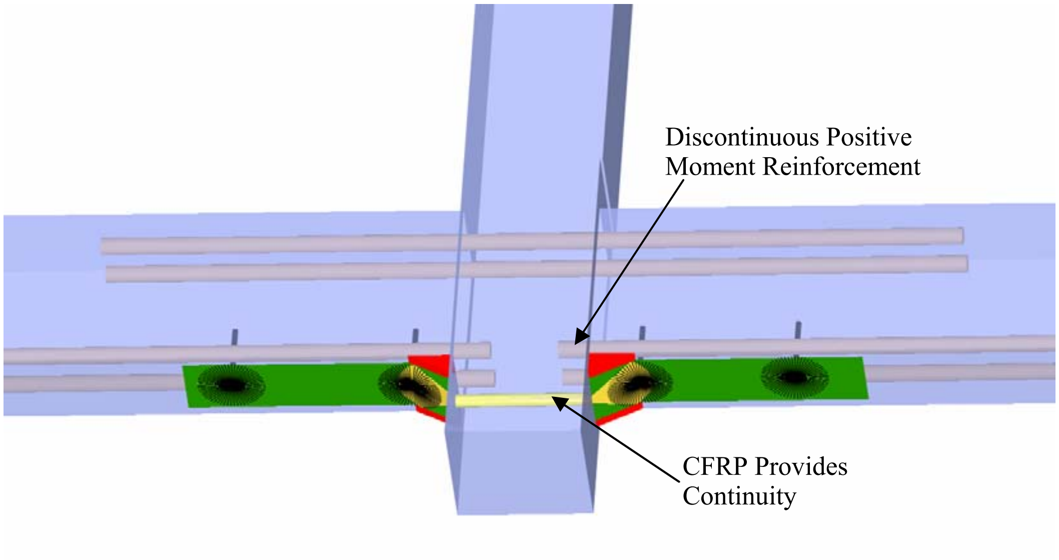
Discontinuous Positive
Moment Reinforcement
CFRP Provides
Continuity

Figure 1-4 CFRP retrofit to provide continuity through positive moment reinforcement

The research presented in this dissertation is limited to retrofits of reinforced concrete beams. The experiments were all conducted statically with load factors to account for dynamic loading. The overall project, not within the scope of this dissertation, will include retrofits to improve the capacity of reinforced concrete columns and dynamic loading of CFRP strengthened beams.

1.2 RESEARCH COMPONENTS

The research was broken into three major components (Figure 1-5):

- Anchorage tests – determine anchorage design parameters critical to utilizing the high tensile strength of CFRP material.
- Continuity tests – determine if CFRP retrofits can provide the continuity and catenary action needed to resist progressive collapse.
- Catenary model - determine a set of equations to predict load-carrying capacity of a beam in catenary action.

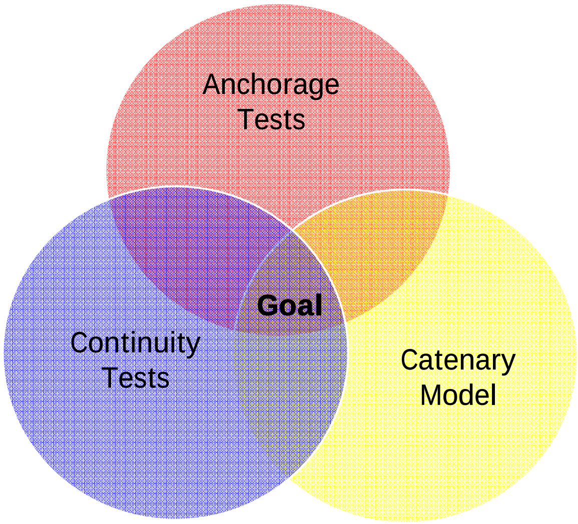

Figure 1-5 Division of research

1.2.1 Anchorage Tests

In order to design the CFRP retrofit to provide continuity, the anchorage of the CFRP must be considered. A serious limitation in the use of CFRP in reinforced concrete buildings comes from the separation of the CFRP sheet from the concrete surface by debonding. The problem of debonding is particularly detrimental because nearly half the CFRP material may be ineffective in increasing the strength of a concrete member [Bonacci et al., 2001].

Furthermore, a height transition (offset in the surface level of the CFRP) will further accentuate the early debonding of CFRP sheets. A height transition occurs when providing continuity of positive moment reinforcement because the hole through the column (where the CFRP will be threaded from one side to the other) cannot be drilled at the level of the bottom surfaces of the beams, Figure 1-6. In order to achieve a greater capacity in the CFRP retrofit, both CFRP anchors (Figure 1-7) and CFRP U-wraps (CFRP sheets wrapped around the sides of the beam) were evaluated as ways of anchoring the longitudinal CFRP sheet. The anchorage tests will also evaluate the best method to overcome the effect of a height transition.

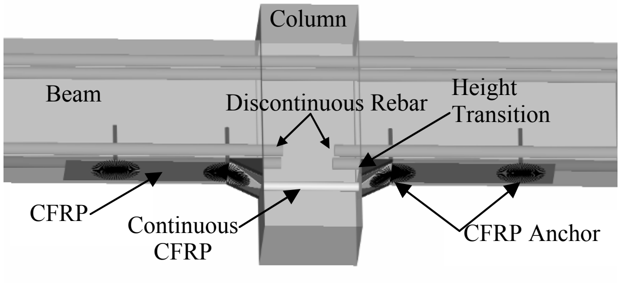
Column
Beam
Discontinuous Rebar
Height Transition
CFRP
Continuous CFRP
CFRP Anchor

Figure 1-6 Use of CFRP at height transitions

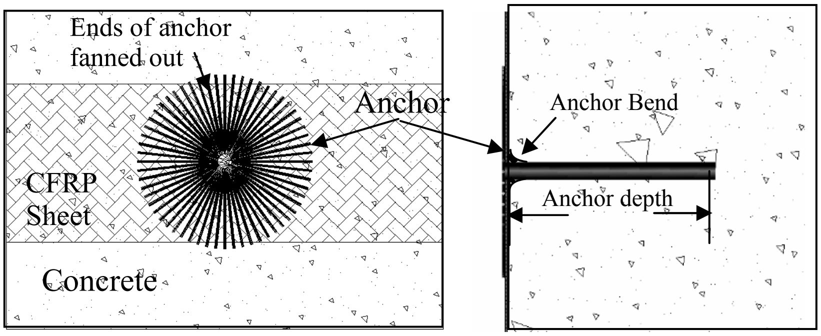
Ends of anchor fanned out
Anchor
Anchor Bend
CFRP Sheet
Anchor depth
Concrete

Figure 1-7 CFRP anchor

The goal of the anchorage tests is to determine simple design recommendations to achieve improved CFRP tensile capacity in the CFRP retrofit to provide continuity to reinforced concrete frames. The parameters evaluated in the anchorage tests are the size, number, and spacing of anchorages (CFRP anchors or U-wraps), slope and height of the transition, material efficiency, type of surface preparation, and type of carbon fiber fabric.

1.2.2 Continuity Tests

The continuity tests evaluate different CFRP retrofit methods to provide continuity and reduce vulnerability to progressive collapse in reinforced concrete frames. The design of a retrofit to provide continuity is based on design details developed during the anchorage tests.

The continuity tests evaluate half-scale specimens of two spans of a reinforced concrete (RC) frame with a center supporting column removed Figure 1-8. The tests are designed to simulate the removal of a perimeter column along an interior span. The tests evaluate the capacity for catenary action of vulnerable RC building beams with discontinuous longitudinal reinforcing steel and the increased capacity achieved by the CFRP retrofit. Additionally, tests will be conducted on a beam with continuous reinforcing steel and a beam strengthened to accommodate the double span through flexure.

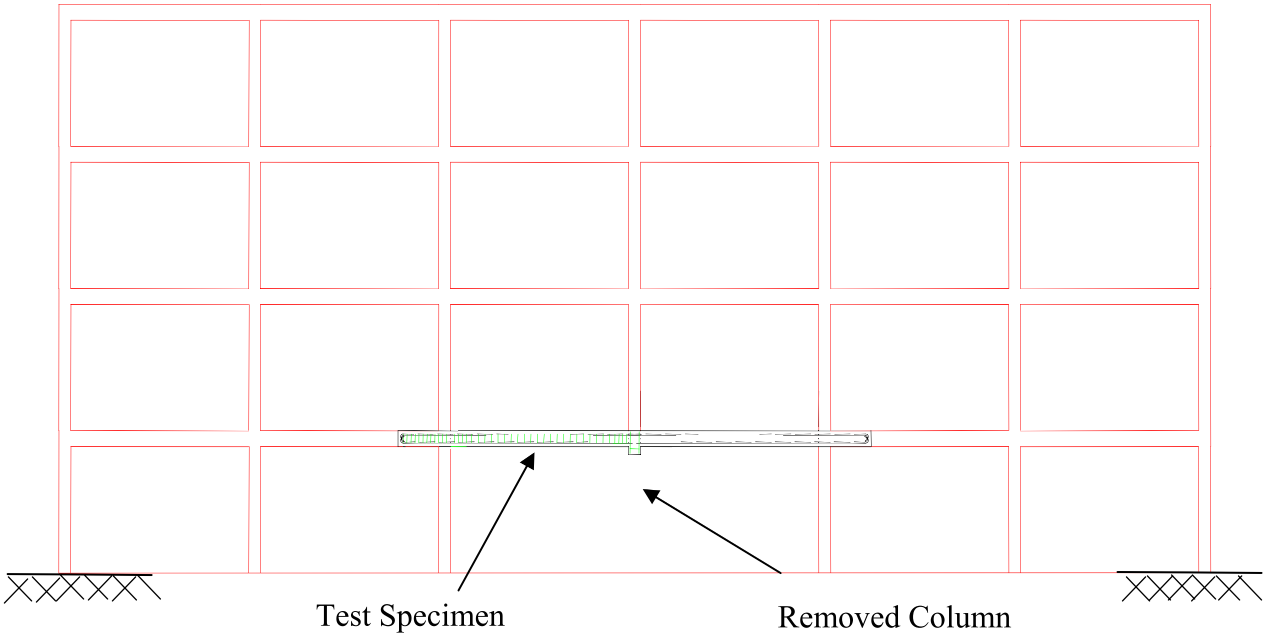

Figure 1-8 Relation of test specimen to prototype building (elevation view)

1.2.3 Catenary Model

In order to apply the experimental results of the continuity tests to reinforced concrete frames, a catenary analysis model was created to understand the process of catenary action. A system of equations was developed in order to predict the load and deflection of a reinforced concrete beam in catenary action. The equations are based on the fundamental concepts of equilibrium, compatibility, and material characteristics. With the knowledge of the load-deflection relationship of a catenary and the axial tension expected, the effect of the catenary on the rest of the structure can be determined.

The anchorage tests form the design basis of the CFRP retrofit and ensure that the capacity of the retrofit can be accurately predicted. The continuity tests determine if the CFRP retrofit is capable of providing continuity and if the retrofit will allow the beam to reach catenary action and sustain a load representing resistance to progressive collapse.

The catenary analysis model forms a set of equations to model catenary action so the results can be applied to reinforced concrete beams in general. All three components work together to deliver the objective of the research: a CFRP retrofit design that may reduce vulnerability to progressive collapse in existing reinforced concrete buildings.

Chapter 2: Progressive Collapse Background

In this chapter, the definition, example and codes pertaining to progressive collapse, the reason why reinforced concrete structures are vulnerable to progressive collapse, and the basis for a retrofit to limit the vulnerability will be discussed.

2.1 PROGRESSIVE COLLAPSE

Progressive collapse is a severe form of collapse to which many structures may be vulnerable. Generally buildings are not designed for abnormal loading conditions that may result in progressive collapse [NIST, 2007]. However, when an unlikely loading event occurs, the injuries and loss of life due to progressive collapse can be severe.

2.1.1 Definition and Causes

Progressive collapse is defined by the U.S. General Services Admistration (GSA) as “a situation where local failure of a primary structural component leads to the collapse of adjoining members which, in turn, leads to additional collapse. Hence the total damage is disproportionate to the original cause.” [GSA, 2003] Other definitions of progressive collapse are similar. ASCE Standard 7-05 defines progressive collapse as “the spread of an initial local failure from element to element resulting, eventually, in the collapse of an entire structure or a disproportionately large part of it.” [ASCE, 2005] Simply put, progressive collapse results in more damage than there is expected to be due to the initiating cause. Limiting the excess damage, or collapsed area, along with a corresponding reduction in loss of life is the focus of this research.

Causes of progressive collapse can be attributed to gas or bomb explosions, collisions (vehicles or airplanes), wind (tornadoes), faulty construction, foundation failure, or other extreme events. In other words, progressive collapse can be caused by any load (typically abnormal) that fails a primary structural component.

2.1.2 Examples

Many structures have exhibited progressive collapse due to an abnormal load. Others have not exhibited progressive collapse in spite of catastrophic loads that could have triggered progressive collapse. The following gives examples pertaining to reinforced concrete (precast or cast-in-place) construction.

2.1.2.1 Ronan Point

One of the earliest and most famous examples of progressive collapse is the collapse of the Ronan Point apartment building in 1968 in the U.K., Figure 2-1 [Nair, 2004]. An accidental explosion caused by a gas leak blew out one of the precast wall panels on the 18th floor triggering the collapse of the upper floors, which was followed by the lower ones due to the additional dead load of the fallen upper floors [Nair, 2004]. The building was a precast concrete wall and floor system with the floors being supported directly by the walls. However, the connections between the walls and floors did not provide any alternate load path for load redistribution leading to the progressive collapse of the structure [NIST, 2007]. Since the Ronan Point collapse, the U.K., and other governments have initiated requirements for structural integrity to aid in the redistribution of loads. For example, in the U.K. precast concrete structures are required to be tied together so that they can either provide an alternate load path or a specific local resistance to withstand an abnormal load [NIST, 2007; Breen, 1975].

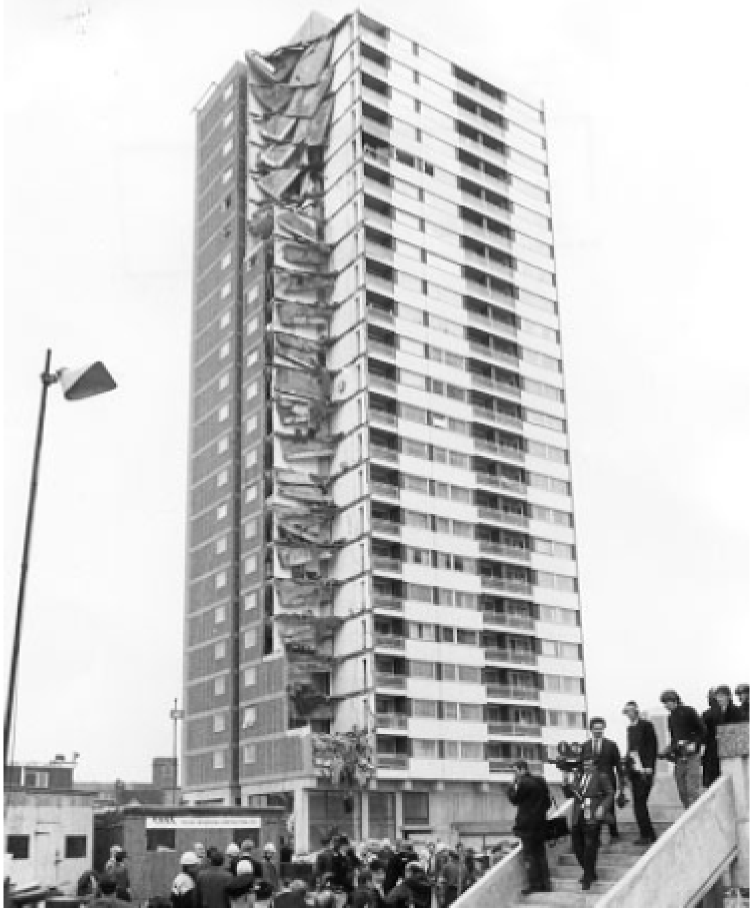

Figure 2-1 Ronan Point collapse [Nair, 2004]

2.1.2.2 Murrah Building

Another famous example of progressive collapse is the Alfred P. Murrah Building in Oklahoma City, Oklahoma. On April 19th 1995, a truck bomb detonated on the North side of the Murrah building causing severe structural damage, Figure 2-2 and Figure 2-3. The building was built in 1974 to 1975 in accordance with the design codes of the day (ACI 318-71) [Sozen et al., 1998]. Column lines were typically spaced at 20 ft. A third-floor transfer girder supported intermediate columns and widened the column spacing to 40 ft for the first two floors, Figure 2-4. A schematic of the third floor transfer girder reinforcement demonstrates discontinuity of reinforcement in both the positive and negative moment reinforcement, Figure 2-5. The blast from the bomb destroyed column

G20 below the transfer girder and may have destroyed or severely damaged columns G24 and G16 on either side [Corley, 2004]. The loss of these columns caused collapse of nearly half the occupiable space in the building.

If the building had been detailed as a special moment frame, so that columns G24 and G16 survived the blast, and had continuity of reinforcement to limit the collapse of floors above, the collapsed area of the structure could have been reduced 50% to 80% [Corley, 2004]. Ninety percent of the 168 people who died in the Murrah building were killed by falling debris; therefore, limiting the collapse of the structure could have saved those lives.

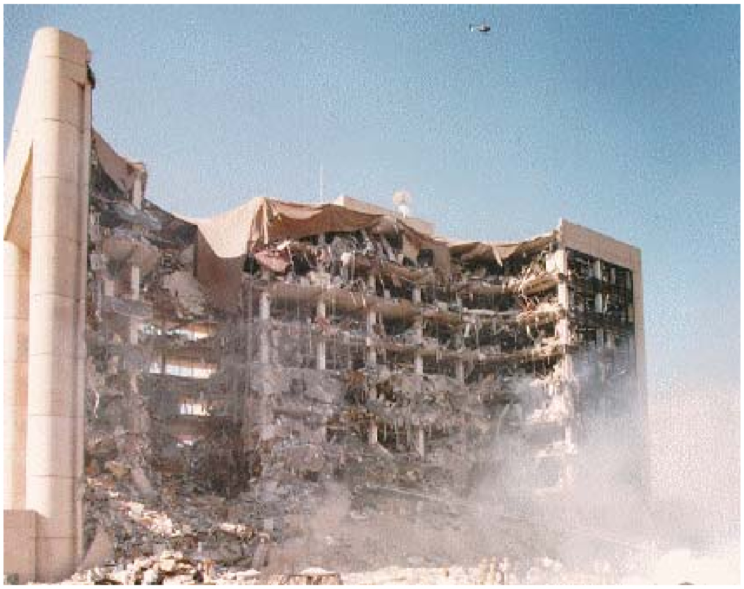

Figure 2-2 Collapse of Murrah building [Crawford, 2002]

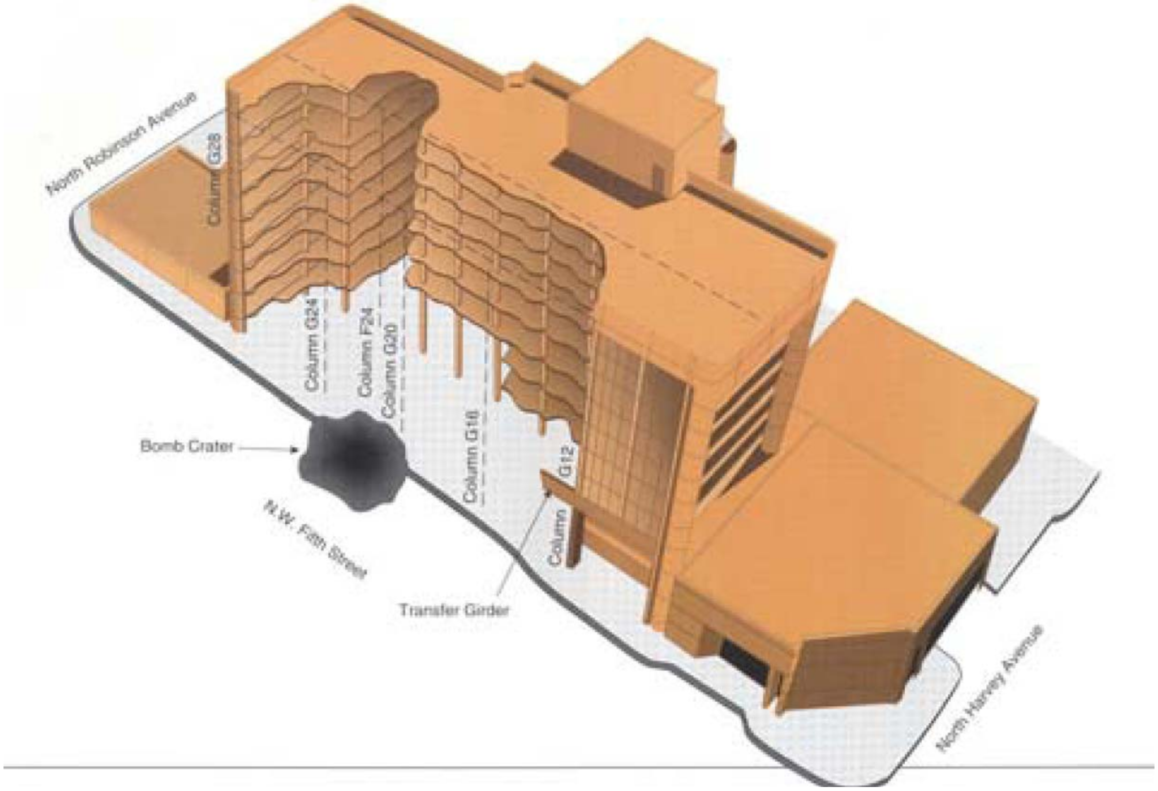
North Robinson Avenue
Column G28
Column G24
Column F24
Column G20
Column G16
Column G12
Bomb Crater
N.W. Fifth Street
Transfer Girder
North Harvey Avenue

Figure 2-3 Collapsed area of Oklahoma City Murrah building [NIST, 2007]

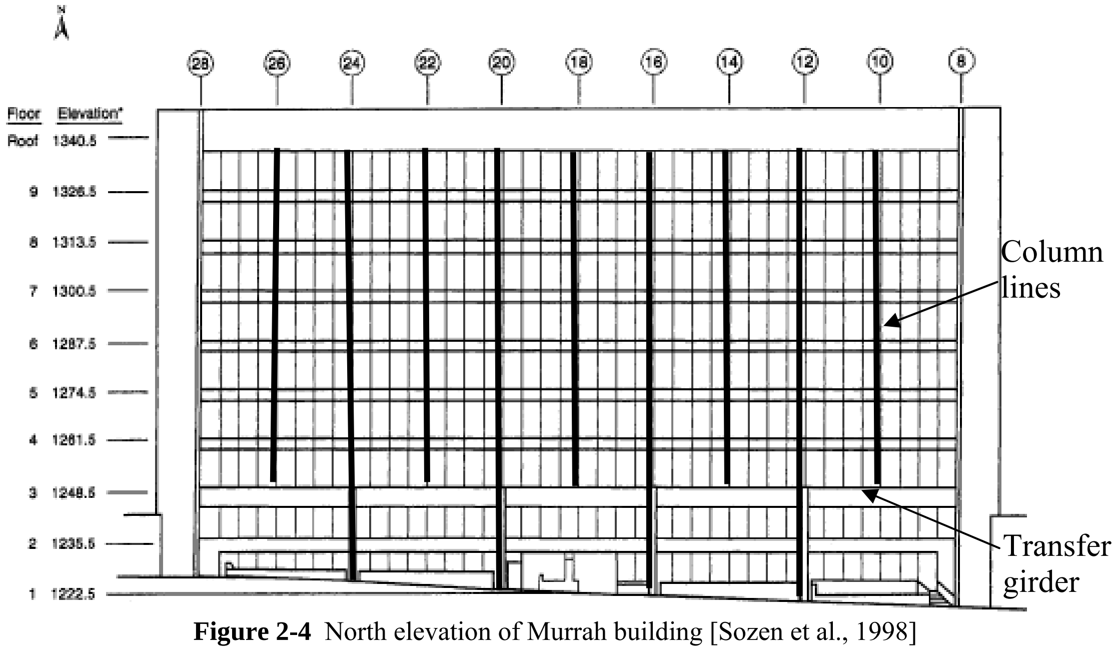
N
28
26
24
22
20
18
16
14
12
10
8
Floor
Elevation*
Roof 1340.5
9 1326.5
8 1313.5
7 1300.5
6 1287.5
5 1274.5
4 1261.5
3 1248.5
2 1235.5
1 1222.5
Column lines
Transfer girder

Figure 2-4 North elevation of Murrah building [Sozen et al., 1998]

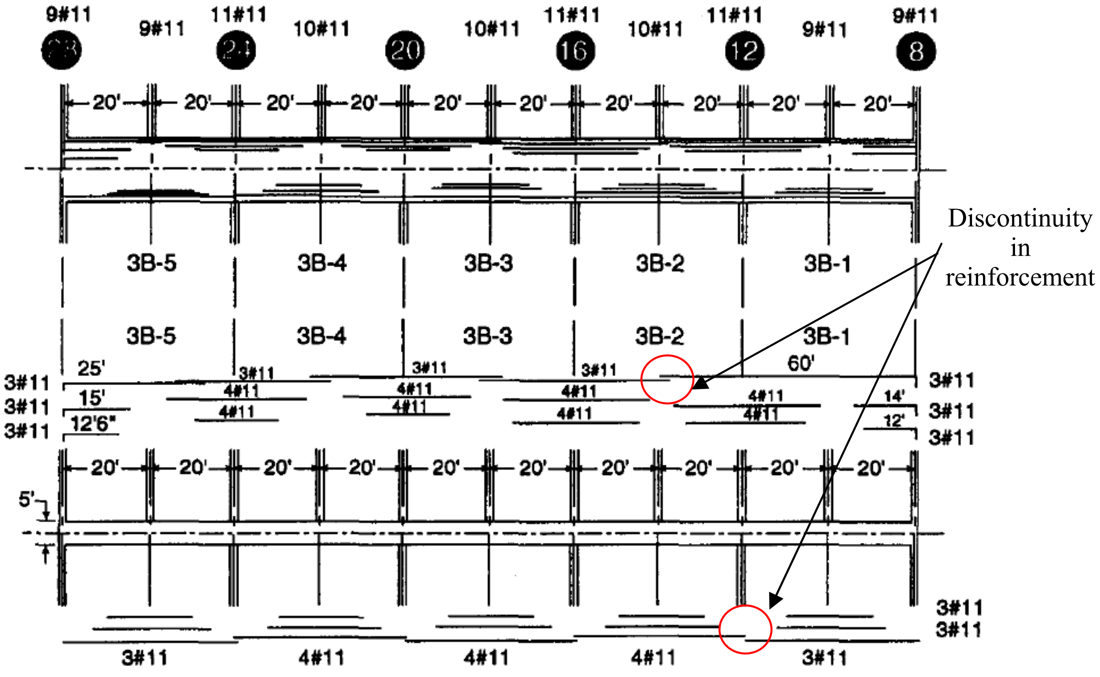
9#11
9#11
11#11
10#11
10#11
11#11
10#11
11#11
9#11
9#11
24
20
16
12
8
20'
3B-5
3B-4
3B-3
3B-2
3B-1
Discontinuity in reinforcement
25'
15'
12'6"
60'
14'
12'
3#11
4#11
5'
3#11
4#11
4#11
4#11
3#11

Figure 2-5 Reinforcement diagram for 3rd floor transfer girder [Sozen et al., 1998]

2.1.2.3 L'Ambiance Plaza

While Ronan Point and the Murrah Building are some of the most famous examples of progressive collapse, many other structures have collapsed. The L'Ambiance Plaza in Bridgeport, Connecticut is an example of a building that collapsed during construction, killing 28 construction workers, Figure 2-6, [Martin et al., 2000]. The building was constructed of post-tensioned floors that were lifted into place on steel columns. Localized failure started when a temporary lifting device at a column failed. The failure progressed throughout the building due to minimal mild reinforcing steel in the slabs, that allowed cracks to grow without restraint, ungrouted post-tensioning tendons, that allowed failure to propagate to all bays, and frame stability that did not provide reserve strength for unusual conditions [NIST, 2007].

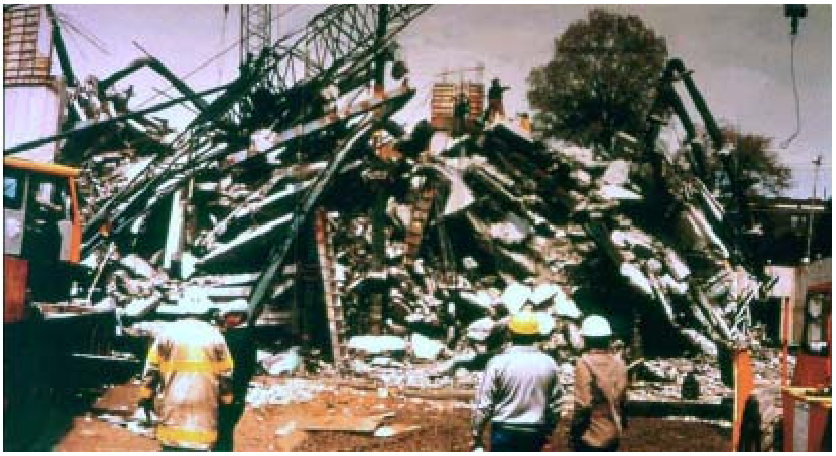

Figure 2-6 L'Ambiance Plaza collapse [NIST, 2007]

2.1.2.4 Pentagon

Conversely, many buildings have suffered severe damage that did not lead to progressive collapse. One example is the limited collapse of the Pentagon Building in Washington, D.C. on September 11th 2001. A plane was flown into the first floor of the building and destroyed 30, first-floor columns and damaged about 20 others along a path that extended approximately 75 ft wide by 230 ft long through the first floor, Figure 2-7 [Mlakar et al., 2003]. Even with the extensive damage to many columns in the first floor, the upper stories remained intact for more than 20 minutes until they collapsed due to fire after the airplane impact, Figure 2-8 and Figure 2-9. According to the Pentagon Building Performance Report [Mlakar et al., 2003], reasons for the performance of the building are:

- "Redundant and alternative load paths of the beam and girder framing system;
- Short spans between columns;
- Substantial continuity of beam and girder bottom reinforcement through the supports;
- Design for 150 psf warehouse live load in excess of service load;
- Significant residual load capacity of damaged spirally reinforced columns;

- Ability of the exterior walls to act as transfer girders."

The survival of the Pentagon building demonstrates the capacity a reinforced concrete building to withstand catastrophic loads if designed with significant redundancy and continuity.

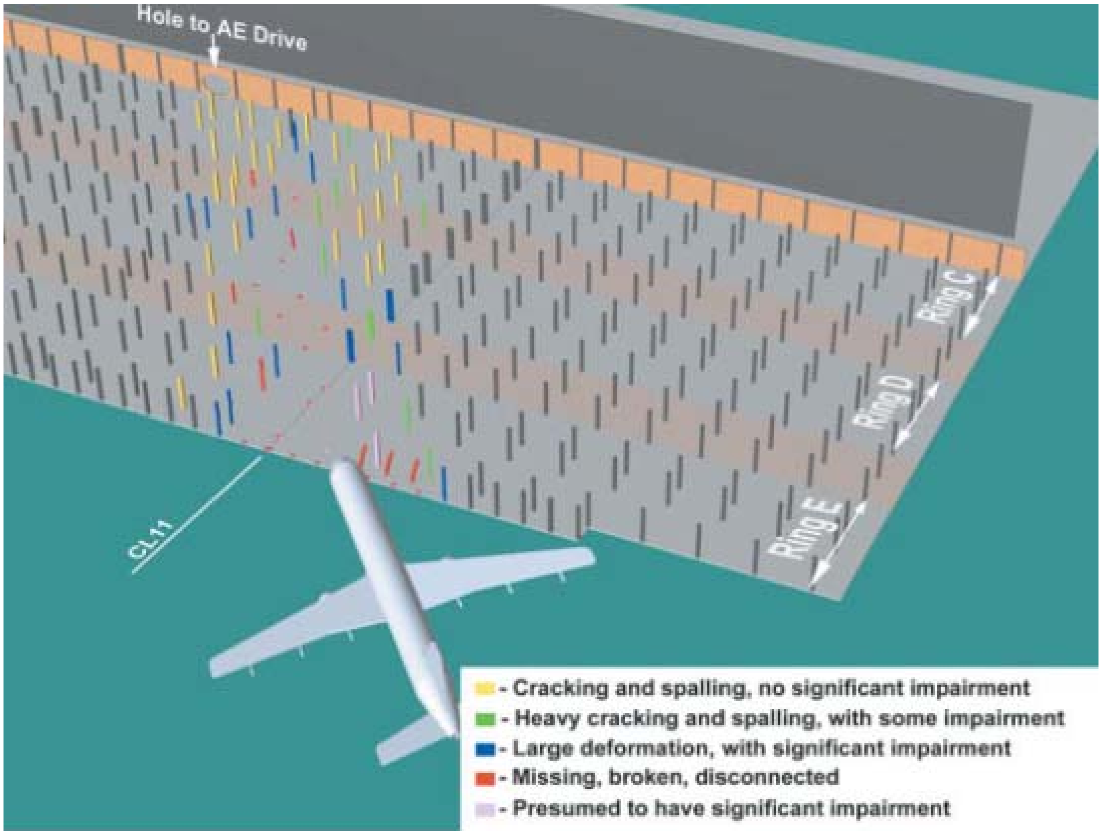
Hole to AE Drive
Ring C
Ring D
Ring E
CL11
🟨 - Cracking and spalling, no significant impairment
🟩 - Heavy cracking and spalling, with some impairment
🟦 - Large deformation, with significant impairment
🟥 - Missing, broken, disconnected
🟪 - Presumed to have significant impairment

Figure 2-7 Damage to first floor columns [Mlakar et al., 2003]

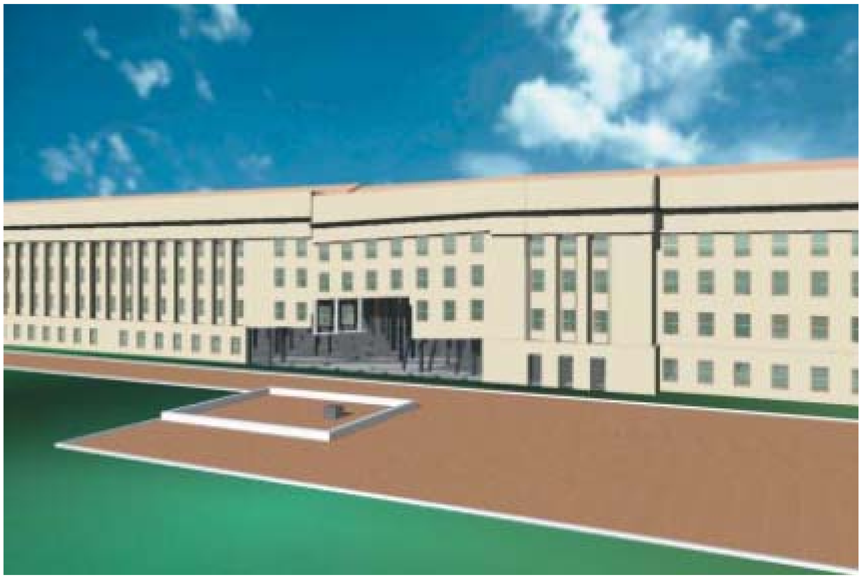

Figure 2-8 Rendering of damaged area of Pentagon before collapse [Mlakar et al., 2003]

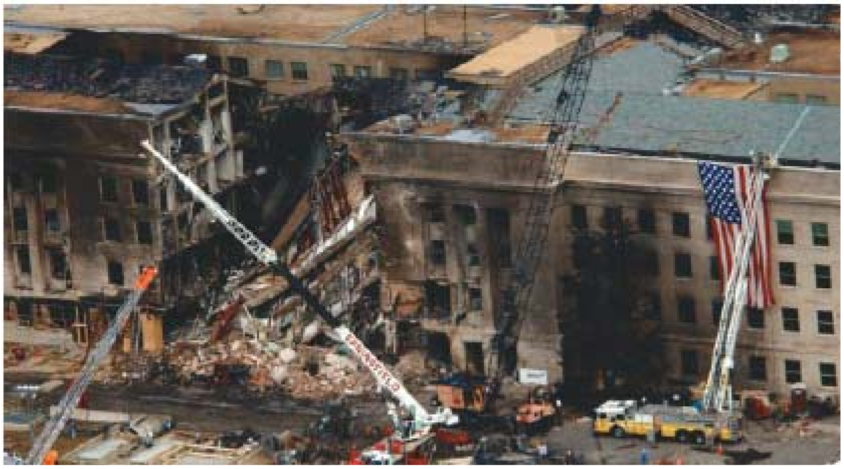

Figure 2-9 Collapse of Pentagon building [Mlakar et al., 2003]

2.1.2.5 Khobar Towers

Another example of a structure that did not exhibit progressive collapse is the Khobar Towers in Dhahran, Saudi Arabia in 1996. The precast panel building was built to the British concrete design code, which included a prescriptive approach for collapse prevention, ductile detailing, and well designed ties between the concrete panels [NIST, 2007]. As a result, the damage due to a very large bomb was limited to the façade and some bays closest to the blast. The collapse did not progress as in the Ronan Point building.

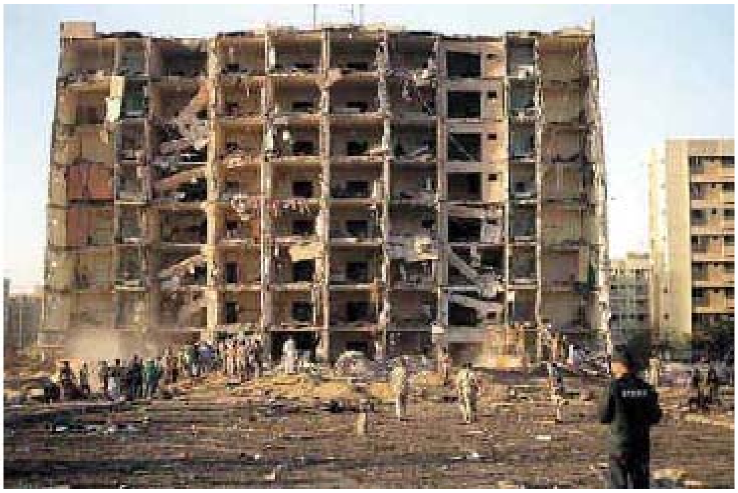

Figure 2-10 Khobar Towers bombing [NIST, 2007]

From the examples of buildings that did and did not exhibit progressive collapse it is clear that an underlying theme of redundancy, continuity, and ductility are effective in reducing progressive collapse.

2.1.3 Standards

The first implementation of standards for progressive collapse was introduced in the U.K. after the 1968 collapse of Ronan Point [NIST, 2007]. The British Standards required consideration of progressive collapse in buildings taller than five stories and provisions for structural ties. In the 1970s the U.S. Department of Housing and Urban Development's Operation Breakthrough examined the problem of progressive collapse in the U.S., focusing on concrete panel structures. Starting in the 1980s, design standards in the U.S., such as the ACI code, began to implement structural integrity provisions. Additionally, ASCE 7 implemented some provisions for general structural integrity. However, these standards did not include specific provisions for resistance against progressive collapse [NIST, 2007].

Agencies of U.S. government, Department of Defense (DoD) and General Services Administration (GSA), have developed some design requirements for progressive collapse [DoD, 2004; GSA, 2003]. Generally, standards for progressive collapse consider three types of approaches:

- *Indirect Design*: Emphasize strength, continuity, redundancy, and ductility; relies on integrated system of tie forces
- *Direct Design – Alternate Load Path:* analyze structure for instantaneous loss of a vertical load bearing member, provide redundant or alternate load path to bridge over failed member; analysis can account for plastic or large deformations including catenary or membrane action
- *Direct Design – Specific Local Resistance:* each member is designed to resist a specific threat

The DoD document *Design of Buildings to Resist Progressive Collapse* (2004) considers both indirect and direct design approaches. For buildings requiring a low level of protection, a system of minimum tie forces is required, Figure 2-11. For example, in reinforced concrete buildings the peripheral ties are required to have the strength of:

Tie Force = Lesser of (4.5 + 0.9*number of stories) or 13.5 kip

Similar requirements exist for other types of ties, and more information can be found in the DoD document.

The direct design approach appears both in the DoD document and the GSA *Progressive Collapse Analysis and Design Guidelines* (2003). Both require the structure to survive the removal of a primary structural component, such as an external column. For static analysis, the loads placed on the structure include a factor for dynamic amplification due to the falling nature of the structure. The static load combinations are given in Table 2-1. For both the DoD and GSA guidelines this amplification factor is 2.

However, some research has indicated that the amplification factor could be reduced to 1.5 [Ruth et al., 2006]. The increased loads must be placed in a tributary area surrounding the removed element.

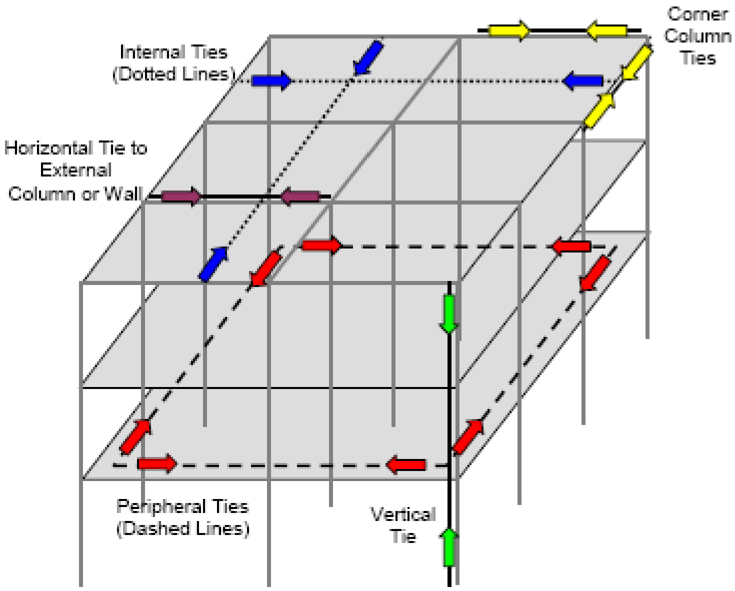
Corner Column Ties
Internal Ties (Dotted Lines)
Horizontal Tie to External Column or Wall
Peripheral Ties (Dashed Lines)
Vertical Tie

Figure 2-11 System of tie forces [DoD, 2003]

Table 2-1 Static load combinations for alternate load path analysis

Code	Static Load Combination
DoD:	2 [(0.9 or 1.2)D + (0.5 L or 0.2S)] + 0.2 W
GSA:	2(D+0.25L)

For a linear static analysis, the GSA guidelines use a demand-to-capacity ratio, generally 2, to account for inelastic deformations. The DoD guidelines require an iterative procedure to account for inelastic loads with acceptance criteria in the form of member deformation limits.

Both methods also include procedures for static inelastic analysis. The procedures allow for use of plastic deformation capacities and material over-strength factors. The inelastic analysis can also include geometric non-linearity, such as tension membrane or catenary action. However, the relative advantages and disadvantages of a catenary system that may hold a floor up compared to one that would break away to prevent damage to the rest of the structure must be evaluated, Figure 2-12. The acceptance criteria are based on member deformation limits. For example, GSA requires a RC beam to have a rotation less than 6 degrees or 0.105 radians. DoD deformation requirements are similar. Both guidelines also include procedures for dynamic analysis of a structure.

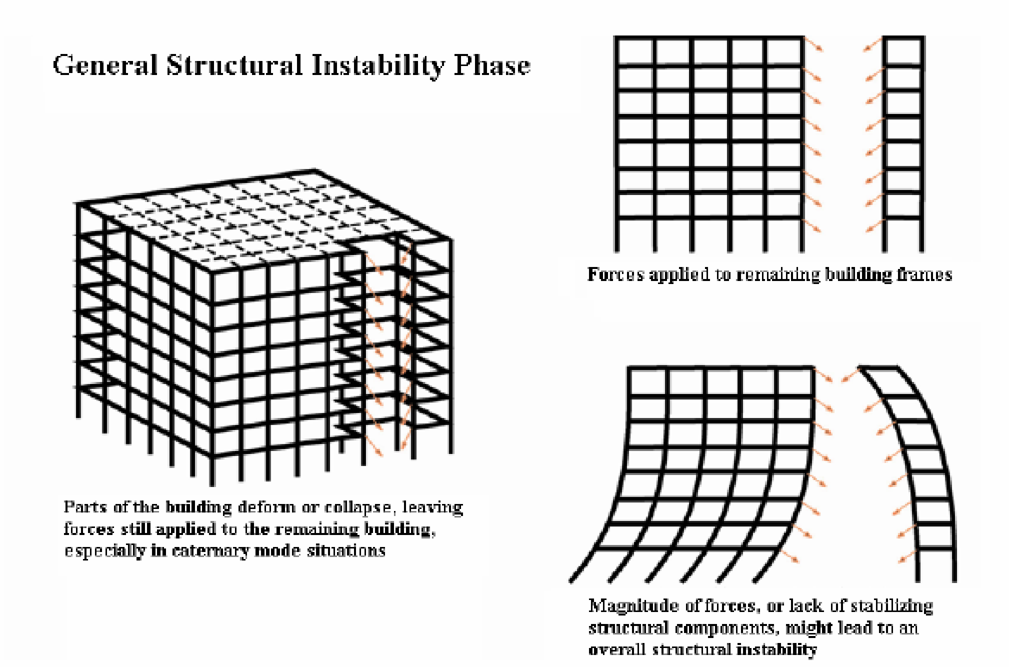
General Structural Instability Phase
Forces applied to remaining building frames
Parts of the building deform or collapse, leaving forces still applied to the remaining building, especially in caternary mode situations
Magnitude of forces, or lack of stabilizing structural components, might lead to an overall structural instability

Figure 2-12 Forces on structure due to catenary loads [NIST, 2007]

2.2 REINFORCED CONCRETE STRUCTURES AND PROGRESSIVE COLLAPSE

One of the major problems with reinforced concrete structures and progressive collapse that is addressed in this research is the lack of continuity of reinforcement, Figure 2-13. The GSA guidelines state “Providing continuous bottom reinforcing steel across the connection is essential to accommodating the double span condition.” However, many older buildings do not have continuous top or bottom reinforcing steel.

The integrity of reinforcement provisions requiring continuous bottom steel were not added until the 1989 American Concrete Institute building code [ACI, 1989]. The current ACI 318 Chapter 7 integrity of reinforcement provisions are [ACI, 2005]:

> *7.13.1—In the detailing of reinforcement and connections, members of a structure shall be effectively tied together to improve integrity of the overall structure.*
>
> *7.13.2.2—Beams along the perimeter of the structure shall have continuous reinforcement consisting of:*
>
> > *a) at least one-sixth of the tension reinforcement required for negative moment at the support, but not less than two bars; and*
> >
> > *b) at least one-quarter of the tension reinforcement required for positive moment at midspan, but not less than two bars.*

Furthermore, the commentary states that "by making a portion of the bottom reinforcement continuous, catenary action can be provided." However, these provisions are not designed to resist progressive collapse, they are just general "good building practices" for structural integrity. There is no assurance that continuity will provide catenary action or resist progressive collapse.

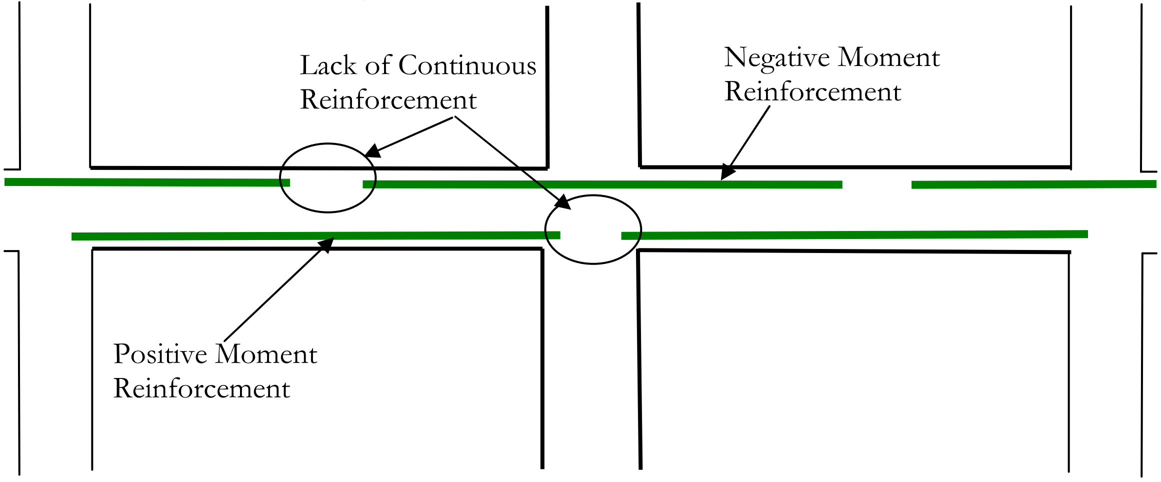
Lack of Continuous Reinforcement
Negative Moment Reinforcement
Positive Moment Reinforcement

Figure 2-13 Lack of continuous reinforcement in RC buildings

The ACI provisions were added in part due to the performance of the failed roof beam in May Co. Parking Garage in after the Whittier Narrows Earthquake in 1987, Figure 2-14 [Degenkolb, 1987]. The continuous positive moment steel over the support pulled out of the bottom of the beam, but was able, through catenary action, to hold up the failed section of the roof. While the continuous reinforcement in this structure was able to support a failed section, in most beams, with better shear reinforcement, the bottom bars would not have pulled out.

The goal of the continuity tests, described in Chapter 5, is to use CFRP to provide the missing continuity and reduce vulnerability to progressive collapse of buildings design according to pre-1989 ACI provisions. However, continuity alone may not be sufficient to develop catenary action or reduce progressive collapse. The GSA guidelines also state "The amount of reinforcement that ACI 318 requires to be continuous may not be sufficient to prevent progressive collapse for instantaneous removal of a column." Therefore, simply following the requirement for continuous reinforcement of the ACI code may not lead to a structure that can resist progressive collapse.

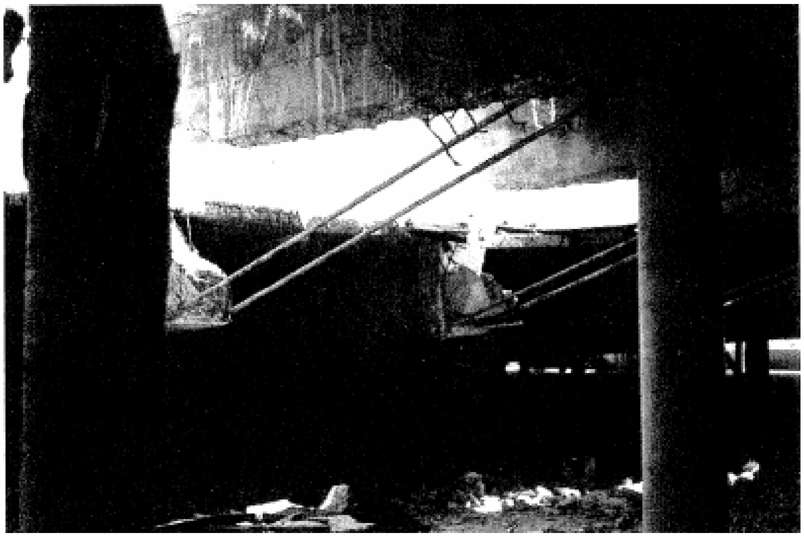

Figure 2-14 Failed roof beam demonstrating continuity of bottom steel [Degenkolb, 1987]

2.3 RESISTANCE TO PROGRESSIVE COLLAPSE

In order to resist progressive collapse, a structure must be able to survive the loss of a primary structural component without additional collapse. The loss of an exterior non-corner column in a reinforced concrete building is considered in this research. For a typical reinforced concrete building, the double span condition created by the loss of a column can be difficult to accommodate. As seen in Figure 2-15, the bending moment significantly increases (approximately 4 times) due to the double span. Furthermore, the moment over the missing column reverses direction, positive where the beam was designed for negative moment. The reversal and increase in moment can be difficult for a beam to accommodate through flexure.

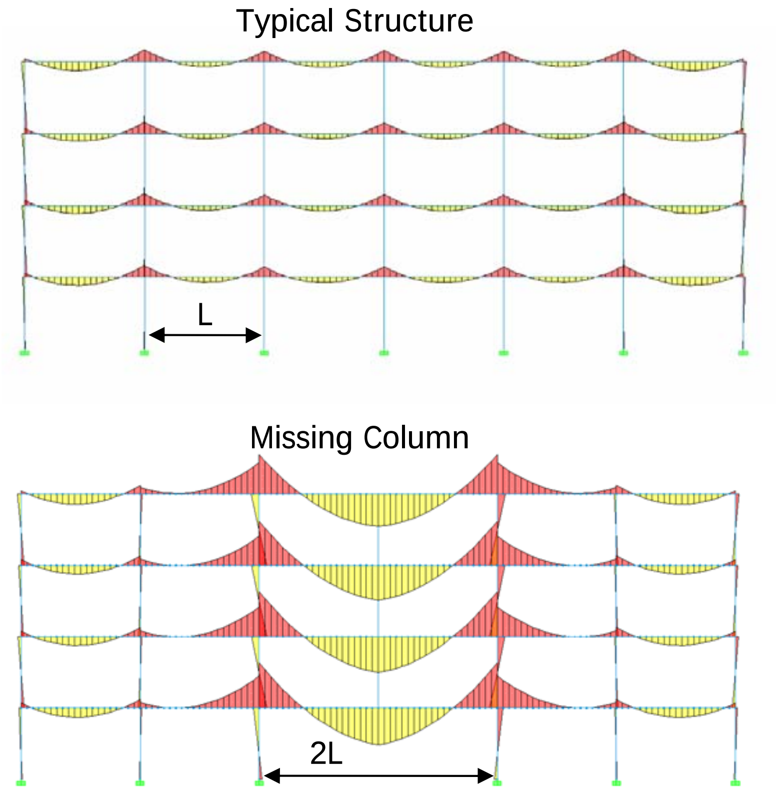

Figure 2-15 Change in bending moment diagram due to loss of column

One way to provide extra capacity to resist progressive collapse is through catenary action. Catenary action, like that used in long-span bridges, resists load by mobilizing axial tension throughout the beam. The tension is then transferred throughout the building, Figure 2-16. However, the catenary tension only becomes effective at large levels of displacement, typically around 7 to 10% of the span length [Wong, 2002]. Based on a typical 20 ft span, the deflection could be as much as 3 to 4 feet. Although, the large deflection means that the structure will be severely damaged, loss of life may be reduced because the catenary action may reduce loss of life from falling debris. However, the rotation of the beam would then be 0.14 to 0.19 radians, which already exceeds the rotation limits for inelastic analysis in most progressive collapse guidelines.

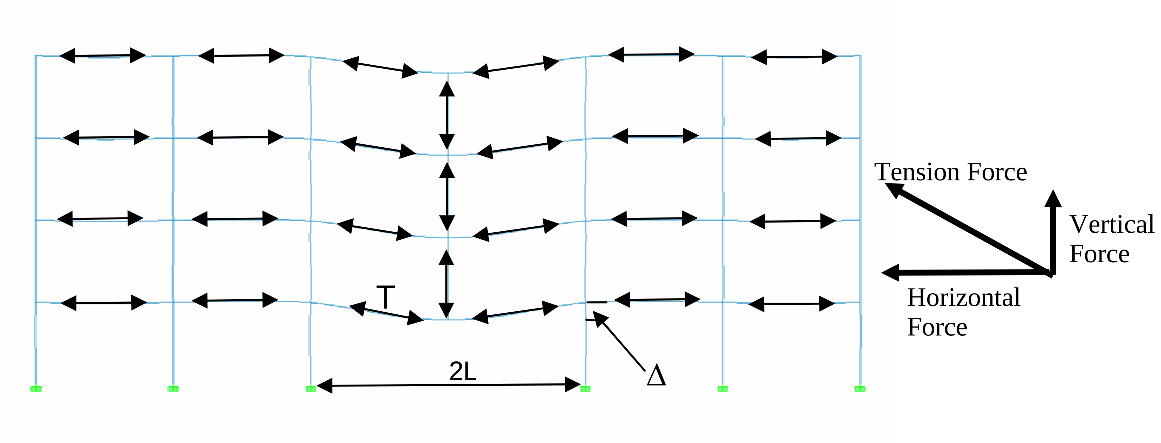

Figure 2-16 Catenary tension forces

In order to develop the catenary tension forces to resist progressive collapse, the reinforced concrete beam must have a line of tension for the force to act along. The tension can be supplied by continuous reinforcement. If the beam does not have continuous reinforcement, the tension line can act through both the negative and positive moment steel if there are sufficient stirrups to transfer the tension force, Figure 2-17. However, this transfer of tension to one side of the beam is not efficient (requires greater deflection to achieve catenary, see Chapter 6) and depends on the size, spacing, and design of the stirrups. The catenary forces can be also be transferred through the positive (Figure 2-18) or negative moment reinforcement (Figure 2-19). The CFRP sheets provide the missing continuity and allow the beam to reach catenary action to resist progressive collapse.

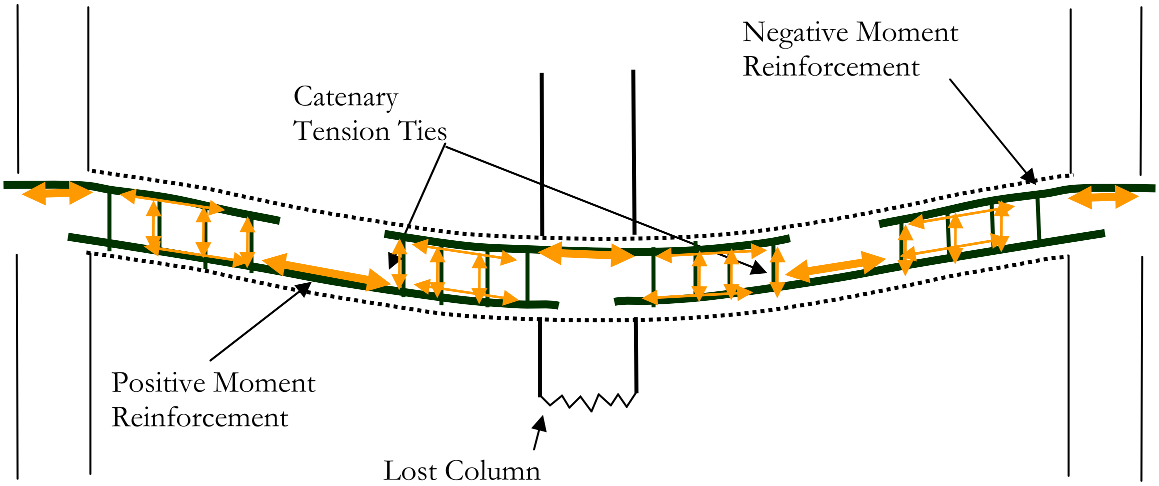
Negative Moment
Reinforcement
Catenary
Tension Ties
Positive Moment
Reinforcement
Lost Column

Figure 2-17 Transfer of catenary forces through stirrups

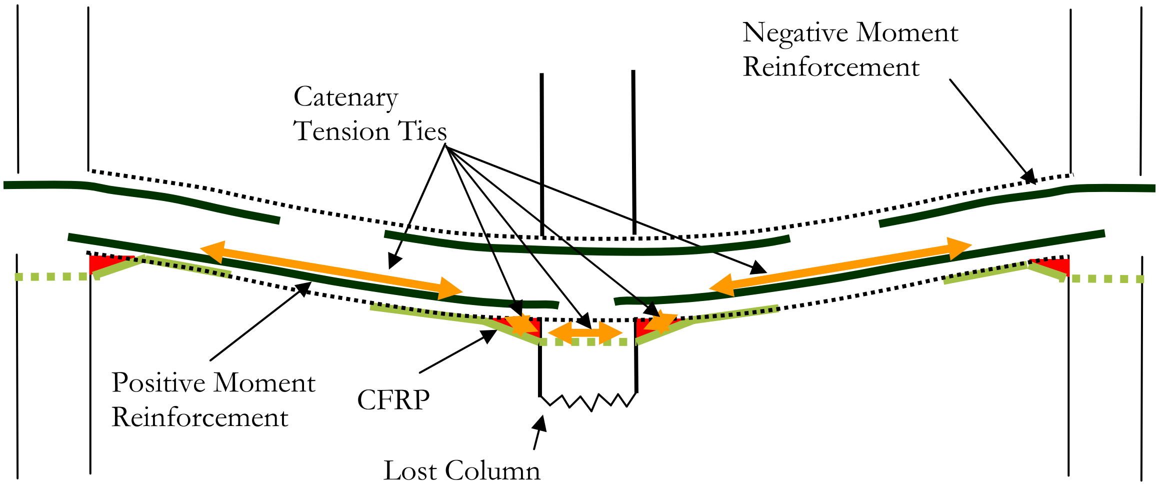
Negative Moment
Reinforcement
Catenary
Tension Ties
Positive Moment
Reinforcement
CFRP
Lost Column

Figure 2-18 Catenary forces provided through the positive moment reinforcement

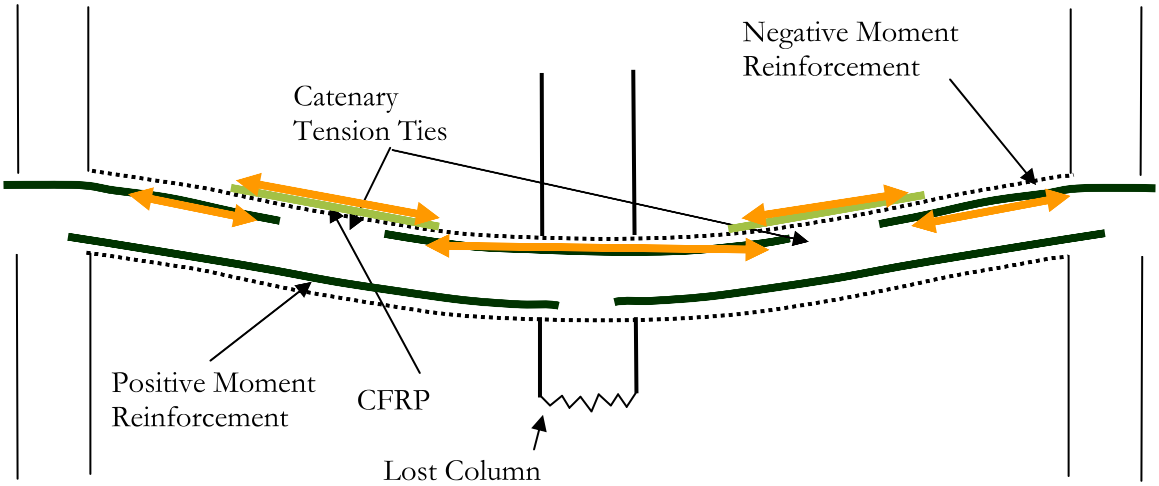

Figure 2-19 Catenary forces provided through the negative moment reinforcement

2.3.1 Previous Research in Catenary Action

There is little previous research on catenary action of reinforced concrete beams. In the 1970s, catenary tests on precast floor strips were conducted at Imperial College in London, Figure 2-20 [Regan, 1975]. The specimens were 14 in. to 28 in. wide and 18 ft long with a central joint between two 9 ft planks representing a lost support. The specimens comprised a 2 in. thick precast panel and a 2 in. thick cast-in-place topping. Details of the ties between the panels varied. For almost all tests, there was an initial compressive arch phase, which was "snapped through" and was followed by a catenary action phase. The majority of the beams failed by tearing out of the bottom bars near the supports at a deflection of 5 to 7% of the double span length (test #5 in Figure 2-21). However, some specimens were able to yield in flexure at the supports before tearing out of the bottom bars. In these cases, the catenary loads were much higher and the ultimate deflection was near 10% of the span length (test #3 in Figure 2-21). The beams eventually failed by fracture of the end rebar due to rotation at the support. For most tests, catenary action started at around 6 to 7 in. of displacement, or slightly greater than the beam depth (4 in.).

The tests also included two specimens that were loaded by sandbags and the central support suddenly pulled out. For one test, the specimen did not fail, but the deflections were 50% greater than for the same load applied to an identical specimen that was loaded with hydraulic jacks. Another specimen failed, although the total weight was only 56% of the ultimate load reached in the hydraulically loaded test.

In his conclusions Regan stated "successful development of a catenary action requires that the members in question posses not only tensile strength but also ductility, which is largely determined by the detailing of the longitudinal reinforcement." The ductility he mentions pertains to, in part, the ability of the concentrated rotation locations (hinges) to not fracture the rebar before catenary action is developed.

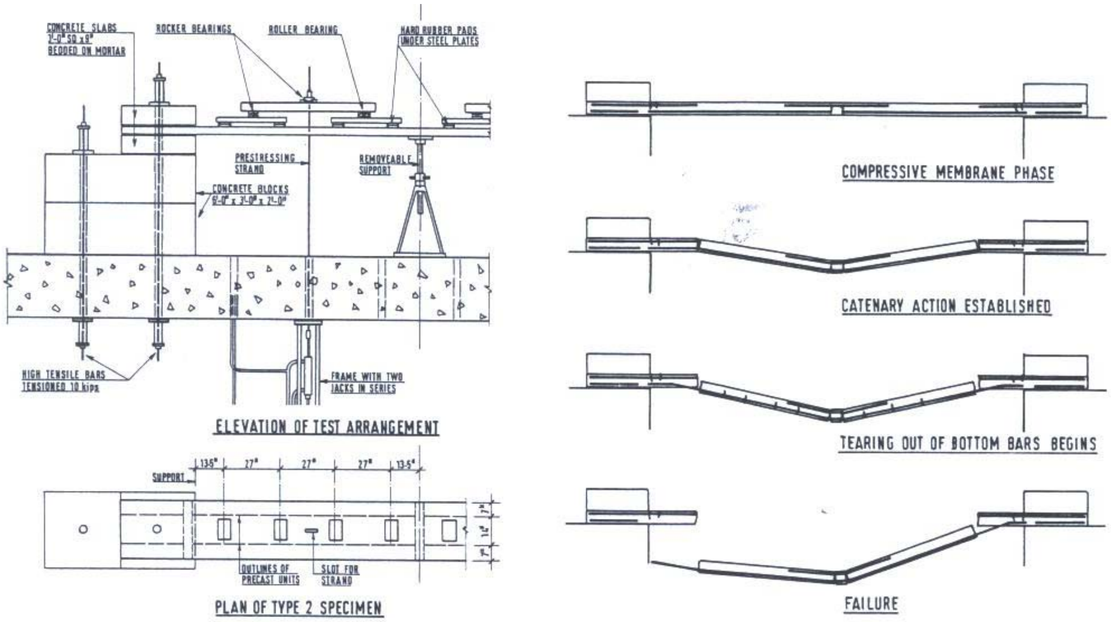
CONCRETE SLABS
7'-0" SQ x 9"
BEDDED ON MORTAR
ROCKER BEARINGS
ROLLER BEARING
HARD RUBBER PADS
UNDER STEEL PLATES
PRESTRESSING
STRAND
REMOVEABLE
SUPPORT
CONCRETE BLOCKS
6'-0" x 3'-0" x 2'-0"
HIGH TENSILE BARS
TENSIONED 10 kips
FRAME WITH TWO
JACKS IN SERIES
ELEVATION OF TEST ARRANGEMENT
13.5"
27"
27"
27"
13.5"
SUPPORT
7"
14"
7"
OUTLINES OF
PRECAST UNITS
SLOT FOR
STRAND
PLAN OF TYPE 2 SPECIMEN
COMPRESSIVE MEMBRANE PHASE
CATENARY ACTION ESTABLISHED
TEARING OUT OF BOTTOM BARS BEGINS
FAILURE

Figure 2-20 Catenary tests of precast floor strips [Regan, 1975]

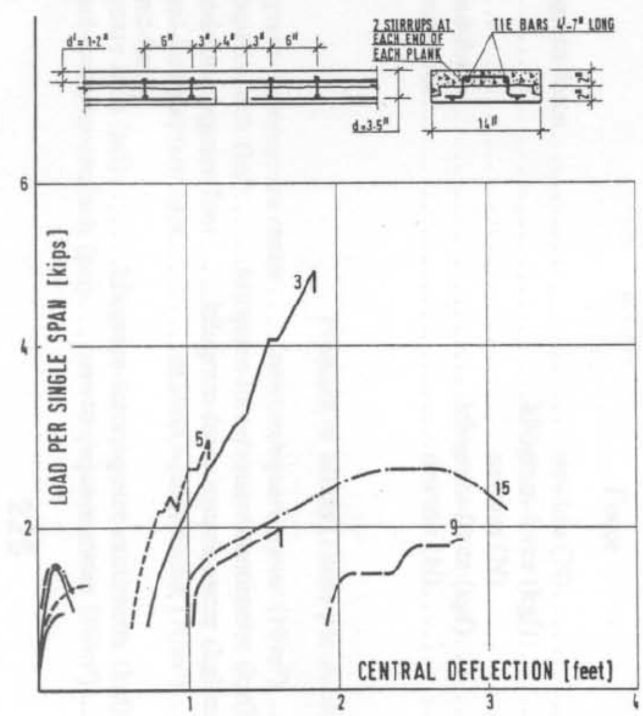

SPEC.	MAIN STEEL	TIE STEEL
3	2 No. 0·31" def.	2 No. 0·31" def.
5	2 No. 0·31" def.	2 No. 0·31" def.
9	2 No. 0·31" def.	2 No. 0·24" plain
15	2 No. 0·16" plain *	2 No. 0·31" def.

* prestressed

Figure 2-21 Results of catenary tests of precast floor strips [Regan, 1975]

There have been other tests of catenary action in the U.K.. Unfortunately, most of these tests were conducted in the early 1970s and reports of the results are hard to acquire. One such series of tests was conducted by Wilford in 1973, Figure 2-22 [Wong, 2002]. Some of the results and pictures appear in a presentation by Wong; however, the original report has not been found. Wong (2002) indicated that catenary action occurs around 7.5 to 10% of the span length.

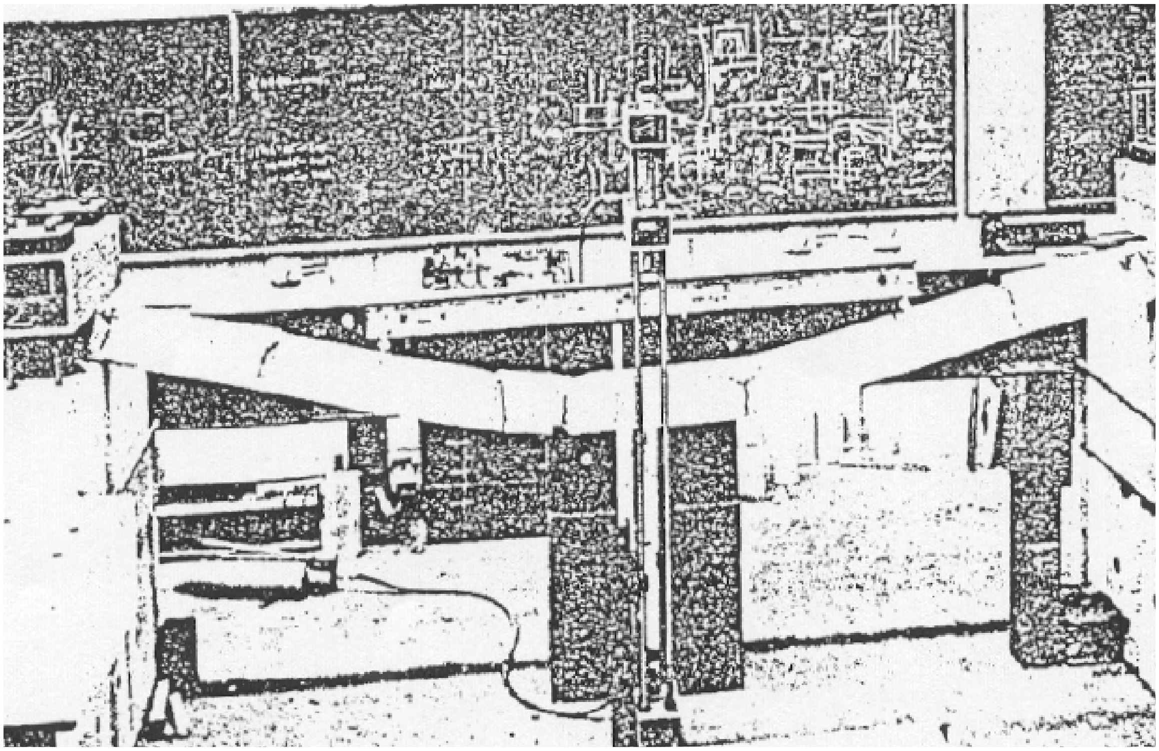

Figure 2-22 Catenary tests conducted by Wilford [Wong, 2002]

Other researchers have attempted to develop equations for catenary action. Izzuddin and Elghazouli (2004) report a series of complex equations to model the catenary response of lightly reinforced concrete members under fire. Their equations describe the presence of a compressive arch effect up to deflections comparable to the beam depth. They also state that the scale of the catenary effect is dependent on the beam depth and the support axial stiffness.

2.3.2 Previous mitigations for progressive collapse

Most codes do not require a building to be retrofitted for progressive collapse unless some other significant upgrade is taking place. However, due to the increased risk of abnormal loads for some buildings, approaches to the mitigation of progressive collapse have been studied.

The easiest and most effective way to reduce vulnerability to progressive collapse is to limit the threat of an abnormal load. For terrorist cases, this can include changes to a building's site layout and security.

However, if the threat cannot be controlled the building's structure must be enhanced. An important step in a progressive collapse mitigation is to determine the performance objective. A life safety performance objective might allow for the large deflections associated to catenary action. A higher performance objective might require a retrofit that is capable of limiting deflections in the building.

One approach to progressive collapse mitigation is to use techniques common in seismic upgrading of buildings, such a wrapping columns, to increase ductility and load capacity [Corley, 2003]. However, any strengthening scheme has to address the implementation problems of existing buildings, such as existing geometry, space limitations, and aesthetics. Generally, most mitigations address the problem of progressive collapse by adding redundancy to a structure. Mitigations can include introducing two-way action in slabs and frames, secondary trusses, Vierendeel action, strong floors, and allowing catenary action to develop [NIST, 2007]. Currently, for concrete frames, mitigation usually means increasing the cross-section of beams by casting more concrete or adding new structural members.

While retrofits to allow catenary action in reinforced concrete frames have not been previously studied, there are some examples for steel frames. Astenah-Asl (2003) studied the use of a steel cable either inside or under the floor slab to withstand the tensile forces generated by the catenary action, Figure 2-23. The tests showed that the installation of the steel cable could increase the maximum load to design load ratio as much as 2 times.

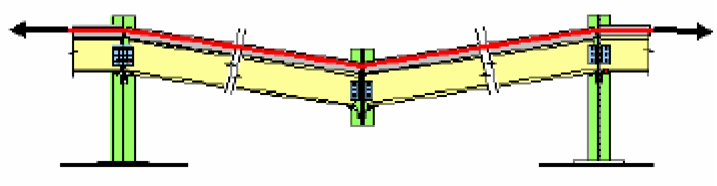

Figure 2-23 Steel cable to develop catenary action [Astenah-Asl, 2003]

Other retrofits for steel frames include means to strengthen the tensile capacity of connections. One such idea is the SidePlate retrofit system, Figure 2-24 [Crawford, 2002]. The system consists of steel plates welded around a connection in order to provide tensile capacity at the connection.

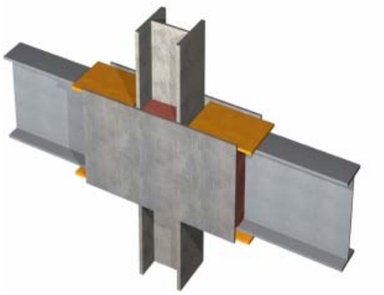

Figure 2-24 SidePlate system for steel frames [Crawford, 2002]

For reinforced concrete frames, there is one example of a seismic retrofit designed to develop yield of the bottom bars (with inadequate splice length) within a beam column connection [Estrada, 1990]. The retrofit consisted of a steel threaded rod inserted through a hole drilled through the column and attached through brackets to steel plates on the beam on either side of the column, Figure 2-25. As with the CFRP retrofit studied in this research, the hole through the column could not be drilled flush with the bottom of the beams. The steel retrofit was able to develop yield of the bottom bars.

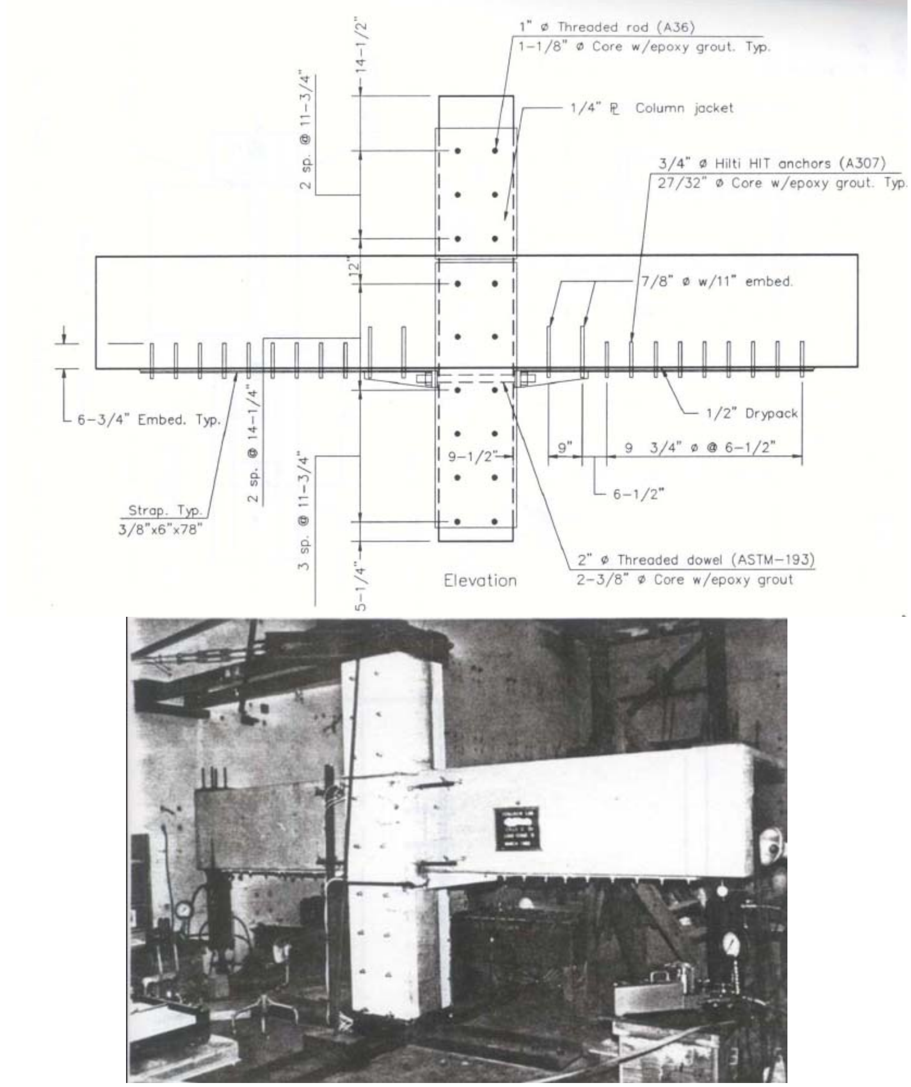
1" ø Threaded rod (A36)
1-1/8" ø Core w/epoxy grout. Typ.
1/4" PL Column jacket
3/4" ø Hilti HIT anchors (A307)
27/32" ø Core w/epoxy grout. Typ.
14-1/2"
2 sp. @ 11-3/4"
12"
7/8" ø w/11" embed.
6-3/4" Embed. Typ.
2 sp. @ 14-1/4"
Strap. Typ.
3/8"x6"x78"
1/2" Drypack
9-1/2"
9"
9 3/4" ø @ 6-1/2"
6-1/2"
3 sp. @ 11-3/4"
5-1/4"
Elevation
2" ø Threaded dowel (ASTM-193)
2-3/8" ø Core w/epoxy grout

Figure 2-25 Steel retrofit to develop yield of bottom bars through a beam column joint [Estrada, 1990]

2.4 SUMMARY

Progressive collapse leads to damage that is disproportionate to the original cause. Examples of progressive collapse include Ronan Point, Murrah Building, and L'Ambiance Plaza. These structures demonstrated a lack of continuity and redundancy that would have allowed the structure to better survive the loss of a primary structural component. Examples of buildings that have suffered severe damage but no progressive collapse include the Pentagon and Khobar Towers. Both of these structures exhibited continuity and redundancy that allowed them to resist progressive collapse.

Although most building codes do not require specific design for progressive collapse, many do apply criteria for general structural integrity (ACI 318, ASCE 7). Some U.S. government agency guidelines exist for designing to resist progressive collapse (DoD, GSA). These guidelines apply either indirect or direct approaches.

Reinforced concrete buildings can be particularly vulnerable to progressive collapse due to lack of continuity in the reinforcement. Although ACI 318 does include provisions requiring continuous reinforcement in perimeter beams, these provisions were not added until the 1989 code and were not intended to provide resistance to progressive collapse.

One way to provide resistance to progressive collapse is by catenary action. The increase and reversal in moment caused by the loss of a column is difficult for most beams to handle through flexure. However, catenary action, comprised of a tensile force with a vertical component, may be able to carry the gravity load of a building. The only drawback is that in order to develop the vertical component of the tensile force, the defections in the beam must be great (7 to 10% of the span length).

From previous research into catenary action, the catenary tension phase is preceded by a compressive arch phase, and catenary action will not begin until the beam has deflected an amount at least equal to its depth. Furthermore, the design and detailing of a beam must be ductile enough so that the beam can reach catenary action without fracturing the rebar.

Although no mitigation method to provide increased continuity and catenary action in reinforced concrete frames has been previously researched, there are some examples for steel frames, including the addition of a steel cable or SidePlate.

Chapter 3: CFRP Background

In this chapter, the characteristics of the carbon fiber reinforced polymer (CFRP) material, CFRP strengthening of reinforced concrete beams, bonding of CFRP to concrete, anchorage of CFRP to concrete, and application procedures will be discussed.

3.1 MATERIAL CHARACTERISTICS OF CFRP

The ability of CFRP to strengthen and provide continuity in RC beams depends on its material characteristics. These characteristics arise from the constituent parts and how they are combined to form the CFRP composite.

By definition, a composite is any type of multiphase material, such as wood, concrete, or steel [Catherall, 1973]. CFRP is a composite material consisting of carbon fibers of high strength and modulus embedded in a matrix with distinct interfaces between them. The combination of fiber and matrix produces a combination of properties that cannot be achieved separately.

3.1.1 CFRP History

Carbon fibers have been around since 1879 when Edison unsuccessfully tried using them as the filament in his electric light bulb [Gill, 1972]. Edison's fibers were manufactured by careful carbonization of cellulose strands such as bamboo or cotton, and therefore lacked the desirable design properties found in carbon fibers today. Afterward, the refractoriness and chemical inertness of carbon fibers were used as insulation in high-temperature furnaces and in the chemical plant industry [Gill, 1972].

Development in carbon fiber reinforced polymers began in the 1960s when the method of manufacture improved to allow for high strength and high modulus fibers. The first work in this area was by Shindo, Fujii, and Sengoku of the Japanese Bureau of

Industrial Techniques [Gill, 1972]. They used polyacrylonitrile (PAN) as a base material to produce carbon fibers with a high degree of molecular orientation. Further researchers refined the process, and today the use of PAN as a base material is common.

The high strength and stiffness properties along with low weight of CFRP have led to numerous uses in the aircraft and aerospace industry [Mallick, 1993]. In 1977, CFRP was used as skins on the vertical fin box and fin leading edge in the F-16 military aircraft. The space shuttle saves an estimated 2,700 lb by using fiber reinforced composites. The very low coefficient of thermal expansion of CFRP has lead to uses in the support structure of space telescopes where temperatures might very from -100 ºC to 100 ºC. The automotive, marine, and sporting goods industries have also found numerous uses for CFRP.

It wasn't until the mid-1980s that CFRP was considered as reinforcement to strengthen concrete beams. The idea of using FRP was developed as an alternative to bonding of steel plates to the tension side of beams. Meier, of the Swiss Federal Laboratory for Materials Testing and Research, tested RC beams strengthened with FRP plates in 1984 and applied FRP to concrete bridges in 1987 [Teng et al., 2001]. Further work by numerous researchers expanded the knowledge of CFRP strengthening of RC beams. In the U.S., initiatives of the National Science Foundation and Federal Highway Administration encouraged development of CFRP strengthening technology in the 1980s and 1990s.

Discoveries from the research led to the development of guidelines involving FRP such as, ACI 440 - *Guide for the Design and Construction of Externally Bonded FRP Systems for Strengthening Concrete Structures* (2002) in the US and Fédération Internationale du Béton (fib-14) *Externally Bonded FRP Reinforcement for RC Structures* (2001) in Europe, as well as codes and guidelines in other countries. With guidance from codes, designers now have the option of using FRP for structural strengthening. However, new research in FRP technology is still expanding the knowledge base regarding CFRP materials.

3.1.2 Carbon Fiber Properties

In the case of CFRP, the carbon exists as a continuous aligned dispersed phase in fibrous form. The fibers are the principle load carrying medium. Carbon fibers are 99.9% pure carbon [Fitzer, 1985]. Structurally they are blend of amorphous carbon and graphitic carbon [Mallick, 1993]. The graphite form leads to the high tensile properties of the fibers. In graphite, carbon atoms are arranged in parallel planes of regular hexagons, Figure 3-1. Within the plane, strong covalent bonds hold the carbon atoms together, while the planes themselves are held by weak van der Walls forces. Carbon fibers are aligned along the strong planes leading to a highly anisotropic material, Figure 3-2. The fibers are very thin with diameters between 6 and 10 μm [Fitzer, 1985]. Properties of commercially available carbon fibers used in structural applications are given in Table 3-1.

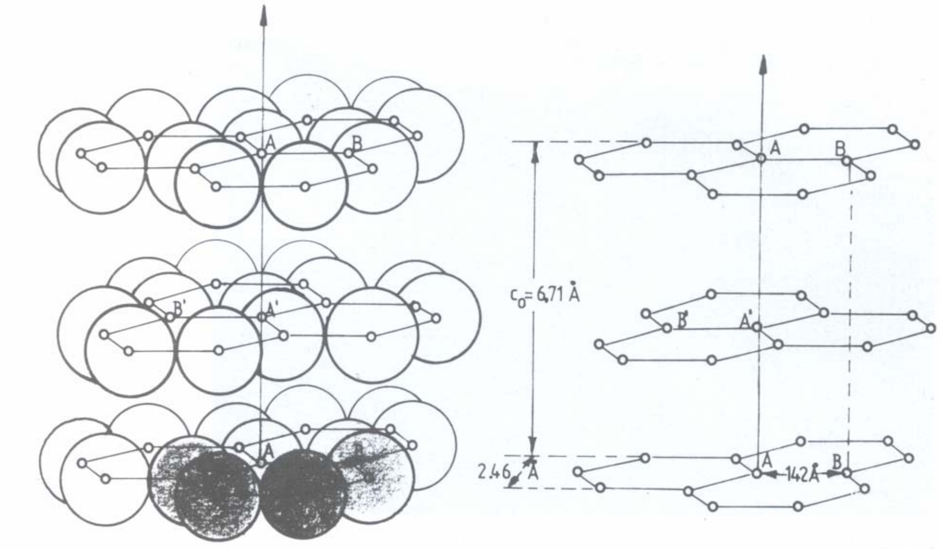

Figure 3-1 Structure of graphite [Fitzer 1985]

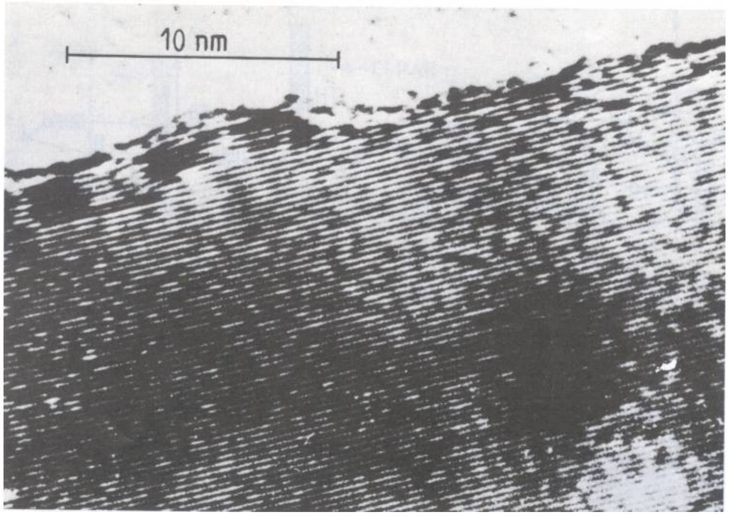

Figure 3-2 High resolution of highly aligned graphite chains in a carbon fiber [Fitzer 1985]

Table 3-1 Properties of commercially available carbon fibers

Carbon fibers	Tensile Strength (ksi)	Tensile Modulus (ksi)	Elongation at break	density (lb/in^3)
Tyfo	550	33,400	1.70%	0.063
Sika	550	34,000	1.50%	0.065

3.1.3 Epoxy Matrix Properties

The matrix in CFRP keeps the fibers in the proper orientation, acts as a load transfer medium between fibers, and protects the fibers. The matrix can be various different types of polymers, though most are thermosetting. The most commonly used are polyester, urethane, methacrylate, vinylester, epoxy, and phenolic [Hollaway et al., 2000].

For CFRP used in structural applications the most common matrix is epoxy. Epoxies have many advantages over other thermosetting matrices [Mallick, 1993]. They have a wide variety of properties depending on the starting materials, curing agents, and modifiers. Volatile materials are absent during cure. They have low shrinkage and excellent resistance to chemical solvents. However, their most important property for structural applications is their excellent adhesion to a wide variety of fibers (such as carbon) and substrates (such as concrete).

Epoxy is a two-part substance composed of a liquid resin and a reactive curing agent. The resin has epoxide groups (three-membered rings of one oxygen atom and two carbon atoms) at the end of each molecule. The curing agent gradually reacts with the resin to transform the liquid into a solid state. Figure 3-3 shows the reaction of an epoxy molecule with the curing agent DETA to form the cross-linked solid state. Generally, the curing agent is added to the resin just prior to embedding the carbon fibers. The curing time, or pot life, allows fibers to be handled and placed before the curing is completely finished. For epoxies common in structural applications, the cure time is about three hours, after this time the epoxy becomes tacky and hard to work with. Final cure may take as long as 72 hours.

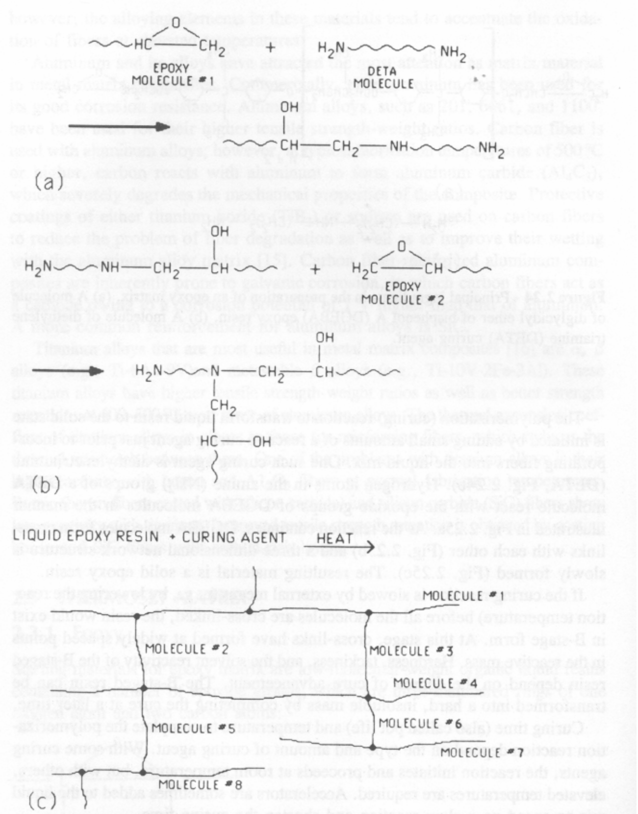
EPOXY MOLECULE #1
DETA MOLECULE
(a)
EPOXY MOLECULE #2
(b)
LIQUID EPOXY RESIN + CURING AGENT
HEAT
MOLECULE #1
MOLECULE #2
MOLECULE #3
MOLECULE #4
MOLECULE #5
MOLECULE #6
MOLECULE #7
MOLECULE #8
(c)

Figure 3-3 Reaction of epoxy components to form cross-linked solid [Mallick, 1993]

The properties of epoxy depend upon the amount of cross-link formation during cure. Typically tensile modulus, glass transition temperature, and chemical resistance improve, but strain at failure and fracture toughness decrease with increasing cross-link density. More information on epoxies can be found in *Fiber-Reinforced Composites* by Mallick (1993). Properties of commercially available epoxies used with CFRP are given in Table 3-2.

Table 3-2 Properties of commercially available epoxies

Epoxies	Tensile Strength (ksi)	Tensile Modulus (ksi)	Elongation at break
Tyfo S	10.5	461	5.00%
Sikadur 300	8	250	3%

3.1.4 CFRP Composite Properties

Once the characteristics of the carbon fiber and epoxy matrix are understood, the two must be combined to form the CFRP composite. There are two main types of CFRP composite used in the strengthening of concrete structures.

One type is pre-impregnated (prepeg) plates, Figure 3-4. In this case the carbon fibers are impregnated in a resin bath and pulled through a forming die at an elevated temperature at the manufacturing facility, Figure 3-5. The advantage to this procedure is that the plates are fabricated with a high degree of quality control, especially in the fiber-to-resin ratio. The disadvantages are that only uniform cross-sections can easily be made and although the plates can be cut to length, they cannot be molded or bent to the existing structure [Brena, 2000].

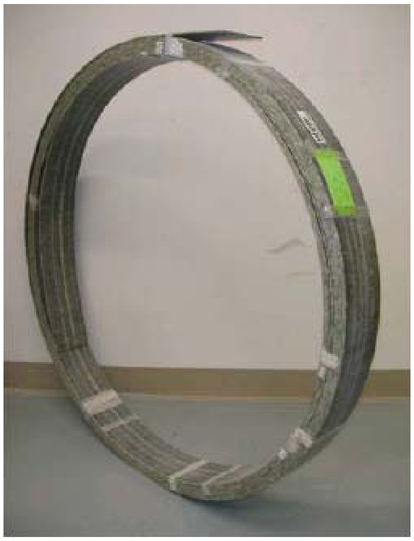

Figure 3-4 Roll of prepeg carbon fiber composite [Lamanna, 2002]

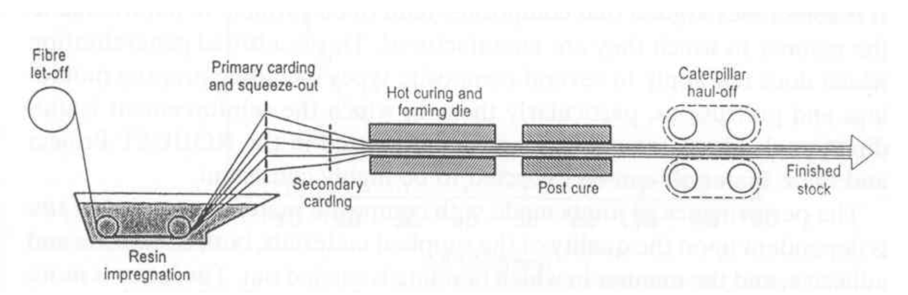
Fibre
let-off
Primary carding
and squeeze-out
Hot curing and
forming die
Caterpillar
haul-off
Finished
stock
Secondary
carding
Post cure
Resin
impregnation

Figure 3-5 Production of prepeg CFRP plates [Hollaway et al., 2000]

The other type is the wet-lay up fabric, in which the carbon fibers are woven into flexible fabric sheets and impregnated with resin at the jobsite, Figure 3-6. This allows the flexible wet fabric to be molded to any desired shape; however, it is difficult to control the fiber-to-resin ratio. The moldability of the wet lay-up sheets (into anchors or pulled through a column) is an important consideration in retrofitting existing buildings. Other important characteristics of CFRP sheets are their speed of construction (CFRP can be applied quickly and reach full strength in 72 hours), aesthetics (low profile of CFRP sheets preserves architectural character of building), and durability (CFRP does not corrode). One disadvantage of CFPR sheets is their high cost, around $30 per square foot installed. Properties of various commercially available CFRP composites are given in Table 3-3.

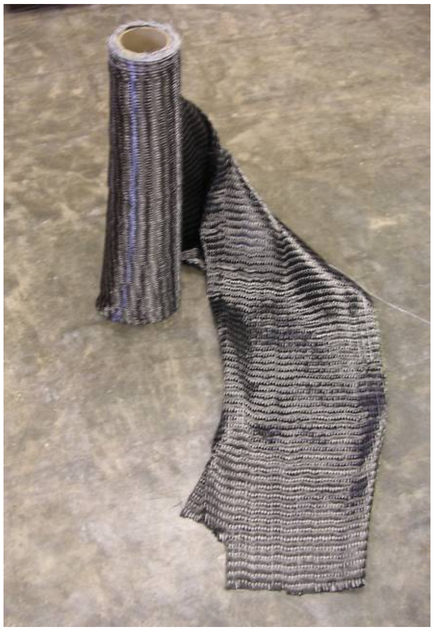

Figure 3-6 Roll of CFRP fabric

Table 3-3 Properties of CFRP composites

CFRP	Tensile Strength (ksi)	Tensile Modulus (ksi)	Elongation at break	Thickness (in.)
Tyfo SCH 35 (fabric)	143	11,400	1.26%	0.035
Tyfo SCH 41 (fabric)	121	11,900	0.85%	0.04
Sikawrap Hex 103C (fabric)	123	10,300	1.12%	0.04
Sika Carbordur (plate)	449	23,900	1.69%	0.047

3.1.5 Standard ASTM Test for CFRP

Because the properties of a CFRP composite can vary with each application, a standard ASTM test D-3039 was developed to uniformly report the properties of the CFRP composite. For this research, rectangular coupons 2 in. wide by 12 in. long were cut from a cured CFRP composite sheet, Figure 3-7. An extra layer of CFRP fabric and steel plate 2 in. by 3 in. was applied to each end to prevent failure in the grip, leaving a 6 in. long gage section. A strain gage was placed in the center of the specimen. The test coupon was placed in a hydraulic testing machine, being careful to avoid misalignment, Figure 3-8. The coupon was loaded at a speed to effect a constant stain rate in the gage section of 0.001 stain per minute.

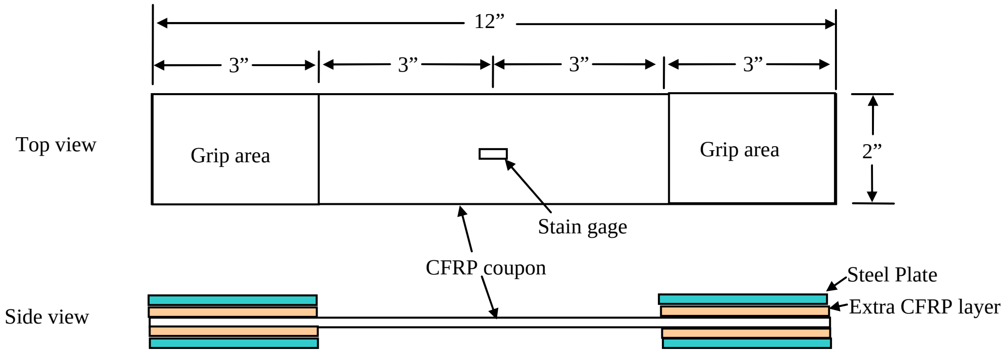
12”
3”
3”
3”
3”
Top view
Grip area
Grip area
2”
Stain gage
CFRP coupon
Steel Plate
Extra CFRP layer
Side view

Figure 3-7 CFRP coupon schematic

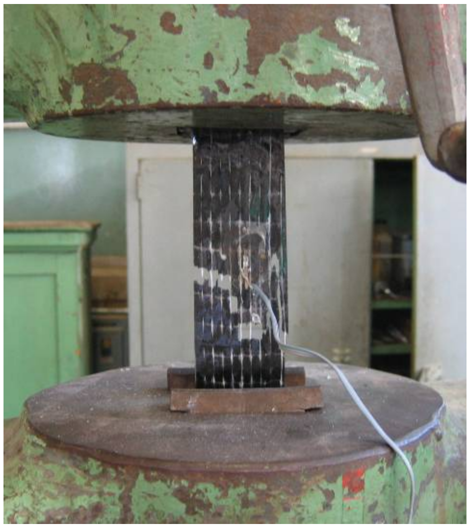

Figure 3-8 CFRP coupons in hydraulic testing machine

3.2 STRUCTURAL STRENGTHENING WITH CFRP

CFRP is very effective in strengthening RC beams to provide continuity and improve redundancy. However, a clear understanding of how this strengthening is achieved and the failure modes and limitations is necessary.

3.2.1 Structural Strengthening

In general, the flexural strengthening of RC beams takes the form of adding more tensile reinforcement. Adding more tensile reinforcement allows the beam to carry more moment by increasing the capacity of the moment couple. For a typical RC beam, applied moment is resisted by a moment couple in the beam consisting of compression on one side and tension on the other. This couple can be seen in Figure 3-9, with the compression contribution coming from the concrete in the top of the beam and the tension coming from the reinforcing steel and CFRP plate at the bottom of the beam. Determination of the strength of the beam is made from a sectional analysis with the forces shown in Figure 3-9 accounting for the fact that the beam may be already stressed before application of the CFRP.

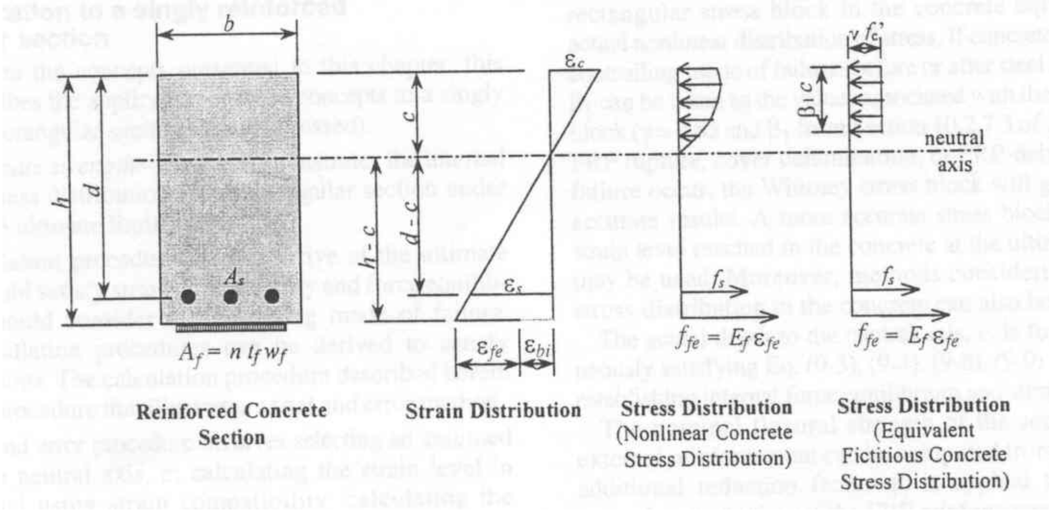

b
ε_c
c
h
d
$d-c$
$h-c$
A_s
ε_s
$A_f = n\, t_f w_f$
ε_{fe}
ε_{bi}
$\gamma f_c'$
$\beta_1 c$
neutral axis
f_s
f_s
$f_{fe} = E_f \varepsilon_{fe}$
$f_{fe} = E_f \varepsilon_{fe}$
Reinforced Concrete Section
Strain Distribution
Stress Distribution (Nonlinear Concrete Stress Distribution)
Stress Distribution (Equivalent Fictitious Concrete Stress Distribution)

Figure 3-9 Moment couple in RC beam [ACI 440, 2002]

3.2.2 CFRP Failure Modes

CFRP structural strengthening systems are designed according to the ACI 318 strength and serviceability requirements. ACI 440 provides guidance on specific design requirements of CFRP. One of these unique requirements is what value to use as the FRP tensile strength. Unlike steel, it’s not simply a matter of finding the ultimate strength of a CFRP fabric; other considerations of the failure mode must be made. The various failure modes of a CFRP strengthened beam are illustrated in Figure 3-10 and Figure 3-11.

Concrete crushing failure arises when the tensile strength of the CFRP is greater than the compressive strength of the concrete. CFRP rupture utilizes the full capacity of the CFRP sheet, however the failure mode is brittle. Shear failure is undesirable and should also be avoided by ensuring the shear strength of the beam is greater than the shear at failure. The loss of composite action (Figure 3-11) is unique to CFRP strengthened beams and difficult to predict (see Section 2.3). Fortunately this failure mode may be limited by newly developed CFRP anchorages.

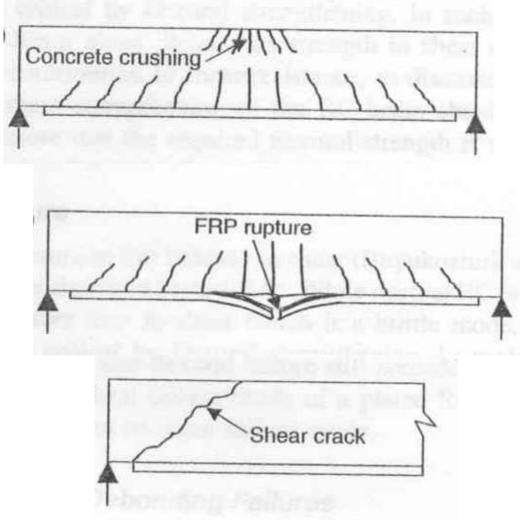

Concrete Crushing

CFRP Rupture

Shear Failure

Figure 3-10 Failure modes in FRP strengthened beams [Teng et al., 2001]

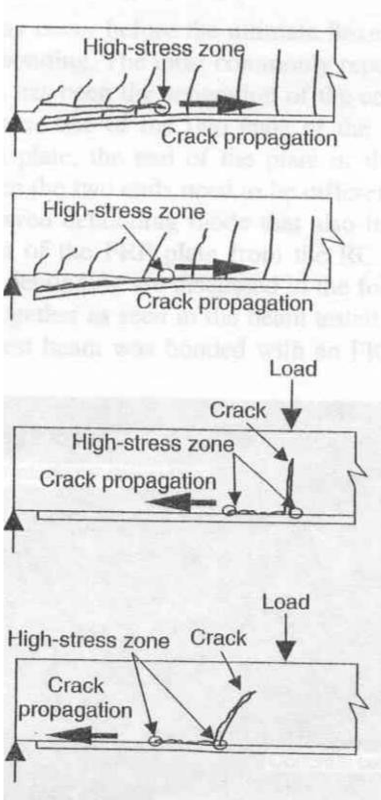
High-stress zone
Crack propagation
High-stress zone
Crack propagation
Load
Crack
High-stress zone
Crack propagation
Load
High-stress zone
Crack
Crack propagation

Loss of composite action between the CFRP and RC beam

Debonding at level of internal reinforcement

Debonding near surface of beam

Debonding due to flexural crack

Debonding due to shear crack

Figure 3-11 Types of debonding or loss of composite action [Teng et al., 2001]

3.3 CFRP DEBONDING

The loss of composite action, also known as debonding or peeling, severely limits the tensile capacity of a CFRP sheet. Debonding of a CFRP sheet can occur by loss of cohesion in the adhesive interface or crack propagation in the concrete [Teng et al., 2001]. The adhesive interface (the epoxy matrix that lies between the carbon fibers and the concrete) is generally very strong and failures here are rare. Most CFRP debonding failures are due to the concrete, with crack propagation occurring in the concrete near the surface of the beam or at the level of the internal reinforcement (Figure 3-12). These failures can occur in one of two ways; failure at the ends of the sheets due to high normal stresses or failure due to a crack offset.

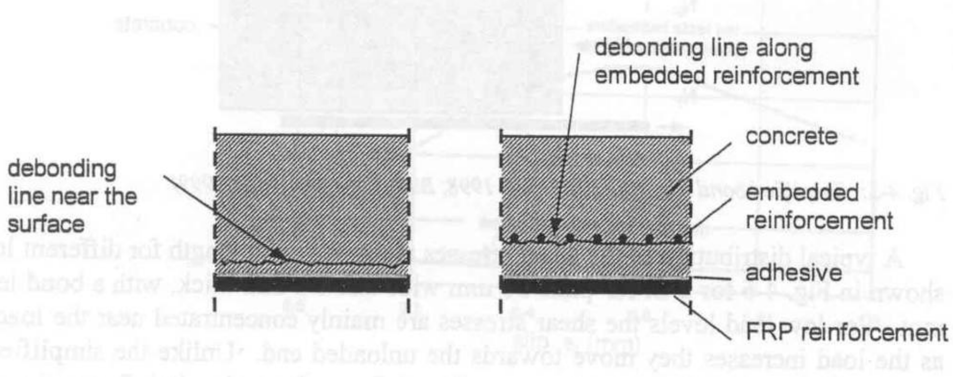
debonding line along
embedded reinforcement
concrete
debonding
line near the
surface
embedded
reinforcement
adhesive
FRP reinforcement

Figure 3-12 Debonding in concrete [fib-14, 2001]

When a beam strengthened with CFRP is loaded, the ends of the CFRP sheet are subjected to high normal and shear stresses as seen in Figure 3-13. The shear stresses cause micro cracking in the concrete adjacent to the adhesive interface. The normal stresses can cause the CFRP sheet to debond or pull away from the concrete. Once the debonding starts it proceeds in an unzipping fashion until most of the CFRP sheet is no longer attached to the RC beam. Debonding due to a crack occurs in a similar manner. For shear cracks, the normal stresses are due to the surface level offset in the crack as seen in Figure 3-14. For flexural cracks, the widening of the crack drives debonding [Teng et al., 2001].

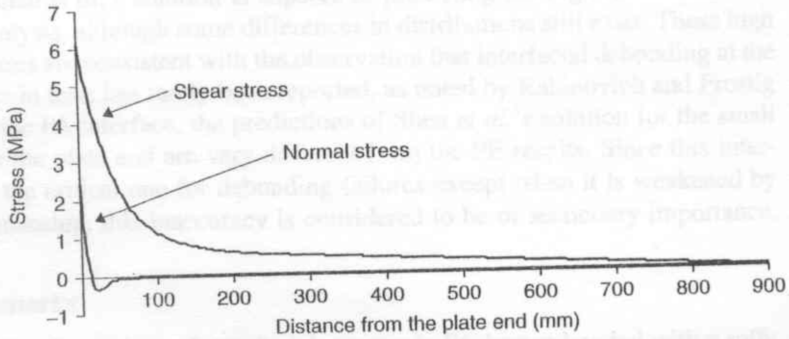

Figure 3-13 Normal and shear stresses at end of CFRP sheet [Teng et al., 2001]

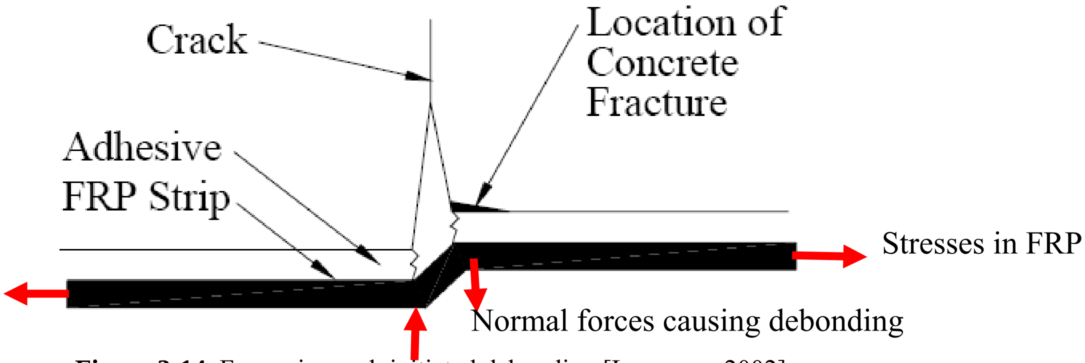
Crack
Location of Concrete Fracture
Adhesive
FRP Strip
Stresses in FRP
Normal forces causing debonding

Figure 3-14 Forces in crack initiated debonding [Lamanna, 2002]

One important feature of the bond strength of CFRP is the notion of an effective bond length [Teng et al., 2001]. Any length beyond the effective bond length cannot increase the tensile force the CFRP sheet can carry. This means that the CFRP sheet may never reach its rupture strength no matter how long the bond length.

A review of experimental tests and analytical models for CFRP bonding found that the equations developed by Teng and Chen were the best in terns of average experimental-to-predicted bond strength ratio (1.58) and percent unsafe design (2.5%) [Toutanji et al., 2006]

A model by Teng and Chen (2001) gives the effective bond length as

$$L_e = \sqrt{\frac{E_p t_p}{\sqrt{f_c'}}}$$ **Equation 3-1**

where E_p and t_p are the stiffness and thickness of the CFRP respectively and f'_c is the concrete compressive strength in units of lb and in. For example, a 0.035 in. thick Tyfo SCH 35 CFRP sheet with a stiffness of 11.4 x 10^6 psi applied to concrete with a strength of 4000 psi, the effective length would be 4.5 in. Teng and Chen also give the ultimate tension force that can be developed in the FRP sheet before debonding as

$$P_u = 0.427 \beta_p \beta_L \sqrt{f'_c} b_p L_e$$ **Equation 3-2**

where β_p is a factor relating to the width of the CFRP versus RC beam, β_L is a reducing factor if the length is less than the effective length, and b_p is the width of the CFRP. For example, a 6 in. width of Tyfo SCH 35 CFRP sheet bonded to an 8 in. wide beam could reach a tension force of 7.5 kip. However, the reported tensile rupture force of the CFRP is 30 kip. This implies that the CFRP would reach only 25% of its tensile capacity.

The FRP guide ACI 440 (2002) also estimates the bonding strength of CFRP; however, their equation is based on an ultimate strain that can be reached in the CFRP before debonding. The strain limit in the FRP is the ultimate rupture strain of the FRP multiplied by a factor κ_m.

$$\kappa_m = \left\{ \begin{array}{l} \dfrac{1}{60\varepsilon_{fu}}\left(1 - \dfrac{nE_f t_f}{2{,}000{,}000}\right) \le 0.9 \; for \quad nE_f t_f \le 1{,}000{,}000 \\ \dfrac{1}{60\varepsilon_{fu}}\left(\dfrac{500{,}000}{nE_f t_f}\right) \le 0.9 \; for \quad nE_f t_f \ge 1{,}000{,}000 \end{array} \right\} < 0.9 \qquad \textbf{Equation 3-3}$$

$$f_{fe} = E_f \varepsilon_{fe} \quad \text{where} \quad \varepsilon_{fe} = \varepsilon_{cu}\left(\frac{h-c}{c}\right) - \varepsilon_{bi} \le \kappa_m \varepsilon_{fu}$$

where E_f is the CFRP modulus, t_f CFRP thickness, n number of layers ε_{fu} CFRP ultimate strain, and ε_{bi} the initial substrate strain (units of lb and in.). For CFRP used in the previous example that has a rupture strain of 0.0126, κ_m is at its maximum of 0.9 and the strain limit would be 0.011. This corresponds to a stress of 130 ksi. The ACI 440 procedure also puts additional limitations and safety factors on the use of FRP, including a cyclic stress limit of $0.55f_{fu}$.

A study of the behavioral trends of CFRP reported that 63% of the beams in the database failed by loss of composite action, 16% by tensile rupture of the FRP, 12% by concrete crushing and 9% by beam shear [Bonacci et al., 2001]. Of the beams that failed by loss of composite action, the average strain in the CFRP sheet was 49% of the rupture strain. Most of the beams that failed by tensile rupture of the CFRP had some form on anchorage of the CFRP sheet. This again demonstrates that RC beams strengthened by

CFRP rarely achieve their full potential unless the CFRP sheet is properly anchored to prevent debonding.

3.4 ANCHORAGE OF CFRP

Due to the severe limitations on tensile capacity caused by debonding, anchoring the CFRP sheets to the RC beam can be advantageous. Furthermore, a good anchorage system may limit the need for surface preparation and produce more reliable results by eliminating variables related to the bond quality of the FRP to the concrete.

For prepeg plates, anchoring can be accomplished by mean of mechanical fasteners shot through the CFRP plate and into the concrete, Figure 3-15. These anchors can develop the full capacity of the plate [Lamanna, 2002]. However, to avoid splitting the plate, plates with transverse fibers should be used, Figure 3-16.

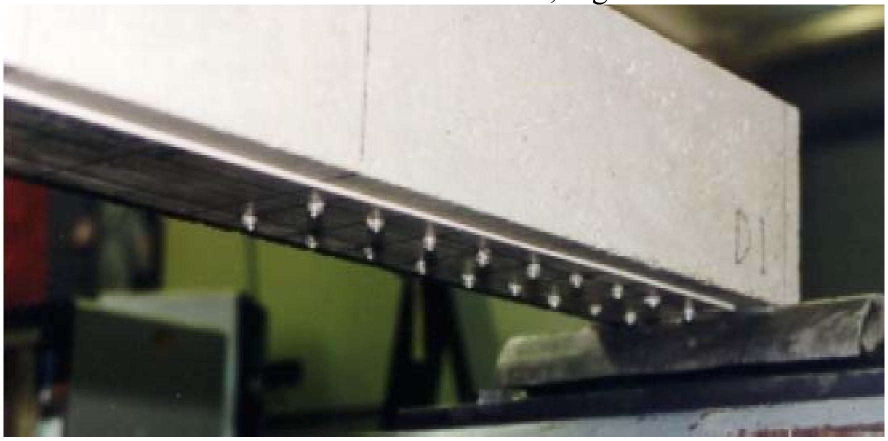

Figure 3-15 Mechanical fastening of prepeg CFRP plate [Lamanna, 2002]

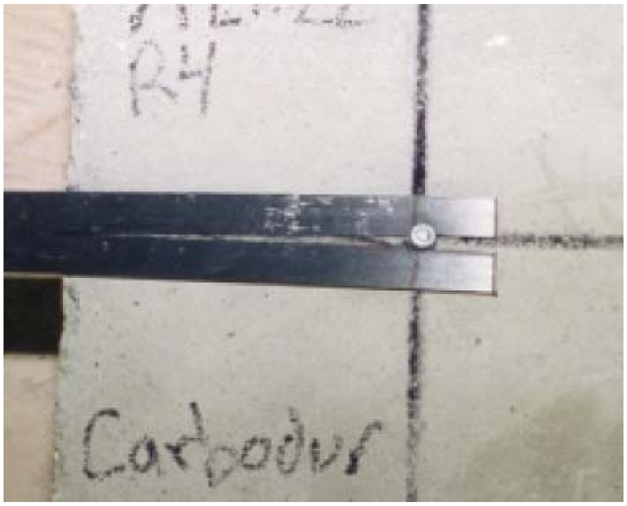

Figure 3-16 Splitting failure of prepeg plate with unidirectional fibers [Lamanna, 2002]

For wet layup systems, several different types of anchorage schemes, including U-wraps (CFRP sheet wrapped around sides of beam) and U-anchors (embedding CFRP into preformed grooves in the concrete) have previously been studied [Bramblett 2001; Khalifa et al. 1999].

Anchoring CFRP sheets by U-wraps simply increases the amount of bonded area of the CFRP sheet, thereby allowing more stress to be developed before debonding, and can be used with both plates and fabrics, Figure 3-17. Although these wraps can be effective, they may require as much CFRP as used in the longitudinal sheet.

U-anchors, shown in Figure 3-18, are also effective, but they anchor the CFRP into the cover of the concrete and may still have debonding issues with cracks at the level of the internal reinforcement.

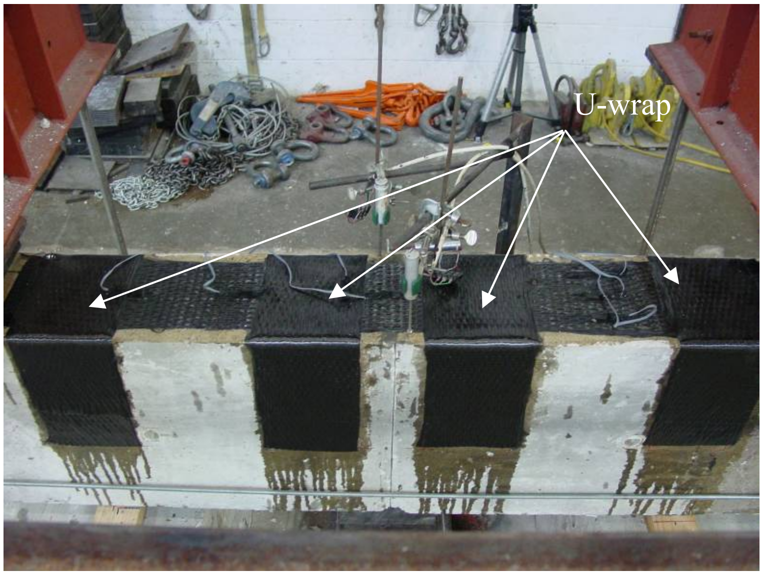

Figure 3-17 U-wrap anchorage on RC beam

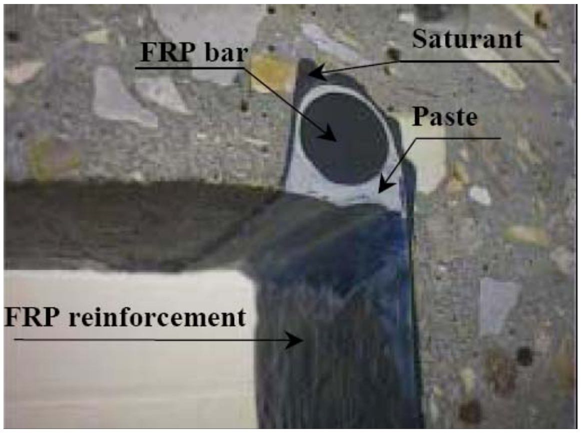

Figure 3-18 U-anchor anchorage [Khalifa, 1999]

3.4.1 Carbon fiber anchors

Carbon fiber anchors, originally developed by the Shimizu Corporation in Japan, offer a new way to anchor CFRP sheets [Jinno et al., 1998]. Carbon fiber anchors are anchors inserted into predrilled holes and fanned out over the CFRP sheet, Figure 3-19. Fiber anchors can be comprised of many types of fibers: araimid, glass, or carbon. In this study, the use of carbon fiber reinforced polymer composites (CFRP) is examined because of their high strength and modulus of elasticity.

The CFRP anchor is made by cutting a strip of the CFRP material, inserting it into a predrilled hole (with the aid of a steel wire to push the CFRP anchor into the concrete hole), then fanning the ends of the anchor over the CFRP sheet, Figure 3-20. The ends of the anchor can be fanned out in a circular fashion as shown in Figure 3-20, or in a pie shape directed along the tension in the CFRP sheet. The CFRP anchors are made from the same material as the sheet and are saturated with epoxy and inserted immediately after the sheet is placed (see Section 3.5). This process ensures that the anchors and sheet form a continuous composite unit.

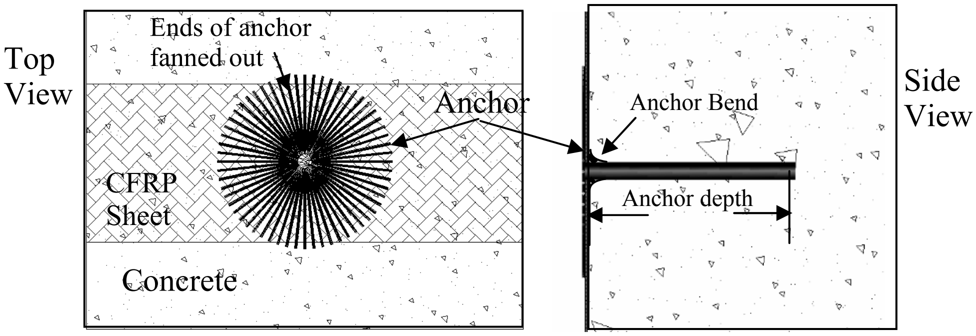

Figure 3-19 CFRP Anchor

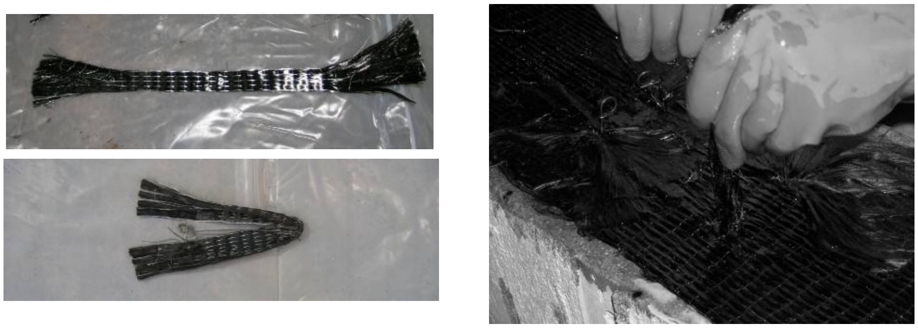

Figure 3-20 Strips of CFRP used to form anchor and inserting anchor into predrilled hole

3.4.2 Previous research

Few experiments have been conducted using the carbon fiber anchors, however some research exists. The required depth into the concrete for full development of the anchor has been studied by Ozedemir and Akyuz (2005). The tests consisted of epoxy coated CFRP strips inserted into predrilled holes and pulled straight out, Figure 3-21. Ozedemir concluded that there is an effective embedment depth (at least 4 inches) beyond which the capacity of the anchors no longer increases and in most cases the full tensile capacity of the anchor is achieved (anchor fracture).

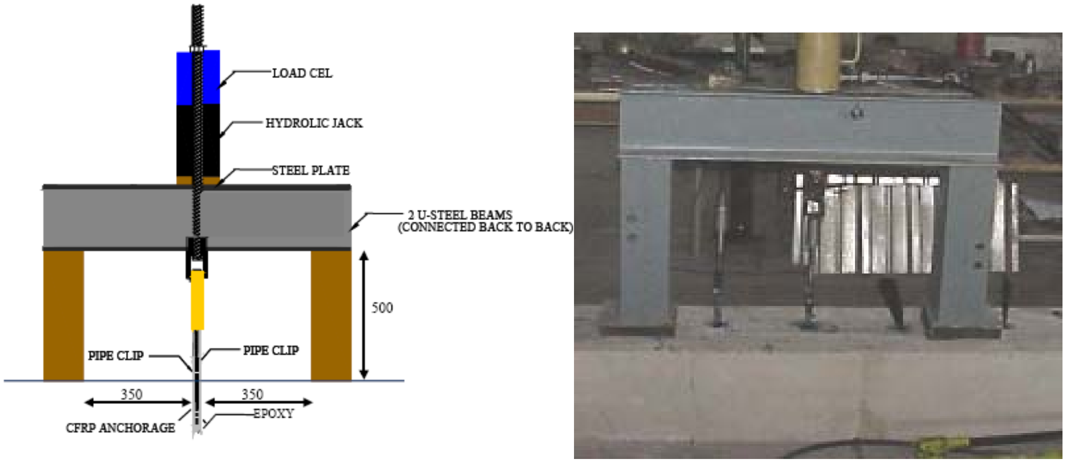

Figure 3-21 Pullout tests by Ozedemir [Ozedemir et al., 2005]

Another important parameter in carbon fiber anchors is the effect of the bend in the anchor as the fibers bend into the concrete hole, Figure 3-19 and Figure 3-22. ACI 440 (2002) recommends that all corners be rounded to a ½ in. diameter. However, a ½ in. diameter is difficult to reach for the anchor holes. Studies by Morphy (1999) on the effect of bend diameter for CFRP stirrups suggest that the radius of the bend be greater than 4 times the anchor diameter or 2 in. Therefore, for a 3/8 in. diameter anchor, the radius would need to be 1.5 in. Unfortunately it is difficult to get this amount of bend radius. Equations developed by JSCE research committee (1997) predict the reduction in CFRP capacity due to a bend, Equation 3-4.

$$\frac{f_a}{f_u} = 0.09\frac{r}{d} + 0.3 \qquad \textbf{Equation 3-4}$$

Where f_a is the stress capacity of the anchor (JSCE did not develop the equation specifically for anchors, but the equation will be used for anchors in this report), f_u is the ultimate CFRP capacity, r is the radius of the bend, and d is diameter of the anchor. A

3/8 in. diameter anchor with a ½ in. radius bend would reach only 42% of its ultimate tensile capacity.

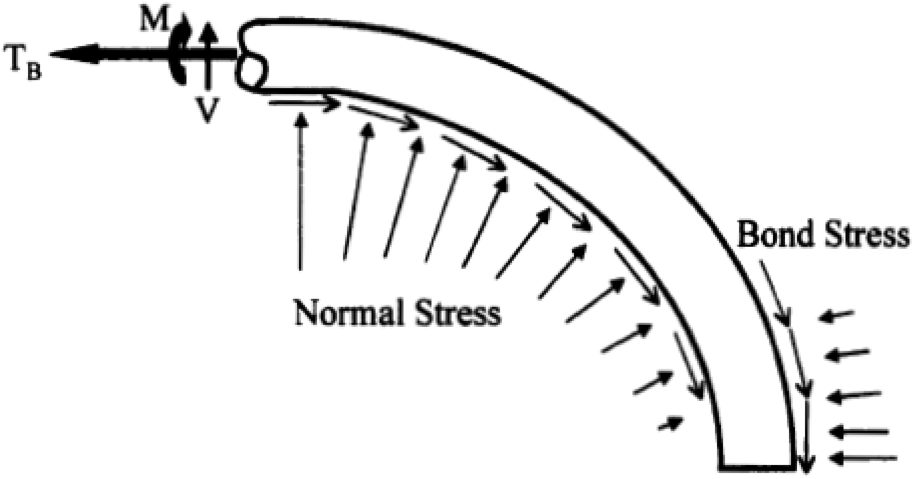

Figure 3-22 Bend in CFRP [Morphy 1999]

The stress transfer mechanism of the carbon fiber sheets has been studied by Kobayashi (2001). If stresses are to be transferred from one CFRP sheet to another using a fan, the fan opening angles should be limited to less than 90 degrees to limit stress concentrations and prevent premature fracture of the CFRP sheet Figure 3-23. This angle is important in the case of providing continuity through the positive moment reinforcement. The CFRP that goes through the column is fanned out onto the beam sheet with an angle less than 60 degrees. Similar fans were then used by Masuo (2001) to wrap columns with a side wall.

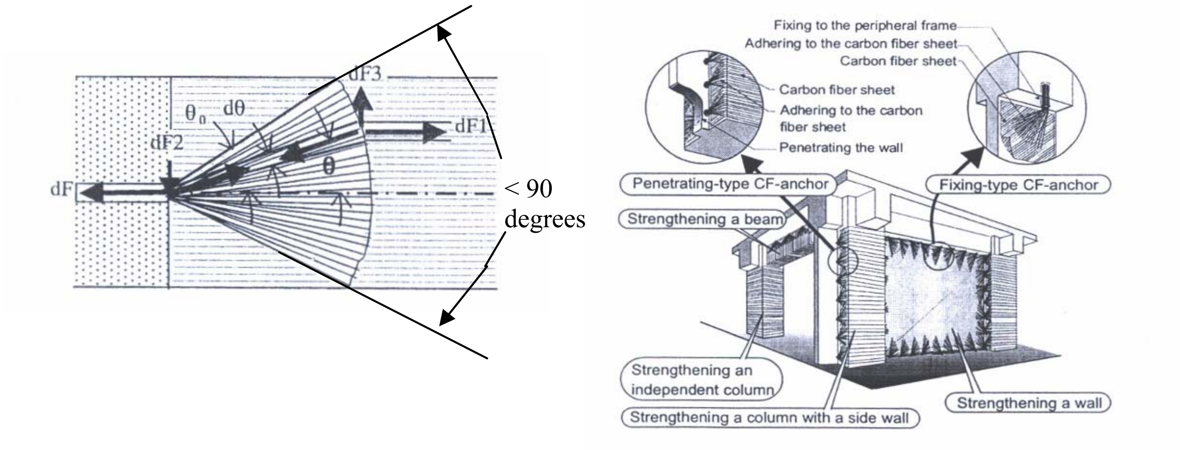
dF3
θ0
dθ
dF1
dF2
θ
dF
< 90
degrees
Fixing to the peripheral frame
Adhering to the carbon fiber sheet
Carbon fiber sheet
Carbon fiber sheet
Adhering to the carbon fiber sheet
Penetrating the wall
Penetrating-type CF-anchor
Fixing-type CF-anchor
Strengthening a beam
Strengthening an independent column
Strengthening a column with a side wall
Strengthening a wall

Figure 3-23 Fan opening angle studied by Koayashi and use of anchor fans [Kobayashi et al., 2001; Masuo et al., 2001]

The effect of a height transition, or offset in surface level of CFRP has not been previously studied. The only mention in the ACI and fib-14 reports is that unevenness, or concrete surface roughness be limited (less than 1/32 inch) due to diverting forces, Figure 3-24. However, when combined with the anchors, limitations in the unevenness or surface offsets may no longer be necessary.

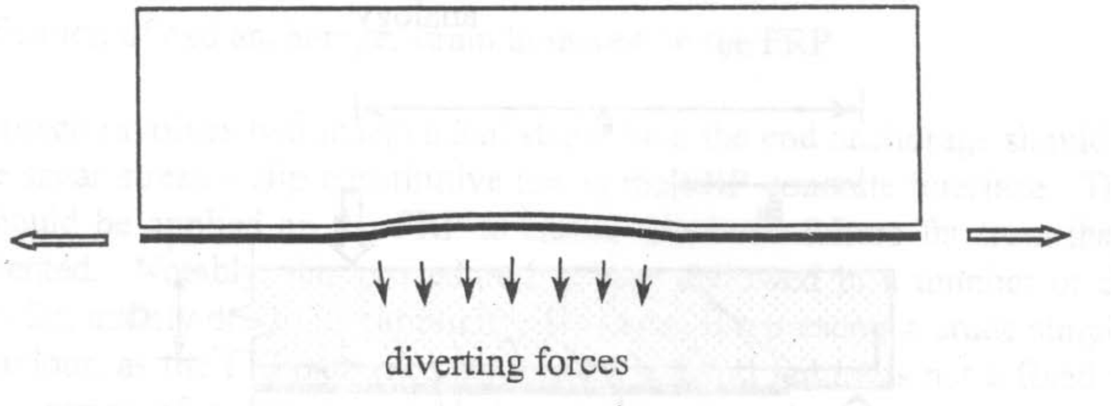
diverting forces

Figure 3-24 Diverting forces due to unevenness of concrete surface [fib-14 2001]

Ibell (2003) studied the use of precured GFRP anchor spikes to anchor a CFRP strip to the curved soffit of a concrete bridge, Figure 3-25. Ibell found that the anchors eliminated the premature debonding due to the curvature of the soffit and increased the capacity of the retrofit by 35% compared to a retrofit without anchors. However, the anchors were not designed to lead to CFRP rupture and no study was conducted on how the design of the anchors affected the retrofit capacity.

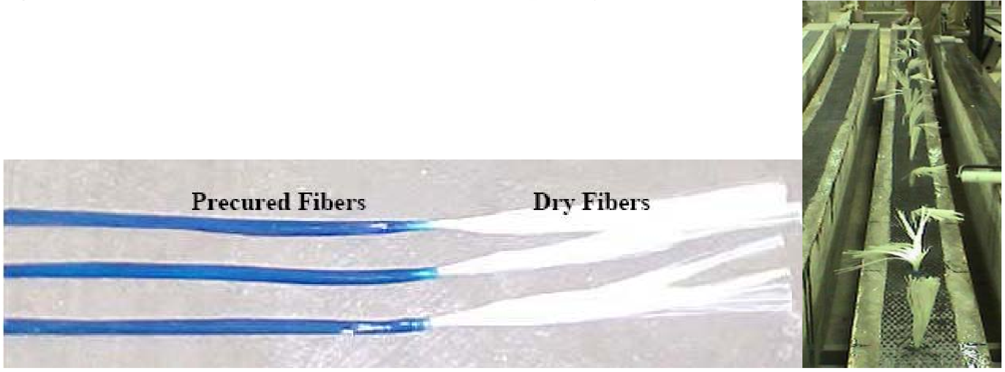

Figure 3-25 GFRP anchor spikes [Ibell et al., 2003]

Burr (2004) briefly reported some initial studies into the shear capacity of carbon fiber anchors for the Fyfe Company, however, no results were reported, Figure 3-26.

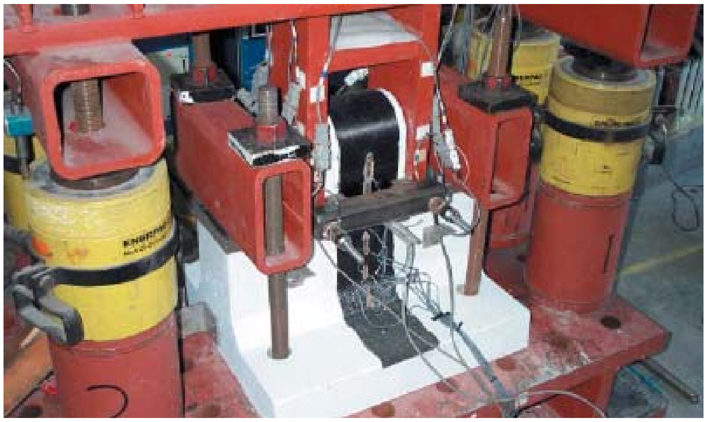

Figure 3-26 Shear test of carbon fiber anchor [Burr, 2004]

Saaticoglu et al. (2005) also used FRP anchors to overcome the effect of a height transition when increasing the lateral capacity of a infill wall whose width was less than that of the surrounding beams, Figure 3-27. Although the anchors preformed well and counteracted the effect of the height transition, the research was not focused on the design parameters of the anchors.

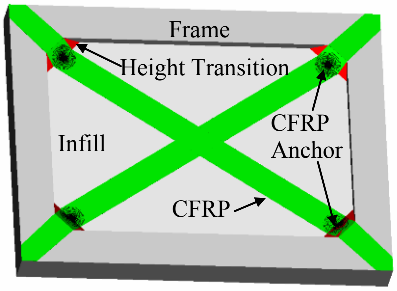

Figure 3-27 Use of FRP anchor on infill wall

Kim (2006) used carbon fiber anchors and U-wraps to examine the rehabilitation of poorly detailed RC structures, Figure 3-28. He applied CFRP to the sides of beams and found the anchors can increase the capacity of the rehabilitation by as much as 1.75 (anchors alone) to 2.2 (anchors with U-wraps) times. Kim is currently conducting tests to evaluate the effect of suddenly applied loads on the CFRP capacity. Early results indicate that CFRP anchors are able to develop the full tensile capacity of the CFRP sheet with impact type loading.

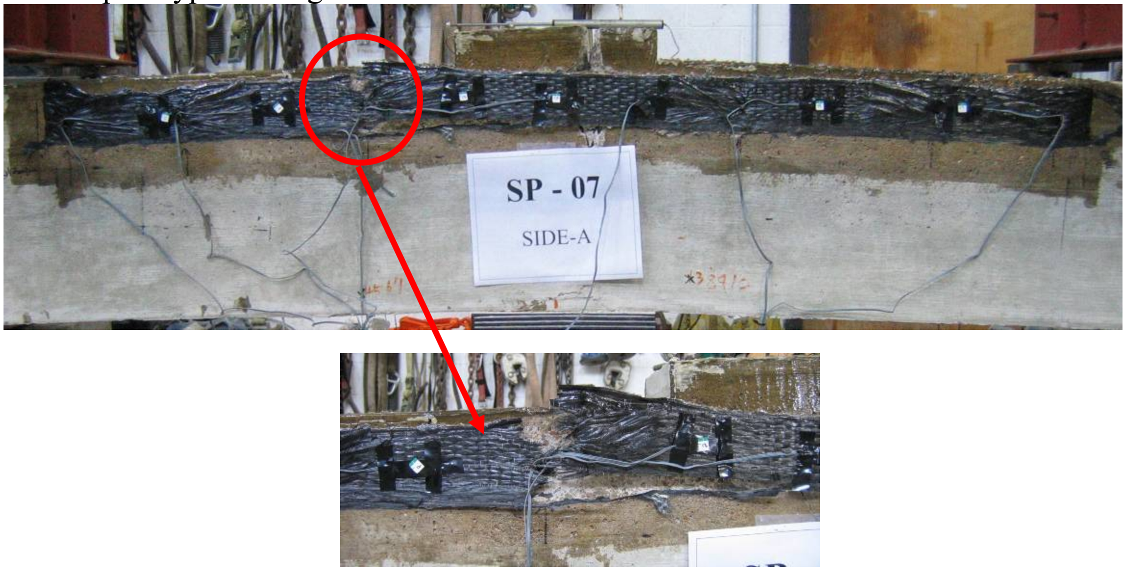

Figure 3-28 Fracture of CFRP with anchors [Kim, 2006]

Major CFRP suppliers, Sika and Fyfe, have designs for carbon fiber anchors [Sika, 2005; Fyfe, 2005b] , Figure 3-29 and Figure 3-30. However, the manufactures have limited design data for their anchors as few tests have been conducted to determine the improved CFRP strengthening of reinforced concrete members with carbon fiber anchors.

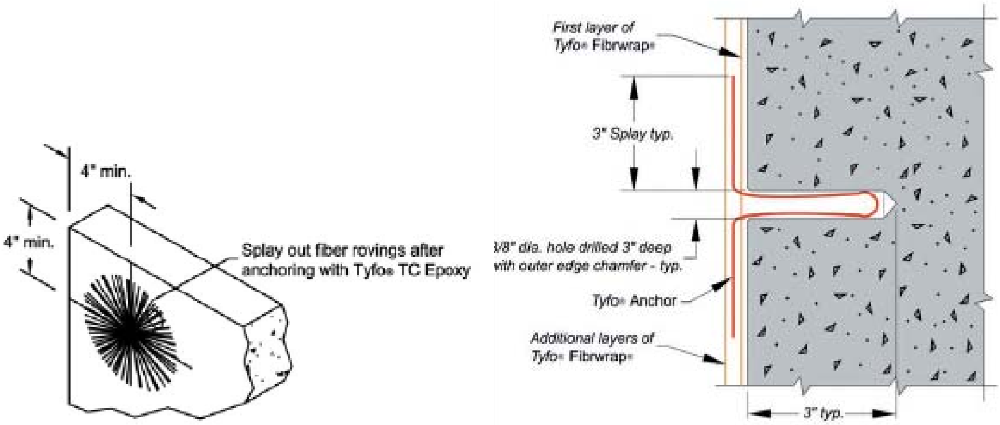
4" min.
4" min.
Splay out fiber rovings after anchoring with Tyfo® TC Epoxy
First layer of Tyfo® Fibrwrap®
3" Splay typ.
3/8" dia. hole drilled 3" deep with outer edge chamfer - typ.
Tyfo® Anchor
Additional layers of Tyfo® Fibrwrap®
3" typ.

Figure 3-29 Fyfe anchors [Burr, 2004]

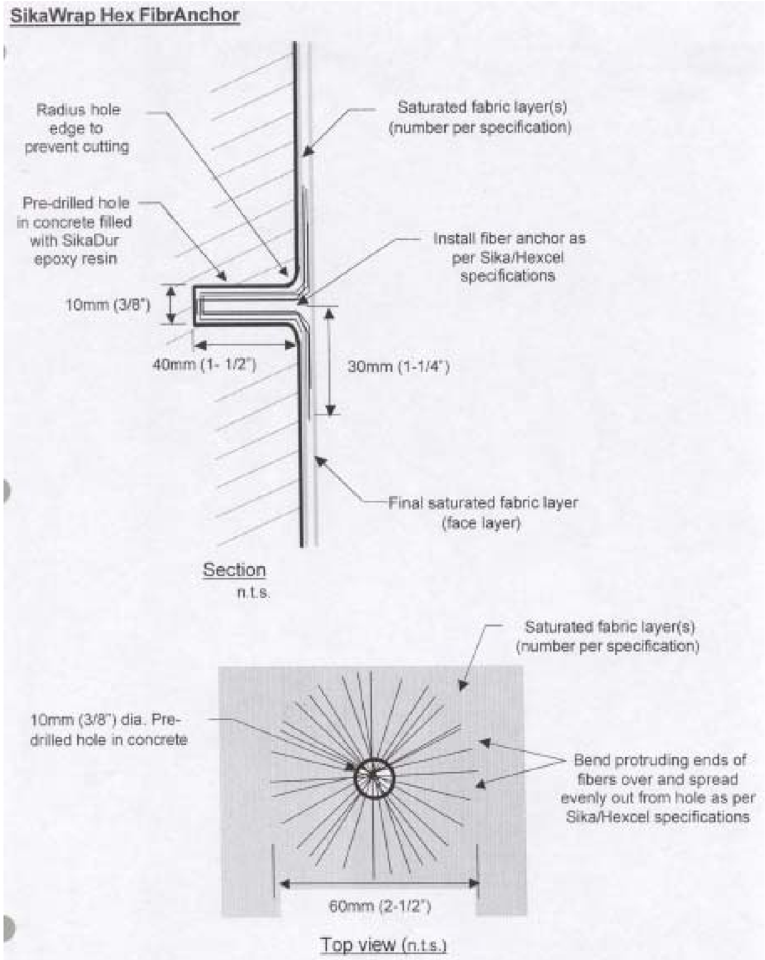
SikaWrap Hex FibrAnchor
Radius hole edge to prevent cutting
Saturated fabric layer(s) (number per specification)
Pre-drilled hole in concrete filled with SikaDur epoxy resin
Install fiber anchor as per Sika/Hexcel specifications
10mm (3/8")
40mm (1- 1/2")
30mm (1-1/4")
Final saturated fabric layer (face layer)
Section
n.t.s.
Saturated fabric layer(s) (number per specification)
10mm (3/8") dia. Pre-drilled hole in concrete
Bend protruding ends of fibers over and spread evenly out from hole as per Sika/Hexcel specifications
60mm (2-1/2")
Top view (n.t.s.)

Figure 3-30 Sika anchors [Sika, 2005]

3.5 CFRP APPLICATION

The first step in applying the CFRP is preparing the surface of the concrete. ACI 440 recommends that the concrete surface be freshly exposed and be free of all loose or unsound materials. The surface preparation can be accomplished by abrasive techniques such as sandblasting. ACI also recommends a concrete surface profile (CSR) of 3 as defined by the ICRI surface profile chips with local out of plane variations less than 1/32 in. For the tests in this report, the surface preparation was accomplished by first grinding the surface using a concrete grinding disk and then sandblasting the surface, Figure 3-31.

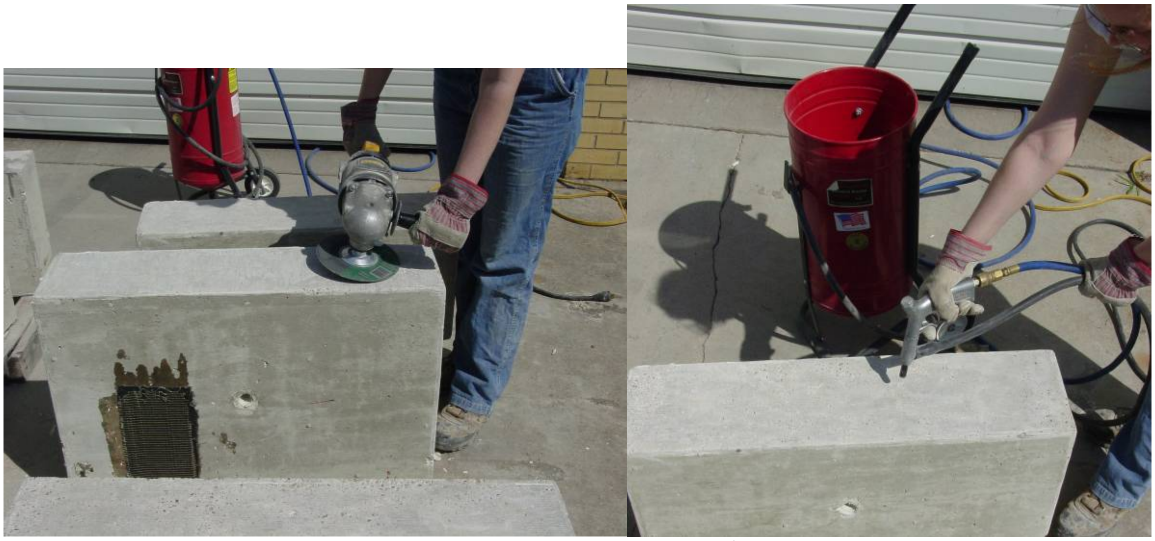

Figure 3-31 Grinding and sandblasting surface preparation

Next, holes were drilled into the concrete where needed. The edges of the holes were rounded over to a radius of ¼ to ½” using a small grinder, Figure 3-32. Dust and debris was removed from the holes by blowing compressed air into the bottom of the holes.

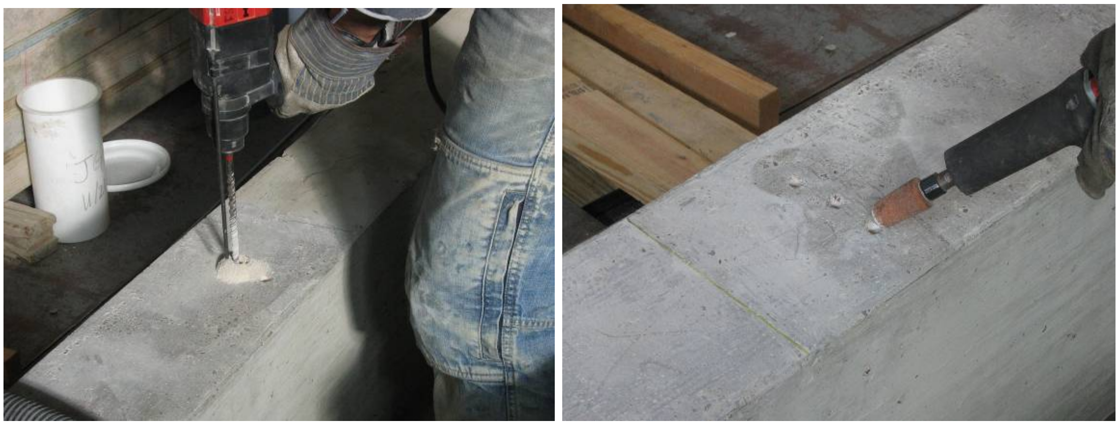

Figure 3-32 Drilling hole in concrete and rounding over edges (courtesy of Insung Kim)

If there was a height transition, a transition ramp was then placed. The ramp was constructed using Tyfo P concrete repair material that consisted of a cement dry powder and a latex solution, Figure 3-33. The surface of the concrete was saturated with water to prevent the dry concrete from pulling moisture from the repair material and weakening the bond to the concrete. To further improve bond some of the latex solution was painted over the concrete surface, Figure 3-33. Next the Tyfo P was mixed and placed onto the concrete then leveled. Figure 3-34.

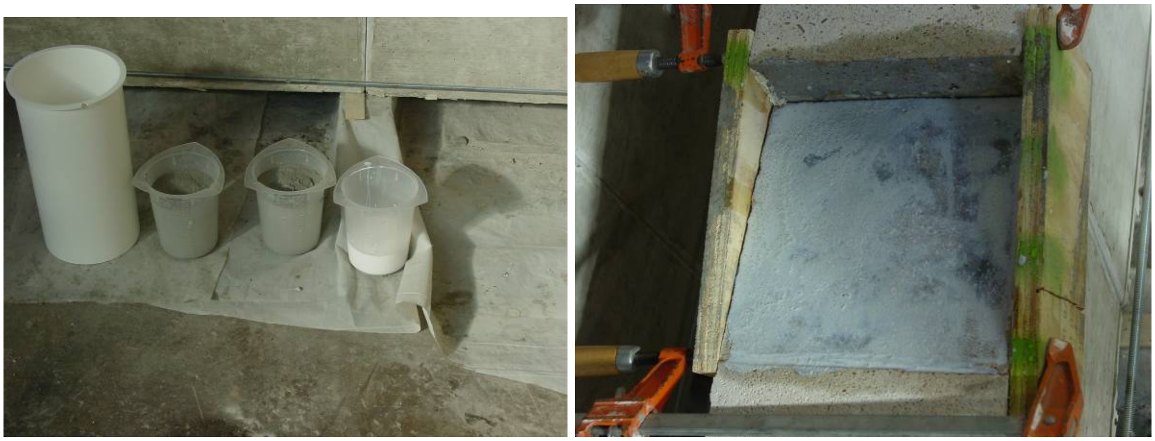

Figure 3-33 Repair material components and painting of concrete with latex solution

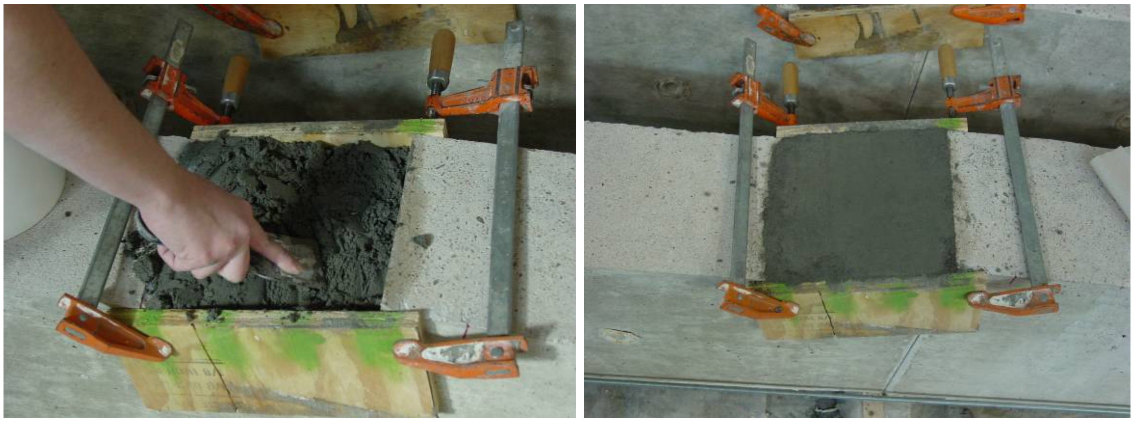
Figure 3-34 Placing and leveling of ramp material

Once the concrete was prepared the CFRP could then be applied. The application of CFRP followed the manufactures' recommendations [Fyfe, 2005a]. The CFRP sheets were cut to length and anchors made. Then the two part Tyfo S epoxy was mixed according to manufacturer recommendations, Figure 3-35. A coating of the epoxy was spread over the concrete and poured into the predrilled anchor holes. Then the CFRP sheets were saturated with epoxy and rolled between two PVC pipes to get an even saturation, Figure 3-36. Next, the saturated sheets were applied and smoothed over the concrete to eliminate air bubbles, Figure 3-37.

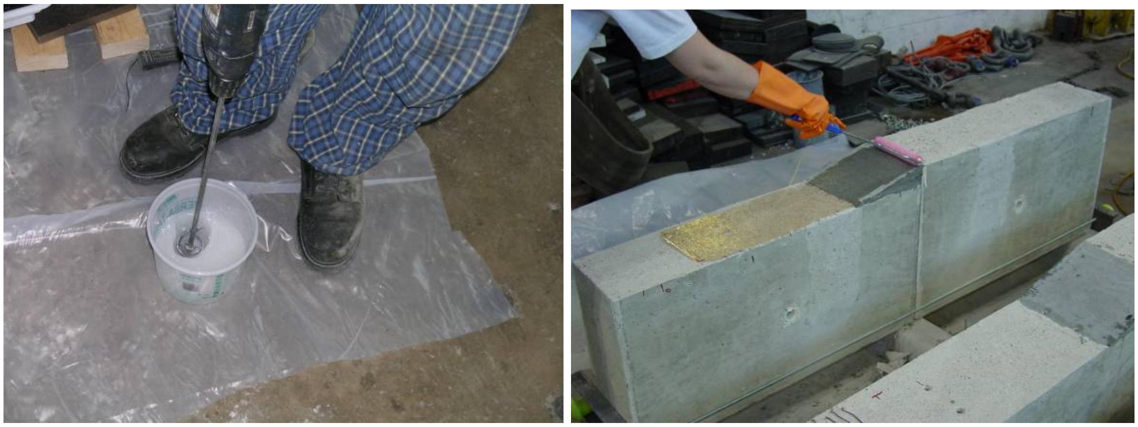
Figure 3-35 Mixing epoxy and saturating concrete surface

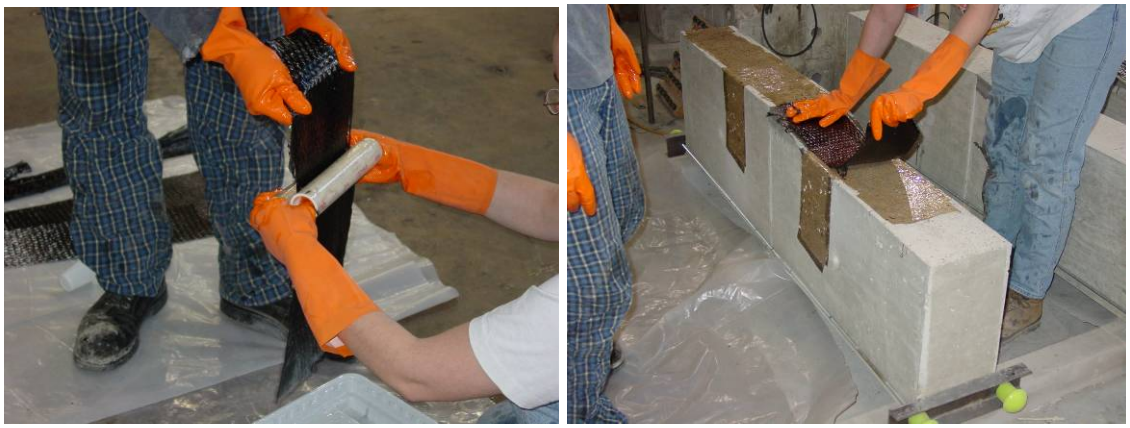

Figure 3-36 Rolling CFRP through PVC pipes and applying to concrete surface

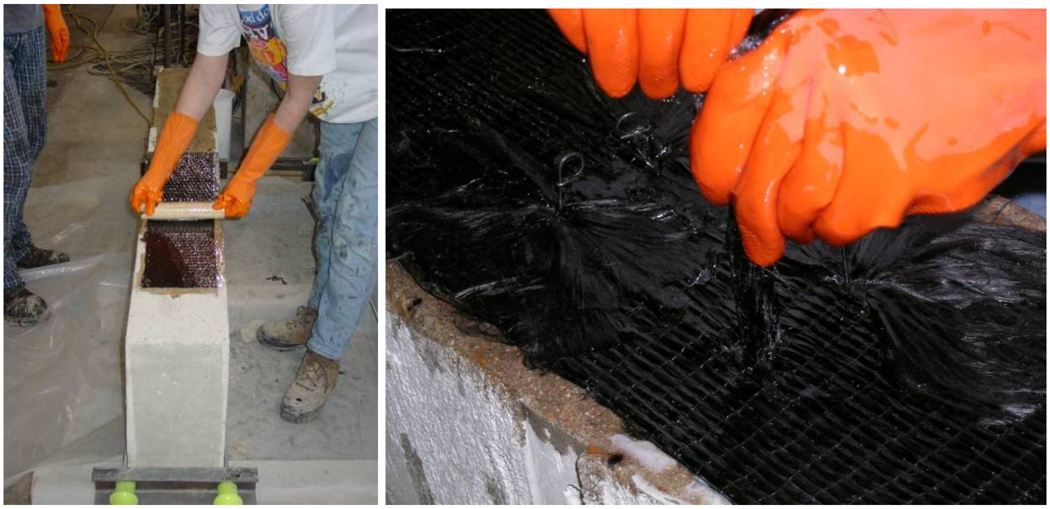

Figure 3-37 Removing air bubbles from CFRP sheet and applying CFRP anchors

The CFRP anchors are made from strips of the carbon fiber fabric, Figure 3-38. The strip of fabric is folded over and attached to a steel wire. The ends of the fabric are separated (cross fibers removed) to aid in the fanning of the anchor over the CFRP sheet. Next the anchor is saturated with epoxy, Figure 3-39. A hole is made in the CFRP sheet to insert the anchor through. The anchor is inserted and the ends of the anchor fanned over the CFRP sheet, Figure 3-40.

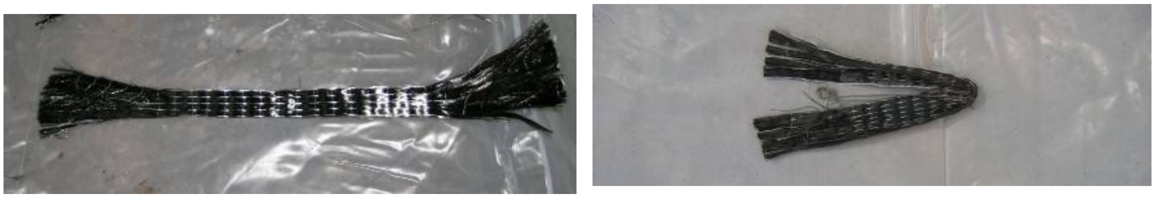

Figure 3-38 Strip of CFRP to make anchor and strip folded over steel wire

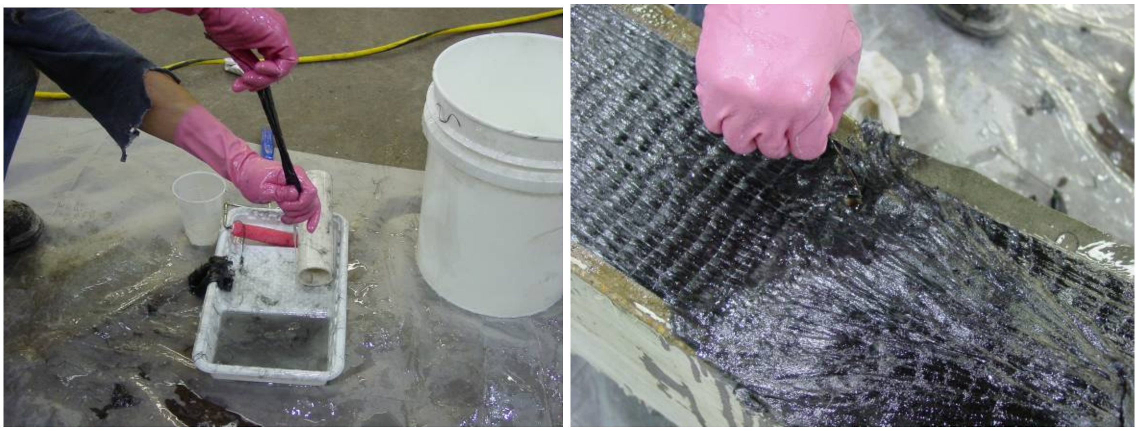

Figure 3-39 Saturating anchor and making hole in CFRP sheet to insert anchor

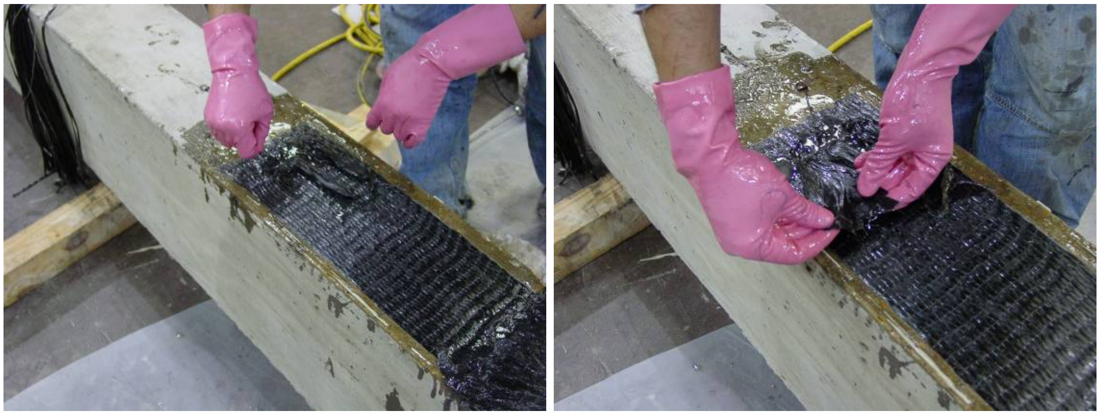

Figure 3-40 Inserting anchor and fanning ends of anchor over CFRP sheet

3.6 SUMMARY

CFRP is comprised of a unidirectional carbon fiber that is made of graphite which provides the strength, and a two-part epoxy matrix that binds the fibers and attaches them to the concrete surface. CFRP's high strength-to-weight ratio, moldability, ease of construction, aesthetics, and durability make it an ideal material to strengthen concrete beams. However, CFRP's high cost and the problem of CFRP debonding from the concrete have limited its use in retrofits. CFRP debonds due to weakness in the concrete surface layer at about 50% its tensile capacity. Equations by Teng and Chen (2001) and ACI 440 (2002) predict the bonding strength of CFRP to concrete.

Anchorage of CFRP to concrete can increase its tensile capacity and reliability. Anchorage can come in the form of mechanical fasteners, U-wraps, U-anchors, or carbon fiber anchors. Carbon fiber anchors consist of fibers inserted into a predrilled hole in the concrete and fanned out over the surface of a CFRP sheet. Although little research has been done with carbon fiber anchors, some studies have given information about possible design parameters. Ozedemir (2005) suggests that anchors be inserted at least 4 in. into the concrete to best secure the anchor into the concrete. Kobayashi (2001) suggests that anchor fans open less than 90 degrees to achieve full tensile capacity and limit stress concentrations. Research by Morphy (1999) and the JSCE (1997) suggest that anchors will lose about half their tensile capacity due to the bend in the anchor. These three suggestions establish the initial design for anchors:

- Inserted at least 4 in. into concrete
- Anchor fans less than 90 degrees
- Twice the cross-sectional area of CFRP in anchors as longitudinal sheet

Suggestions by manufactures and ACI detail the application process of CFRP.

Chapter 4: Anchorage Tests

Forty anchorage tests were conducted to determine design parameters critical to utilizing the high tensile strength of CFRP materials. In this chapter, the test setup, results, and conclusions from the anchorage tests will be discussed.

4.1 INTRODUCTION

As discussed in Chapter 3, a serious limitation in the use of CFRP on reinforced concrete comes from separation of the CFRP sheet from the concrete surface by debonding. A study of experimental results by Bonacci and Maalej (2001) indicated that CFRP debonded on average at 50% of its tensile capacity. Therefore, nearly half the CFRP is ineffective in increasing the strength of a concrete member.

Furthermore, a height transition (offset in the surface level of the CFRP) will further accentuate the early debonding of CFRP sheets. An example of a height transition occurs when providing continuity of positive moment reinforcement through a column because the hole drilled through the column (where the CFRP will be threaded through from one side to the other) cannot be drilled at the level of the bottom surfaces of the beams, Figure 4-1.

In order to utilize the high tensile capacity of CFRP sheets and to compensate for the effect of a height transition, both CFRP anchors (Figure 4-2) and CFRP U-wraps were evaluated as ways of anchoring a CFRP sheet.

The goal of the anchorage tests was to develop simple design recommendations for CFRP retrofits to provide continuity to reinforced concrete beams. The parameters evaluated in the anchorage tests were the size, number, and spacing of anchorages (CFRP anchors or U-wraps), slope and height of the transition, material efficiency, type of surface preparation, and type of carbon fiber fabric.

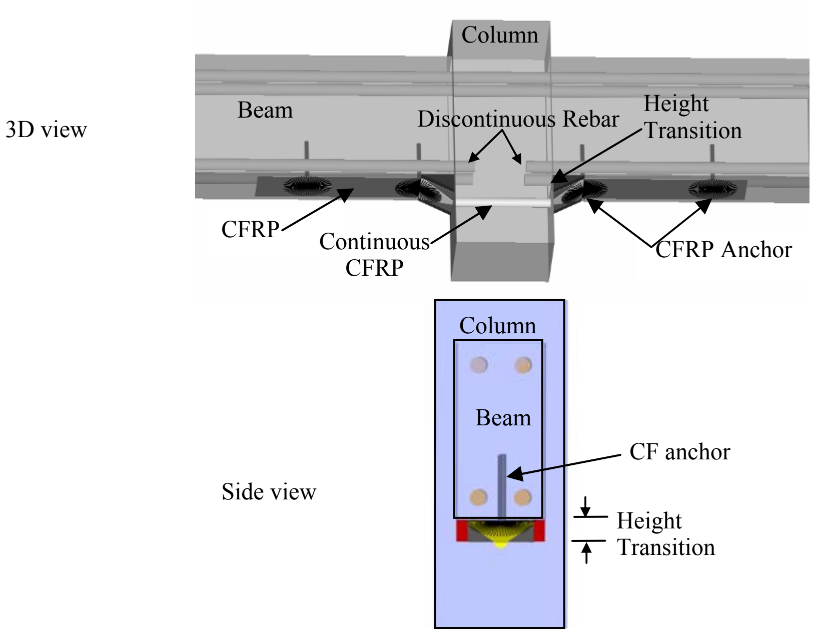
3D view
Column
Beam
Discontinuous Rebar
Height Transition
CFRP
Continuous CFRP
CFRP Anchor
Side view
Column
Beam
CF anchor
Height Transition

Figure 4-1 Use of CFRP at height transitions

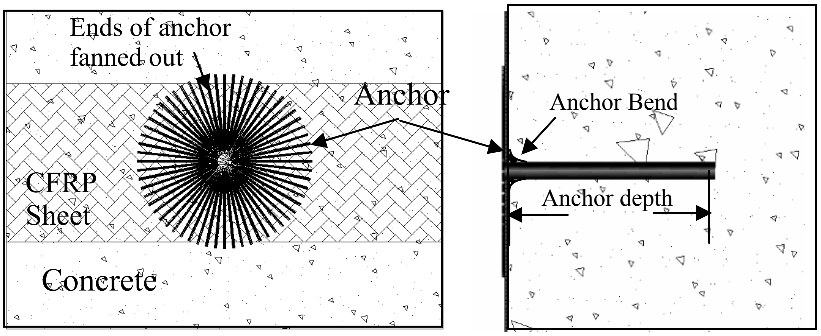
Ends of anchor fanned out
Anchor
CFRP Sheet
Concrete
Anchor Bend
Anchor depth

Figure 4-2 CFRP anchor

4.2 TEST SETUP

The specimens and test setup were designed to allow for a controlled evaluation of the anchorage of the CFRP sheet with and without a height transition, Figure 4-3. The test setup was designed as a reinforced concrete beam in bending with a preexisting crack at mid-span. The test setup simulated the condition of using CFRP to provide continuity across critical sections of a reinforced concrete beam. Tests with no height transition simulated the case where CFRP provides continuity through the negative moment reinforcing bars. The tests with a height transition simulated the case of providing continuity through the positive moment reinforcing bars.

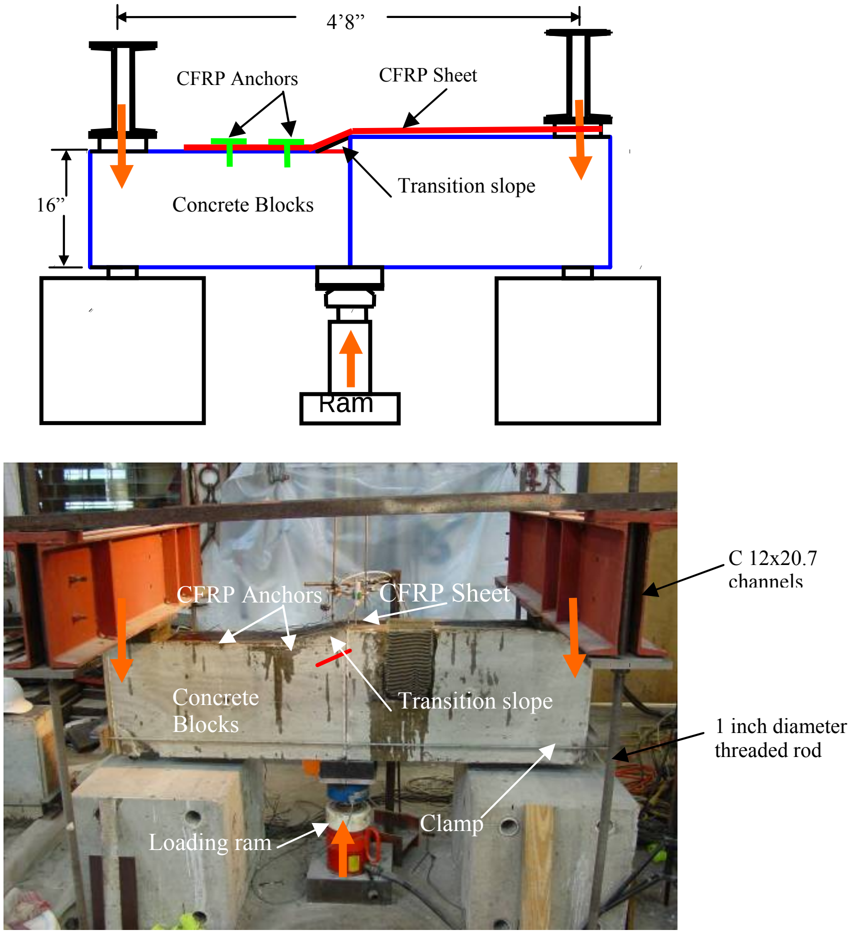
4’8”
CFRP Anchors
CFRP Sheet
16”
Concrete Blocks
Transition slope
Ram
CFRP Anchors
CFRP Sheet
Concrete Blocks
Transition slope
Loading ram
Clamp
C 12x20.7 channels
1 inch diameter threaded rod

Figure 4-3 Test setup

Most of the test specimens consisted of two 8 in., wide by 32 in. long blocks of reinforced concrete connected by a CFRP sheet. The height of the blocks was 16 in. for one block and 16 in. plus transition height for the other. The connected blocks were loaded at mid-span by a 60 ton ram. Simple support reaction were provided at both ends through use of back to back steel C 12x20.7 channels connected to the lab floor though 1 in. diameter threaded rod, Figure 4-3. The support reactions were 4 ft 8 in. apart.

A clamp comprised of threaded rod and small channels, clamped the blocks together for CFRP application and moving the blocks into the test setup. The clamp was applied at the base of the blocks where it would not provide any resistance during testing.

The use of two separate blocks of concrete created the crack to initiate debonding at a controlled point and ensured that all tensile resistance was provided by the CFRP sheet. The tension in the CFRP sheet could then be determined by evaluation of the moment at midspan (PL/4) and moment resistance ($T_{CFRP}d$) as in Equation 4-1 (see also free body diagram in Figure 4-4).

$$T_{CFRP} = \frac{PL}{4d}$$ **Equation 4-1**

where T_{CFRP} is the tension in the CFRP sheet, P is the load in the loading ram, L is the distance between support reactions (4 ft 8 in.) and d is the height of the blocks[1].

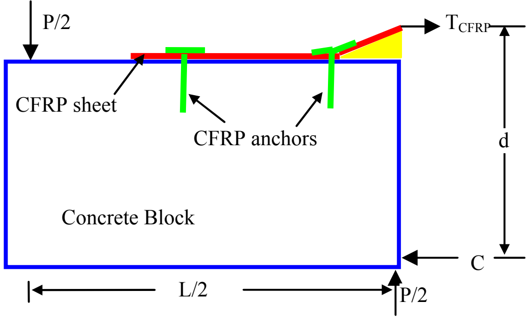

Figure 4-4 Free body diagram of half of test specimen

The blocks were cast with two #5 reinforcing bars at the top and bottom and four # 3 stirrups. The blocks were cast with a hole through the center for lifting and rotating the blocks. Rotating the blocks enabled the use of both the top and bottom surfaces in the anchorage tests. In general, blocks were cast ten at a time in two five-block groups.

---

[1] d is actually the distance between the CFRP sheet and the centroid of the compressive stress block in the concrete. For a tension of 30 k, the height of the concrete compressive stress block is only 1 in. and d is the height of the block minus ½ in. For calculation simplicity, d is taken as the total height of the block and the error in the tension calculation is less than 3%.

Pictures of the formwork and rebar for the blocks can be found in Figure 4-5. Four earlier tests used 10 in. and 12 in. high blocks.

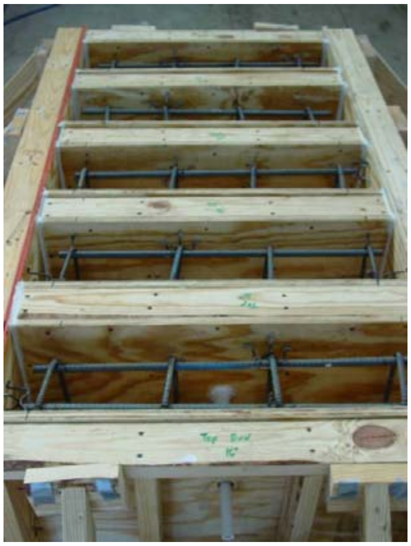

Figure 4-5 Concrete block formwork and rebar

4.2.1 CFRP layout

The CFRP was applied according to the procedure presented in Section 3.5. The tension surfaces of typical test specimens are shown in Figures 4-6 and 4-7. The tests with no height transition between the blocks consisted of a single 6 in. wide CFRP sheet applied across the concrete blocks with anchors (if any) at 5 in. and 19 in. from centerline. The anchors were fanned in a pie shape directed along the tension in the CFRP sheet.

Tests with a height transition between the blocks simulated the CFRP application shown in Figure 4-1. The transition slope was constructed using a polymer modified cement repair mortar (Tyfo P) with a bonding strength greater than the concrete substrate and suitable for overhead applications (see Section 3.5 and Figure 3-34). A CFRP sheet was then applied to the beam concrete block and transition slope. Another CFRP sheet was fanned over the beam sheet and bundled onto the column block, Figure 4-7. The opening of the fan was kept to less than 90 degrees as recommended by Kobayashi (2001) (see Chapter 3). Fanning of the column sheet over the beam sheet transfers stresses in the column sheet into the beam sheet. The bundling of the column sheet simulates inserting the sheet into a hole drilled through the column. In the actual structure, the sheet would be extended through the column to the beam on the other side of the column. However, these tests simulate only one side of the beam column joint, and the sheet on the column block was secured under the reaction point to simulate the anchorage of the sheet on the other side of the column. Anchors (if any) were then inserted at the end of the transition slope and 21 in. from the center. The anchors at the end of the transition slope were fanned in a circular fashion due to the need to resist normal forces (due to bend in CFRP sheet) at that location.

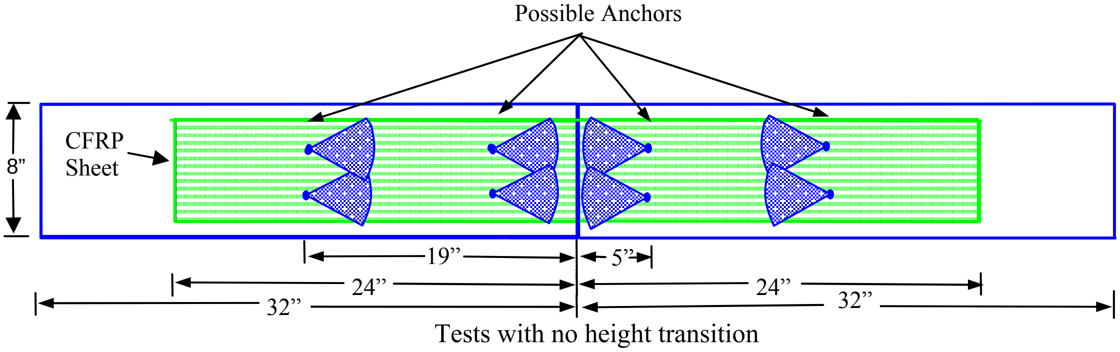
Possible Anchors
CFRP Sheet
8"
19"
5"
24"
24"
32"
32"
Tests with no height transition

Figure 4-6 CFRP application with no height transition

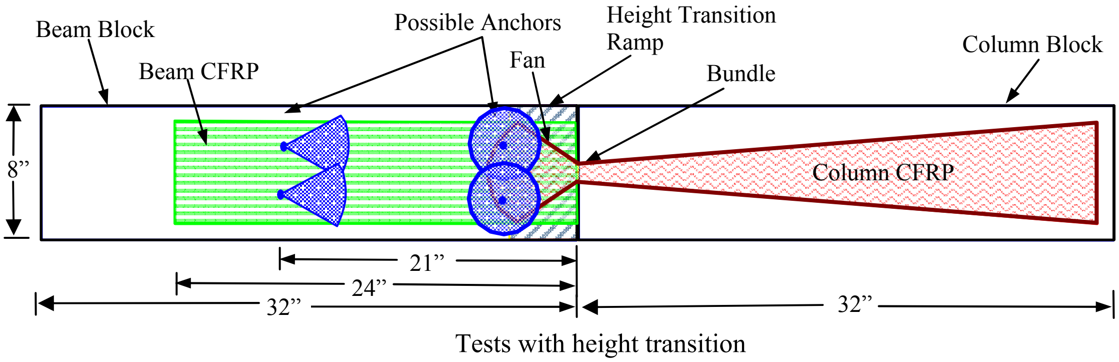
Beam Block
Beam CFRP
Possible Anchors
Fan
Height Transition Ramp
Bundle
Column Block
Column CFRP
8"
21"
24"
32"
32"
Tests with height transition

Figure 4-7 CFRP application with height transition

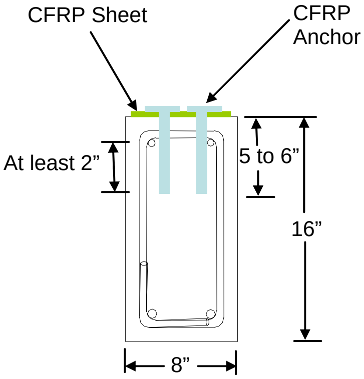

Figure 4-8 CFRP anchor depth

All anchors were inserted to a depth of 5 to 6 in. to ensure at least a 2 in. depth into the core of the concrete (interior of the first layer of reinforcing steel), Figure 4-8. Inserting anchors into the core of the concrete ensures that stresses are transferred to concrete surrounding the reinforcing steel and that failure does not occur by separation of the concrete cover. The anchor depth is also greater than the 4 in. effective depth suggested by Ozedemir (2005).

All of the edges of the predrilled concrete holes were rounded to limit stress concentrations (see anchor bend in Figure 4-2). Even with the rounded edges, equations from a JSCE research committee report (1997), presented in Chapter 3, predict that the loss of strength of the anchors due to the bend would at least 50%. Therefore, the total cross-sectional area of all anchors needs to be comprised of a cross-sectional area greater than that of the longitudinal sheet. The size of the anchor[2] in relation to the diameter of the hole drilled in the concrete and actual width of the CFRP sheet used to make the anchor are given in Table 4-1.

---

[2] the size of the anchor is notated by the size of hole drilled in the concrete, the actual cross-sectional area of the anchor can be computed by multiplying the width of the CFRP sheet used to make the anchor by the thickness of the CFRP sheet

All U-wraps were 6 in. wide and extended 10 in. down the sides of the concrete block. The 10 in. bonding length on the side of the concrete block is greater than the effective length of 5 in. given by the Teng and Chen equation presented in Chapter 3. The designation for each test based on the test parameters is given in Table 4-2.

Table 4-1 Anchor sizes

Anchor Size	Diameter of hole drilled in concrete (in)	Width of CFRP sheet used to make anchor (in)
5/8	5/8	6
9/16	5/8	4
1/2	1/2	3
3/8	3/8	2

Table 4-2 Specimen designation: ab-dce

Parameter	Possible Values	Designation
a) Slope of Transition	none	0
	1:2	2
	1:4	4
b) Height of Transistion	0 in	0
	1 in	1
	2 in	2
	3 in	3
c) Anchorage of sheet	none	n
	U-wraps	u
	2 anchors	2
	4 anchors	4
	6 anchors	6
d) Surface Preparation	grinding	g
	sandblasting	s
e) Test number with similar parameters		1,2…n

4.2.2 Instrumentation

Instrumentation of the anchorage tests consisted of three linear potentiometers, one load cell, one pressure transducer, and numerous strain gages on the CFRP. The displacement measurements were taken at the center crack between the concrete blocks. Two pots measured the vertical displacement, and one pot measured the opening of the crack between the concrete blocks, Figure 4-9. A load cell and pressure transducer measured the load in the loading ram. Stain gages measured the strain in the CFRP sheet (see Section 4.3.2.5 and Appendix A).

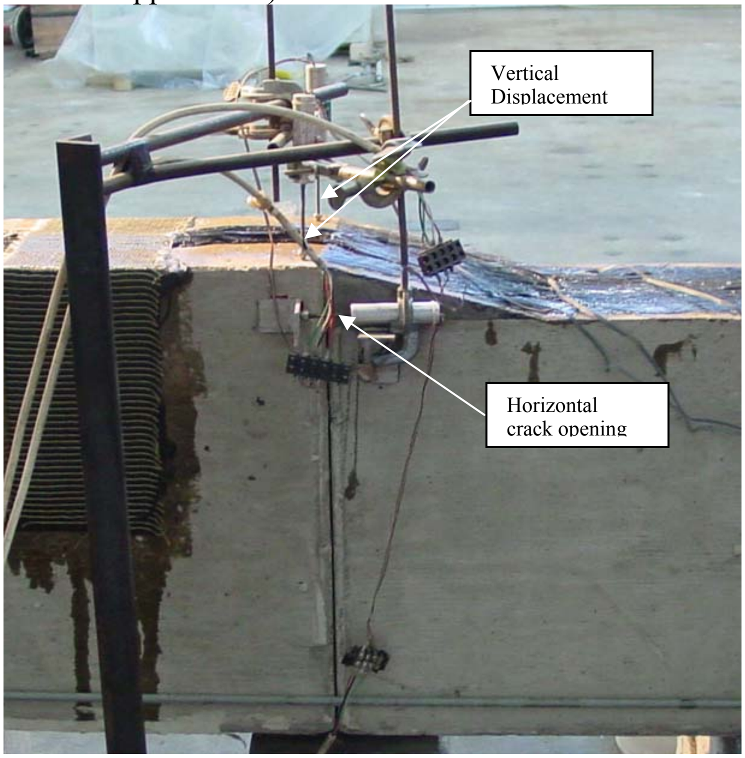

Figure 4-9 Measurement of vertical displacement and horizontal crack opening

4.2.3 Material Properties

The concrete blocks had an average nominal compressive strength of 3400 psi as determined from standard ASTM cylinder tests on 6 in. diameter by 12 in. high cylinders. At least four cylinders were tested for each casting of concrete, and cylinder tests occurred as near as possible to testing dates of the specimens.

Both the manufacturer's properties and results of ASTM D-3039 standard tests (see Section 3.1.5) of the CFRP material are given in Table 4-3, photos in Figure 4-10. For both the SCH-35 fabric and SCH-41 fabric, six coupons were constructed and tested. The same roll of CFRP fabric was used throughout the anchorage tests and the coupons for each type of fabric. However, a different batch of epoxy was made for each application of CFRP. CFRP coupons were made for two different applications of epoxy (three coupons each) for each type of fabric.

For each type of fabric, one coupon had an undesirable failure due to misalignment in the testing machine or grips. The results reported are the average properties for the five remaining coupons ± the standard deviation. The results show close agreement between the manufacturer's reported values and the measured values during testing. The relatively low standard deviation in the test data indicates material consistency.

Table 4-3 CFRP fabric properties (ASTM D-3039)

	SCH 35		**SCH 41**	
Property	**Nominal**[a]	**Measured**	**Nominal**[a]	**Measured**
Tensile Strength (ksi)	143	170±18	143	125±8
Tensile Modulus (ksi)	11,400	12,520±1900	13,900	12,949±1460
Elongation at break	1.26%	1.32%±0.18%	1.00%	0.97%±0.10%
Thickness (in.)	0.035	0.035	0.04	0.04

a)Provided by Manufacturer's data sheets

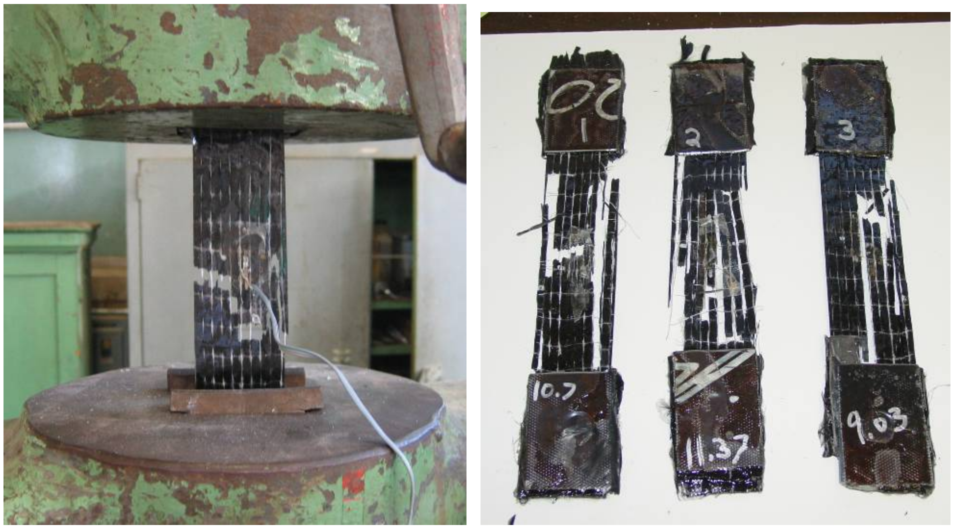

Figure 4-10 FRP coupons tested in accordance with ASTM D-3039

4.3 TEST RESULTS

The goal of the anchorage tests was to determine simple design recommendations for the use of CFRP sheets to provide continuity to reinforced concrete beams. The tests with no height transition were focused on the design of the anchorage. Tests with a height transition evaluated the effect of the slope and height of the transition, as well as the surface preparation and type of carbon fabric.

4.3.1 Tests With No Height Transition

The test results for all specimens with no height transition are presented in Table 4-4 and a graph of results for selected specimens in Figure 4-11. The efficiency of CFRP material usage is defined in Equation 4-2 and is directly comparable to the material cost of the CFRP strengthening scheme. The efficiency describes the percentage of total CFRP capacity actually being utilized in strengthening the concrete member (providing additional tensile reinforcement). A higher efficiency would indicate an anchorage system that would require less material to achieve a given strength.

$$Efficiency \equiv \left(\frac{V_{LS}}{V_T}\right) * \left(\frac{T_{\max}}{T_{ult}}\right) \qquad \textbf{Equation 4-2}$$

Where

T_{max} = Maximum measured tension in CFRP sheet

T_{ult} = Ultimate tensile capacity of CFRP sheet (determined from coupon tests, Table 4-3)

V_{LS} = Volume of Longitudinal CFRP sheet (thickness * width * length)

V_T = Total Volume of CFRP (thickness * width * length of all CFRP sheets used in retrofit)

In order to keep comparisons of tests with and without a height transition consistent, the efficiency represents the CFRP on the beam side of the concrete blocks.

The volume for all longitudinal sheets is comprised of a 6 in. by 24 in. sheet. For example, specimen 00-6s1 contained a 6 in. wide by 24 in. long by 0.035 in. thick longitudinal CFRP sheet on the beam block (V_{LS} = 5 in^3). The six anchors were made from 2 in. by 9 in. long by 0.035 in. thick CFRP sheets (V in anchors = 3.8 in^3, V_T = 8.8 in^3). T_{max} was 32 k and T_{ult} was 32 k. Therefore the efficiency was 57%.

An efficiency of 1 would indicate that all of the CFRP is at its ultimate tensile strength and being utilized in strengthening the concrete member. However, use of anchors ensures that V_{LS}/V_T will always be less than 1.

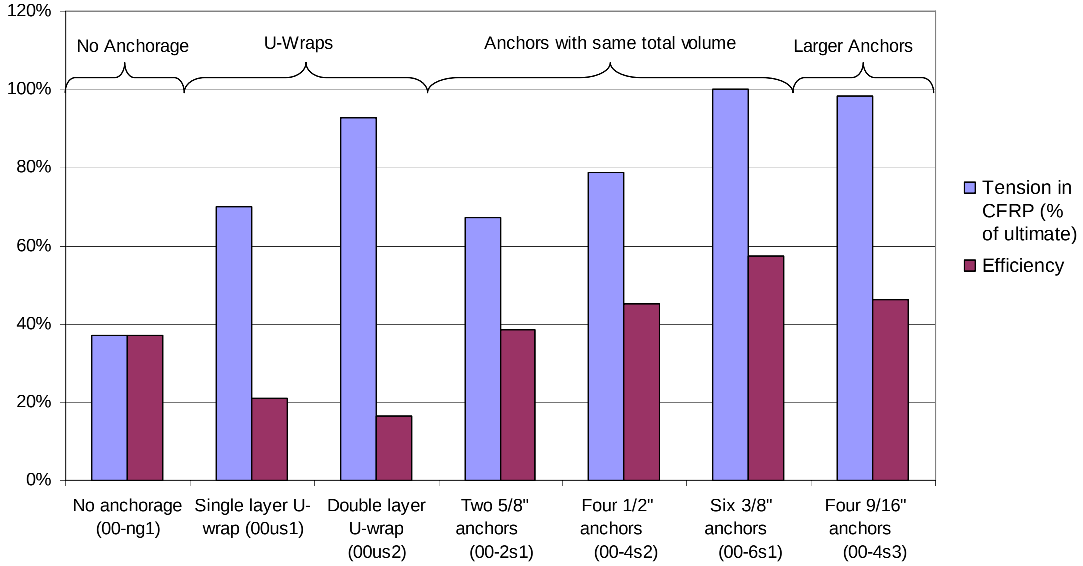

Figure 4-11 Maximum tension and efficiency of CFRP

Table 4-4 Test results for no height transition

Test #	Slope	Height difference	Type of Fabric	Anchorage	Diagram	Depth of beam	Surface preparation	f'c (psi)	Load at Failure (kip)	Tension in CFRP at Failure (kip)	Tension in CFRP (% of ultimate)	Area of CFRP (ft^2)	Retrofit Effectiv-eness	Failure Mode
00-ng1	none	0"	SCH-35	none	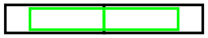	10"	grinding	3400	11.88	11.88	37%	0.67	37%	Debonding
00-ns1	none	0"	SCH-35	none	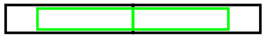	16"	sandblast	3100	12.07	10.56	33%	1.00	33%	Debonding
00-us1	none	0"	SCH-35	U wraps 6" wide at 5" and 19"	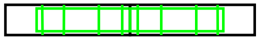	16"	sandblast	3300	25.55	22.36	70%	3.33	21%	debond of flat FRP, shear of U wrap
00-us2	none	0"	SCH-35	Double U wrap 6" wide at 5" and 19"	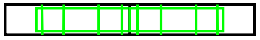	18"	sandblast	3300	33.8	29.58	93%	5.67	16%	Fracture
00-2s1	none	0"	SCH-35	2 3/8" anchor at 3"	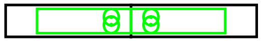	18"	sandblast	3100	15.02	11.68	37%	1.38	27%	Shear off corner of block and debonding
00-2s2	none	0"	SCH-35 sheet SCH-41 anchors	5/8" anchor at 5" and 19"	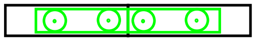	18"	sandblast	3400	27.5	21.39	67%	1.75	38%	Fracture anchor, partly debond
00-4g1	none	0"	SCH-35	2 3/8" anchor at 3"and at 6"	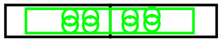	12"	grinding	3400	24.19	20.16	63%	1.08	39%	Shear failure in concrete block
00-4s1	none	0"	SCH-35	2 3/8" anchor at 5"and at 19"	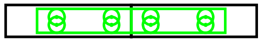	18"	sandblast	3300	27.21	21.16	66%	1.50	44%	Fracture of 4.5" width, debonding of 1.5"
00-4s2	none	0"	SCH-35 sheet SCH-41 anchors	Two 1/2" anchors at 5" and 19"	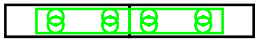	16"	sandblast	3400	28.73	25.14	79%	1.75	45%	Fracture
00-4s3	none	0"	SCH-35 sheet SCH-41 anchors	2 9/16" anchors at 5" and 19"	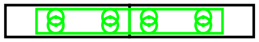	18"	sandblast	3400	40.38	31.41	98%	2.13	46%	Fracture
00-6s1	none	0"	SCH-35	3 3/8"anchors at 5" and at 19"	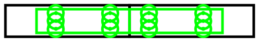	16"	sandblast	3300	36.5	31.94	100%	1.75	57%	Fracture

4.3.1.1 No Anchorage

The results of tests 00-ng1 and 00-ns1 show that without additional anchorage the CFRP sheets debonded at less than 40% of their ultimate tensile capacity[3], Figure 4-12. The Teng and Chen model for FRP debonding (presented in Chapter 3) would give the CFRP an effective length of 4.5 in. and a capacity of 7.5 k. The maximum measured tension in the two tests was 11.9 k and 10.6 k, indicating that the Teng and Chen equation was conservative. The strain distribution at 80% of maximum load shows a concentration of strain just above the center crack, Figure 4-13. At maximum load, the strain is fairly uniform throughout a length of about 12 in. from the center crack. The distribution of strain could have been caused by micro cracking in the concrete just below the CFRP sheet prior to debonding.

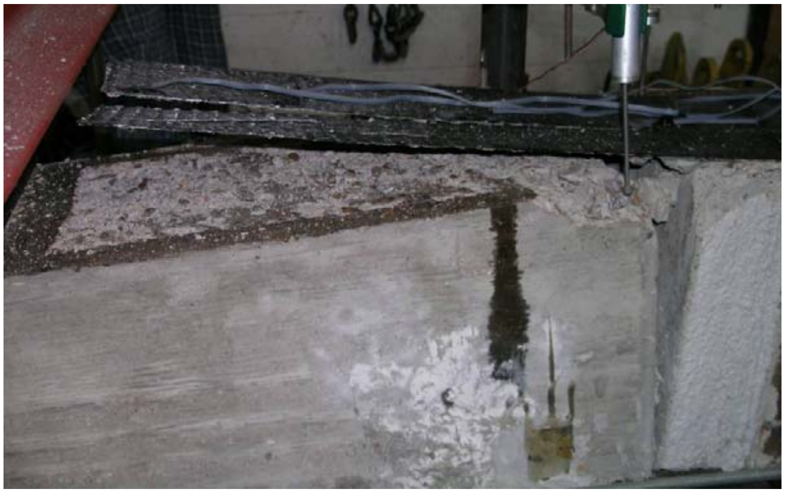

Figure 4-12 Debonding of CFRP

---

[3] Ultimate or nominal tensile capacity is determined from coupon tests presented in Table 4-3, for SCH-35 fabric the value would be 31.9 k, for SCH-41 fabric 30 k. The ultimate tensile capacity is intended to represent the point at which the CFRP fractures.

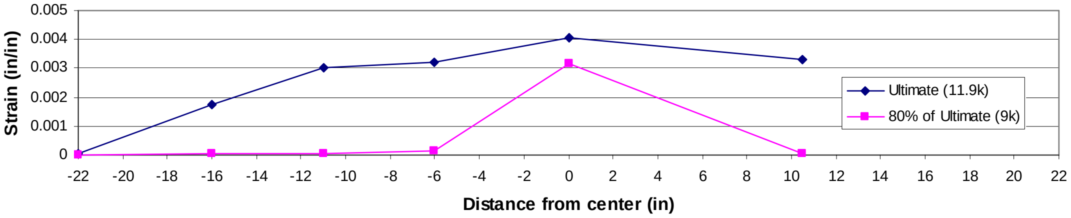

Figure 4-13 Strain distribution for test 00-ns1

4.3.1.2 U-wraps

Two single layer U-wraps on either side of the "crack" increased the tension in the CFRP sheet to 70% of ultimate tensile capacity with the longitudinal sheet debonding and the U-wrap failing in shear[4] (00-us1), Figure 4-14. The shearing of the U-wrap allowed the CFRP sheet to slip under the U-wrap and increase the deformation capacity of the retrofit, Figure 4-15. The ultimate displacement of 00-us1 reached 0.8 in., much higher than 00-ns1 at 0.25 in. or 00-6s1 at 0.6 in.

Two double layer U-wraps reached 93% of ultimate tensile capacity (00-us2) with a tension of 29.6 k at failure. The sheet failed by FRP fracture just above the center crack between the concrete blocks, Figure 4-16. However, the CFRP retrofit efficiency was reduced to 16% due to the excess of CFRP material being used in the U-wraps. For the 1 ft^2 of material in the longitudinal sheet, and extra 4.7 ft^2 was added in the U-wraps to anchor the longitudinal sheet. The low efficiency of U-wrap anchorage shows that U-wraps are not a materially efficient method to improve the capacity of CFRP retrofits.

---

[4] U-wrap shear strength is based on epoxy holding individual fibers together, when epoxy bond breaks due to shear forces, fibers are able to slide relative each other.

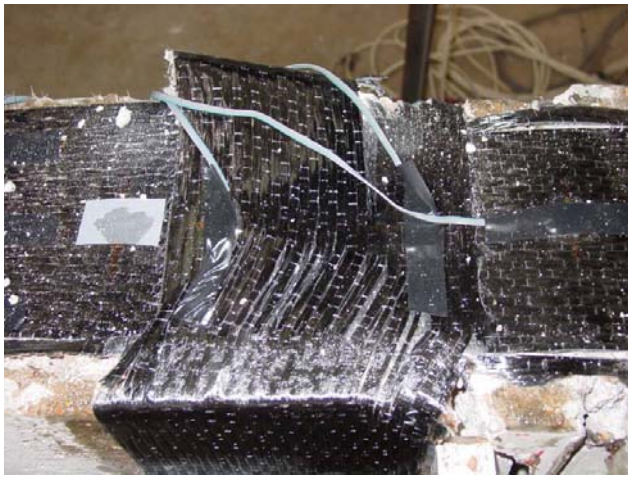

Figure 4-14 Shear failure of U-wrap

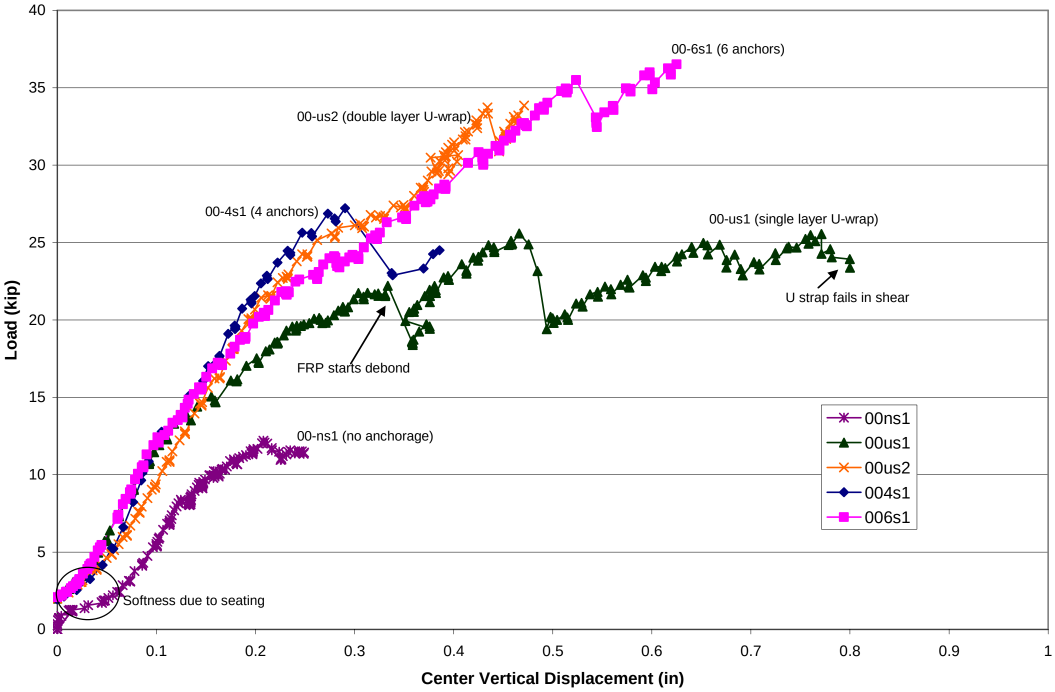

Figure 4-15 Deformation capacity of various retrofits

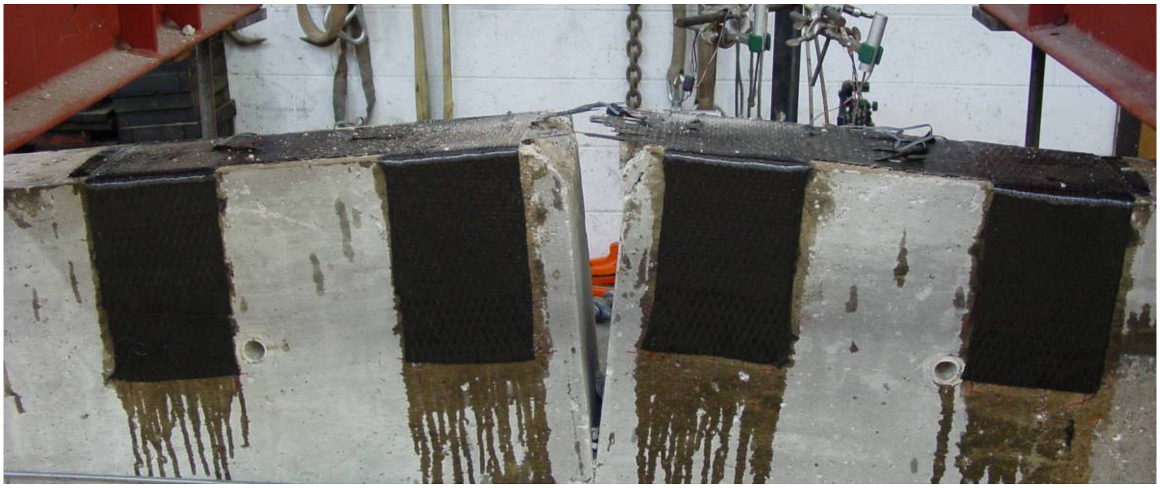

Figure 4-16 Failure by FRP fracture of retrofit with double layer U-wraps (00-us2)

4.3.1.3 CFRP Anchors

CFRP anchors allowed the CFRP sheets to utilize their full tensile capacity and maximized the material efficiency of the CFRP retrofit, but the number and size of anchors played a critical role. In the first series of CFRP anchor tests, anchors had the same total cross sectional area in each row, but were divided into 1, 2, or 3 anchors. The total cross sectional area for each anchor row was equal to the cross sectional area of the longitudinal sheet (6 in. wide by 0.35 in. thick). This gives a total cross-sectional area of anchors twice as much as the cross-sectional area of the longitudinal sheet to compensate for the loss of anchor strength due to the anchor bend. A table of the anchor sizes (not equivalent to actual anchor diameter), width of CFRP sheet used to make the anchor, diameter of hole drilled in the concrete can be found in Table 4-1.

A 5/8 in. diameter single anchor in each row was not able to fully develop the CFRP sheet's tensile capacity (00-2s2) reaching only 67% of ultimate tensile capacity in the CFRP sheet. Failure of the specimen occurred by anchor fracture and debonding, Figure 4-17. Fracture of the anchor occurred at the location where the anchor bent as it extended from the concrete hole to fan out over the CFRP sheet. The low maximum load for this test may be due to the fact that the anchor was not able to distribute stresses to the entire width of the CFRP sheet.

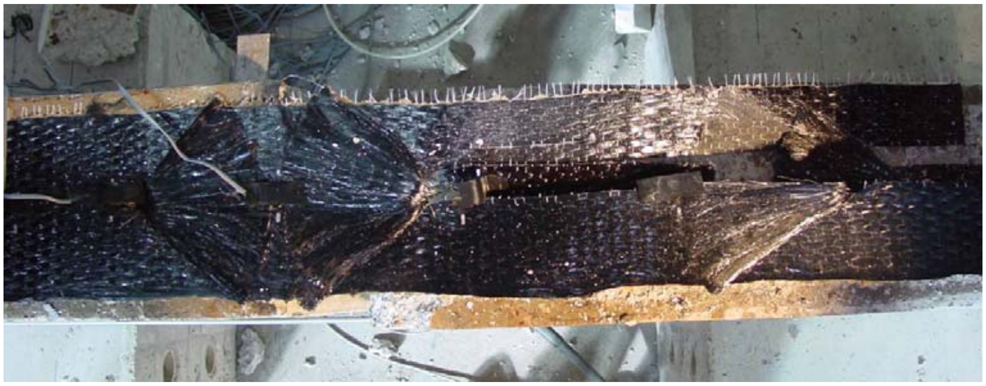

Figure 4-17 Failure by debonding and partial FRP fracture of retrofit with one anchor per row (00-2s2)

Two ½ in. diameter anchors in each row increased the tension in the CFRP sheet at failure to 79% of ultimate tensile capacity (00-4s2). Although the failure occurred by CFRP fracture, the specimen only reached 25 k of tension in the CFRP sheet. The reduced tension at fracture may be due to the fact that the fracture occurred along half of the CFRP sheet on one side of the block then along the other half on the other side of the block, Figure 4-18. The splitting of the fracture between two blocks could be indicative of a lack of uniform stress distribution across the CFRP sheet, with fracture occurring on one side followed by fracture on the other side. The reduced capacity could also be due to the fact that SCH-41 fabric was used in the anchors rather than SCH-35 in the previous tests (see Section 4.3.2.2).

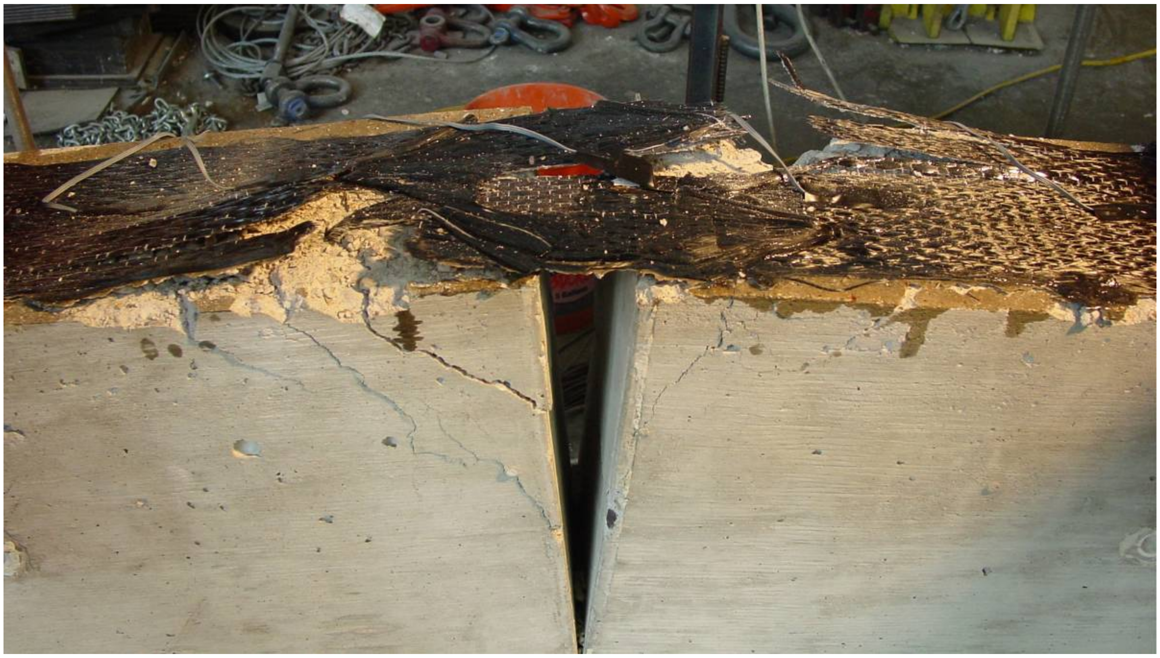

Figure 4-18 Failure by FRP fracture of retrofit with two anchors per row (00-4s2)

Three 3/8 in. diameter anchors in each row were able to develop the CFRP sheet's ultimate tensile capacity and led to CFRP sheet rupture at 32 k of tension in the CFRP sheet (00-6s1). The specimen failed by CFRP fracture just behind the first row of anchors, Figure 4-19. In Figure 4-20 the strains in the CFRP sheet at maximum load are shown. The highest strain (0.012) occurred just above the crack between the concrete blocks and was greater than the strain at fracture as determined by standard ASTM tests of the CFRP (0.0097). The strain dropped to 0.007 after the first row of anchors and then to near zero after the last row of anchors. The drop in strain after each row of anchors demonstrates the effectiveness of force transfer to the concrete by each row of anchors. The consistency of the strain between rows demonstrates that little force was transferred from the CFRP directly to the concrete surface through bonding. The anchors also increased the efficiency of the CFRP retrofit to 57%. The retrofit required only an additional 0.75 ft^2 of CFRP material to anchor the 1 ft^2 CFRP sheet.

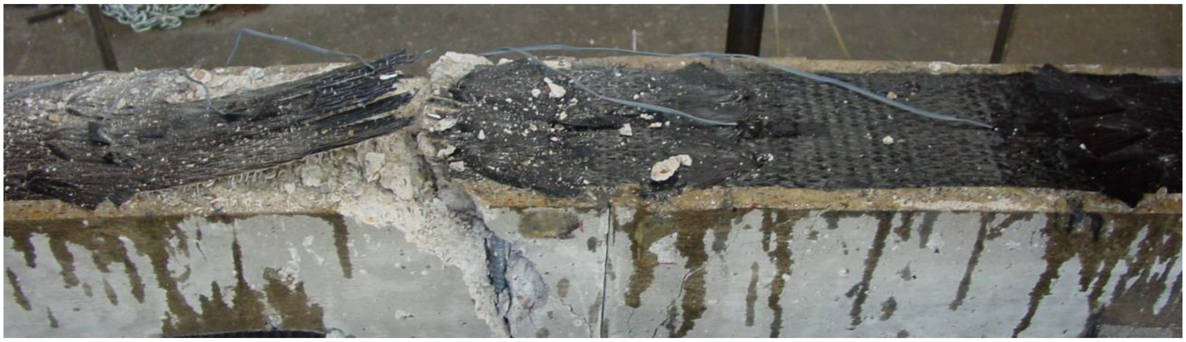

Figure 4-19 Failure by FRP fracture of retrofit with three anchors per row (00-6s1)

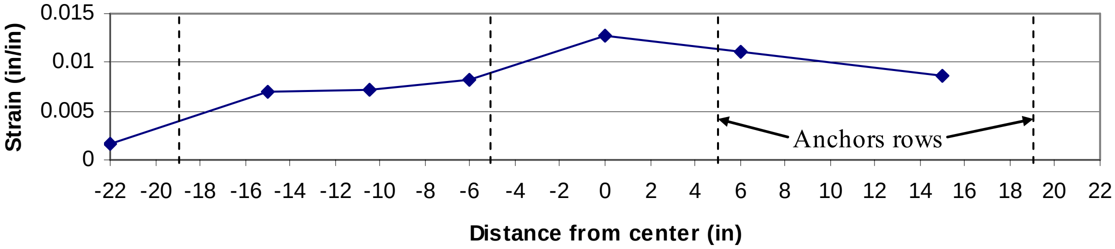

Figure 4-20 Strains in CFRP for test 00-6s1

The progression of tests with the same total volume of CFRP but increasing anchor numbers and decreasing anchor sizes indicates that a greater number of smaller and more closely spaced anchors are more effective in fully developing the tension capacity of the CFRP sheet. The distribution of more anchors across the width of the CFRP sheet resulted in better distribution of tension across the CFRP sheet and reduced stress concentrations at the anchors.

However, increasing the size of each anchor by 33% to 9/16 in. diameter allowed the CFRP sheet to reach 98% of capacity with only two rows of two anchors (00-4s3). Failure occurred by CFRP fracture just before the first row of anchors, Figure 4-21. Although the efficiency of this test was reduced to 46% due to the larger anchors, reducing the number of anchors may reduce installation time and installation cost.

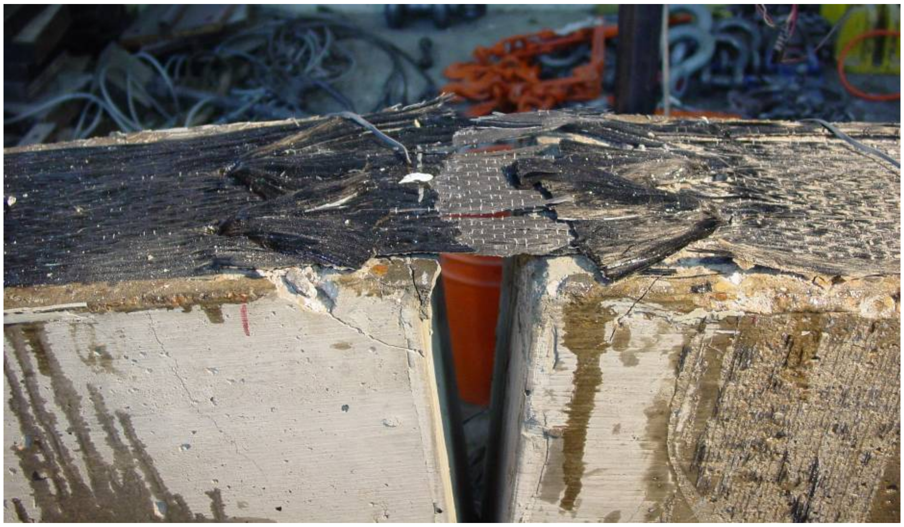

Figure 4-21 Failure by CFRP fracture for retrofit with two larger anchors per row (00-4s3)

4.3.1.4 Other Issues

Two tests had undesirable failure modes. The first had two anchors in one row (00-2s1). Because both anchors were located in front of the first stirrup, the corner of the concrete block simply fractured off and the rest of the CFRP sheet debonded at 37% of ultimate, Figure 4-22. The other test consisted of two rows of two anchors and used in 12 in. high blocks that had no stirrups (00-4g1). The concrete blocks failed in shear at 63% of the ultimate tensile capacity, Figure 4-23. The results of these two tests illustrate the importance locating the anchors where forces can be transferred into the concrete and of ensuring sufficient shear capacity in members that are strengthened flexurally.

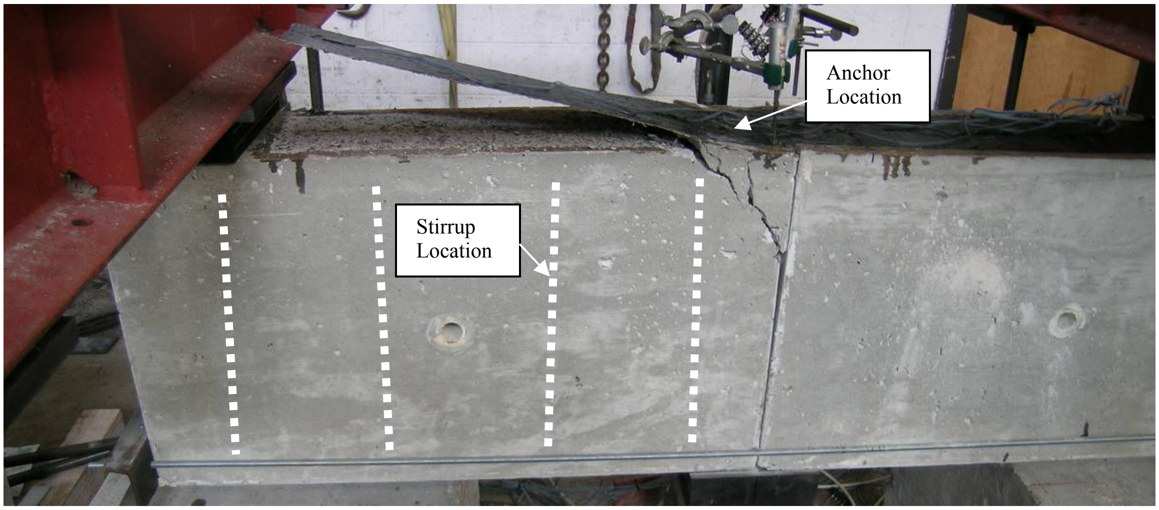

Figure 4-22 Failure by concrete fracture and debonding for retrofit with one row of two anchors (00-2s1)

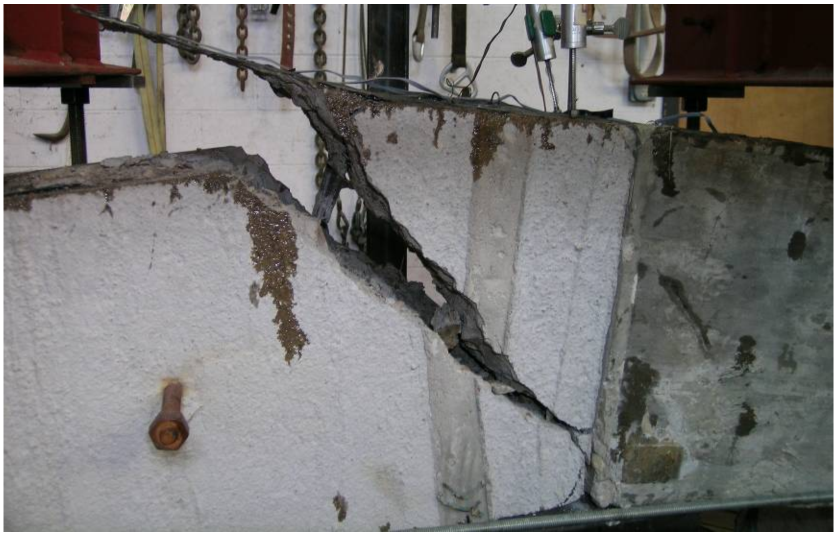

Figure 4-23 Failure by shear in concrete block (00-4g1)

Although carbon fiber anchors in these tests only increased the efficiency of the CFRP retrofit from 40% to 57%, most CFRP retrofits, comprised of longer lengths of longitudinal CFRP sheets, will have higher efficiencies. The higher efficiency is due to a higher ratio of the CFRP volume in the longitudinal sheet, which allows more of the CFRP material to be utilized as the tension resistance element and less to be required in the anchors. For example, a 20 ft long CFRP retrofit on a beam with two rows of anchors at each end would have a CFRP volume ratio and efficiency of 85%.

4.3.2 Tests With Height Transition

A height transition accentuates the debonding of a CFRP sheet. The height transition can occur when providing continuity of the positive moment reinforcement because the hole through the column cannot be drilled flush with the bottom of the beam. Use of carbon fiber anchors and a transition slope can enhance utilization of CFRP tensile capacity. The results for the tests with the height transition are presented in Table 4-5.

4.3.2.1 Slope of Transition

In order to determine the best slope for the transition ramp a series of tests were conducted using a 1 to 2 slope or a 1 to 4 slope with different types of CFRP anchorage. The tests can be compared to the tests with no height transition as shown in Figure 4-24.

The steepness of a 1 to 2 (height to length) transition slope proved detrimental to the capacity of the CFRP sheet. With no anchors, failure occurred by debonding at 14% ultimate tensile capacity, less than half the capacity of specimens with no height transition (22-ns1). For tests with anchorage, the CFRP fractured at approximately half its ultimate tensile capacity. With U-wraps, failure occurred by FRP fracture at 41% ultimate tensile capacity (22-us1). With CFRP anchors, failure occurred by fracture at 64% of ultimate tensile capacity (22-6s1). The fracture of the CFRP occurred at the top or bottom of the transition slope where the stress concentration due to the bend in the CFRP was the greatest, Figure 4-25.

Table 4-5. Test results for tests with height transition

Test #	Slope	Height difference	Type of Fabric	Anchorage	Diagram	Depth of blocks	Surface preparation	f'c (psi)	Load at Failure (kip)	Tension in CFRP at Failure (kip)	Tension in CFRP (% of ultimate)	Area of CFRP (ft^2)	Retrofit Effectiv-eness	Failure Mode
22-ng1	1:2	2"	SCH-35	none	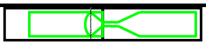	10"/12"	grinding	3400	7.17	5.98	19%	0.67	19%	Debonding
22-ns1	1:2	2"	SCH-35	none	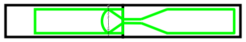	16"/18"	sandblast	3100	5.17	4.52	14%	1.00	14%	Debonding
22-us1	1:2	2"	SCH-35	U-wrap, 6" wide	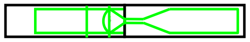	16"/18"	sandblast	3100	14.79	12.94	41%	2.17	19%	Fracture
22-2g1	1:2	2"	SCH-35	2 3/8" anchors at ramp	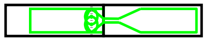	10"/12"	grinding	3400	12.02	10.02	31%	0.92	23%	FRP fracture around anchor and peeling
22-4s1	1:2	2"	SCH-35	2 3/8" anchors at ramp and at 5"	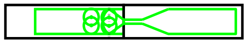	16"/18"	sandblast	3100	11.92	10.43	33%	1.50	22%	Fracture
22-6s1	1:2	2"	SCH-35 sheet SCH-41 anchors	3 3/8" anchors at 4" and at 21"	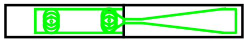	16"/18"	sandblast	3400	22	19.25	60%	1.50	40%	Fracture
42-ns1	1:4	2"	SCH-35	none	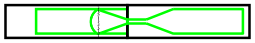	16"/18"	sandblast	3600	14.6	12.78	40%	1.00	40%	Debonding
42-ns2	1:4	2"	SCH-35	none	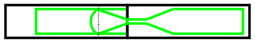	16"/18"	sandblast	3400	13.55	11.86	37%	1.00	37%	peeling of 15"
42-us1	1:4	2"	SCH-35	U-wrap, 6" wide	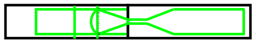	16"/18"	sandblast	3300	24.04	21.04	66%	2.17	30%	debond of flat FRP, shear of U wrap
42-us2	1:4	2"	SCH-35	Double U-wrap at ramp	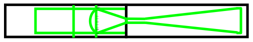	16"/18"	sandblast	3600	27.25	23.84	75%	3.33	22%	Slipping under U-wrap
42-us3	1:4	2"	SCH-35	Double U-wrap at ramp and single at	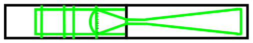	16"/18"	sandblast	3600	32.6	28.53	89%	4.50	20%	Fracture
42-cs1	1:4	2"	SCH-35	U-wrap and 2 3/8" anch. at ramp, 2	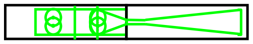	16"/18"	sandblast	3600	33.8	29.58	93%	2.67	35%	Fracture
42-4s1	1:4	2"	SCH-35	2 3/8" anchors at 8"and at 21"	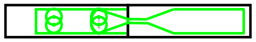	16"/18"	sandblast	3300	21.2	18.55	58%	1.50	39%	Premature fracture in column sheet
42-4s2	1:4	2"	SCH-35	2 3/8" anchors at 8"and at 21"	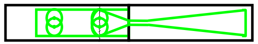	16"/18"	sandblast	3600	26.78	23.43	73%	1.50	49%	Fracture around anchor
42-4s3	1:4	2"	SCH-35 sheet SCH-41 anchors	2 1/2" anchors at 8"and at 21"	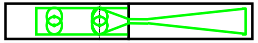	16"/18"	sandblast	3400	25.06	21.93	69%	1.75	39%	Fracture in column bundle
42-4s4	1:4	2"	SCH-35 sheet SCH-41 anchors	2 1/2" anchors at 8"and at 21"	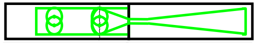	16"/18"	sandblast	3400	22.57	19.75	62%	1.75	35%	Fracture in column bundle
42-4s5	1:4	2"	SCH-41	2 9/16" anchors at 8" and 19"	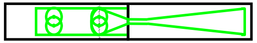	16"/18"	sandblast	3600	33.85	26.33	88%	2.13	41%	Fracture
42-6s1	1:4	2"	SCH-35	3 3/8" anchors at 8"and at 21"	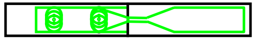	16"/18"	sandblast	3300	15.6	13.65	43%	1.75	24%	Premature fracture in column sheet
42-6s2	1:4	2"	SCH-35	3 3/8" anchors at 8"and at 21"	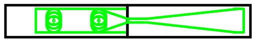	16"/18"	sandblast	3600	38.4	33.60	105%	1.75	60%	Fracture
42-6s3	1:4	2"	SCH-35 sheet SCH-41 anchors	3 3/8" anchors at 8"and at 21"	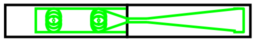	16"/18"	sandblast	3400	24.47	21.41	67%	1.75	38%	Anchor Fracture
42-6s4	1:4	2"	SCH-35 sheet SCH-41 anchors	3 1/2" anchors at 8" and at 21"	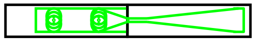	16"/18"	sandblast	3400	38.67	33.84	106%	2.13	50%	Fracture
42-6s5	1:4	2"	SCH-41	3 1/2" anchors at 8" and at 21"	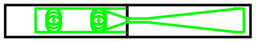	16"/18"	sandblast	3400	34.8	30.45	102%	2.13	48%	Fracture
42-6s6	1:4	2"	SCH-41	3 1/2" anchors at 8" and at 21"	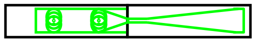	16"/18"	sandblast	3400	40.26	31.31	104%	2.13	49%	Fracture

Table 4-5 continued

Test #	Slope	Height difference	Type of Fabric	Anchorage	Diagram	Depth of blocks	Surface preparation	f'c (psi)	Load at Failure (kip)	Tension in CFRP at Failure (kip)	Tension in CFRP (% of ultimate)	Area of CFRP (ft^2)	Retrofit Effectiv-eness	Failure Mode
42-6n1	1:4	2"	SCH-35 sheet SCH-41 anchors	3 3/8" anchors at 8"and at 21"	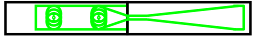	16"/18"	none	3400	18.7	16.36	51%	1.75	29%	Anchor Fracture
42-6n2	1:4	2"	SCH-41	3 1/2" anchors at 8" and at 21"	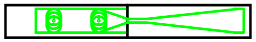	16"/18"	none	3400	34.02	29.77	99%	2.13	47%	Fracture
41-ns1	1:4	1"	SCH-35	none	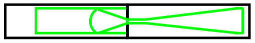	16"/17"	sandblast	3600	9.54	7.86	25%	1.00	25%	Debonding
43-ns1	1:4	3"	SCH-35	none	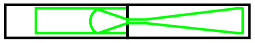	16"/19"	sandblast	3600	15.86	11.69	37%	1.00	37%	Debonding
41-6s1	1:4	1"	SCH-35 sheet SCH-41 anchors	3 1/2" anchors at 8" and at 21"	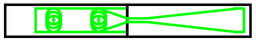	16"/17"	sandblast	3600	39.29	34.38	108%	2.13	51%	Fracture

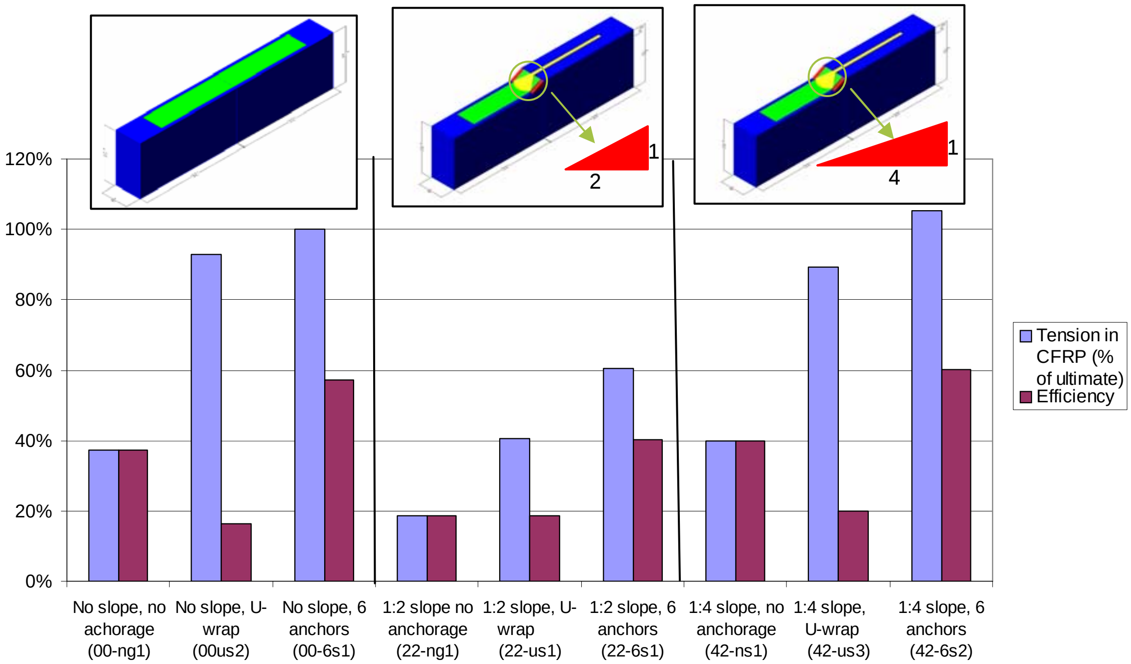

Figure 4-24 Effect of slope of transition

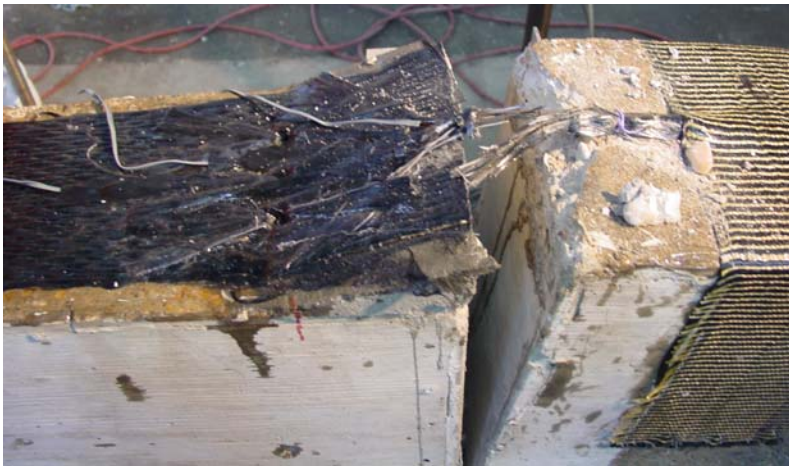

Figure 4-25 Fracture of CFRP at top of transition slope in test 22-6s1

The results for a shallower 1:4 slope mirrored the results for no height transition and allowed the CFRP to reach full capacity when adequate anchorage was provided. Without any anchorage, failure occurred by debonding at 40% and 37% of ultimate tensile capacity (42-ns1, 42-ns2). With U-wraps, failure occurred by FRP fracture at

89% tensile capacity (42-us3). With anchors, failure occurred at 105% ultimate tensile capacity[5] (42-6s2). Therefore, the effect of an offset in surface level, or height transition, can be counteracted by use of at least a 1 to 4 slope connecting the two surface levels.

4.3.2.2 Type of Fabric

Two types of CFRP fabric (Tyfo® SCH-35 and SCH-41) were donated by Fyfe Co. LLC. Both have the same reported tensile strength (143 ksi) and almost the same elastic modulus (11,400 ksi and 13,900 ksi respectively), Table 4-3. However, material tests indicated some difference in the tensile strength of the fabrics (SCH-35 fabric 170 ksi and SCH-41 125 ksi). Furthermore, the SCH-35 fabric had a higher elongation at break of 1.26% versus 1.00% for the SCH-41 fabric. The differences in the fabric may have caused SCH-41 fabric to be weaker in cases where the CFRP is bent, such as in the anchors. The anchors with the SCH-41 fabric fractured in test 42-6s3 where the anchors were the same size and at the same location as in test 42-6s2, that had SCH-35 anchors Figure 4-26. The fracture of the anchor occurred at the location where the anchor was bent as it extended from the concrete hole to fan out over the CFRP sheet (Figure 4-27). To compensate for the difference in strength, the volume of SCH-41 fabric used in the anchors was increased by 33% (42-6s4) in order to achieve the same anchor capacity as the SCH-35 fabric.

Only one roll of each type of fabric was donated, therefore all tests and coupons used the same carbon fiber material. Each CFRP application used the same procedure and same personnel to ensure consistency among the tests. The weakness found in the SCH-41 fabric may be particular to that roll of fabric. Results for anchor strength from different rolls of the same type of fabric, or different types of fabric, may vary. Therefore, it is important to verify the anchor strength of different rolls of CFRP fabric.

---

[5] Ultimate or nominal tensile capacity is computed from the coupon tests presented in Table 4-3, results from specimen tests showed CFRP fracture between 93% and 108% of the ultimate tensile capacity due to variations in the CFRP application.

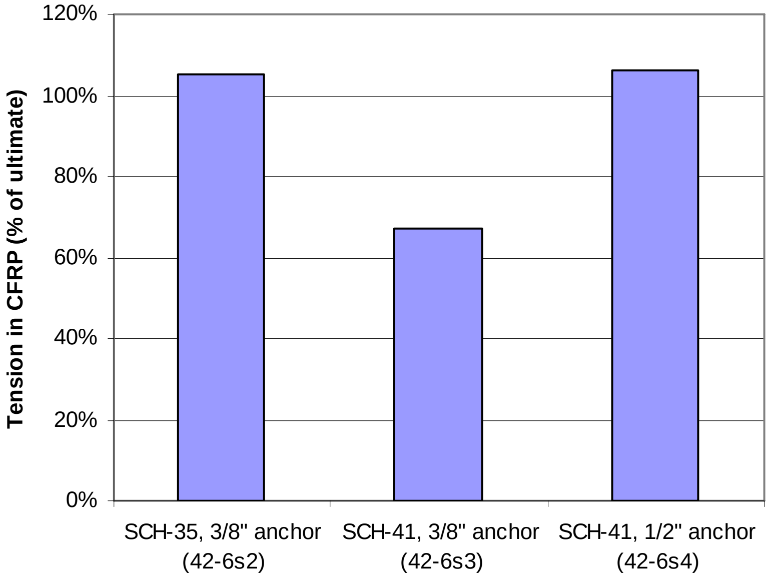

Figure 4-26 Effect of type of CFRP fabric

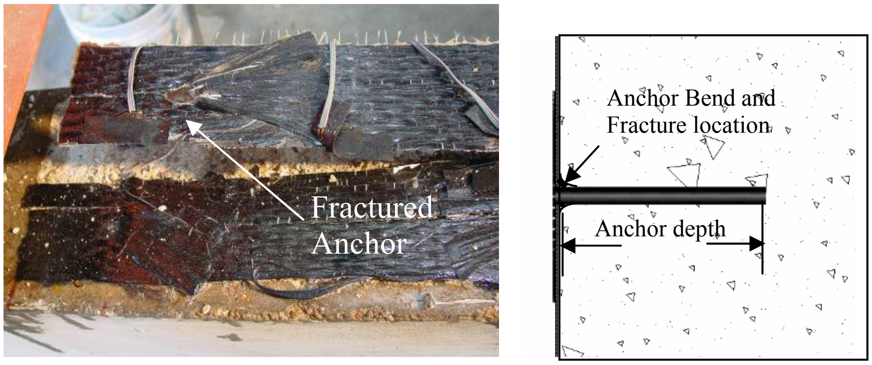

Figure 4-27 Fracture of CFRP anchor

4.3.2.3 Surface Preparation

The effect of surface preparation on the tensile capacity of an anchored CFRP sheet was evaluated in tests 42-6n1 and 42-6n2. A layer of plastic wrap was placed between the CFRP sheet and the concrete to eliminate bond between the CFRP and the concrete. Test 42-6n1, with 3/8 in. diameter anchors, reached only 55% of capacity as compared to 71% capacity when the CFRP was bonded to the concrete (42-6s3), Figure 4-28. However, test 42-6n2 with larger ½ in. diameter anchors was able to reach 99% of capacity and fracture the CFRP sheet, Figure 4-29.

The performance of 42-6n1 and 42-6n2 indicates that although bond to the concrete can supplement the maximum load, when the anchors are large enough, the anchors can transfer all the tensile force from the CFRP sheet into the concrete without any CFRP bonding to the concrete. Furthermore, even in tests with anchors where bond was provided between the CFRP and the concrete, the CFRP sheet often debonded from the concrete prior to reaching maximum load. Therefore, the use of anchors may reduce the need for extensive surface preparation because CFRP bond to the concrete is no longer critical to achieving the desired capacity of the CFRP retrofit. Anchors may increase the reliability of CFRP retrofits by reducing uncertainties relating to the quality of the surface preparation and bonding strength. However good quality control is still needed to realize maximize performance for the CFRP sheets.

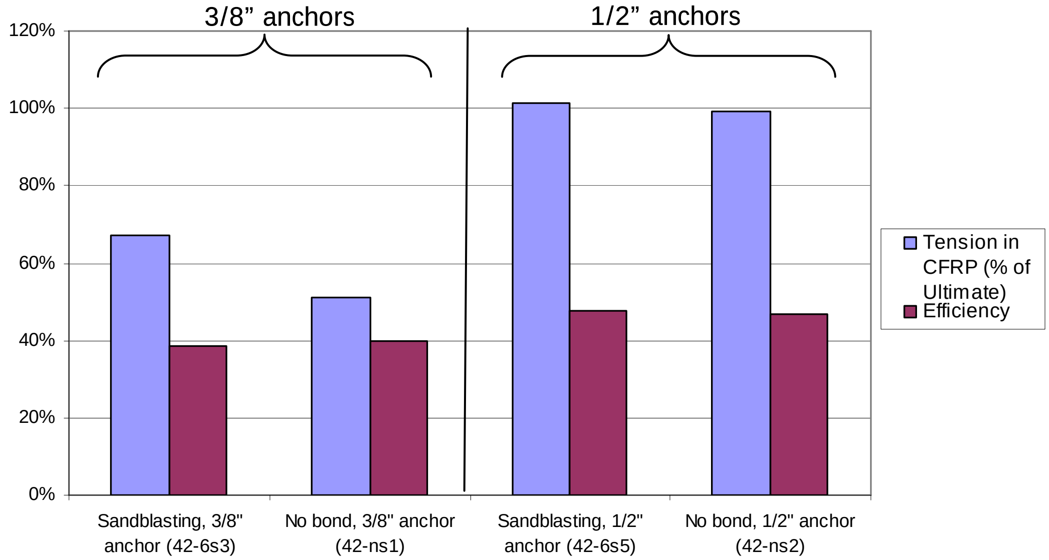

Figure 4-28 Effect of surface preparation

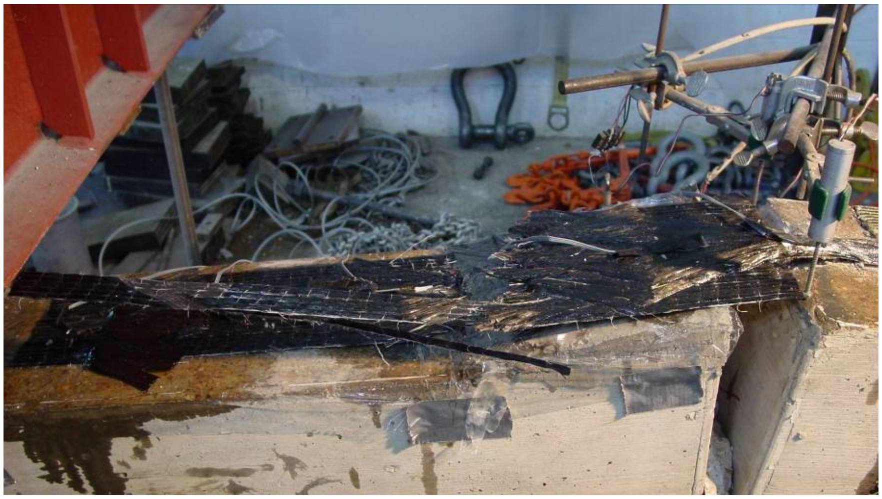

Figure 4-29 Failure of test 42-6n2

4.3.2.4 Height Difference

In the last set of tests, the effect of the height difference (1, 2, and 3 in.) in the height transition with a 1:4 slope was studied, Figure 4-30. When ½ in diamter anchors were used, the full capacity of the CFRP sheet was reached regardless of the height difference. With a 1 in. height difference failure occurred by FRP fracture at 108% of ultimate tensile capacity (41-6s1), Figure 4-31. With a 3 in. height difference failure occurred by FRP fracture at 93% of ultimate tensile capacity (43-6s1), Figure 4-32. The differences between the failure loads may be due to the fact that for a 1:4 slope and a 3 in. height difference the transition ramp was 12 in. long, whereas for a 1 in. height difference it was only 4 in. long. The length of the transition ramp on a short concrete block (24 in.) may have impacted the failure of the CFRP sheet. When unanchored, less than 45% of the ultimate tensile capacity was reached in any test (41-ns1, 42-ns1, 43-ns1). Therefore, the amount of the height difference between surface levels of the CFRP did not significantly affect the capacity of the CFRP sheet when the sheet was anchored and a shallower than 1:4 transition slope was provided.

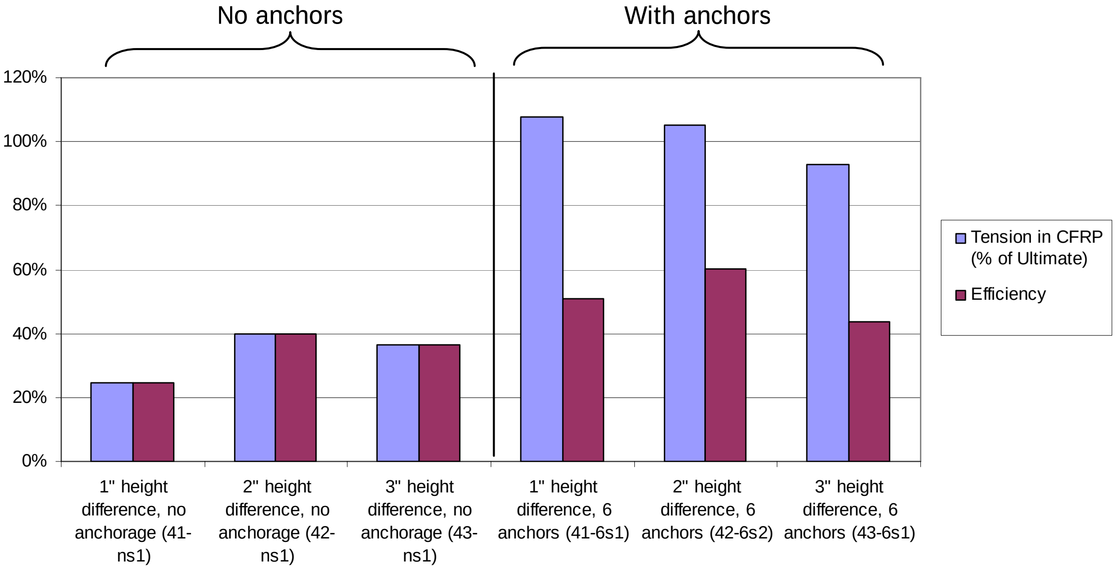

Figure 4-30 Effect of height difference

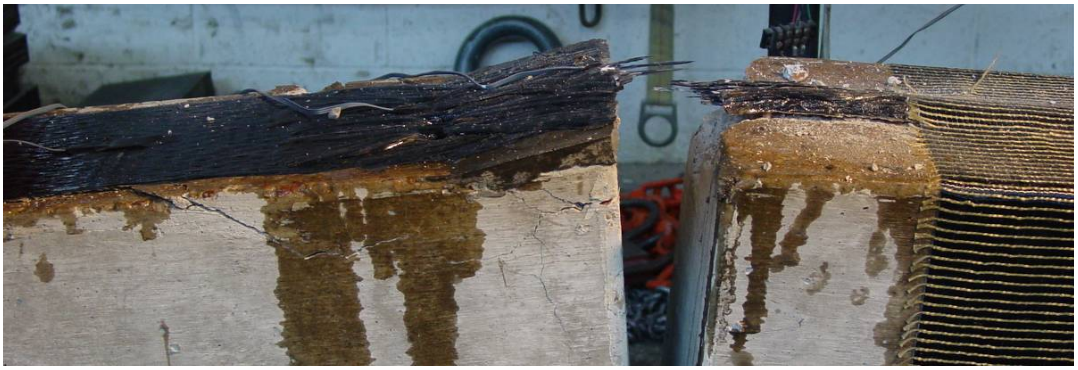

Figure 4-31 Failure of 41-6s1 with 1” height difference

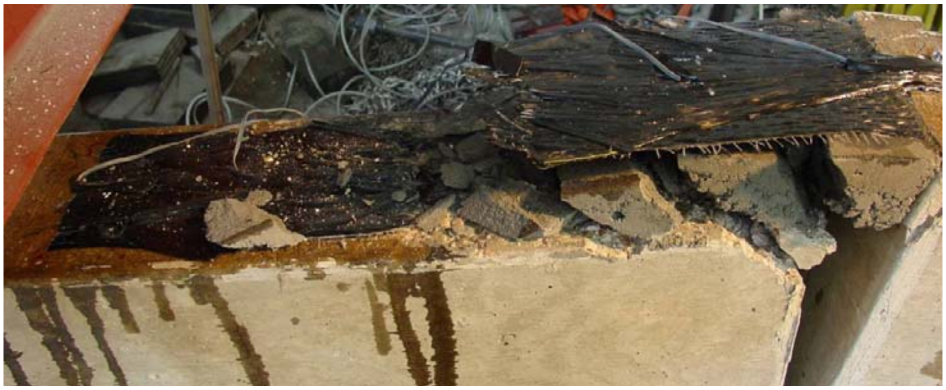

Figure 4-32 Failure of 43-6s1 with 3” height difference

4.3.2.5 Strains

The first two tests 22-ng1 and 22-2g1 used a large number of strain gages in order to determine the best locations for strain measurement, Figure 4-33. Most gages were in rows of 3 gages spread across the width of the CFRP sheet. Data from these gages showed that the strain was fairly uniform across the width of the CFRP sheet, Figure 4-34. Therefore, future gages were only placed along the centerline of the CFRP sheet.

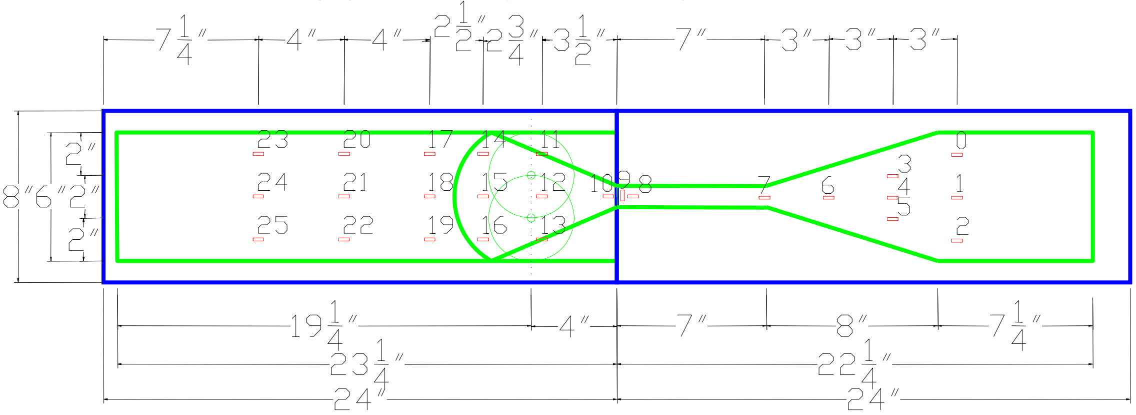

Figure 4-33 Example of strain gage locations on 22-2g1

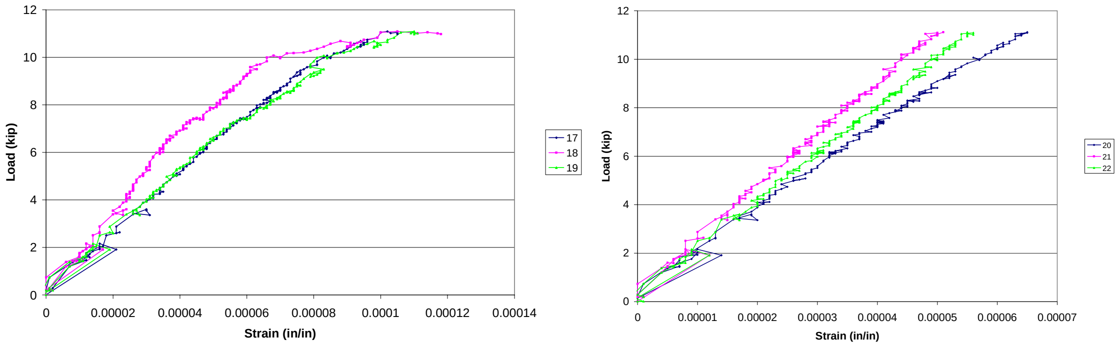

Figure 4-34 Strain distribution across CFRP sheet in 22-2g1

The strain distribution for three tests with three anchors per row and a 1 to 4 transition slope is shown in Figure 4-35. Each of these tests reached the full capacity of the CFRP. The maximum strain in each case was recorded at the bottom of the transition slope (gage 3) and ranged from 0.006 to 0.008. Although the recorded strains did not reach the CFRP fracture strain from materials tests (0.01), placement of the gages at the bottom of the transition slope was difficult and the gages may not have recorded the actual maximum strain.

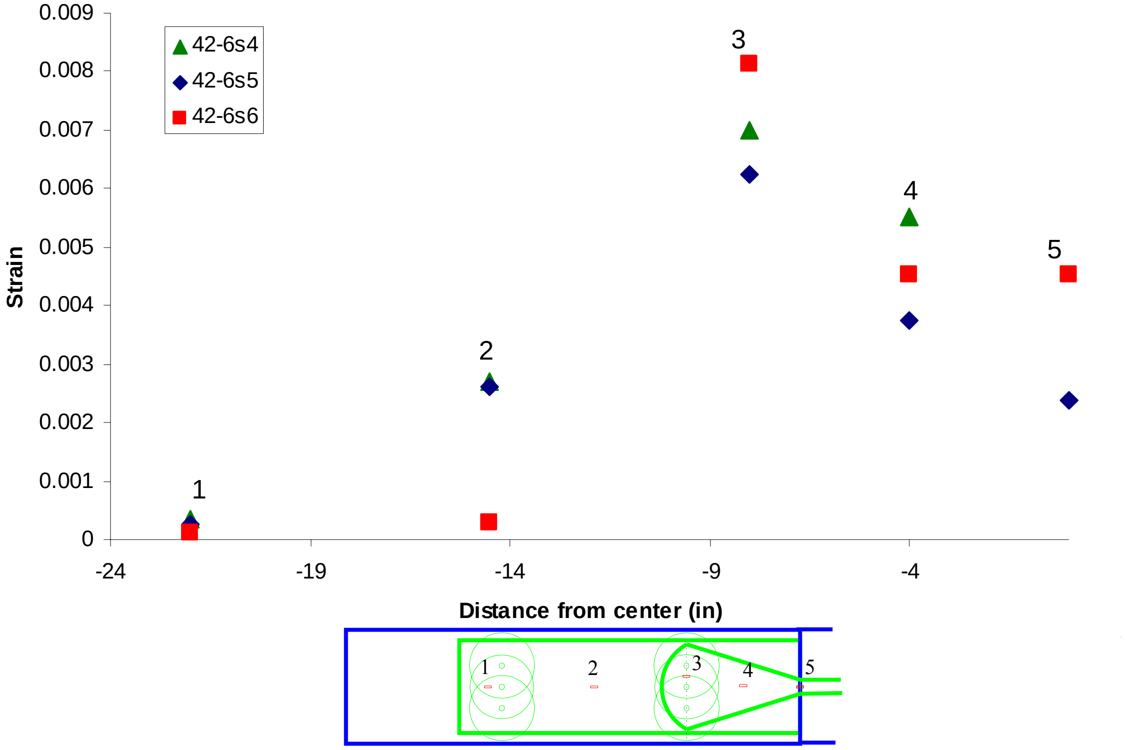

Figure 4-35 Distribution of strains at CFRP fracture for tests with 6 anchors

The strain reading for tests with a 1 to 2 transition slope are given in Figure 4-36. These strains indicate a higher strain at the bottom of the transition slope (0.007 and 0.01) but also a compressive strain at the top of the slope (-0.002 and -0.017). The compressive strains are caused by the concave bend of the CFRP at the top of the transition slope and the fact that the CFRP was bundled at that location causing a great amplification of the bend (strain gage was placed on top of CFRP bundle), Figure 4-37. The compressive strain is not likely the strain throughout the CFRP at that location, just the strain on top of the bundle.

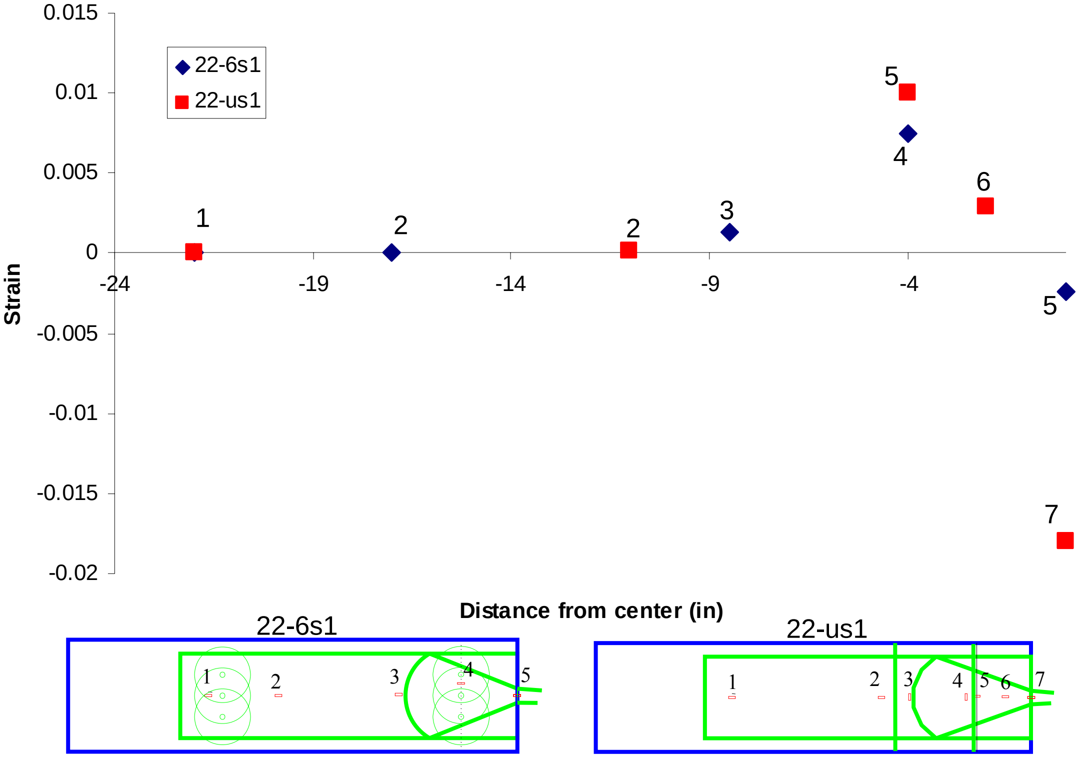

Figure 4-36 Distribution of strains at CFRP fracture for tests with 1 to 2 transition slope

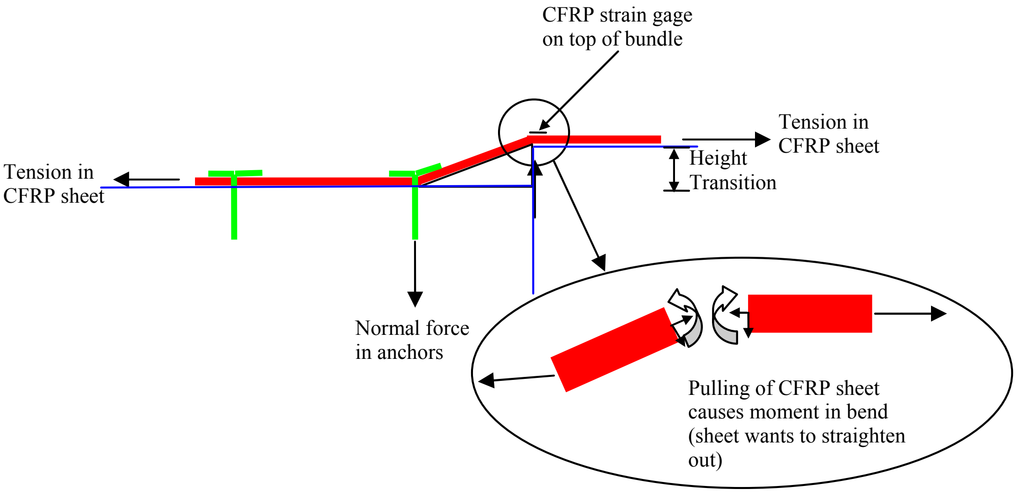
CFRP strain gage
on top of bundle
Tension in
CFRP sheet
Tension in
CFRP sheet
Height
Transition
Normal force
in anchors
Pulling of CFRP sheet
causes moment in bend
(sheet wants to straighten
out)

Figure 4-37 Forces in CFRP sheet

4.3.2.6 Other Issues

In order to create the fan of the column sheet, Figure 4-7, the cross fibers in the CFRP sheet were removed. This allowed the carbon fiber to remain straight as they fanned open. However, the cross fiber were not removed throughout the entire column sheet. For two tests, 42-4s1 and 42-6s1 this created a stress concentration due to the bunching of the carbon fiber and led to premature failure. For all subsequent tests, the cross fibers were removed throughout the entire length of the column sheet, Figure 4-38.

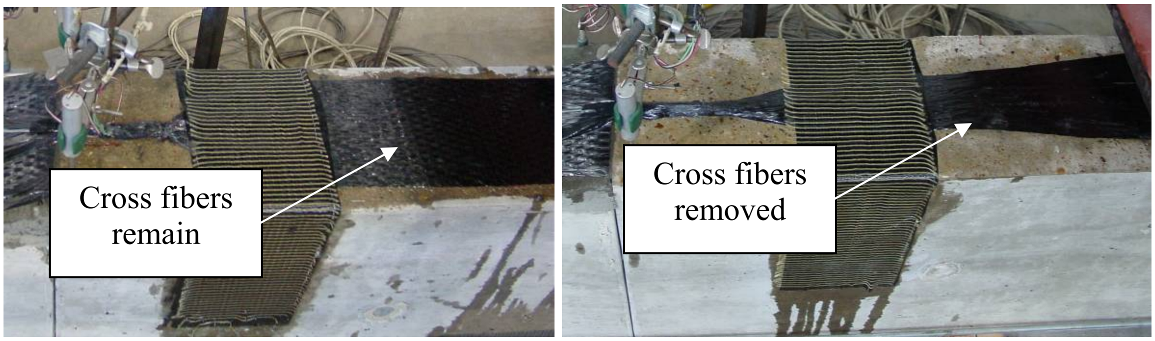

Figure 4-38 Cross fibers in column sheet

One specimen, 42-cs1, consisted of a combination of two rows of two 3/8 in. CFRP anchors and a 6 in. wide U-wrap. A similar specimen with only anchors (42-4s2) reached only 73% of tensile capacity. The addition of a U-wrap in 42-cs1 increased the tensile capacity to 93% with the CFRP fracturing. The test indicated that both anchors and U-wraps can be used together if needed.

Most specimens in the anchorage study consisted of different CFRP schemes in order to test different parameters. However, a few tests studied the same CFRP retrofit scheme in order to address the repeatability of tests. These tests were 42-ns1 and 42-ns2, which had similar tensile capacities of 40% and 37%, and 42-6s5 and 42-6s6, which again had similar tensile capacities of 102% and 104%. The similar results for tests with the same retrofit scheme indicate that the tests are repeatable.

4.4 CONCLUSIONS

Forty tests were conducted on specimens designed to evaluate anchorage design parameters critical to utilizing the high tensile strength of CFRP materials. Results from the testing program are:

- Unanchored CFRP sheets utilized only about 37% of their tensile capacity before debonding. The efficiency of material usage was 37%.
- U-wraps allowed the CFRP sheet to reach full tensile capacity but required greater amounts of material that reduced material efficiency to 16%.
- CFRP anchors allowed the CFRP sheet to reach full tensile capacity and increased efficiency of material usage to 57%. Different types and designs of CFRP retrofits may have higher efficiencies.
- Anchor rows with a greater number of smaller and more closely spaced anchors were more effective at distributing stress across the CFRP sheet. Each of several rows of anchors was effective in transferring tensile forces into the concrete.
- The adverse effect of a height transition was eliminated by the use of at least a 1:4 transition slope.
- The properties of carbon fiber fabric had an impact on the ultimate capacity in cases where the CFRP was bent, such as in the anchors. Different types of CFRP fabric may exhibit different behavior in anchor strength.
- Carbon fiber anchors reduced the need for extensive surface preparation because CFRP bond to the concrete was no longer critical to achieving the desired capacity of the CFRP retrofit.
- The amount of height difference did not affect the CFRP capacity when CFRP sheets were fully anchored.

- Additional tests with a wider range of parameters (anchor size, number, CFRP sheet width, etc.) are needed to develop a complete design methodology.

The overall conclusion is:

- Carbon fiber anchors enabled improved utilization of the tensile capacity of a CFRP sheet and thereby increased the strengthening capacity of a CFRP retrofit with or without a height transition. Anchors also improved the efficiency of material usage in CFRP retrofits, requiring less CFRP material for a greater strengthening capacity.

From the tests, the general design philosophy for use of CFRP sheets to provide continuity in reinforced concrete frames is:

- Use two rows of anchors with the cross-sectional area in each row equal to 1.3 times the cross-sectional area of the longitudinal sheet.
- Use a larger number of smaller more closely spaced anchors in each row.
- Use a 1:4 or shallower slope on all height transitions.
- Surface preparation and amount of height difference is not critical.

Chapter 5: Continuity Tests

Eight continuity tests evaluate different load paths to develop continuity and catenary action in reinforced concrete beams. The test setup, test results, and conclusions will be covered in this chapter.

5.1 INTRODUCTION

As discussed in Chapter 2, reinforced concrete buildings may be vulnerable to progressive collapse due to a lack of continuity of reinforcing steel. If the column support between spans of a reinforced concrete frame were removed accidentally or by a blast, the lack of continuity may lead to progressive collapse. CFRP can be used to provide the missing continuity. The CFRP can provide continuity through the positive[6] moment reinforcement by means of a CFRP sheet applied through a hole drilled in the column and attached to CFRP sheets applied on the bottom of the beams on either side of the column as shown in Figure 5-1. Because the hole through the column cannot be drilled flush with the bottom of the beam, there is an offset in the surface level of the CFRP. Alternatively, the CFRP can be used to provide continuity through the negative moment reinforcement, Figure 5-2.

The CFRP could be applied to the sides of the beam. However, based on the advice from the industry advisory panel for this project, this option was discarded because applying CFRP on the sides would still have the a problem of going around the column if the column were not the same size as the beam, both sides may not be accessible due to building cladding, and CFRP on the bottom or top is at a more extreme position to increase moment capacity. The purpose of the CFRP along the top or bottom of the beam is to provide continuity through the reinforcement on that side of the beam.

---

[6] Positive and negative moment are as defined in the ACI-318 code

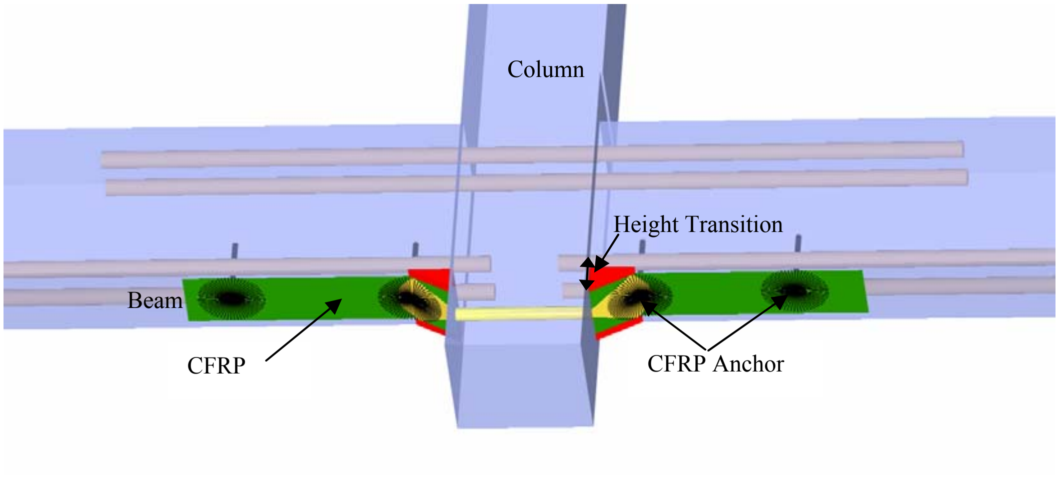
Column
Height Transition
Beam
CFRP
CFRP Anchor

Figure 5-1 Use of CFRP to provide continuity through the positive moment reinforcement

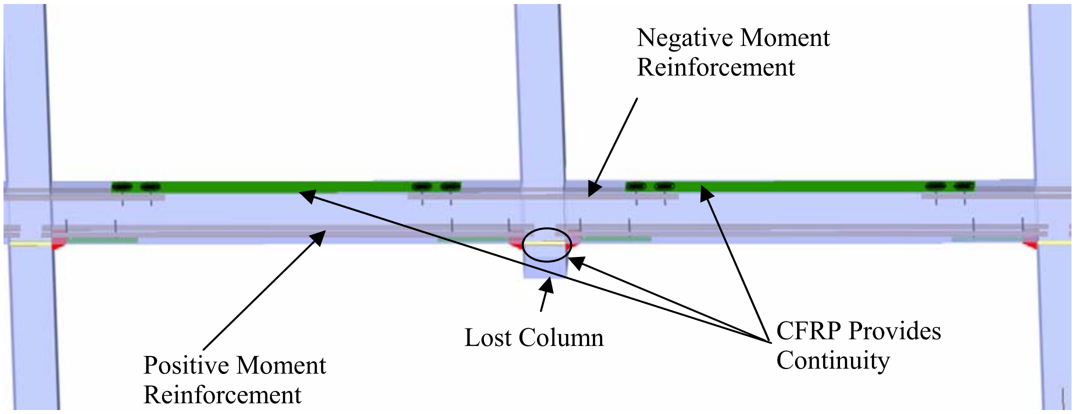
Negative Moment
Reinforcement
Lost Column
CFRP Provides
Continuity
Positive Moment
Reinforcement

Figure 5-2 CFRP to provide continuity

Eight half-scale tests of two spans of a reinforced concrete (RC) frame with a center supporting column removed were conducted to study the ability of CFRP to provide continuity and reduce vulnerability to progressive collapse. The tests evaluated the capacity for catenary action of vulnerable RC building beams with discontinuous reinforcing steel and the increased capacity achieved through the use of a CFRP retrofit. The continuity and catenary action provided by the CFRP retrofit should reduce the vulnerability of reinforced concrete buildings to progressive collapse. Additionally, tests were conducted to evaluate the capacity for catenary action of a well-designed beam with continuous reinforcing steel and the ability to strengthen a beam to accommodate the double span through flexural action. As discussed in Chapter 2, the development of catenary action requires large displacement and as such only satisfies a life safety performance criterion. Limiting the displacements by a retrofit for flexural action may be able to achieve a higher performance objective.

The tests were designed to simulate the behavior of adjacent spans after removal of a non-corner perimeter column. The relationship of test specimen to the full scale structure is shown in Figure 5-3. The 3 ft sections on the ends of the test specimen were designed to simulate the support from the rest of the structure. The support from the structure does not include the effect of the slab or the upper story column. During a blast event the slab may be damaged, or depending on the design may not be connected to the beam in such a way that it can resist vertical loads. The upper story column may not be able to resist tension loads depending on the splicing of the reinforcement. Therefore, the test specimen only considered the resistance of the beam itself.

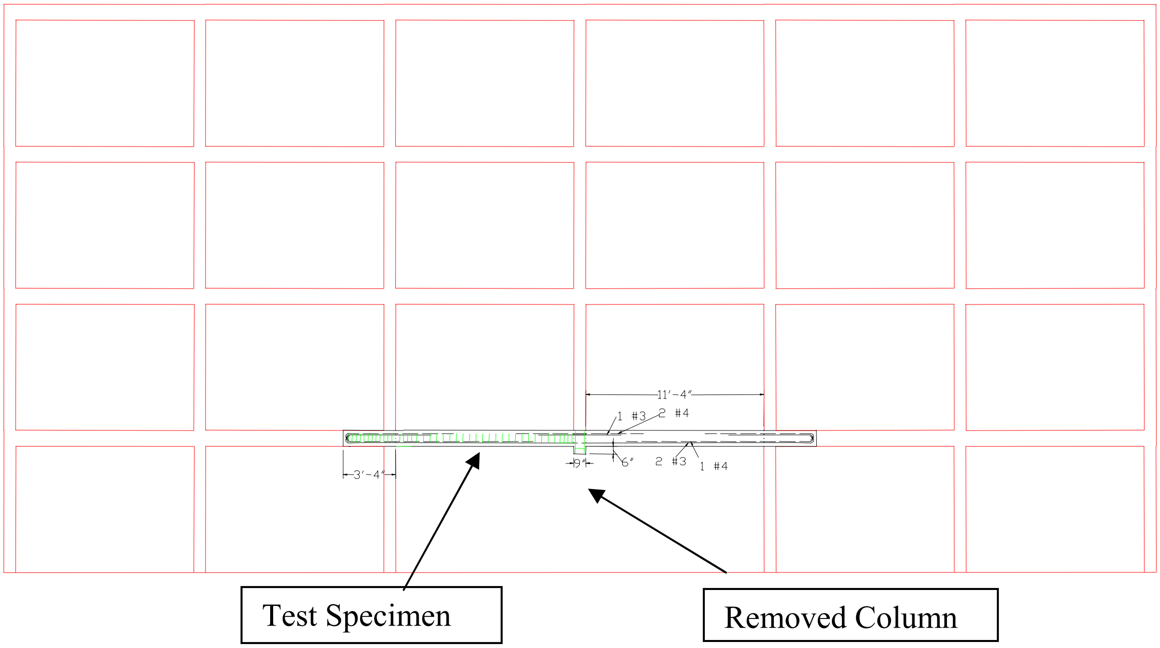

Figure 5-3 Relationship of test specimen to prototype building

For ease of testing, the test specimen was turned upside-down. All future figures and discussion will refer to the test specimen in its test position (upside-down from the prototype structure).

5.2 SPECIMEN DESIGN

The test specimen was designed to represent a double span of a reinforced concrete beam typical in 1970s buildings. The prototype building had span lengths of 24 ft with 12 by 24 in. beams. The beams were reinforced with 0.8% longitudinal steel area, based on a review of typical 1970's building practices [ACI-315, 1974]. The positive and negative moment steel was designed in accordance with the 1971 ACI code. Details of the design can be found in Appendix B.

The test specimen was half scale with a 12 in. by 6 in. cross section, 9 in. by 8 ½ in. column stub, and 30 ft length. The 30 ft length consisted of two half scale 12 ft spans and an additional 3 ft span on each end to provide restraint during testing. The reinforcement consisted of #3 (0.11 in^2) and #4 (0.2 in^2) reinforcing bars equivalent to half-scale versions of the prototype beam. The reinforcement for the beam design, shown in Figure 5-4 and Figure 5-5, is discontinuous in both the negative moment and positive moment regions. Cutoff locations for the reinforcement were based on typical building practice and adhere to the 1971 ACI code. The beam contained transverse reinforcement consisting of #3 stirrups with 90º hooks sufficient to prevent shear failure in the beam during testing and provide some confinement and additional ductility near the ends of the span. Although the level of shear reinforcement may be greater than typical 1970's practice, actual beams may be retrofitted to improve shear capacity if a deficiency exists. The column stub in the center of the beam represented the remnants of a removed column. The stub contained one # 3 stirrup located 3 in. above the positive moment rebar.

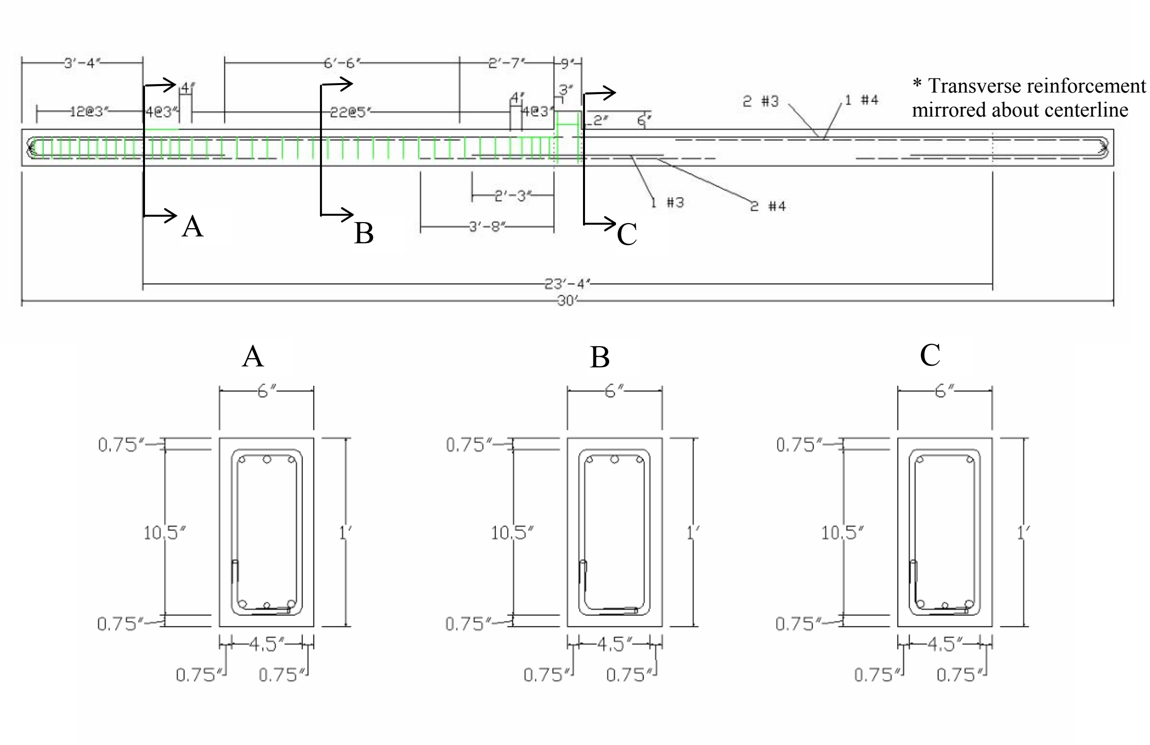
3′-4″
6′-6″
2′-7″
9″
4″
3″
4″
12@3″
4@3″
22@5″
4@3″
2″
6″
2 #3
1 #4
* Transverse reinforcement mirrored about centerline
2′-3″
3′-8″
1 #3
2 #4
A
B
C
23′-4″
30′
A
B
C
6″
0.75″
10.5″
1′
0.75″
4.5″
0.75″
0.75″

Figure 5-4 Reinforcement design of test specimen (shown in test position)

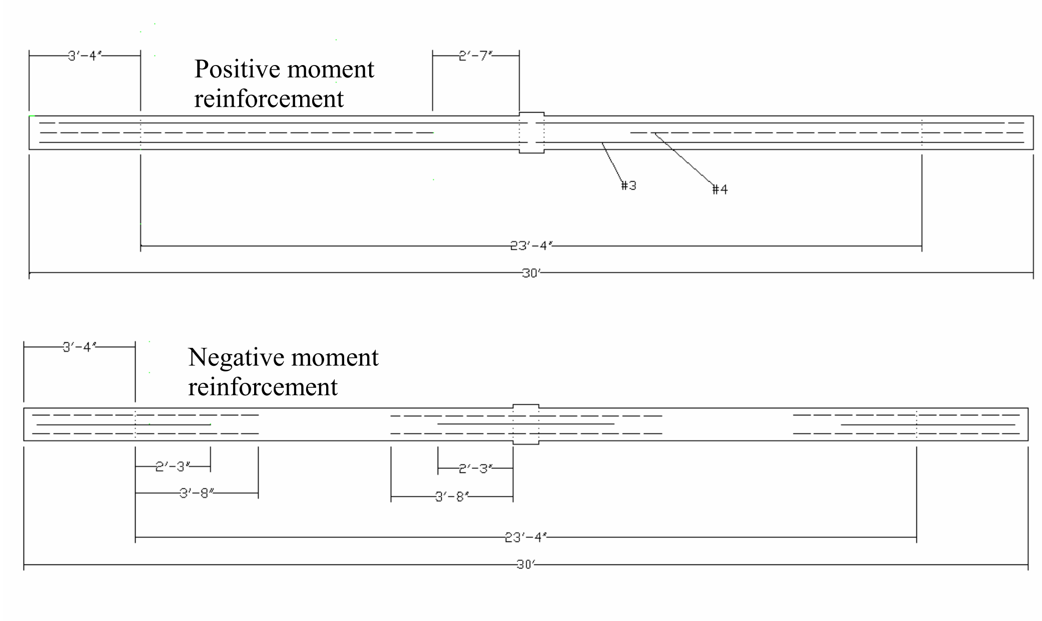
3′-4″
Positive moment reinforcement
2′-7″
#3
#4
23′-4″
30′
3′-4″
Negative moment reinforcement
2′-3″
3′-8″
2′-3″
3′-8″
23′-4″
30′

Figure 5-5 Reinforcement cutoff locations

5.3 TEST SETUP

A schematic and photo of the test setup are shown in Figure 5-6 and Figure 5-7. The setup was designed to simulate the vertical, axial, and rotational restraint provided at the ends of the beam by the rest of the structure (assuming the rest of the structure is able to provide fixed restraint), as well as a system to apply loads to the beam through large deflections. The beam was tested in an inverted position for ease of testing.

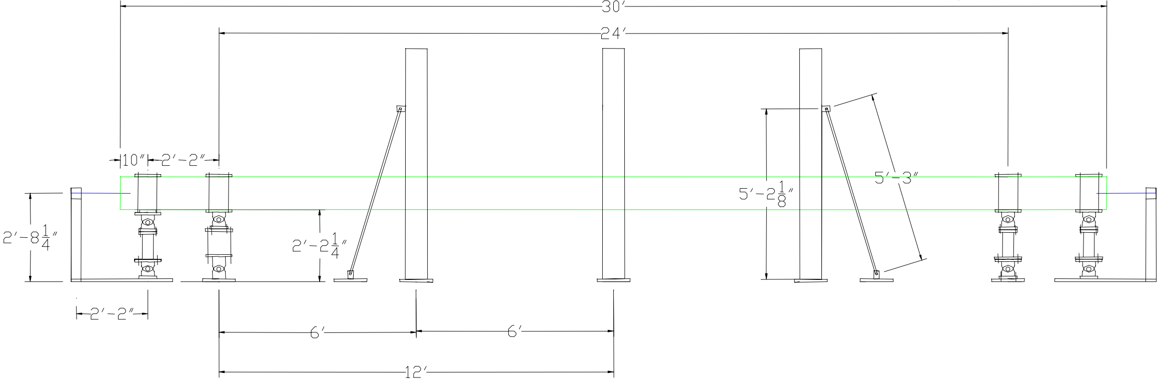
30′
24′
10″
2′-2″
2′-8¼″
2′-2¼″
5′-2⅛″
5′-3″
2′-2″
6′
6′
12′

Figure 5-6 Schematic of test setup

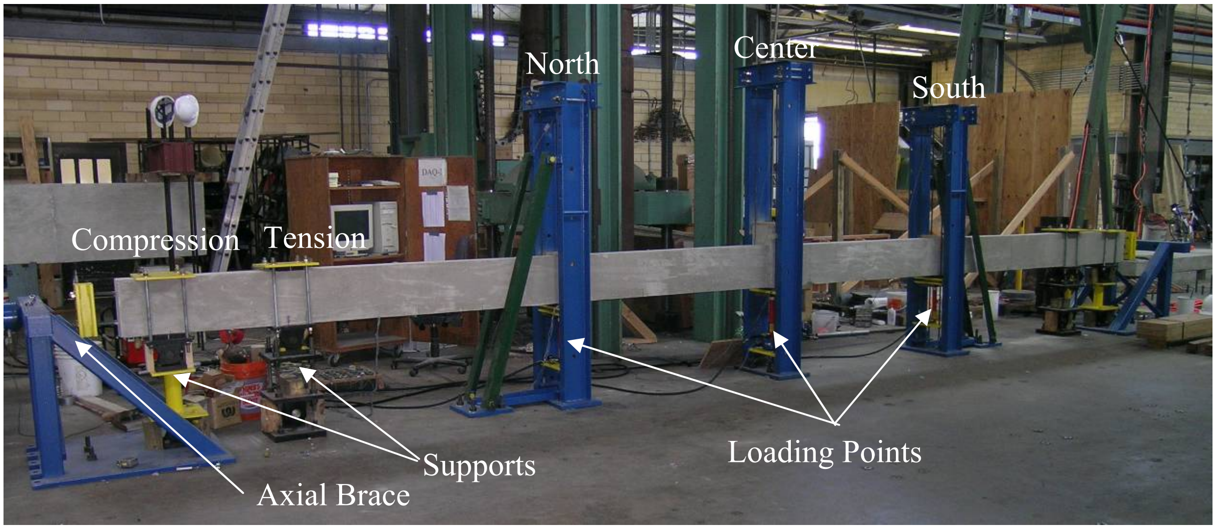
North
Center
South
Compression
Tension
Supports
Axial Brace
Loading Points

Figure 5-7 Photo of test setup

The design uniform load on the beam represents the maximum load that would be allowed by design under the ACI 318-71 code for the size and reinforcement layout in the beam (the beam is not over-designed). Over-design of the beam would lead to better progressive collapse resistance, as in the pentagon building (see Chapter 2). The uniform load (1.4 DL + 1.7 LL) was 3.9 k/ft on the full-scale beam and 1.9 k/ft on the half-scale beam. A uniform load of 1.7 k/ft on the half-scale beam represents the 2 times dead load plus 25% live load recommended by the GSA guidelines to resist progressive collapse [GSA, 2003]. Three point loads spaced at 6 ft were applied to represent the nearly uniform load present in the real structure, Figure 5-8. A load of 5 k per loading point represents the dead load plus 25% live load. A load of 10 k per loading point represents the 2 times dead load plus 25% live load suggested by the GSA guidelines for progressive collapse prevention. The dead and live loads include the weight and loads on a tributary area of the slab.

The specimens are tested in an inverted position. Therefore, the self-weight of the beam during testing acts opposite of the direction of gravity in the prototype building. The self-weight of the beam is approximately 0.35 kip per loading point. The load data reported does not account for this self-weight of the beam.

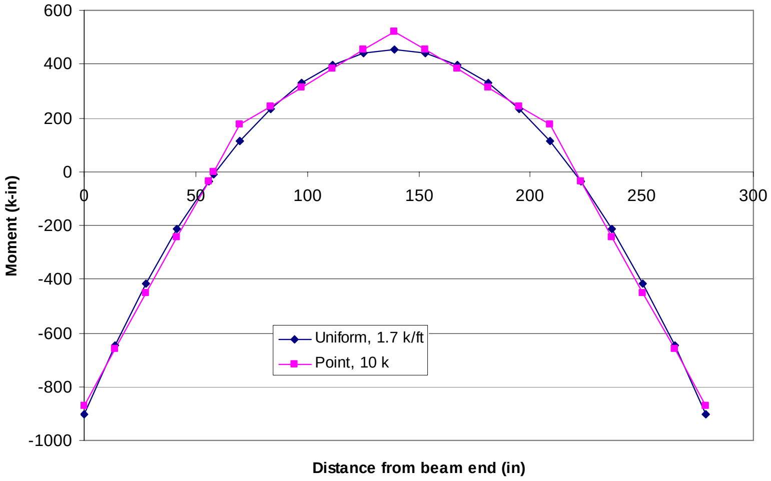

Figure 5-8 Comparison of uniform and 3 point loads

Due to the large deflections anticipated during testing (up to 10% of span length or 3 ft), a system of movable loading plates was devised to allow for repositioning of the loading ram during testing, Figure 5-9. The plates were supported by four ½ in. diameter threaded rods hung from the top of the channel columns. The columns consisted of C 8x18.75 channels and were welded to a base plate attached to the lab floor. The North and South loading points had a pivot point to allow for rotation of the beam during loading, Figure 5-10.

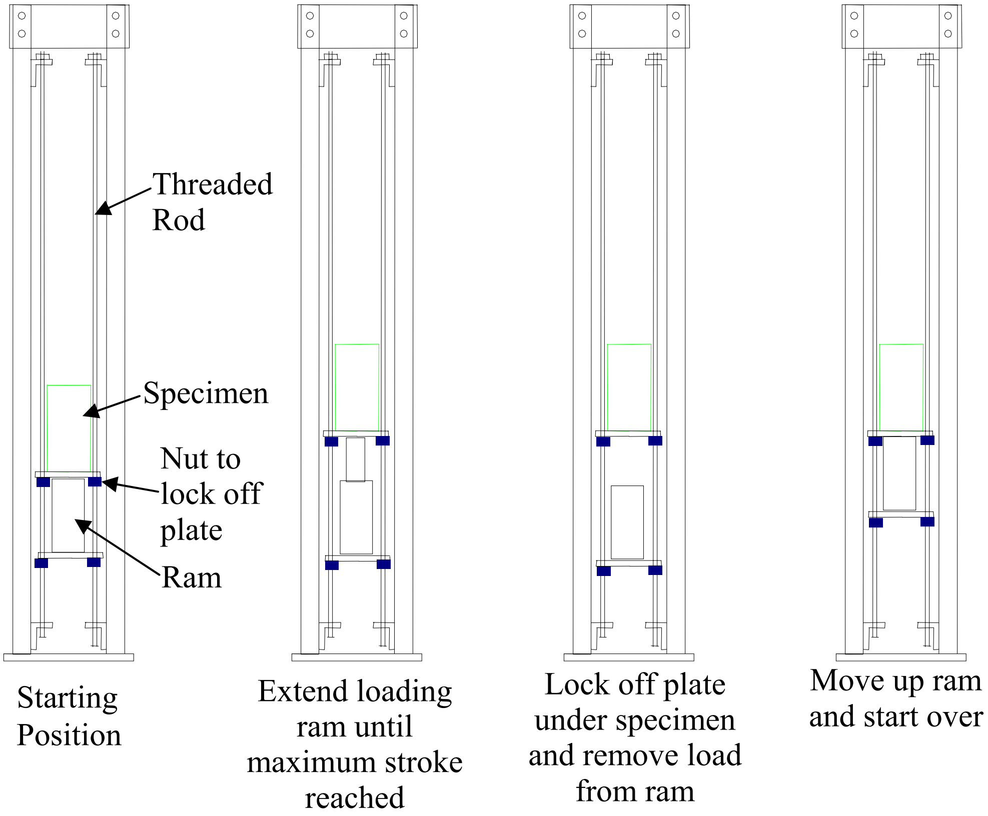
Threaded Rod
Specimen
Nut to lock off plate
Ram
Starting Position
Extend loading ram until maximum stroke reached
Lock off plate under specimen and remove load from ram
Move up ram and start over

Figure 5-9 Movable loading plates to allow for large deflections

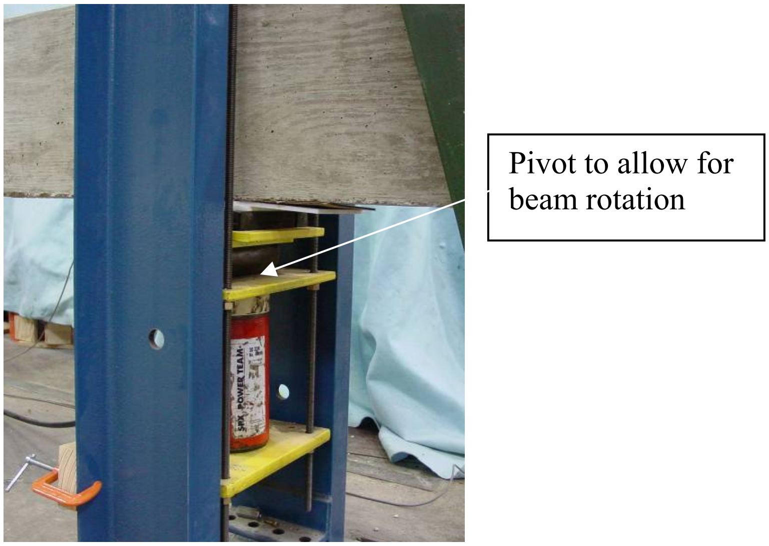

Figure 5-10 Photo of loading point

The specimen was fixed at both ends by using two supports spaced at 26 in. to provide moment resistance, Figure 5-11 and Figure 5-12. The supports had hinges at both ends to remove any axial restraint from the vertical supports and ensure that the axial restraint (coming from the axial brace) could be accurately measured. The tension support also contained a load cell under the top plate to measure the moment at the supports.

Axial restraint was provided by an axial brace at both ends of the specimen. Axial tensile resistance was provided through rebar extending from the end of the concrete beam to a yellow transfer plate to a 7/8 in. diameter threaded rod connected to the axial brace bolted into the lab floor, Figure 5-13. The extended rebar was comprised of #4 threaded dowel-in bars with 5/8 in. diameter threaded ends. Restraint against compression loads was provided by filling in gaps with spacers of wood 4x4s and metal plates, Figure 5-14. Two load cells measured the compression and tension loads.

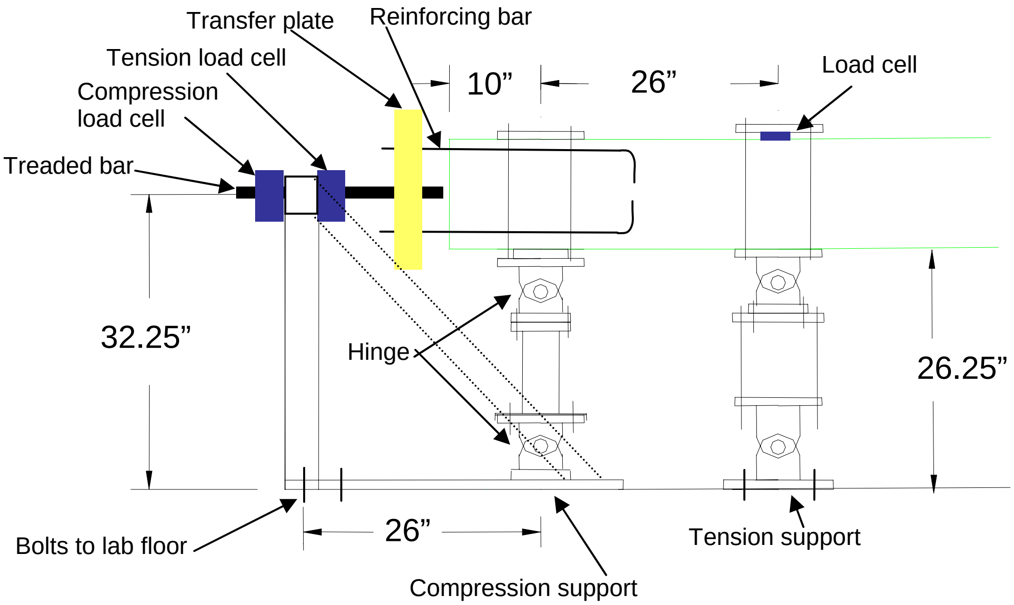
Transfer plate
Reinforcing bar
Tension load cell
Compression load cell
Treaded bar
10”
26”
Load cell
32.25”
Hinge
26.25”
Bolts to lab floor
26”
Tension support
Compression support

Figure 5-11 Schematic of restraint at end of beam

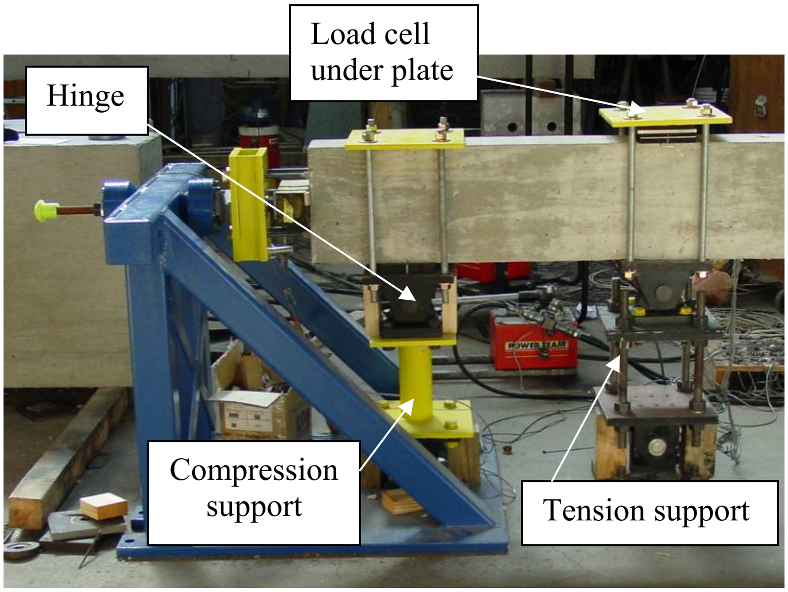
Load cell under plate
Hinge
Compression support
Tension support

Figure 5-12 Supports to provide moment resistance

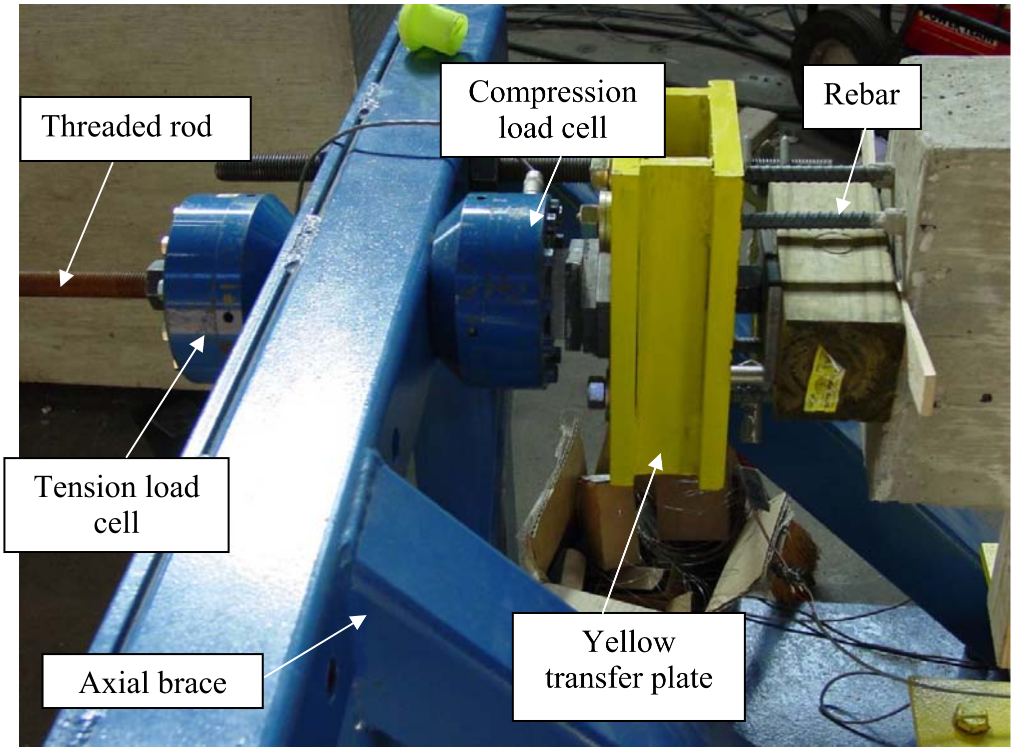
Threaded rod
Compression load cell
Rebar
Tension load cell
Axial brace
Yellow transfer plate

Figure 5-13 Axial restraint and measurement

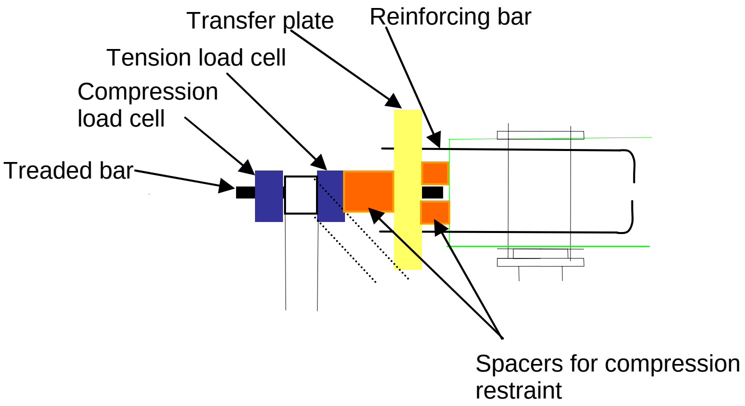
Transfer plate
Reinforcing bar
Tension load cell
Compression load cell
Treaded bar
Spacers for compression restraint

Figure 5-14 Spacers for compression restraint

A rotational restraint was also provided at the specimen column stub by a 1 5/8 in. diameter rod that was machined with roller bearings on each end to roll against the sides of the channel columns during testing, Figure 5-15. The rotational restraint simulates the restraint provided by the upper story column and ensures that hinges can form on both sides of the column stub. Restraint against twisting of the beam, or lateral movement, was provided with plywood spacers on the center column and braces (green) on the North and South columns, Figure 5-16.

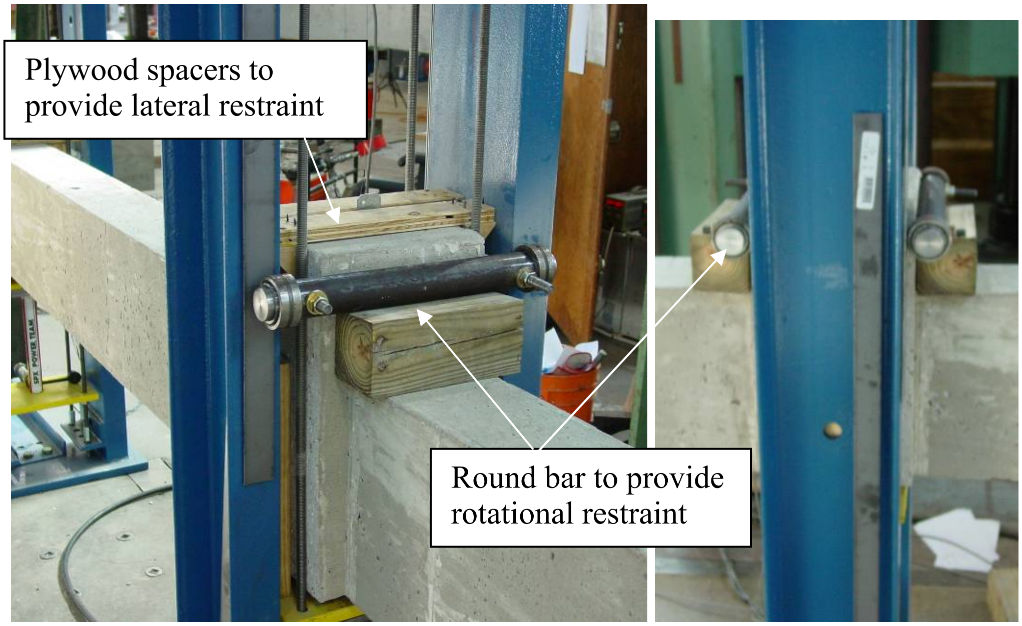
Plywood spacers to provide lateral restraint
Round bar to provide rotational restraint

Figure 5-15 Rollers to provide rotational restraint at column stub

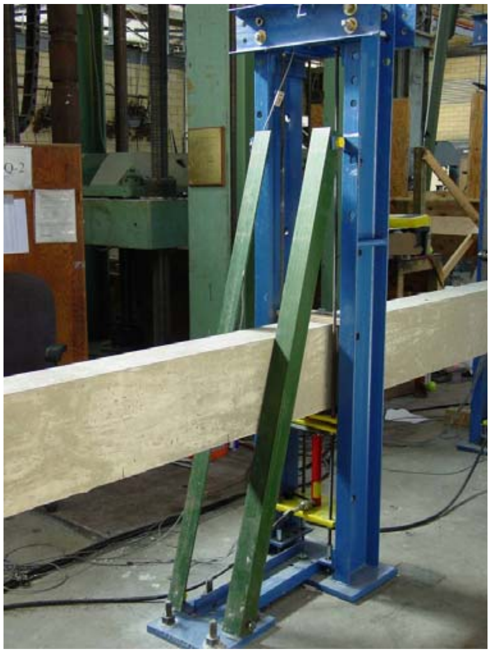

Figure 5-16 Braces (green) to provide lateral restraint and support North and South blue columns

5.4 INSTRUMENTATION

Instrumentation for the continuity tests included five load cells, five displacement transducers, and numerous strain gages on the rebar and CFRP, Figure 5-17.

Two load cells were located at one end to measure the axial tension and compression forces, Figure 5-13. One load cell was located under the center loading point to monitor the applied loads on the test specimen. All three loading rams were connected to the same manifold so the hydraulic pressure in each ram was equal. A pressure transducer on the pump gave the pressure in the hydraulic lines and provided a check on the load cell readings from the center ram. Two load cells were located on the tension supports at each end to determine the moment at the ends of the beam, Figure 5-12.

Displacement measurements were taken through the use of string potentiometers located above each loading point. Two linear potentiometers were also used to measure the horizontal movement at the ends of the beam.

Strain gages were placed throughout the specimen on both the rebar and CFRP. Gage locations can be found in Appendix C.

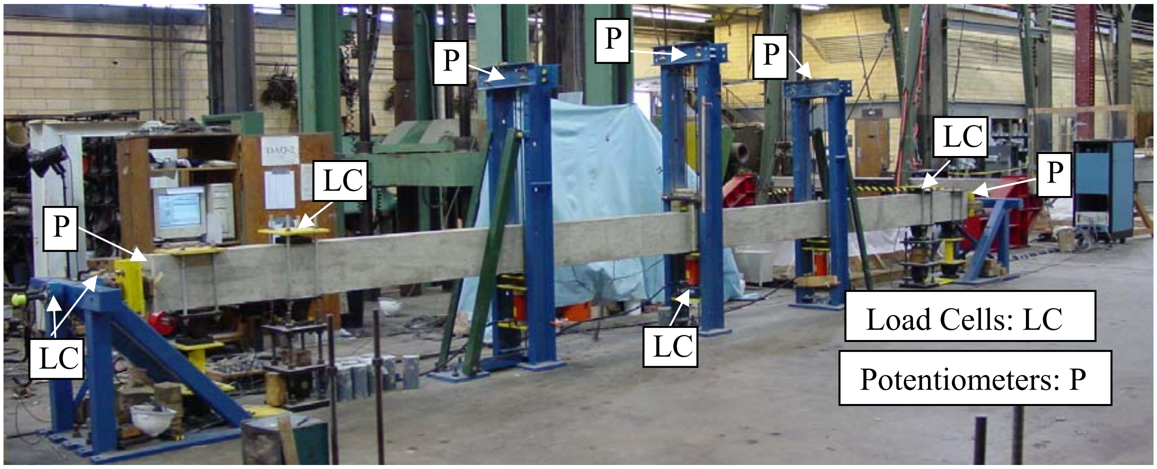

Figure 5-17 Instrumentation locations

5.5 TEST RESULTS

Eight specimens were tested, Table 5-1. The first specimen was used as a shake-down test to identify problems in the test setup. The test led to changes in the axial load measurement, axial restraint, and rotation of center column and will not be included in the results. The other specimens were designed to evaluate the catenary response of a beam with no continuous reinforcement, with continuous reinforcement, with CFRP retrofits to provide continuity through the positive or negative moment reinforcement, and with a CFRP retrofit to increase the flexural capacity of the beam.

Table 5-1 Test specimen designation

Specimen Designation	Specimen Description
NR-1	No Retrofit, shake-down test
NR-2	No Retrofit
PM-1	Positive Moment retrofit, provided continuity of 2 #3 positive moment bars
PM-2	Positive Moment retrofit, provided continuity of all positive moment bars
NM-1	Negative Moment retrofit, 10 in CFRP width
NM-2	Negative Moment retrofit, 6 in CFRP width
FR-1	Flexural retrofit
CR-1	Continuous Reinforcement, beam meeting ACI 318-05 Chapter 7 requirements

The materials used for each of the test specimens were the same, except for the concrete. The properties of the CFRP material are shown in Table 5-2 and discussed in Chapter 4. Based on tensile tests, the #3 and #4 rebar had a yield stress of 63 ksi and a tensile strength of 100 ksi, Figure 5-18. The specimens were cast 2 or 3 at a time. The concrete compressive strength for each specimen is given in Table 5-3. The concrete delivered for casting for specimens NR-1 and NR-2 produced unexpectedly poor quality concrete. The concrete for other castings provided nearly the same strength concrete.

Table 5-2 CFRP fabric properties

Property	SCH 41	
	Nominal$_a$	Measured
Tensile Strength (ksi)	143	133±8
Tensile Modulus (ksi)	13,900	13,270±1770
Elongation at break	1.00%	1.01%±0.10%
Thickness (in)	0.04	0.04

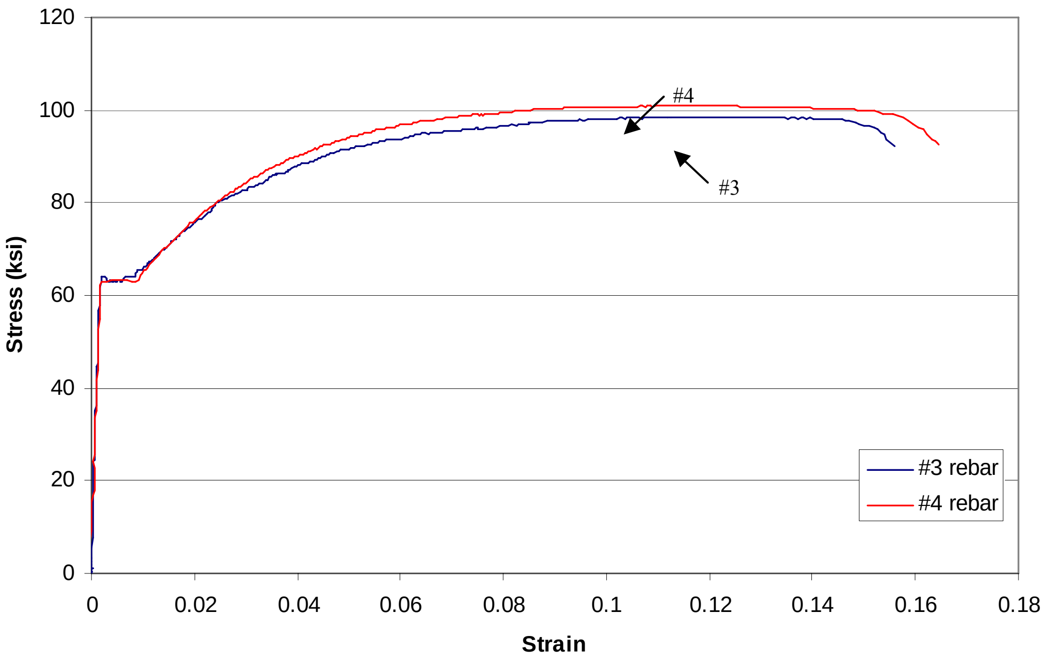

Figure 5-18 Stress vs strain for reinforcing bar

Table 5-3 Concrete compressive strength per specimen

Specimen	f'$_c$ (psi)
NR-1	1700
NR-2	1700
PM-1	4900
PM-2	4900
NM-1	4900
NM-2	5300
FR-1	5300
CR-1	5300

5.5.1 NR-2 – No Retrofit

Specimen NR-2 was not retrofitted and demonstrated the capacity of the beam without any continuous reinforcement. The specimen reached 2.3 k per loading point before hinges developed on either side of the column and at the ends of the negative moment reinforcement, Figure 5-19. After the hinges developed the load dropped to about 1 k and remained at that level as deformations increased. Because no reinforcement crossed the tension side of the hinge locations, the cracks continued to open widely and the beam deflected as a mechanism comprised of rigid blocks connected at the hinge locations. The rotation of the blocks caused axial compression in the beam until the beam reached around 17 in. of center displacement or 5% of the span length, Figure 5-20. The axial compression phase followed by catenary tension at 5% of the span length is the same type of behavior reported by Regan (1975).

After the compression phase, the catenary effect created axial tension in the beam allowing it to carry more vertical load. The catenary tension was carried by the positive moment steel near the ends of the beam and then transferred by the stirrups to the negative moment steel at the column line (see Figure 2-17 in Chapter 2). The maximum vertical load per loading point was 5.2 k with 14.6 k axial tension measured in the tension load cell and a displacement at the center load point of 24.6 in. The load carried through catenary action was nearly twice the load reached before the hinges formed but still less than the 10 k recommended by GSA to resist progressive collapse. The test was stopped at 5.2 k due to a tension failure at the end of the beam due to poor concrete consolidation in that area during casting (photo in Appendix C).

The poor quality concrete (f'_c of 1700 psi) had little impact in this test because hinges formed at the ends of the reinforcing bars and the hinge capacity was not significantly influenced by the strength of the concrete. The greatest impact the concrete strength had was at the end of the beam where the extended reinforcing bars that connect to the axial brace were able to pull out of the poorly consolidated and weak concrete.

The design of the beam provided extra capacity in the stirrups (#3 stirrups at 5 in. spacing with 90º hooks) due to scaling issues (smallest size of deformed rebar available was #3). If the design of the stirrups had been properly scaled, they may have not have been able to transfer the catenary tension loads between the positive to the negative moment reinforcement.

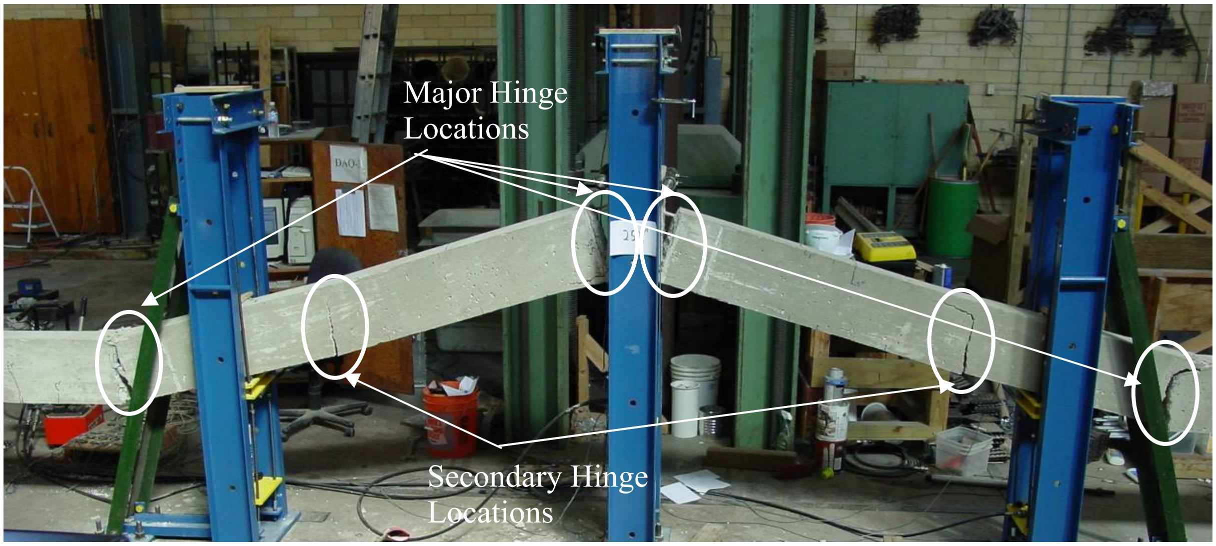

Figure 5-19 Failure of specimen NR-2

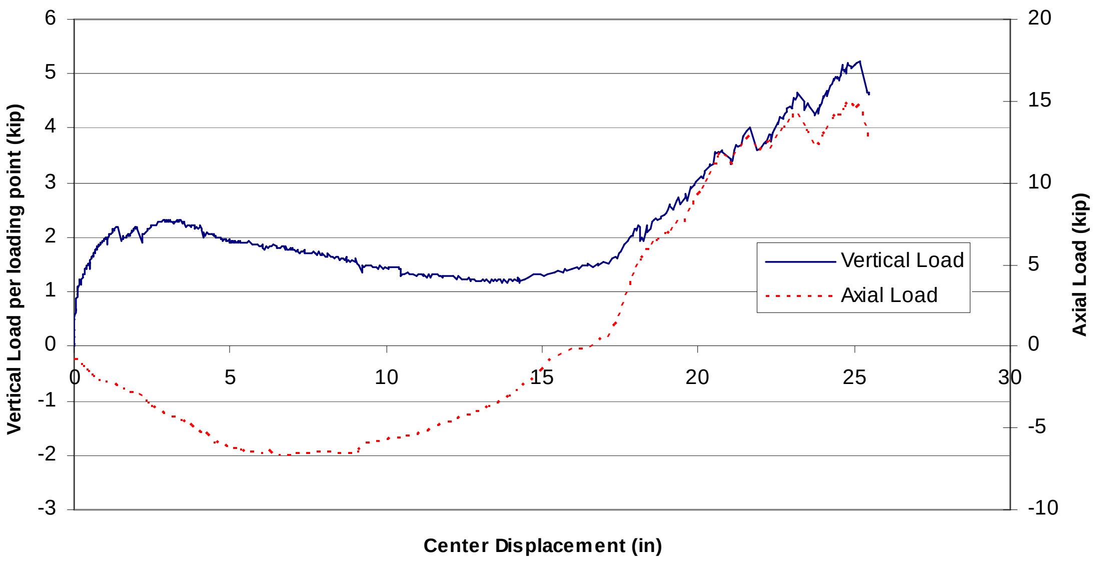

Figure 5-20 Vertical and axial loads versus displacement for NR-2

5.5.2 PM-1 – Positive Moment Retrofit

The purpose of the positive moment retrofit was to provide continuity of reinforcement through the column using the two #3 reinforcing bars that extended only 3 in. into the column. To provide ductility, the retrofit was designed so that hinging would be controlled by yielding in the rebar rather than fracture of the CFRP retrofit. In order to force a hinge to form just beyond the end of the CFRP sheet, the required moment capacity at a section at the center of the column was 260 k-in and require a CFRP sheet which corresponds to an area of 0.24 in^2. Details of the design process can be found in Appendix B. The anchorage design of the retrofit was based on the results from the anchorage tests – two rows of anchors with a cross-sectional area of each row equal to 1.33 times the cross-sectional area of the longitudinal sheet. Additionally, the amount of CFRP going through the column was also increased by 1.33 times to adjust for the weakness of the CFRP fabric at bends (see Section 4.3.2.2).

For the retrofit, a 7 in. wide sheet of CFRP fabric along the beam, a 9 1/2 in. wide sheet through the column, and 4.75 in. wide strips in the two anchors in each row were used, Figure 5-21. The symbol for the anchors in Figure 5-21 is circular though, the anchors were fanned in a pie shape directed along the tension in the CFRP sheet (see Figure 4-7) or in a circular fashion at the bottom of the transition slope. All anchors were inserted at least 6 in. into the concrete. Use of U-wraps could have avoided drilling holes in the concrete; however, results from the anchorage tests (Chapter 4) show that they are not an efficient way to anchor the CFRP sheet. A hole was drilled through the column (Figure 5-22) and the CFRP sheet was pulled through (Figure 5-23) then fanned out on top of the beams on either side, Figure 5-24. Transition ramps with a 1 to 4 slope, like the ones used in the anchorage tests, were also applied (see Section 2.5). The last row of anchors was placed at a distance (22" from the column face) greater than the 14" development length for a #3 rebar to ensure full transfer of forces from the CFRP to the rebar.

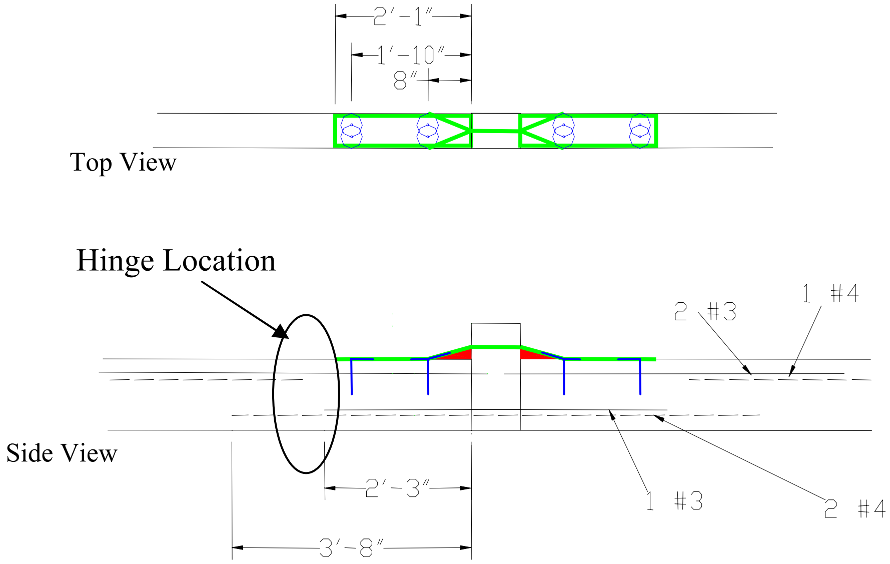

Figure 5-21 Design of CFRP retrofit for PM-1

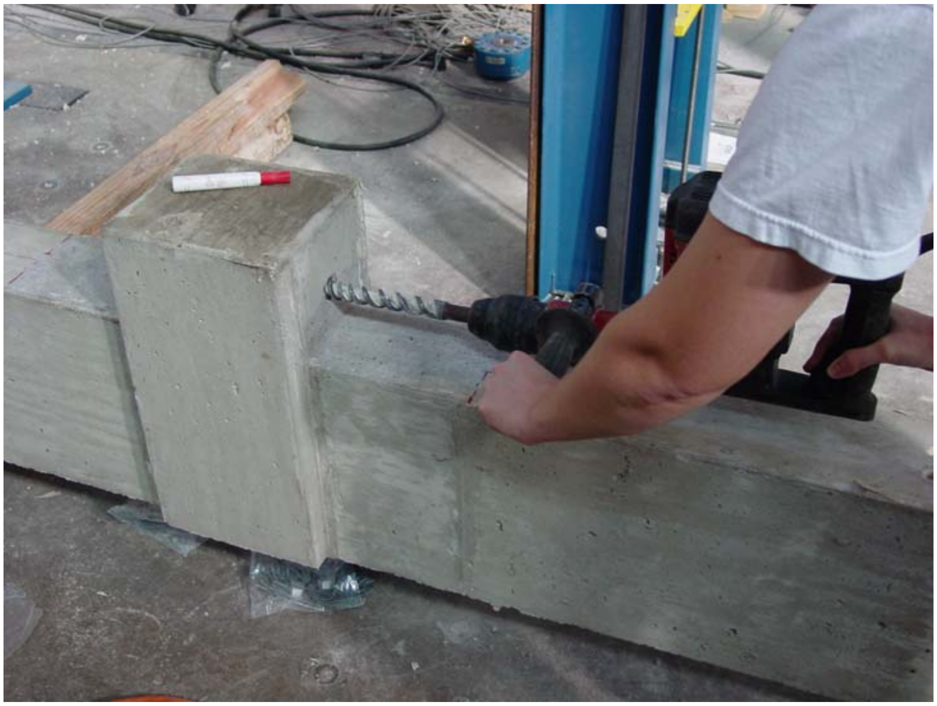

Figure 5-22 Drilling hole through column

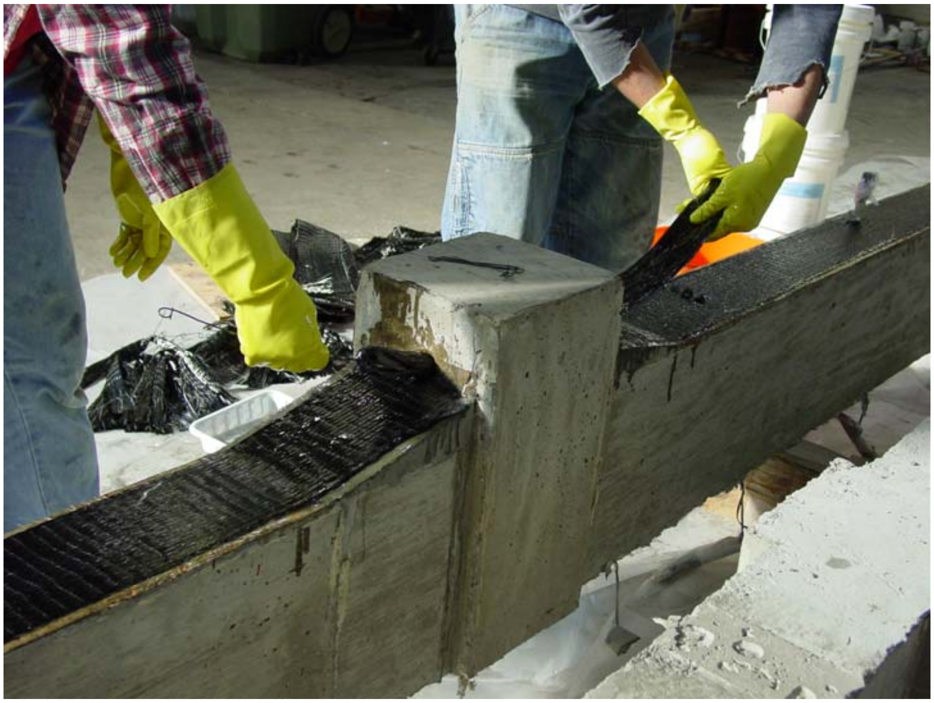

Figure 5-23 Pulling CFRP through hole in column

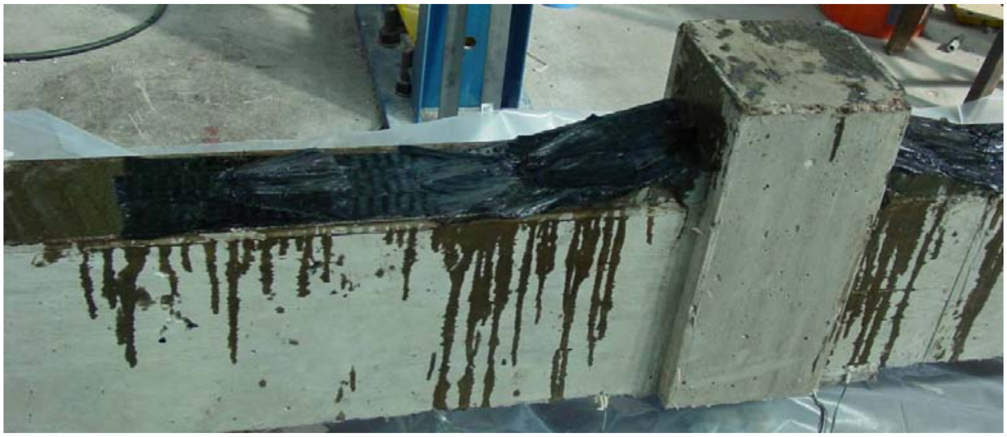

Figure 5-24 CFRP retrofit for PM-1

During testing of specimen PM-1, hinges started to form at the ends of the CFRP retrofit and the ends of the negative moment reinforcement. Eventually the #3 positive moment bars yielded and then fractured at the end of the CFRP retrofit at a vertical load of 5.5 k and displacement of 10 in., Figure 5-25 and Figure 5-26. Using equations developed by Mattock and Corley (1966), the section at the end of the retrofit should have a rotational capacity of 0.098 radians. In order to develop catenary action a rotation of 0.13 radians would be needed. As Regan (1975) pointed out, a beam not only needs tensile strength, it must also have sufficient ductility to reach catenary action.

The load then dropped and the beam eventually went into catenary action similar to that of specimen NR-2, but with hinges at the end of the CFRP sheet rather than at the column. The test was stopped at 24 in. of displacement when the vertical load rams became misaligned due to excess rotation of the center column.

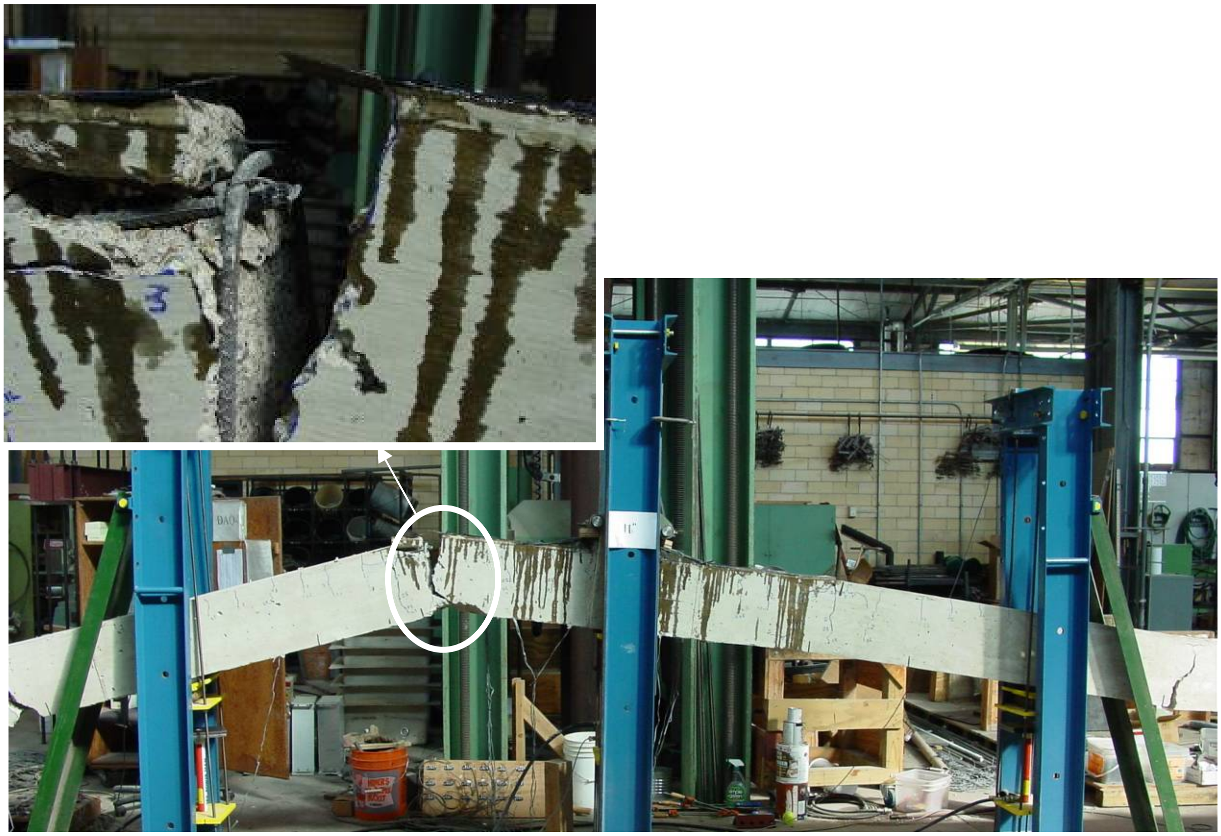

Figure 5-25 Failure of PM-1 by fracture of rebar

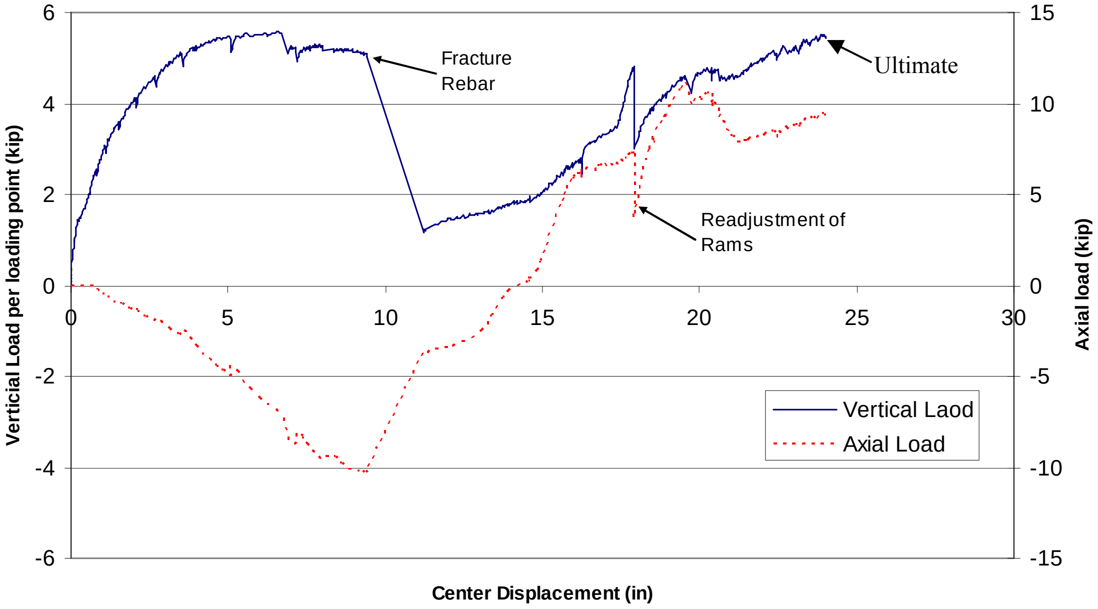

Figure 5-26 Vertical and axial loads for PM-1

The strains in the positive moment steel at rebar fracture and ultimate deflection are shown in Figure 5-27. Unfortunately, several of the gages were not working during the test and yielding and fracture of the positive moment rebar was not monitored. The maximum measured strain in the CFRP prior to fracture of the rebar was 0.005, Figure 5-28. At the same time, reading of 0.002 and 0.003 occurred at gages 2 and 7 just beyond the transition slope. When compared to the results from the anchorage tests, in which strains of around 0.008 at the bottom of the transition slope and 0.003 at the gage just beyond (gages 2 and 7) were measured, the strain in the CFRP just prior to rebar fracture indicate that the material was near its ultimate tensile capacity and was being used efficiently. After rebar fracture, the CFRP strains on the North side of the beam dropped due to the redistribution of moment.

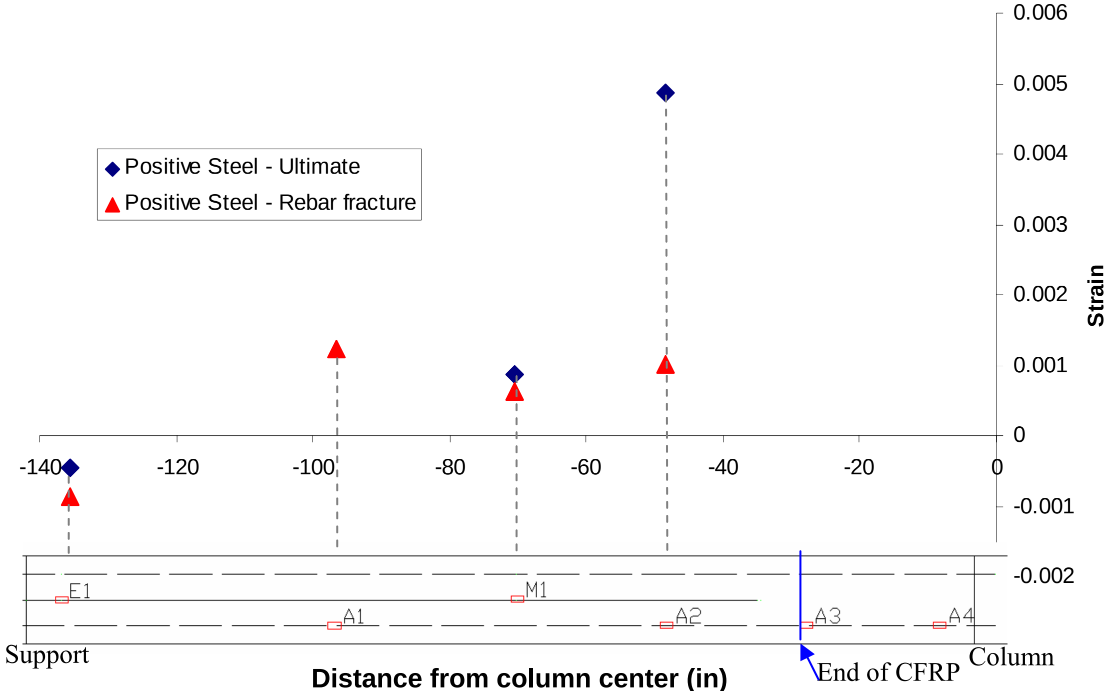

Figure 5-27 Strains in positive moment steel for PM-1

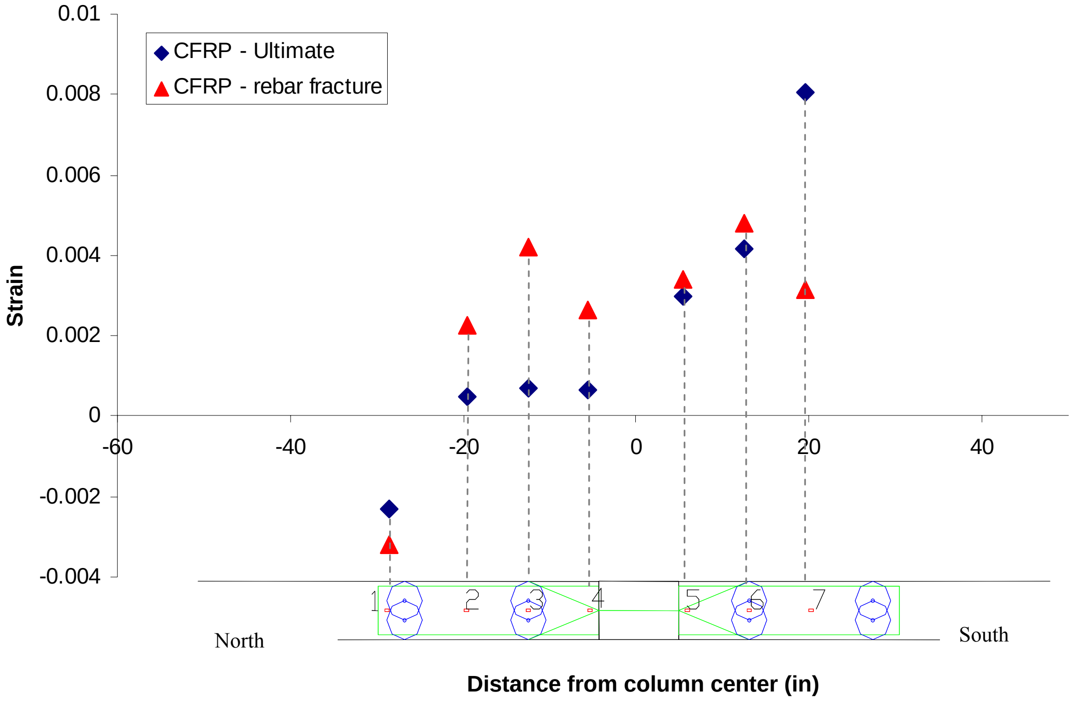

Figure 5-28 Strains in CFRP for PM-1

5.5.3 PM-2 – Positive Moment Retrofit

In specimen PM-2, the CFRP sheet was extended to develop the additional #4 positive moment bar. The moment capacity of the section at the end of the CFRP sheet consisted of the two #3 bars and one #4 bar. The location and increased capacity of this section required a moment capacity of 510 k-in at the column line. Therefore, a 12 in. wide sheet of CFRP fabric (0.48 in^2) along the beam, a 15.5 in. wide sheet through the column, and 7.75 in. wide strips in the two anchors in each row were applied, Figure 5-29 and Figure 5-30. Three rows of anchors were used instead of two due to the increased length of the CFRP sheet. Design details can be found in Appendix B.

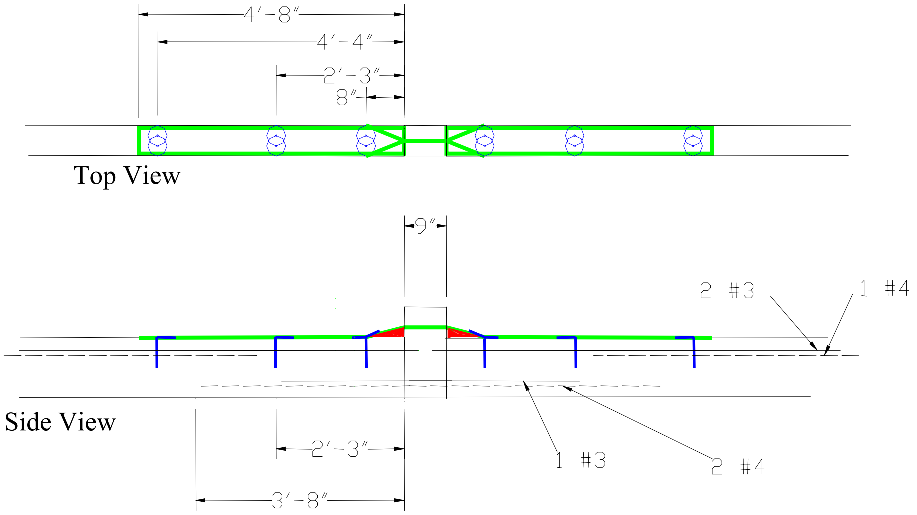

Figure 5-29 Design of CFRP retrofit for PM-2

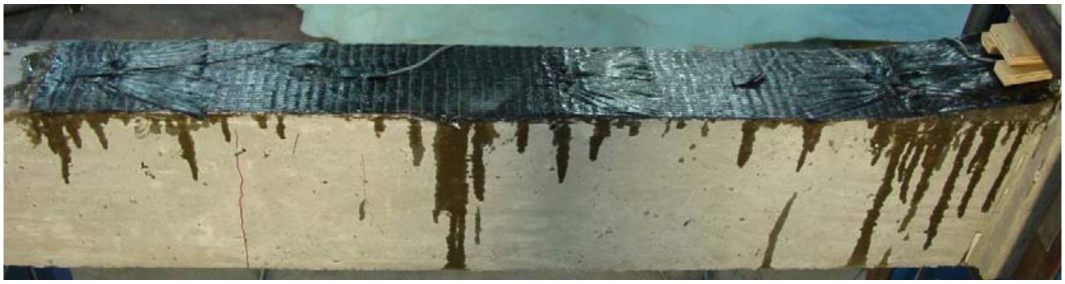

Figure 5-30 CFRP retrofit for PM-2

As specimen PM-2 was loaded, hinges started to form at the ends of the CFRP sheet and at the supports. At 6 k per loading point, the CFRP fractured at the end of the transition slope, Figure 5-31 and Figure 5-32. Strains in the CFRP just prior to fracture indicate high strains at the face of the column (0.004) but not near the fracture strain of the CFRP of 0.01, Figure 5-33. There was no gage at the bottom of the transition slope where the fracture occurred. The #4 gage at the bottom of the transition slope on the other side of the column recorded a strain of 0.011 before it broke at 5 k of vertical load. As was found in the anchorage tests, it is difficult to place a gage on the transition slope and get an accurate strain reading. Strain readings at gages 3 and 7 agree with readings from the anchorage tests at CFRP fracture (see Section 4.3.2.6). Therefore, the fracture of the CFRP was not necessarily premature, but more CFRP was needed in the design to force the hinge to form at the end of the CFRP sheet.

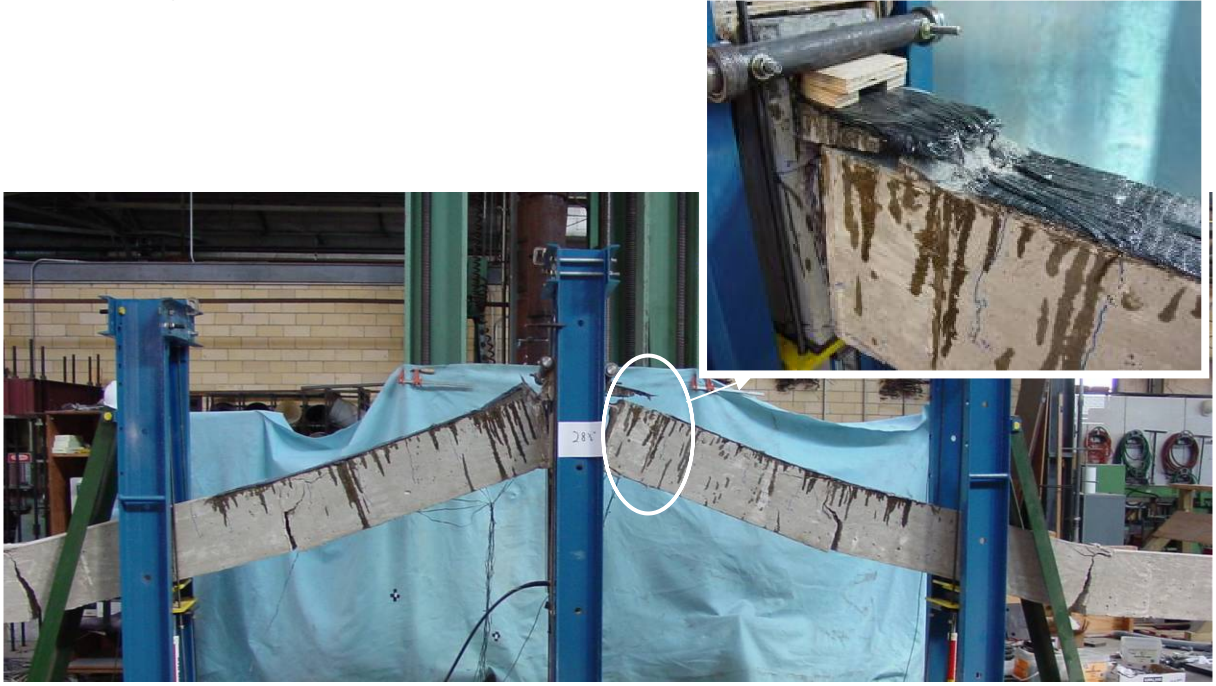

Figure 5-31 Final state of PM-2

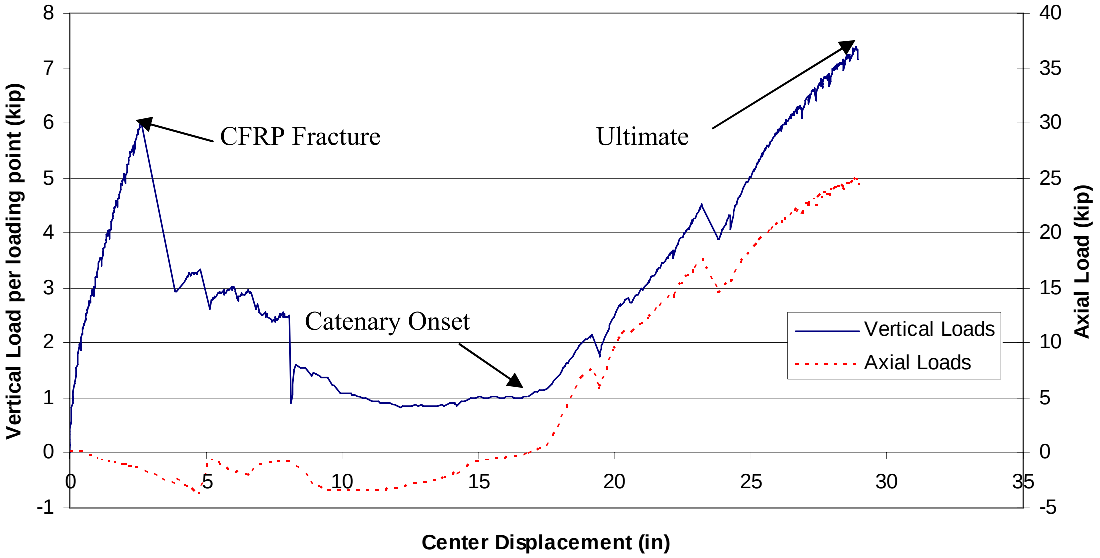

Figure 5-32 Vertical and axial load versus displacement for PM-2

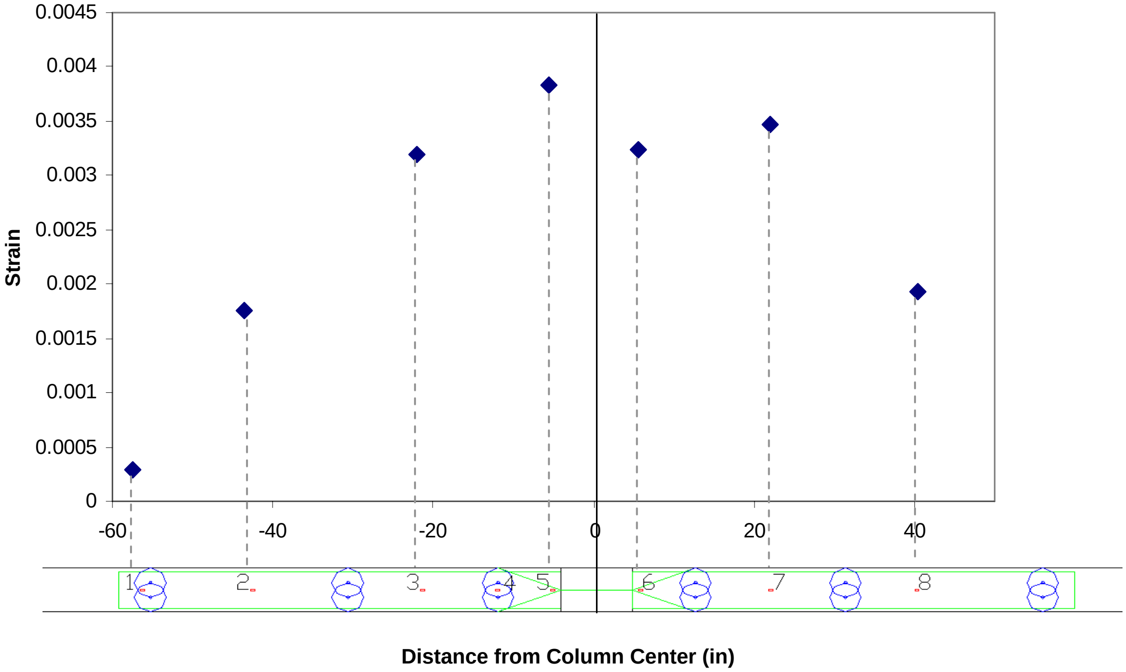

Figure 5-33 Strain in CFRP prior to fracture for PM-2

Strains in the positive moment reinforcing bars are shown in Figure 5-34. A strain of 0.0018 (close to the yield strain of 0.002) at M1 (66 in. from column face) indicate that a hinge was close to forming just beyond the end of the CFRP sheet (56 in. from column face) prior to CFRP fracture. If the CFRP had not fractured, the hinge would have continued to form and the rebar may have fractured, as in PM-1, at about 6.8 k of load per loading point (see calculations in Appendix B).

Although the 6.8 k per loading point is not 10 k per loading point recommended by the GSA to resist progressive collapse, if the anticipated dead and live loads were less so that 2(DL +0.25LL) requirement was less than 10 k per loading point (beam was over-designed) and the dynamic increase factor of 2 reduced (see Chapter 2) the 6.8 k that could have been reached by the positive moment retrofit could be enough to resist progressive collapse.

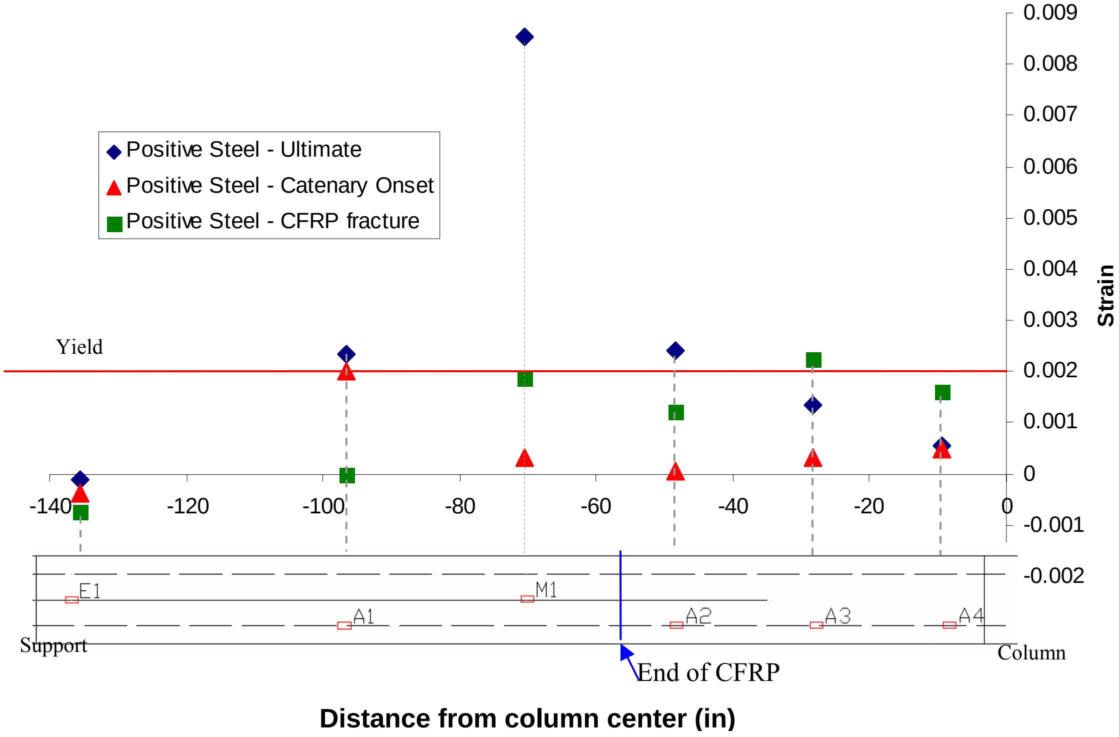

Figure 5-34 Strains in positive moment steel in PM-2

After the CFRP fractured, the specimen behaved in the same manner as specimen NR-2 with wide cracks on either side of the column and at the ends of the negative moment steel. Due to changes in the test setup, the specimen, now behaving as an unretrofitted specimen, was able to reach a higher load and displacement than NR-2. The specimen eventually reached 7.3 k per load point with 24.3 k in axial tension and 28.9 in. of displacement, Figure 5-32.

Due to the high axial tension at ultimate deflection, the strains in the rebar were beyond yield along most of the length of the beam. One exception was near the ends of the discontinuous positive moment steel near the column line (A3 and A4), indicating that the catenary tension forces had been transferred through the stirrups to the negative moment steel. The other exception is at the very end of the beam (E1) where the strain was in compression due to the bending in that region. The greatest strain (0.0085 at M1) was recorded in a location where all the catenary tension forces were being carried through the positive moment reinforcement. The measured axial tension from the load cell at the end of the beam is 25 k and is close to the yield strength of the positive moment steel of 26.5 k (0.42 in^2 * 63 ksi), again indicating that in the center sections of the beam the positive moment steel was carrying all the catenary tension stresses. The yielding of the positive moment reinforcement may have caused greater displacements in catenary action.

Strains in the negative moment reinforcement are shown in Figure 5-35. The strains in gages E2 and E3 were high due to the bending at support. The strains in gages near the column were high due to the tension from catenary action. Although not all gages recorded yield strains, the catenary tension force of 25 k is approaching the yield strength of the three negative moment reinforcing bars (32.1 k).

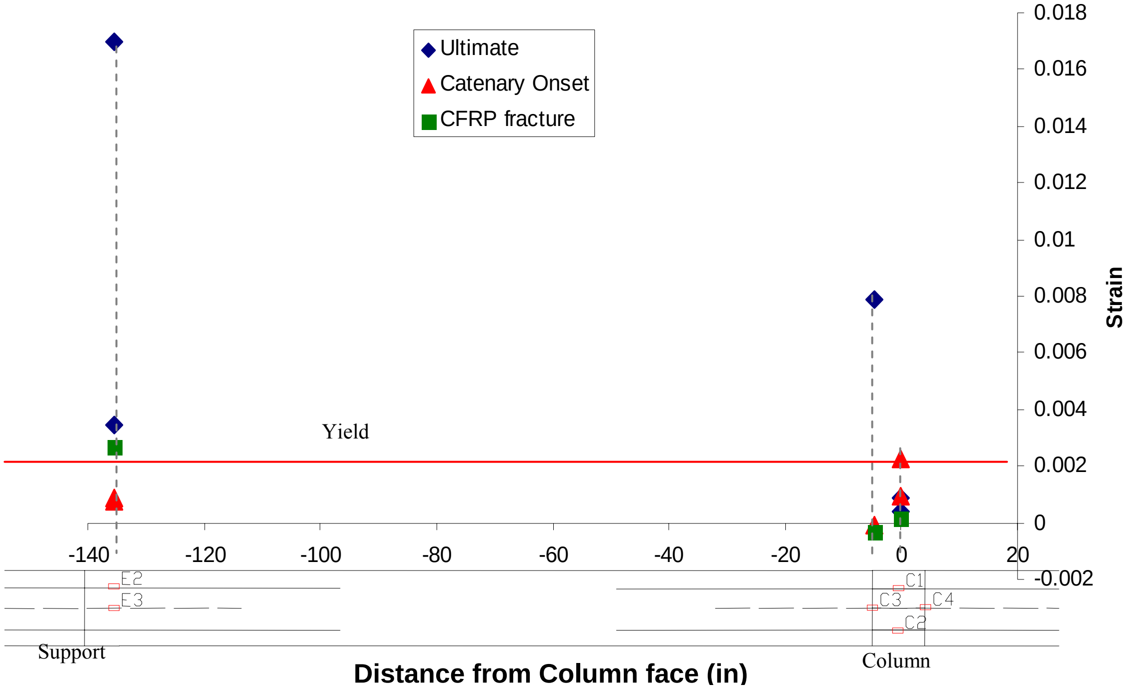

Figure 5-35 Strains in negative moment reinforcement in PM-2

Although PM-2 was able to reach a higher load and displacement than NR-2, the 7.3 k per loading point was still less than the 10 k (2 times dead plus 25% live load) recommended by the GSA guidelines to withstand progressive collapse. The test was stopped due to misalignments of the loading rams due to the high displacements. However, the yielding of the positive moment reinforcement may have increased catenary displacement, and the beam may have eventually been able to reach the 10 k vertical load level (see Chapter 6).

5.5.4 NM-1 – Negative Moment Retrofit

A retrofit that provided continuity through the negative moment reinforcement was also studied. The amount of CFRP applied was based on the fracture strength of the 2 #4 bars (44 k) to ensure that the tensile capacity of the CFRP would be able to exceed that of the reinforcement under catenary action. A 10 in. wide sheet (double layer of 5 in. wide sheets) of CFRP was applied to the bottom of the beam, Figure 5-36. Anchors consisting of 6.75 in. wide strips in 5/8 in. diameter holes anchored the CFRP sheet. The location and spacing of the anchor rows was based on the development length of a #4 rebar (19 in.) to ensure that the CFRP would be able to transfer all stresses into the rebar. Details of the design can be found in Appendix B.

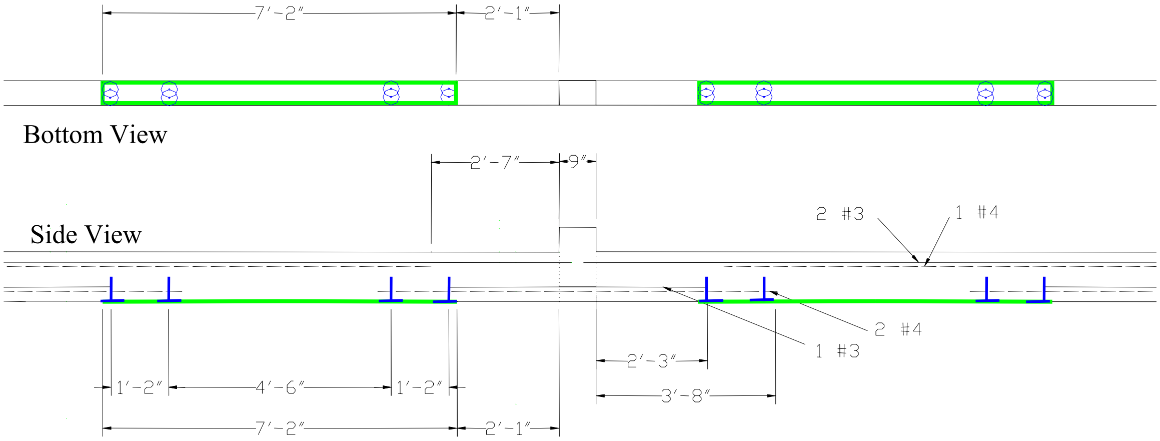

Figure 5-36 Design of CFRP retrofit for NM-1

The specimen preformed well and was able to reach the desired 10 k per loading point at 30.6 in. of displacement and 32.4 k of axial load, Figure 5-37 and Figure 5-38. At 32.4 k axial load, the threaded rod connecting the end of the specimen to the blue axial brace fractured, Figure 5-39.

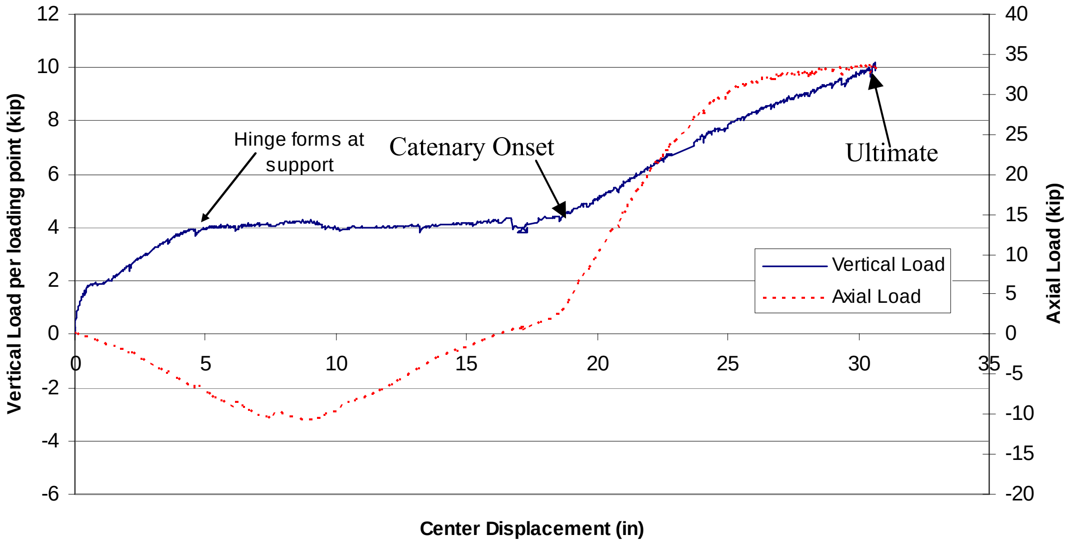

Figure 5-37 Vertical and axial loads for NM-1

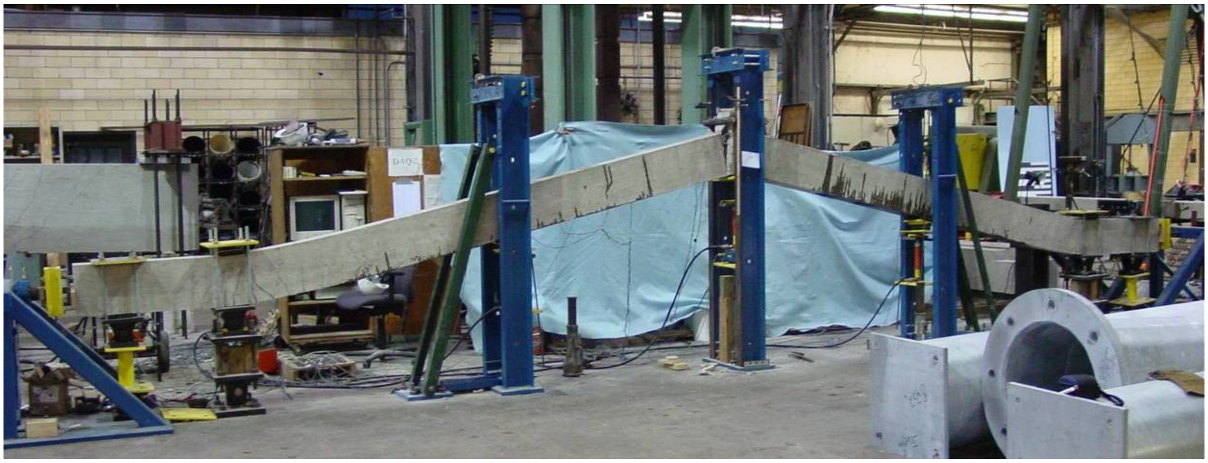

Figure 5-38 Final state of specimen NM-1

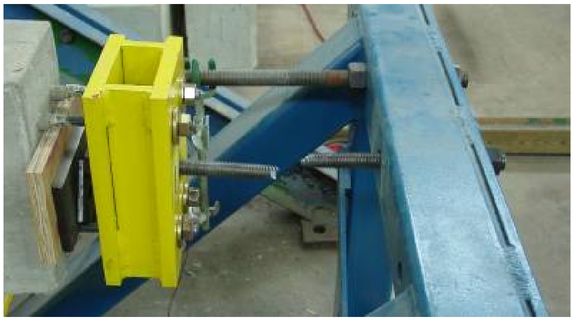

Figure 5-39 Fracture of threaded rod at 32 k axial tension

Because there was no continuity of positive moment reinforcement at the column line, a wide crack formed next to the column stub and the #3 bars pulled out of the column, Figure 5-40. The specimen was able to reach about 4 k load per load point when hinges began to form at the supports, Figure 5-41. Both the measured moment of 420 k-in from the load cells under the tension support and the moment based on strain gage readings (see data in Appendix C) agree with the design capacity analysis of the section at the support and the plastic analysis that indicates the section will hinge at about 4 k load per load point (see Appendix B).

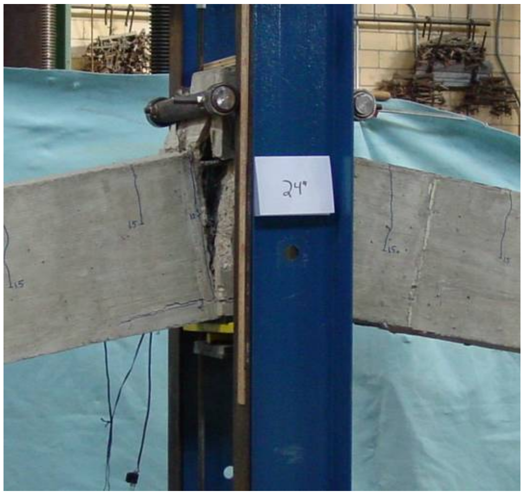

Figure 5-40 Wide crack and pulling out of #3 bars at column line

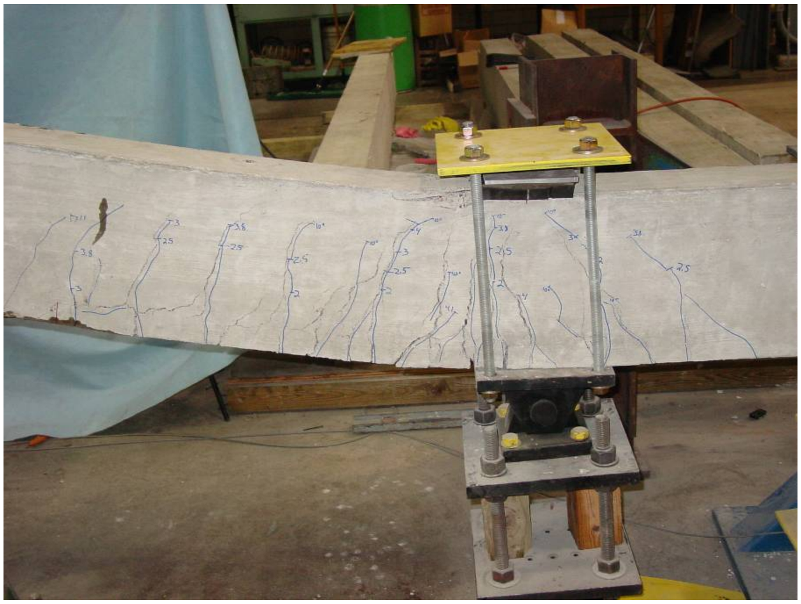

Figure 5-41 Hinging at support

At ultimate deflection, the hinges at the supports underwent 0.21 radians of rotation based on the center displacement. Based on equations by Mattock and Corley the rotational capacity of the section was only 0.11 radians [Corley, 1966]. This rotational capacity is enough to allow the beam to reach catenary action. Once catenary starts, the tension or shear in the beam may increase the hinge length and further increase the rotational capacity of the section leading to the 0.21 radians of rotation measured with no fracture of the rebar.

The strains in the positive and negative moment reinforcement are shown in Figure 5-42 and Figure 5-43. At hinge formation, the strains in the negative moment rebar near the support were 0.0027 and 0.0032 with a strain of -0.0012 in the positive moment rebar at E1. These strains again indicate formation of a hinge near the support. At ultimate, strains throughout the positive moment rebar were nearing yield except near the discontinuity at the column line and the support as in specimen PM-2. The presence of significant yielding in the beam indicates that the stiffness of the beam will decrease as vertical load is increased.

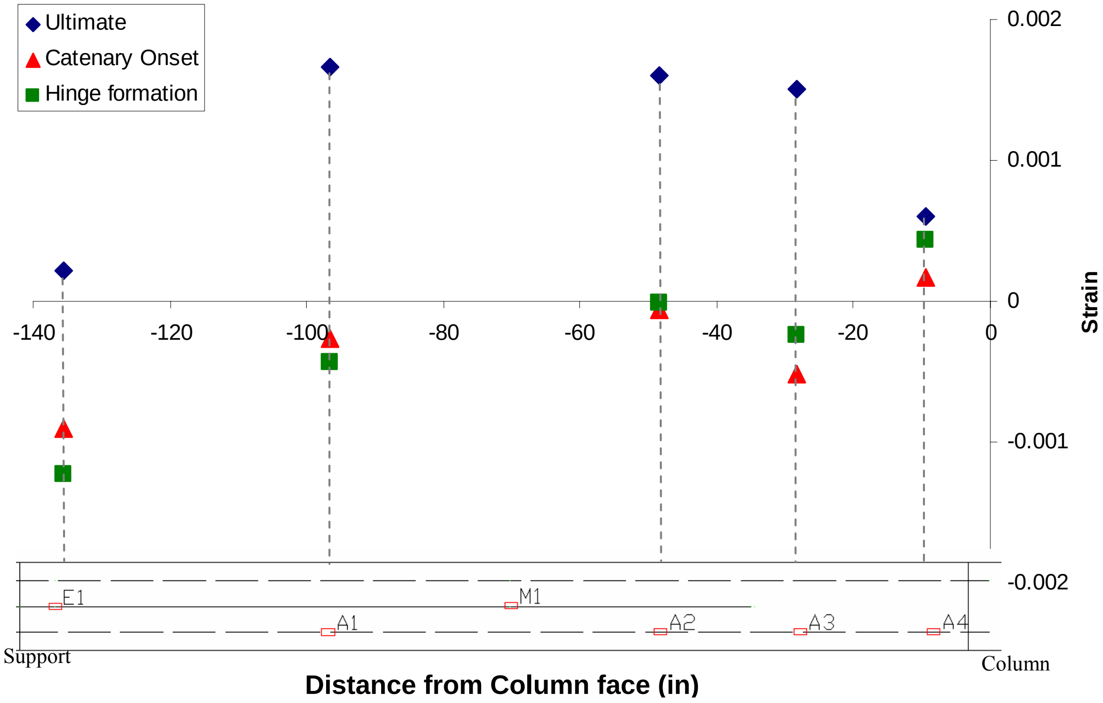

Figure 5-42 Strains in positive moment rebar for NM-1

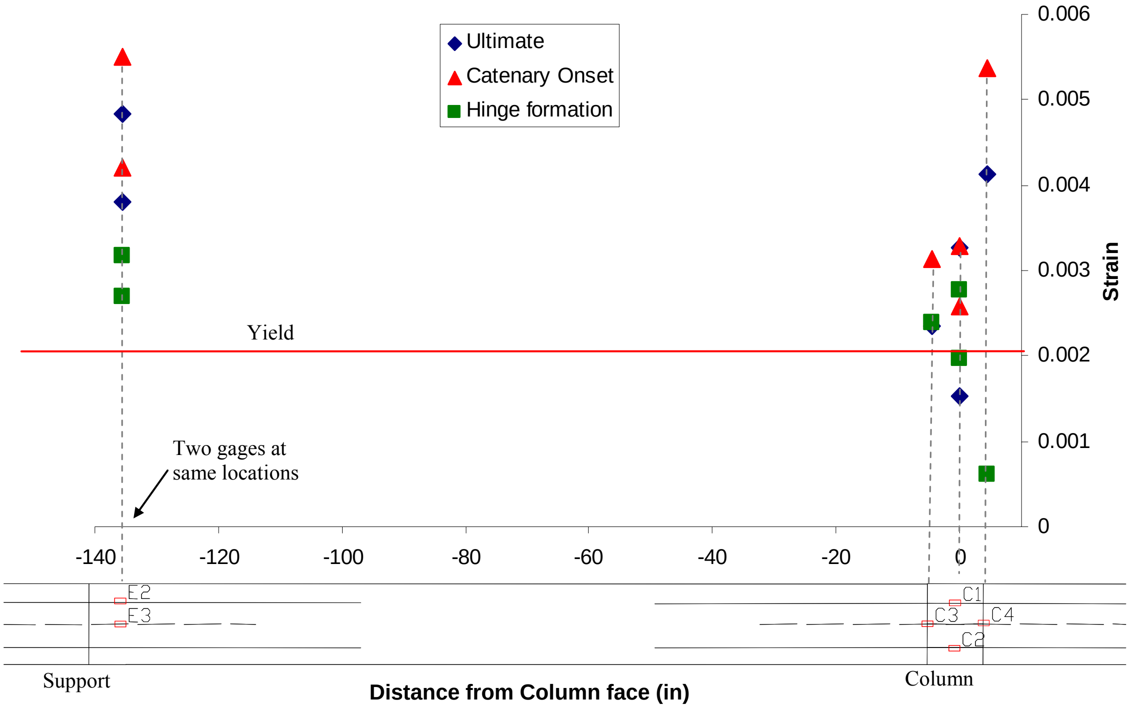

Figure 5-43 Strains in negative moment reinforcement for NM-1

The strains in the CFRP are shown in Figure 5-44. At ultimate the highest strain recorded was 0.0035 at gage 1. This reading is much lower than the ultimate strain of the CFRP material of 0.01, indicating that more CFRP material was used than was needed and a reduced area of CFRP could be used on the next specimen.

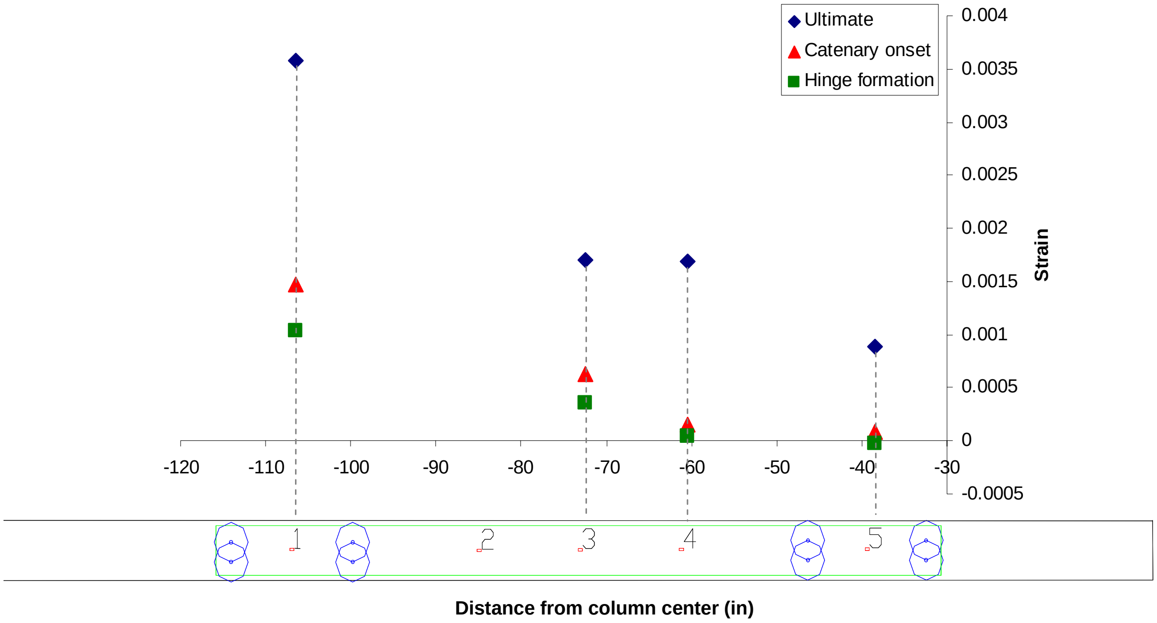

Figure 5-44 Strains in CFRP for NM-1

5.5.5 NM-2 – Negative Moment Retrofit

A second negative moment retrofit with a reduced area of CFRP was tested. A stronger threaded rod at the end of the specimen was installed to prevent failure in the test setup. For this retrofit the amount of CFRP applied was adjusted to account for hinges forming near the supports that would limit the amount of moment at the end of the CFRP sheet to 270 k-in. Additionally, in order to achieve the desired vertical load, catenary tension would be less than 32 k. To achieve 270 k-in moment capacity and to ensure CFRP sheet tensile capacity greater than 32 k, a CFRP sheet width of 6 in. was used. Anchors consisting of 4 in. wide strips in ½ in. diameter holes anchored the CFRP sheet.

The location and spacing of the anchor rows was the same as for specimen NM-1. A detailed design can be found in Appendix B.

The specimen preformed almost identically to NM-1 and was able to reach the desired 10.8 k per loading point at 32.3 inches of displacement and 36.6 k axial tension, Figure 5-45. As with specimen NM-1, a wide crack formed at the column stub and hinges formed at the supports at 4 k load per load point. At 36.6 k of axial tension, the CFRP fractured, Figure 5-46 and Figure 5-47.

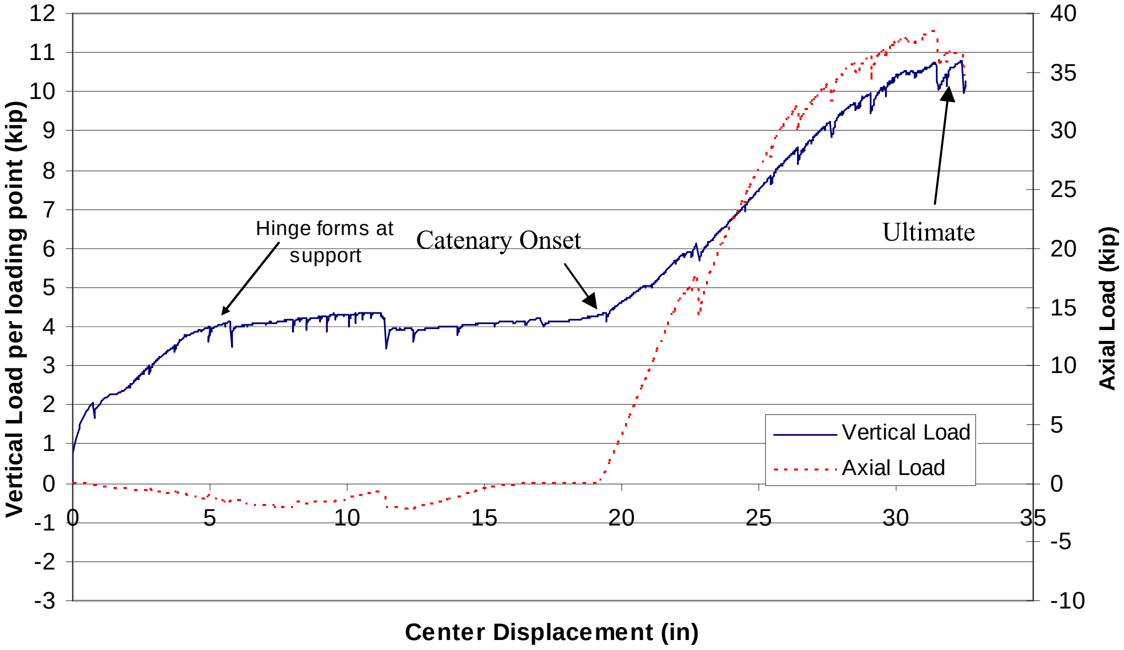

Figure 5-45 Vertical and Axial loads for NM-2

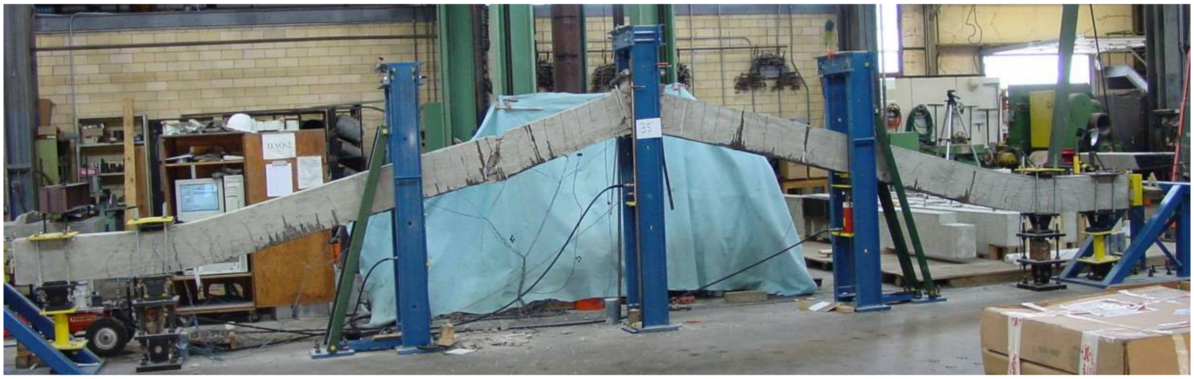

Figure 5-46 Final state of specimen NM-2

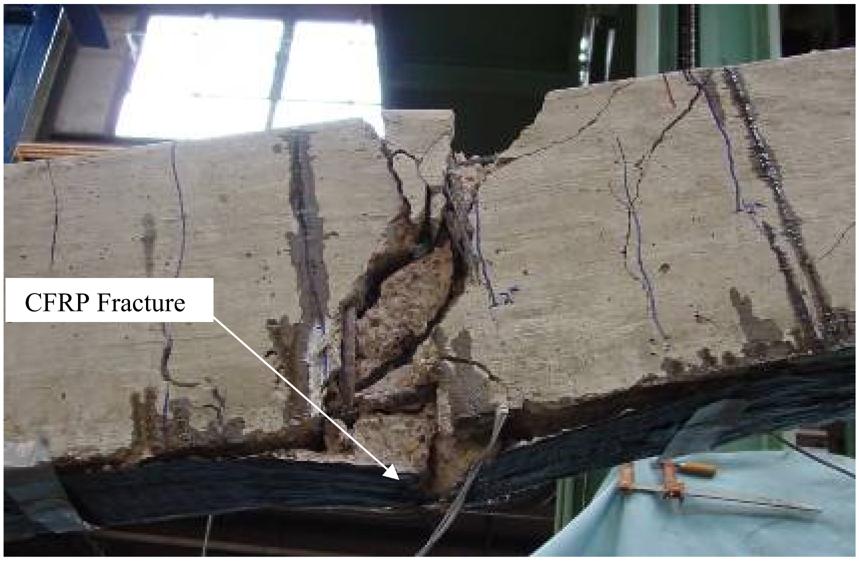

Figure 5-47 Fracture of CFRP at 36 k axial tension in NM-2

Strains at the ultimate load and deflection (10.8 k, 32.3 in.) in the positive moment rebar were well above yield through the middle section of the beam, Figure 5-48. At ultimate vertical load, cracks were present throughout the entire depth of the concrete beam. The strains at ultimate in the negative moment reinforcement were also above yield, Figure 5-49. With yielding in the positive and negative moment reinforcement under catenary action, it is not likely the beam will be able to support additional vertical load without substantial deflection. Yielding of the reinforcement may be the reason for the leveling out of the vertical and axial load versus displacement curves near the end of the test.

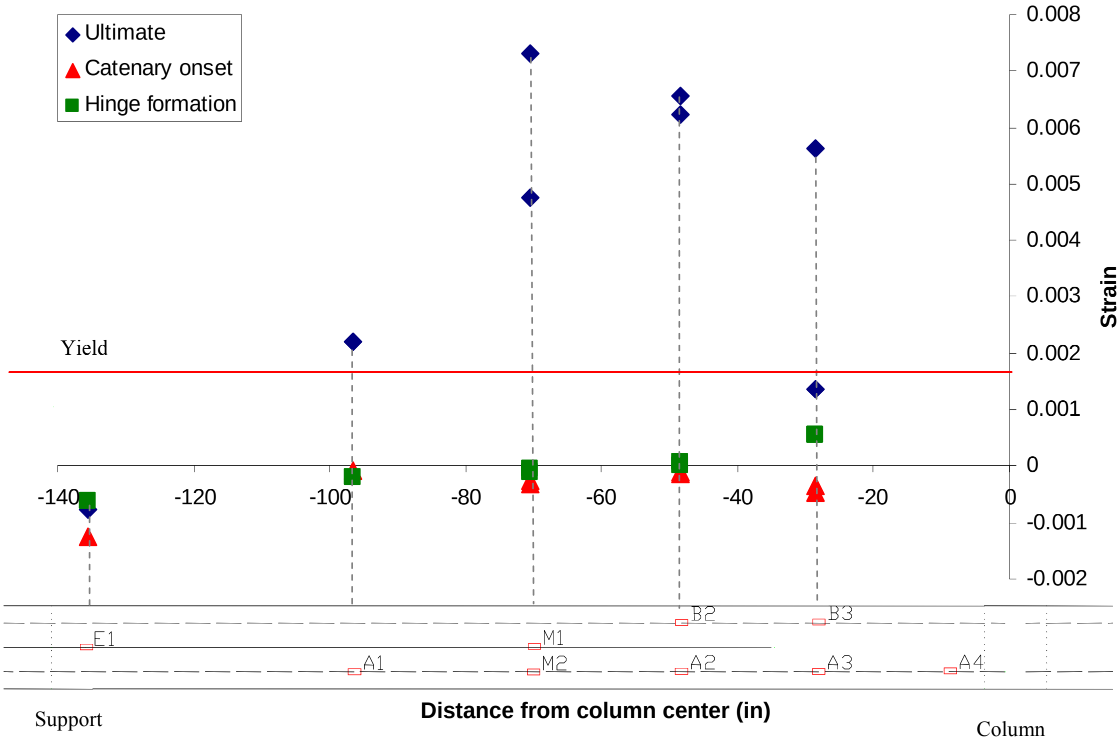

Figure 5-48 Strains in positive moment reinforcement for NM-2

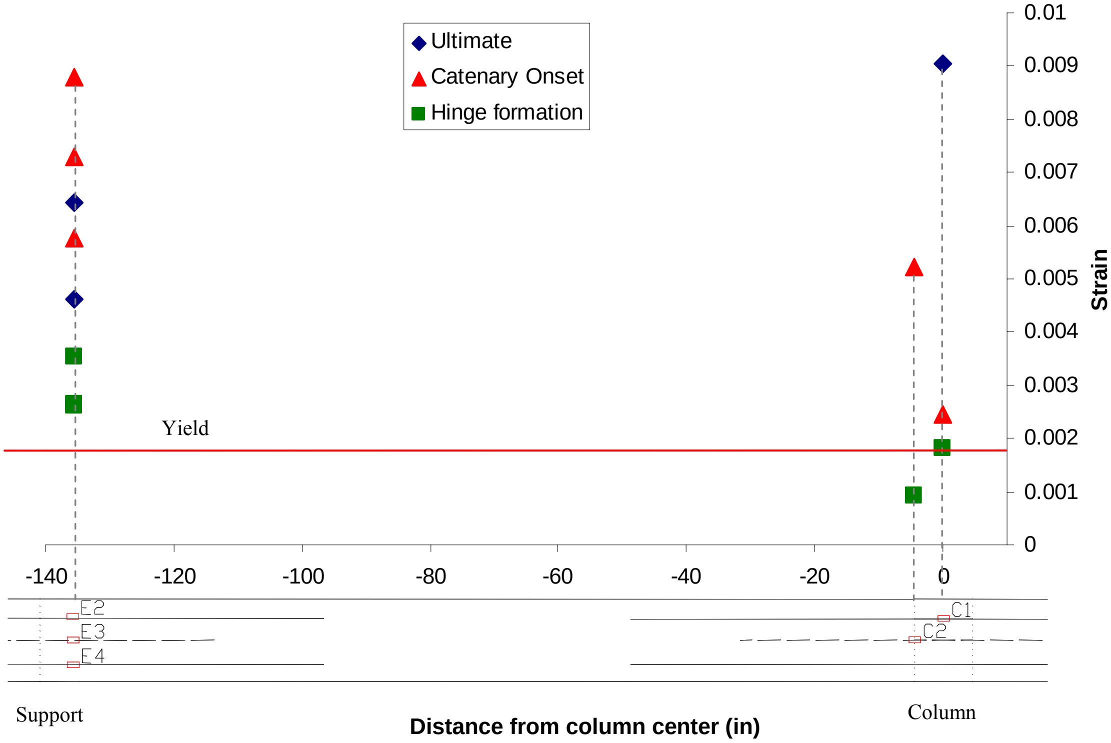

Figure 5-49 Strains in negative moment reinforcement for NM-2

The CFRP fractured at a location just behind a row of anchors with a nearby gage (gage 5) recording a strain of 0.0091, Figure 5-47 and Figure 5-50. The total axial load on the beam was 36.6 k; the capacity of the 6 in. wide CFRP sheet was 30 k. The remaining axial load capacity came from the positive moment rebar. At the time of CFRP fracture, the reinforcement was beyond yield (Figure 5-48), with a tension capacity of 13.2 k. The combined tension capacity from the reinforcement and CFRP was 43.2 k, exceeds the tension at which the CFRP fractured.

The fact that the CFRP fractured just after all the rebar had yielded and the beam was able to reach the desired 10k of vertical load per load point illustrates the efficiency of the amount of CFRP applied. Furthermore, the fact that the CFRP was able to reach at least 90% of its strain capacity confirmed the design detail developed during the anchorage tests.

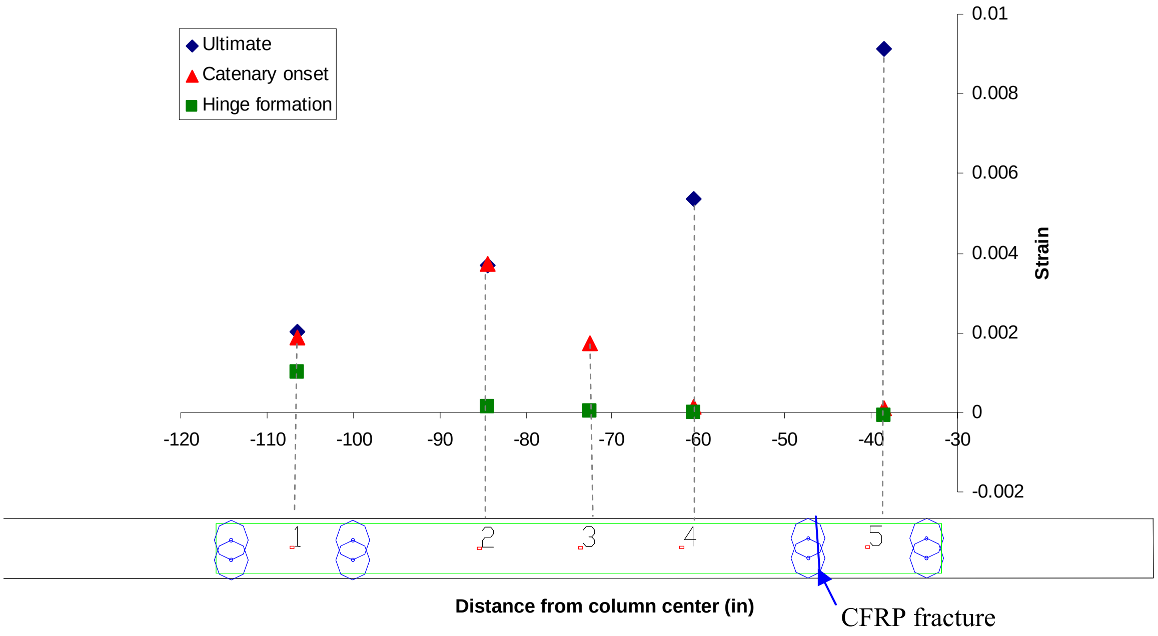

Figure 5-50 Strains in CFRP for NM-2

Additionally for test NM-2, linear potentiometers (pots) were added at the North support location to measure the rotation of the beam. The pots were spaced 10 in. apart and measured rotation over a length of 10 in., Figure 5-51. Based on the data from the pots, the 10 in. section of the hinge rotated by 0.09 radians or 5.2 degrees. The total rotation of the hinge based on the center deflection was 0.22 radians. The difference in the rotations indicates that the hinge length was much longer than 10 in., or the distance between layers of reinforcement. The longer hinge length is also illustrated by the crack distribution shown in Figure 5-52. Furthermore, although the Mattock and Corley (1966) rotational capacity equation used a hinge length of 2d, the result was only 0.11 radians. The remainder of the rotational capacity could be due to shear or axial tension increasing the hinge length. A similar pot was located to measure the opening of the crack next to the column stub, Figure 5-53. This pot measured an opening of 2.6 in., with a corresponding rotation at the section of 0.23 radians.

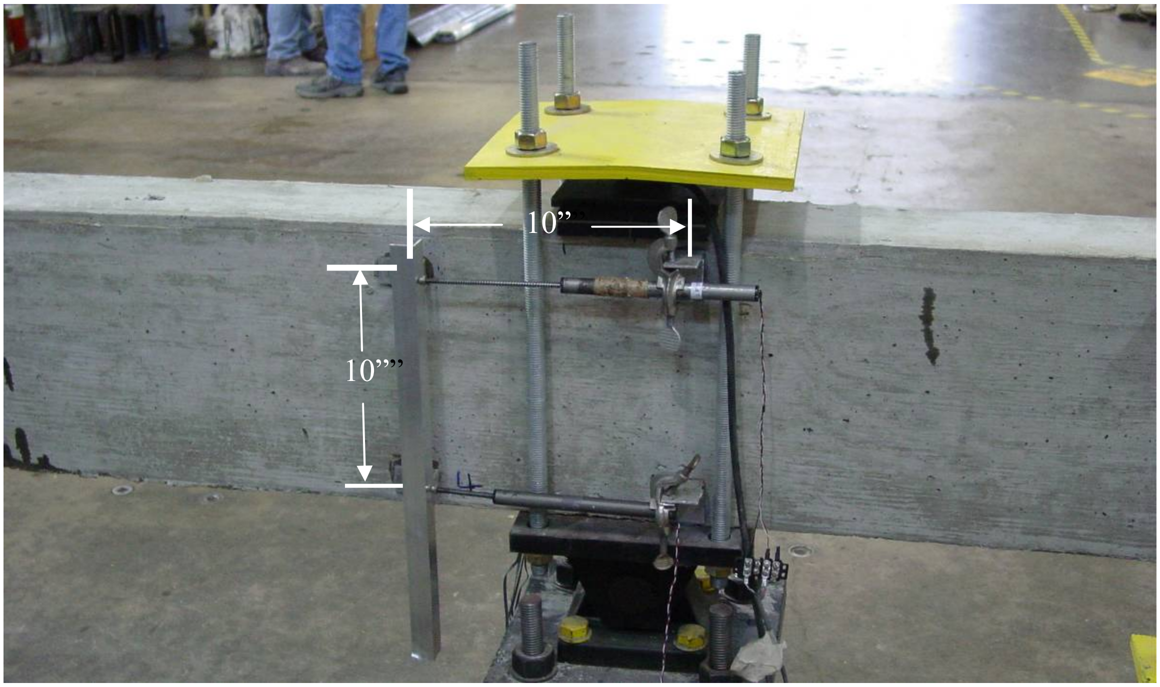

Figure 5-51 Linear pots to measure hinge rotation

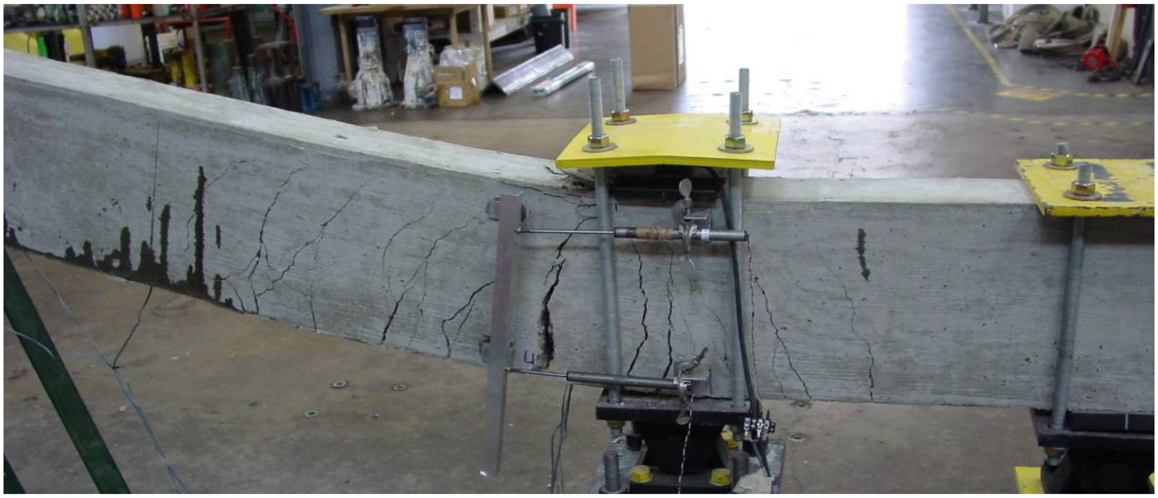

Figure 5-52 Distributed cracking in hinge region

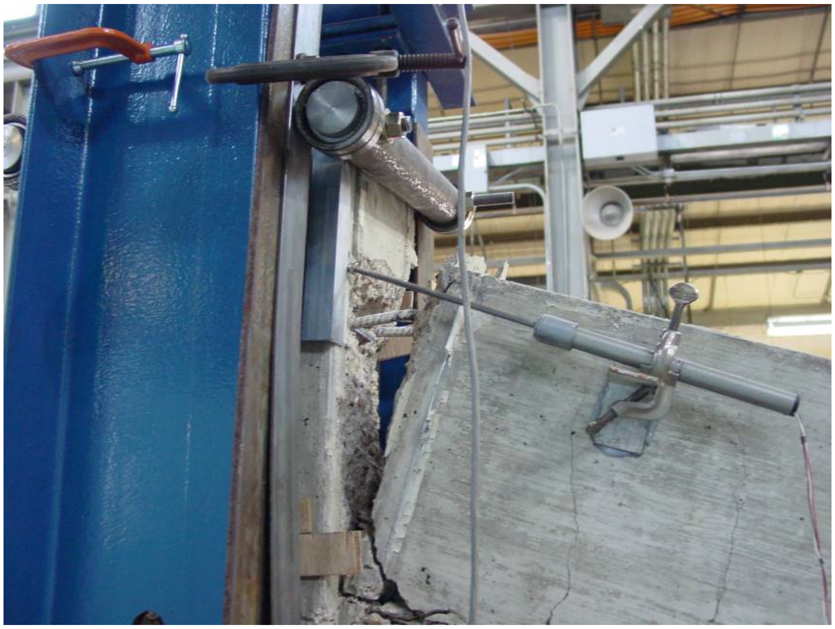

Figure 5-53 Linear pot to measure crack opening

5.5.6 FR-1 – Flexural Retrofit

Although the negative moment retrofits were able to reach catenary action and carry the desired 10 k per load point, a retrofit that does not rely on catenary action and limits deflection may be desirable in some cases. Such cases would include buildings requiring a higher performance objective such as hospitals that may need to remain functional after an abnormal load. Therefore, a beam was strengthened to carry the vertical load through flexure. A comparison was made as to whether it would require less CFRP to strengthen only the positive moment capacity and allow hinges to form at the supports, or to strengthen both the positive and negative moment capacity and allow no hinging to occur. It was determined that strengthening both sides of the beam would require the least amount of CFRP material.

The design procedure for the beam is given in Appendix B and the final design is shown in Figure 5-54. The design required numerous layers of CFRP sheets and rows of anchors to nearly double the moment capacity of some sections. The total area of CFRP applied on this beam was 54 ft^2, or 4.5 times the amount required for NM-2.

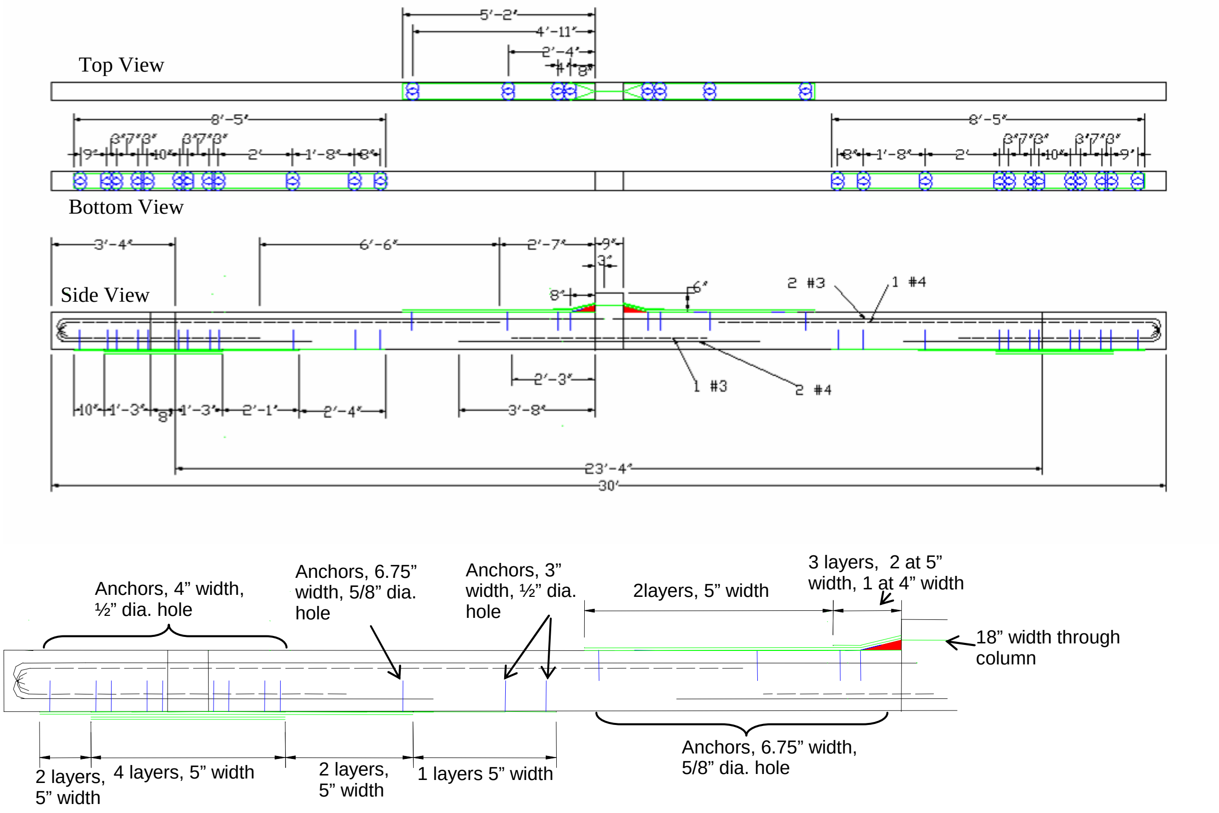
Top View
5′-2″
4′-11″
2′-4″
4″ 8″
8′-5″
3″7″3″
3″7″3″
9″
10″
2′
1′-8″
8″
8′-5″
Bottom View
Side View
3′-4″
6′-6″
2′-7″
9″
3″
8″
6″
2 #3
1 #4
1 #3
2 #4
2′-3″
10″
1′-3″
8″
1′-3″
2′-1″
2′-4″
3′-8″
23′-4″
30′
Anchors, 4” width, ½” dia. hole
Anchors, 6.75” width, 5/8” dia. hole
Anchors, 3” width, ½” dia. hole
2layers, 5” width
3 layers, 2 at 5” width, 1 at 4” width
18” width through column
2 layers, 5” width
4 layers, 5” width
2 layers, 5” width
1 layers 5” width
Anchors, 6.75” width, 5/8” dia. hole

Figure 5-54 Design of CFRP retrofit for FR-1

The specimen was able to reach the desired 10 k per load point at only 6 in. of deflection, Figure 5-55. At this level the anchors at the end of the positive moment CFRP sheet fractured, Figure 5-56. The anchors at this location were designed for a 6 in. wide sheet rather than the 10 in. side sheet that was continued from the previous section. As a result, the anchors fractured rather than the sheet, but they were able to carry the anticipated load (the beam reached 10 k per loading point). After the anchors fractured, the vertical load again increased to 9.4 k at 9 in. of displacement when the negative moment CFRP sheet fractured, Figure 5-57. Although the negative moment CFRP fractured toward the end of the sheet (at the end of the negative moment reinforcement) debonding was present throughout most of the CFRP sheet. Finally at 6 k per load point and 10.6 in. of displacement, the #3 bars (West bar followed by East bar) fractured, Figure 5-58. The specimen developed catenary action and picked up axial tension at about 12 in. of displacement. Due to the unbalanced fracture (failures on only one side of the beam) the rotation of the center column was too great to continue and the test was stopped.

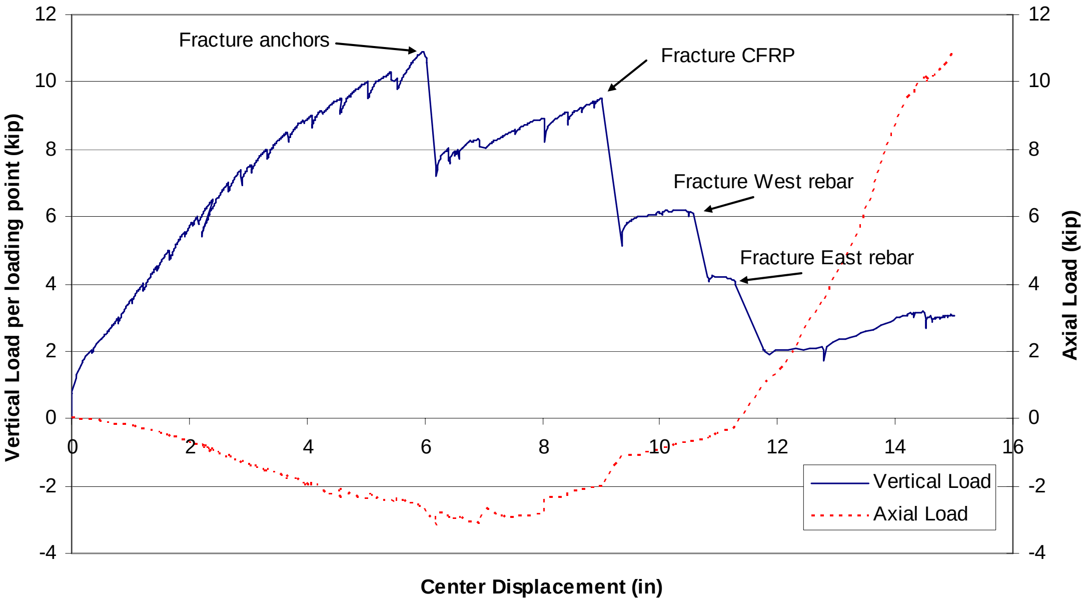

Figure 5-55 Vertical and axial load versus displacement for FR-1

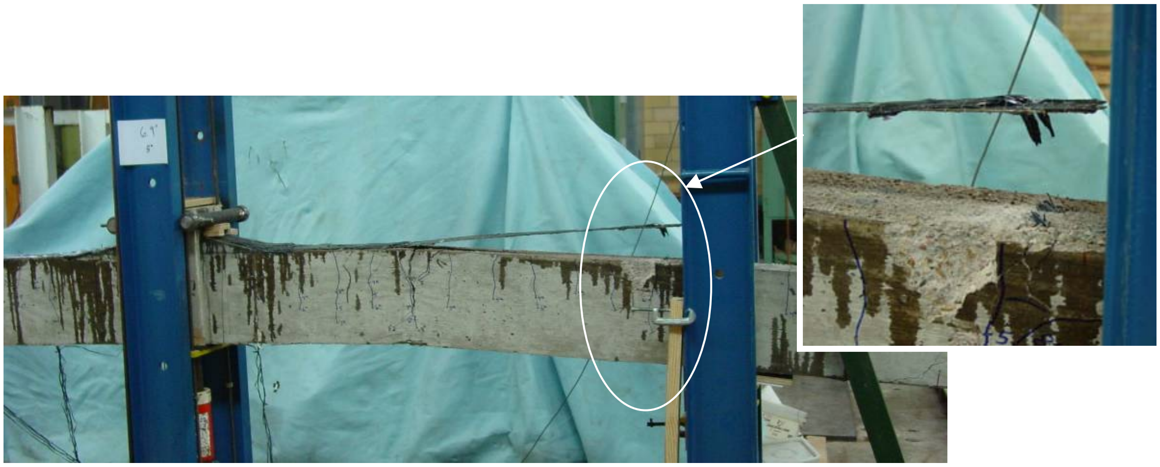

Figure 5-56 Fracture of anchors at end of positive moment reinforcement

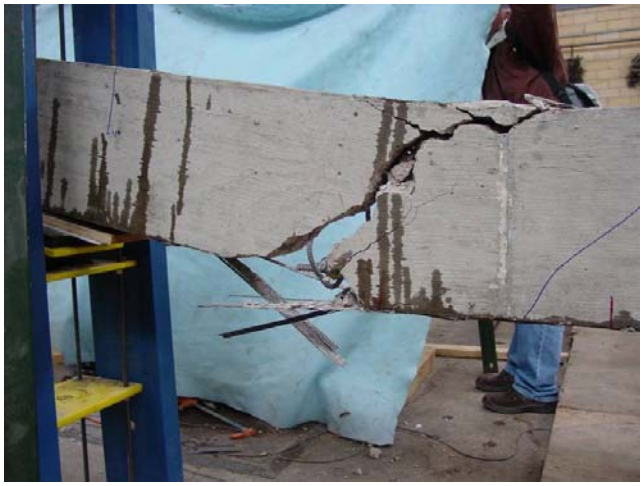

Figure 5-57 Fracture of negative moment CFRP

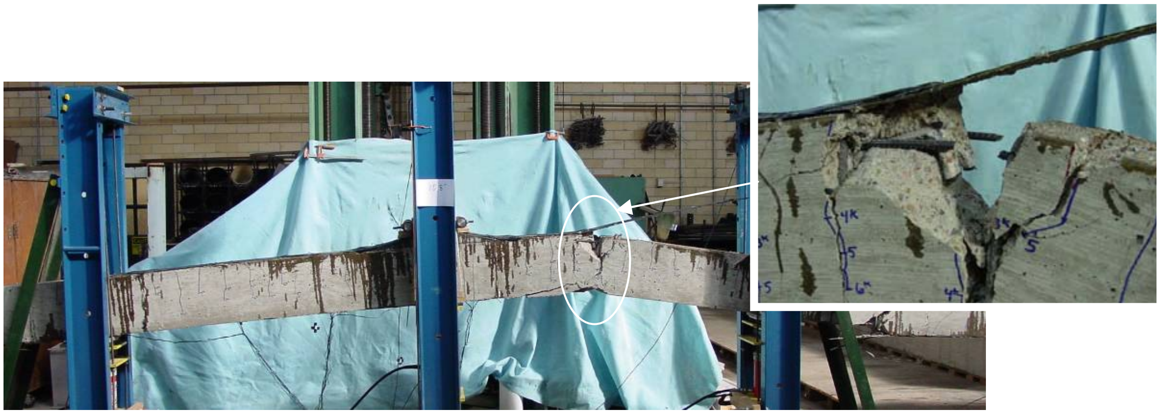

Figure 5-58 Fracture of rebar

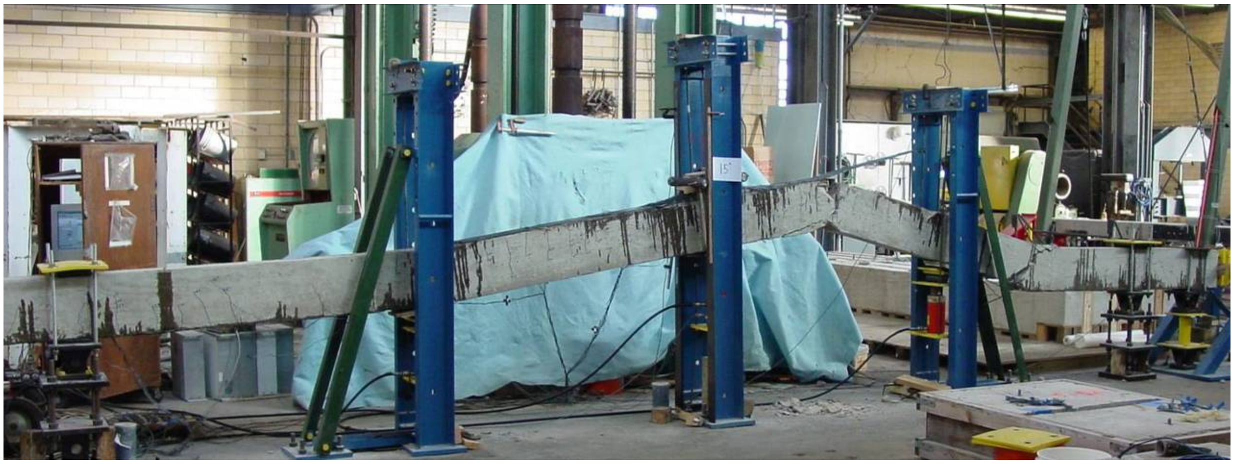

Figure 5-59 Final state of FR-1

The strains in the positive and negative moment reinforcement are given in Figure 5-60 and Figure 5-61. The highest strains in the positive moment reinforcement were recorded in gages M1 and M2. CFRP was provided at that location, and the reinforcement had to resist all the bending moment. For the negative moment reinforcement, high strains exist at the support due to the high moment demand (870 k-in) even though 4 layers of 5 in. wide CFRP was provided. At the column, low strains were observed because of the section is under positive moment at that location.

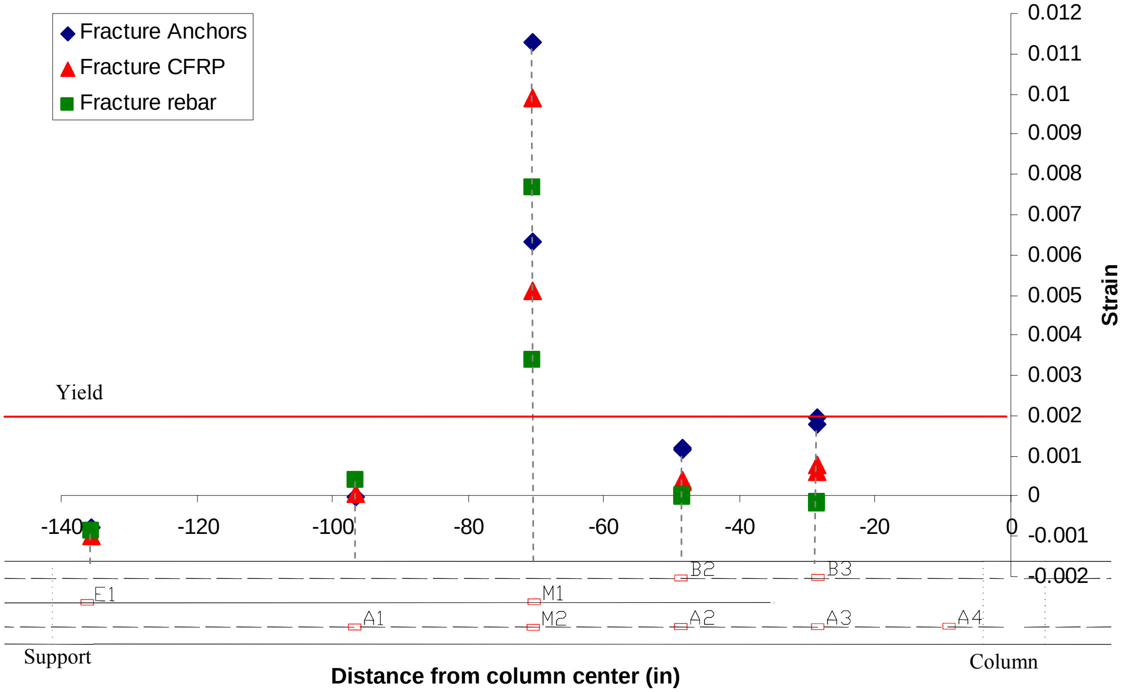

Figure 5-60 Strains in positive moment reinforcement for FR-1

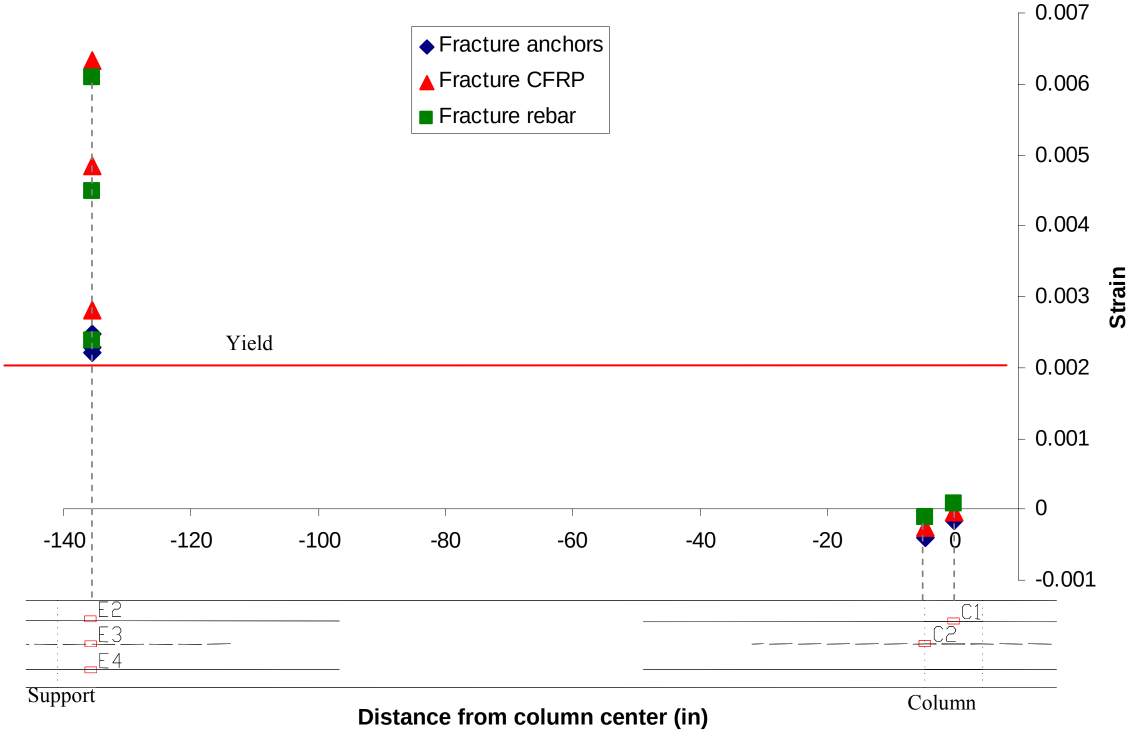

Figure 5-61 Strains in negative moment reinforcement for FR-1

Strains in the CFRP are given in Figure 5-62 and Figure 5-63. Although gages were placed on the North side of the specimen, it was the South side that experienced all the damage. Even so, the gages on the undamaged side of the specimen did experience high strains. For the CFRP at the support, a high strain of 0.008 was recorded at gage 4 when the CFRP fractured at the same location on the South side of the specimen. Additionally, all the strains are fairly high (above 0.004) indicating that although different sections had different numbers of CFRP layers, the design of the CFRP was efficient and all sections were highly stressed. For the column CFRP, a strain of 0.005 was recorded at gage 5 when the last row of anchors fractured on the south side of the specimen. The strain indicates that the tension in that section of CFRP was about 30 k, which was the design capacity of the anchors. A high strain of 0.008 also exists at gage 10 just before the anchors fractured. The high strain indicates that the CFRP was efficiently designed and if the anchors had not failed the CFRP would have fractured at that location.

The high strains throughout the CFRP indicate how well the design details developed from the anchorage tests worked on this beam. Although numerous layers of CFRP were applied, and moment demands varied throughout the length of the CFRP, the anchors delivered their desired performance and allowed the CFRP to reach much higher strains and tensional forces throughout the retrofit. In fact much of the CFRP along the support and some along the column debonded during the test, but the anchors transferred forces from the CFRP to the concrete and maintained the section’s moment capacity.

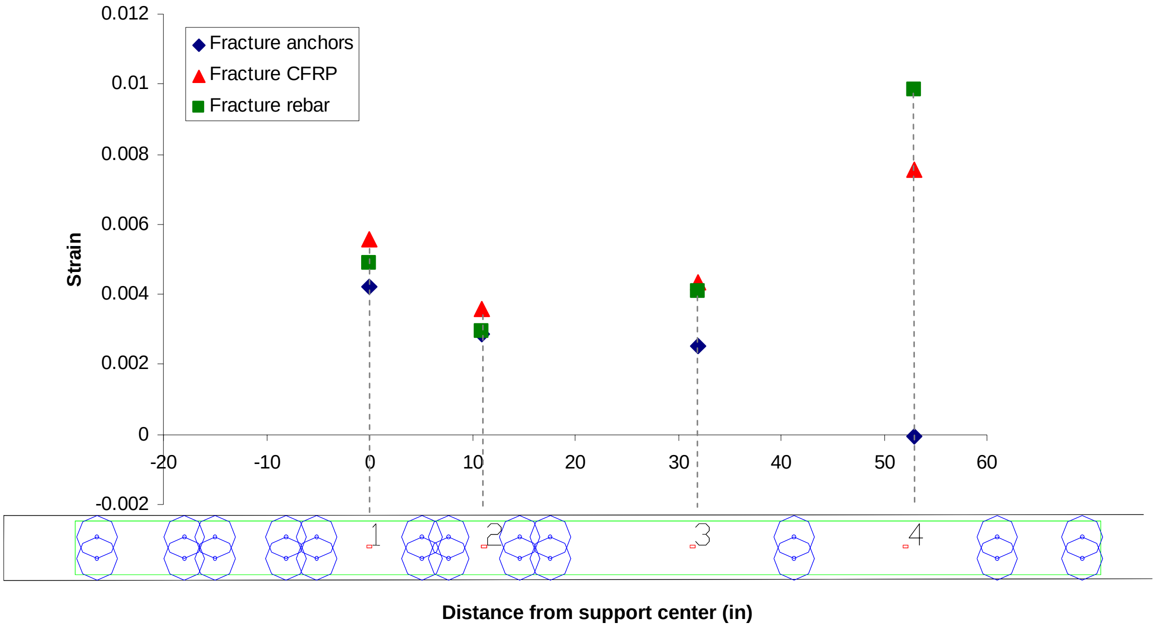

Figure 5-62 Strains in CFRP over support region for FR-1

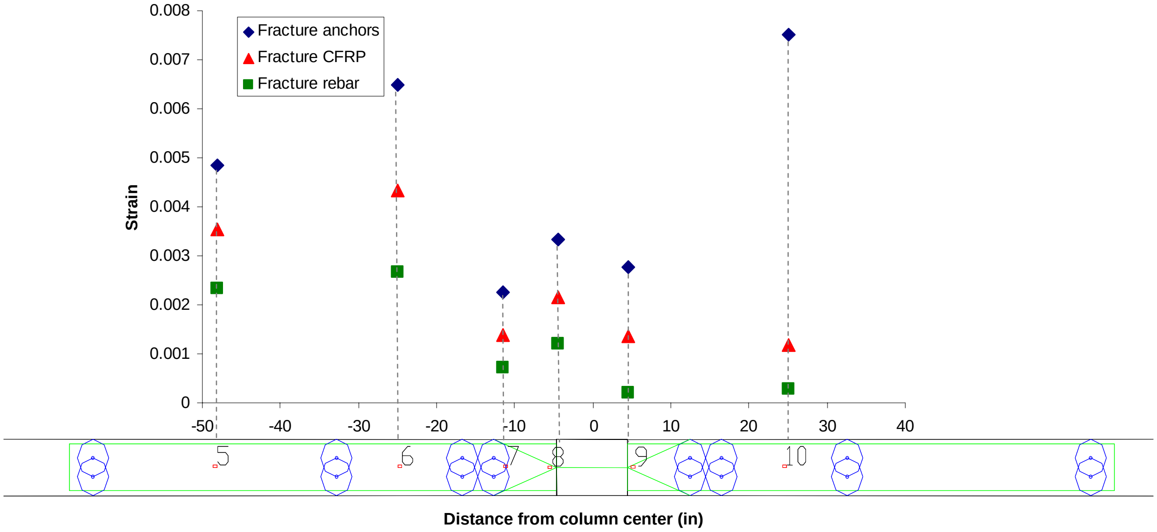

Figure 5-63 Strains in CFRP over column region for FR-1

5.5.7 CR-1 Continuous Reinforcement

The final test considered the catenary capacity of a beam designed according to current ACI Chapter 7 guidelines for continuous reinforcement. The design for the beam contained 18 in. splices of the #3 bars at the column and at the midspans, Figure 5-64.

An amount greater than the ACI required continuity steel was provided in both cases. One half of the positive moment steel (two #3 bars) was continuous across the column line, ACI requires 1/4 continuous. One-quarter of the negative moment steel (one #3 bar) was continuous across the midspans of the beam, ACI requires 1/6 continuous.

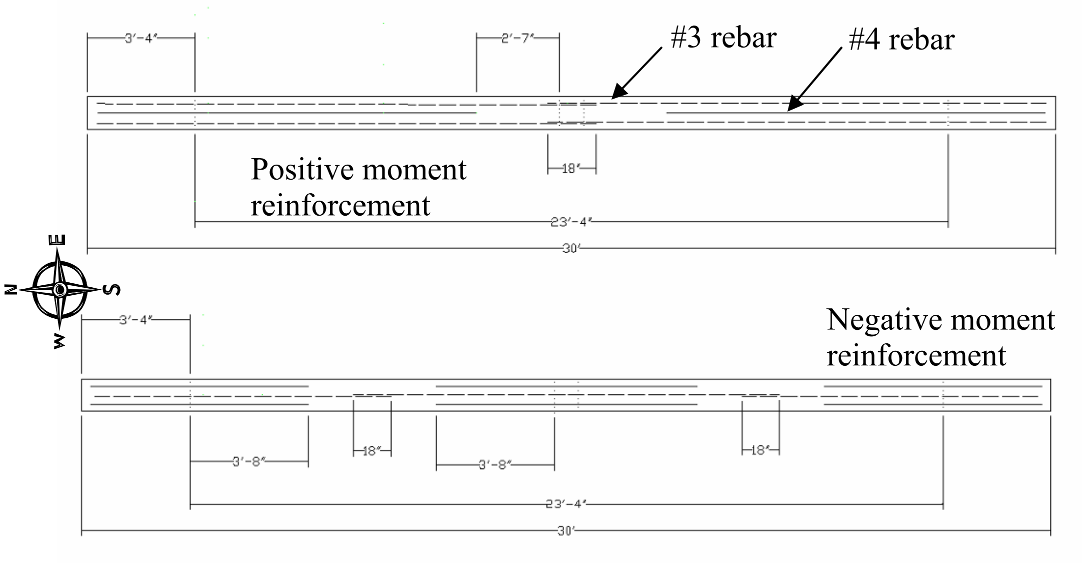

Figure 5-64 Design of specimen CR-1

The beam reached 5 k load per load point when hinges began to form next to the column stub, Figure 5-65. At 10.5 in. of displacement the East #3 positive moment rebar, followed by the West rebar fractured, Figure 5-66. As with PM-1, the rebar fractured due to the high rotation demand at that section. Based on the equations of Mattock and Corley the rotation capacity of that section is 0.098 radians. In order to reach catenary action (18 in. displacement), the required rotation would be 0.13 radians. Although the available rotation is close to the required rotation, both the failure in PM-1 and CR-1 indicate that the section does not have enough rotational capacity to reach catenary action.

The load then dropped to 3 k per load point until 16 in. of displacement was reached and the South negative moment rebar followed by the North rebar fractured, Figure 5-67. The reinforcing bars fractured due to the high moment demand at that section. In order for sections at the support to hinge at 420 k-in (as in NM-1 and NM-2) a section at the fracture location has a moment of 200 k-in. The capacity of this section was only 92 k-in. If the area of reinforcement had been larger (0.32 in^2) to allow hinges to form at the support, the reinforcement would have remained intact until catenary action was reached. However, in order to reach the desired 10 k load per load point to resist progressive collapse, the tension capacity of the rebar would need to be about 30 k (see specimen NM-2 whose CFRP capacity was 30 k), requiring a reinforcement area of 0.5 in^2. However, if strain hardening is considered with a steel strength of 100 ksi, only 0.3 in^2 would be needed, corresponding to a little more than half of the negative moment reinforcement continuous (1/4 was provided, 1/6 required by ACI 318). After fracture of the continuous rebar the beam behaved like NR-2 that had no continuous reinforcement.

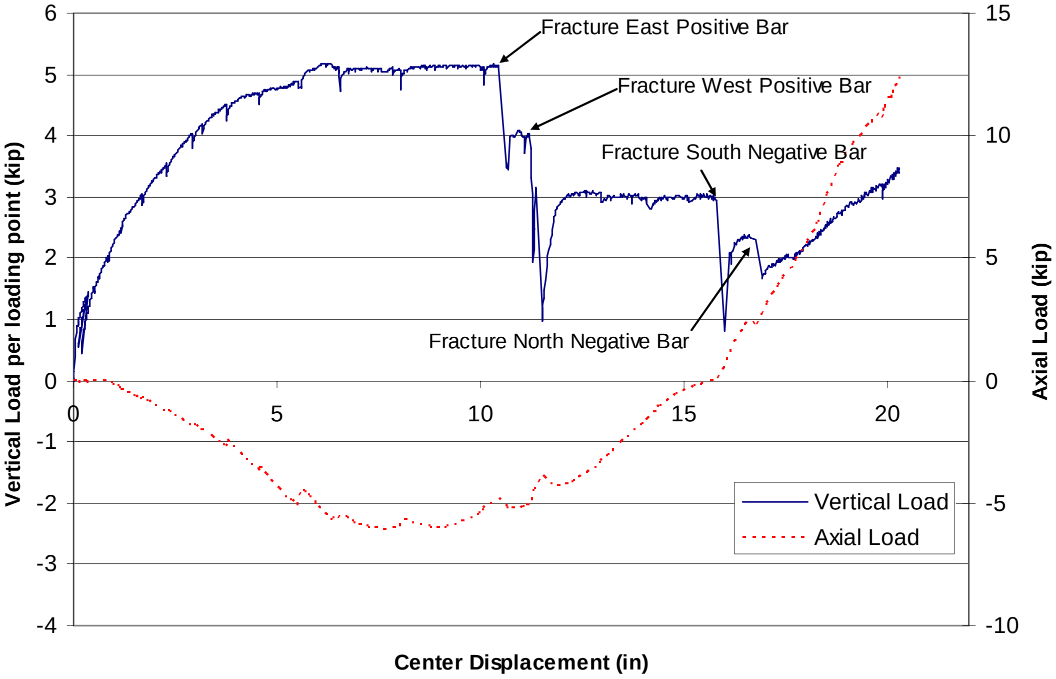

Figure 5-65 Vertical and axial load versus displacement for CR-1

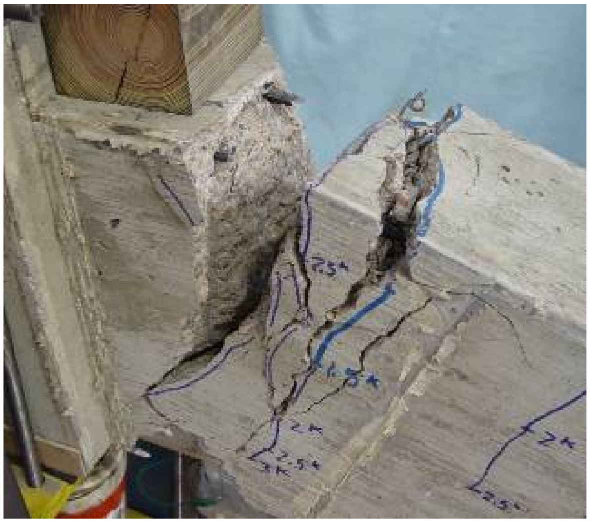
2.5k
1.5k
2k
2.5k
3k
2k
2.5k

Figure 5-66 Fracture of positive moment rebar

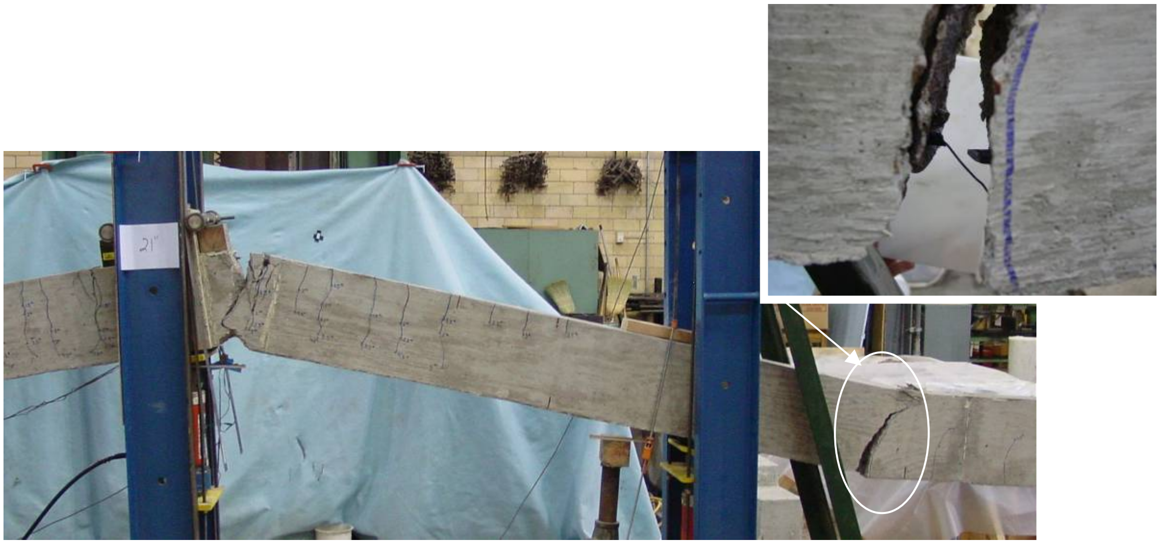

Figure 5-67 Fracture of negative moment rebar

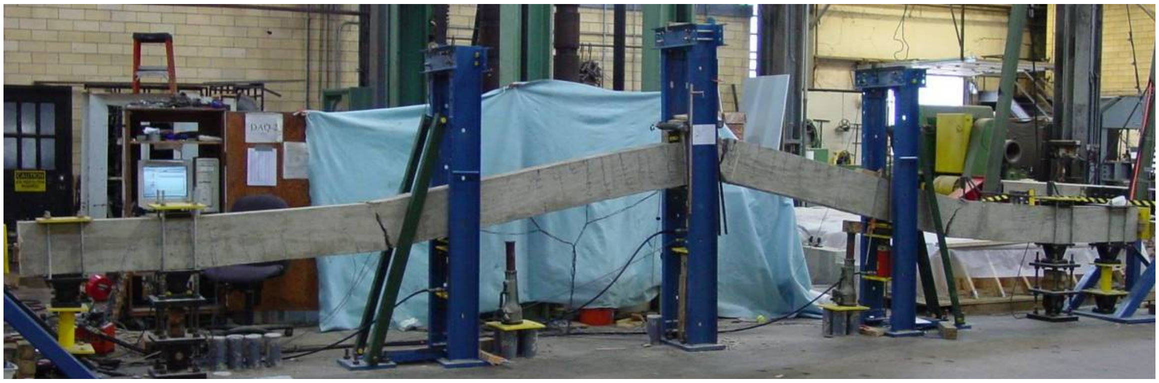

Figure 5-68 Final state of CR-1

Strains in the positive moment reinforcement are given in Figure 5-69. Although the rebar fractured at a location just past the end of the splice on the South side of the column, the gage near the same location on the North side of the column barely exceeded yield. It is likely that the rebar on the South side yielded first and limited the strains in nearby locations. High strains were recorded in gage B3, though gage A3 did not record high strains. For the negative moment reinforcement, strains were high at E2, E3, and E4 due to the hinging in the area, Figure 5-70. Unfortunately gage T1, located at the point where the negative moment reinforcement fractured, ceased to work before the reinforcement fractured. However, at a load of 4 k and displacement of 10 in., the gage recorded a strain of 0.014 indicating that the rebar was well on its way to fracture.

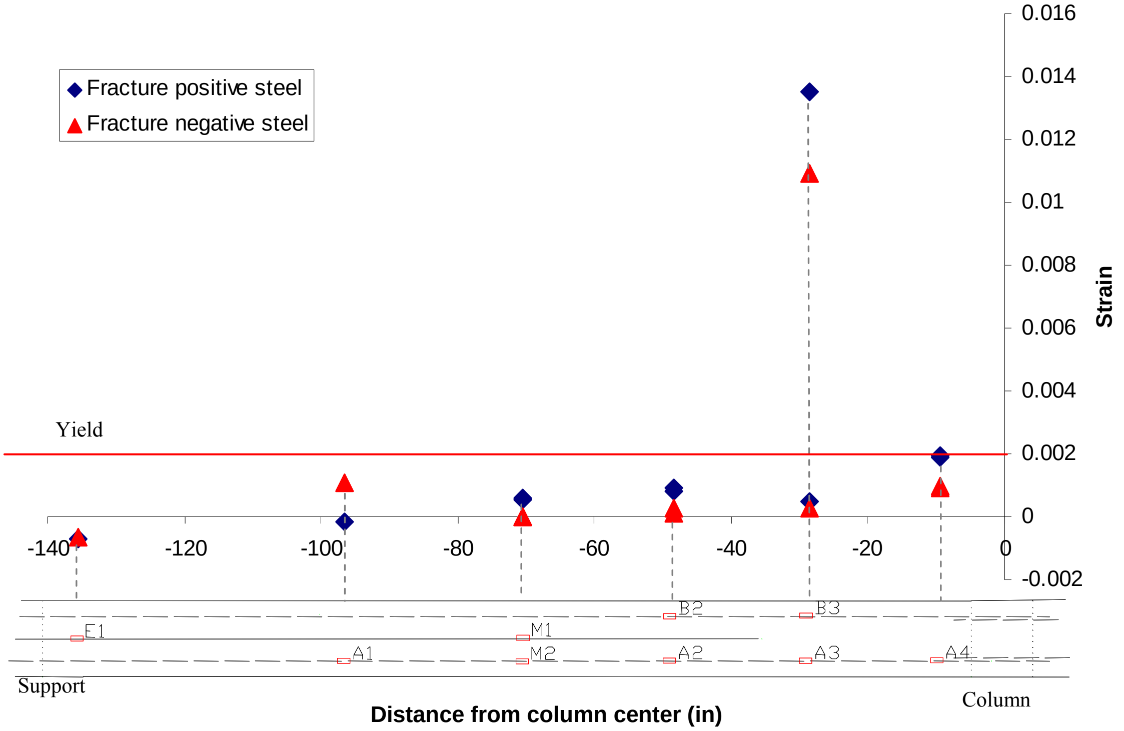

Figure 5-69 Strains in positive moment reinforcement for CR-1

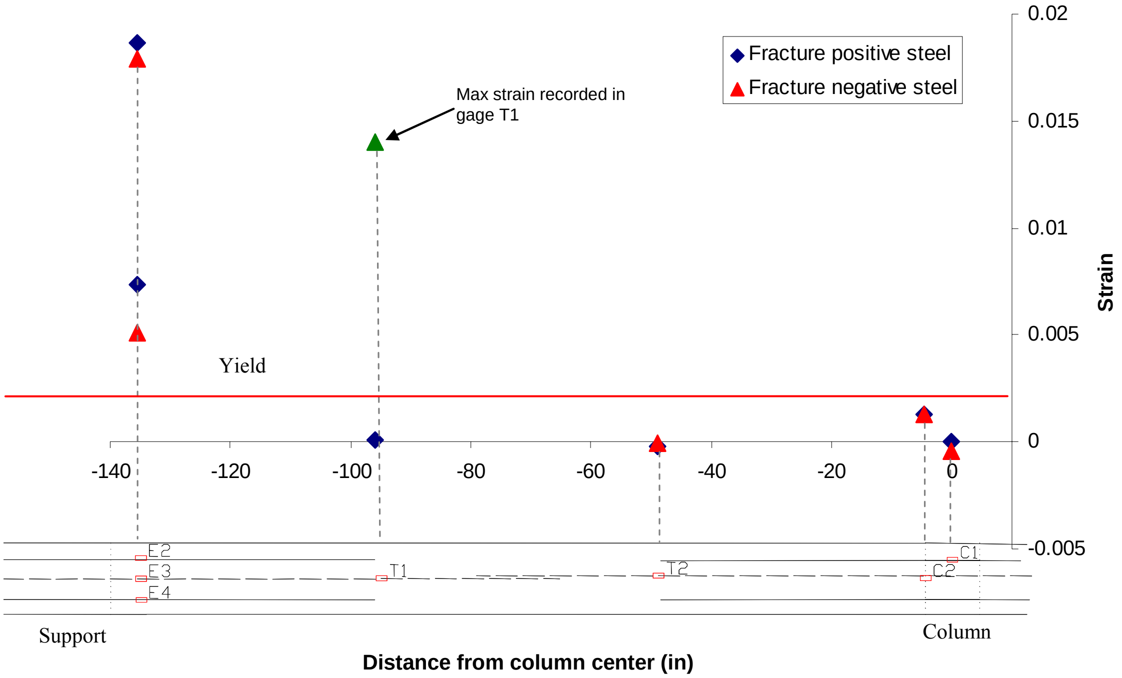

Figure 5-70 Strains in negative moment reinforcement for CR-1

5.6 TEST COMPARISONS

A comparison of the vertical load versus displacement for all tests is shown in Figure 5-71. The improved behavior of the negative moment retrofits over the positive moment retrofits and un-retrofitted specimen is apparent by both reaching the desired 10 k of load per loading point and retaining a high load carrying capacity throughout the test. A comparison of the axial load versus displacement for all tests is shown in Figure 5-72. Although the reinforcement or retrofit of specimens was different, they all follow a similar axial load versus displacement curve. The curve consists of a compression phase followed by a catenary tension phase starting at 15 to 18 in. of displacement. The similarity of the curves indicates that the catenary response of the beam depends more on the beam geometry than on the reinforcement or retrofit. However, the retrofit of the NM-1 and NM-2 beams allowed them to reach an axial load corresponding to the 10 k per load point needed to resist progressive collapse.

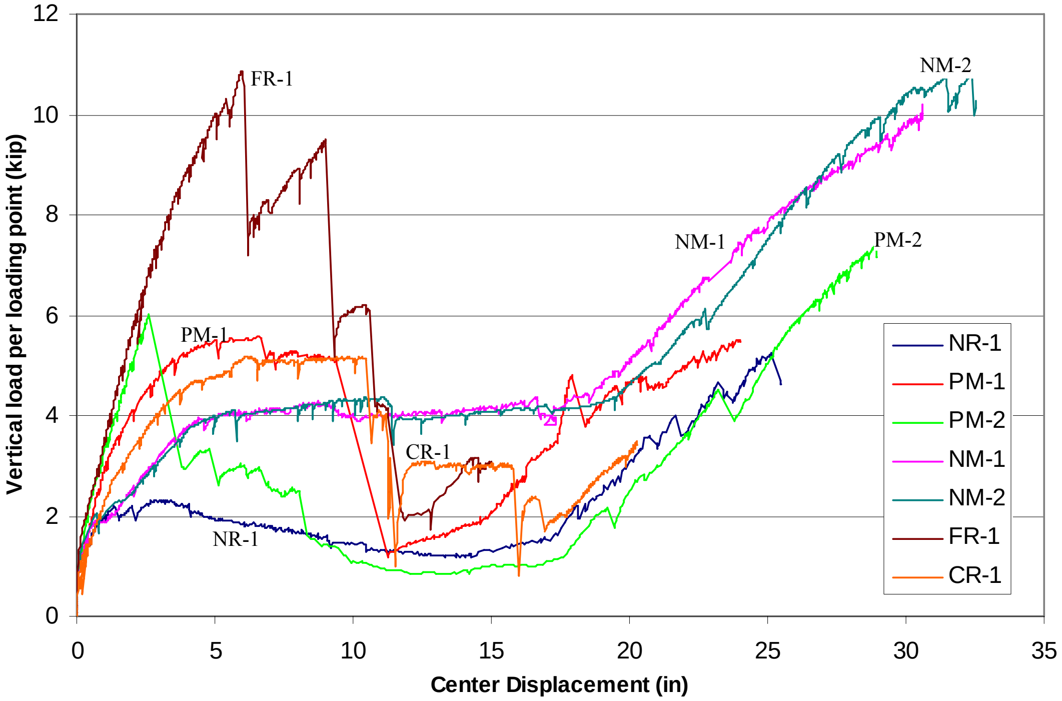

Figure 5-71 Vertical load versus displacement for all tests

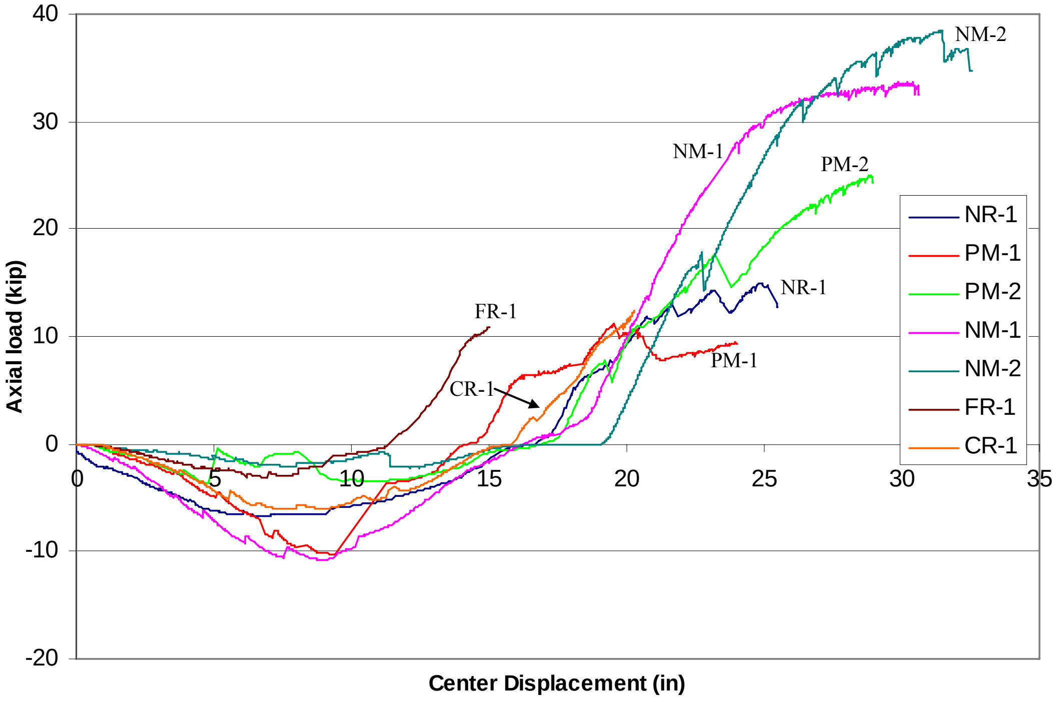

Figure 5-72 Axial load versus displacement for all tests

One objective of the tests was to determine if CFRP sheets can be used to establish continuity similar to that of beams with reinforcement detailed as required by ACI 318. Comparison of PM-1 and CR-1 clearly show very similar behavior and indicate that the CFRP was able to provide comparable continuity even if continuity insufficient to reach 10 k per load point to resist progressive collapse as required by GSA guidelines, Figure 5-73. Furthermore, the two negative moment retrofits, NM-1 and NM-2, show identical results confirming the repeatability of the tests, Figure 5-74.

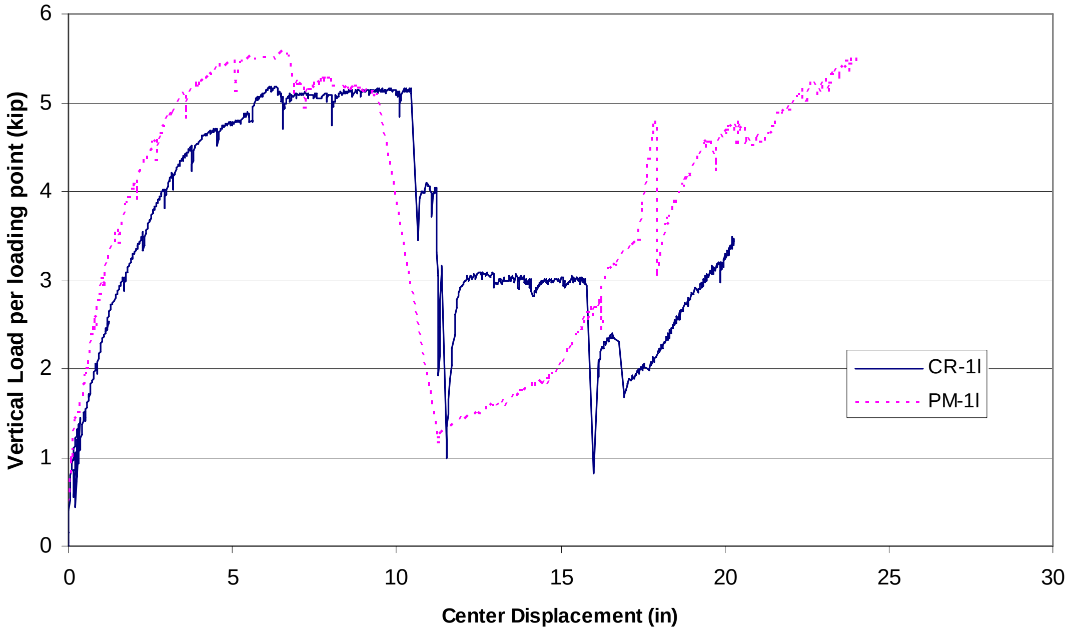

Figure 5-73 Comparison of PM-1 and CR-1

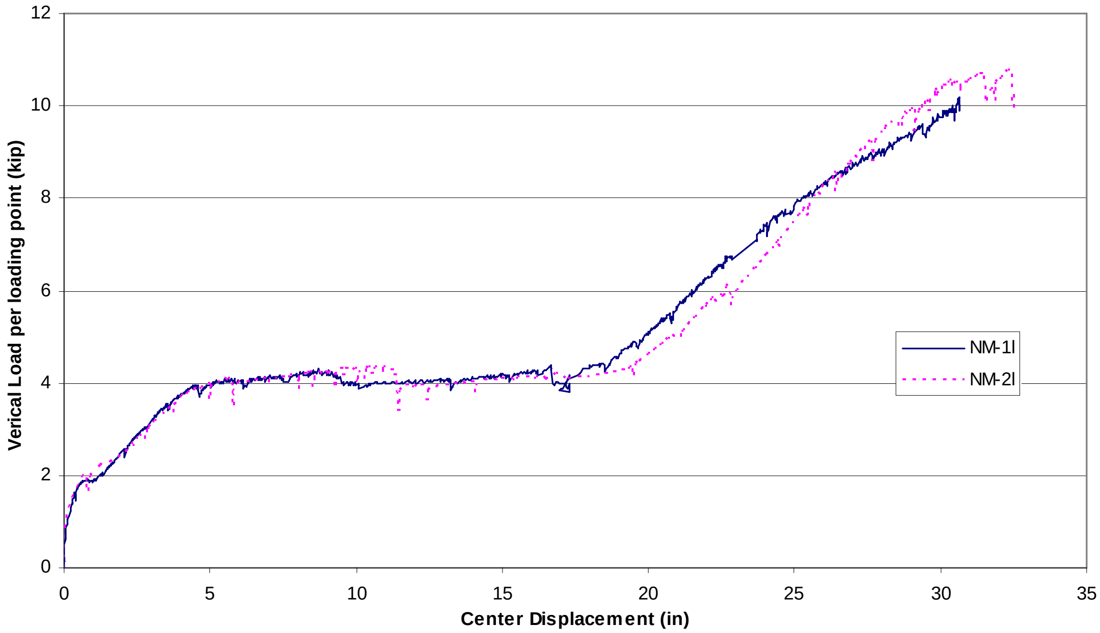

Figure 5-74 Comparison of NM-1 and NM-2

5.7 CONCLUSIONS

Eight specimens (one not reported) were tested to determine the ability of CFRP materials to provide continuity and reduce vulnerability to progressive collapse, Table 5-4. The capacity for catenary action of vulnerable RC building beams with discontinuous reinforcing steel and the increased capacity achieved by the CFRP retrofit were evaluated. Additionally, tests were conducted on a beam with continuous reinforcing steel and a beam strengthened to accommodate the double span through flexure.

Table 5-4 Results of continuity tests

Test	Maximum Load per Load Point (k)	Deflection at Max Load (in)	Deflection at Beginning of Catenary (in)	Max Axial Tension (k)	Area of CFRP (ft^2)	Intermediate Failure	State at End of Testing
NR-2	5.2	24.6	17	14.6	None	Hinge formation at 2.3 k and 3 in.	Failure of beam end due to poor concrete
PM-1	5.5	23.8	14	9.3	6.3	Rebar fracture at 5 k and 10 in.	Test stopped due to misalignment
PM-2	7.3	28.9	18	24.3	18	CFRP fracture at 6 k and 2.6 in.	Test stopped due to high displacements and misalignment
NM-1	10.0	30.6	17	32.4	16	Hinging at support at 4 k and 5 in.	Failure of test setup (fracture of threaded rod)
NM-2	10.8	32.3	19	36.6	12	Hinging at support at 4 k and 5 in.	Fracture of CFRP
FR-1	10.9	6.0	11	10.8	54	Fracture of CFRP at 10.9 k and 6 in.	Continued fracture of CFRP and rebar
CR-1	5.0	10.5	16	12.4	none	Fracture of pos. mom. rebar at 5 k and 10.5 in.	Continued fracture of rebar

The un-retrofitted specimen, NR-2, developed hinges and was able to carry significant load (5.2 k vertical load per loading point) due to catenary action. The catenary tension was transferred from the positive moment steel through the stirrups to the negative moment steel. However, the catenary action did not initiate until around 17 in. or 5% of the span length of displacement.

CFRP was used to provide continuity through the positive moment reinforcement and was able to increase the capacity of the beam before catenary action developed. However, the CFRP retrofit on specimen PM-1 caused a concentrated hinge at the end of the CFRP sheet to develop at 4 k of vertical load and eventually led to fracture of the rebar. Continuity of reinforcement was lost and the beam behaved like an un-retrofitted specimen. The PM-2 retrofit provided continuity through an extra #4 bar reached 6 k of vertical load before the CFRP fractured. If the CFRP had not fractured, a hinge would have formed at the end of the CFRP sheet at about 6.8 k of vertical load. Neither of the positive moment retrofits were able to reach the representative 2 times dead plus 25% live load recommended by the GSA guidelines.

CFRP can also be used to provide continuity through the negative moment reinforcement. NM-1 and NM-2 were able to reach the representative 2 times dead plus

25% live load recommended by the GSA guidelines. In both tests a hinge formed at the support that had sufficient ductility to allow the beam to reach catenary action. After catenary action started, the CFRP had sufficient tensile capacity (at least 30 k) to carry the high axial loads due to the catenary action.

A retrofit that strengthened the beam flexurally required 54 ft^2 of CFRP (4.5 times the amount of CFRP for NM-2) and was also able to reach the representative 2 times dead plus 25% live load recommended by the GSA guidelines at only 6 in. of deflection. Although, the retrofit preformed as desired the large amount of CFRP required may make this option unfeasible for a life safety performance objective. For critical buildings (such as hospitals), requiring a better performance, limiting the deflections and damage may be desirable.

A beam with continuous reinforcement (exceeding the ACI Chapter 7 requirements) was not able to reach the representative 2 times dead plus 25% live load recommended by the GSA guidelines. Hinges formed at the face of the column at 5 k of vertical load, which led to fracture of the positive moment reinforcement due to the limited rotational capacity of that section. Furthermore, the continuous negative moment reinforcement also fractured. After fracture of the continuous reinforcement the beam behaved as NR-2 without ever having reached catenary action.

The design philosophy for the carbon fiber anchors developed during the anchorage tests worked extremely well for the catenary tests. The anchors allowed for the development of high strains and fracture in the CFRP.

In general, the catenary test results agreed with previous results reported by Regan (1975), including the importance of ductility (or rotational capacity) to achieve catenary action, a compressive arch phase followed by a catenary tension phase, and catenary action starting at a deflection slightly greater than the beam depth.

The overall conclusion based on the continuity tests is:

- CFRP, if designed correctly (placed in locations that do not cause rebar fracture before catenary action is developed), may be able to reduce vulnerability to progressive collapse.

The specific conclusions based on the continuity tests are:

- Beams without continuous reinforcement can reach catenary action, if the catenary forces can be transferred between the positive and negative moment reinforcement.
- CFRP can be used to provide continuity in the positive moment reinforcement, however, continuity may not lead to improved progressive collapse resistance if the beam does not have sufficient rotational ductility to reach catenary action.
- CFRP also can be used to provide continuity in the negative moment reinforcement, and may cause the beam to have improved rotational ductility (force hinge development at more ductile sections that are able to reach catenary action before fracture of the rebar) to reach catenary action.
- CFRP can be used to improve the flexural resistance of a beam to a point where it would resist progressive collapse. Such a retrofit would limit deflections and provide a higher performance objective, but require a much greater amount of CFRP.
- Beams with continuous reinforcement (exceeding to Chapter 7 of the ACI 318 code) may not have improved progressive collapse resistance due to limited ductility in the beam (beam may not be able to reach catenary action before rebars fracture).

Chapter 6: Catenary Model

The development of a catenary action model, comparison of that model to the continuity test results, and use of the model to represent the response of the prototype structure will be discussed in this chapter.

6.1 MODEL DEVELOPMENT

A catenary action analysis model was created to understand the mechanisms governing catenary action. A system of equations was developed to characterize the load and deflection relationship of a reinforced concrete beam in catenary action. The equations are based on the fundamental concepts of equilibrium, compatibility, and material characteristics. With the knowledge of the load-deflection relationship of a catenary and the axial tension expected, the effect of the catenary action on the rest of the structure can be determined.

The analysis model was based on the results of the continuity tests. These results were broken into two sections. Case 1 was based on the negative moment retrofits and Case 2 based on no retrofit. Both cases involve solving equations for equilibrium and compatibility.

6.1.1 Case 1 (Retrofitted)

For case 1, the catenary model has flexural moment resistance at the support and no moment resistance at centerline. This case applies to specimens NM-1 and NM-2, where a hinge at the support provided moment resistance and a wide crack at the center of the beam (due to discontinuous positive moment reinforcement) provided little moment resistance. In Figure 6-1, an idealization of NM-2 is shown. The beam deforms as a rigid block between the support and center column. The CFRP and the negative moment reinforcement provide a continuous tension tie for catenary action. As with the tests, everything is inverted, upward deflection in the figures is actually downward deflection in a real structure.

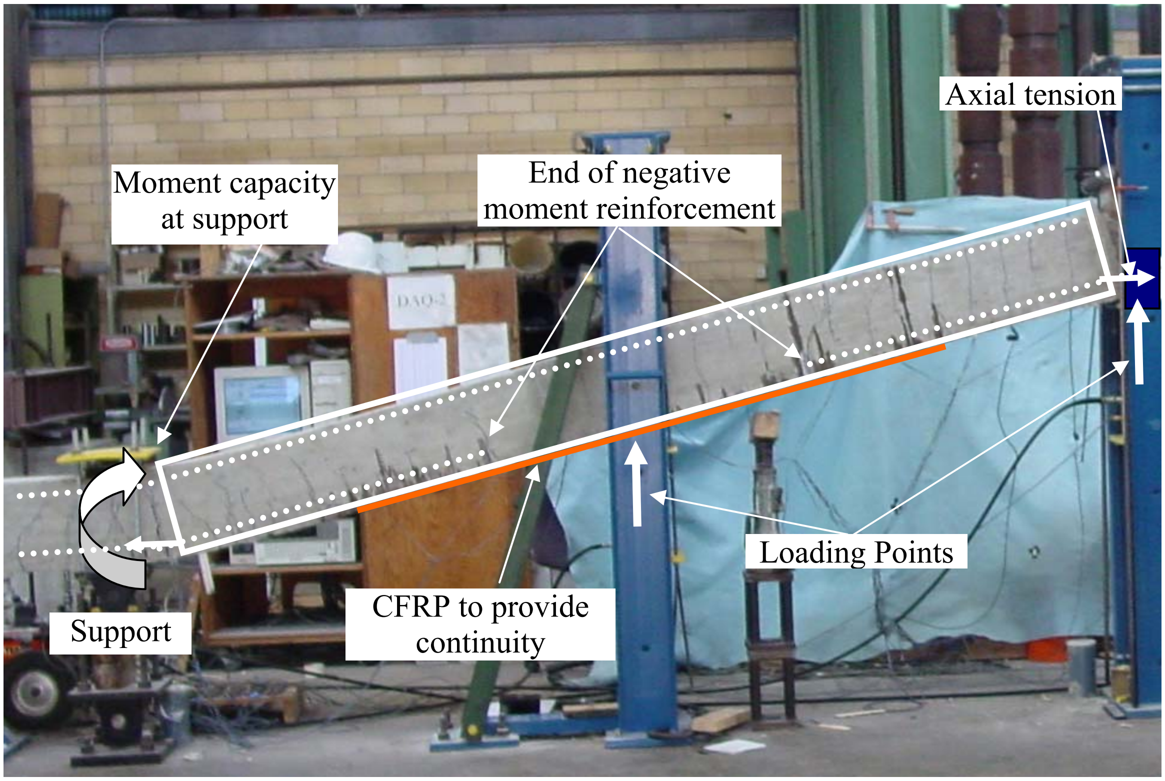
Axial tension
Moment capacity at support
End of negative moment reinforcement
Loading Points
Support
CFRP to provide continuity

Figure 6-1 Idealization of specimen NM-2 for case 1

6.1.1.1 Equilibrium

The equilibrium equation for this case is based on the assumption that the beam deforms as a rigid block with a specified flexural moment resistance at the support and no moment resistance at centerline. In Figure 6-2, a free body of case 1 is illustrated. The beam model is symmetric about the centerline, or removed column, and only half of the beam is modeled. From equilibrium and neglecting bending within the concrete block and the beam's self weight, the sum of the moments about the support point is:

$$M + A\Delta - P\frac{L}{2} - \frac{P}{2}L = 0$$ **Equation 6-1**

The value of axial tension can be expressed by rearranging Equation 6-1.

$$A = \frac{PL - M}{\Delta} \geq 0$$ **Equation 6-2**

where M is the nominal flexural capacity of the hinge at the support, A is the axial tension, Δ is the center deflection, P is the point load, and L is the length of the modeled half of the beam(support to centerline). For general cases, the term PL would be replaced by the moment resulting from loads on the beam (for example, $\omega L^2/2$ for a uniform load ω). If the resisting moment M is greater than the applied moment PL, the axial force A is zero or in compression and catenary action has not yet begun. Therefore, catenary action does not begin until the beam has formed a mechanism and can no longer carry additional vertical loads in a flexural manner, or PL > M. The equation is only valid after catenary action has begun and Δ is greater than 0.

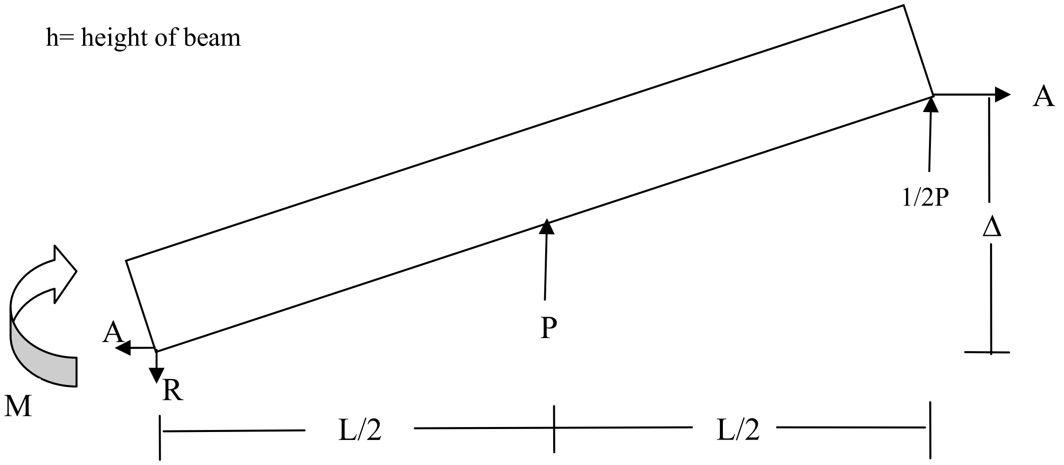

Figure 6-2 Free body diagram of case 1

6.1.1.2 Compatibility

In order to determine the catenary response of the beam, the axial extension of the beam also must be taken into account. The axial extension (δL) is due to geometry, support movement, and beam elongation. The components of axial extension can be determined from the applied loads and geometry of the beam (see Section 6.1.1.3). The elongated length of the beam is the hypotenuse of a right triangle with legs of the original length L and center displacement Δ, Figure 6-3.

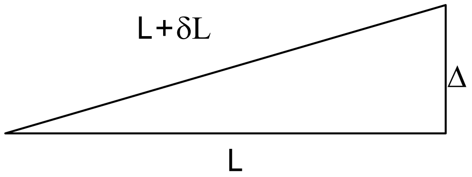

Figure 6-3 Deflection compatibility

Therefore, the deflection of the beam that satisfies compatibility is:

$$\Delta = \sqrt{(L + \delta L)^2 - L^2} \qquad \textbf{Equation 6-3}$$

Equation 6-2 and Equation 6-3 are expressed in terms of Δ and P and can be solved simultaneously for different values of load P to give the catenary response of the beam.

6.1.1.3 Axial Extension

The amount of axial tension and beam deflection is highly dependent on the axial extension in the beam. Any axial movement that does not require axial force (such as extension due to geometry or slip in the connection) must be overcome before catenary action can develop. Therefore, catenary action will not begin until the beam is sufficiently restrained axially. As a result, all sources of axial extension must be taken into consideration.

The first source of axial extension is due to the rotation of the beam. As the beam rotates, its horizontal projection increases until it reaches the length of the diagonal of the beam (Figure 6-4). After the maximum extension is reached, the horizontal projection of the beam decreases as the beam continues to rotate. The catenary effect does not occur until after the beam has reached its maximum extension, or until the deflection is equal to the height of the beam (Δ = h). Although, deflections until 2 times the beam height show a positive value of extension, the rotation of the block causes movement at the support and compression in the beam that effectively shortens the beam. Therefore, after the maximum extension is reached at h, the beam may experience axial tension to overcome the support movement and compression. Therefore, the extension due to geometry is:

δg =extension due to geometry, maximum extension occurs when Δ = h

$$\delta g = h * \sin\theta - L * (1 - \cos\theta)$$ **Equation 6-4**

Where:

$$\theta = \tan^{-1}\left(\frac{\Delta}{L}\right)$$ **Equation 6-5**

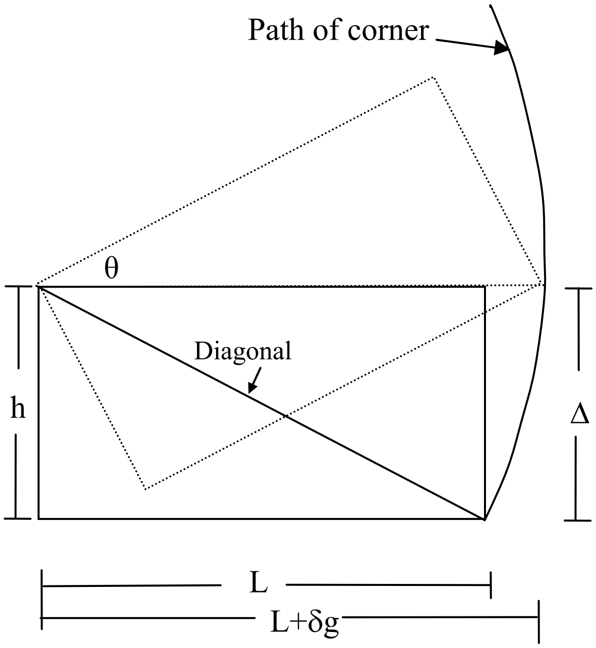

Figure 6-4 Extension due to geometry

The second source is due to the support movement. The values for this extension are based on the measured axial movement at the ends of the beam. For real buildings, the values will be based on the stiffness of the surrounding frame. The first term in Equation 6-6 is a static value representing the movement in the supports. Although every effort was made to ensure that connections at the ends of the beam were tight, some movement could not be avoided. Additionally, the compressive arch phase forces the ends of the beam outward, and this extension must be overcome before the catenary starts to act. For most specimens, the axial extension was measured relative to the axial brace (Figure 6-5). For specimens, FR-1 and NM-2, the extension was measured relative to the lab floor (Figure 6-6).

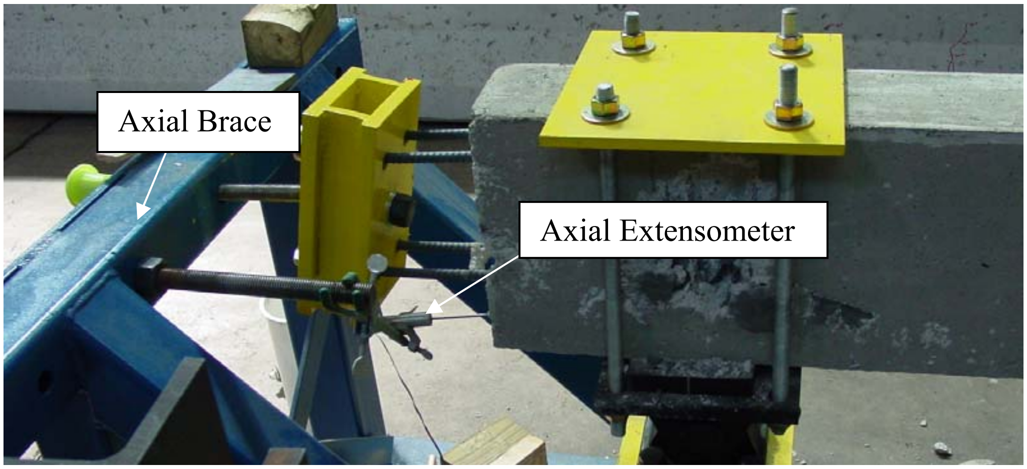
Axial Brace
Axial Extensometer

Figure 6-5 Axial extension measurement from brace

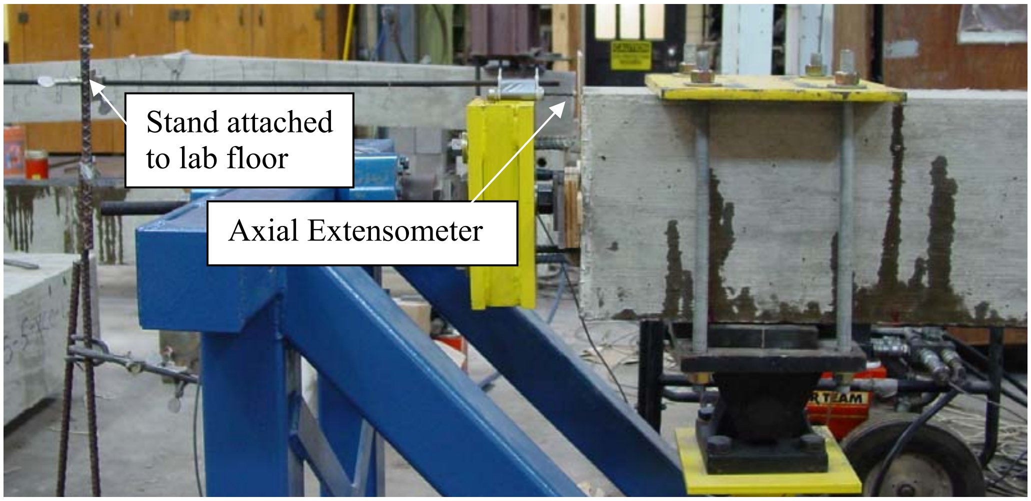
Stand attached to lab floor
Axial Extensometer

Figure 6-6 Axial extension measurement from floor

The results from the axial extensometer in test NM-2 are shown in Figure 6-7. The results from specimen NM-2 include the displacement due to the compressive arch phase because the measurements were taken relative to the lab floor. From the measurements, it was estimated that the static support movement is equal to the average maximum displacement in the compressive phase or 0.32 in.

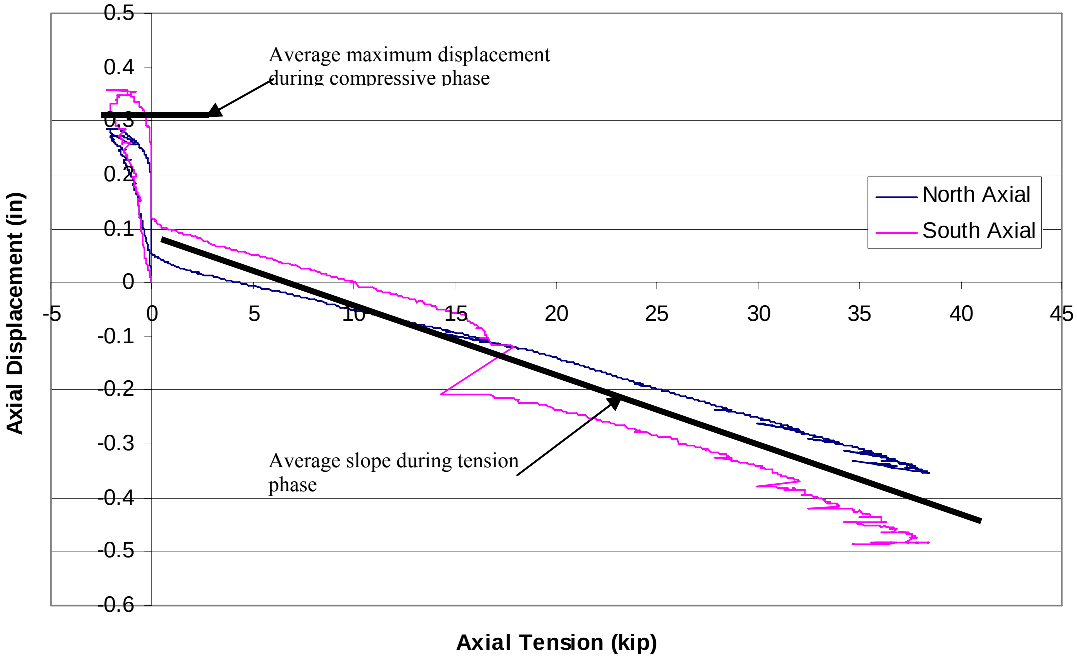

Figure 6-7 Measured axial displacements versus axial tension for specimens NM-2

The remainder of the support movement is due to movement or stretching of support members under axial tension. This value is based on the average slope of the axial displacement versus axial tension measured during the catenary phase, 0.013*Axial tension. Therefore, the extension due to support movement becomes the sum of static movement and movement due to axial tension.

δs =extension due to support movement

$$\delta s = 0.32 + 0.013A \qquad \textbf{Equation 6-6}$$

The last source of axial extension is due to elongation within the beam. However, the actual tension in different sections of the beam varies (see strain diagrams in Chapter 5) and is not equal to the measured axial tension due to effects of bending moments. In the early stages of catenary action, the steel across the wide center crack has yielded and elongated. As more axial tension is placed on the beam, a larger percentage of the steel yields and the beam elongates axially. Eventually the reinforcing steel along the entire length of the beam yields. Unfortunately, the distribution of yielding through the beam is difficult to determine. To estimate beam elongation, it is necessary to approximate the state of yielding in the beam.

Based on the unique elongation properties of different sections of the beam, analysis for beam elongation is broken up into 3 sections, Figure 6-8. For case 1, the three sections are the crack section (yielded rebar), reinforced concrete section, and CFRP sections.

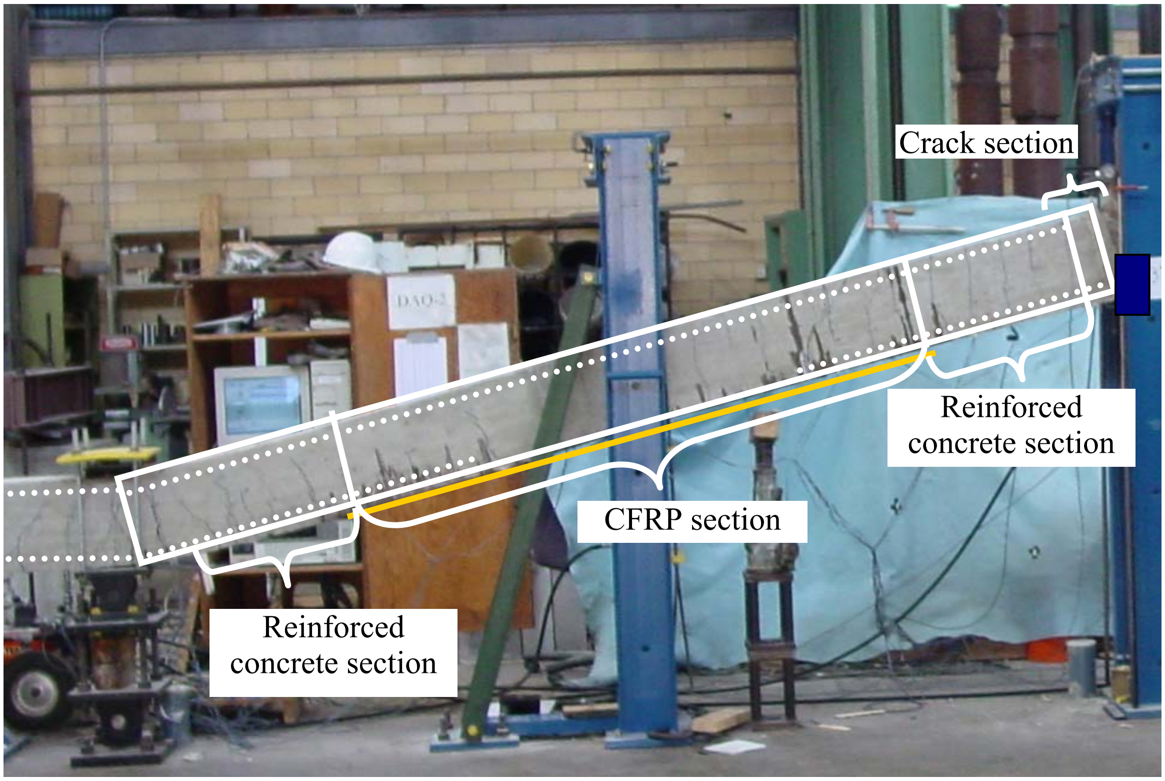

Figure 6-8 Division of beam for elongation analysis

The first section is at the wide crack. Gages at the center of the column stub and face of the column stub showed yielding when catenary action began. The yielding was likely to be due to bending in that area. Figure 6-9 gives the values of strain for gages at the column face and center of column when catenary action began for specimens NM-1 and NM-2. The value of strain was greatest at the column face and decreased on either side. Assuming strains decrease linearly along the bar from the column face, the length of yielded rebar is assumed to be approximately 10 in. The 10 in. value also corresponds to the distance between reinforcing bars. The elongation due to the wide crack is the sum of the approximate elongation that occurs before catenary action and the elongation due to additional axial load.

$$\delta_{crack} = e_i + \frac{AL_y}{E_{st}A_s}$$ **Equation 6-7**

Where the first term, e_i, represents the average value of elongation before catenary action begins (~ 0.1 in.), and the second term represents the continued elongation with L_y representing the yielded length of rebar (10 in.), A_s the area of steel (.51in^2), and E_{st} the strain hardening modulus (0.02Es = 600 ksi).

The rebar is also yielded at the support hinge. However, this elongation is accounted for by the geometric extension due to rotation of the blocks.

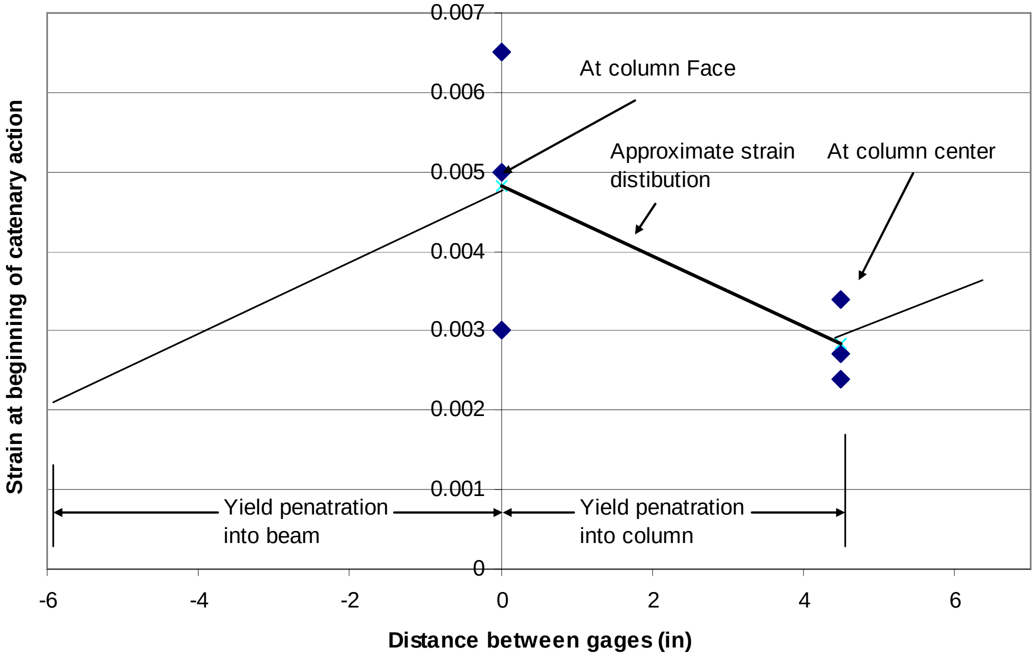

Figure 6-9 Determination of initial length of yielded reinforcement

As the beam picks up axial tension due to catenary action, the tension measured by the load cell at the end of beam may not represent the actual tension in all sections of the beam due to effects of bending moments and sharing of tensile forces between layers of reinforcement. A graph of the axial load in which yield began versus distance from the column face, shown in Figure 6-10, illustrates the variation of yielding throughout the beam. In order to account for the progression of yielding throughout the beam an additional term increases the length of yielded rebar after the axial tension has reached the yield strength of the negative moment reinforcement. After the axial tension is greater than that associated with yield of the negative moment reinforcement, the additional term is

$$\delta_y = \frac{[L_y + L_i(A - yield)]A}{E_{st}A_s}$$

Equation 6-8

where L_i is the additional length of yielded rebar per kip.

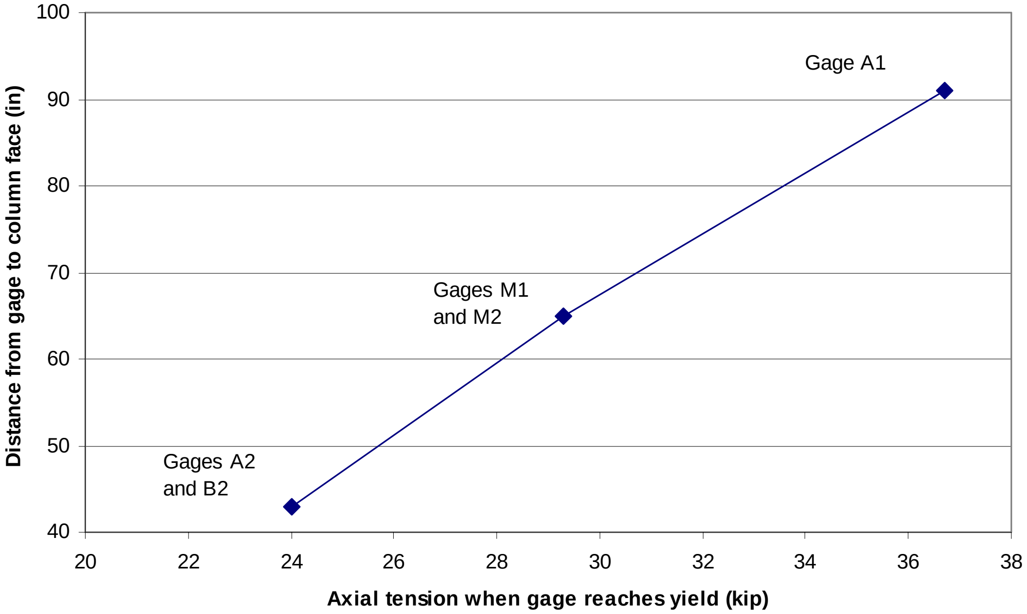

Figure 6-10 Variation of yielding along beam (NM-2)

The second section is the elongation of the reinforced concrete sections. The elongation is approximated by using a Ramberg-Osgood model for the steel stress-strain curve until the stress in the steel is equal to the fracture stress (100 ksi) [Izzuddin, 2004].

$$\varepsilon_s = \frac{\sigma_s}{E_s} + \frac{\varepsilon_{sp}}{\sigma_{sp}^{n_s}} \sigma_s^{n_s}$$ **Equation 6-9**

where ε_s is the steel strain, σ_s the steel stress (A/A_s), E_s the elastic modulus (30,000 ksi), ε_{sp} and σ_{sp} the stress and strain in the plastic region (0.01, 63 ksi), and n_s a parameter equal to 4. A comparison of the model to measured stress strain data for a #4 rebar is given in Figure 6-11. The elongation in the reinforced concrete section is then

$$\delta_{concrete} = \varepsilon_s * l_c$$ **Equation 6-10**

Where l_c is the length of the concrete region. For case 1, one concrete section has a length of 27 in. with A_s of 0.51 in^2 (negative moment steel only) and the other section has a length of 27 in. with A_s of 0.93 in^2 (both positive and negative moment steel).

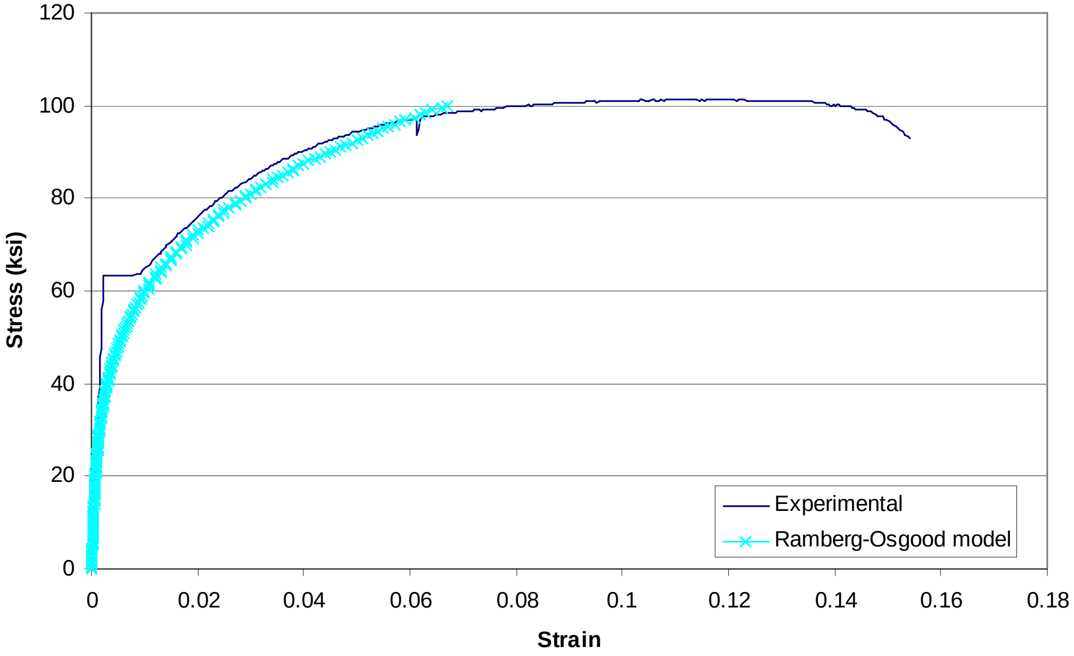

Figure 6-11 Comparison of Ramberg-Osgood and experimental stress strain curves for reinforcing bar

The third section is the CFRP section. The stress-strain curve for CFRP is linear, so the elongation becomes

$$\delta_{CFRP} = \frac{A * l_{CFRP}}{E_{CFRP} * A_{CFRP}}$$ **Equation 6-11**

Where l_{CFRP} is the length of the CFRP section (80 in.), E_{CFRP} is the CFRP modulus (14,000 ksi) and A_{CFRP} is the area of CFRP (0.24 in^2).

Therefore, the axial elongation in the beam is

$$\delta e = \delta_{crack} + \delta_y + \delta_{Concrete} + \delta_{CFRP}$$ **Equation 6-12**

The total axial extension then becomes

$$\Delta L = \delta g + \delta s + \delta e$$ **Equation 6-13**

The catenary action equations were implemented into a MathCad sheet for solving. The sheet and example calculations are given in Appendix D.

6.1.2 Case 2 (Un-retrofitted)

Case 2 is based on the catenary response of the un-retrofitted beams. These beams formed a wide crack at the column face as well as at the end of the negative moment reinforcement and have little moment resistance at either end, Figure 6-12. The set of equations for this case involves some simple manipulation of the equations for case 1.

The greatest change occurs in the equation for equilibrium due to a hinge forming at the end of the negative moment reinforcement that has little moment resistance. For the test specimens, the length of the beam changes from 144 in. to 91.5 in., or the distance from the end of the negative moment reinforcement to the column face. Furthermore, the location of the axial restraint at the end of the beam changes because the restraint is from the positive moment reinforcement rather than the negative moment as in case 1. Therefore, the moment due to axial load is $A^*(\Delta\text{-}d)$, where d is the distance between the levels of reinforcing steel (10 in.).

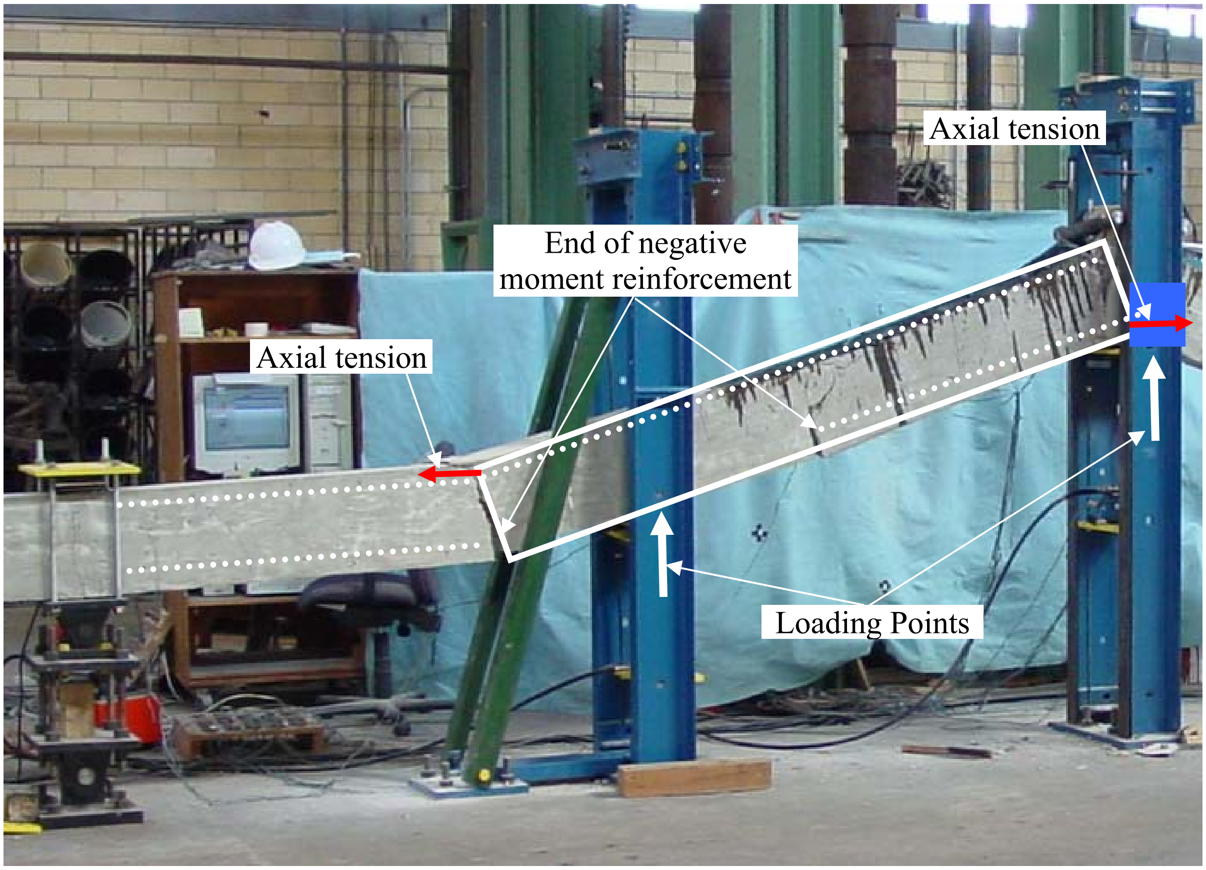
Axial tension
End of negative moment reinforcement
Axial tension
Loading Points

Figure 6-12 Idealization for case 2

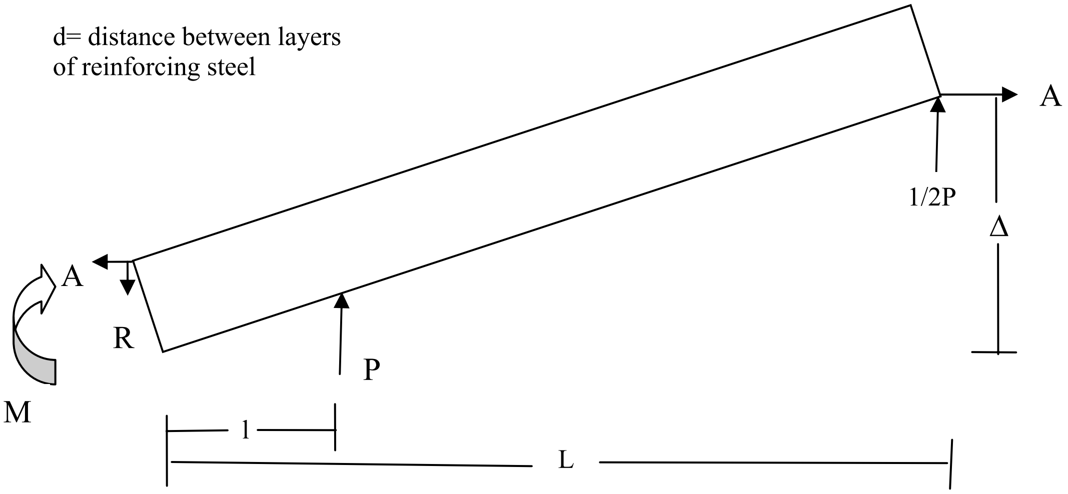
d= distance between layers of reinforcing steel
A
1/2P
Δ
A
R
P
M
l
L

Figure 6-13 Free body diagram of case 2

Taking the sum of the moments about the reaction point

$$0 = M + A(\Delta - d) - Pl - 0.5PL$$ **Equation 6-14**

Where l is the distance to the first point load or 24 in., and L is 91.5 in. The term d is taken as the distance between the layers of reinforcing steel (10 in.). Due to rotation of the beam, d should be vertical projection or dcosθ, but the difference is minor and is ignored for simplicity. The term M in the equation reflects both the small moment capacities at the ends of the beam as well as the moment overcome due to self weight (80 kip-in). Therefore, the equation for the axial tension becomes

$$A = \frac{P * (l + 0.5L) - M}{\Delta - d}$$ **Equation 6-15**

The second change from case 1 occurs in the axial extension of the beam. There are 2 crack sections (one at each end) with a total length of yielded rebar, L_y, equal to 20 in. and the elongation before catenary e_i increases to 0.3 in. Due to the long lengths of rebar, the transfer of tension force between the positive and negative moment reinforcement, and bending in the beam, the distribution of axial tension in the reinforcement is not constant. The actual tension in a given section of reinforcement may be above yield even though the measured axial tension at the ends of the beam is not. Therefore, for this case the term for additional yielded rebar length is included even though the average value of axial tension (A) is less than yield. After A reaches yield, the length of yielded rebar per kip (L_i) is increased to from 1 to 2 in. order to account for faster spreading of yielded rebar length under higher axial loads and to fit the measured test data.

Additionally, there are 3 reinforced concrete sections with a length and area of 48 in. and 0.42 in^2 (center), 44 in. and 0.51 in^2 (left), and 44 in. and 0.47 in^2 (right)[7]. The remaining equations (for geometry and support movement) are the same as for case 1. Sample calculations for this model are given in Appendix D.

---

[7] Area of rebar is average of positive and negative moment rebar because axial tension is being transferred by the stirrups from positive to negative moment rebar in this section

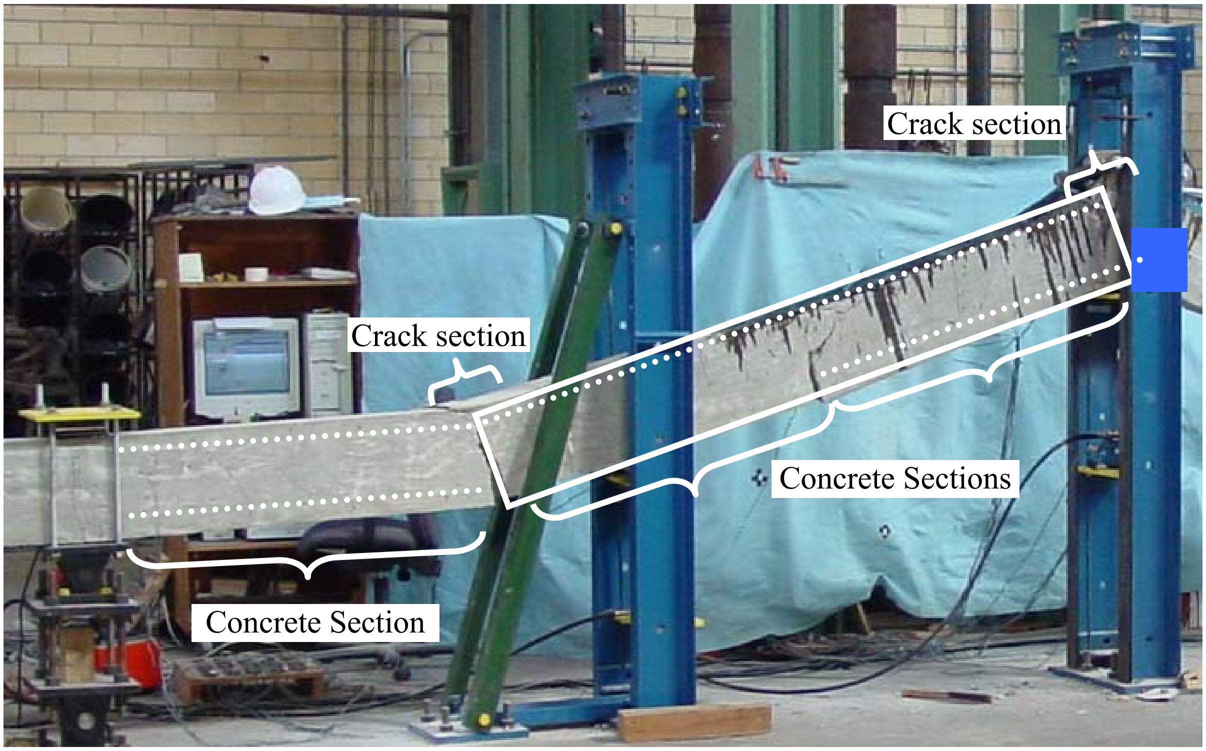

Figure 6-14 Division of beam for elongation analysis, case 2

6.2 COMPARISON WITH TEST RESULTS

The system of equations was solved using a MathCad sheet (Appendix D). The results of the system of equations for case 1 (retrofitted) and the measured values during testing of specimens NM-1 and NM-2 are given in Figure 6-15 and Figure 6-16. The results are calculated after action catenary begins, or after the applied moment (PL) becomes greater than the resisting moment (M). Once the axial load is no longer 0, the equations calculate the deflection at which the catenary begins. The calculated curves end when the reinforcement or CFRP fractures in tension.

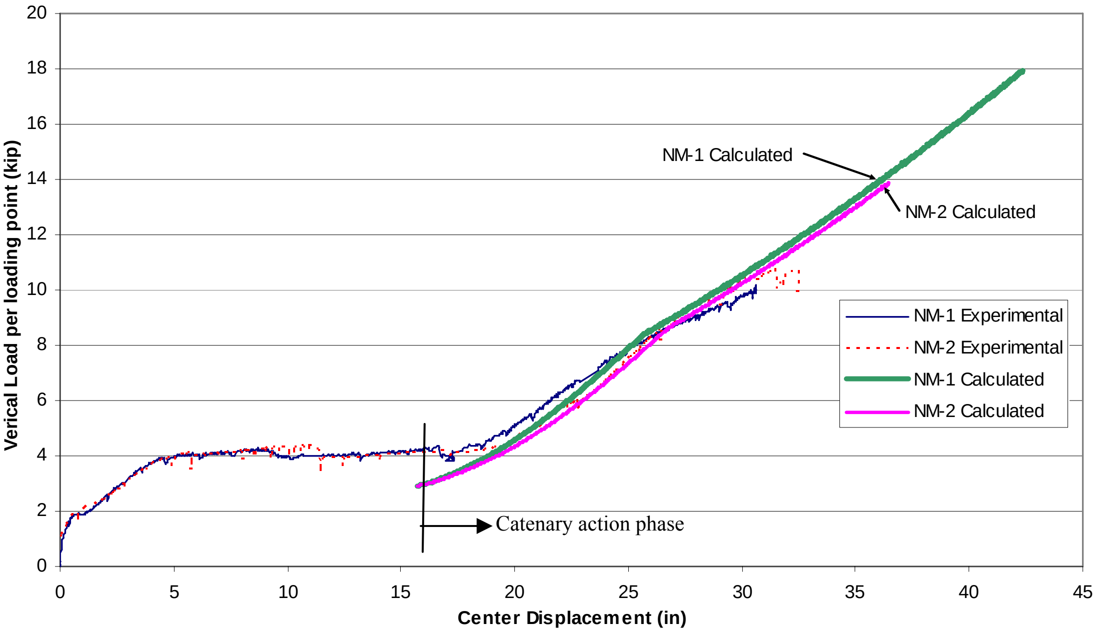

Figure 6-15 Vertical load versus deflection for specimens NM-1 and NM-2 and analysis model

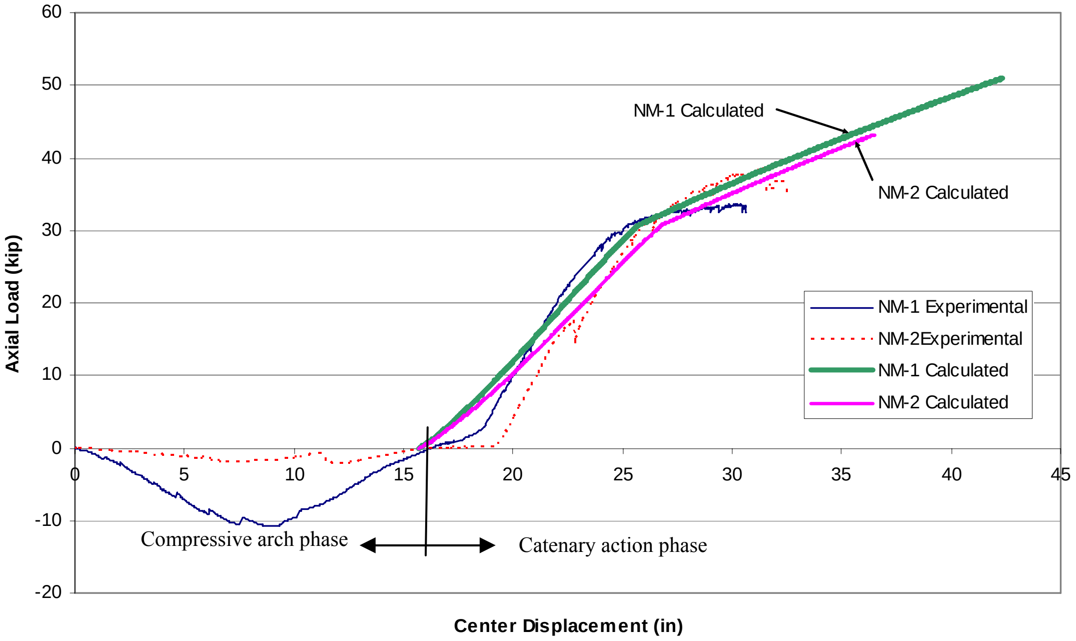

Figure 6-16 Axial tension versus deflection for specimens NM-1 and NM-2 and analysis model

The catenary action analysis model was able to accurately characterize the behavior of the test specimens in catenary action. In fact, the calculated curve for NM-2 is almost on top of the experimental curve. However, the axial tension at which the CFRP fracture is calculated from the combined ultimate capacity of the CFRP (30k for NM-2, 6 in. wide CFRP sheet) and yield of the positive moment reinforcement (13.2k) is greater than the measured axial tension at CFRP fracture (36.6k) in test NM-2 (see Section 5.5.5). The difference in axial tension capacity leads to a difference in the maximum vertical load carrying capacity. For NM-1, the CFRP capacity was 50 k (10 in. wide CFRP sheet) and was close to the fracture strength of the negative moment reinforcement (51k). Therefore, the calculated curve ends at an axial load of 51 k, representing fracture of the negative moment reinforcement. The comparison of calculated and experimental results for the axial load versus deflection is not as close as the vertical load results, but the calculated curve does capture the effect of yielding rebar on the catenary.

The results of the system of equations for case 2 (un-retrofitted) and the measured values during testing of specimens NR-2 and PM-2 are given in Figure 6-17 and Figure 6-18.

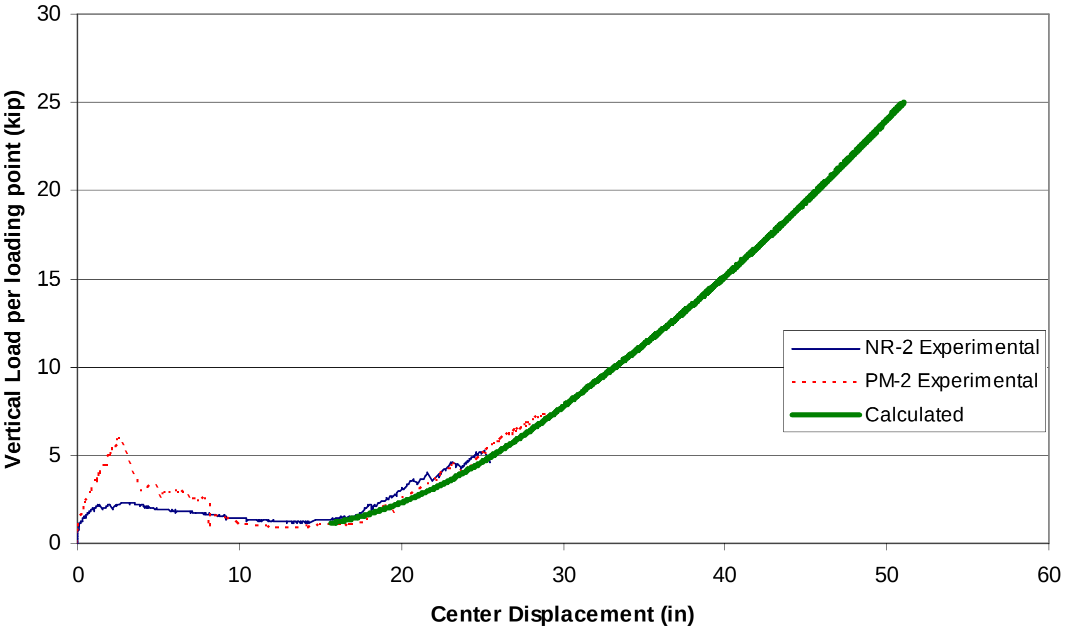

Figure 6-17 Vertical load vs. displacement curves for spec NR-2 and PM-2 and analysis model

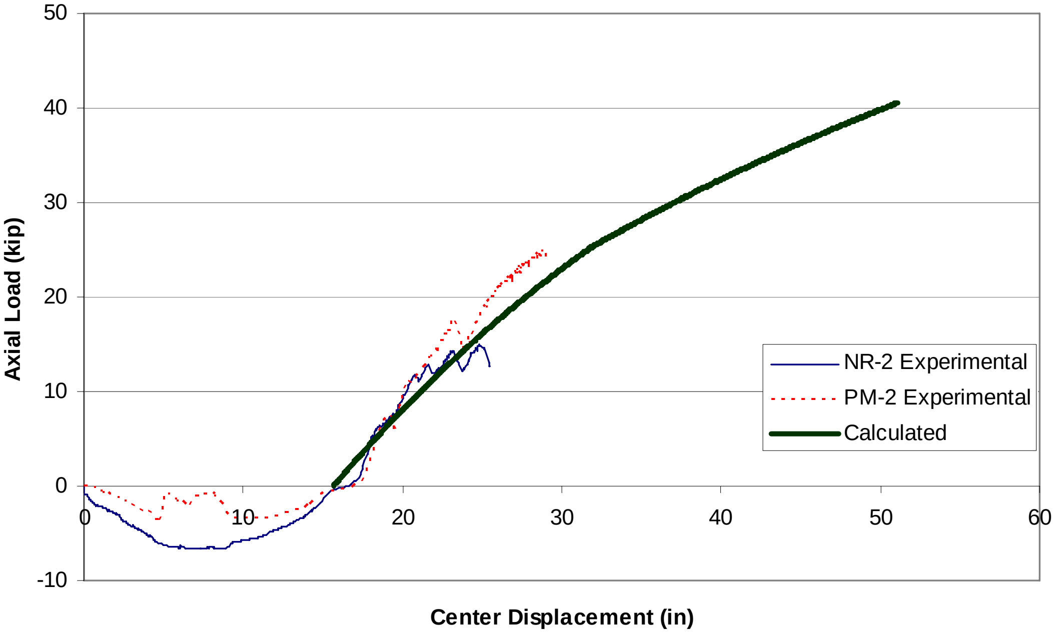

Figure 6-18 Axial tension vs. displacement curves for spec NR-2 and PM-2 and analysis model

Again the experimental and calculated results are very close of the vertical load versus deflection curves and not quite as close for the axial load versus deflection curves.

Both calculated curves for the retrofitted and un-retrofitted cases indicate that the beam can reach a high level of vertical load carrying capacity before the rebar fractures under axial tension. However, none of the experimental tests reached such high vertical loads and it is difficult to say that the calculations are accurate beyond the range of the tests.

Comparisons of case 1 and case 2 are shown in Figure 6-19 and Figure 6-20. The figures show that the retrofitted case, case 1, maintains a higher vertical load carrying capacity per displacement. However, due to the shortened length of the catenary (length of rotating concrete block 91.5 in. for case 2 as compared to 144 in. for case 1) for case 2, the vertical load vs displacement curve for case 2 crosses case 1 at 43 in. of displacement. Furthermore, the un-retofitted case is able to achieve a higher vertical load carrying capacity before the rebar fractures. However, the analysis does not consider failure of the stirrups. Depending on the detailing of the un-retrofitted beam, axial tension forces may not be able to be transferred by the stirrups from the positive to the negative moment reinforcement at high levels of axial tension.

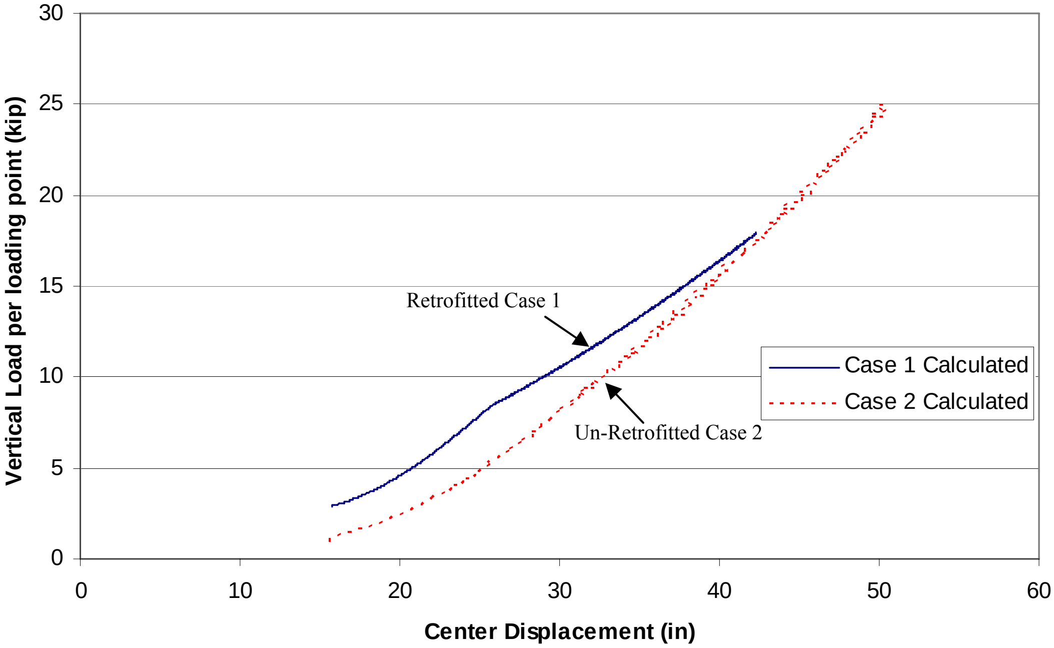

Figure 6-19 Comparison of case 1 and case 2 vertical load vs displacement

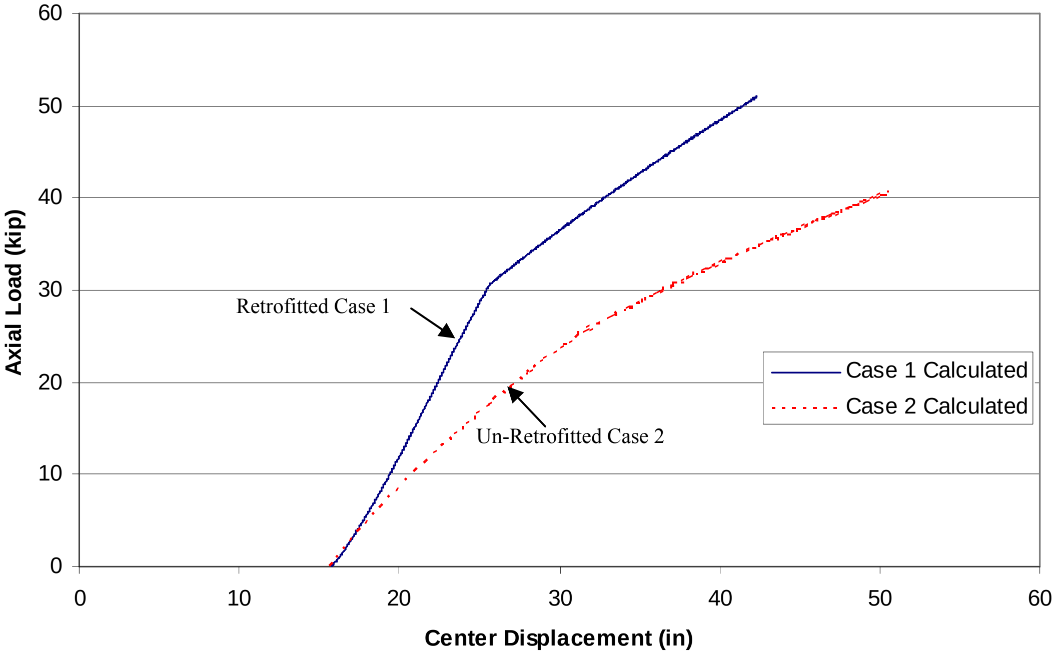

Figure 6-20 Comparison of case 1 and case 2 axial load vs displacement

6.3 PARAMETRIC STUDY

Many of the values in the catenary equations are based on the test data. A parametric study was conducted to determine the influence of the parameters on the catenary response of the beam. The study was conducted with the case 1 model. The curves were calculated to the point where the rebar fractured in tension. The mainly experimentally based parameters (parameters chosen to fit test data) were in the equation to determine elongation of the beam.

The first parameter considered was the value of L_i (additional length of yielded rebar per kip after yield) in Equation 6-8. Increasing L_i from 1 to 4 in. per kip increases the deflection at rebar fracture from 42 to 48 in.; however, at the 10 kip vertical load level reached in the tests, the increase is only 29 in. to 30.7 in., Figure 6-21. Although there is a difference in the predicted displacement and axial load, the difference is less than 2 in. and 2 kip.

Similar results were found for parameter, L_y (initial yielded length of the rebar) also in Equation 6-8. A change in Ly from 6 to 24 in. does not change the displacement or axial load at which catenary action begins, but it does change the displacement and axial load at the 10 kip vertical load level. However, the change is less than 4 in. and 4 kip, Figure 6-22. Therefore, the influence of beam elongation under yielding affects the stiffness of the beam or the slope of the load displacement curve.

The last parameter considered was e_i (initial elongation of the beam). Again, changing the value of e_i from 0.1 to 0.4 in. changes the displacement and axial load less than 1 in. or 1 kip, Figure 6-23. The minor influence of these parameters indicates that although they were chosen to fit the test data, the accuracy of the analysis model is not dependent on them. Furthermore, changes in the yielding of the beam (changes in L_i and

L$_Y$) do not greatly affect the point at which catenary action begins but do affect the slope of the load (vertical and axial) displacement curves.

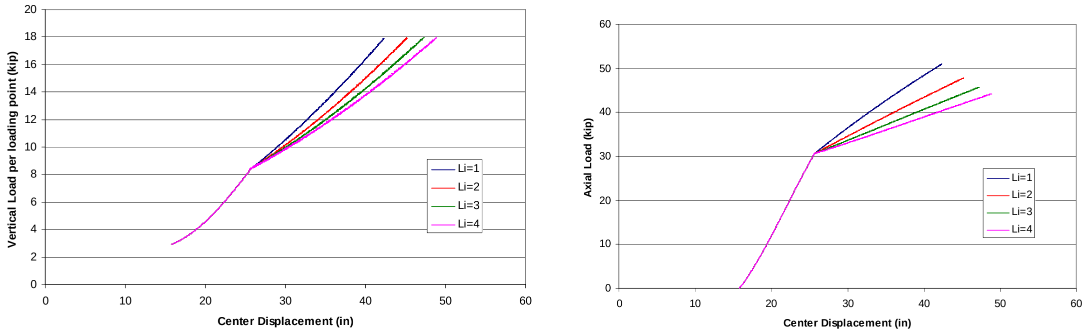

Figure 6-21 Influence of parameter L_i on catenary response

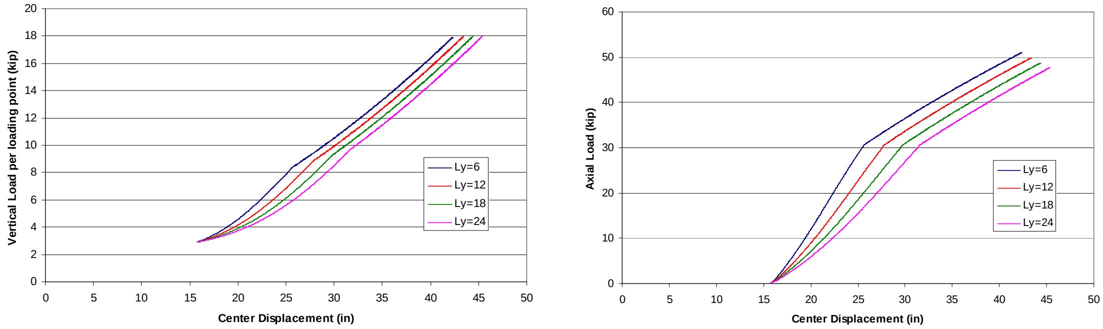

Figure 6-22 Influence of parameter L_y on catenary response

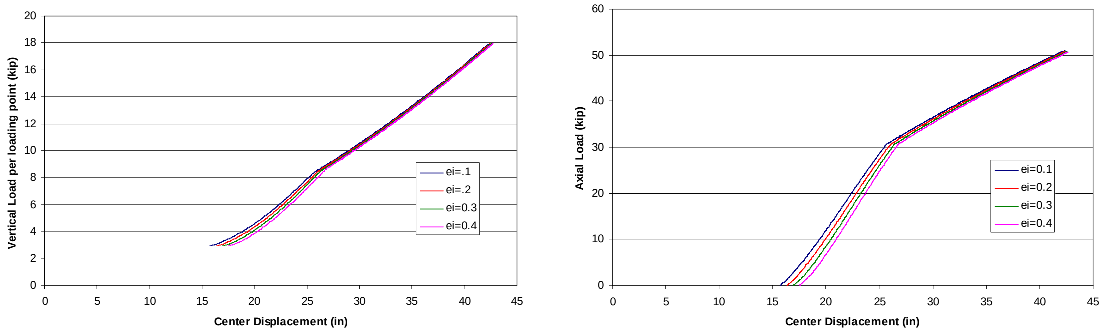

Figure 6-23 Influence of parameter e_i on catenary response of beam

Additionally, a parametric study was conducted to evaluate the influence of the height and length of the beam on catenary response. Changing the height of the beam from 12 to 18 in. changes the displacement at which catenary begins from 15.7 in. to 20.9 in., Figure 6-24. The difference in catenary displacement, 5.2 in., is about the same as the difference in beam height, 5 in., indicating that the catenary displacement is directly dependent on the beam height. Changing the length of the beam from 132 to 156 in. did not have significant impact (less than ½ in.) on the displacement at which catenary begins; however, the displacement at the 10 kip vertical load level changed by 4.2 in. and the axial load by 3.2 kip, Figure 6-25. Therefore, a change in beam length changes the slope of the load-displacement curve.

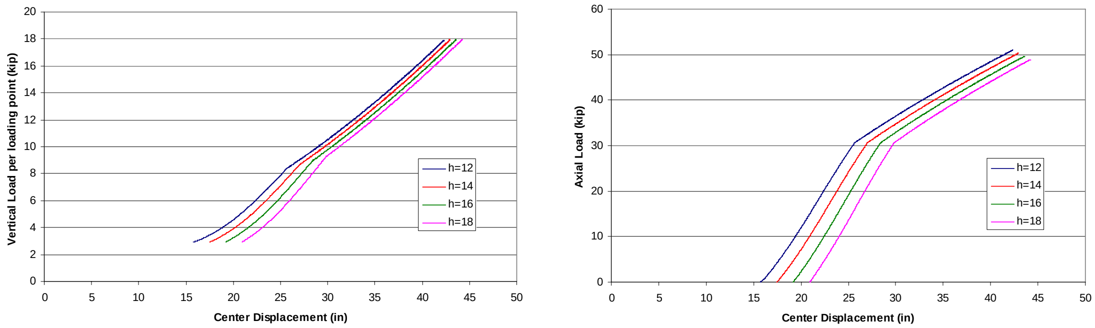

Figure 6-24 Influence of beam height on catenary response

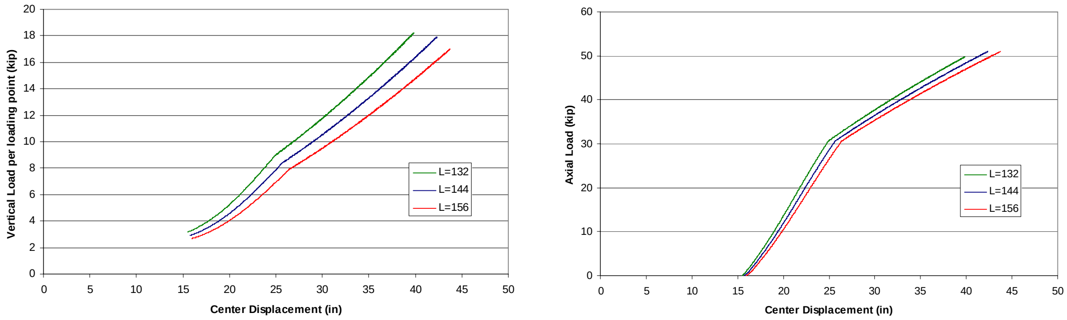

Figure 6-25 Influence of beam length on catenary response

6.4 APPLICATION TO PROTOTYPE STRUCTURE

With a few simple modifications to the models, cases 1 and 2 can be applied to most reinforced concrete building beams. The first step is performing a plastic analysis of the double span under consideration and determining the locations of the plastic hinges. Based on the locations of the hinges, it can be determined whether or not the hinge has enough rotational ductility to reach catenary action. For example, a hinge just past a rebar cutoff point would have no residual capacity, Figure 6-26. A hinge forming in a location where the rebar can be developed on either side may have enough ductility to survive until catenary action begins and the moment capacity of that section needs to be included in the equilibrium equation, Figure 6-27.

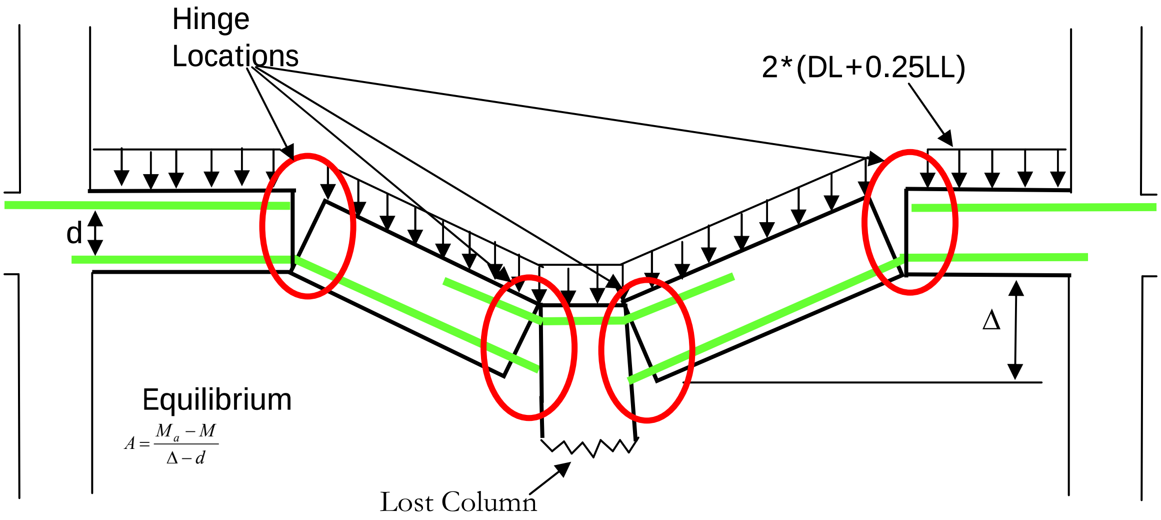
Hinge Locations
2*(DL+0.25LL)
d
Δ
Equilibrium
$A = \frac{M_a - M}{\Delta - d}$
Lost Column

Figure 6-26 Determination of hinge locations for beam without retrofit

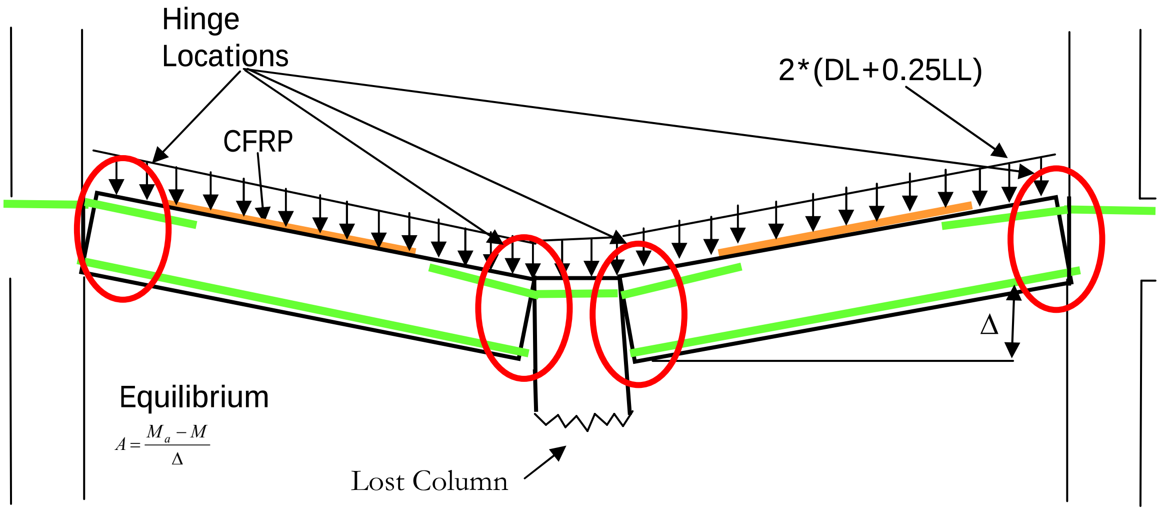
Hinge Locations
CFRP
2*(DL+0.25LL)
Δ
Equilibrium
$A = \frac{M_a - M}{\Delta}$
Lost Column

Figure 6-27 Determination of hinge locations for beam with CFRP retrofit

With the determination of the hinge locations, either Case 1 or Case 2 can be applied to the double span under consideration. It is important to check the rotational limit of all hinges and make sure they are able to achieve the level of deflection calculated by the catenary analysis.

Next, the equation for equilibrium can be written. In this case, the applied moment M_a is the moment at the end of the beam caused by the uniform load and is equal to $\omega L^2/2$. Terms for other loading conditions can be similarly modified.

Then, the axial extension terms can be modified to account for the structural characteristics of the building under evaluation. The equations for the extension due to geometry and beam elongation do not change.

The extension due to support movement can be modified to account for the support conditions. In a model of the building under consideration, remove the double span and place horizontal loads, representing the axial tension in the beam at the connections. The amount of axial tension is equal to the yield strength of the continuous rebar.

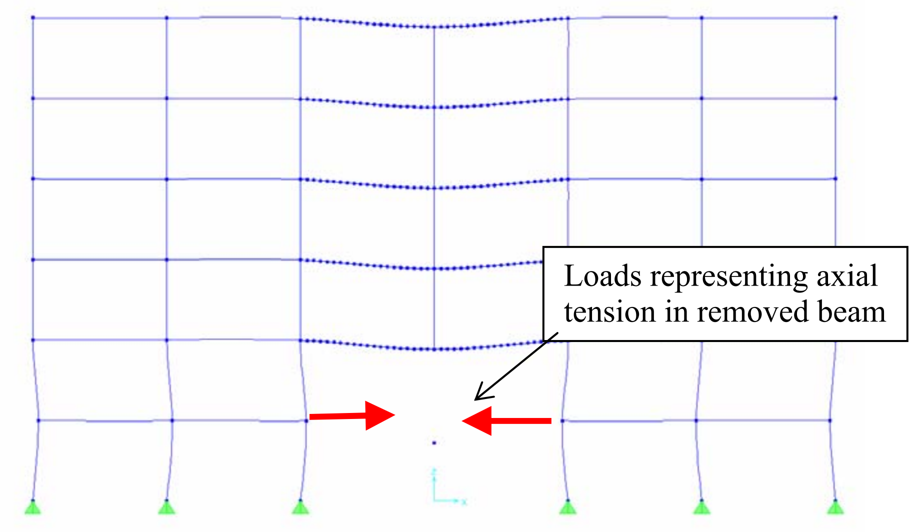

Figure 6-28 Application of representative axial loads

The amount of inward deflection of the beam column joints gives the amount of expected support movement. The extension due to support movement equation is then

$$\delta s = \frac{d}{T_y} * A$$ **Equation 6-16**

Where *d* is the inward deflection of the beam column joints, and T_y is the yield strength of the continuous rebar.

For example, in the prototype building for the test specimens the double span under consideration frames into a structure with 18x18 in. columns. The yield strength of the negative moment steel is 120 kip (2 in^2*60 ksi). Application of the representative axial loads as in Figure 6-28 gives an inward deflection of the beam column joints of 2.1 in. without the presence of slabs and 0.07 in. with the presence of slabs in bays other the one undergoing catenary action. The d/T_y term for the extension due to support movement would range from 0.02 to 0 depending on the presence of slabs.

Finally, the equations for equilibrium and axial elongation can be combined and the catenary response of the building determined. The catenary calculations were carried out for the prototype building. The building was 5 stories with 6 bays of 24 ft spans that consist of 12 by 24 in. beams and 18 by 18 in. columns. The center column on the first floor was removed to analyze the vulnerability to progressive collapse of the building, Figure 6-29.

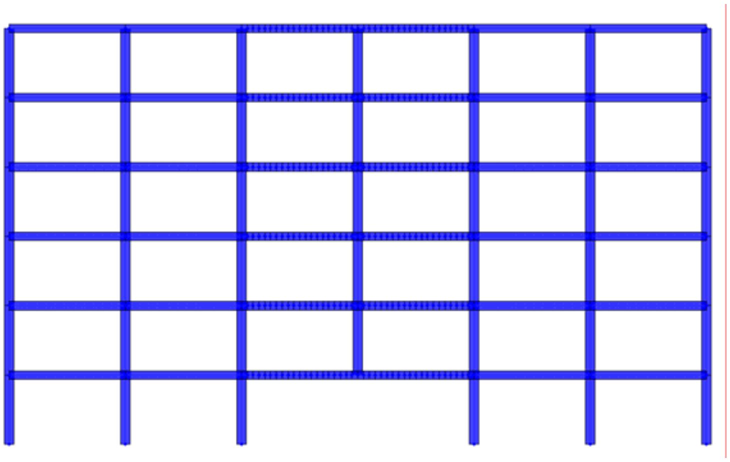

Figure 6-29 Prototype building with center column removed

Catenary calculations were conducted for both the un-retrofitted building and a CFRP retrofit similar to NM-1 and NM-2. The results of the calculations are shown in

Figure 6-30 and Figure 6-31. For this beam, the load representing resistance to progressive collapse, or 2(DL+0.25LL), would be 0.28 k/in. The retrofitted beam was able to achieve this load at 62 in. of displacement and 136 kip of axial load. The un-retofitted beam reached 0.28 k/in at 71 in. of displacement and 80 kip of axial load. The retrofit was able to reduce the deflection of the beam by 9 in., although it also resulted in more axial tension in the beam. Furthermore, the capacity of the un-retrofitted beam matched the retrofitted beam at 0.38 k/in of uniform load. The steepness of the un-retrofitted load deflection curve is due to the reduced length of the catenary because the hinges form at the ends of the negative moment reinforcement rather than at the beam-column connections, see Figure 6-26 and Figure 6-27.

It may not be economical to retrofit every beam in a building when that retrofit only saves 9 in. of displacement in catenary action. However, it must be remembered that the response of the un-retrofitted beam in this case is highly dependent on the design details in the building. The design of the stirrups and longitudinal reinforcement must be such that they can transfer the catenary tension forces from the positive to the negative moment reinforcement and back in order for catenary action to form in a beam with no continuous reinforcement. Furthermore, none of the un-retrofitted test specimens reached a load corresponding to resistance to progressive collapse (they were stopped due to problems in the test setup) and although analysis indicates the beam can reach such a load other unknown factors may limit the beam strength.

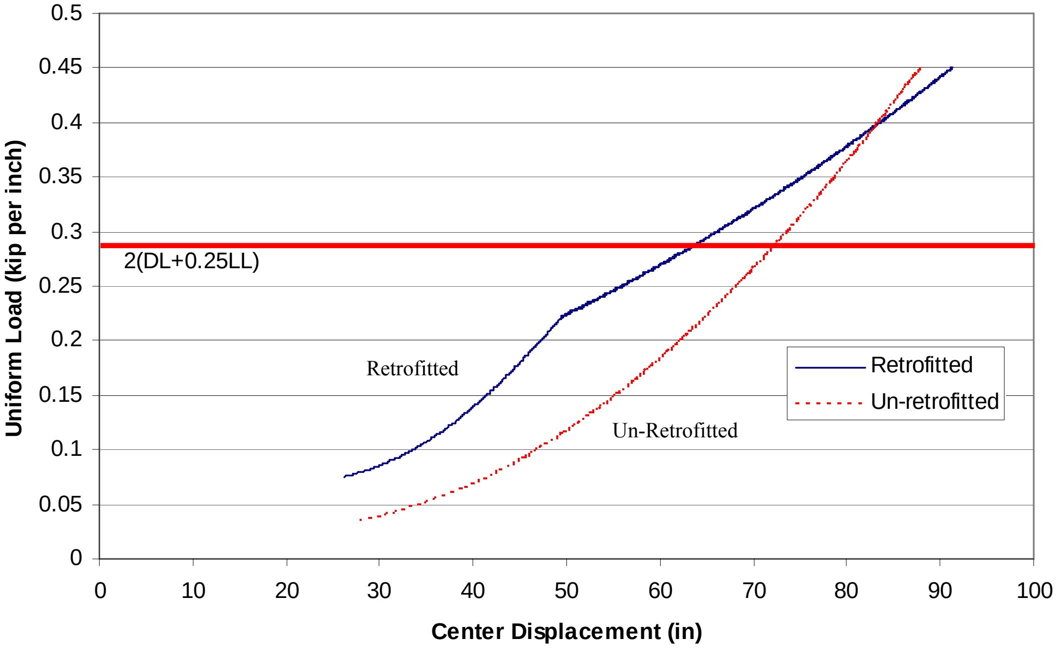

Figure 6-30 Results of catenary analysis on prototype beam, uniform load vs displacement

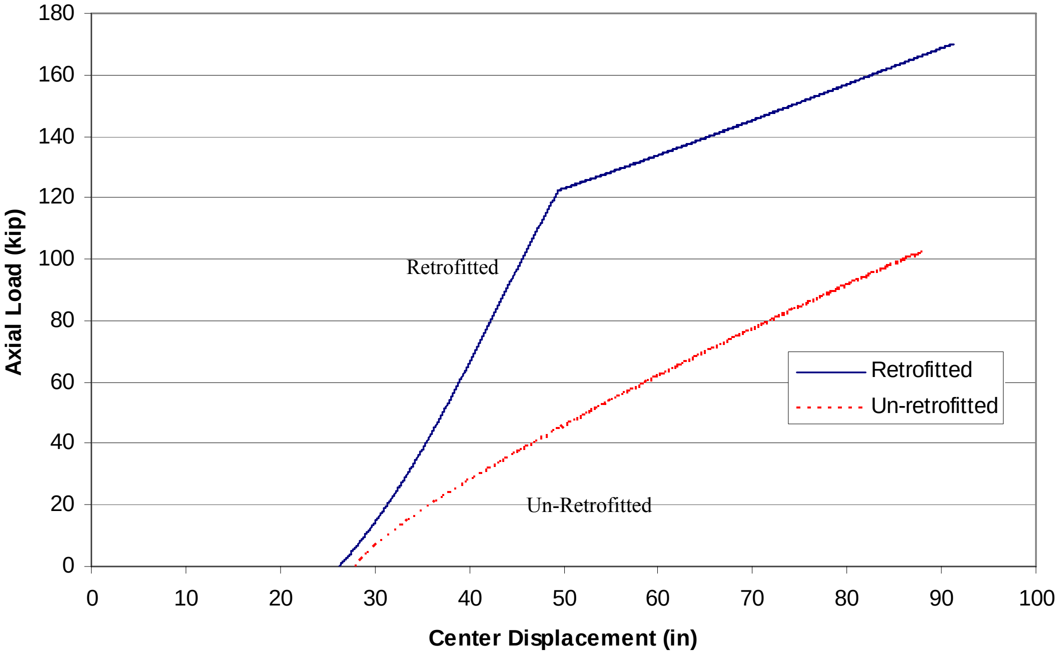

Figure 6-31 Results of catenary analysis on prototype beam, axial load vs displacement

The last step in a catenary analysis is to determine the effect of the catenary on the rest of the structure. For this purpose, a 3D model of the building was constructed in SAP 2000, Figure 6-32. The center two bays of the structure (bays in which the beams would be experiencing catenary action) were removed and representative axial loads determined from catenary analysis of the beams were placed at the corresponding connections, Figure 6-33.

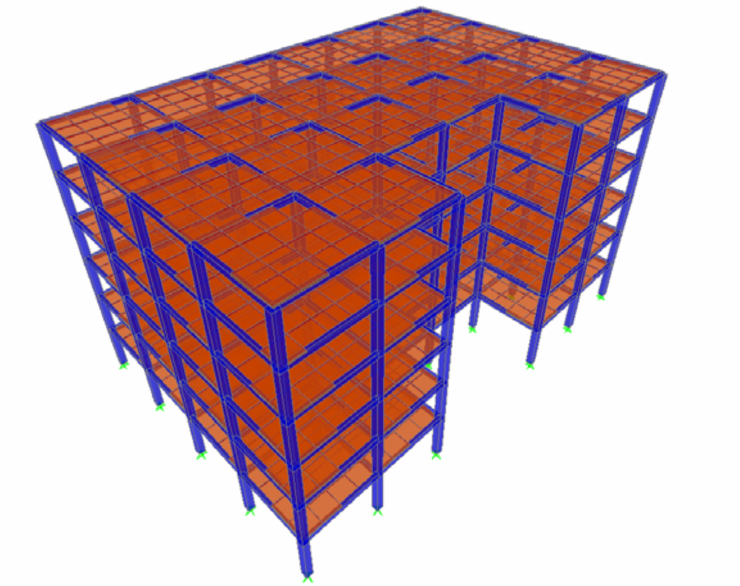

Figure 6-32 3D model of prototype building

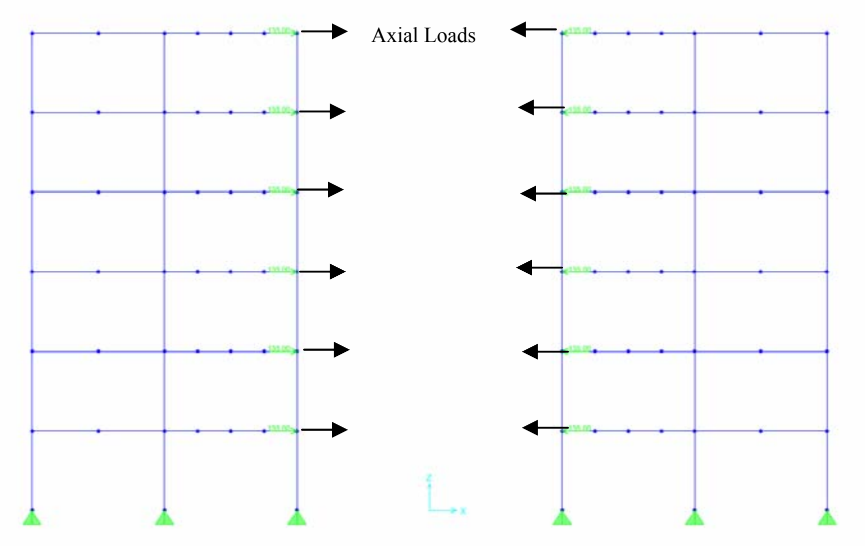

Figure 6-33 Application of axial loads representing catenary response of beams

The resulting forces in the structure are shown in Figure 6-34 through Figure 6-37. All of the results include the presence of the floor slabs. The maximum defection in the frames is a 0.06 in. inward movement at the top floor, Figure 6-34. The maximum moment in the columns is 1376 kip-in in the top column and 1068 kip-in in the bottom column, Figure 6-35. These moments are well within the capacity of an 18 by 18 in. column. The stresses in the floor show a maximum compressive stress of approximately 0.6 ksi, Figure 6-36 and Figure 6-37. With the presence of floor slabs, the building is able to withstand the catenary forces and collapse does not progress.

Without the presence of the floor slabs the forces in the remaining frame would be much more severe. An elastic moment of 16,000 kip-in was calculated at the bottom columns. These forces may be enough to collapse to the rest of the building.

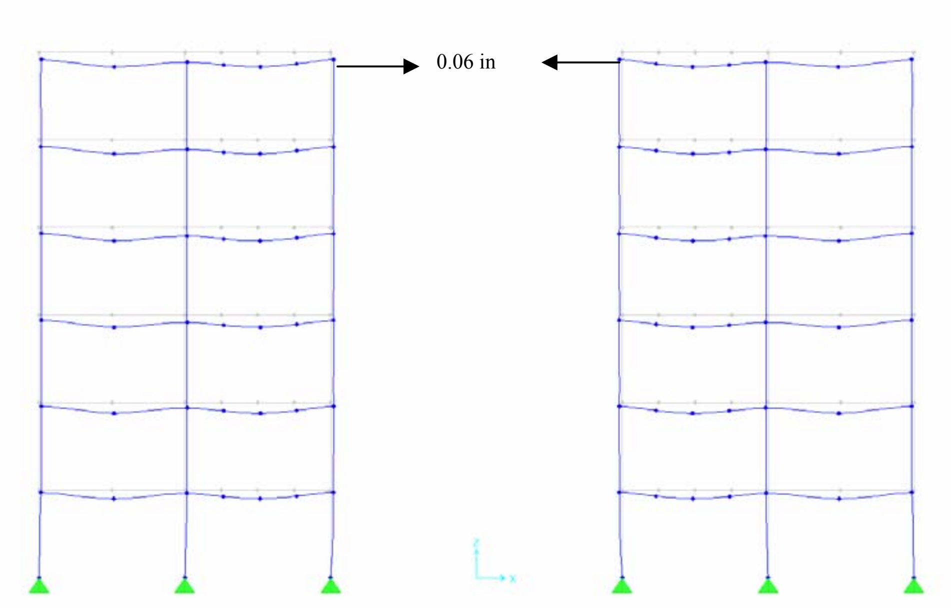

Figure 6-34 Displacements in prototype building

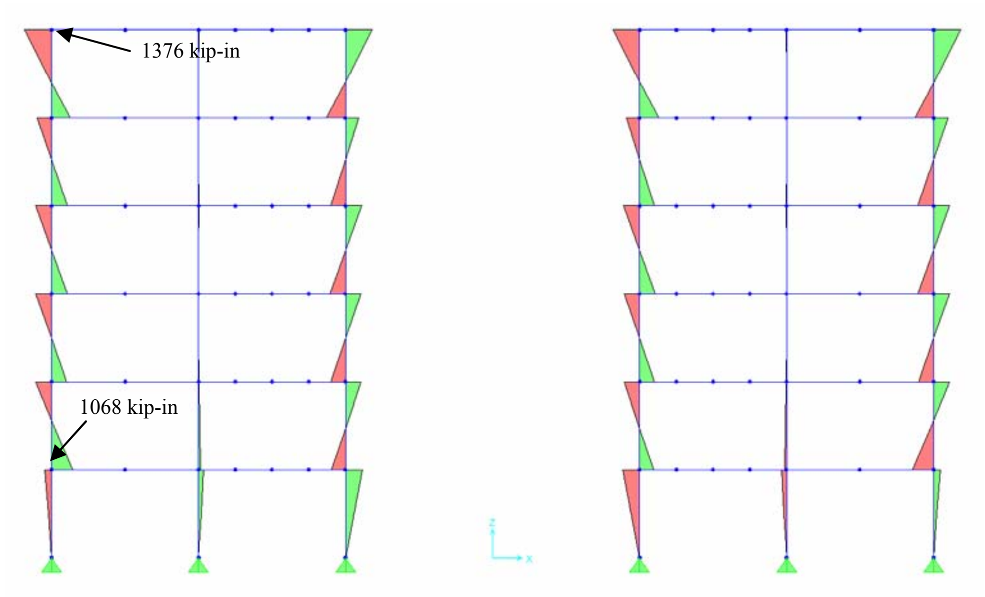
1376 kip-in
1068 kip-in

Figure 6-35 Moment diagrams for columns

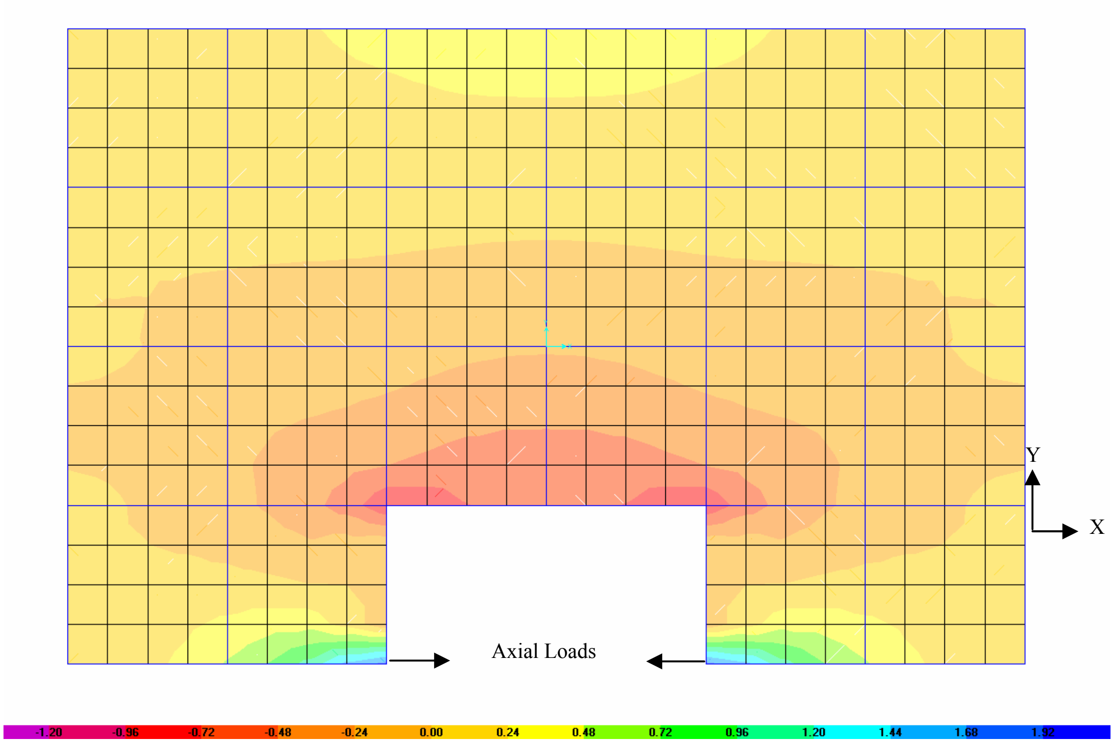

Figure 6-36 X direction stresses in first floor (ksi)

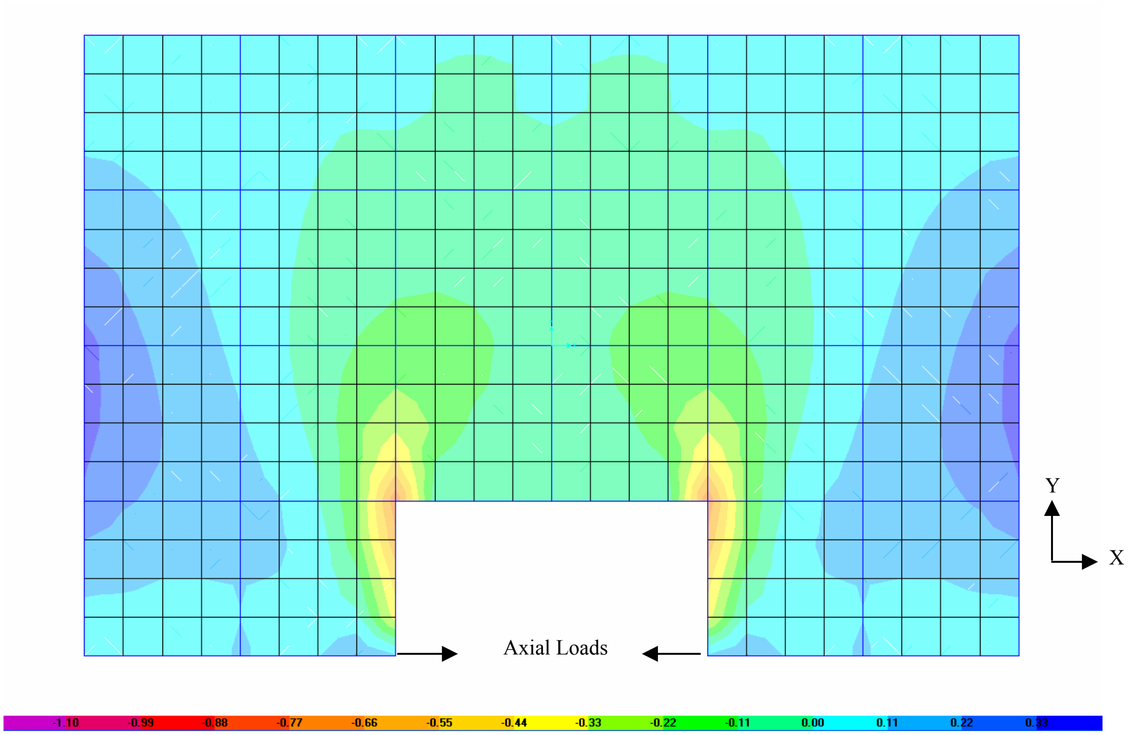

Figure 6-37 Y direction stresses in first floor (ksi)

Furthermore, the previous example considered removal of a center column such that the remaining bays on each side had enough lateral restraint to withstand the forces from catenary action. If a column next to the corner column were considered for removal in progressive collapse analysis, the outer column line of the building may not have the capacity to restrain the catenary action forces, Figure 6-38.

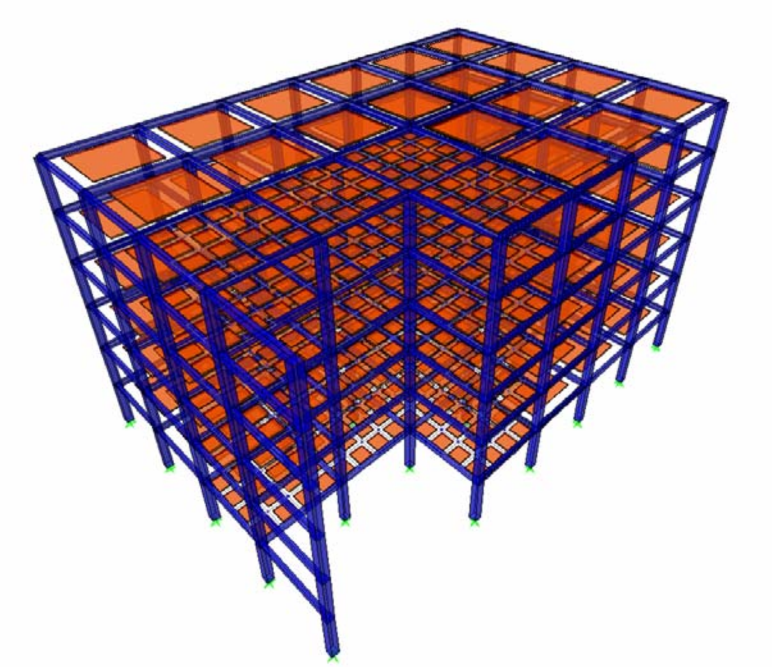

Figure 6-38 Removal of column next to corner for progressive collapse analysis

6.5 CONCLUSIONS

A system of equations was successfully developed to characterize the load and deflection relationship of a reinforced concrete beam in catenary action. The equations were based on the fundamental concepts of equilibrium, compatibility, and material characteristics and the measured response of the test specimens. The equations considered two cases, the retrofitted beam with a moment resistance at one end and an un-retrofitted beam with no moment resistance at either end. For both cases, an equilibrium equation was determined based on a free-body diagram in which the concrete beam behaved as a rectangular block. Equations for the axial elongation of the beam were based on the geometry of the rotating rectangular block, support movement, and elongation within the beam. These equations were combined and solved simultaneously to give the catenary response of the beam. Comparisons with the calculated and measured response showed very close agreement. A parametric study was also conducted to determine the influence of various parameters on the catenary response of a beam. From the analytical study, various conclusions can be made about the catenary response of reinforced concrete beams.

- Catenary action begins after the beam has formed a failure mechanism, or the beam is no longer able to sustain additional vertical loads in a flexural manner
- A reinforced concrete beam can be modeled a rigid rectangular blocks between the hinge locations
- The deflection at which catenary action begins is directly dependent on the height of the beam.
- The stiffness, or slope of the load-deflection curve, is dependent on the axial elongation of the beam, which is largely dependent on the length of the beam (determines elongation due to geometry) and yielding in the beam (determines beam elongation).

The catenary equations were then applied to the full-scale prototype structure. The results indicated that if the details of the building allowed catenary action for the un-retrofitted beam, retrofitting the building would decrease catenary displacements by only 9 in.. However, if the design details did not allow for catenary action in the un-retrofitted beam, the retrofit may be able to reduce vulnerability to progressive collapse.

The axial loads caused by catenary action were then applied to a 3D model of a reinforced concrete building. The model showed that the building would be able to withstand the loads generated by catenaries if the slabs were included in the analysis.

Chapter 7: Summary and Conclusions

Reinforced concrete buildings may be vulnerable to progressive collapse due to a lack of continuity of longitudinal reinforcing steel in the beams. The use of carbon fiber reinforced polymer (CFRP) to retrofit existing reinforced concrete beams and provide the missing continuity needed to resist progressive collapse was investigated.

7.1 SUMMARY OF RESULTS

The research was divided into three main components: anchorage tests, continuity tests, and a catenary model. Forty anchorage tests, eight continuity tests, and one analysis model were constructed and evaluated to develop a CFRP retrofit scheme that would reduce vulnerability of progressive collapse in reinforced concrete buildings. The CFRP retrofit was designed to provide continuity through either the negative or positive moment reinforcement. The continuity was in turn able to allow the beam to develop catenary action and reduce the risk of progressive collapse.

7.1.2 Anchorage Tests

The anchorage tests formed the design basis of the CFRP retrofit and ensured that the capacity of a retrofitted beam can be accurately predicted. The anchorage tests also evaluated how carbon fiber anchors improve the use of CFRP sheets to strengthen reinforced concrete members.

The anchorage tests consisted of two rectangular blocks of concrete connected only by a CFRP sheet. The connected blocks were loaded as a simple beam with a point load at midspan, thereby putting tension in the CFRP sheet. The blocks were either of the same height (to simulate providing continuity through the negative moment reinforcement) or had a height difference (to simulate providing continuity of the positive moment reinforcement through a beam-column joint).

Eleven specimens did not have a height difference between the blocks and focused on the design (size, number, and spacing) of the carbon fiber anchors. The efficiency of material usage with carbon fiber anchors and U-wraps (sheets wrapped around the sides of a beam) was also studied. The tests found that unanchored CFRP sheets utilized less than 40% of their tensile capacity before debonding. U-wraps allowed the CFRP sheet to reach its full tensile capacity, but required much greater amounts of material (than the anchors) that reduced the efficiency of material usage. CFRP anchors allowed the CFRP sheet to reach its full tensile capacity and increased the efficiency of material usage. Finally, a greater number of smaller and more closely spaced anchors were more effective, and each of several rows of anchors was effective in transferring tensile forces into the concrete.

Twenty-nine specimens had a height difference between the blocks and were used to evaluate the effect of the slope and height of the transition, type of CFRP fabric, and surface preparation. The tests found that the adverse effect of a height transition was eliminated by the use of a 1:4 or shallower transition slope. Anchors with a different type of CFRP fabric (but similar properties) did not perform as well as another fabric. Tests with no bond between the CFRP and the concrete were able to reach the full tensile capacity of the CFRP sheet when anchors were used. Therefore, carbon fiber anchors reduced the need for extensive surface preparation because CFRP bond to the concrete was no longer critical to achieving the desired capacity of the CFRP retrofit. Finally, tests with varying height differences were able to reach the same load when anchors and a 1 to 4 transition slope were provided.

The general design approach, developed through the anchorage tests of CFRP sheets with anchors, is:

- Use two rows of carbon fiber anchors with the cross-sectional area in each row equal to 1.3 times the cross-sectional area of the longitudinal sheet.
- Use a larger number of smaller, more closely spaced anchors.
- Use a transition slope shallower than 1:4 on all height transitions.
- Surface preparation is not critical if anchors are used.
- Amount of the height difference in a height transition is not critical.

7.1.2 Continuity Tests

Eight specimens were tested to determine the ability of CFRP to provide continuity and reduce vulnerability to progressive collapse. The test specimen and setup simulated a double span of a reinforced concrete frame with the center supporting column removed. The development of catenary action of vulnerable RC building beams with discontinuous reinforcing steel was studied. The increased capacity that would be achieved by using a CFRP retrofit was evaluated. Additionally, tests were conducted on a beam with continuous reinforcing steel in excess of that specified by ACI 318-05 and a beam strengthened with CFRP to accommodate the double span through flexure.

The un-retrofitted specimen was able to carry significant load (5 k vertical load per loading point) due to catenary action. The catenary tension was transferred from the positive moment steel through the stirrups to the negative moment steel. However, the catenary action did not initiate until around 17 in. or 5% of the span length of vertical displacement was reached at the mid-span of the double span beam.

CFRP was used to provide continuity through the positive moment reinforcement in a reinforced concrete beam and was able to increase the capacity of the beam before catenary action developed. However, the hinge that formed at the end of the CFRP sheet did not have enough rotational ductility to reach catenary action before the reinforcement fractured. Continuity of reinforcement was lost and the beam reverted to behavior like that of an un-retrofitted specimen. Neither of the positive moment retrofits were able to reach the representative 2(DL + 0.25LL) recommended by the General Services Administration progressive collapse guidelines to resist progressive collapse.

CFRP was also used to provide continuity through the negative moment reinforcement. The negative moment retrofits were able to reach the representative load to resist progressive collapse. In both tests, a hinge formed at the support and had sufficient ductility to allow the beam to reach catenary action. After catenary action started, the CFRP had sufficient tensile capacity (at least 30 kips) to carry the high axial loads needed for catenary action.

A retrofit that strengthened the beam through flexure used 4.5 times the amount of CFRP as was used for the negative moment retrofits. The flexural retrofit was also able to reach the representative 2 times (dead plus 25% live load) recommended by the GSA guidelines at a much lower level of deflection. Although, the retrofit preformed as desired it required a large amount of CFRP.

A beam with continuous reinforcement (exceeded the ACI-318 Chapter 7 requirements) was not able to reach the representative load to resist progressive collapse. The continuous reinforcement did not have enough rotational ductility to reach catenary action before fracture of the reinforcing bars. After fracture of the continuous reinforcement, the beam reverted to behavior similar to an un-retrofitted beam.

7.1.3 Catenary Model

A system of equations was developed to characterize the load and deflection relationship of a reinforced concrete beam in catenary action. The equations were based on the fundamental concepts of equilibrium, compatibility, and material characteristics as well as the measured response of the continuity test specimens. The equations considered two cases, the retrofitted beam with a moment resistance at the support and an un-retrofitted beam with negligible moment resistance at either end. For both cases, an equilibrium equation was determined based on a free-body diagram in which the concrete beam behaved as a rectangular block. Equations for the axial elongation of the beam were based on the geometry of the rotating rectangular block, support movement, and elongation within the beam. These equations were combined and solved simultaneously to give the catenary response of the beam. The catenary action analysis model was able to accurately predict the catenary response of the test specimens. A parametric study was also conducted to determine the influence of various parameters on the catenary response of the beam.

The catenary equations were then applied to a full-scale prototype structure. The results indicated that if the details of the transverse reinforcement allowed catenary action in the un-retrofitted beam, a CFRP retrofit would decrease catenary displacements by only 9 in. However, if the design details did not allow for catenary action in the un-retrofitted beam, the retrofit may be able to reduce vulnerability to progressive collapse.

The axial loads caused by catenary action were then applied to a 3D model of a reinforced concrete building. The model showed that the building would be able to withstand the loads generated by catenaries if the slabs were included in the analysis.

7.2 CONCLUSIONS

The conclusions drawn from the results of the research program are:

- Carbon fiber anchors improved utilization of the tensile capacity of a CFRP sheet and thereby increased the capacity of a CFRP retrofit with or without a height transition. Anchors also improved the efficiency of material usage in CFRP retrofits, requiring less CFRP material for the same strengthening capacity.

- Beams without continuous reinforcement can reach catenary action if the catenary tension forces can be transferred between the positive and negative moment reinforcement (bottom and top steel).
- CFRP can be used to provide continuity in the positive and/or negative moment reinforcement.
- A CFRP retrofit, if designed correctly (placed in locations that do not cause rebar fracture before catenary action develops), may be able reach catenary action and reduce vulnerability to progressive collapse.
- A CFRP retrofit can also be designed to resist progressive collapse through flexural action. The retrofit may limit deflections and provide a higher performance objective (than retrofits that rely on catenary action), but may require a much greater amount of CFRP.
- Catenary action begins after the beam has formed a flexural failure mechanism, or the beam is no longer able to sustain additional vertical loads in a flexural manner.
- The deflection at which catenary action begins is directly dependent on the height of the beam.
- The stiffness, or slope of the load deflection curve, is dependent on the axial elongation of the beam, which is largely dependent on the length of the beam (determines elongation due to geometry) and yielding in the beam (determines beam elongation).

The overall conclusion is:

- A CFRP retrofit can reduce vulnerability to progressive collapse in reinforced concrete buildings.

7.3 FUTURE RESEARCH

Future research still needs to be conducted on:

- Carbon fiber anchors - additional anchorage tests with a wider range of parameters (anchor size, number, CFRP sheet width, type of CFRP fabric, etc.) are needed to develop a complete design methodology. Standard tests need to be developed to determine anchor strength and ensure consistency between experiments.
- Dynamic impact on CFRP retrofit – tests need to be conducted where the progressive collapse load is applied dynamically. All tests in this research were static with a dynamic amplification factor of 2 recommended by both the GSA and DoD. The amplification factor may be overly conservative, and the CFRP retrofit may behave differently under a dynamic load.
- Capacity of other members to aid in resistance to progressive collapse analysis - Tests need to be conducted to evaluate the capacity of slabs or columns above the removed column to help with progressive collapse resistance.
- Influence of stirrup design – Tests need to be conducted with various stirrup designs to determine the influence of the stirrups on the ability of beam with non-continuous reinforcement to reach catenary action.
- Improved catenary analysis model – Models need to be created to better simulate axial tension and yielding of reinforcement throughout beam (additional catenary action tests with measurements of beam elongation could improve model parameters) and include the entire building under progressive collapse.

Appendix A

Data From Anchorage Tests

Tests Without Height Transition 208

- 00-ng1 208
- 00-4g1 210
- 00-ns1 212
- 00-2s1 214
- 00-us1 216
- 00-4s1 218
- 00-6s1 220
- 00-us2 222
- 00-2s2 224
- 00-4s2 226
- 00-4s3 228

Tests With Height Transition 230

- 22-ng1 230
- 22-2g1 232
- 22-ns1 234
- 22-us1 236
- 22-4s1 238
- 42-us1 240
- 42-4s1 242
- 42-6s1 244
- 42-ns1 246
- 42-4s2 248
- 42-us2 250
- 42-6s2 252

42-us3 254
42-cs1 256
42-ns1 258
42-4s3 260
42-4s4 262
42-6n1 264
22-6s1 266
42-6s3 268
42-6s4 270
42-6s5 272
42-6n2 274
42-4s5 276
42-6s6 278
41-ns1 280
43-ns1 282
41-6s1 284
43-6s1 286

TESTS WITHOUT HEIGHT TRANSITION

00-ng1

Test Date: July 11th, 2005
No height transition
No anchors
Grinding surface preparation
SCH-35 fabric

Specimen Design:

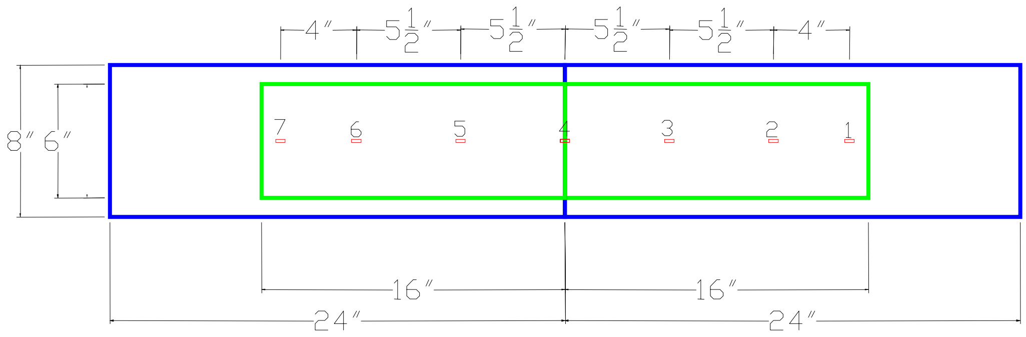
4″
5 1/2″
5 1/2″
5 1/2″
5 1/2″
4″
8″
6″
7
6
5
4
3
2
1
16″
16″
24″
24″

Test Data:

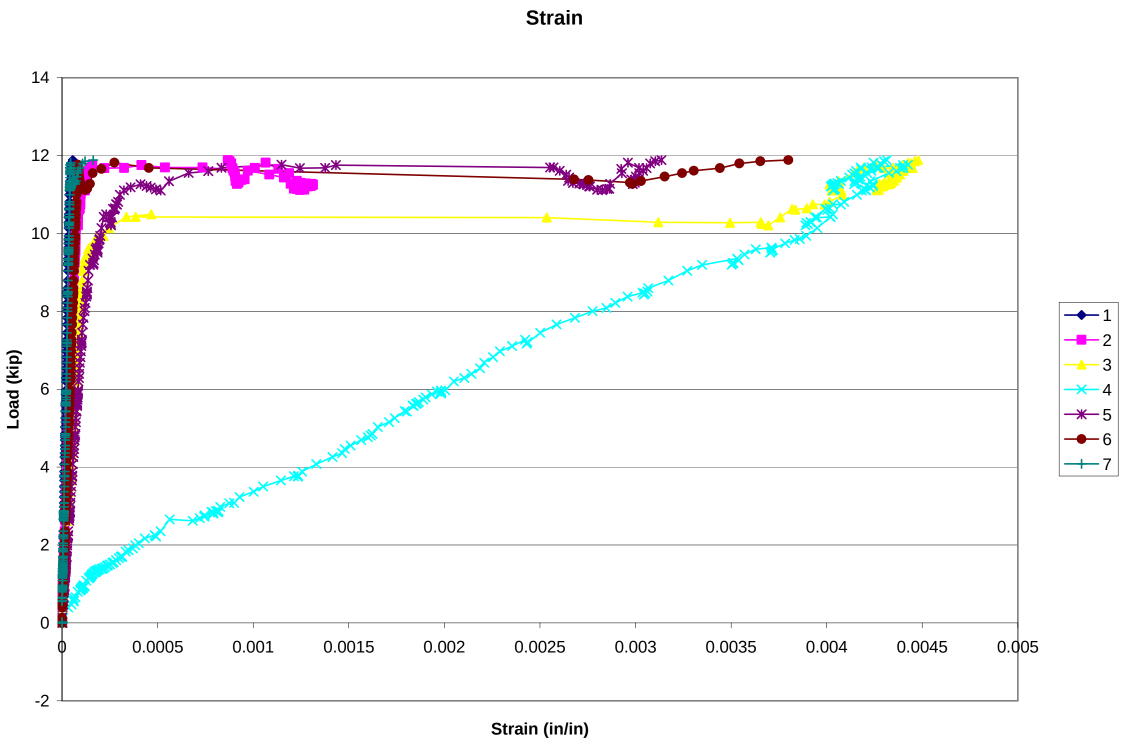

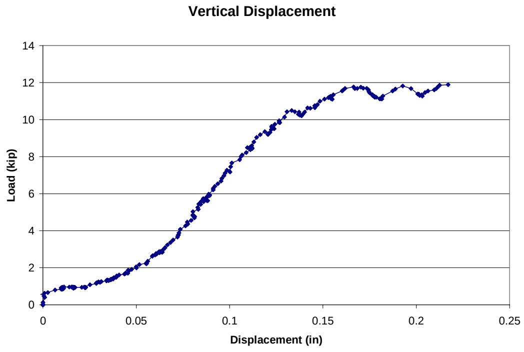

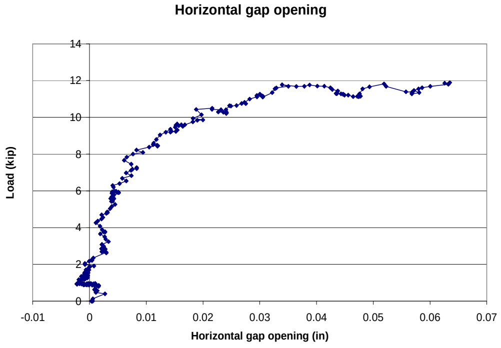

Photographs:

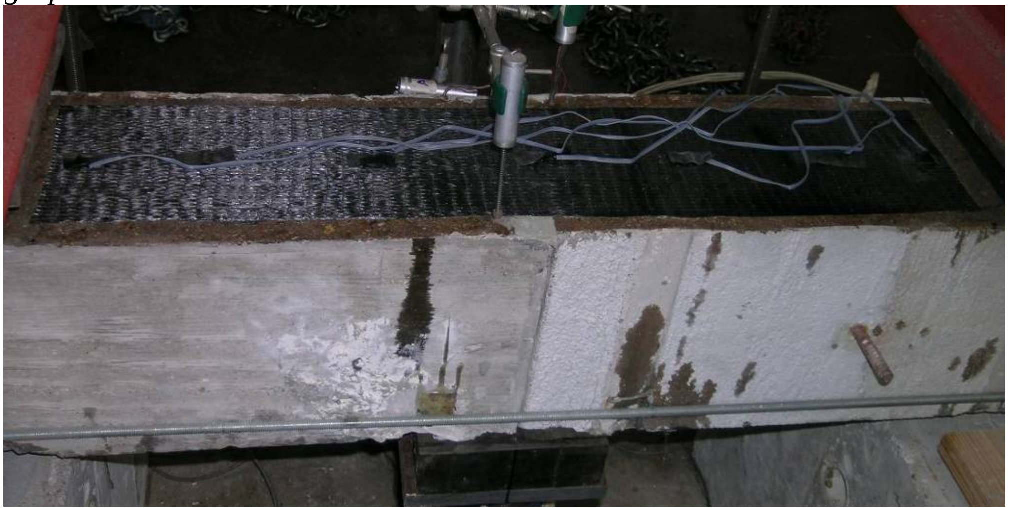

Before Testing

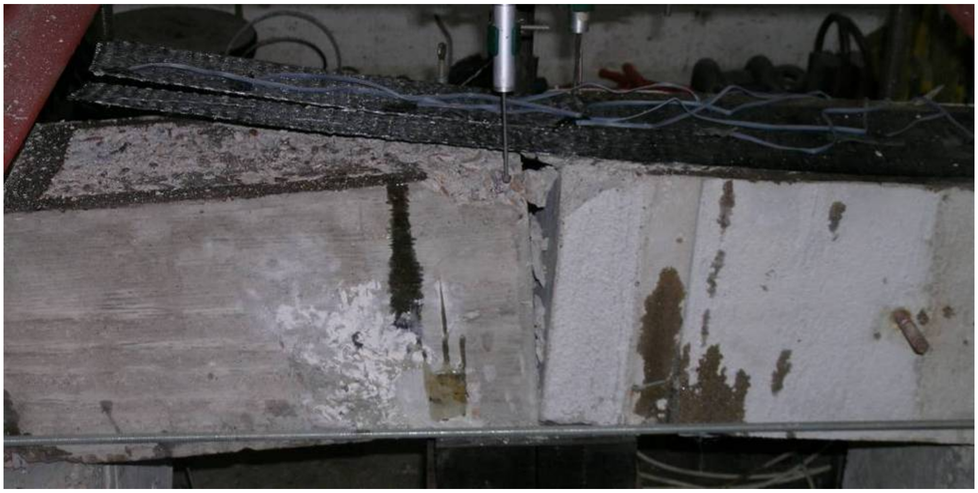

After Testing: Failure by Debonding

00-4g1

Test Date: July 15th 2005
No height transition
Two rows of 2 anchors at 3 and 6”, 1 ½” width sheet, 3/8” diameter concrete hole
Grinding surface preparation
SCH-35 fabric

Specimen Design:

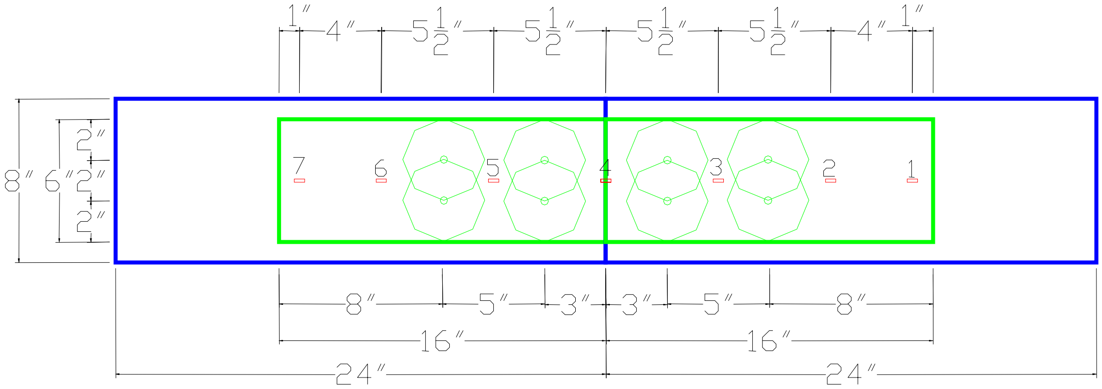

1"
4"
5 1/2"
5 1/2"
5 1/2"
5 1/2"
4"
1"
8"
6"
2"
2"
2"
7
6
5
4
3
2
1
8"
5"
3"
3"
5"
8"
16"
16"
24"
24"

Test Data:

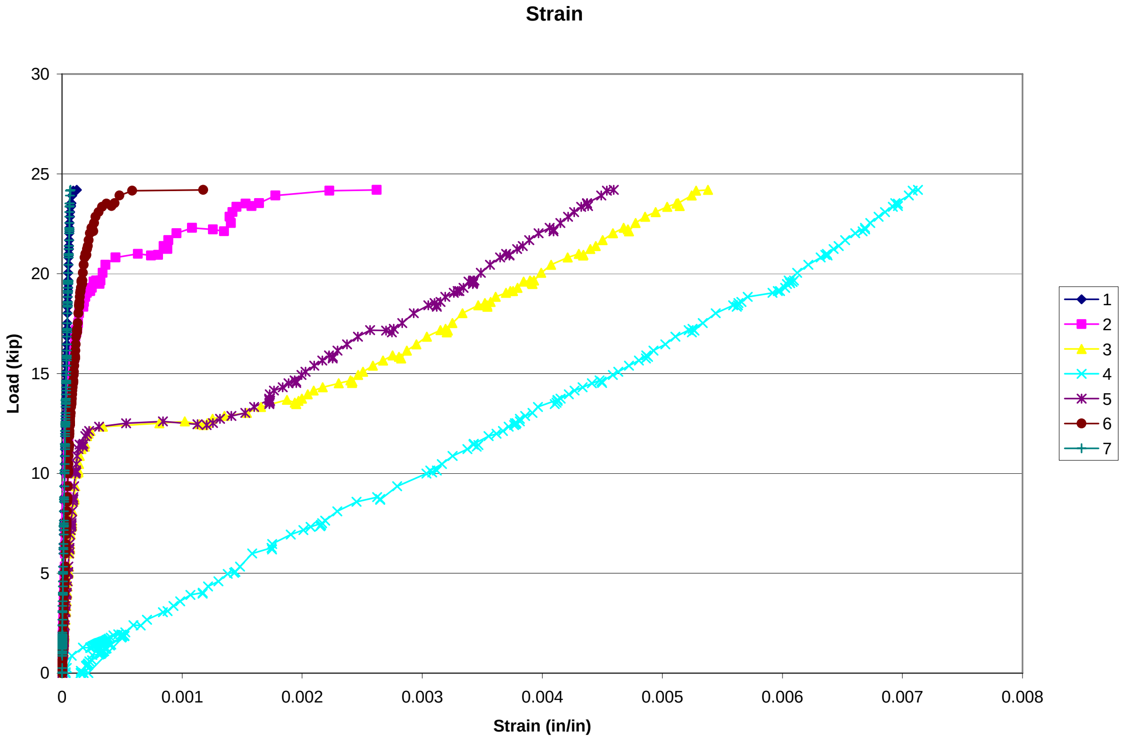

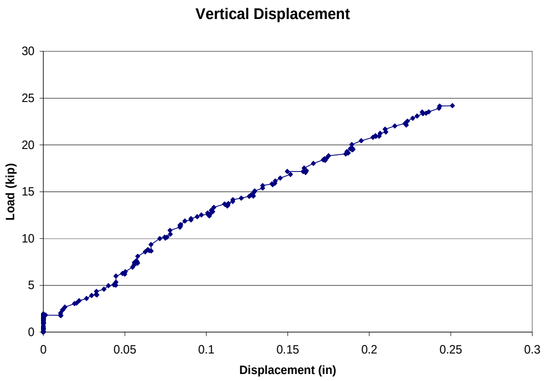

Vertical Displacement

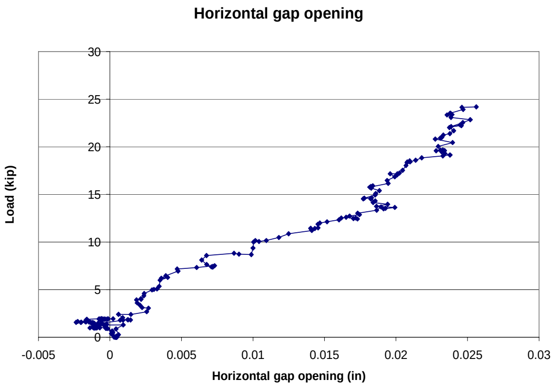

Horizontal gap opening

Photographs:

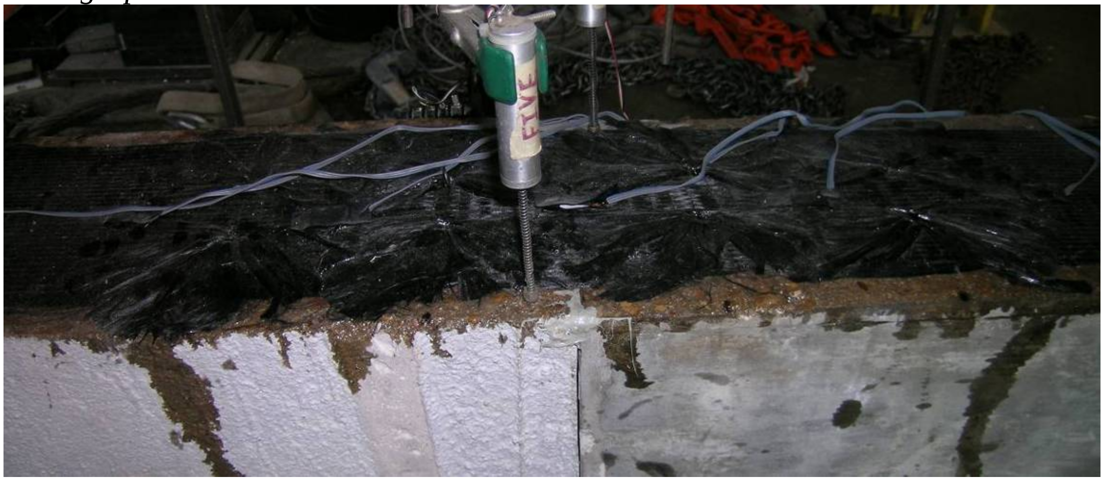

Before Testing

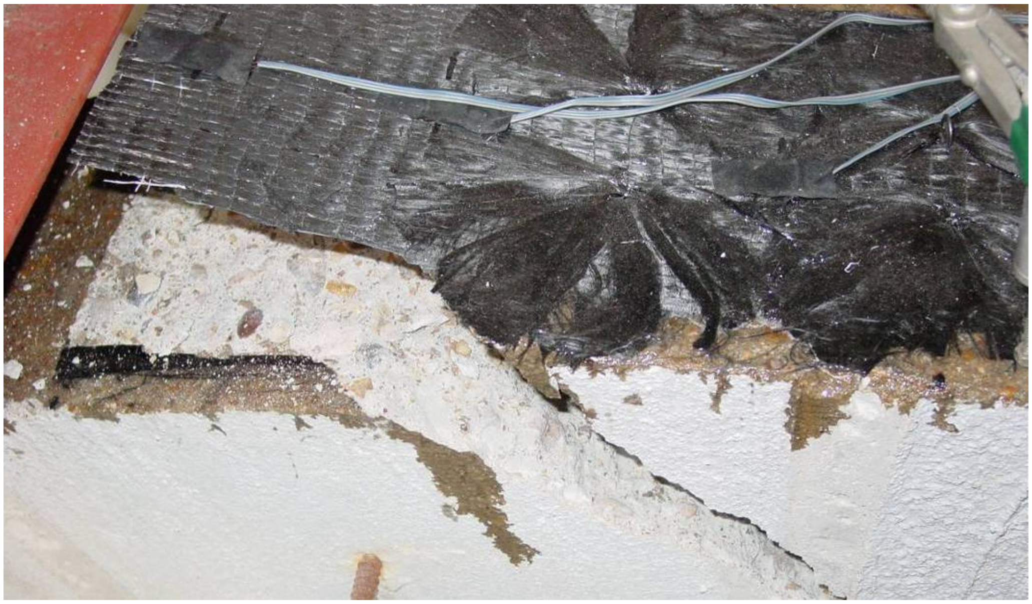

After Testing: Failure by shear in concrete block

00-ns1

Test Date: July 28th 2005
No height transition
No anchors
Sandblasting surface preparation
SCH-35 fabric

Specimen Design:

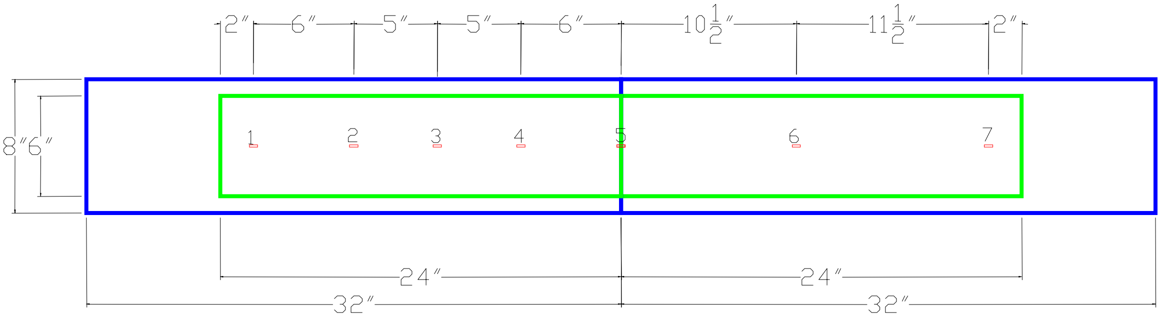
2"
6"
5"
5"
6"
10 1/2"
11 1/2"
2"
8"
6"
1
2
3
4
5
6
7
24"
24"
32"
32"

Test Data:

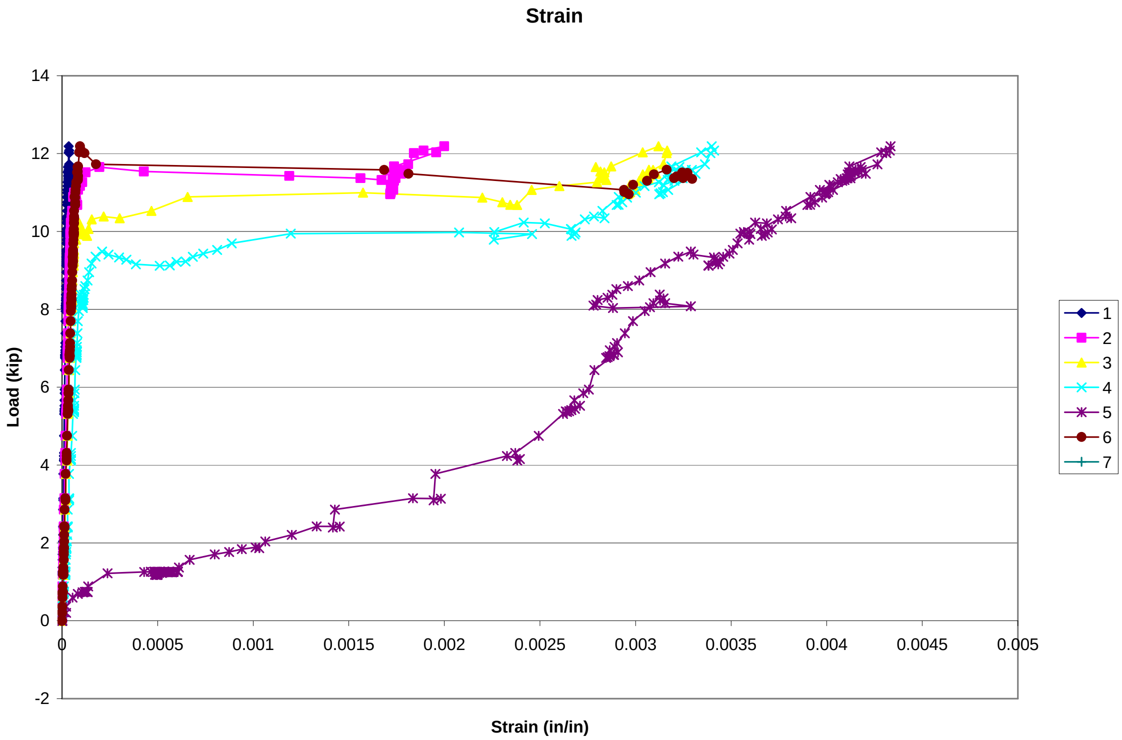

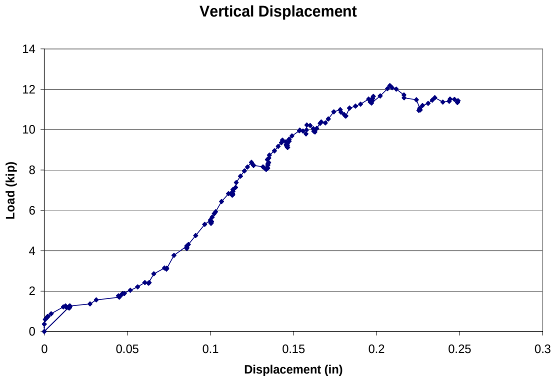

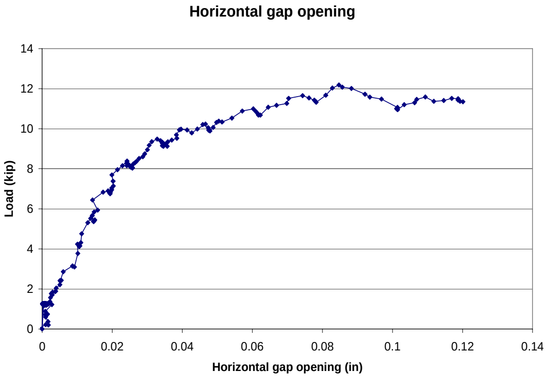

Photographs:

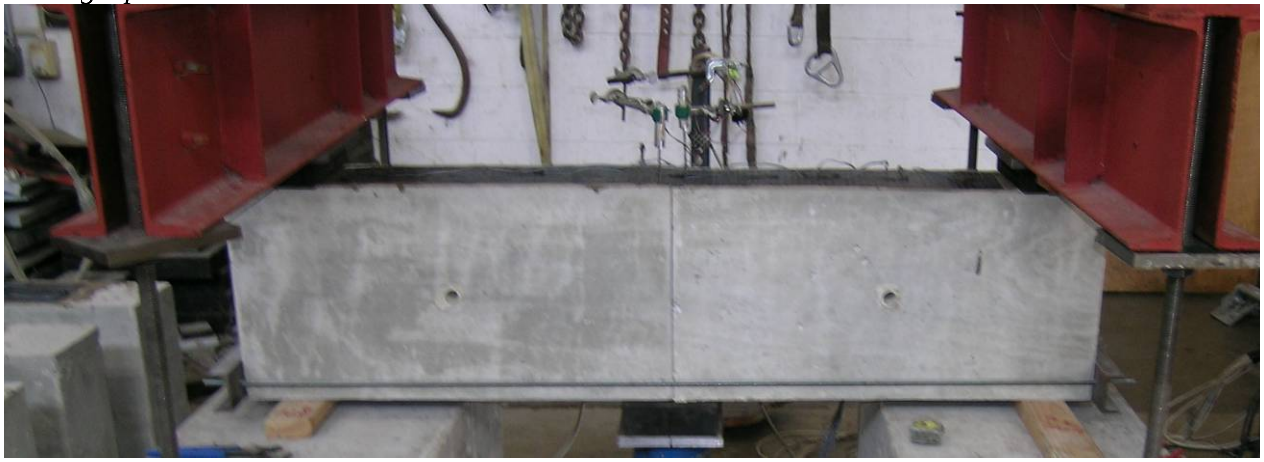

Before Testing

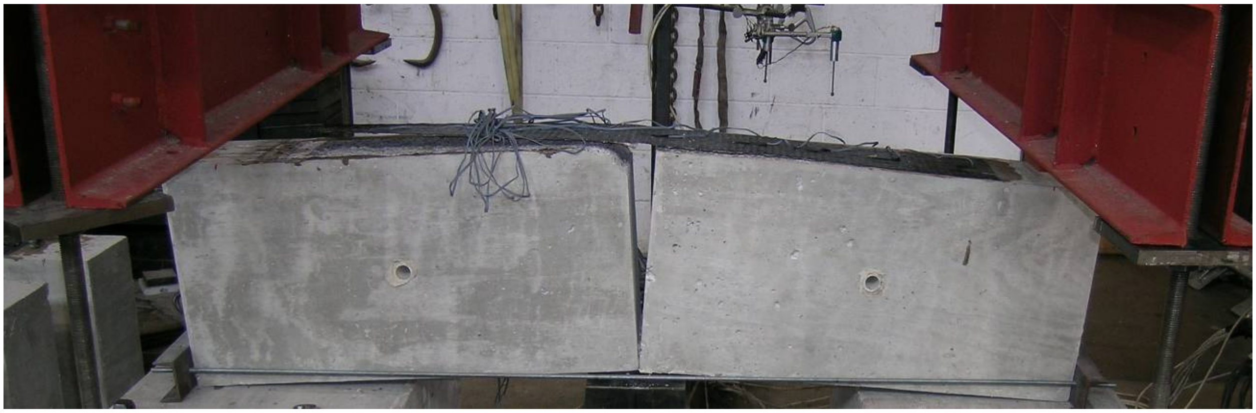

After Testing: Failure by debonding

00-2s1

Test Date: July 29th 2005
No height transition
One row of two anchors, 1 ½” width sheet, 3/8” diameter concrete hole
Sandblasting surface preparation
SCH-35 fabric

Specimen Design:

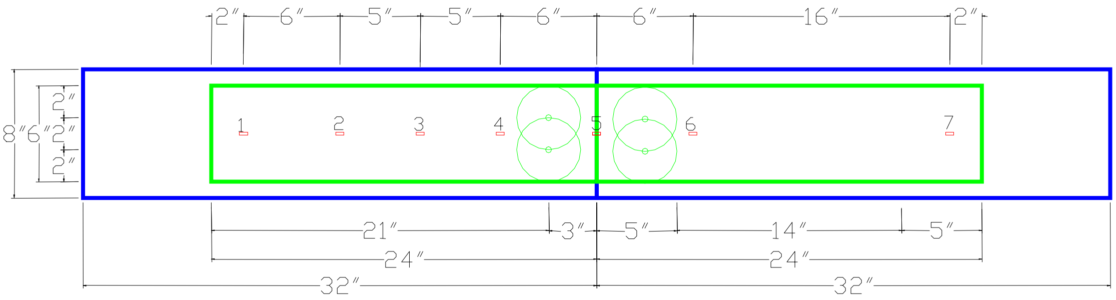
2″
6″
5″
5″
6″
6″
16″
2″
8″
6″
2″
2″
2″
1
2
3
4
5
6
7
21″
3″
5″
14″
5″
24″
24″
32″
32″

Test Data:

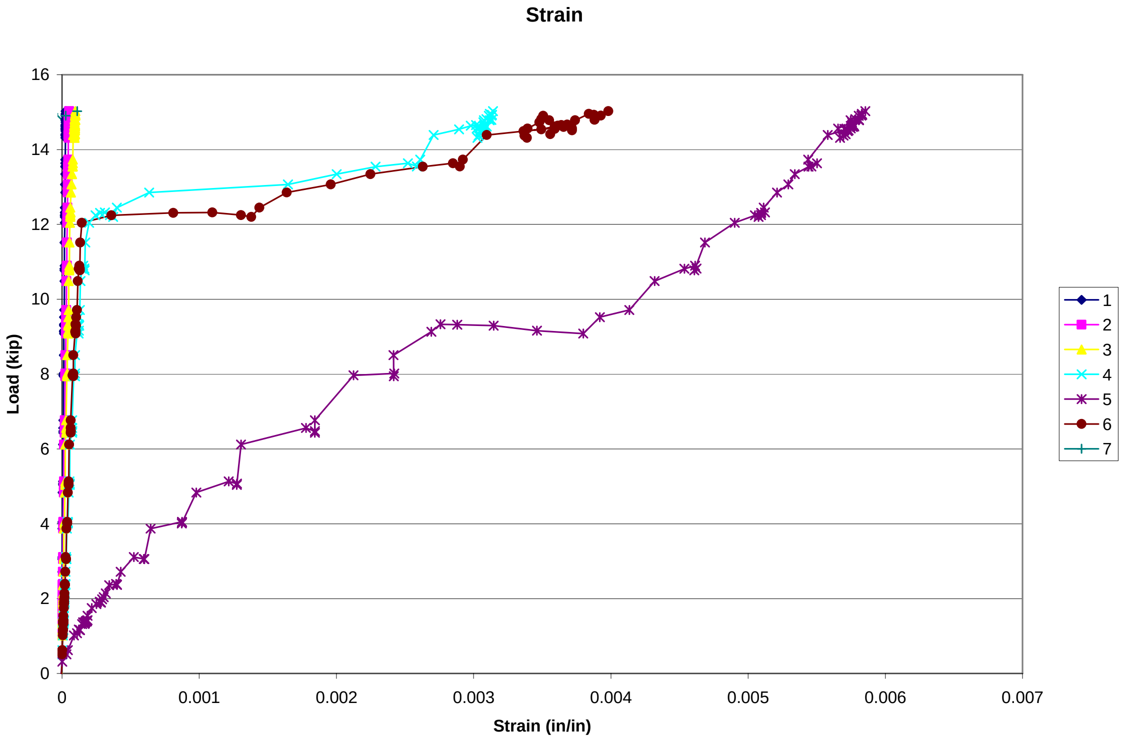

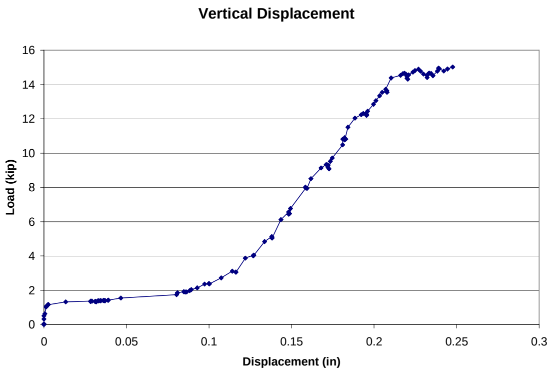

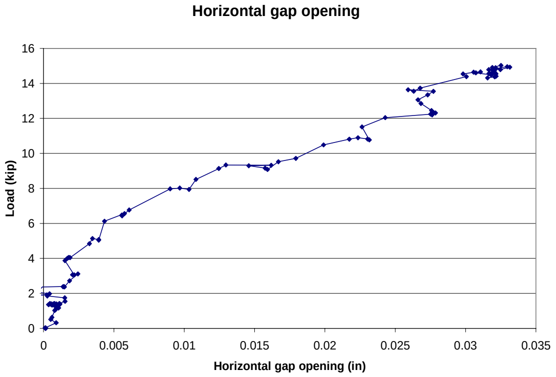

Photographs:

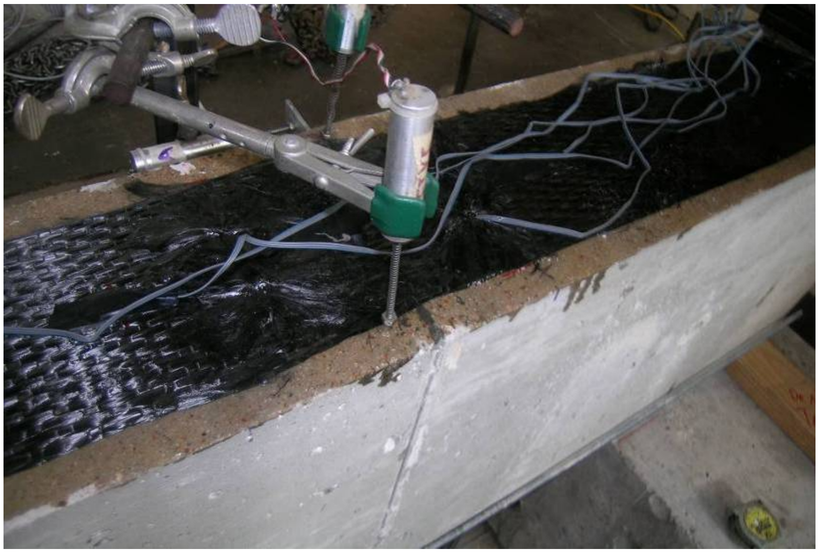

Before Testing

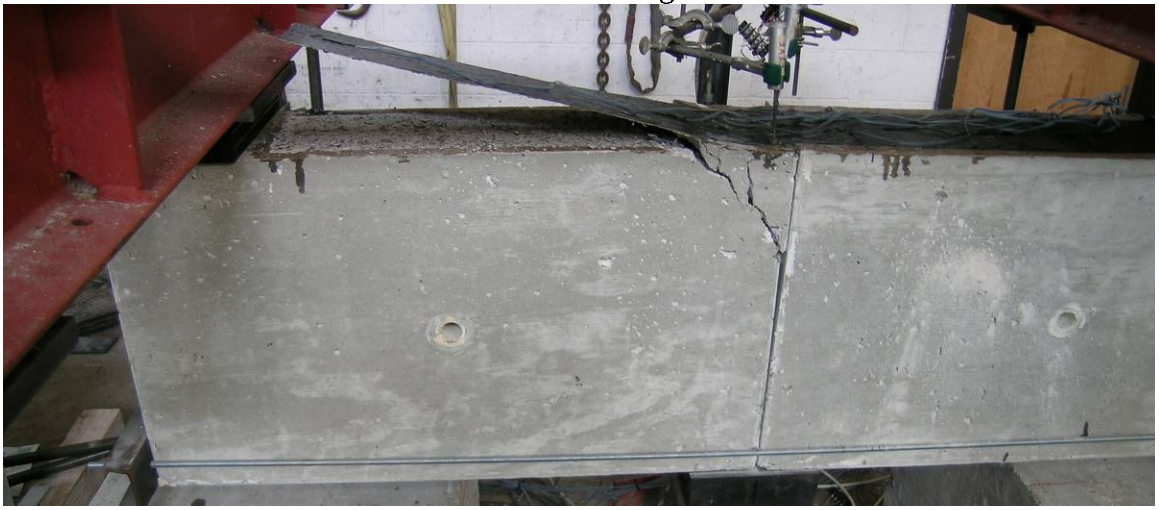

After Testing: Failure by corner crack and debonding

00-us1

Test Date: September 27th 2005
No height transition
Two single layer U-wraps, 6” width sheet
Sandblasting surface preparation
SCH-35 fabric

Specimen Design:

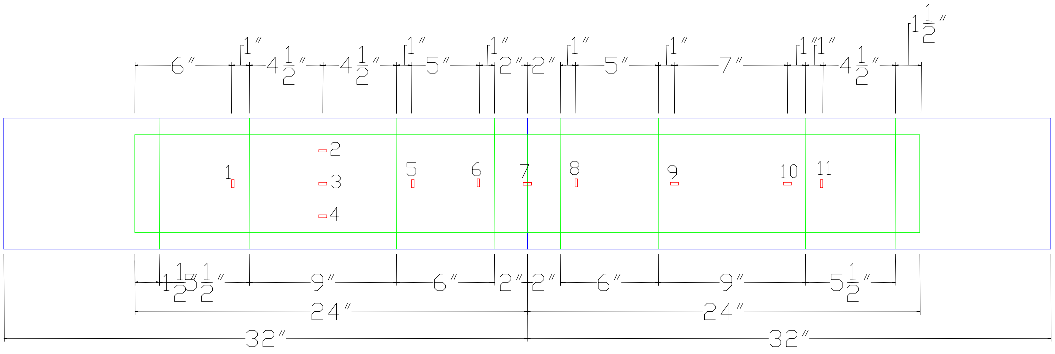

6″
1″
4 1/2″
4 1/2″
1″
5″
1″
2″
2″
1″
5″
1″
7″
1″
1″
4 1/2″
1 1/2″
1
2
3
4
5
6
7
8
9
10
11
1 1/2″
3 1/2″
9″
6″
2″
2″
6″
9″
5 1/2″
24″
24″
32″
32″

Test Data:

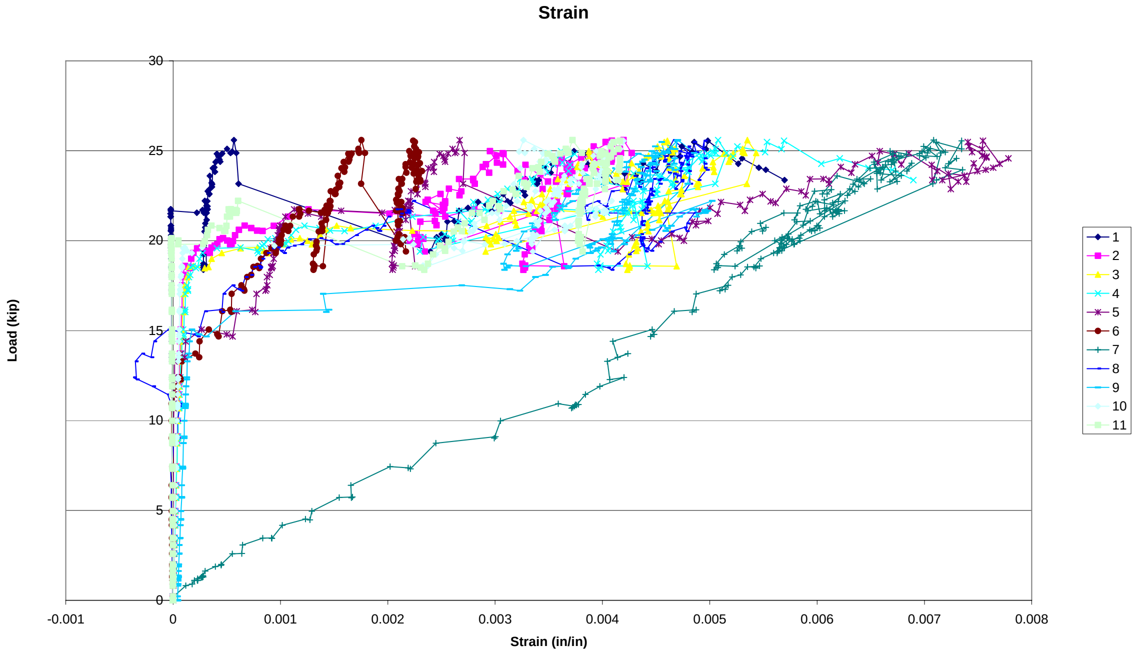

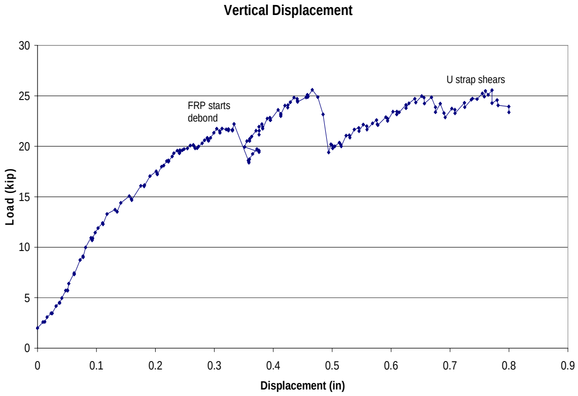

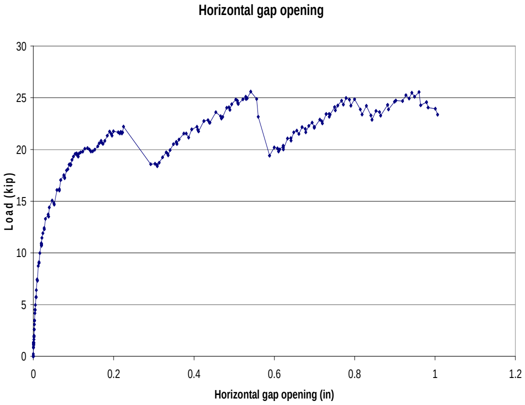

Photographs:

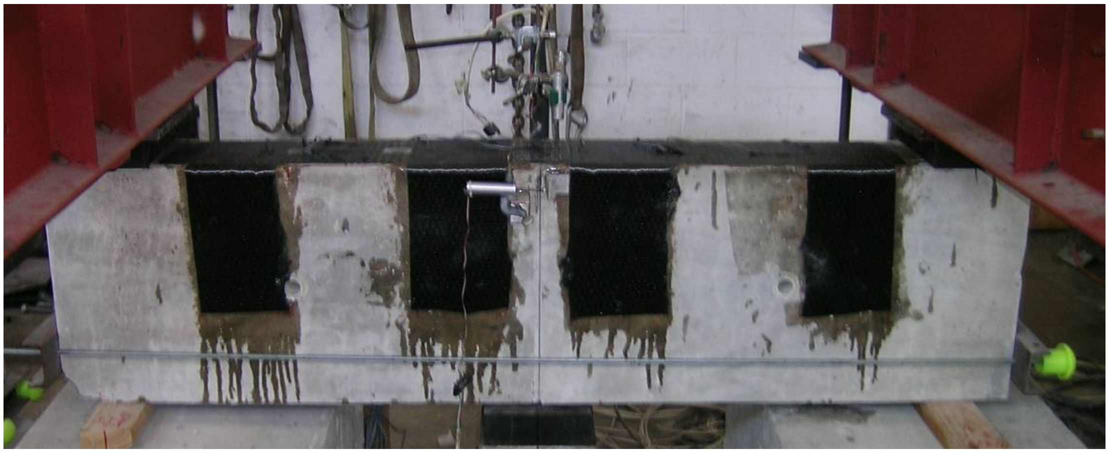

Before Testing

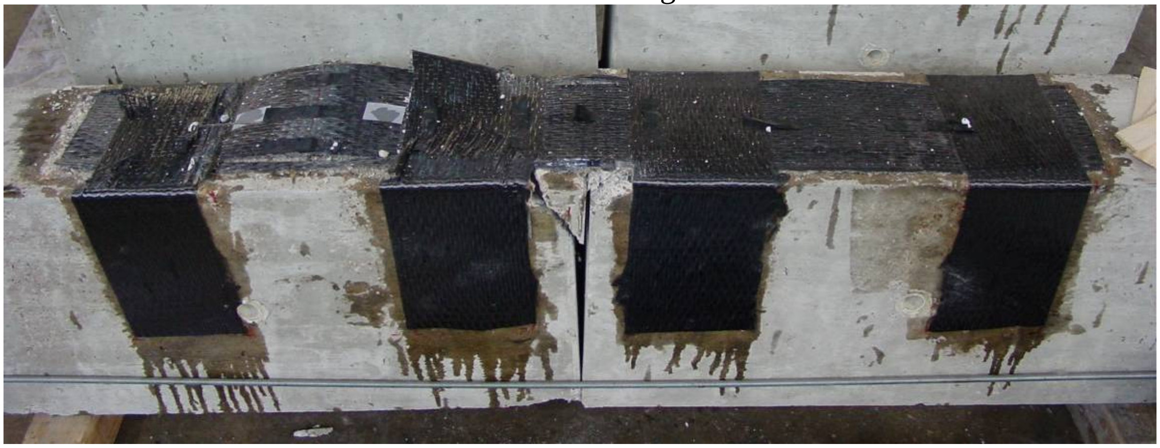

After Testing: Failure by U-wrap shear

00-4s1

Test Date: September 27th 2005
No height transition
Two rows of two anchors, 2” width sheet, 3/8” diameter concrete hole
Sandblasting surface preparation
SCH-35 fabric

Specimen Design:

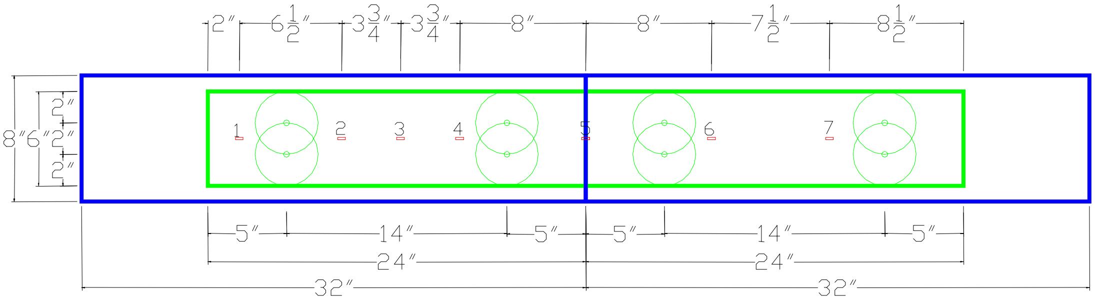

2″
6 1/2″
3 3/4″
3 3/4″
8″
8″
7 1/2″
8 1/2″
8″
6″
2″
2″
2″
1
2
3
4
5
6
7
5″
14″
5″
5″
14″
5″
24″
24″
32″
32″

Test Data:

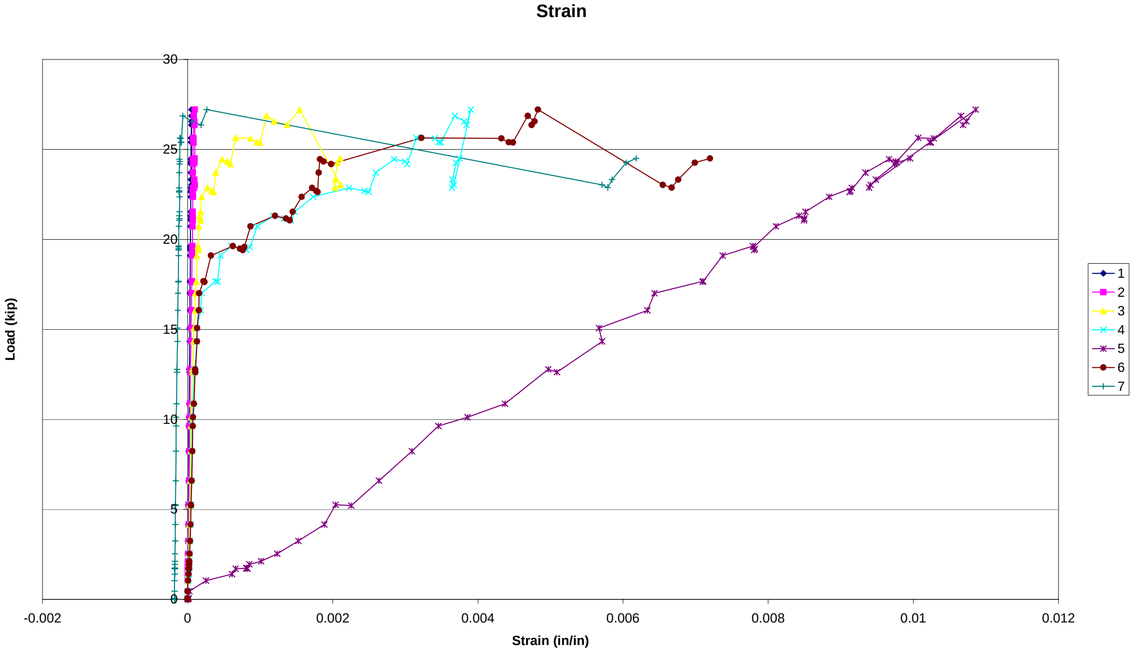

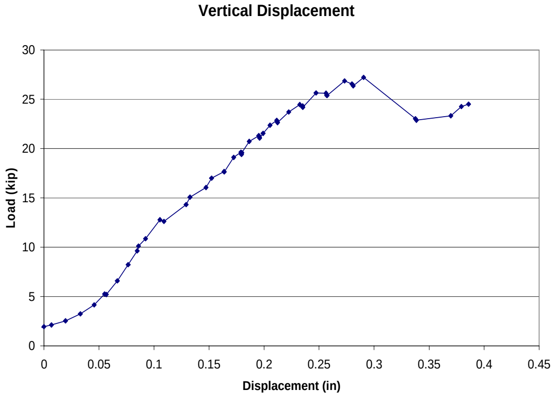

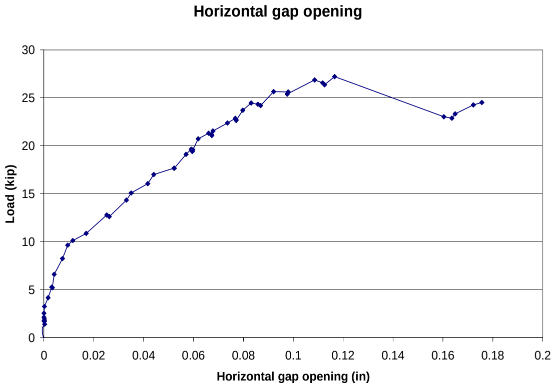

Photographs:

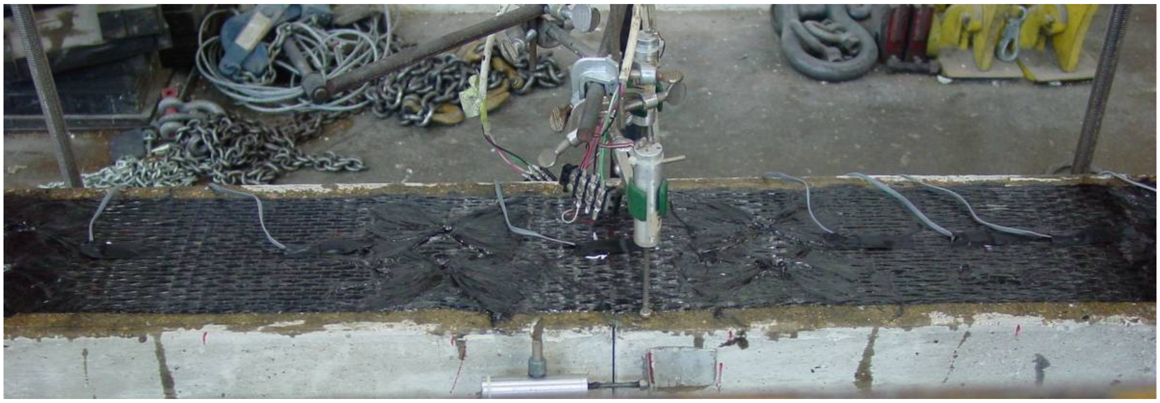

Before Testing

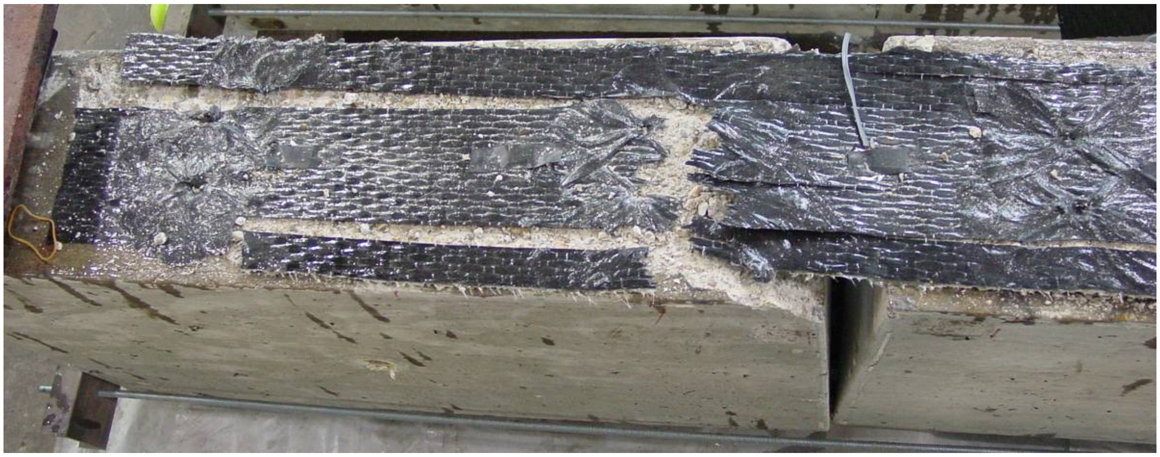

After Testing: Failure by partial debonding and fracture

00-6s1

Test Date: November 28th 2005
No height transition
Two rows of three anchors, 2” width sheet, 3/8” diameter concrete hole
Sandblasting surface preparation
SCH-35 fabric

Specimen Design:

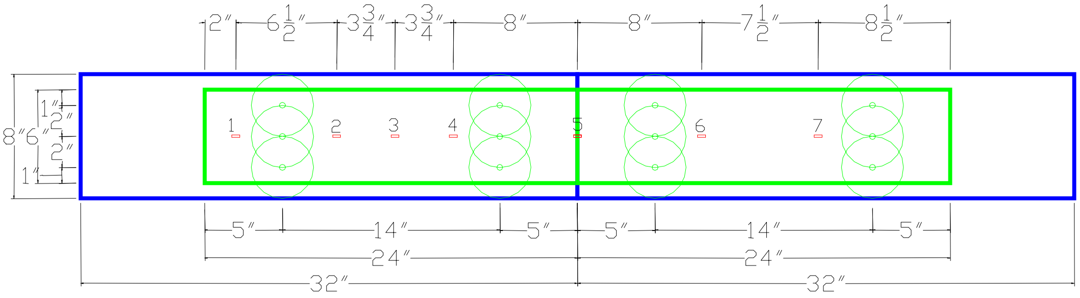
2″
6½″
3¾″
3¾″
8″
8″
7½″
8½″
8″
6″
1″
2″
2″
1″
1
2
3
4
5
6
7
5″
14″
5″
5″
14″
5″
24″
24″
32″
32″

Test Data:

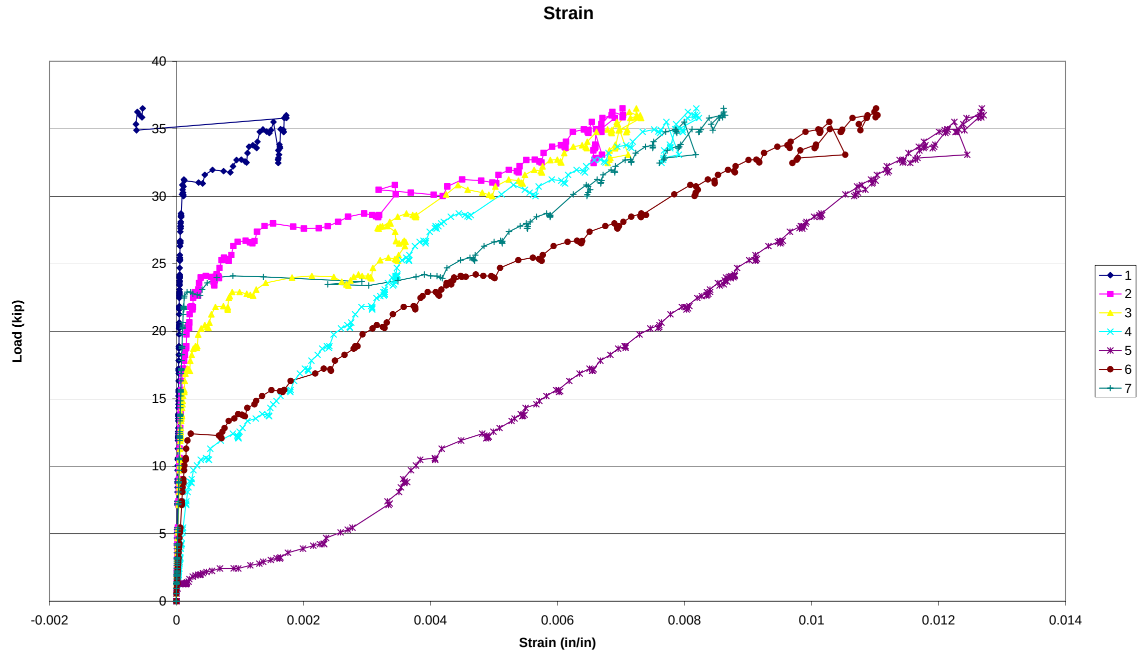

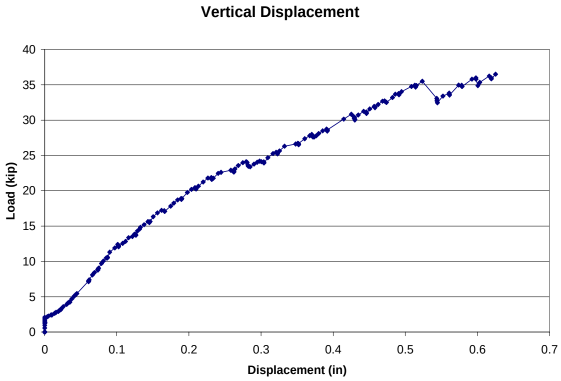

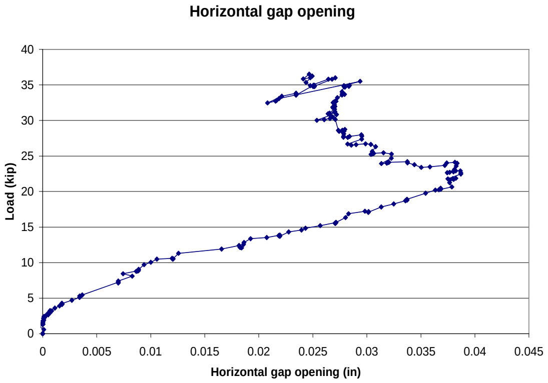

Photographs:

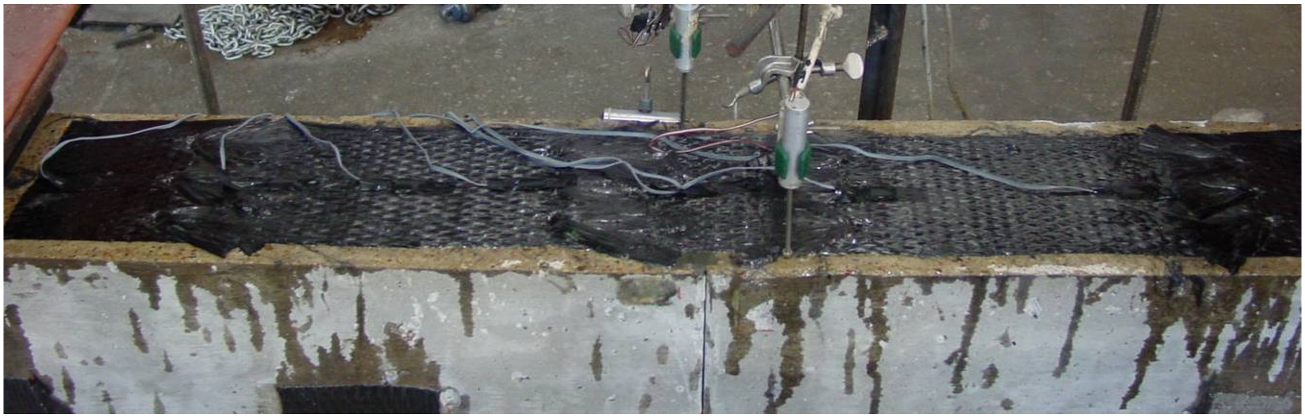

Before Testing

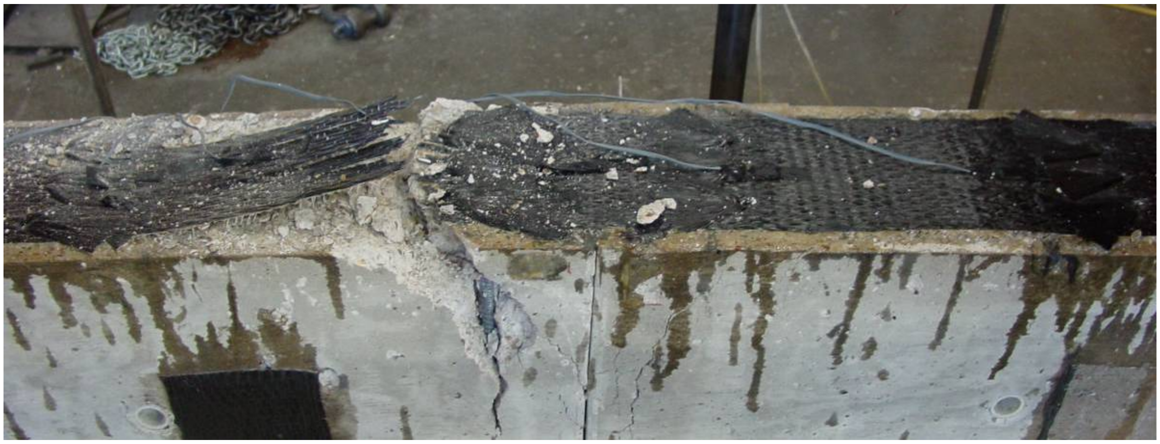

After Testing: Failure by FRP fracture

00-us2

Test Date: November 1st 2005
No height transition
Two double layer U-wraps, 6” width sheet
Sandblasting surface preparation
SCH-35 fabric

Specimen Design:

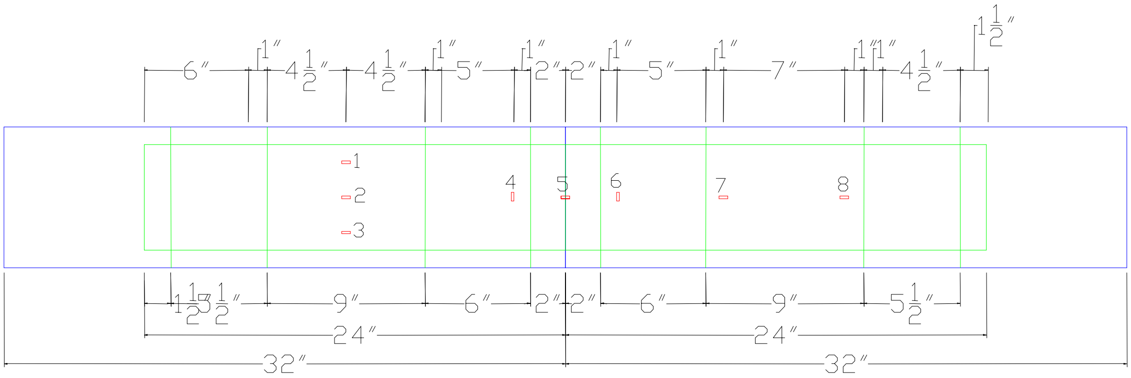
6″
1″
4 1/2″
4 1/2″
1″
5″
1″
2″
2″
1″
5″
1″
7″
1″
1″
4 1/2″
1 1/2″
1
2
3
4
5
6
7
8
1 1/2″
3 1/2″
9″
6″
2″
2″
6″
9″
5 1/2″
24″
24″
32″
32″

Test Data:

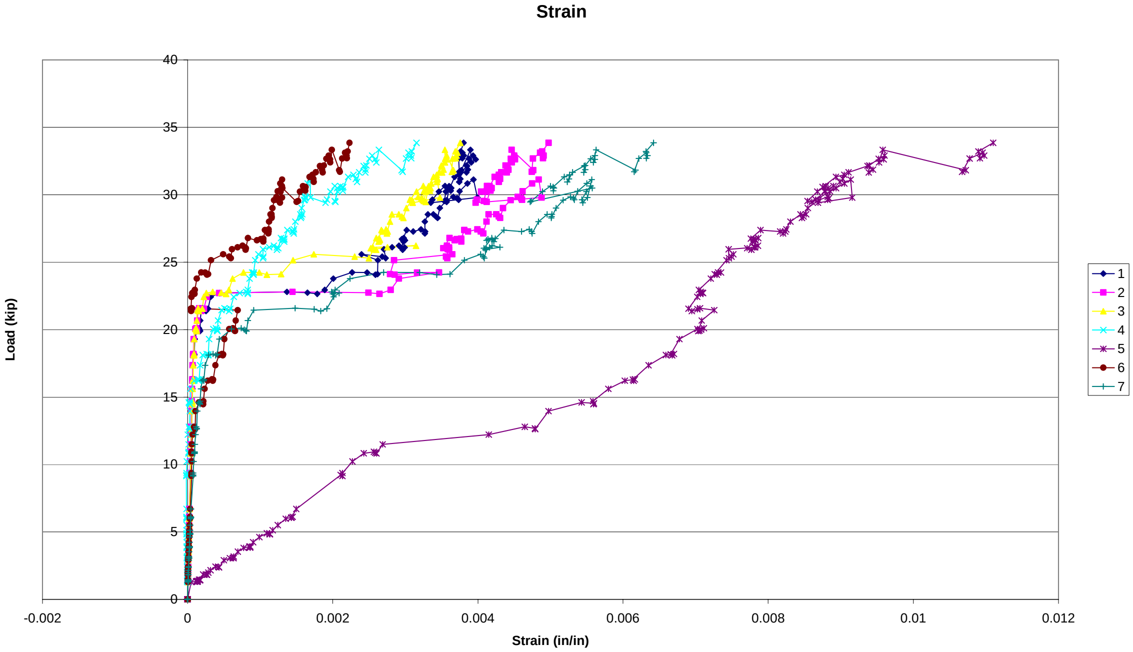

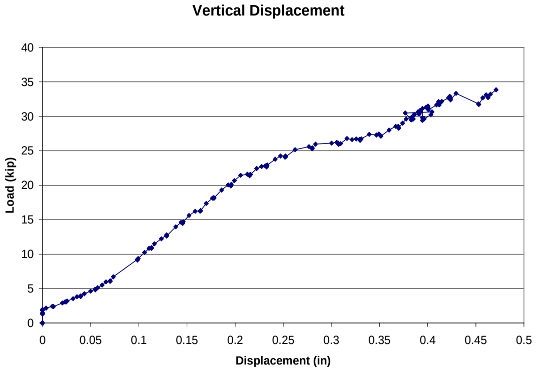

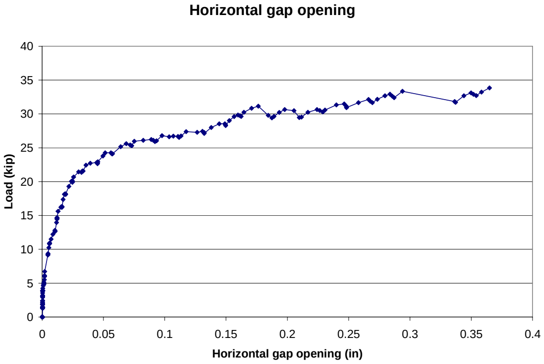

Photographs:

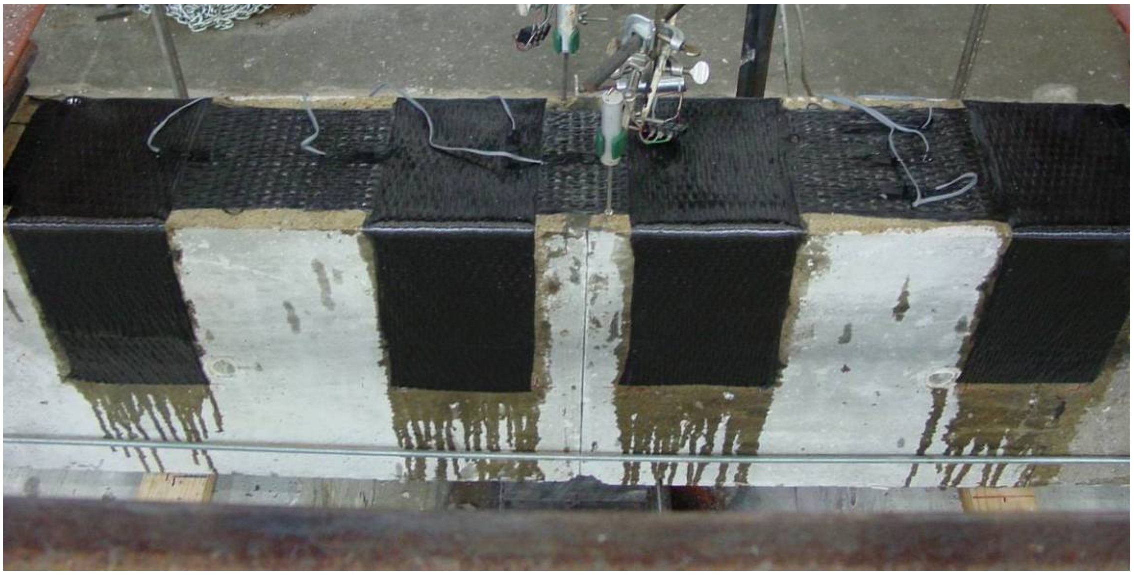

Before Testing

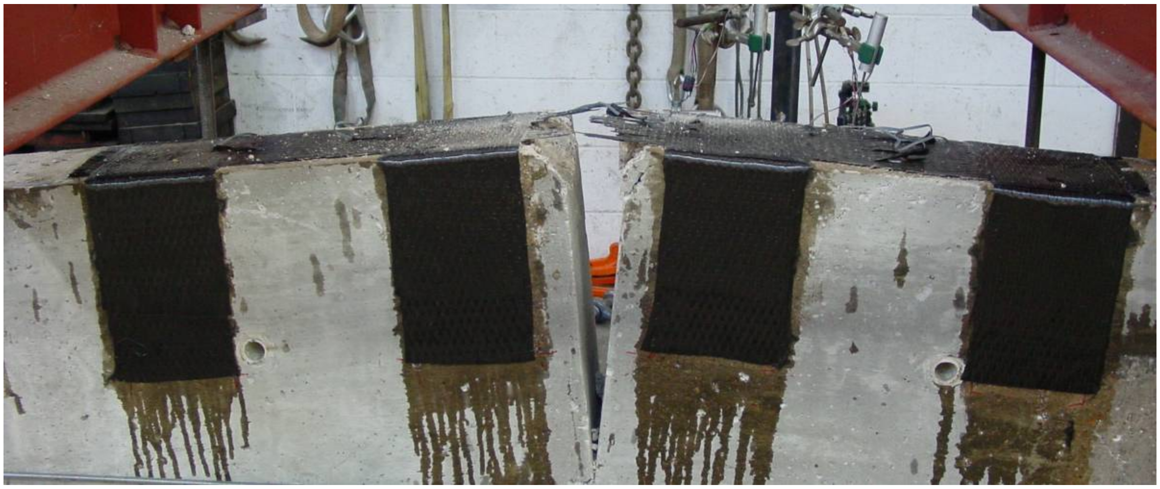

After Testing: Failure by FRP fracture

00-2s2

Test Date: January 24th 2006
No height transition
Two rows of one anchor, 6” width sheet, 5/8” concrete hole
Sandblasting surface preparation
SCH-35 fabric sheet, SCH-41 fabric anchors

Specimen Design:

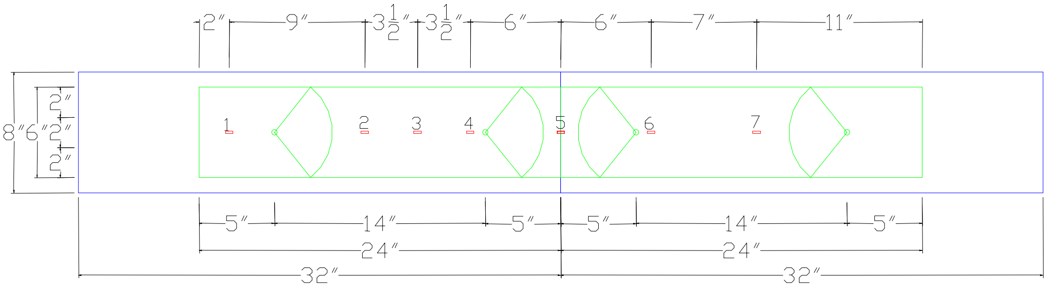
2″
9″
3½″
3½″
6″
6″
7″
11″
8″
6″
2″
2″
2″
1
2
3
4
5
6
7
5″
14″
5″
5″
14″
5″
24″
24″
32″
32″

Test Data:

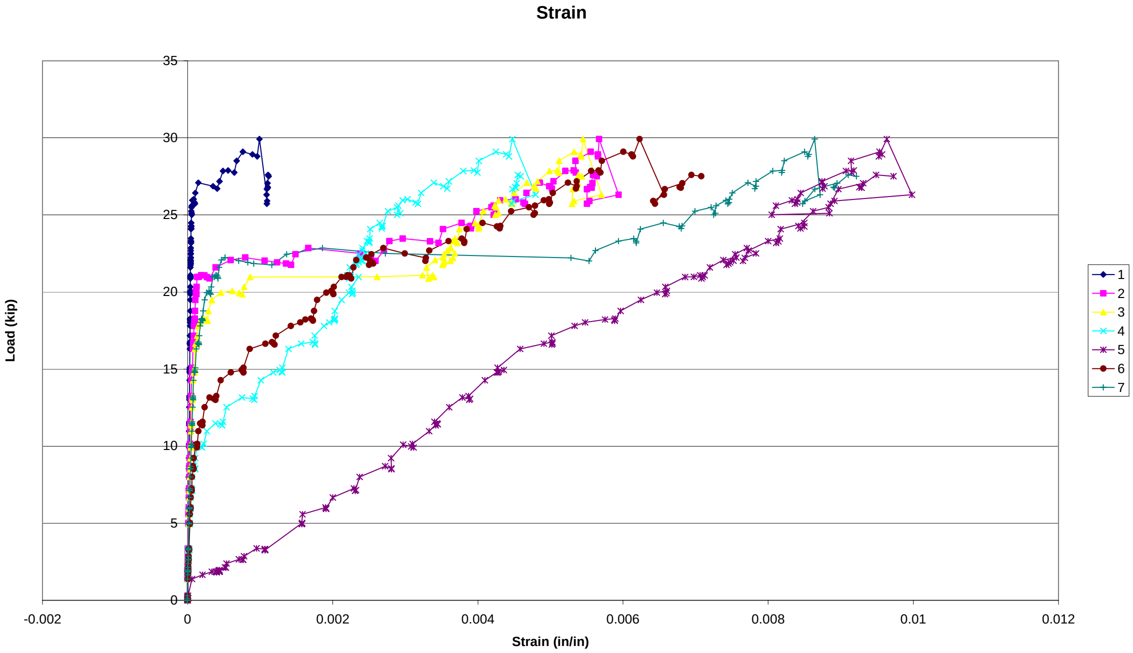

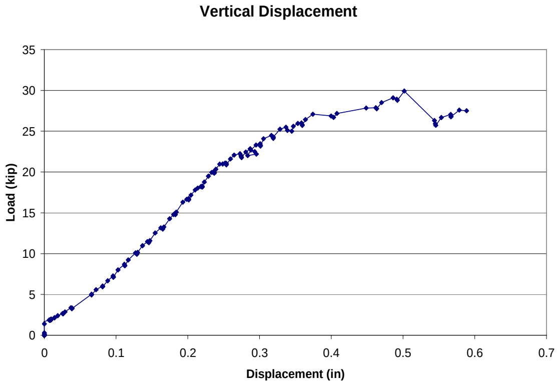
Vertical Displacement

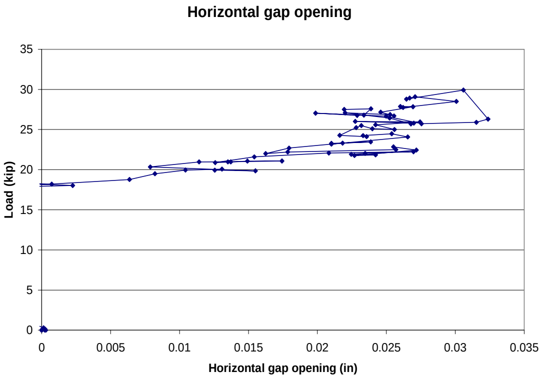
Horizontal gap opening

Photographs:

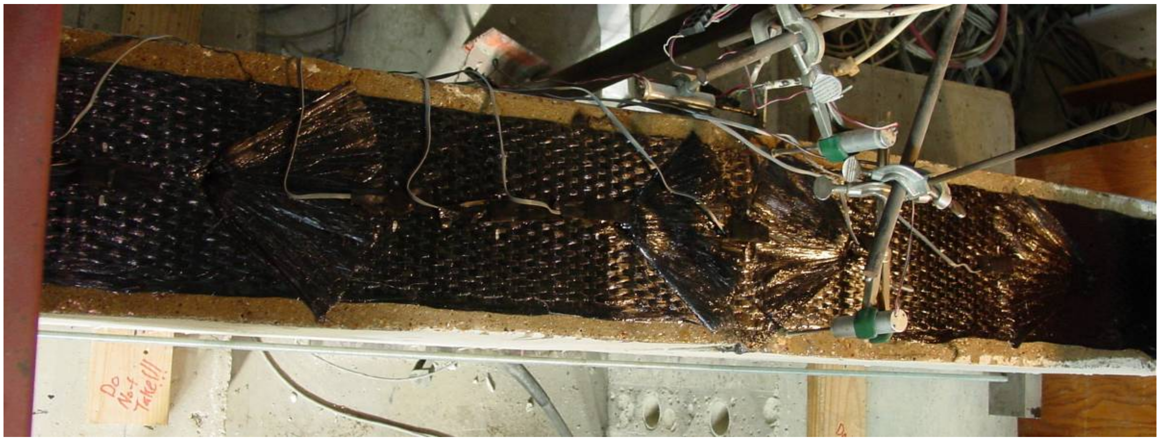

Before Testing

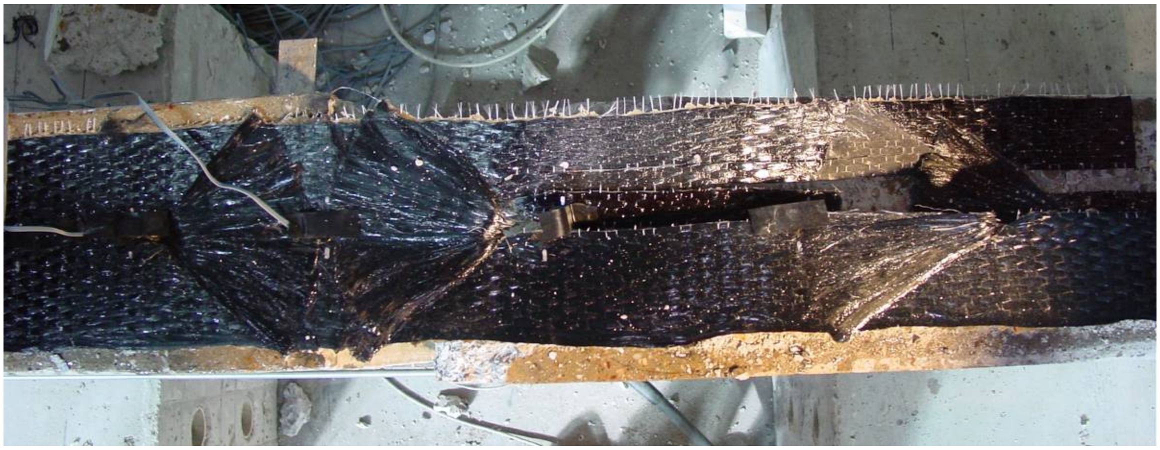

After Testing: Failure by debonding and FRP fracture

00-4s2

Test Date: January 24th 2006
No height transition
Two rows of one anchor, 3” width sheet, 1/2” concrete hole
Sandblasting surface preparation
SCH-35 fabric sheet, SCH-41 fabric anchors

Specimen Design:

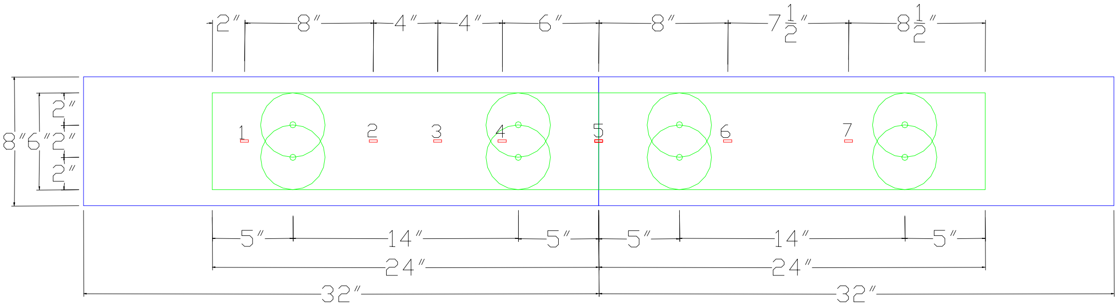
2"
8"
4"
4"
6"
8"
7 1/2"
8 1/2"
8"
6"
2"
2"
2"
2"
1
2
3
4
5
6
7
5"
14"
5"
5"
14"
5"
24"
24"
32"
32"

Test Data:

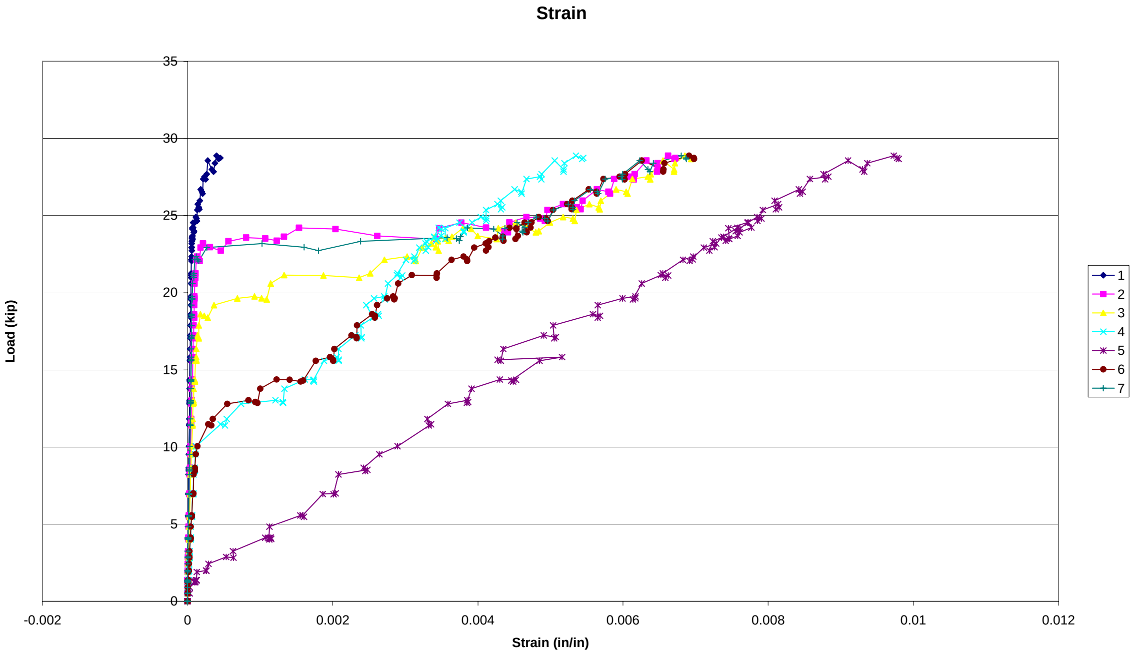

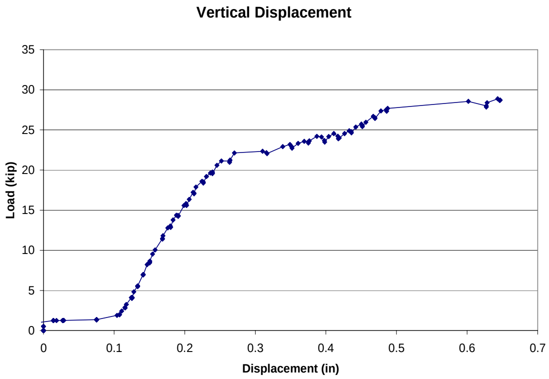

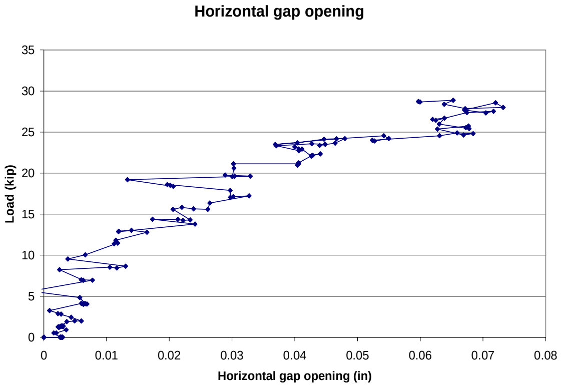

Photographs:

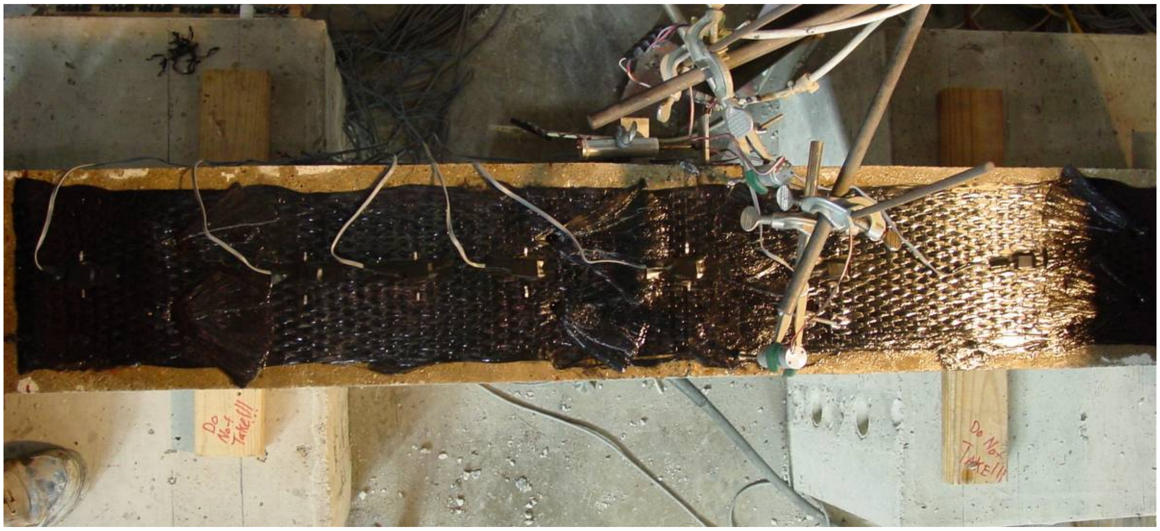
Do Not Take!!
Do Not Take!!

Before Testing

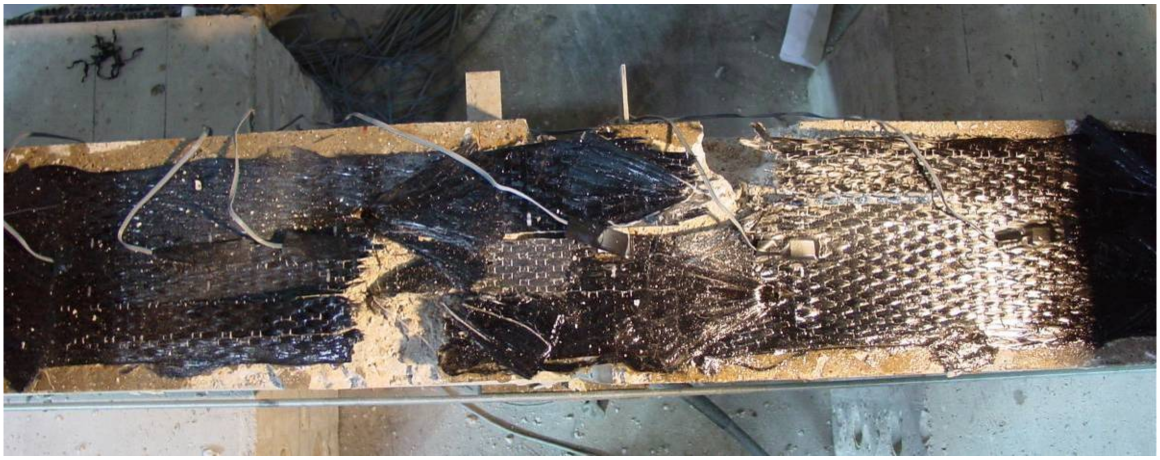

After Testing: Failure by FRP fracture

00-4s3

Test Date: March 21st 2006
No height transition
Two rows of one anchor, 4” width sheet, 5/8” concrete hole
Sandblasting surface preparation
SCH-35 fabric sheet, SCH-41 fabric anchors

Specimen Design:

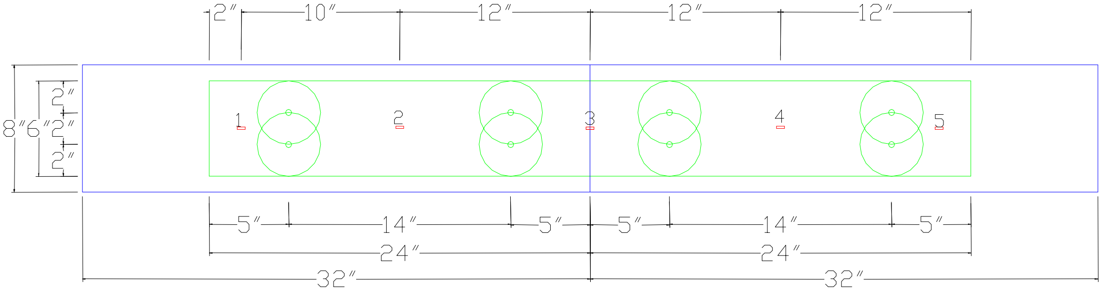

2″
10″
12″
12″
12″
8″
6″
2″
2″
2″
1
2
3
4
5
5″
14″
5″
5″
14″
5″
24″
24″
32″
32″

Test Data:

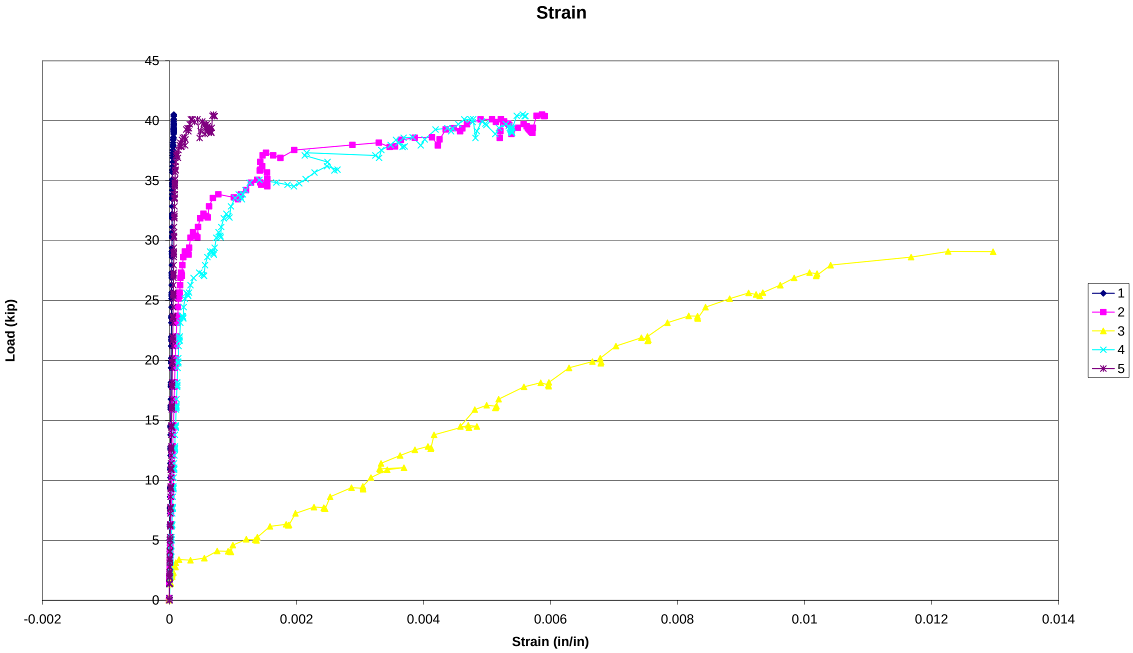

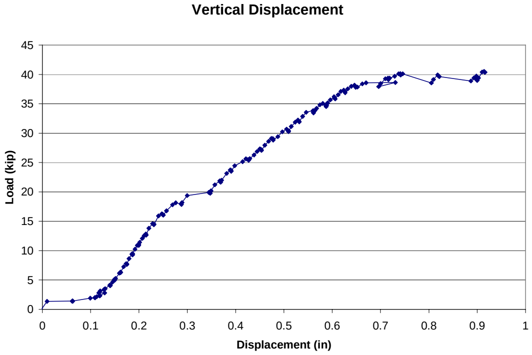

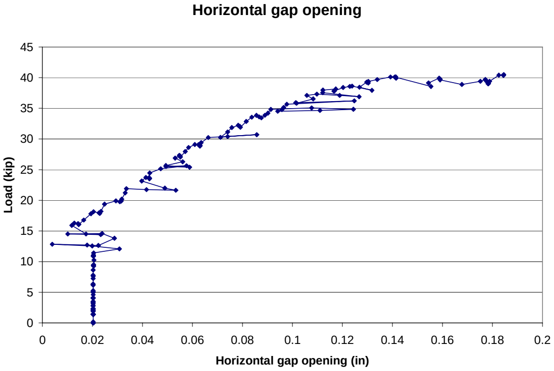

Photographs:

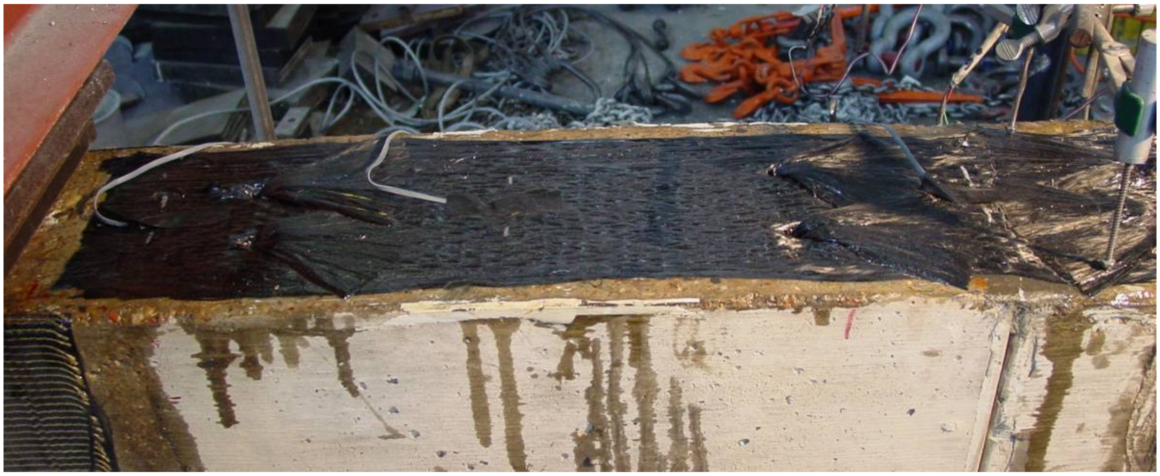

Before Testing

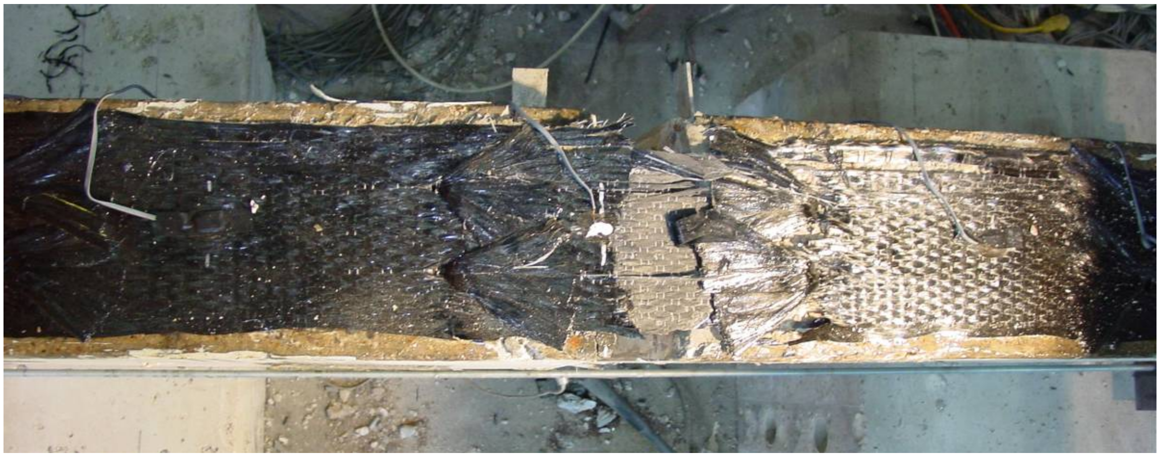

After Testing: Failure by FRP fracture

TESTS WITH HEIGHT TRANSITION

22-ng1

Test Date: May 10th, 2005
2” height transition
1 to 2 slope
No anchors
Grinding surface preparation
SCH-35 fabric

Specimen Design:

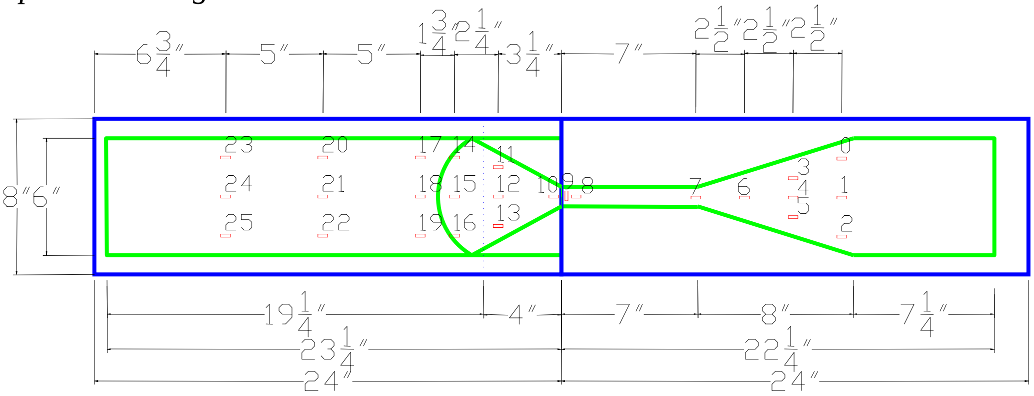
6 3/4″
5″
5″
1 3/4″
2 1/4″
3 1/4″
7″
2 1/2″
2 1/2″
2 1/2″
8″
6″
23
20
17
14
11
24
21
18
15
12
10
9
8
7
6
3
4
5
0
1
2
25
22
19
16
13
19 1/4″
4″
7″
8″
7 1/4″
23 1/4″
22 1/4″
24″
24″

Test Data:

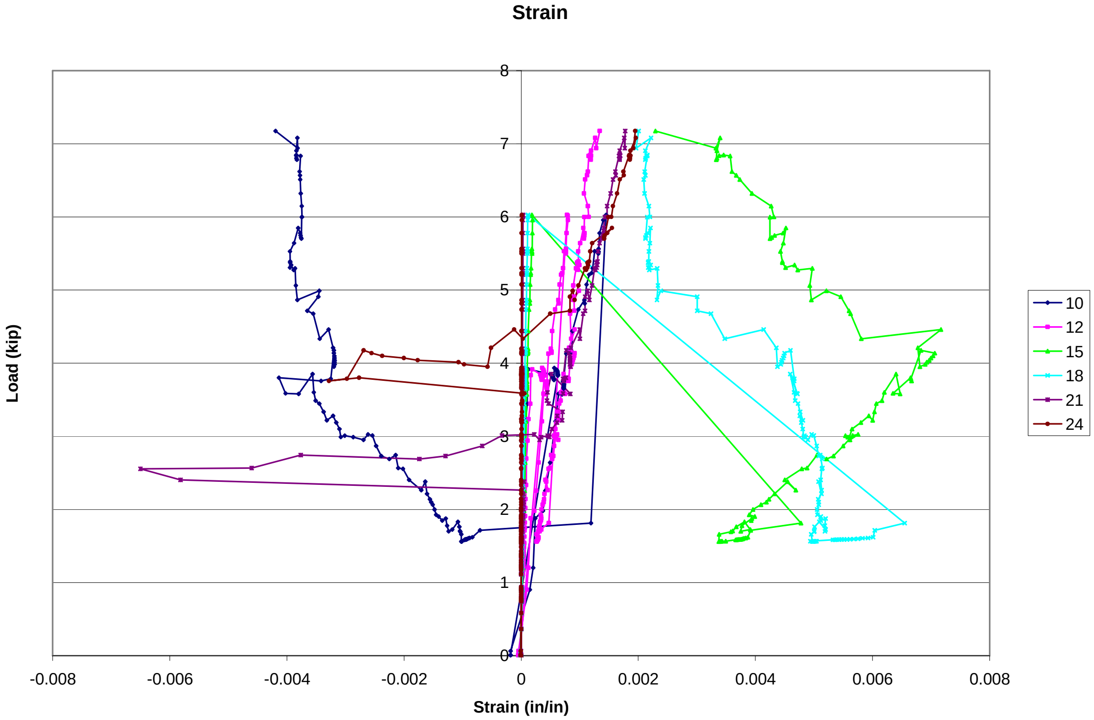

Vertical displacement data not available

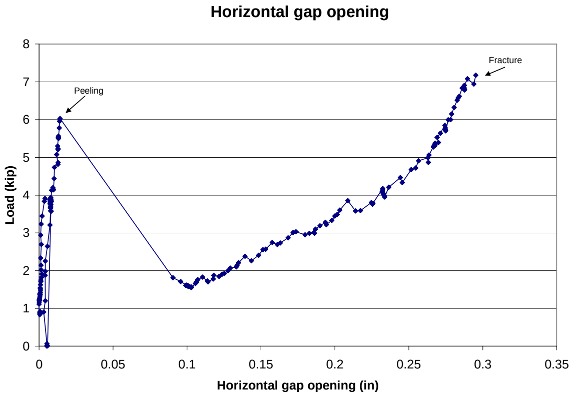

Photographs:

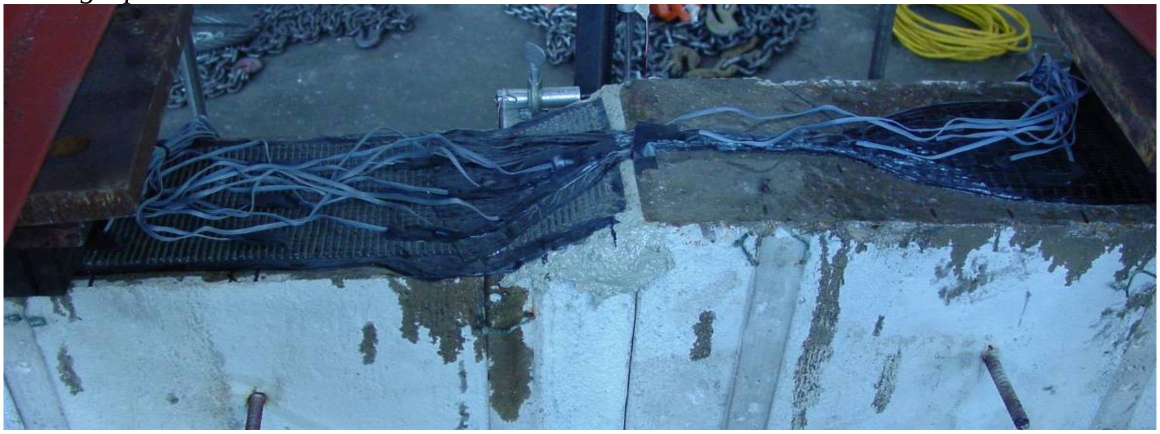

Before Testing

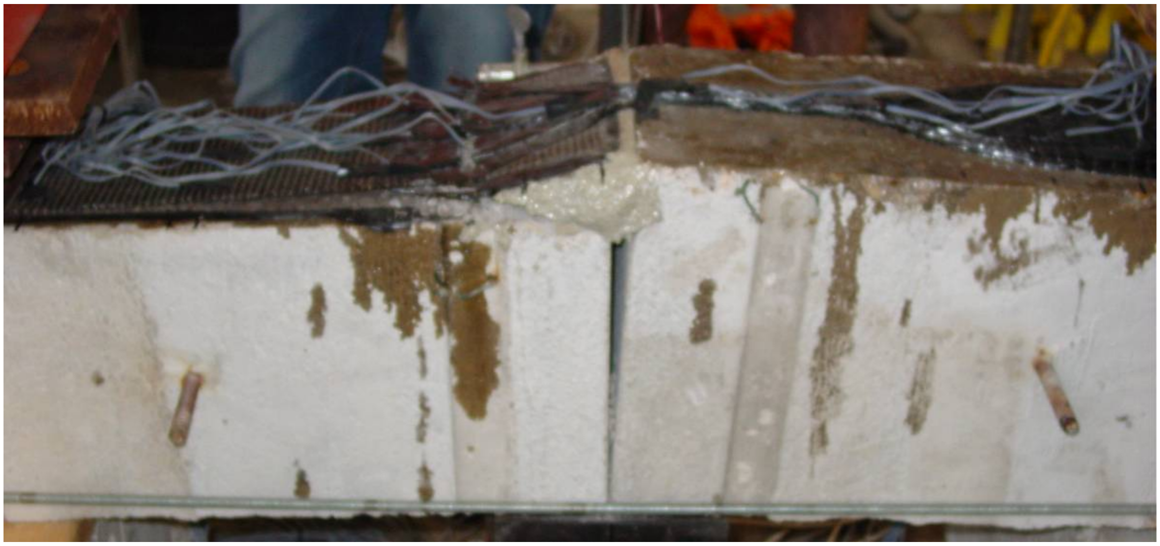

After Testing: Failure by Debonding

22-2g1

Test Date: July 29th, 2005
2” height transition
1 to 2 slope
2 anchors at end of ramp, 1 ½” width sheet, 3/8” diameter concrete hole
Grinding surface preparation
SCH-35 fabric

Specimen Design:

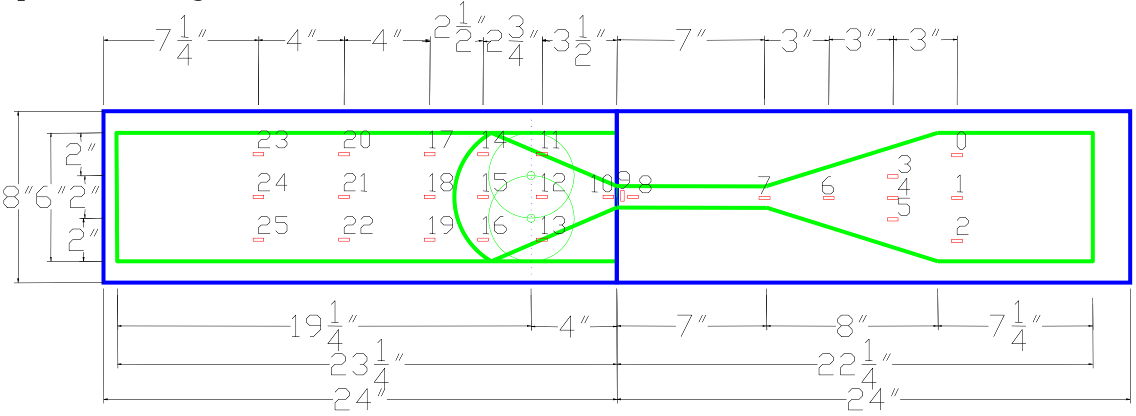
7 1/4"
4"
4"
2 1/2"
2 3/4"
3 1/2"
7"
3"
3"
3"
8"
6"
2"
2"
2"
23
20
17
14
11
0
24
21
18
15
12
10
9
8
7
6
3
4
5
1
25
22
19
16
13
2
19 1/4"
4"
7"
8"
7 1/4"
23 1/4"
22 1/4"
24"
24"

Test Data:

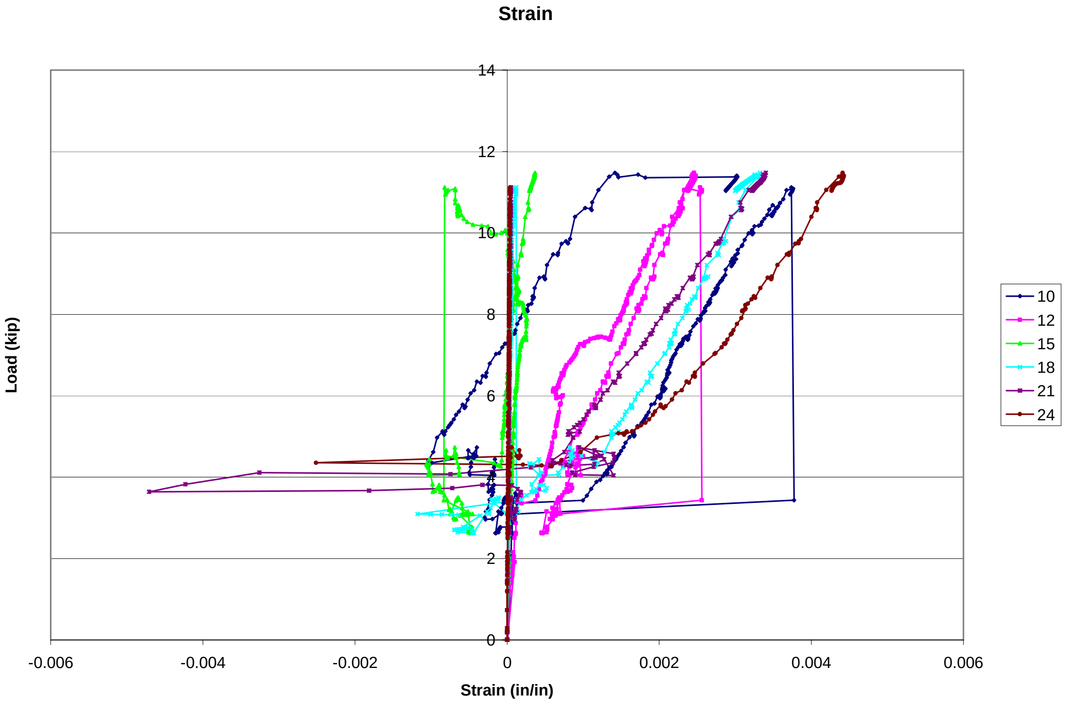

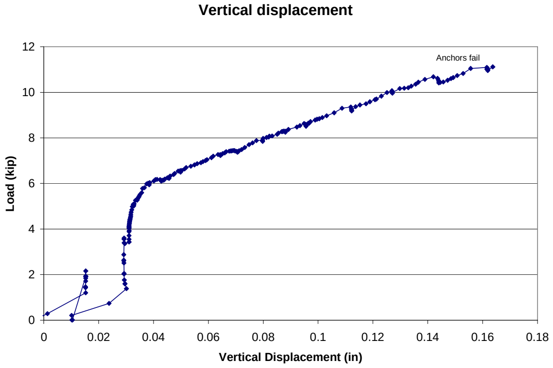

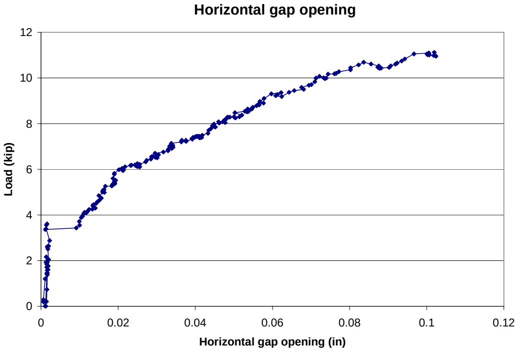

Photographs:

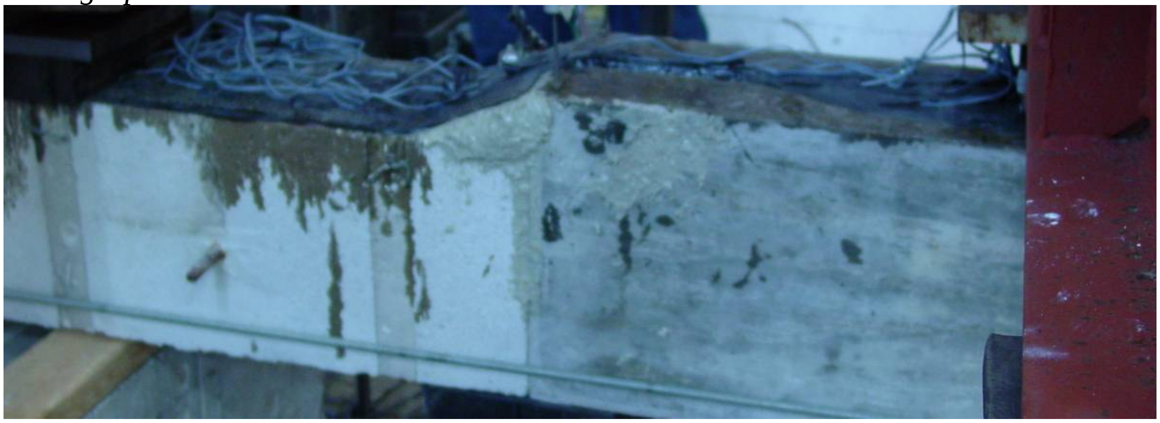

Before Testing

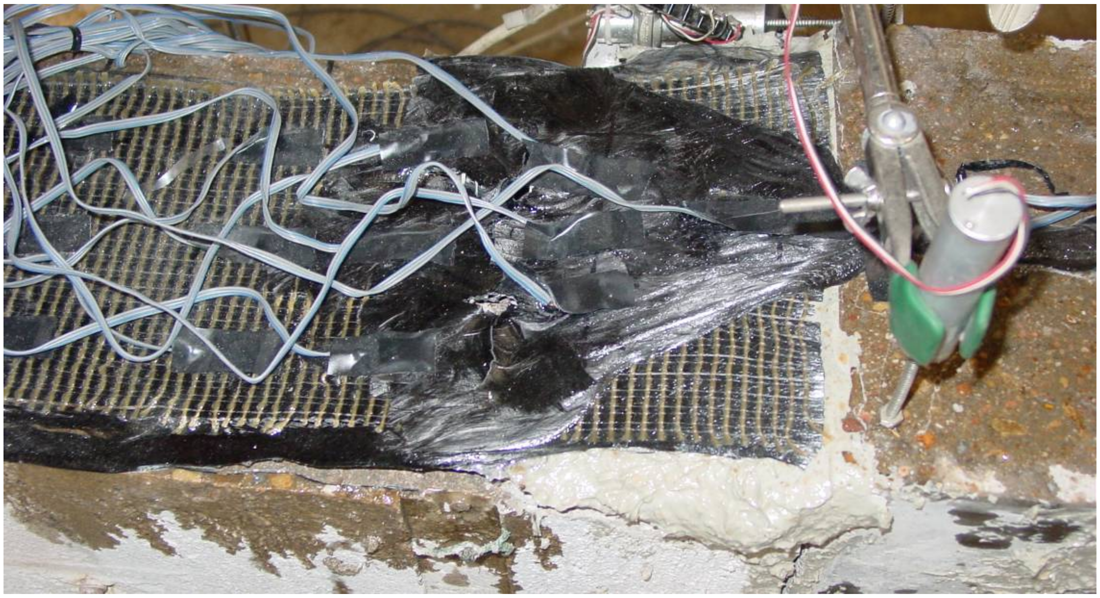

After Testing: Failure by anchor fracture

22-ns1

Test Date: July 29th, 2005
2” height transition
1 to 2 slope
No anchors
Sandblasting surface preparation
SCH-35 fabric

Specimen Design:

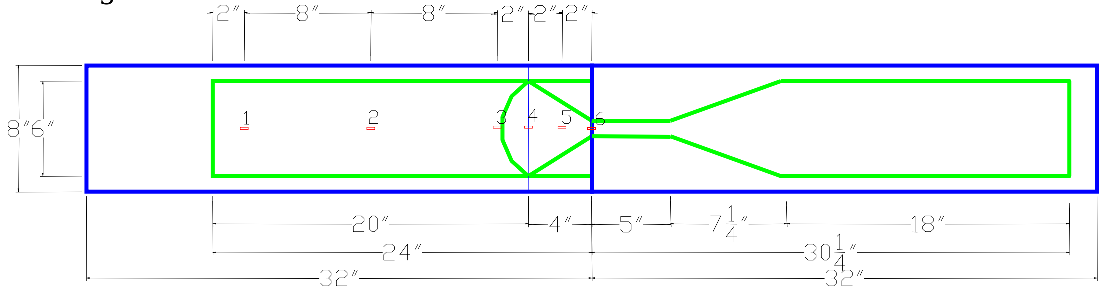

2″
8″
8″
2″
2″
2″
8″
6″
1
2
3
4
5
6
20″
4″
5″
7 1/4″
18″
24″
30 1/4″
32″
32″

Test Data:

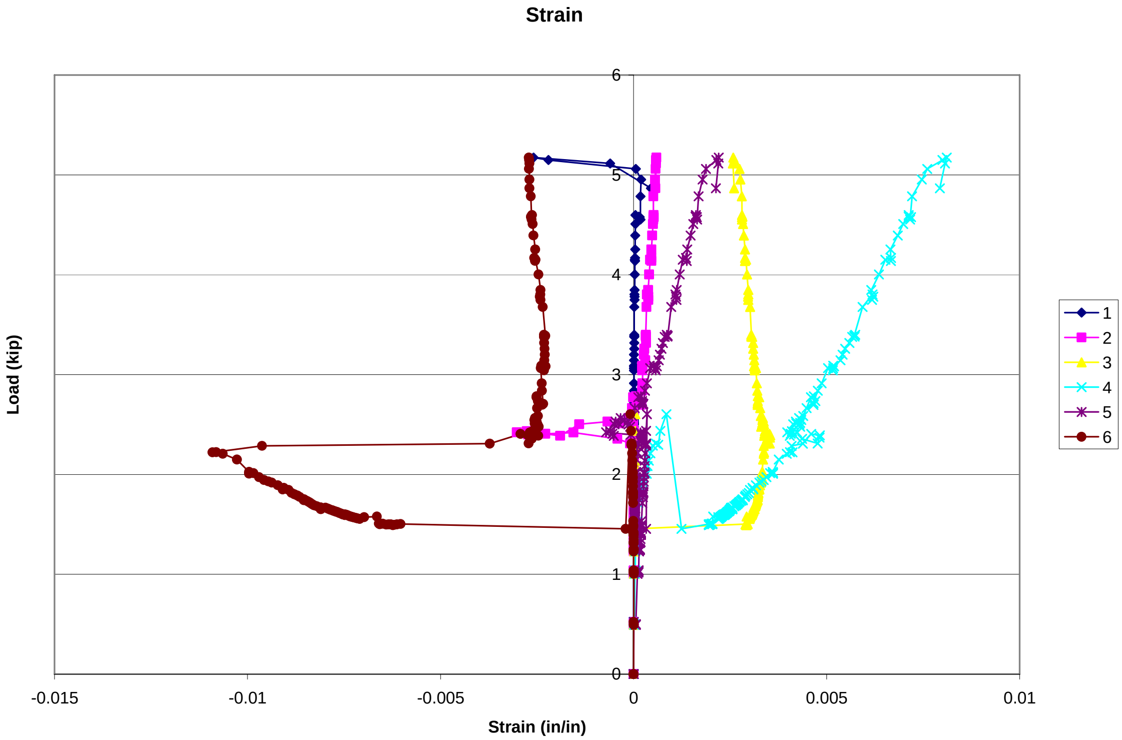

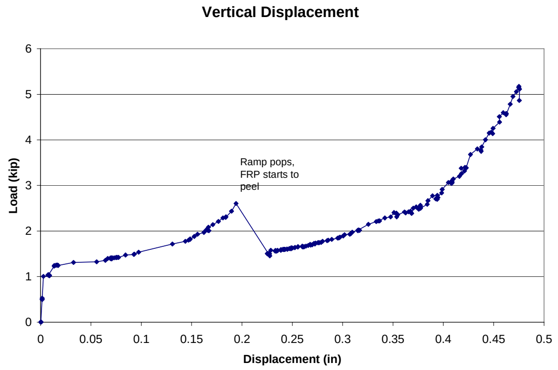

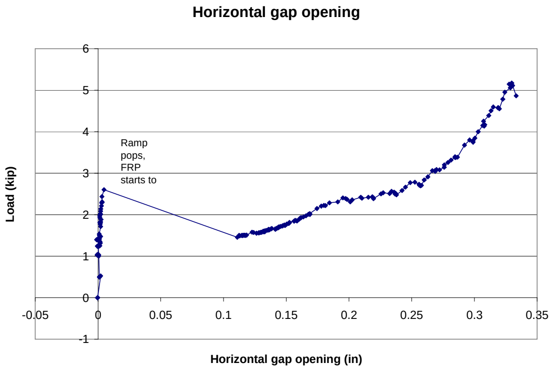

Photographs:

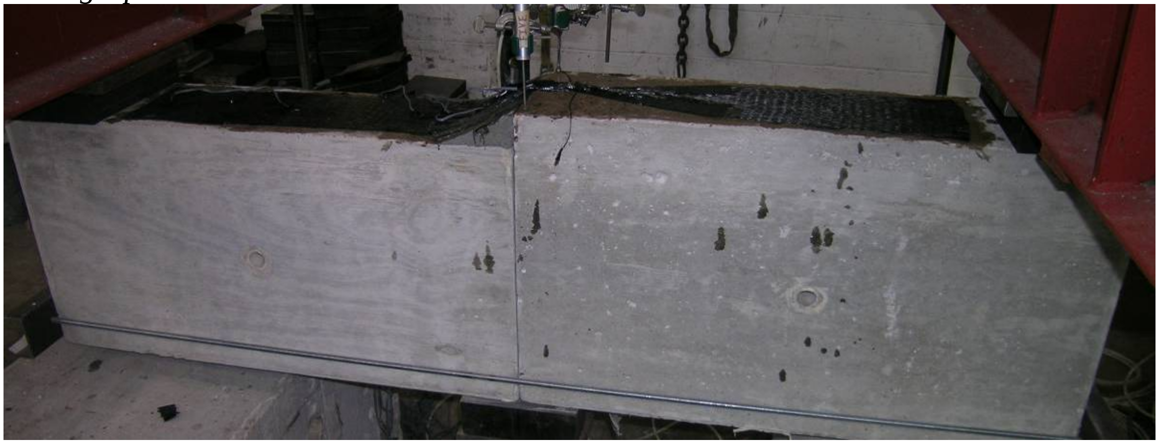

Before Testing

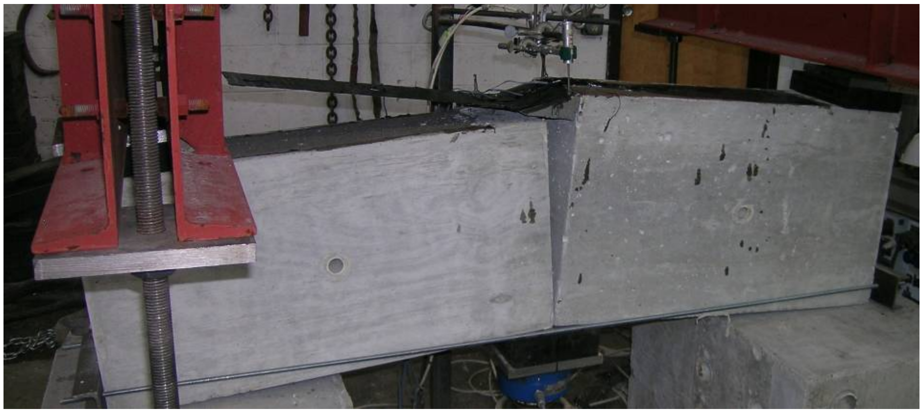

After Testing: Failure by Debonding

22-us1

Test Date: August 3rd, 2005
2” height transition
1 to 2 slope
Single layer 6” wide U wrap anchorage
Sandblasting surface preparation
SCH-35 fabric

Specimen Design:

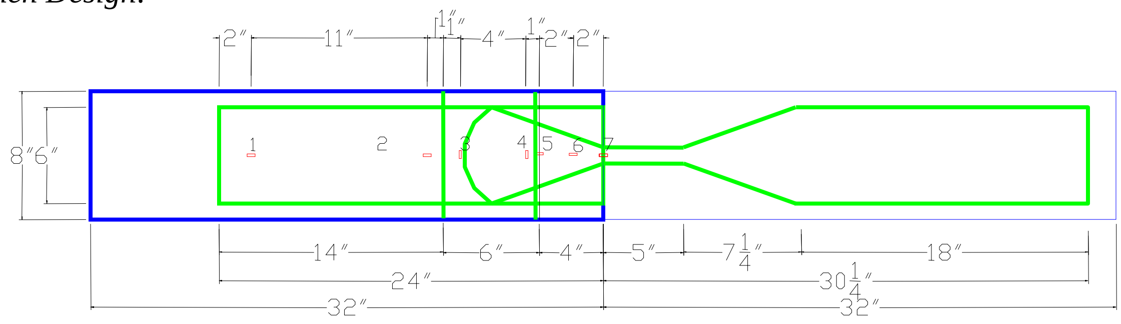
2″
11″
1″
1″
4″
1″
2″
2″
8″
6″
1
2
3
4
5
6
7
14″
6″
4″
5″
7 1/4″
18″
24″
30 1/4″
32″
32″

Test Data:

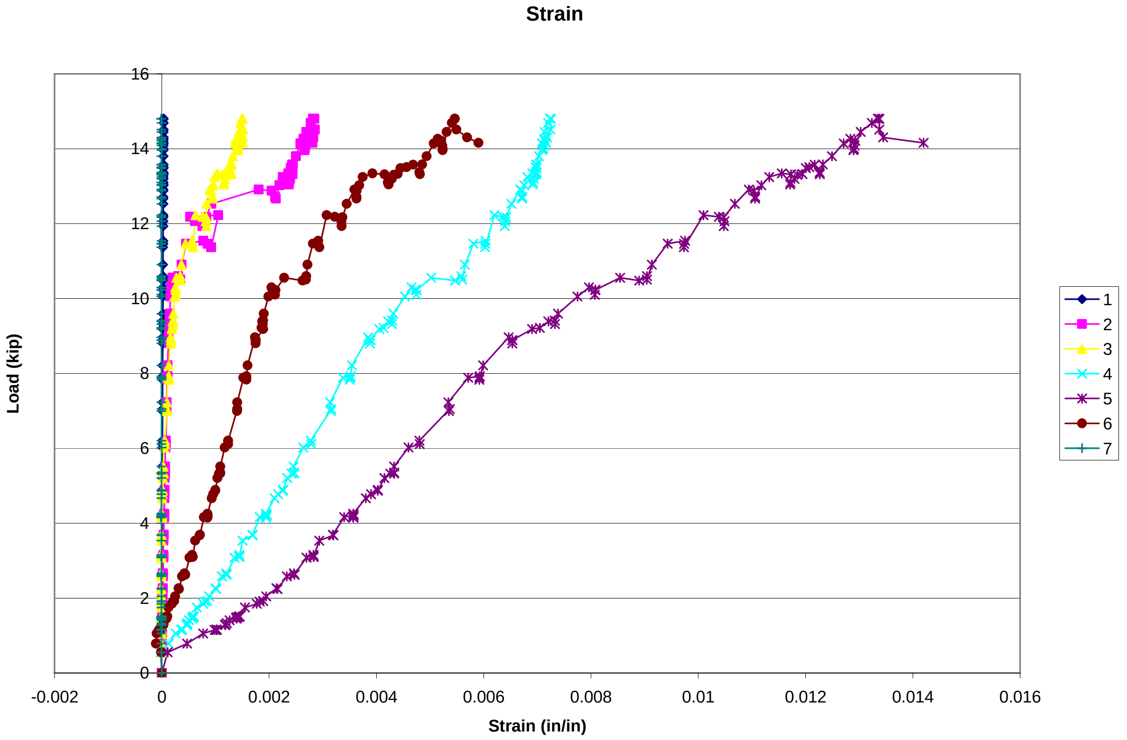

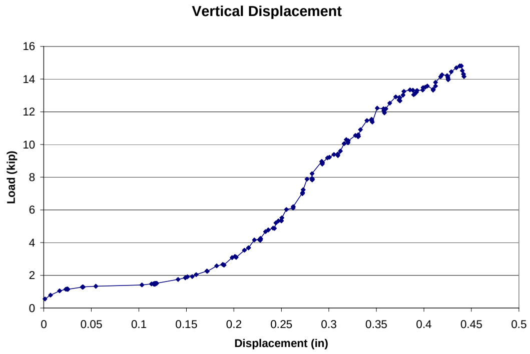

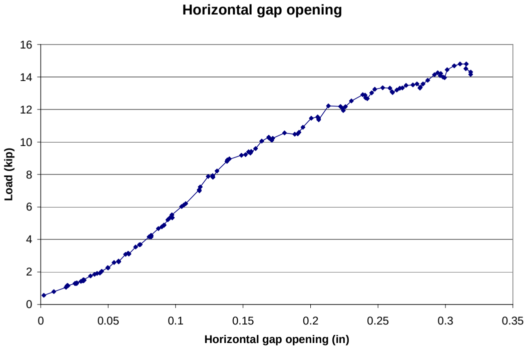

Photographs:

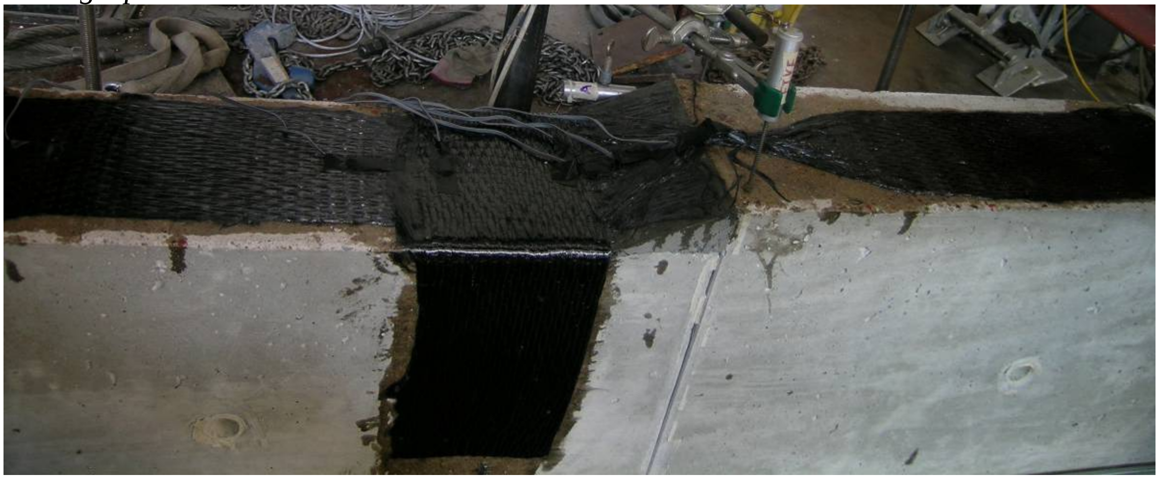

Before Testing

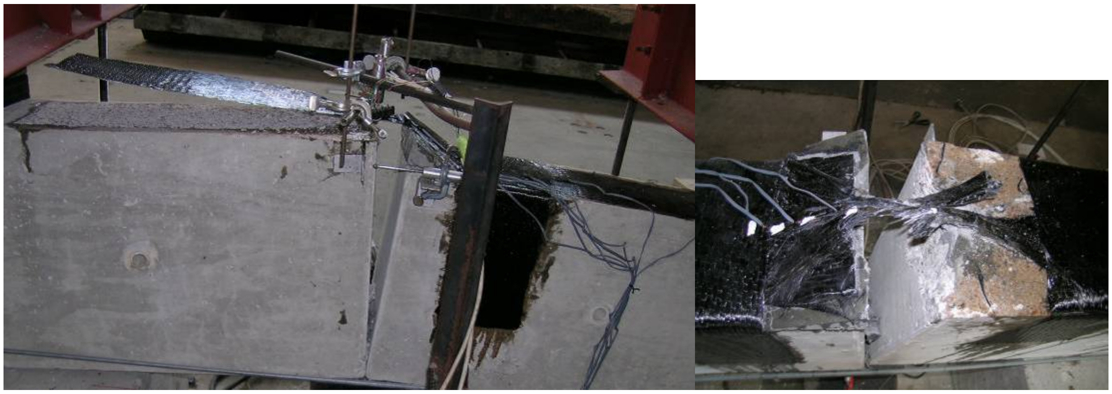

After Testing: Failure by Debonding, After Retest by FRP Fracture

22-4s1

Test Date: August 3rd, 2005
2” height transition
1 to 2 slope
2 anchors at ramp, 2 anchors at 5”, 1 ½” width sheet, 3/8” diameter concrete hole
Sandblasting surface preparation
SCH-35 fabric

Specimen Design:

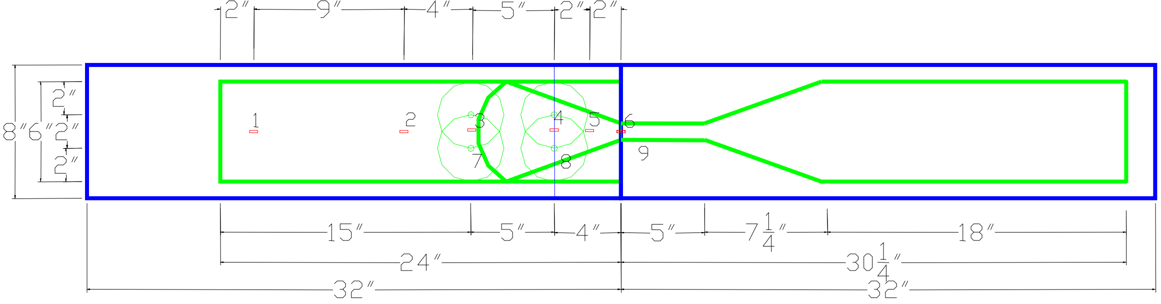
2″
9″
4″
5″
2″
2″
8″
6″
2″
2″
2″
1
2
3
4
5
6
7
8
9
15″
5″
4″
5″
7 1/4″
18″
24″
30 1/4″
32″
32″

Test Data:

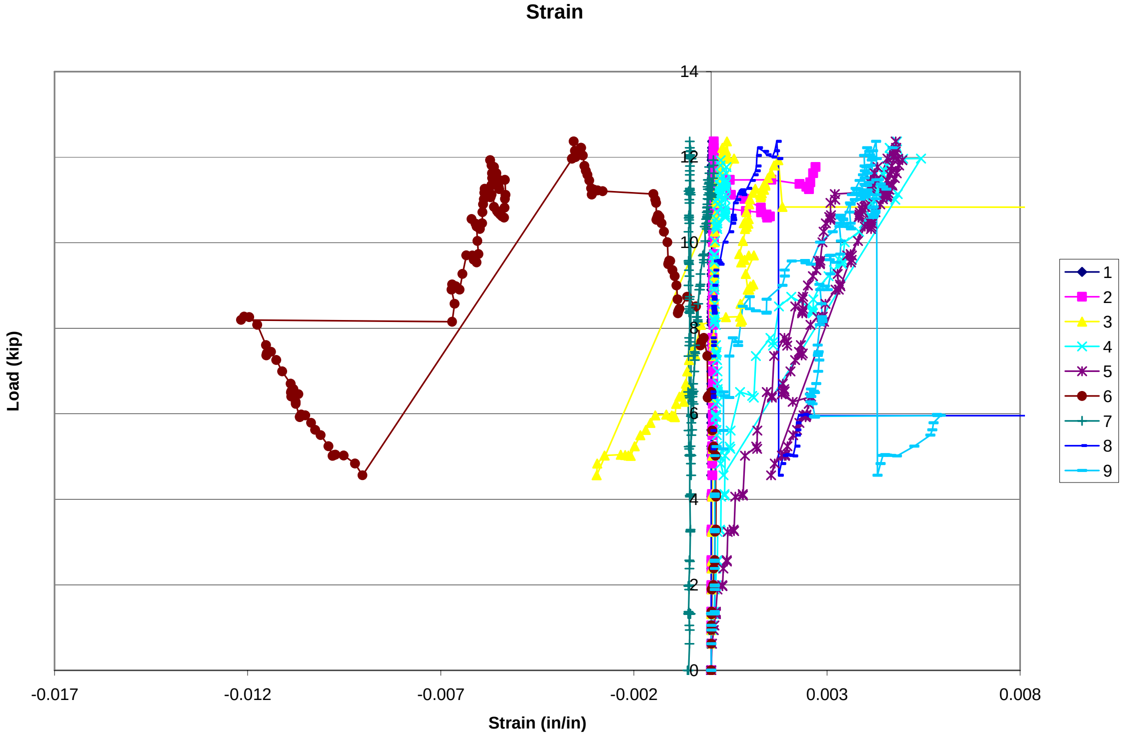

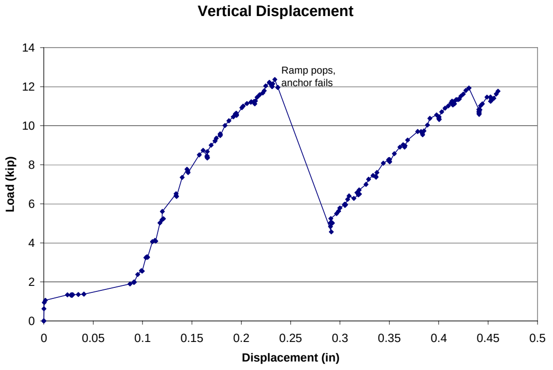
Vertical Displacement

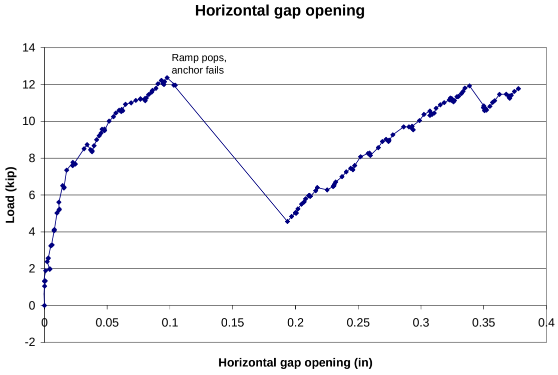
Horizontal gap opening

Photographs:

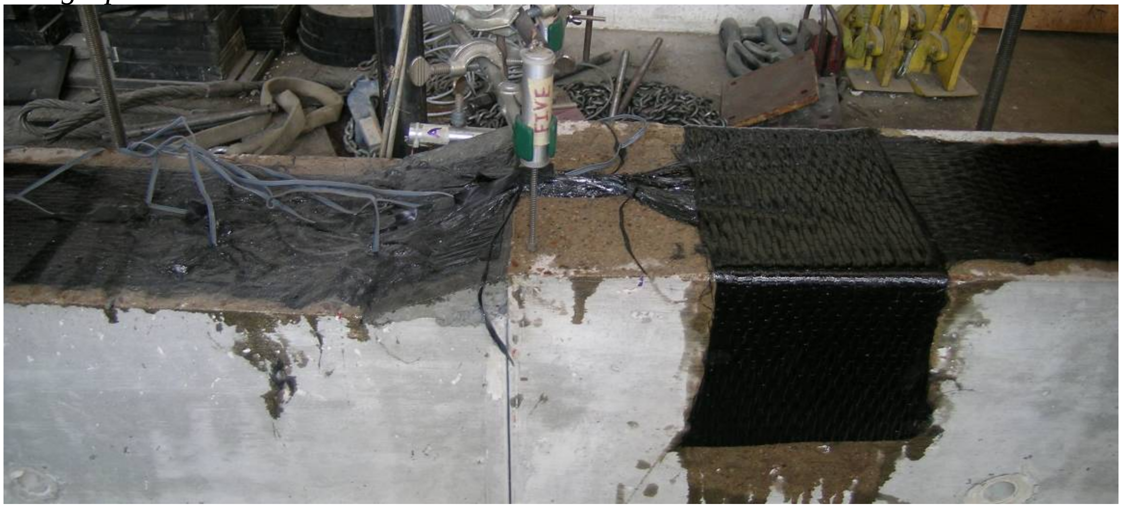

Before Testing

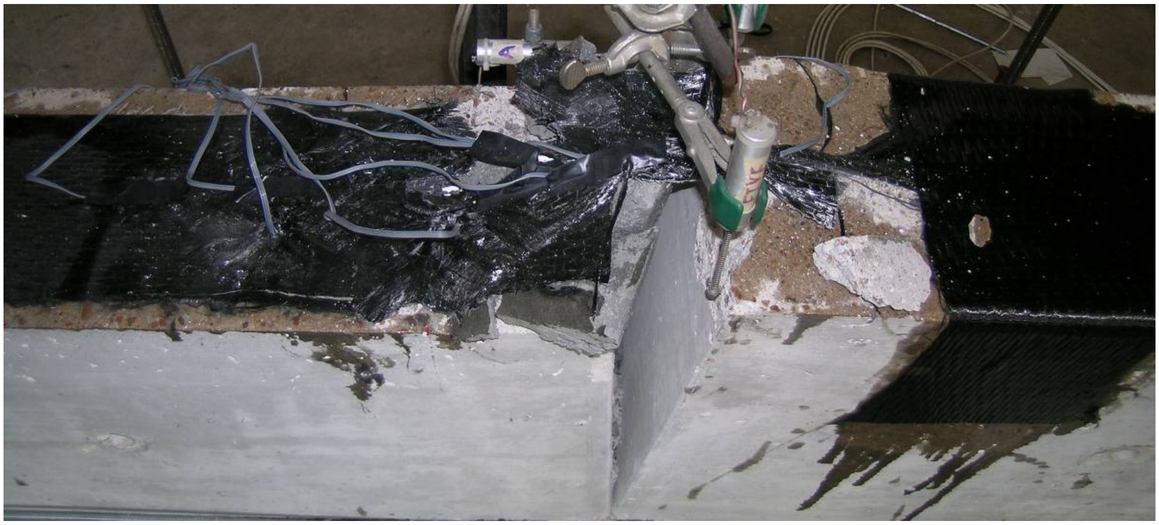

After Testing: Failure by FRP Fracture

42-us1

Test Date: September 20th, 2005
2” height transition
1 to 4 slope
Single layer 6” wide U-wrap at ramp
Sandblasting surface preparation
SCH-35 fabric

Specimen Design:

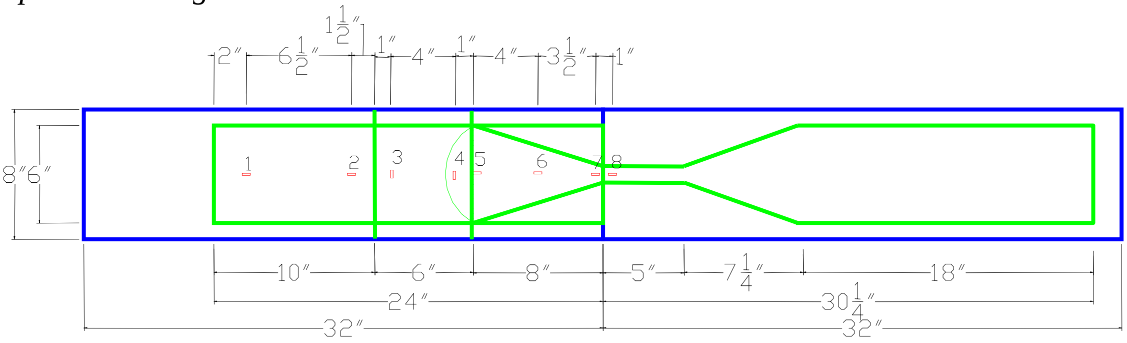

2″
6 1/2″
1 1/2″
1″
4″
1″
4″
3 1/2″
1″
8″
6″
1
2
3
4
5
6
7
8
10″
6″
8″
5″
7 1/4″
18″
24″
30 1/4″
32″
32″

Test Data:

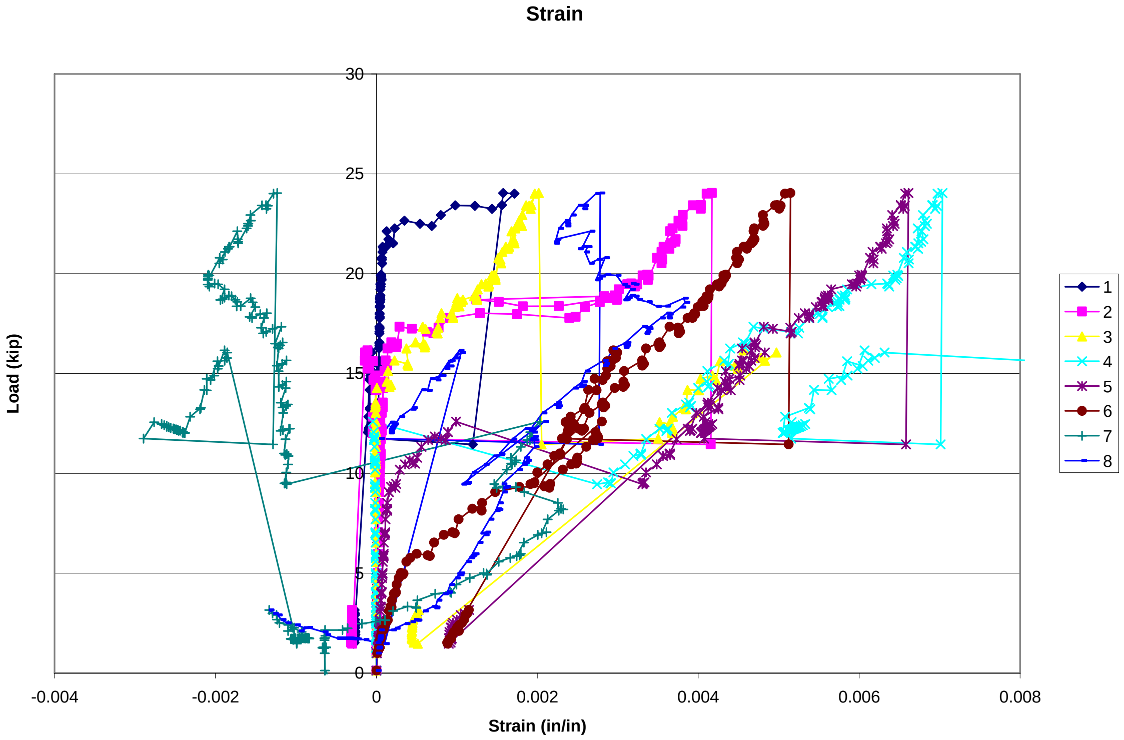

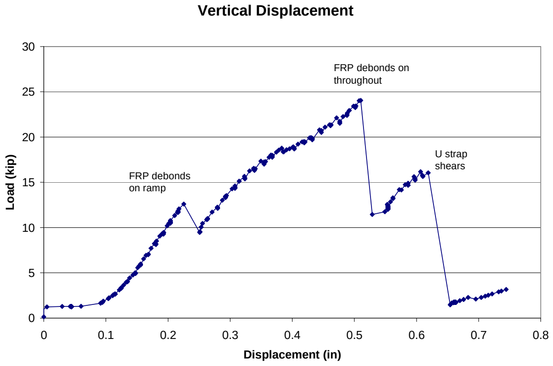

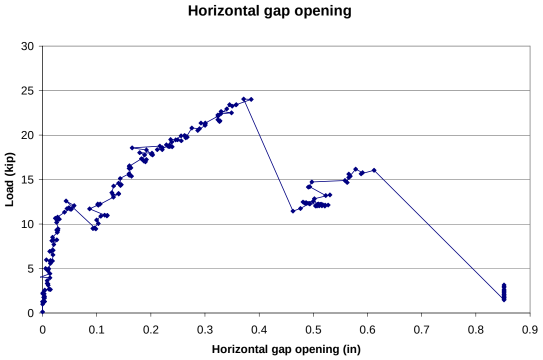

Photographs:

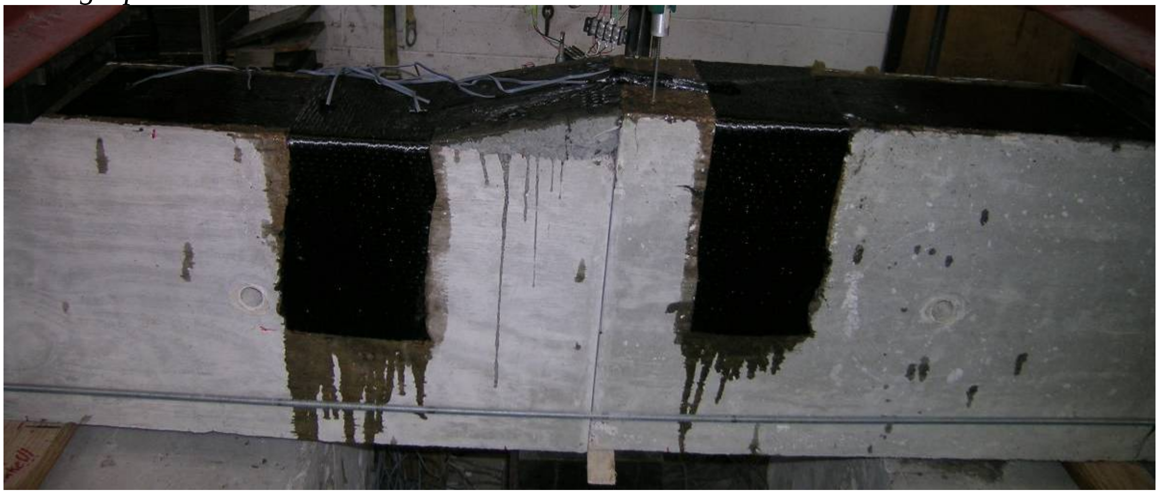

Before Testing

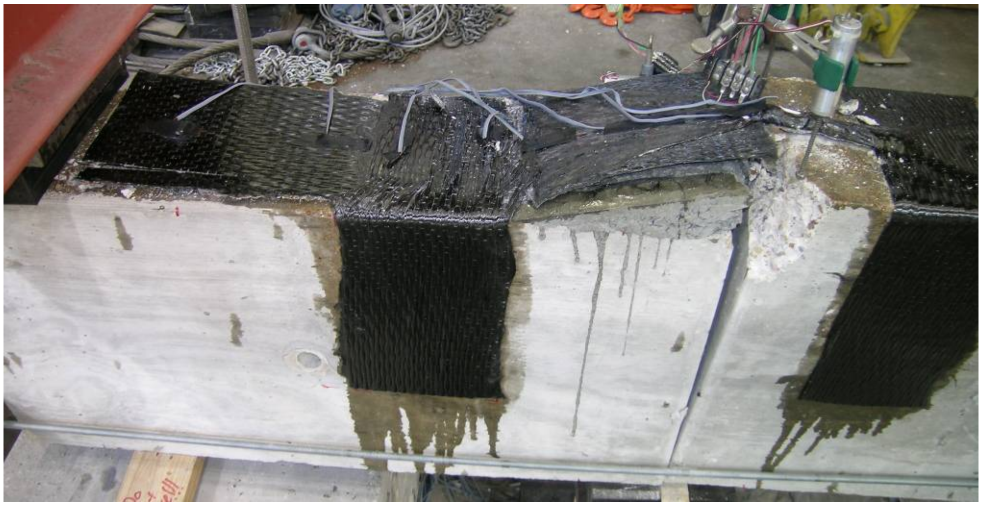

After Testing: Failure by U-wrap shear

42-4s1

Test Date: November 28th, 2005
2” height transition
1 to 4 slope
2 anchors at ramp, 2 anchors at 21”, 2” width sheet, 3/8” diameter concrete hole
Sandblasting surface preparation
SCH-35 fabric

Specimen Design:

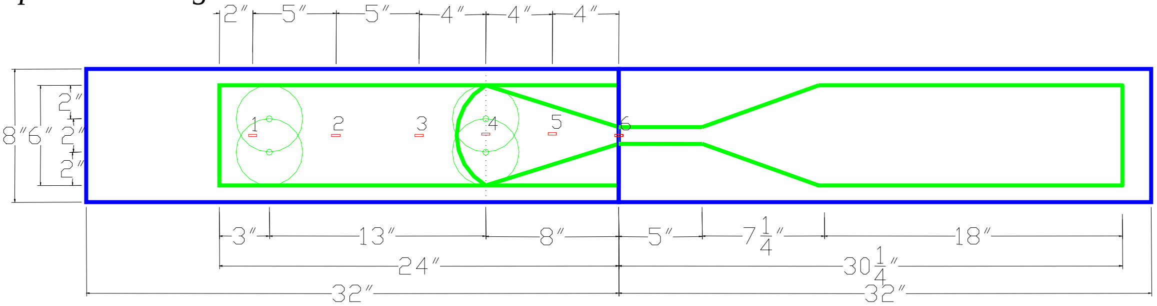

2″
5″
5″
4″
4″
4″
8″
6″
2″
2″
2″
1
2
3
4
5
6
3″
13″
8″
5″
7 1/4″
18″
24″
30 1/4″
32″
32″

Test Data:

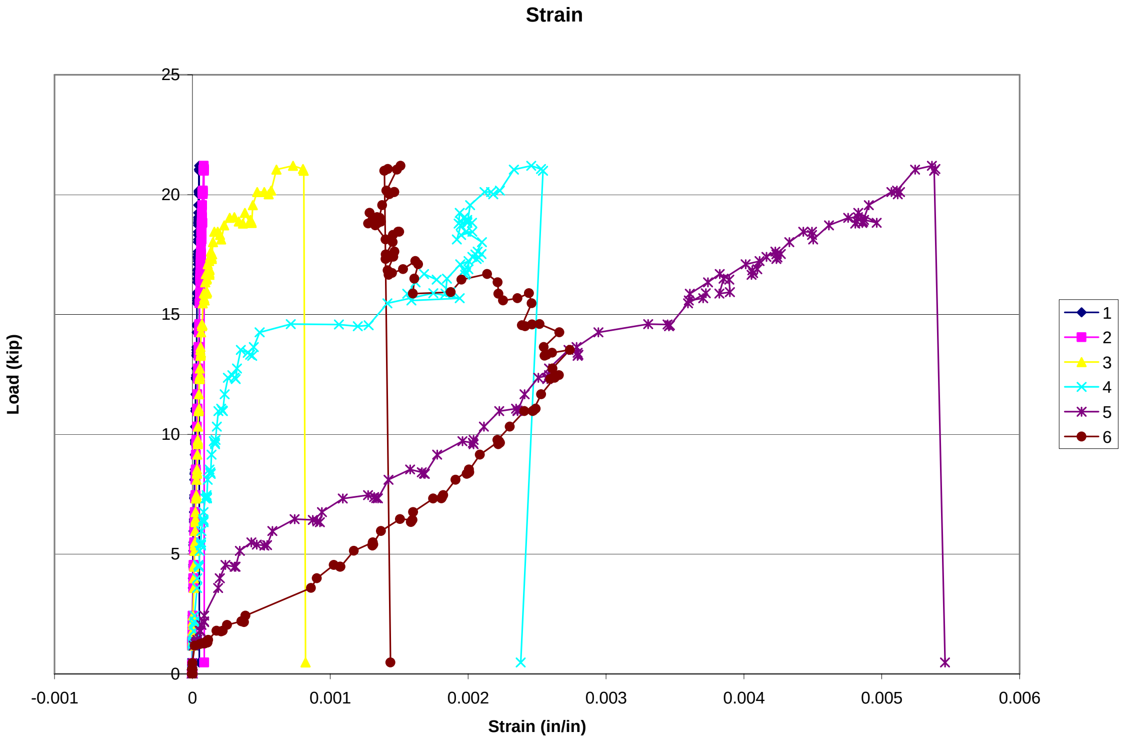

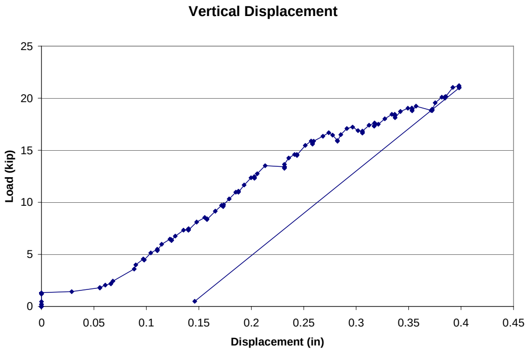

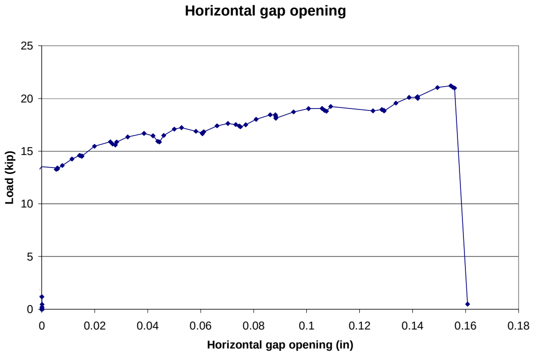

Photographs:

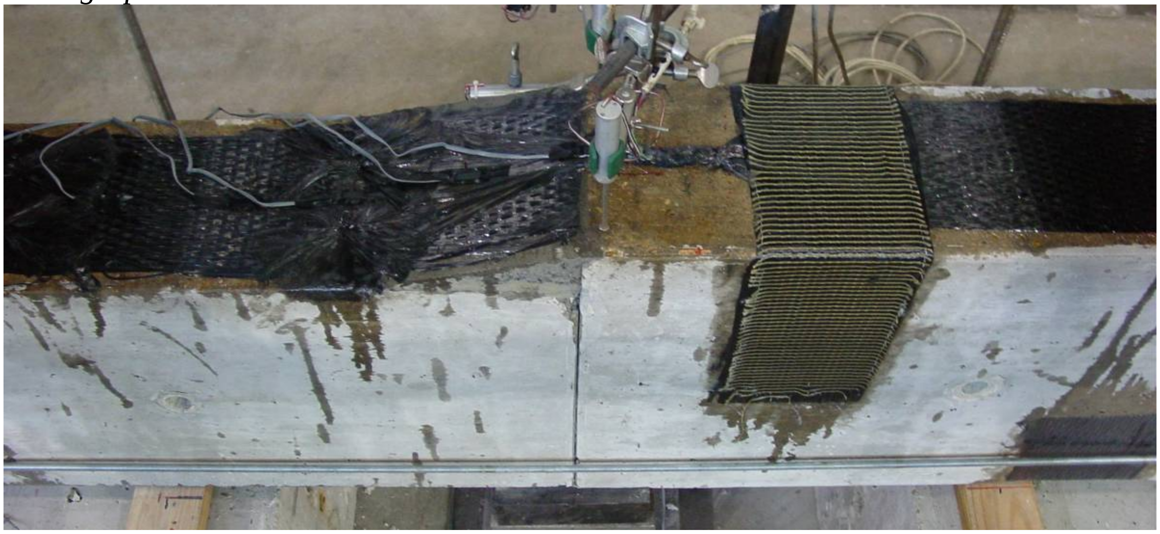

Before Testing

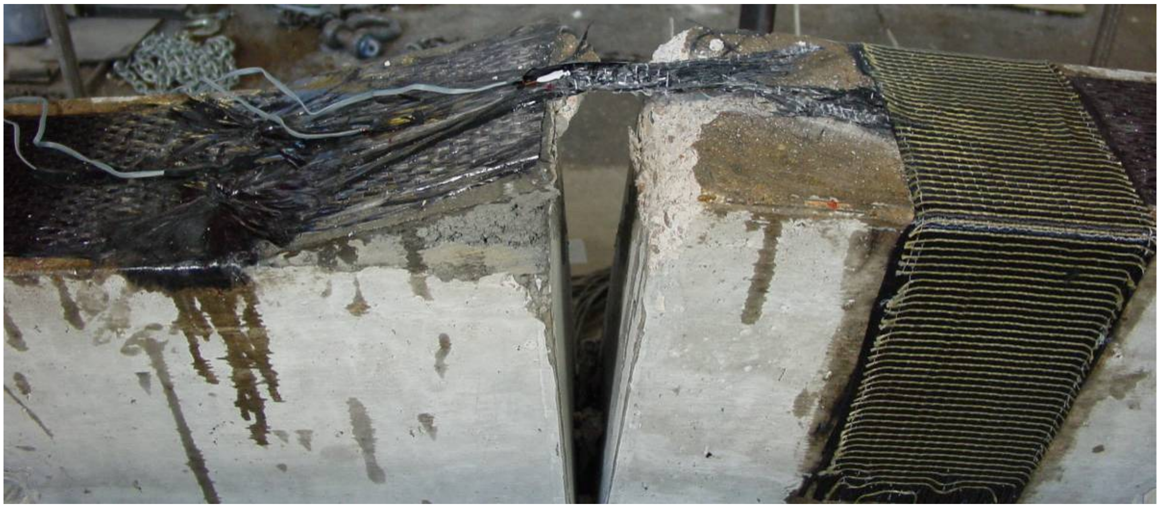

After Testing: Failure by premature fracture in column part

42-6s1

Test Date: November 28th, 2005
2” height transition
1 to 4 slope
3 anchors at ramp, 3 anchors at 21”, 2” width sheet, 3/8” diameter concrete hole
Sandblasting surface preparation
SCH-35 fabric

Specimen Design:

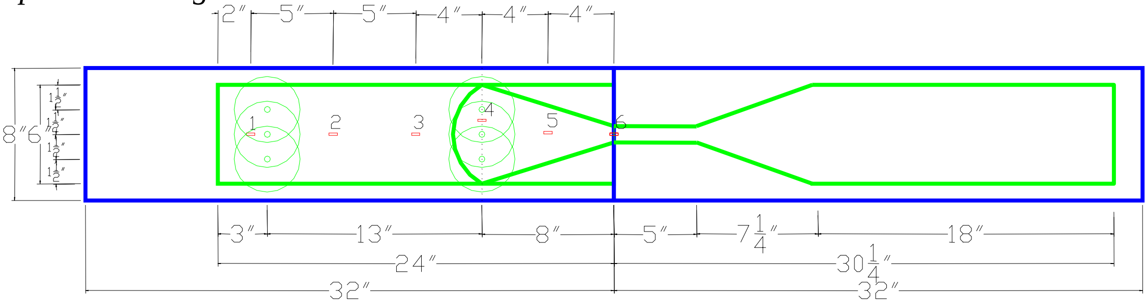

2″
5″
5″
4″
4″
4″
8″
6″
1½″
1½″
1½″
1½″
1
2
3
4
5
6
3″
13″
8″
5″
7¼″
18″
24″
30¼″
32″
32″

Test Data:

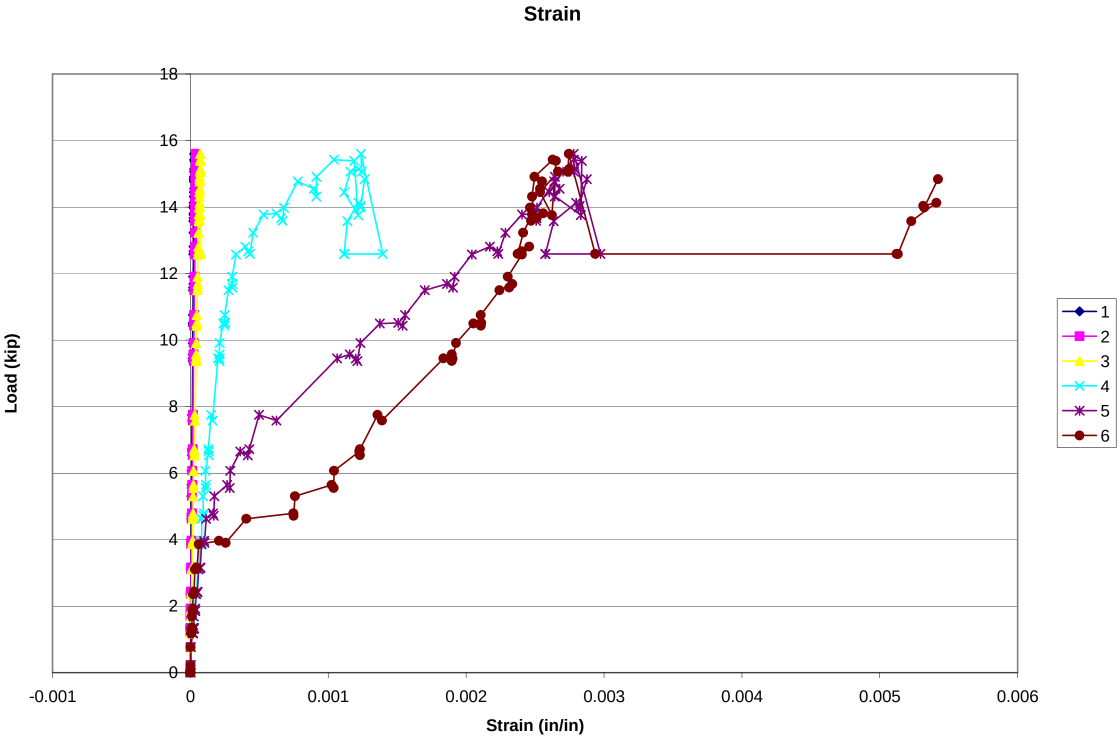

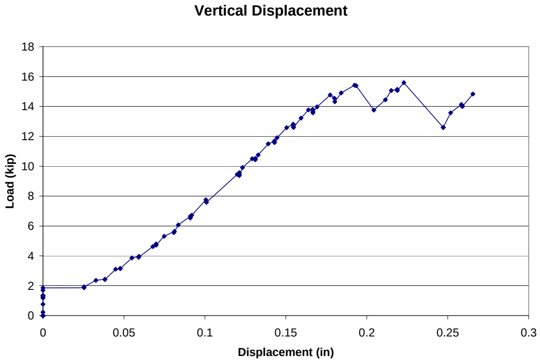

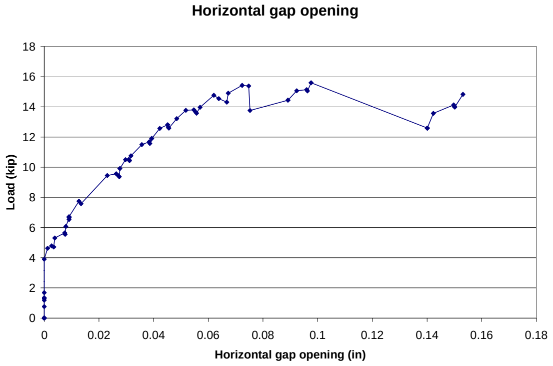

Photographs:

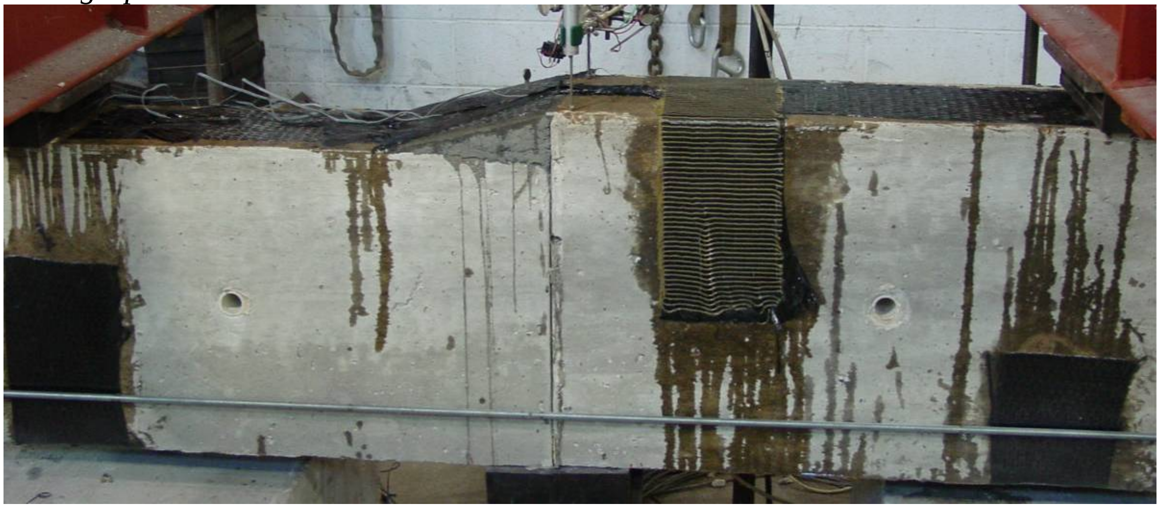

Before Testing

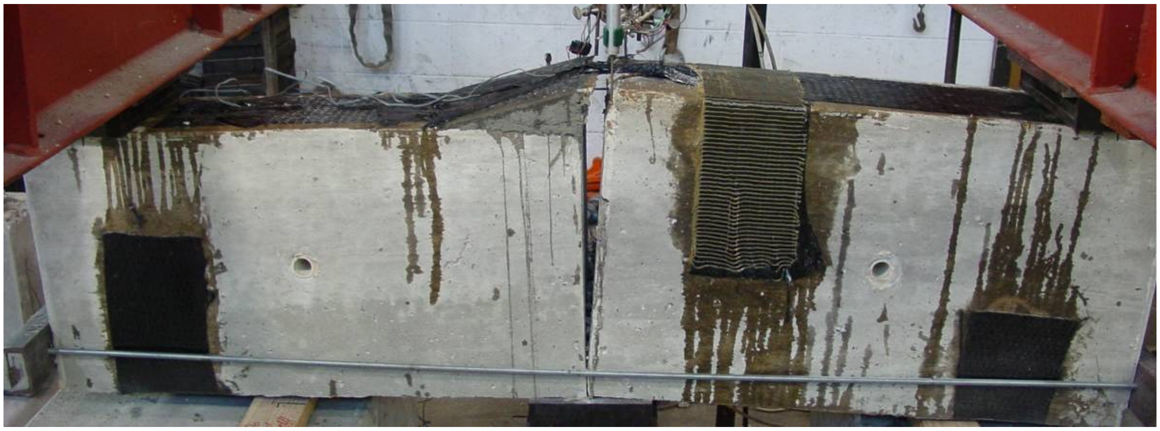

After Testing: Failure by premature fracture in column part

42-ns1

Test Date: December 6th, 2005
2” height transition
1 to 4 slope
No anchorage
Sandblasting surface preparation
SCH-35 fabric

Specimen Design:

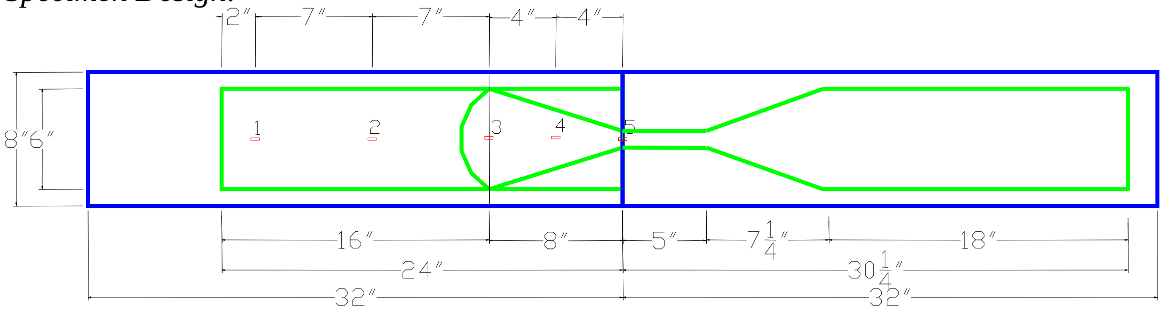

2″
7″
7″
4″
4″
8″
6″
1
2
3
4
5
16″
8″
5″
7 1/4″
18″
24″
30 1/4″
32″
32″

Test Data:

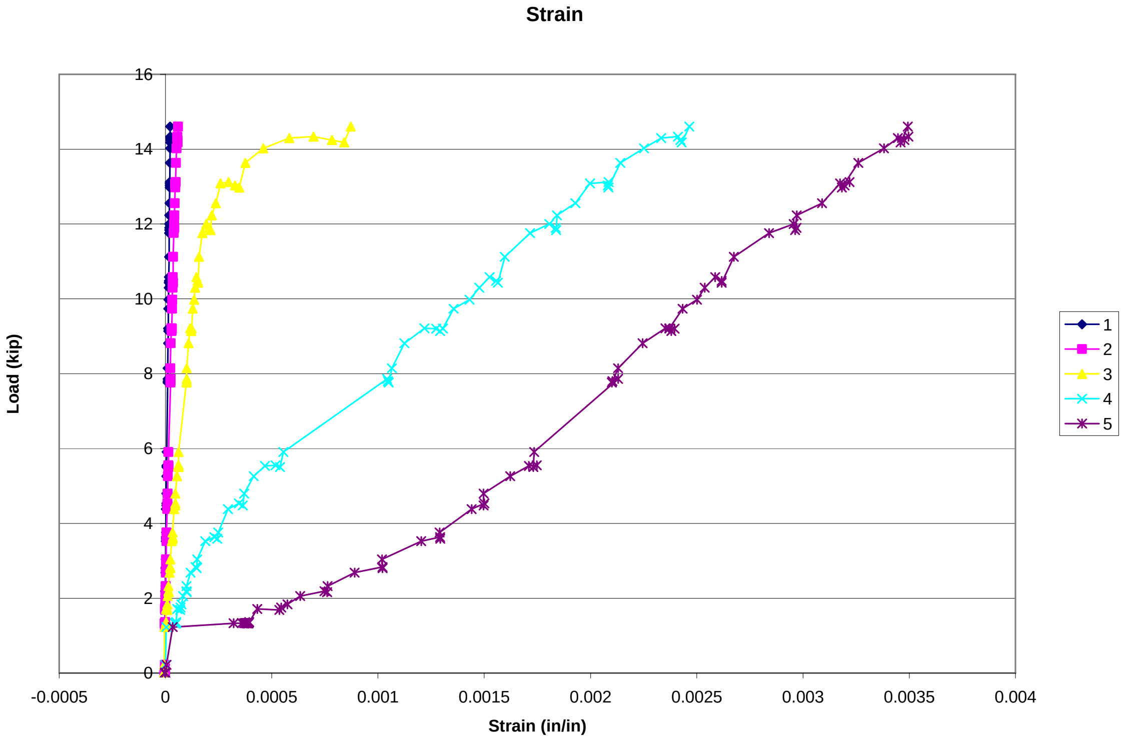

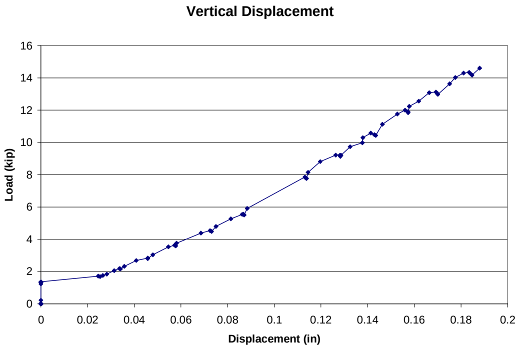

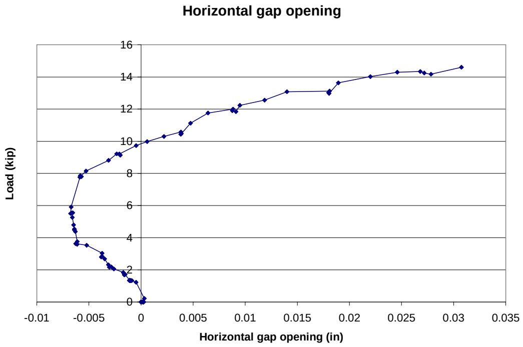

Photographs:

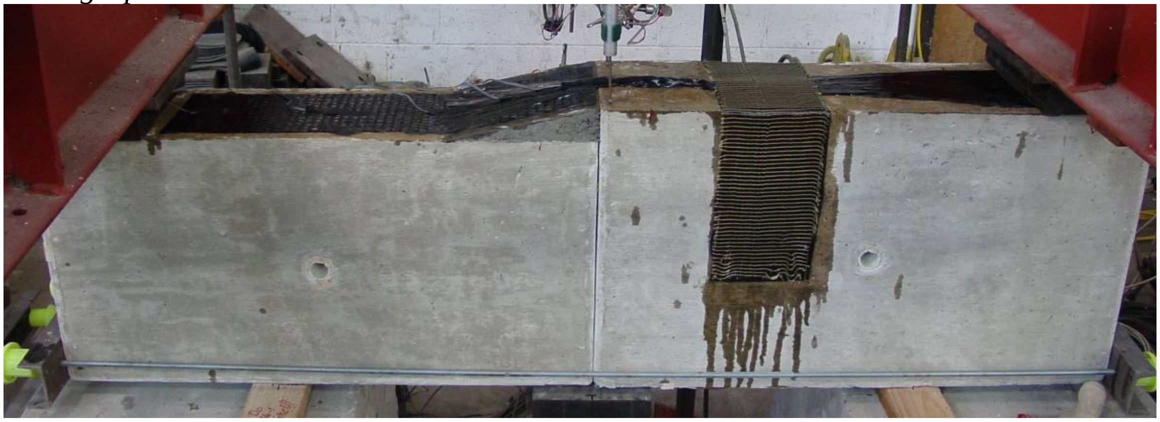

Before Testing

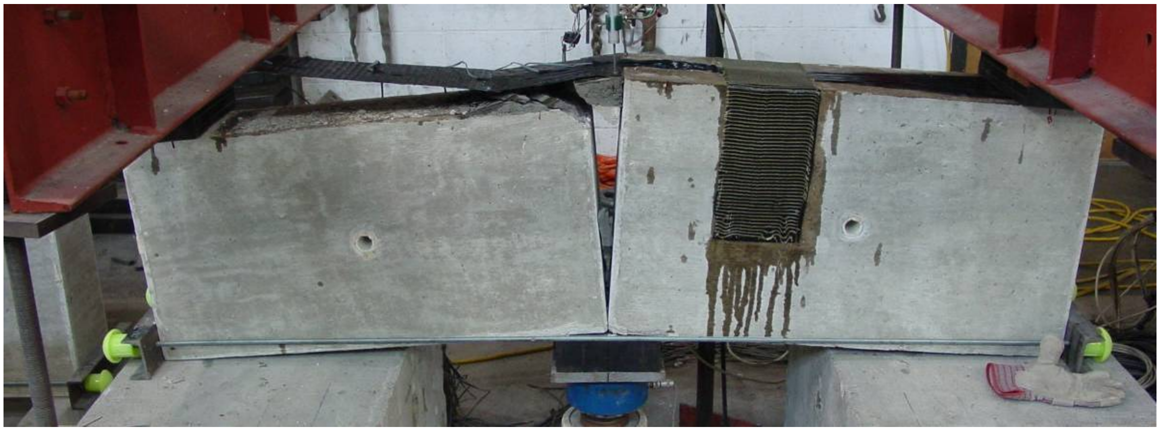

After Testing: Failure by debonding

42-4s2

Test Date: December 6th, 2005
2” height transition
1 to 4 slope
2 anchors at ramp, 2 anchors at 21”, 2” width sheet, 3/8” diameter concrete hole
Sandblasting surface preparation
SCH-35 fabric

Specimen Design:

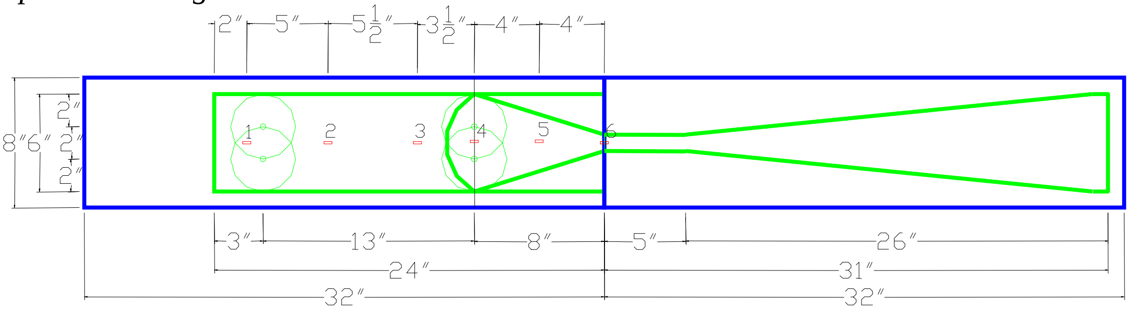
2″
5″
5 1/2″
3 1/2″
4″
4″
8″
6″
2″
2″
2″
1
2
3
4
5
6
3″
13″
8″
5″
26″
24″
31″
32″
32″

Test Data:

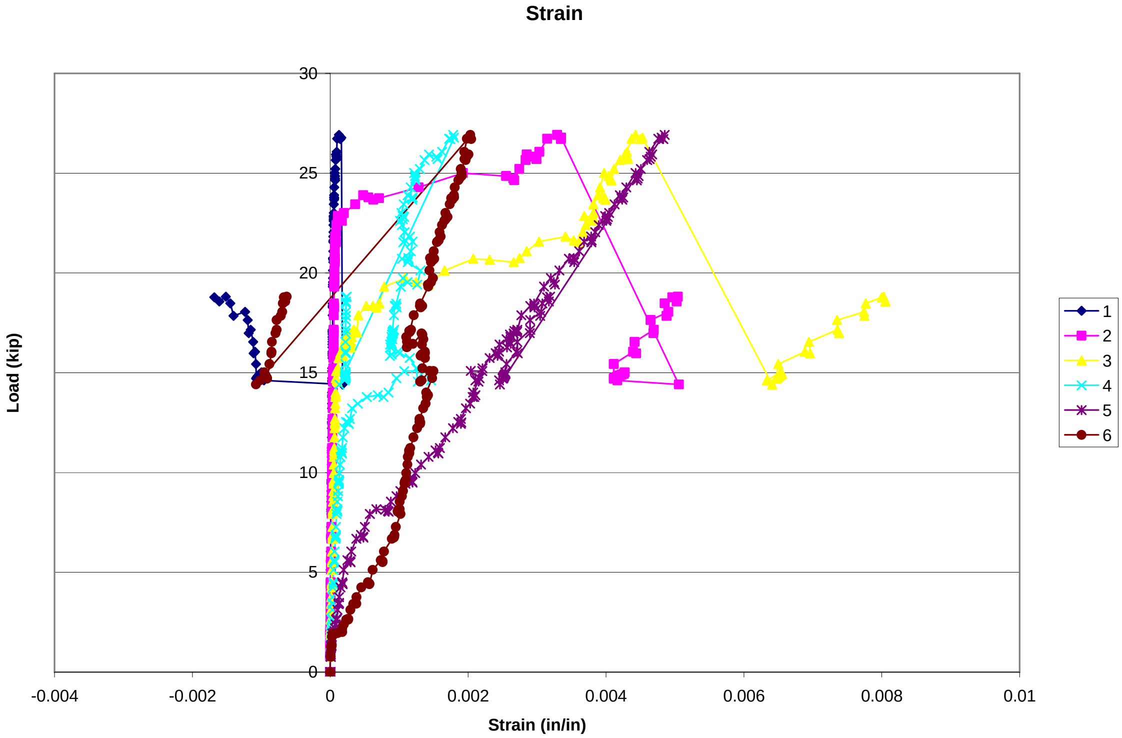

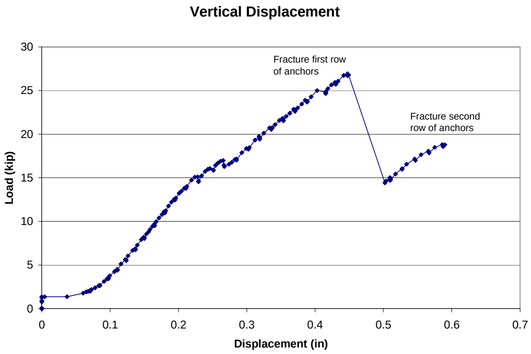

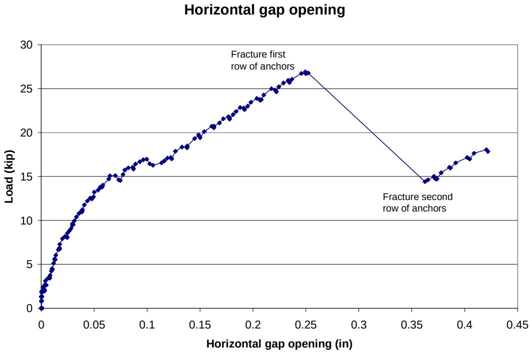

Photographs:

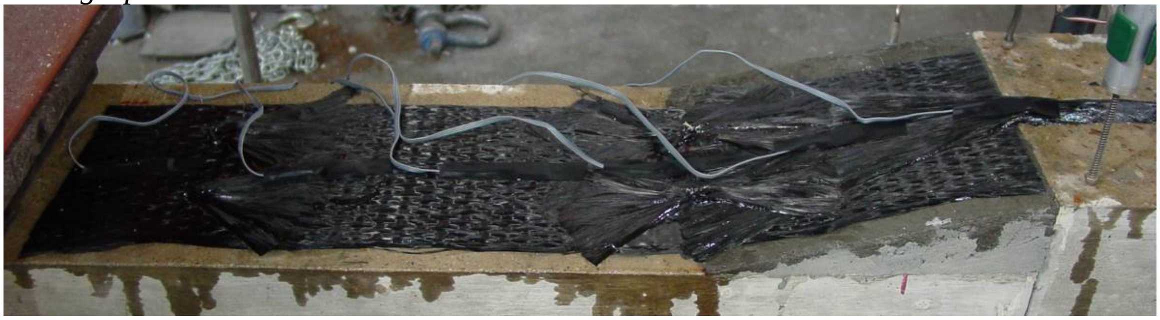

Before Testing

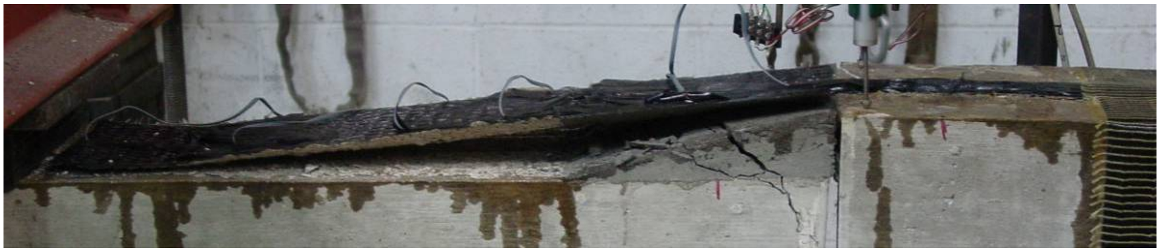

Fracture first row of anchors

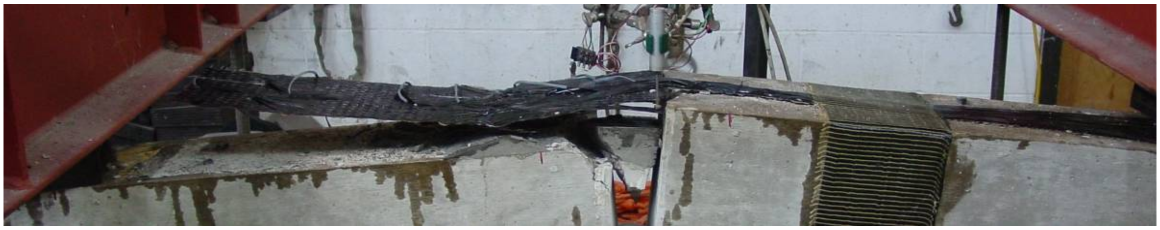

After Testing: Failure by anchor fracture

42-us2

Test Date: December 6th, 2005
2” height transition
1 to 4 slope
Double layer 6” wide U-wrap at ramp
Sandblasting surface preparation
SCH-35 fabric

Specimen Design:

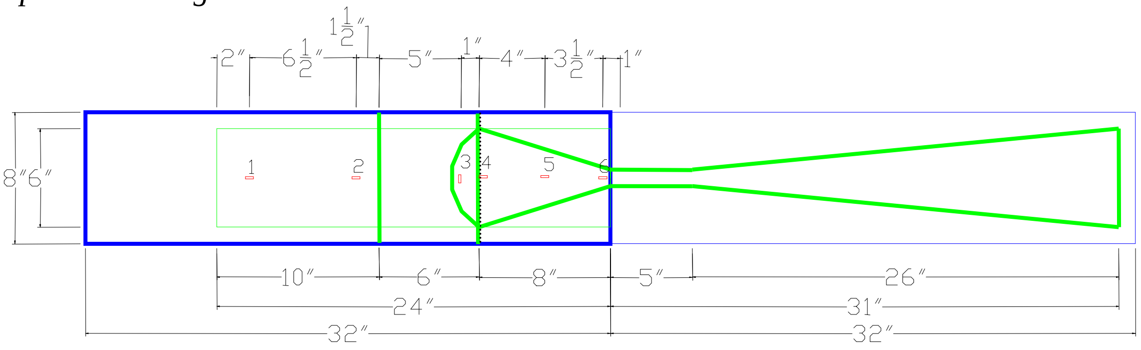

1 1/2″
2″
6 1/2″
5″
1″
4″
3 1/2″
1″
8″
6″
1
2
3
4
5
6
10″
6″
8″
5″
26″
24″
31″
32″
32″

Test Data:

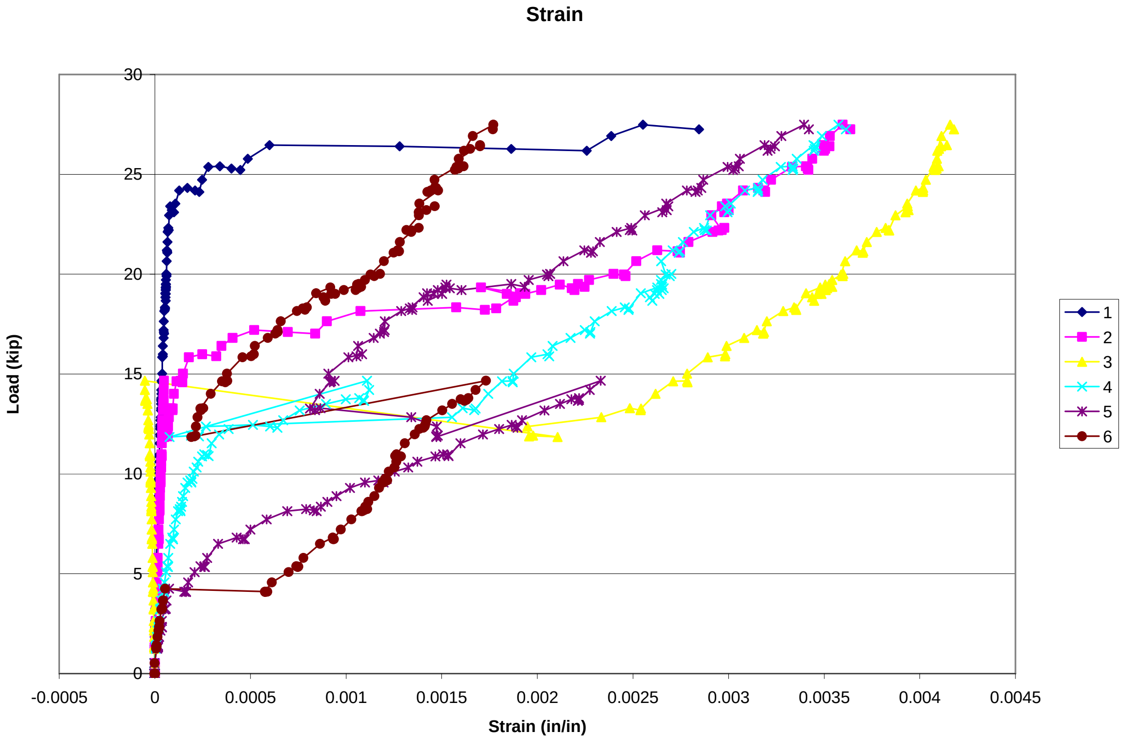

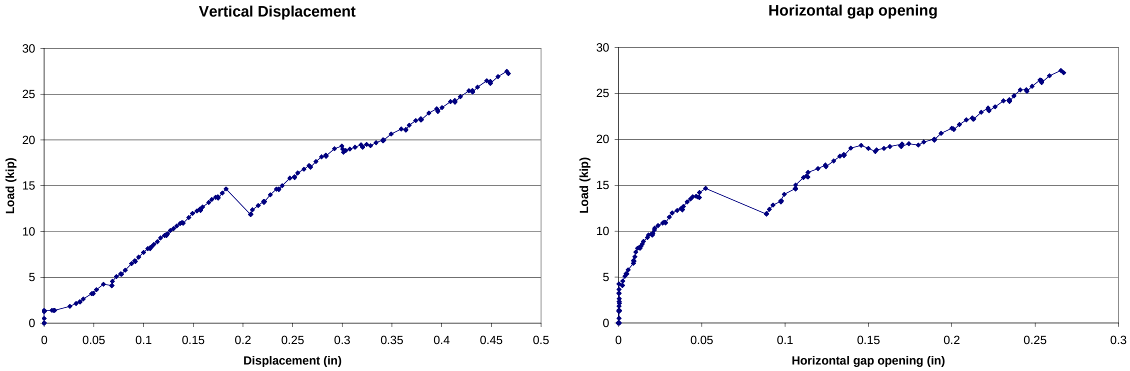

Photographs:

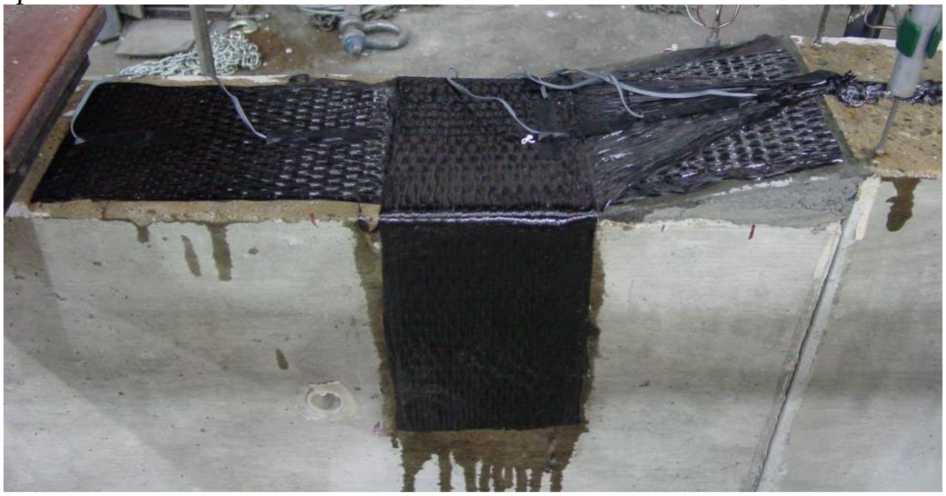

Before Testing

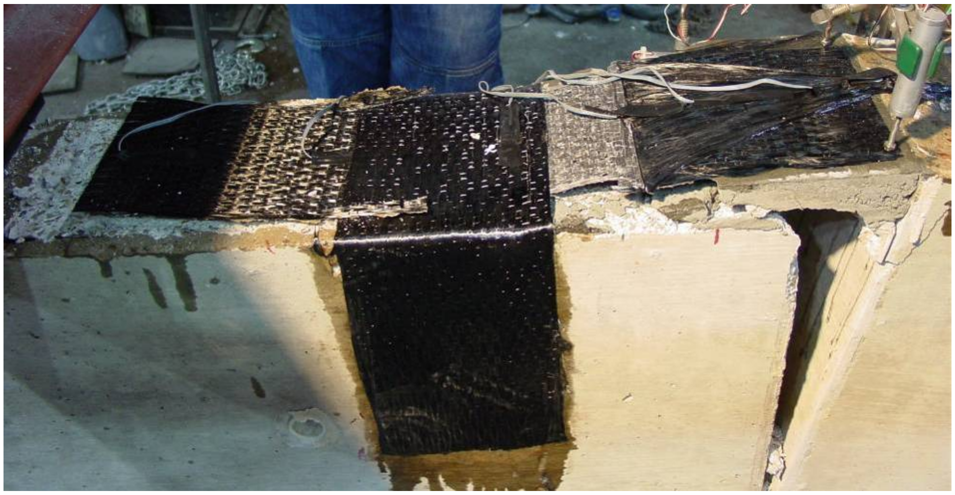

After Testing: Failure by FRP sheet slipping under U-wrap

42-6s2

Test Date: December 14th, 2005
2” height transition
1 to 4 slope
3 anchors at ramp, 3 anchors at 21”, 2” width sheet, 3/8” diameter concrete hole
Sandblasting surface preparation
SCH-35 fabric

Specimen Design:

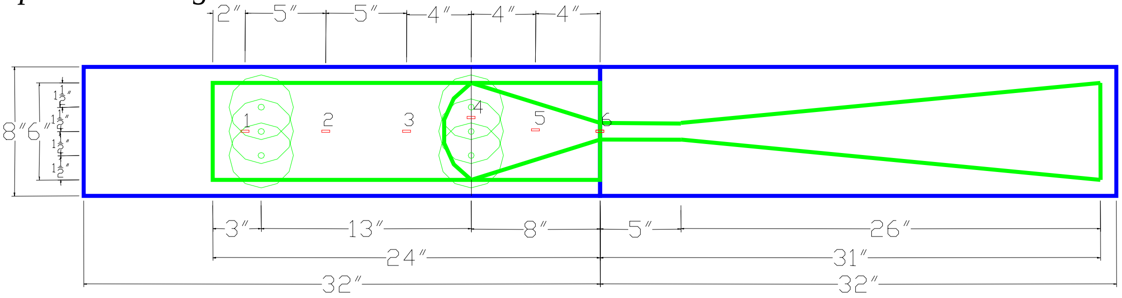

2″
5″
5″
4″
4″
4″
8″
6″
1½″
1½″
1½″
1½″
1
2
3
4
5
6
3″
13″
8″
5″
26″
24″
31″
32″
32″

Test Data:

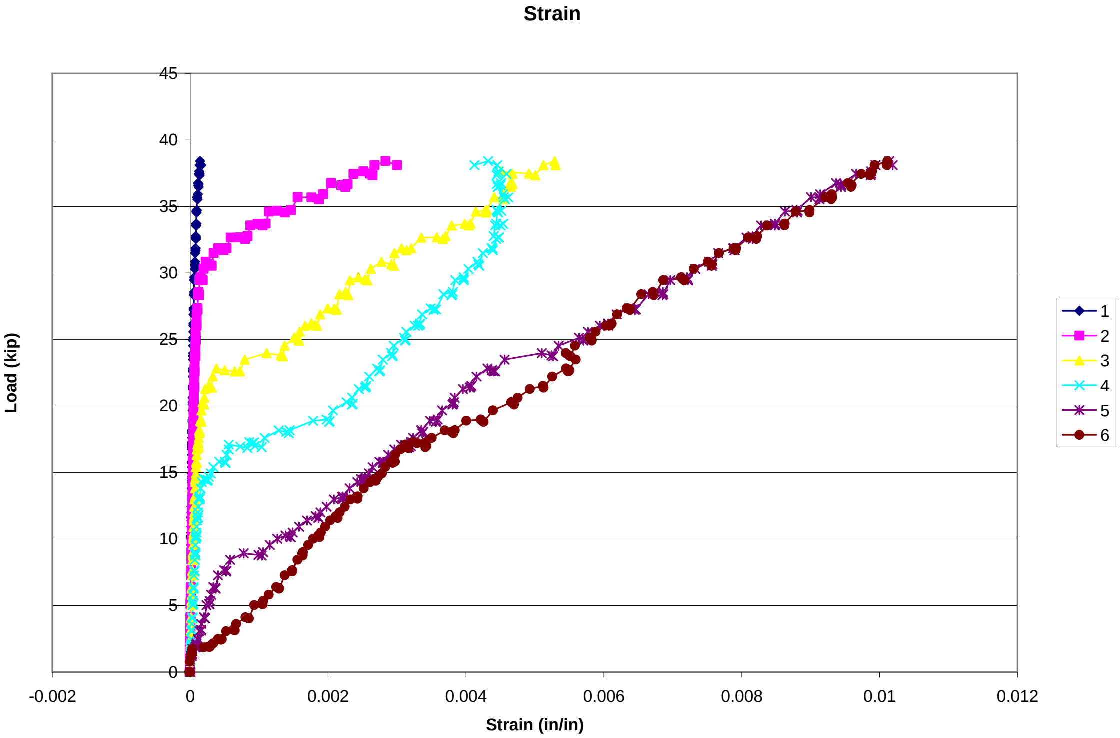

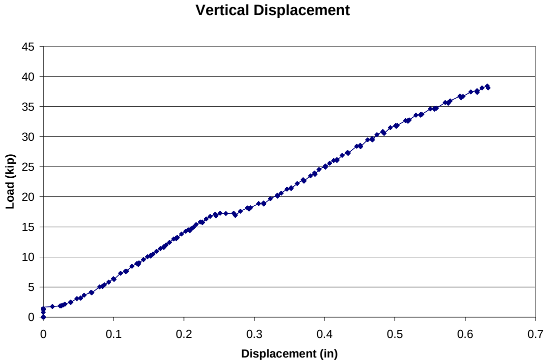
Vertical Displacement

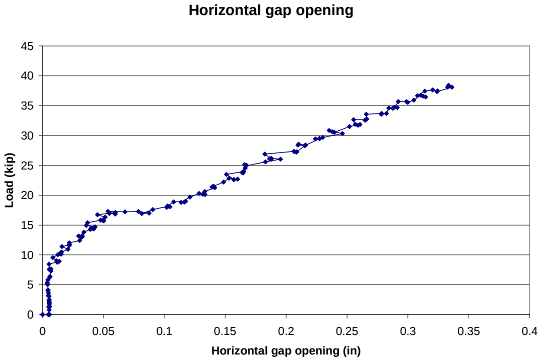
Horizontal gap opening

Photographs:

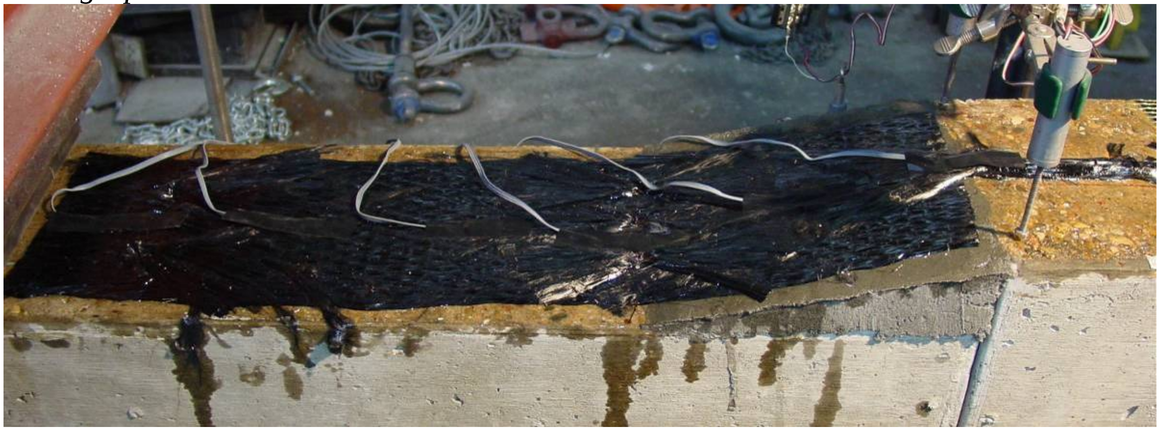
Before Testing

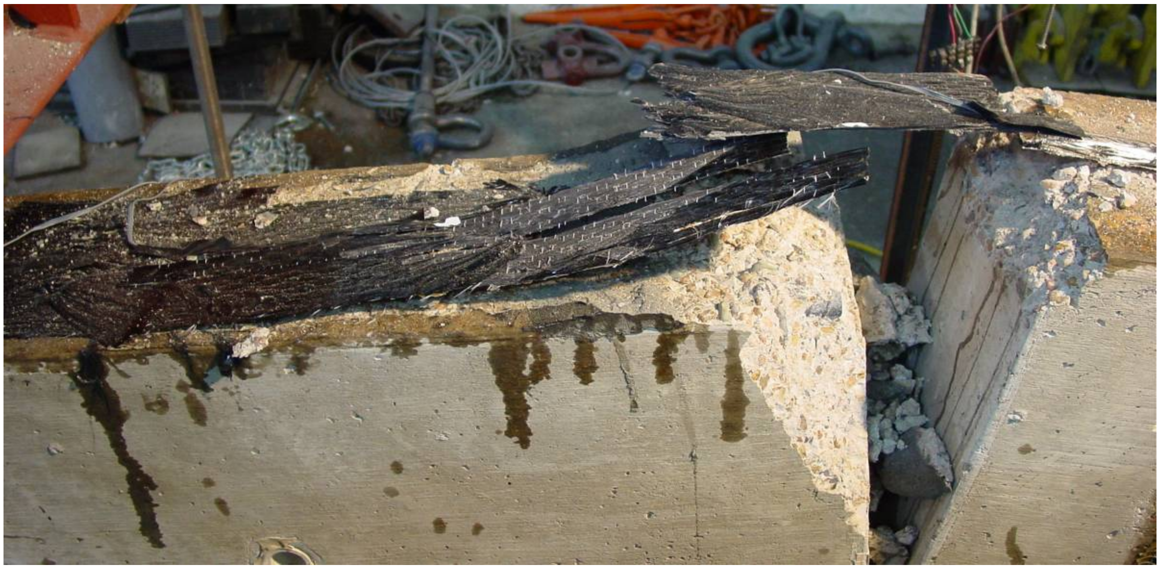
After Testing: Failure by FRP fracture

42-us3

Test Date: December 14th, 2005
2” height transition
1 to 4 slope
Double layer 6” wide U-wrap at ramp, single layer 6” wide U-wrap at 21”
Sandblasting surface preparation
SCH-35 fabric

Specimen Design:

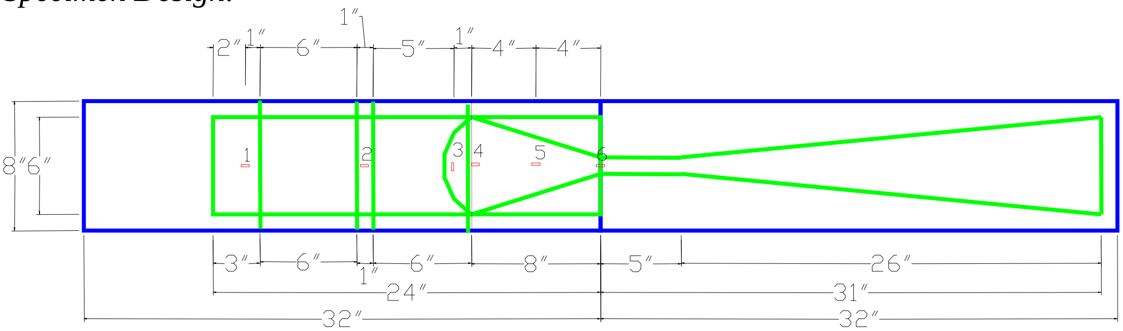
1″
2″
1″
6″
5″
1″
4″
4″
8″
6″
1
2
3
4
5
6
3″
6″
1″
6″
8″
5″
26″
24″
31″
32″
32″

Test Data:

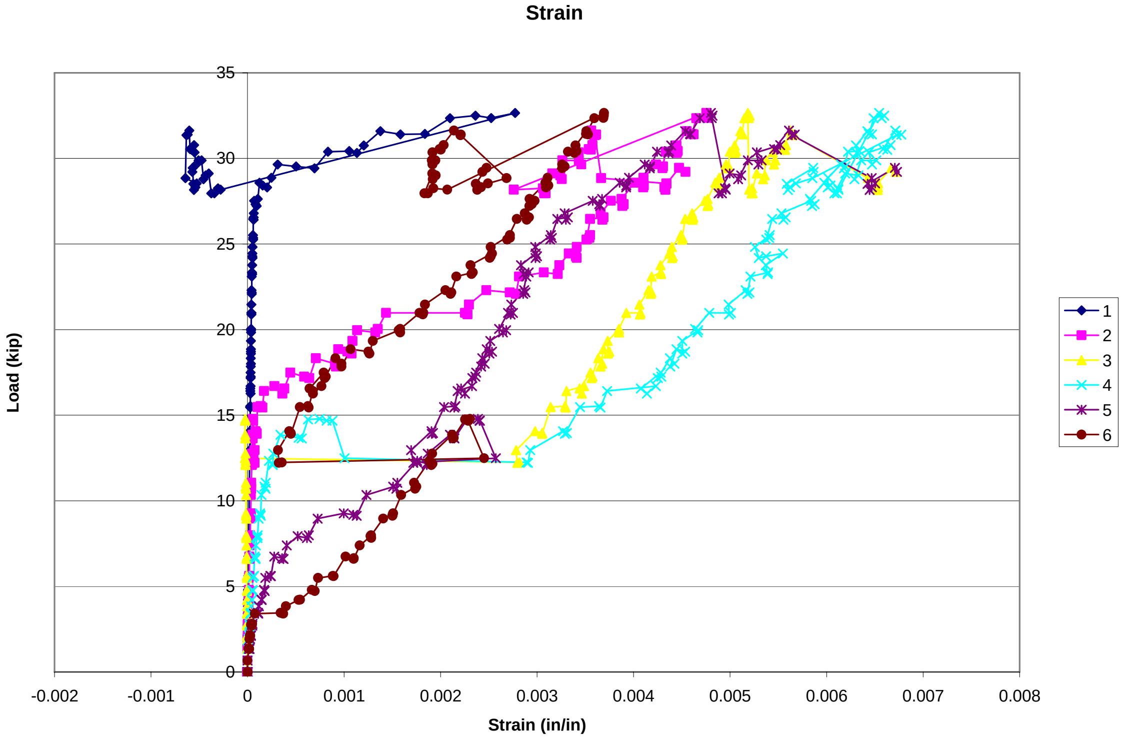

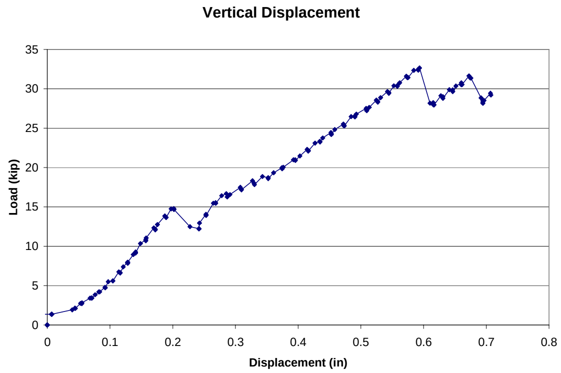

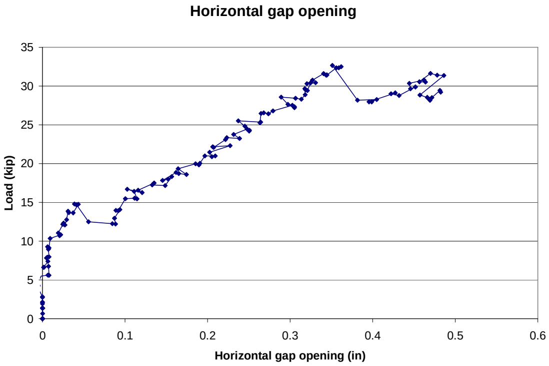

Photographs:

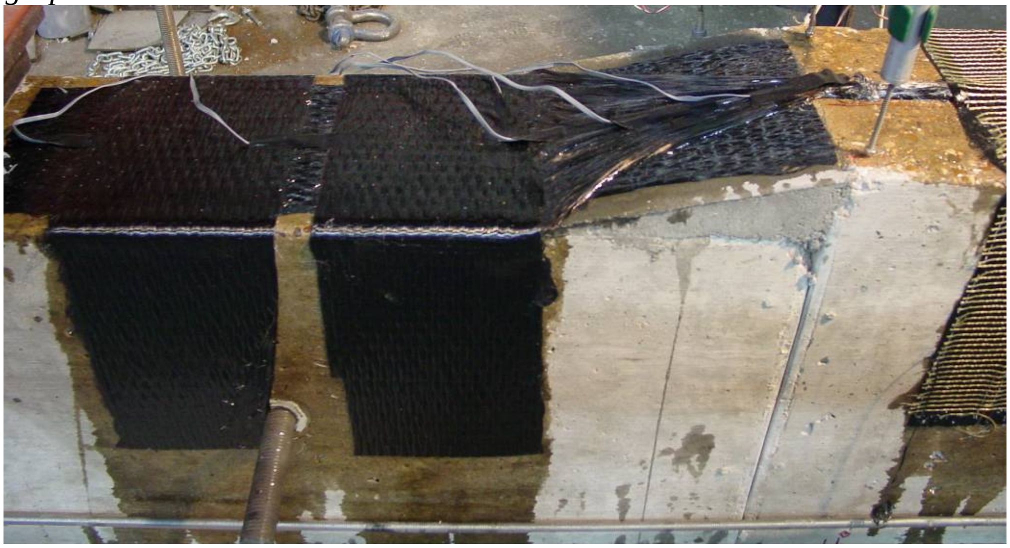

Before Testing

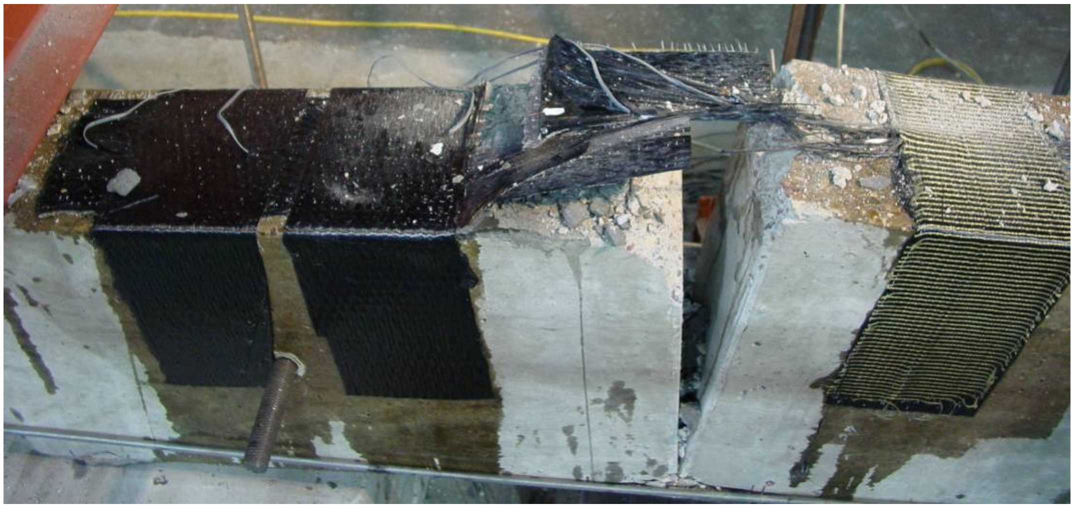

After Testing: Failure by FRP fracture

42-cs1

Test Date: December 14th, 2005
2” height transition
1 to 4 slope
2 anchors at ramp, 2 anchors at 21”, 2” width sheet, 3/8” diameter concrete hole
Single layer 6” wide U-wrap at ramp
Sandblasting surface preparation
SCH-35 fabric

Specimen Design:

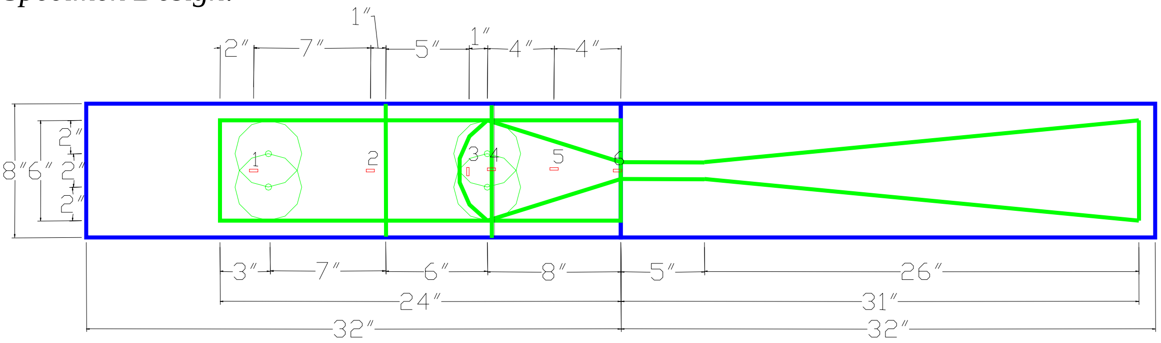
1″
2″
7″
5″
1″
4″
4″
8″
6″
2″
2″
2″
1
2
3
4
5
6
3″
7″
6″
8″
5″
26″
24″
31″
32″
32″

Test Data:

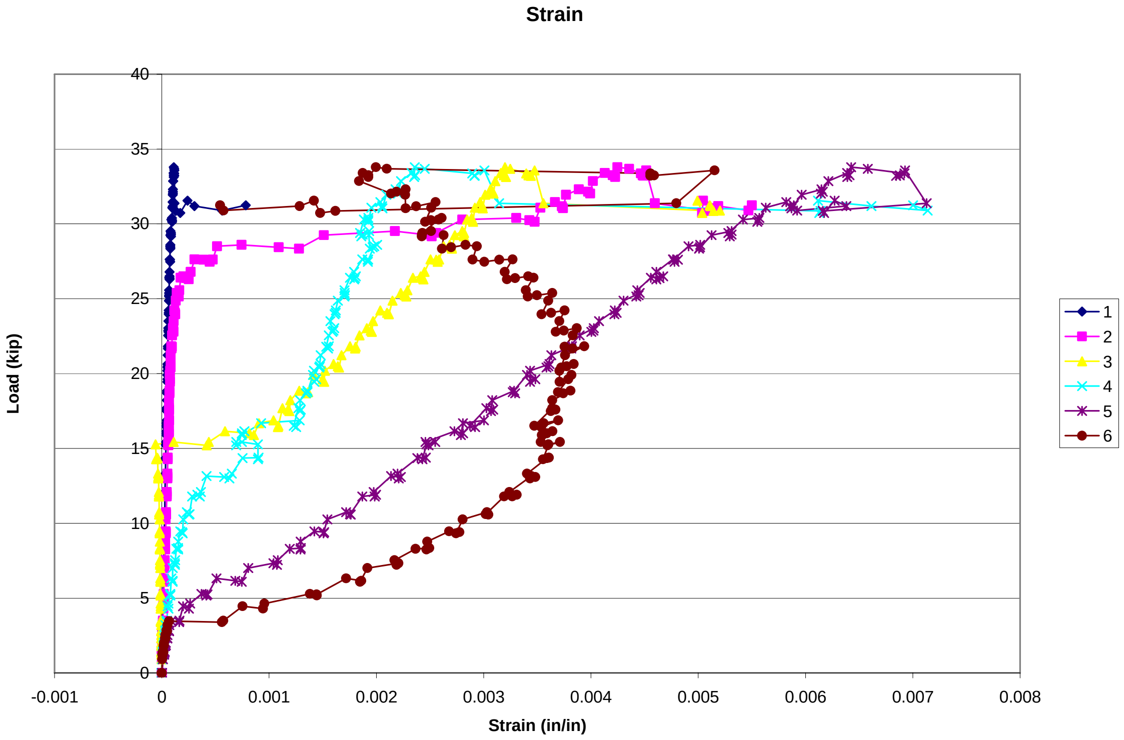

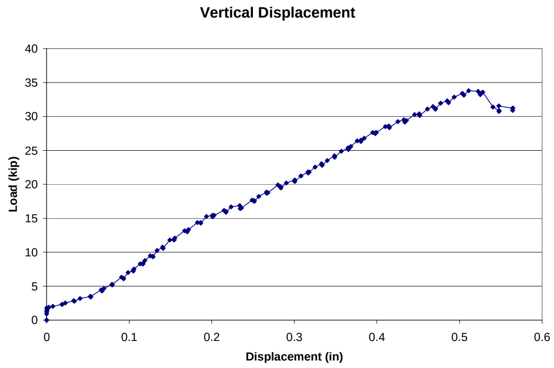

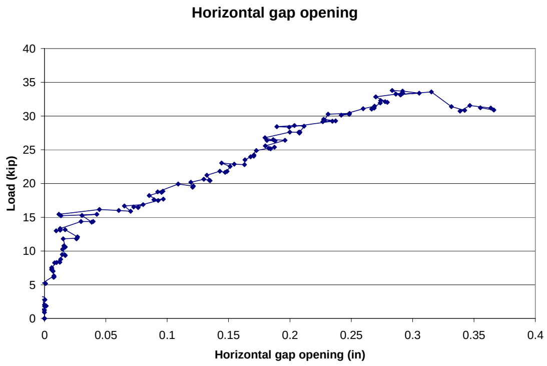

Photographs:

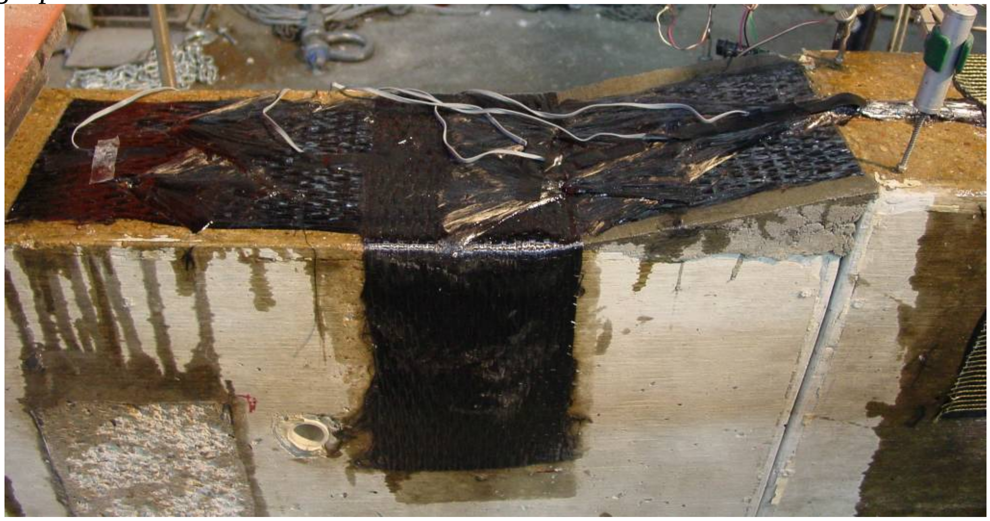

Before Testing

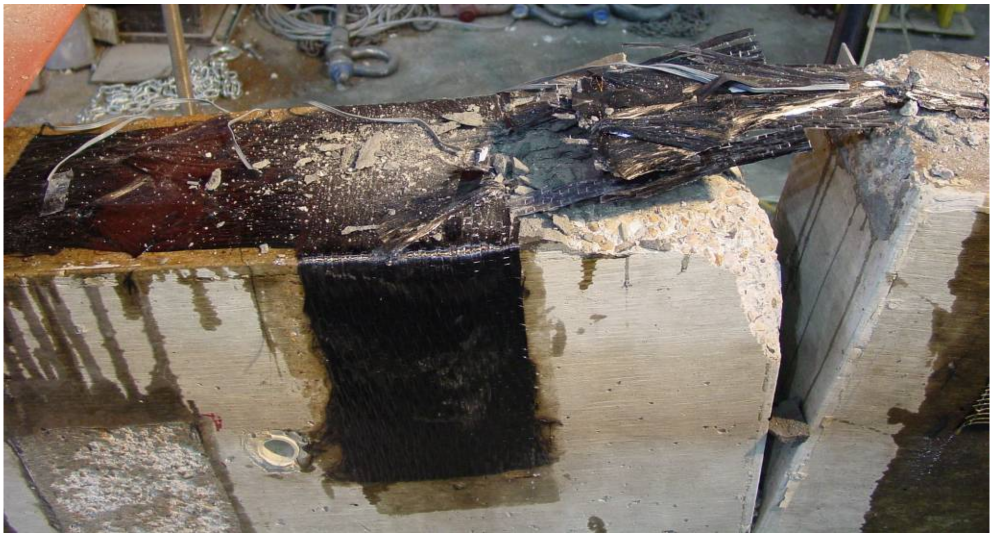

After Testing: Failure by FRP fracture

42-ns1

Test Date: January 24th, 2006
2" height transition
1 to 4 slope
No Anchorage
Sandblasting surface preparation
SCH-35 fabric beam sheet, SCH-41 fabric column sheet

Specimen Design:

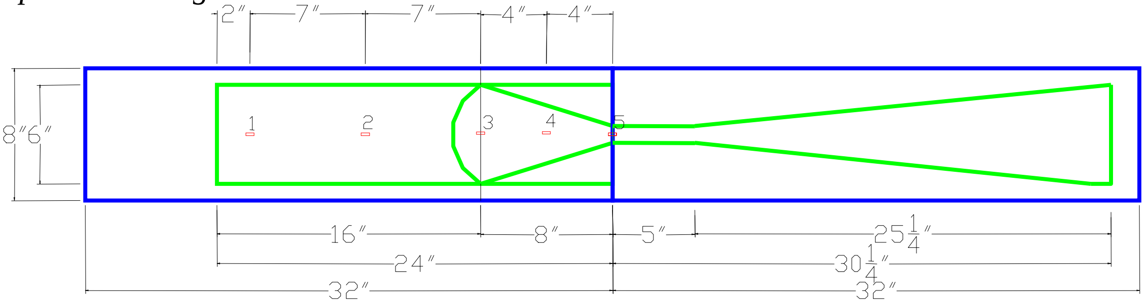
2"
7"
7"
4"
4"
8"
6"
1
2
3
4
5
16"
8"
5"
25 1/4"
24"
30 1/4"
32"
32"

Test Data:

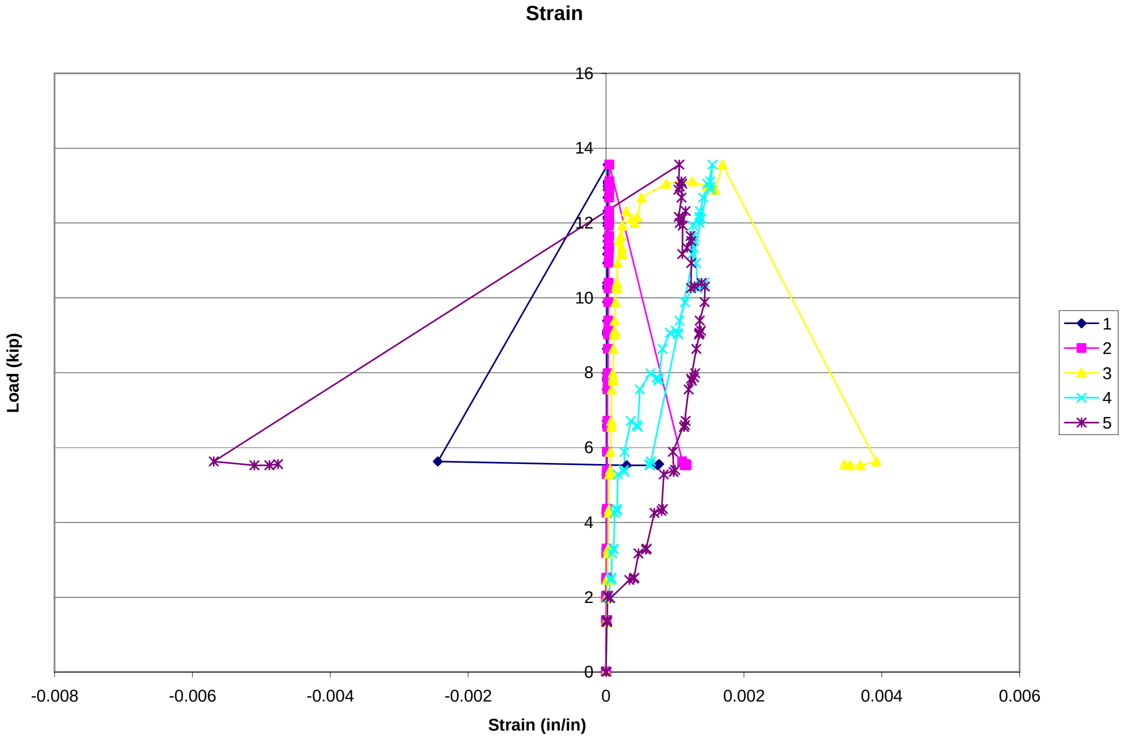

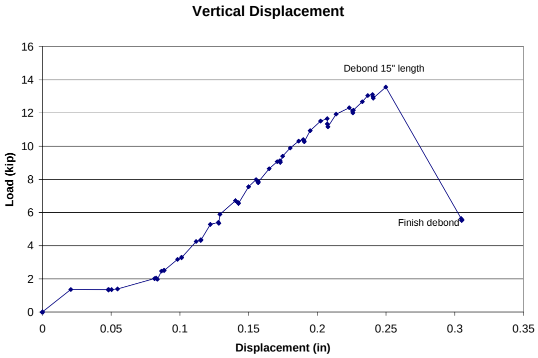

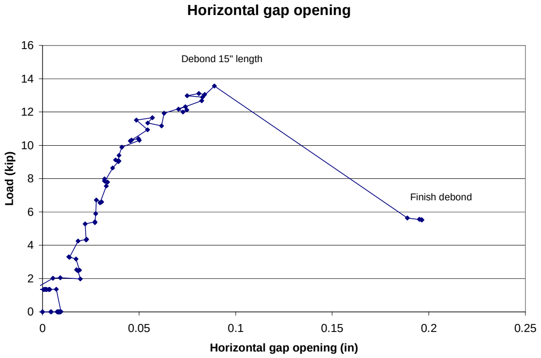

Photographs:

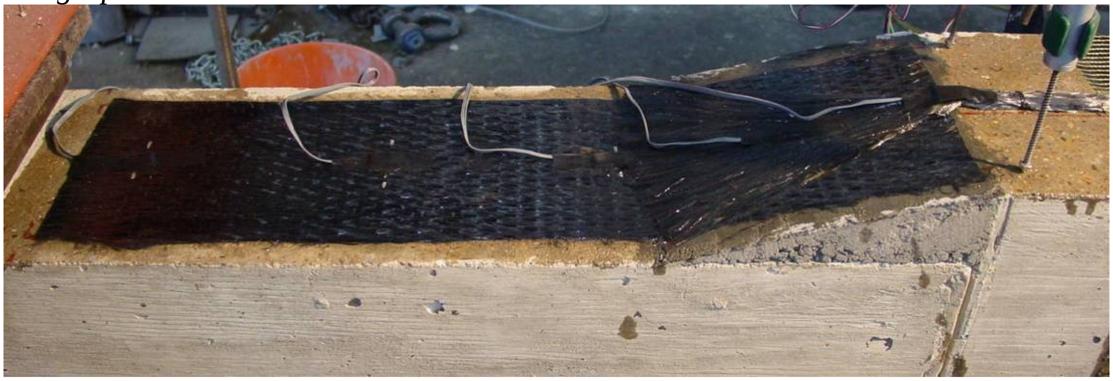

Before Testing

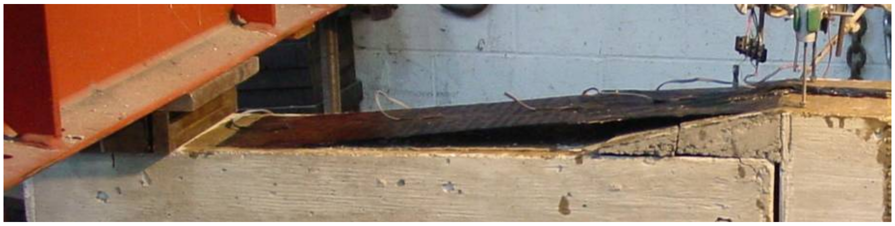

Debond 15” length

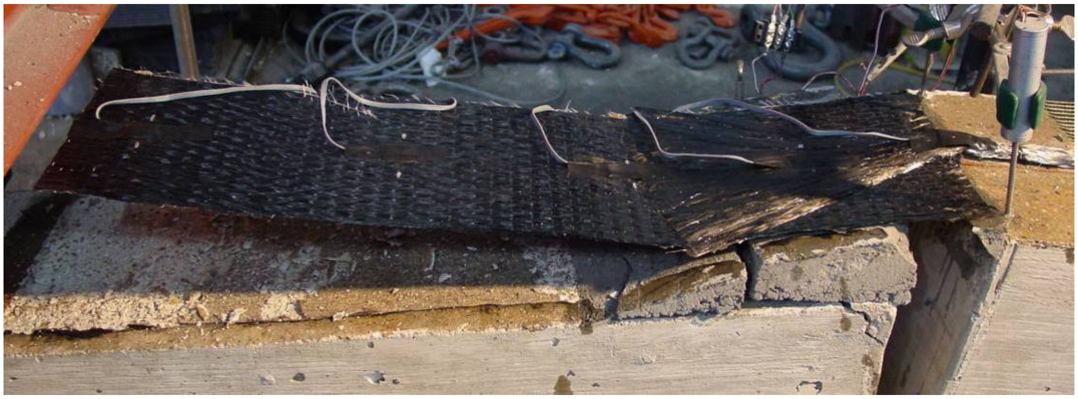

After Testing: Failure by debonding

42-4s3

Test Date: January 24th, 2006
2” height transition
1 to 4 slope
2 anchors at ramp, 2 anchors at 21”, 3” width sheet, 1/2” diameter concrete hole
Sandblasting surface preparation
SCH-35 fabric sheet, SCH-41 fabric anchors and column sheet

Specimen Design:

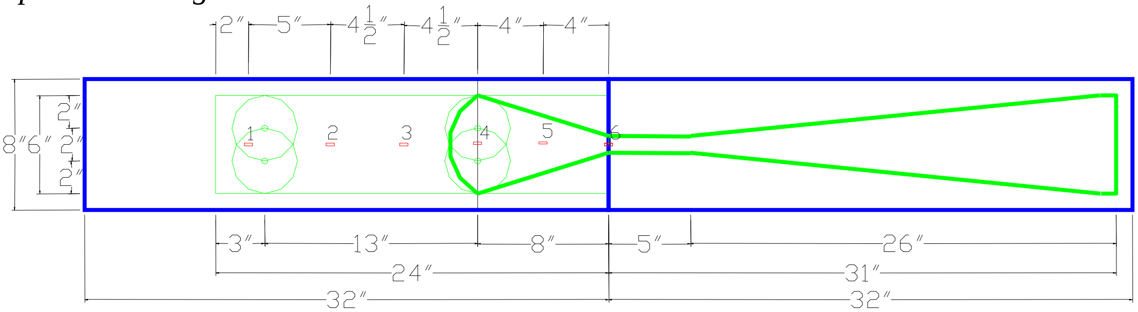
2″
5″
4 1/2″
4 1/2″
4″
4″
8″
6″
2″
2″
2″
1
2
3
4
5
6
3″
13″
8″
5″
26″
24″
31″
32″
32″

Test Data:

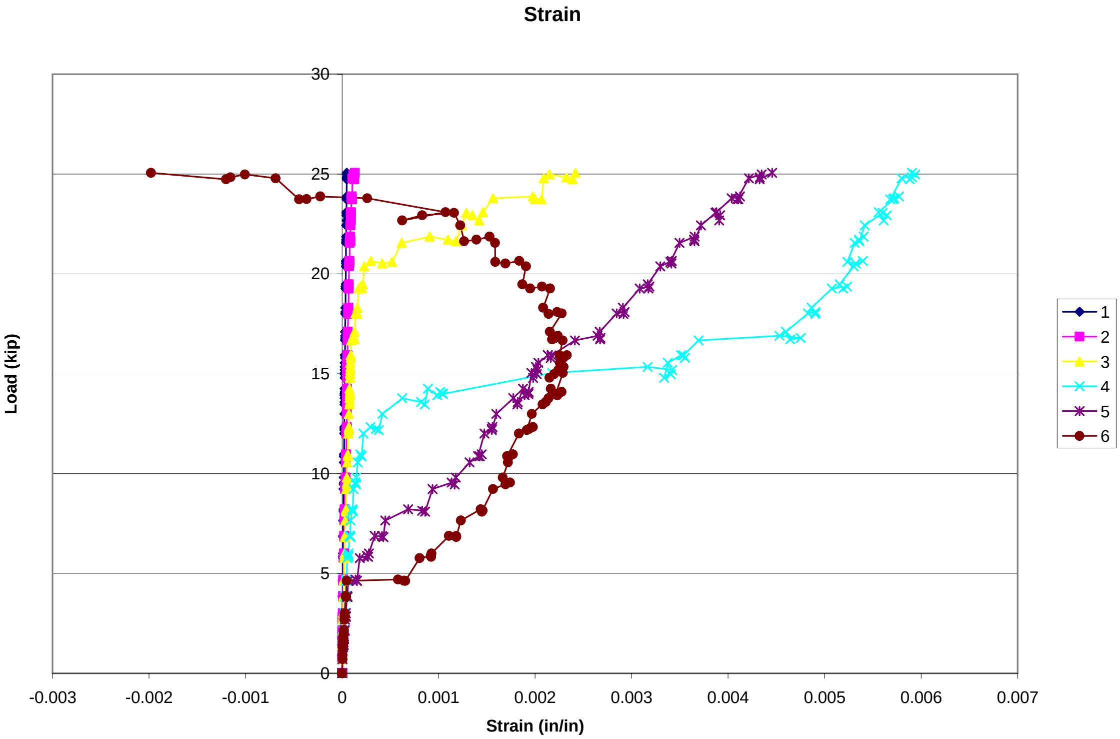

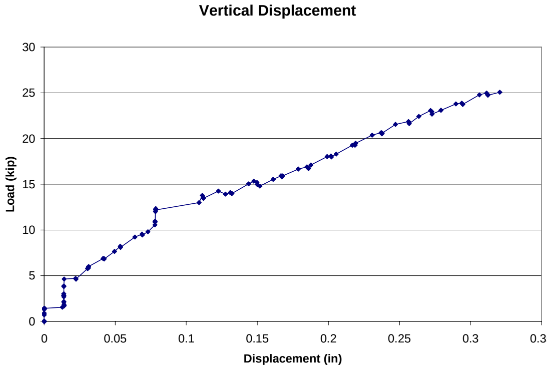
Vertical Displacement

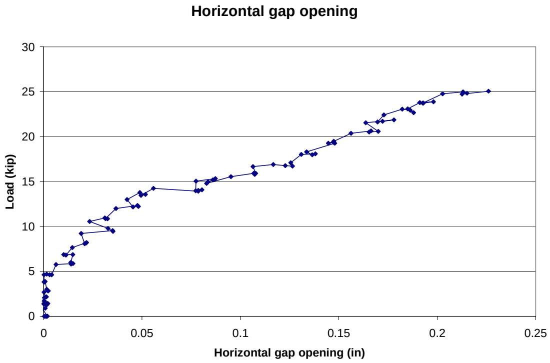
Horizontal gap opening

Photographs:

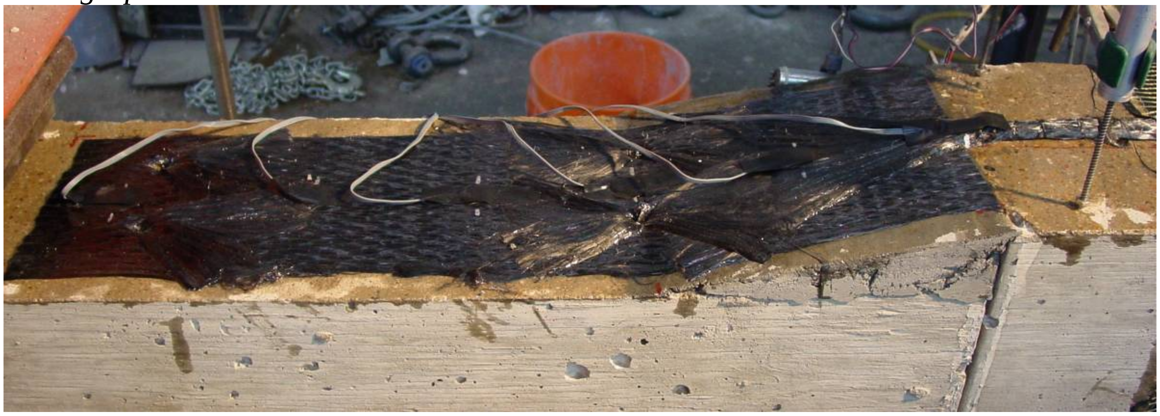
Before Testing

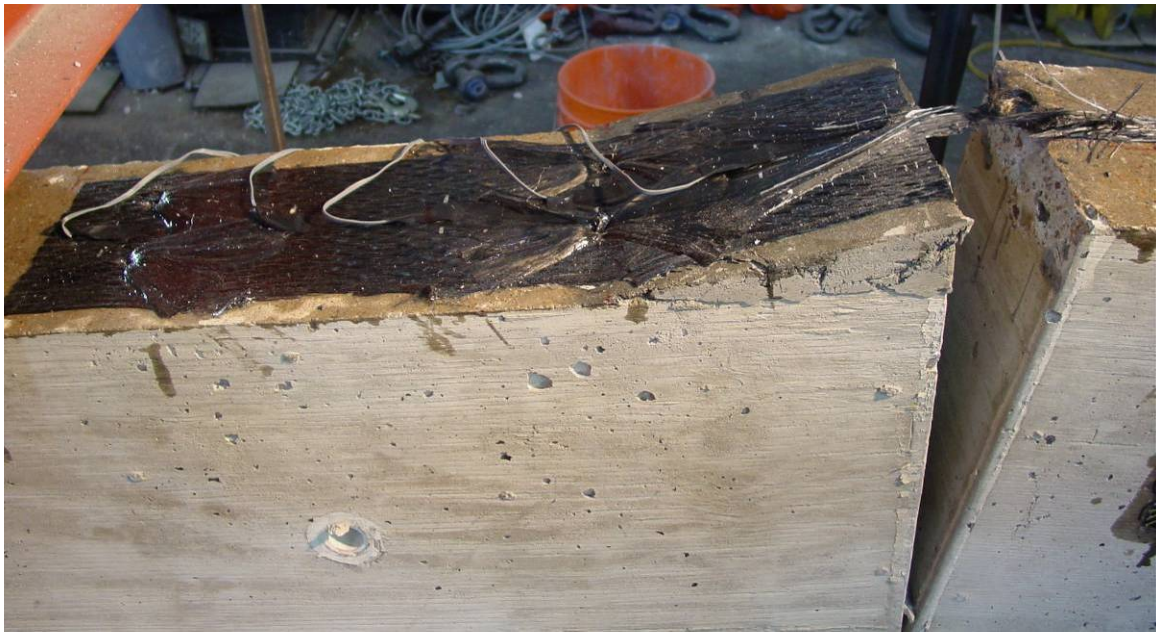
After Testing: Failure FRP fracture in column bundle, insufficient saturation

42-4s4

Test Date: February 6th, 2006
2” height transition
1 to 4 slope
2 anchors at ramp, 2 anchors at 21”, 3” width sheet, 1/2” diameter concrete hole
Sandblasting surface preparation
SCH-35 fabric sheet, SCH-41 fabric anchors and column sheet

Specimen Design:

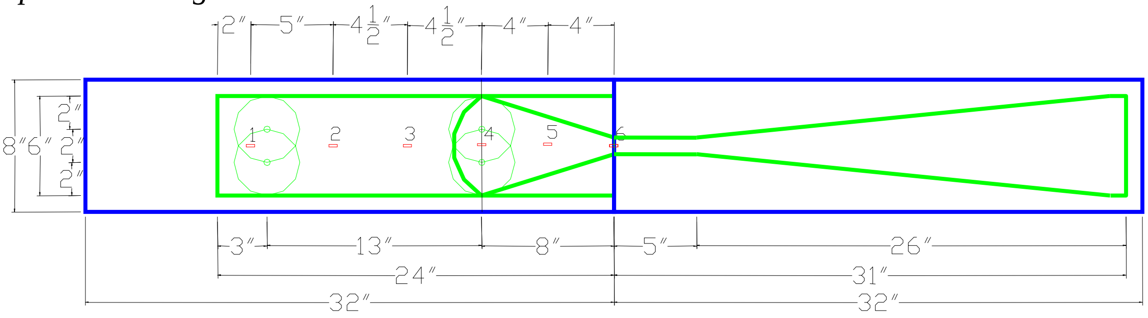
2″
5″
4 1/2″
4 1/2″
4″
4″
8″
6″
2″
2″
2″
1
2
3
4
5
6
3″
13″
8″
5″
26″
24″
31″
32″
32″

Test Data:

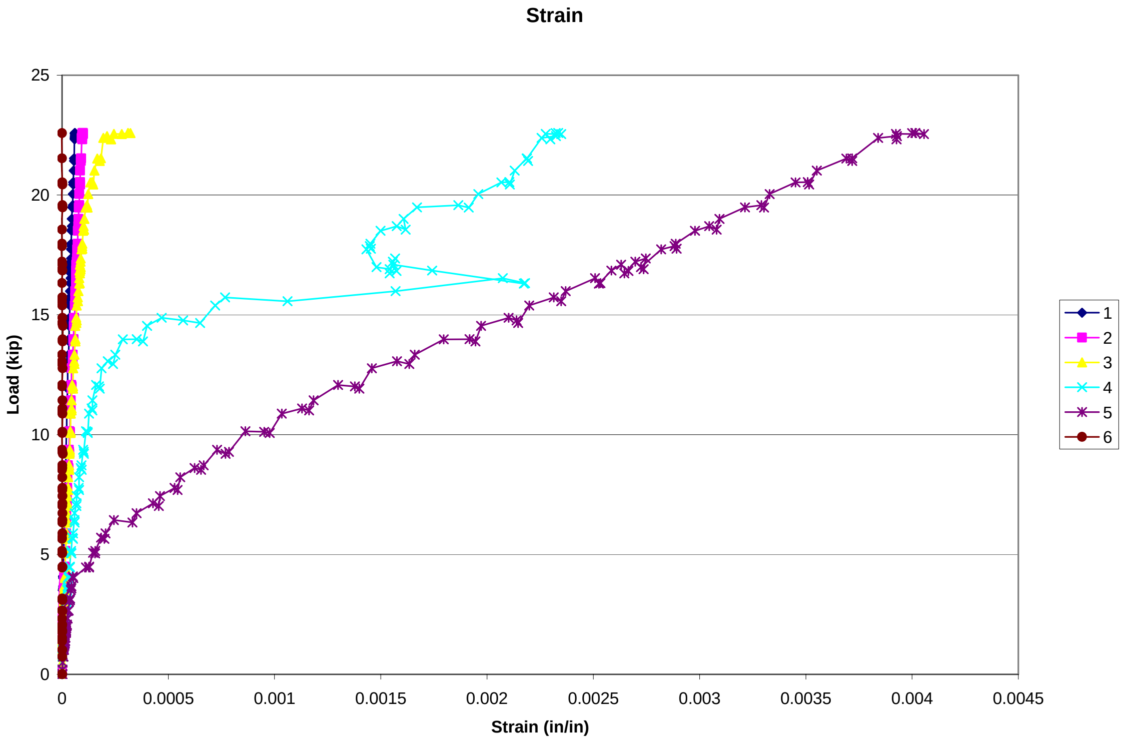

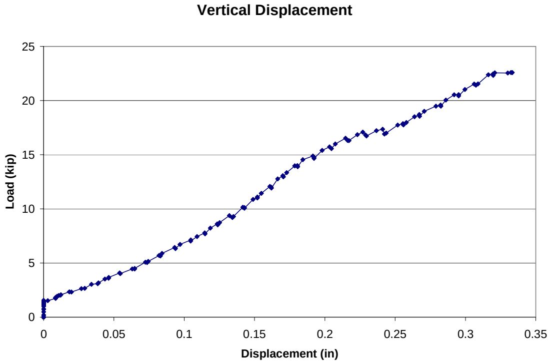

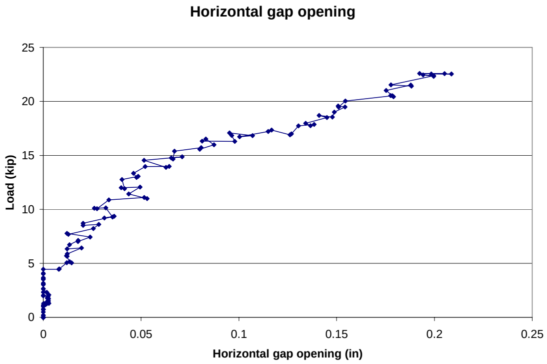

Photographs:

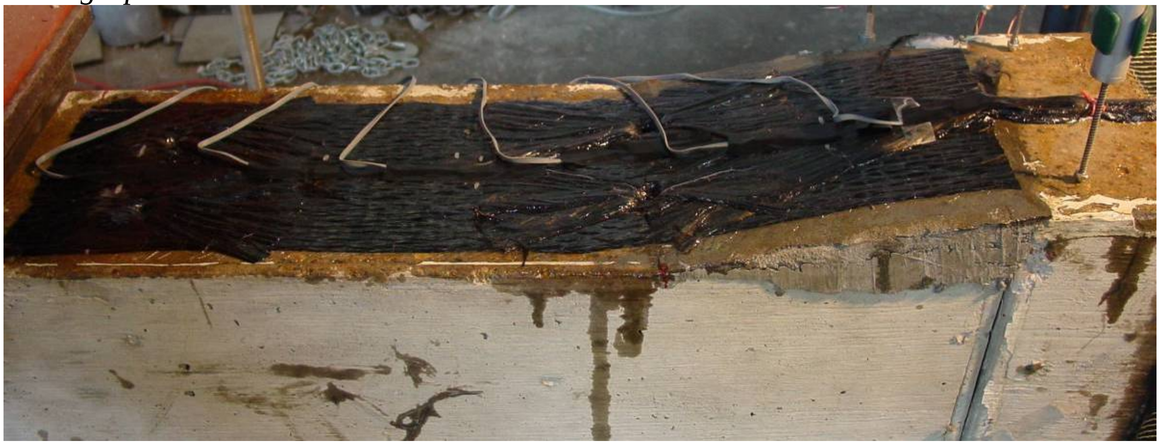

Before Testing

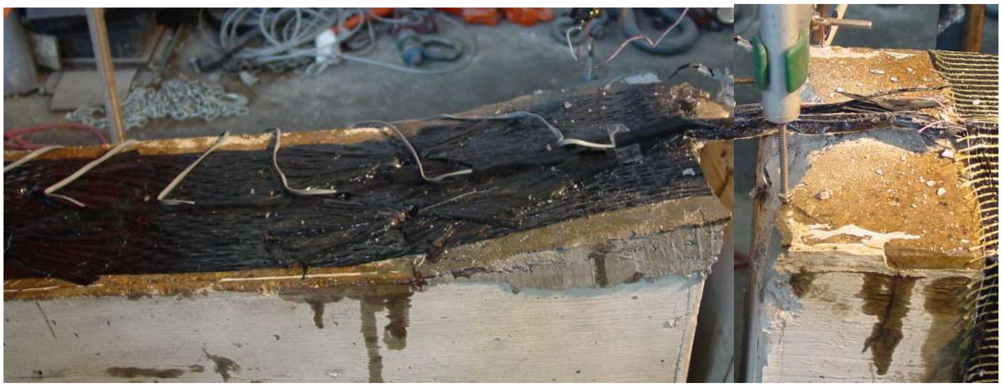

After Testing: Failure by FRP fracture of column bundle

42-6n1

Test Date: February 14th, 2006
2” height transition
1 to 4 slope
3 anchors at ramp, 3 anchors at 21”, 2” width sheet, 3/8” diameter concrete hole
No bond, plastic sheet between FRP and concrete
SCH-35 fabric beam sheet, SCH-41 fabric anchors and column sheet

Specimen Design:

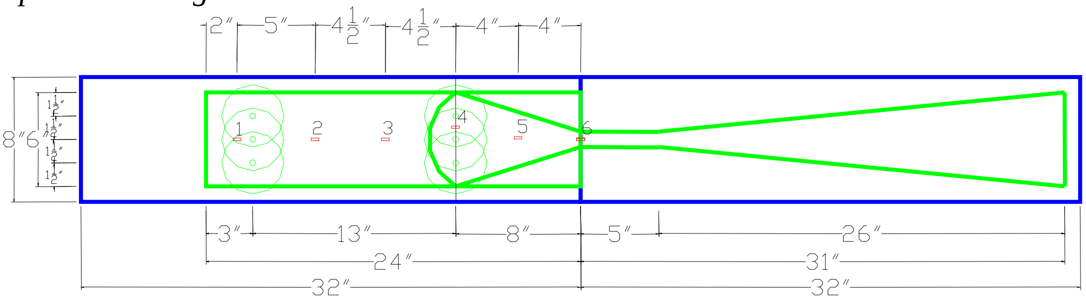
2″
5″
4 1/2″
4 1/2″
4″
4″
8″
6″
1 1/2″
1 1/2″
1 1/2″
1 1/2″
1
2
3
4
5
6
3″
13″
8″
5″
26″
24″
31″
32″
32″

Test Data:

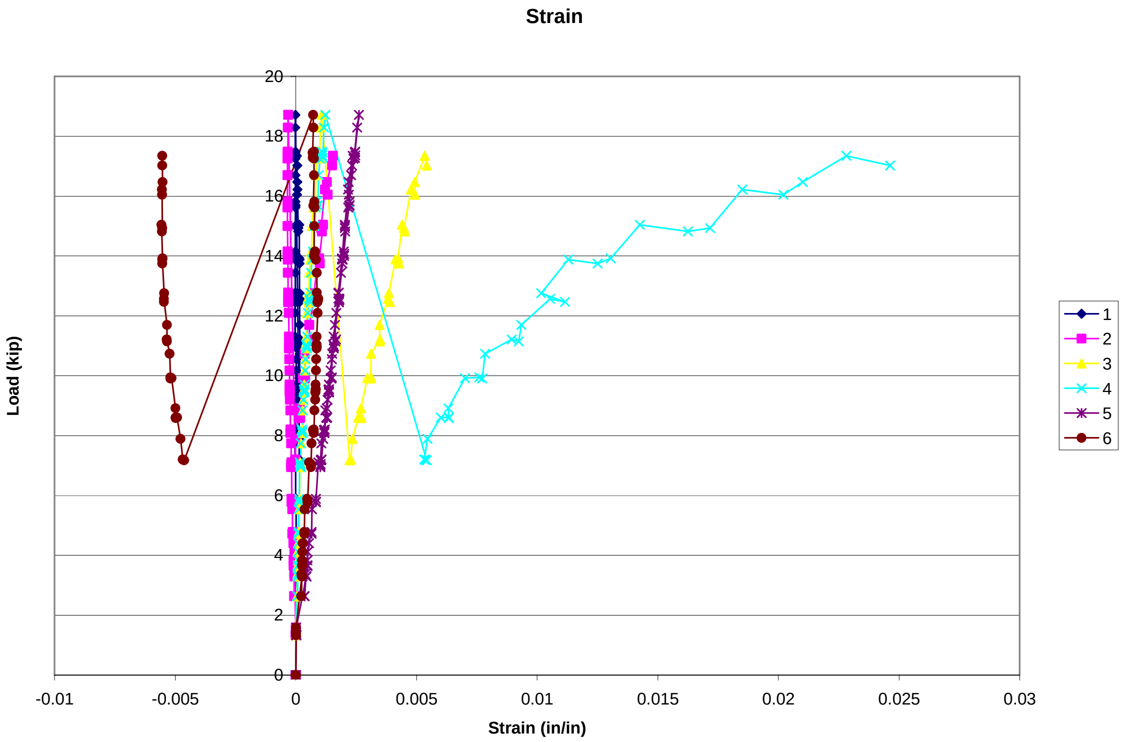

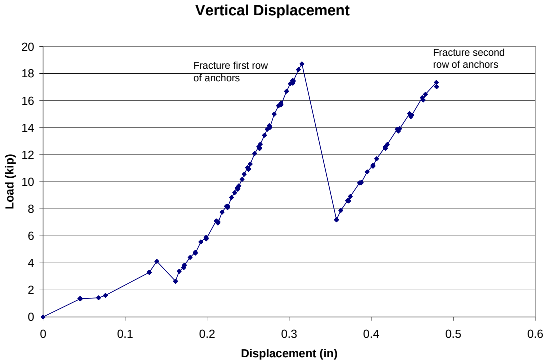
Vertical Displacement

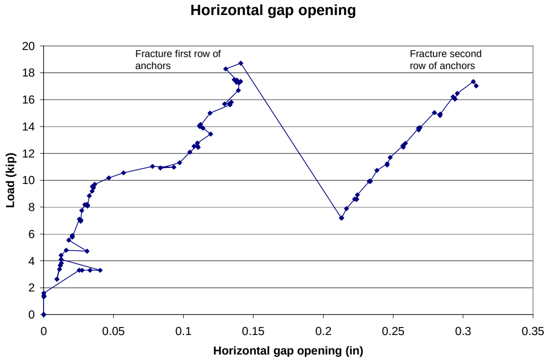
Horizontal gap opening

Photographs:

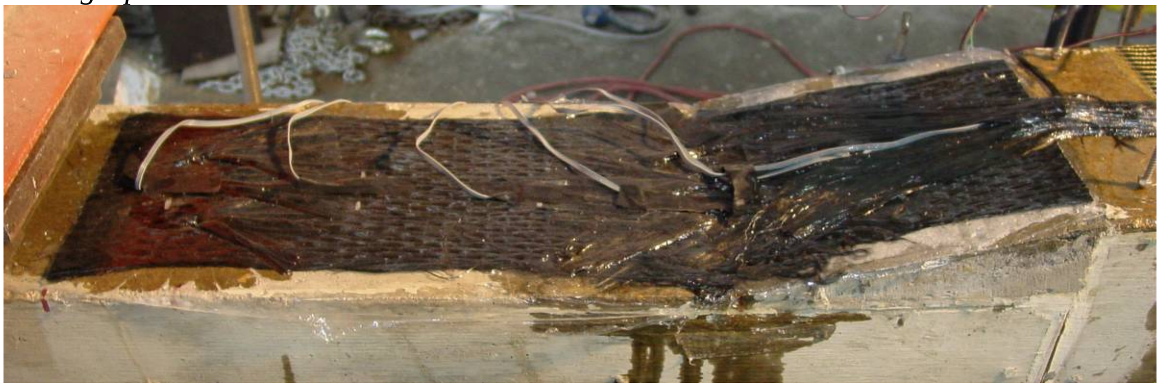

Before Testing

Fracture first row of anchors

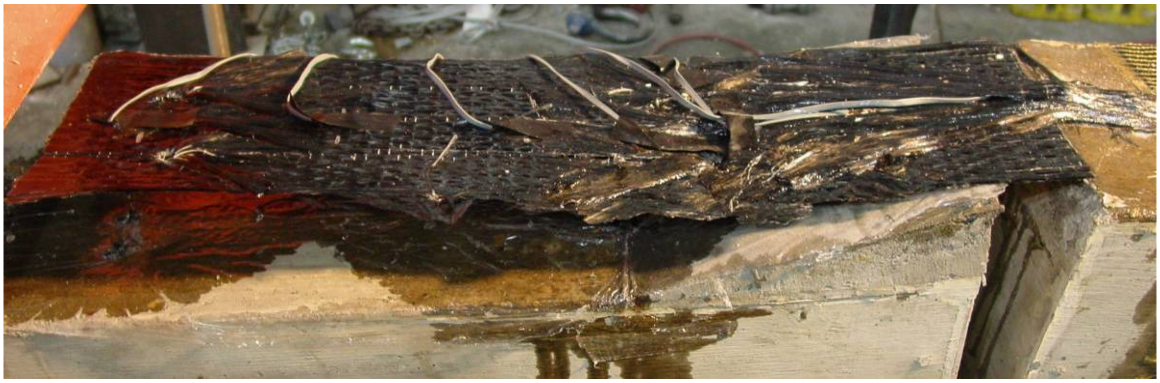

After Testing: Failure by anchor fracture

22-6s1

Test Date: February 7th, 2006
2” height transition
1 to 2 slope
3 anchors at ramp, 3 anchors at 21”, 2” width sheet, 3/8” diameter concrete hole
Sandblasting surface preparation
SCH-35 fabric beam sheet, SCH-41 fabric anchors and column sheet

Specimen Design:

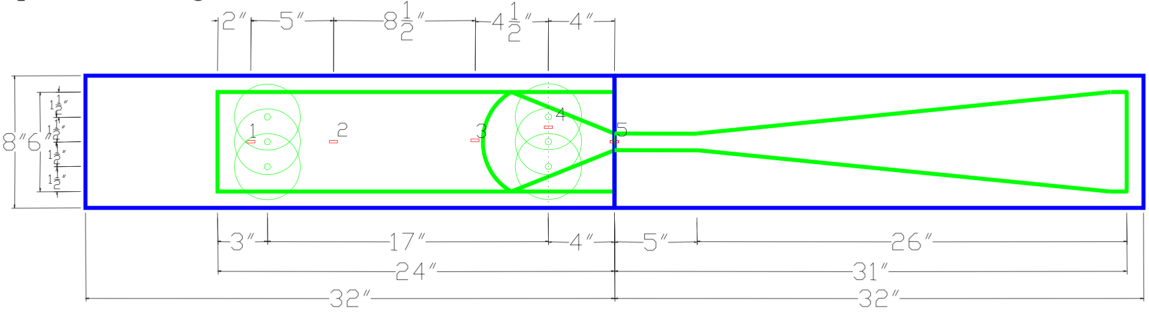
2″
5″
8½″
4½″
4″
8″
6″
1½″
1½″
1½″
1½″
1
2
3
4
5
3″
17″
4″
5″
26″
24″
31″
32″
32″

Test Data:

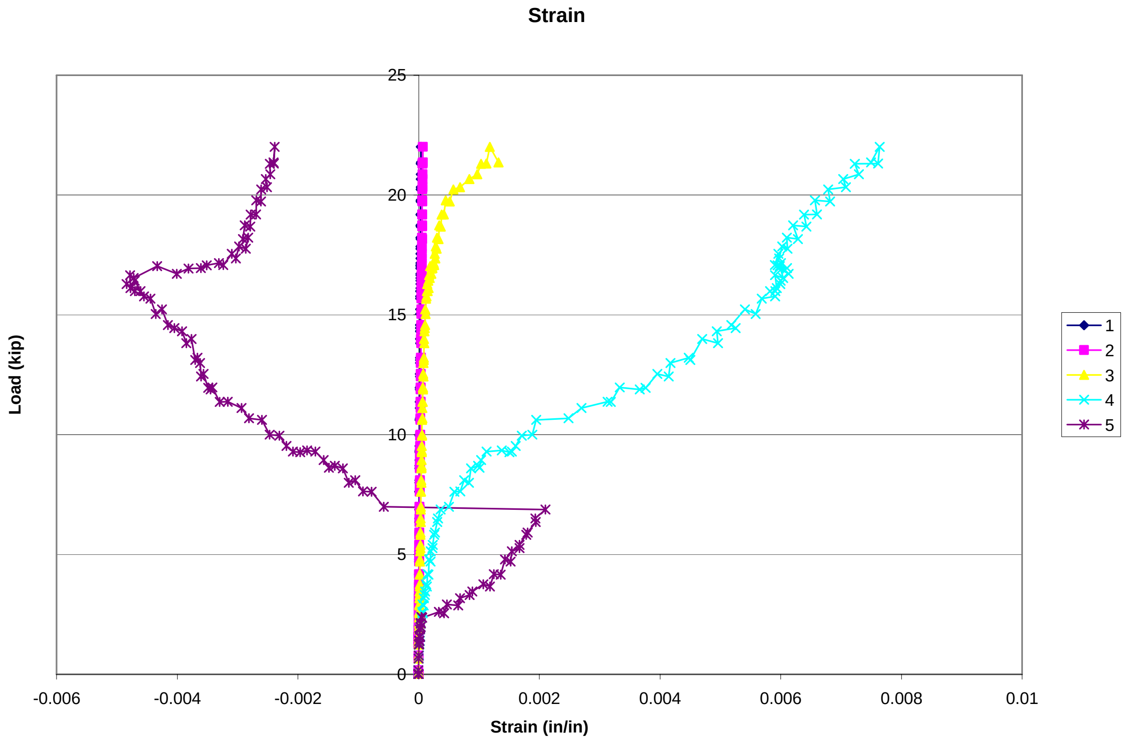

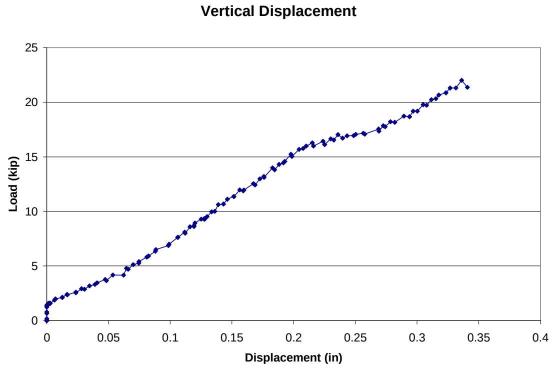

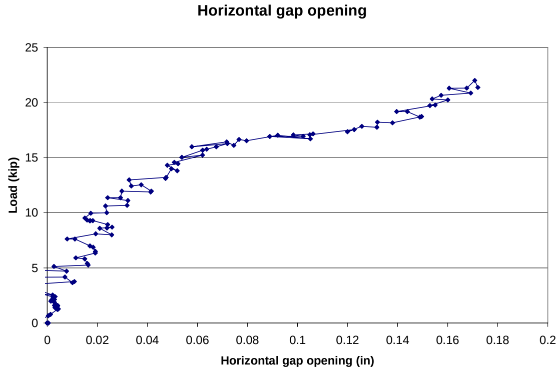

Photographs:

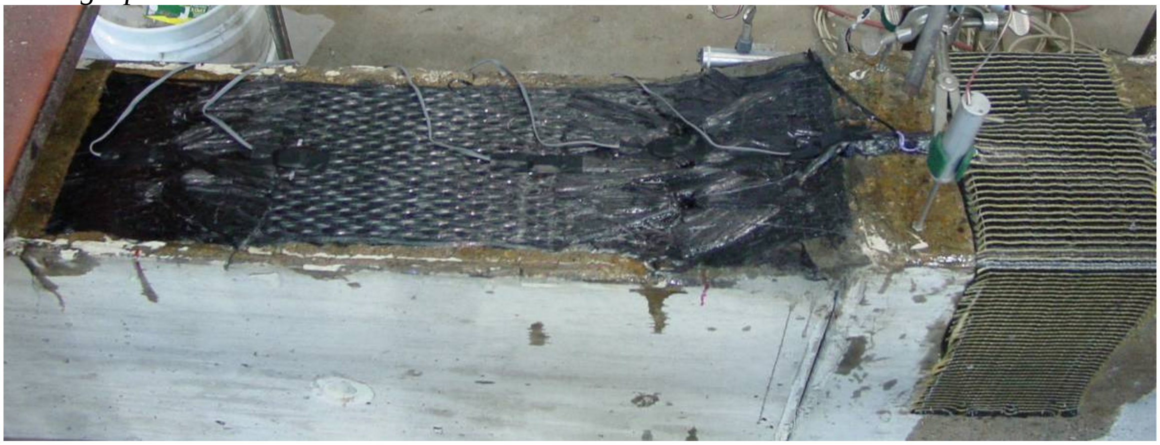

Before Testing

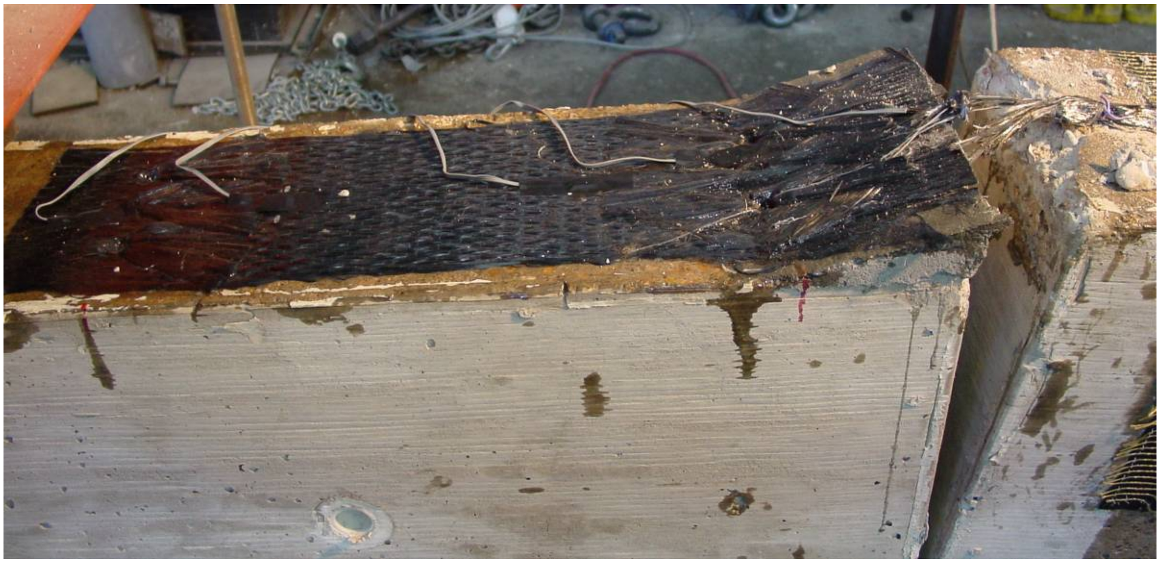

After Testing: Failure by FRP fracture

42-6s3

Test Date: February 14th, 2006
2” height transition
1 to 4 slope
3 anchors at ramp, 3 anchors at 21”, 2” width sheet, 3/8” diameter concrete hole
Sandblasting surface preparation
SCH-35 fabric beam sheet, SCH-41 fabric anchors and column sheet

Specimen Design:

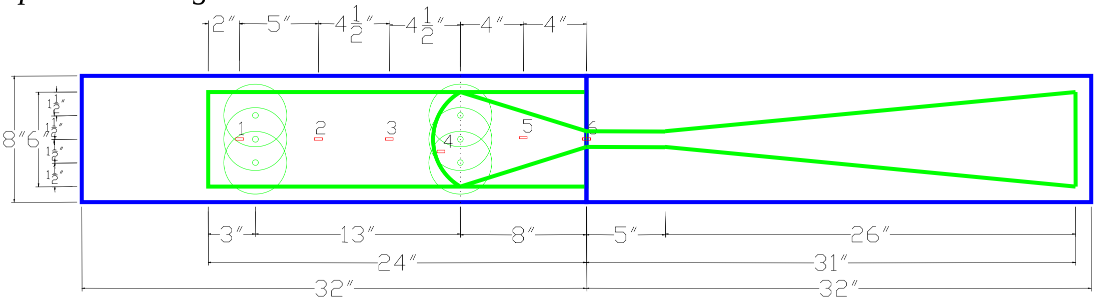

2″
5″
4 1/2″
4 1/2″
4″
4″
8″
6″
1 1/2″
1 1/2″
1 1/2″
1 1/2″
1
2
3
4
5
6
3″
13″
8″
5″
26″
24″
31″
32″
32″

Test Data:

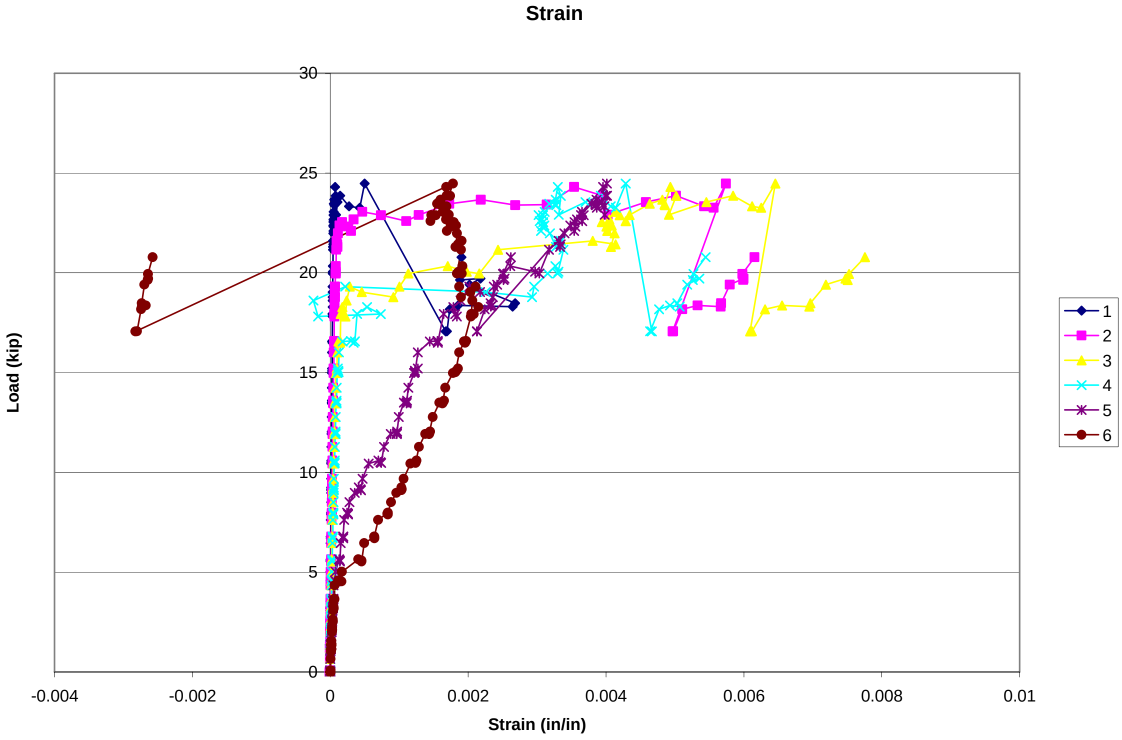

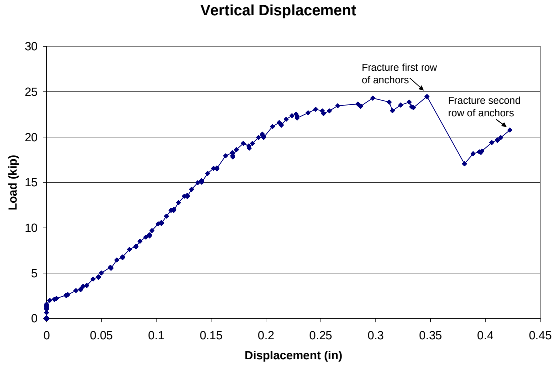

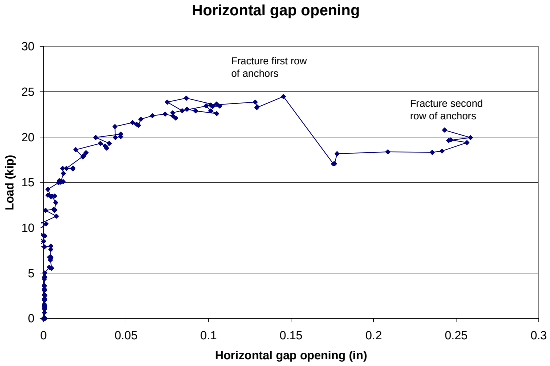

Photographs:

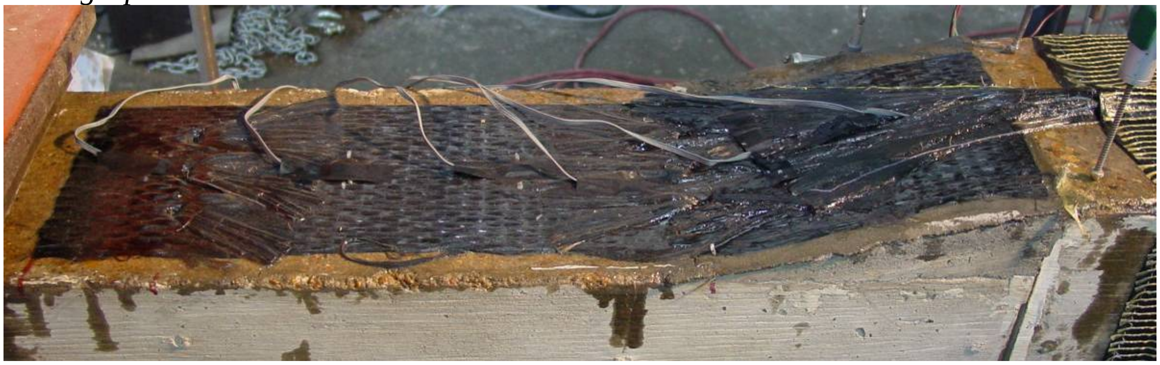

Before Testing

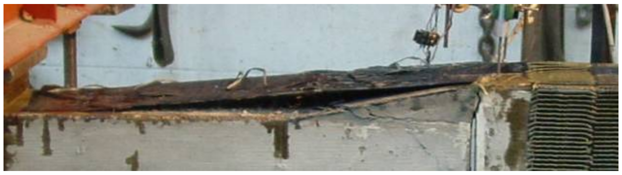

Fracture first row of anchors

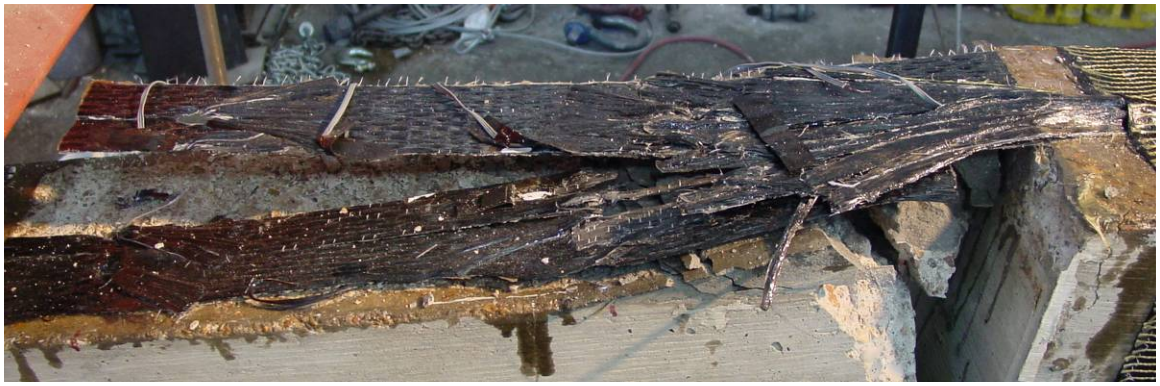

After Testing: Failure by anchor fracture

42-6s4

Test Date: February 28th, 2006
2" height transition
1 to 4 slope
3 anchors at ramp, 3 anchors at 21", 2 2/3" width sheet, 1/2" diameter concrete hole
Sandblasting surface preparation
SCH-35 fabric beam sheet, SCH-41 fabric anchors and column sheet

Specimen Design:

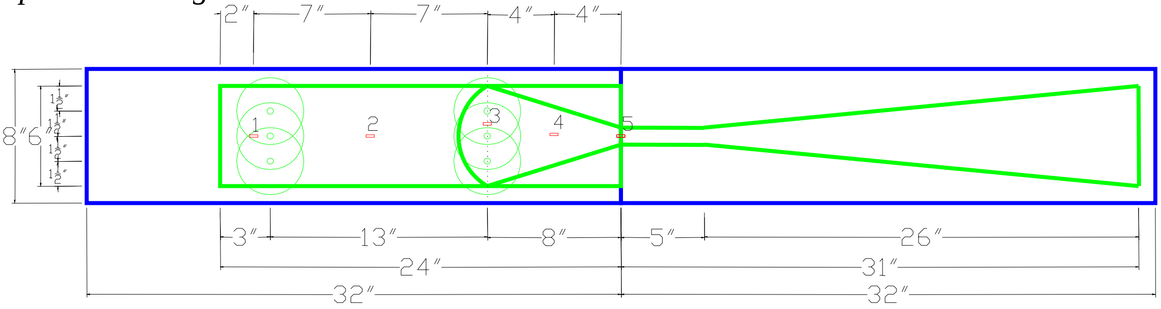

2"
7"
7"
4"
4"
8"
6"
1½"
1½"
1½"
1½"
1
2
3
4
5
3"
13"
8"
5"
26"
24"
31"
32"
32"

Test Data:

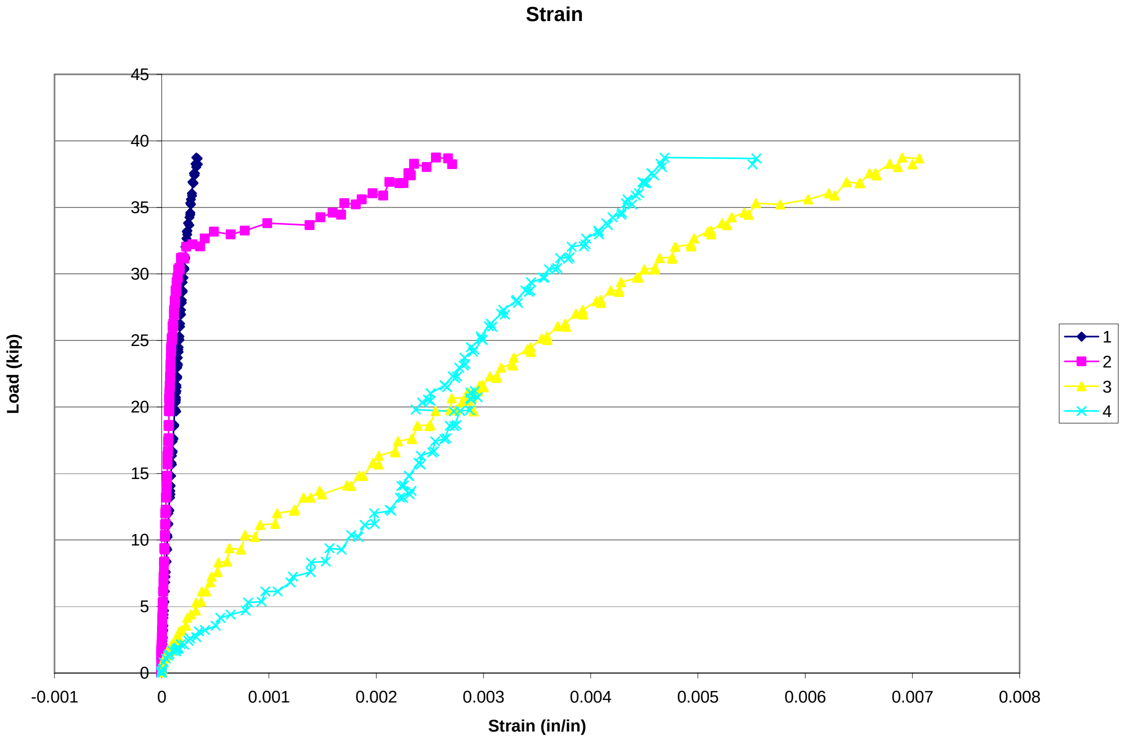

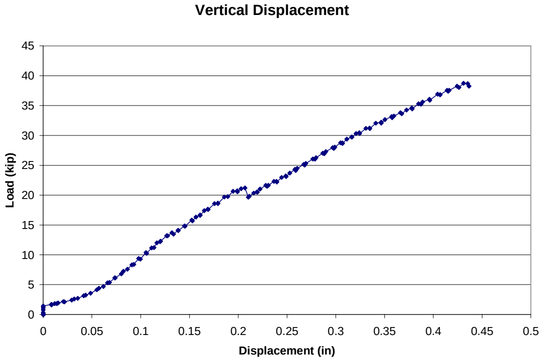

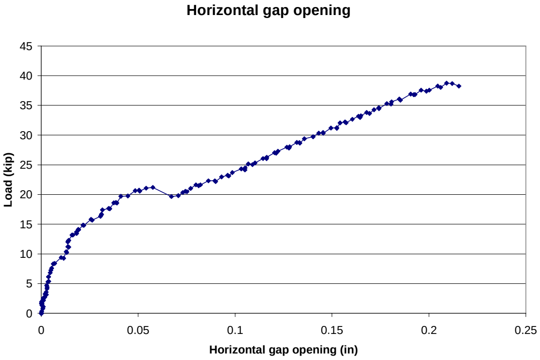

Photographs:

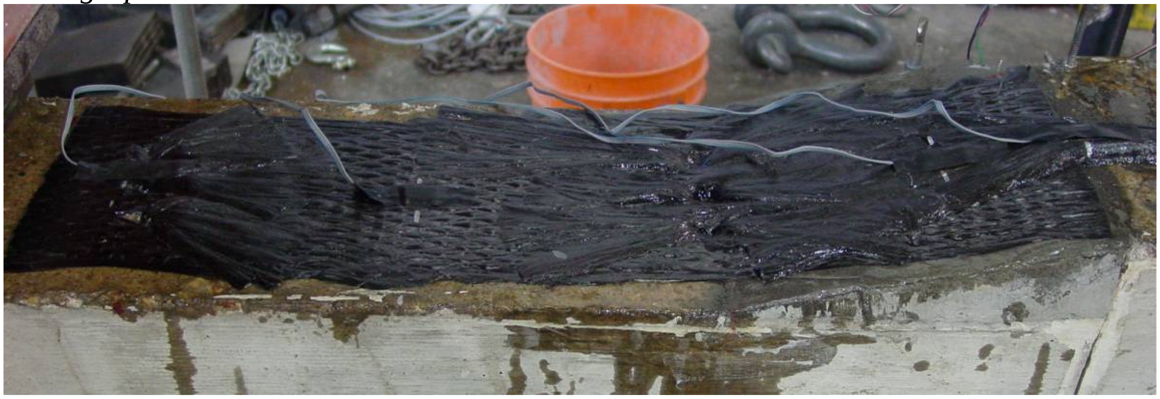

Before Testing

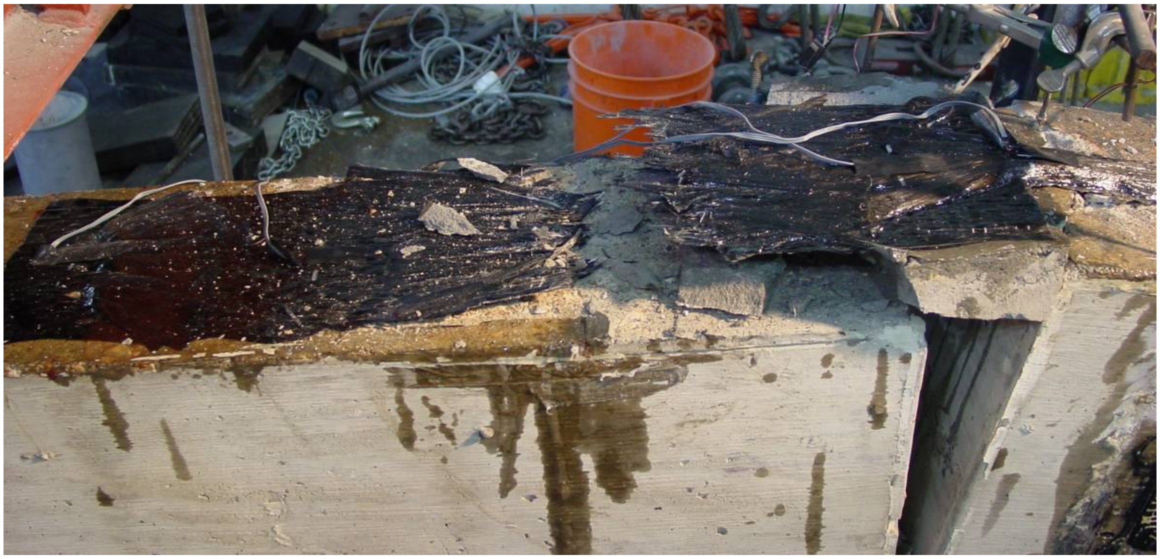

After Testing: Failure by FRP fracture

42-6s5

Test Date: March 21th, 2006
2” height transition
1 to 4 slope
3 anchors at ramp, 3 anchors at 21”, 2 2/3” width sheet, 1/2” diameter concrete hole
Sandblasting surface preparation
SCH-41 fabric

Specimen Design:

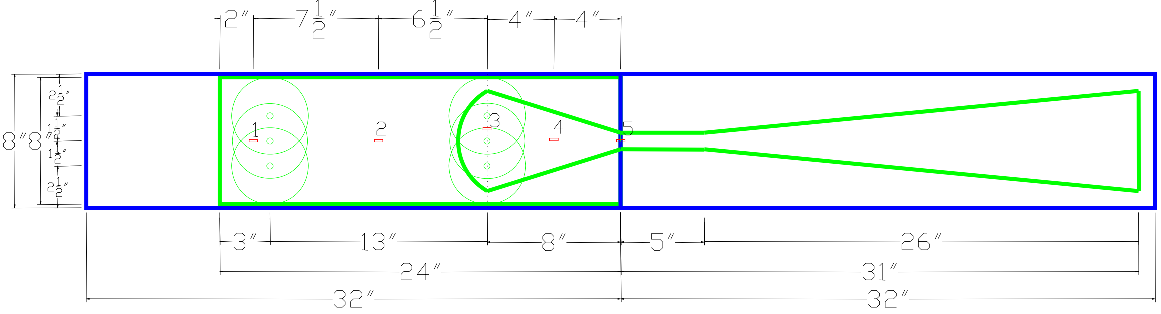
2″
7 1/2″
6 1/2″
4″
4″
8″
8″
2 1/2″
1 1/2″
1 1/2″
2 1/2″
1
2
3
4
5
3″
13″
8″
5″
26″
24″
31″
32″
32″

Test Data:

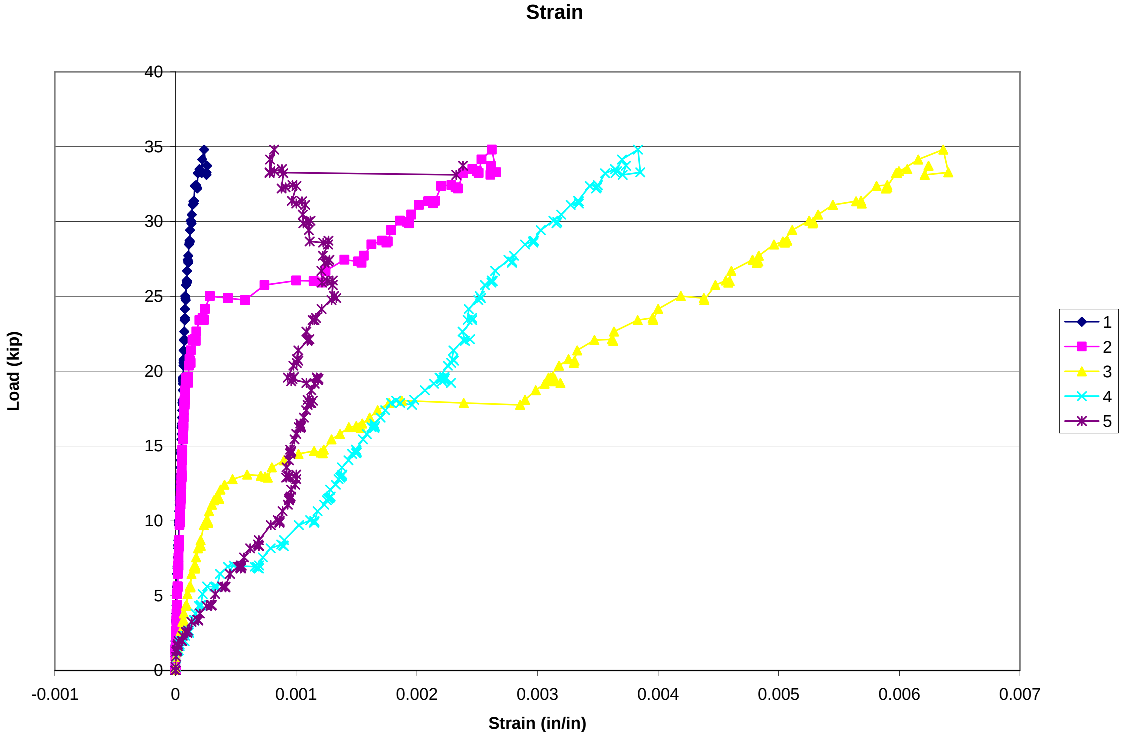

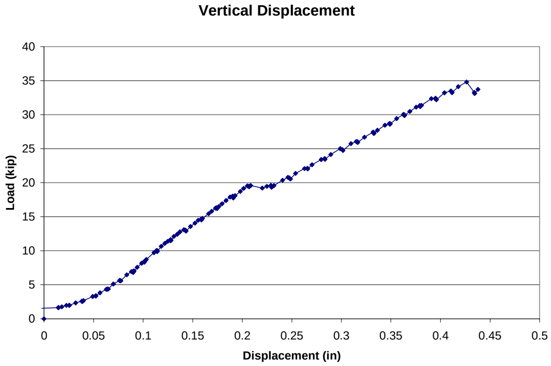
Vertical Displacement

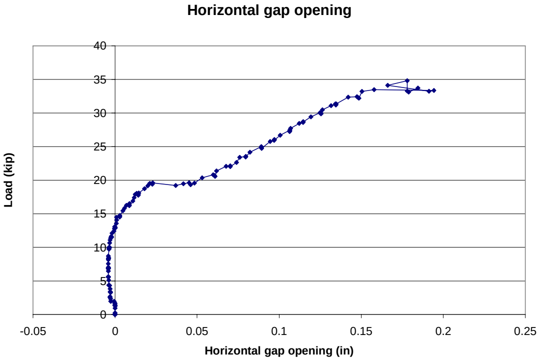
Horizontal gap opening

Photographs:

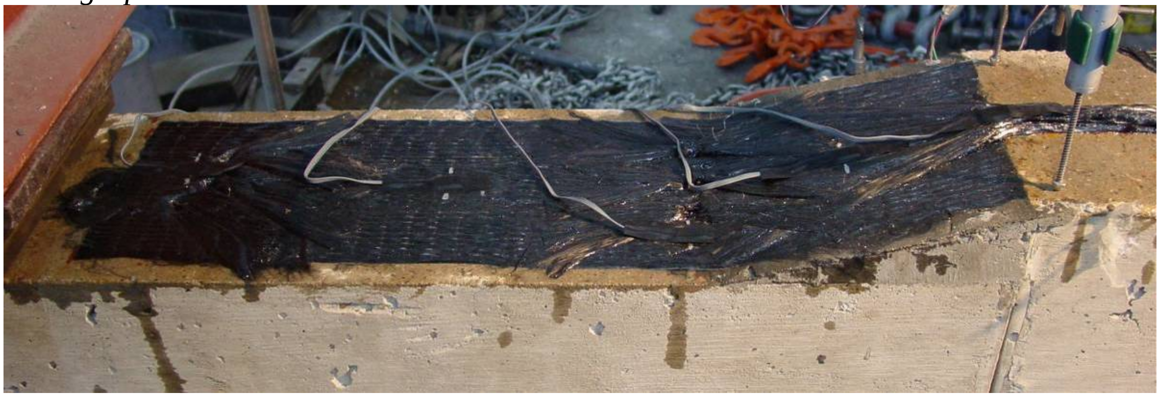
Before Testing

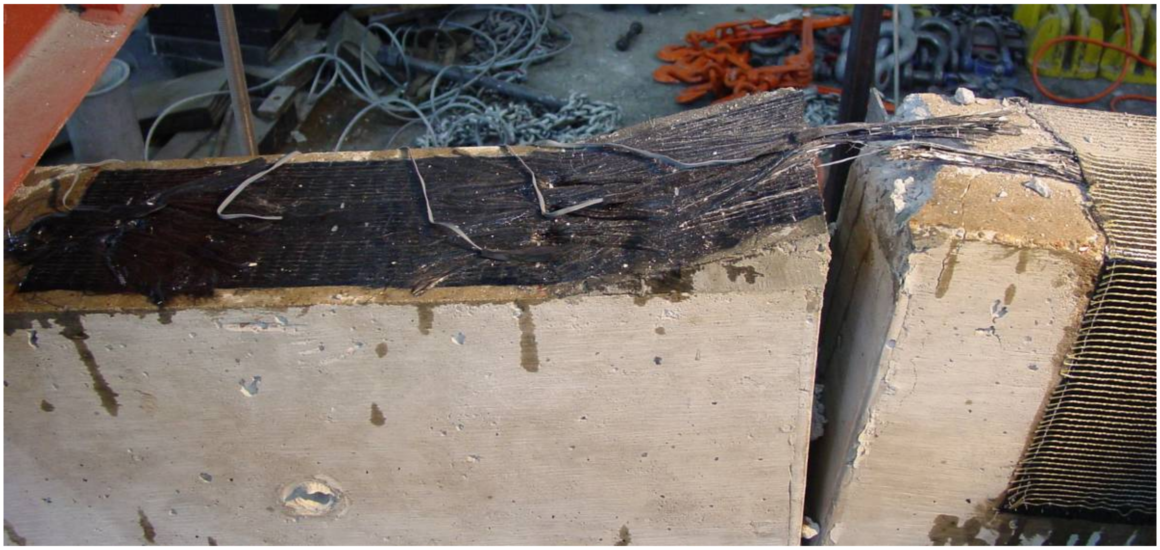
After Testing: Failure by FRP fracture

42-6n2

Test Date: March 21th, 2006
2” height transition
1 to 4 slope
3 anchors at ramp, 3 anchors at 21”, 2 2/3” width sheet, 1/2” diameter concrete hole
No bond, plastic sheet between FRP and concrete
SCH-41 fabric

Specimen Design:

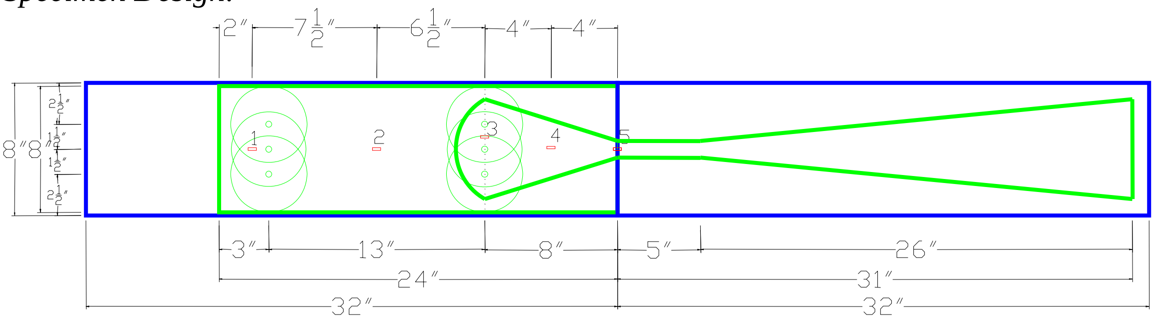
2″
7 1/2″
6 1/2″
4″
4″
8″
8″
2 1/2″
1 1/2″
1 1/2″
2 1/2″
1
2
3
4
5
3″
13″
8″
5″
26″
24″
31″
32″
32″

Test Data:

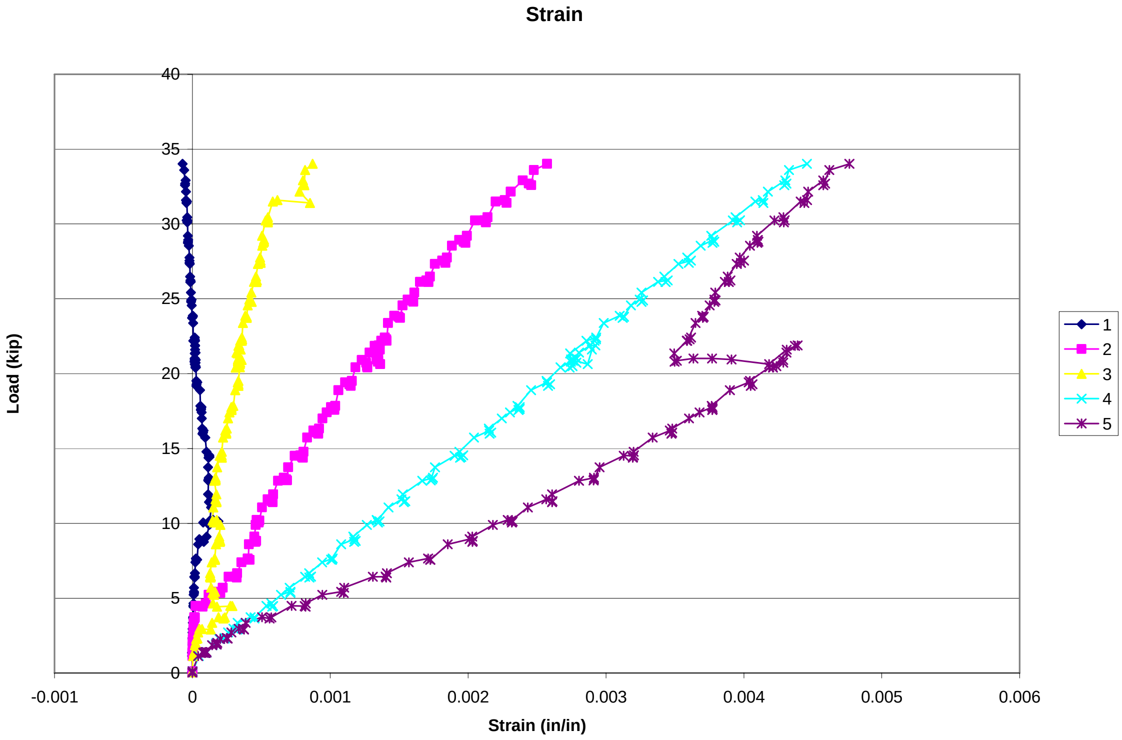

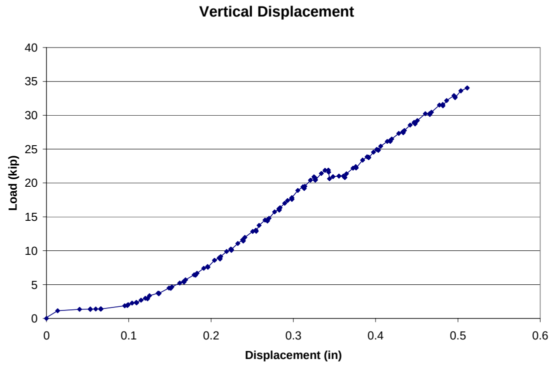

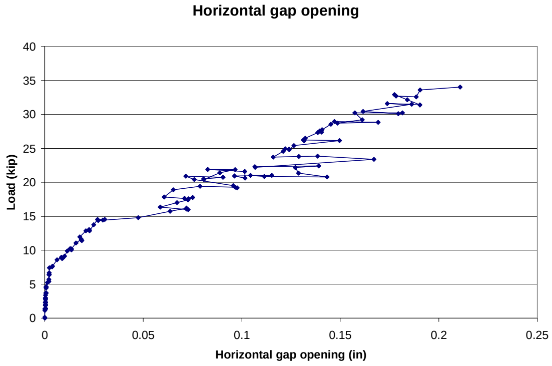

Photographs:

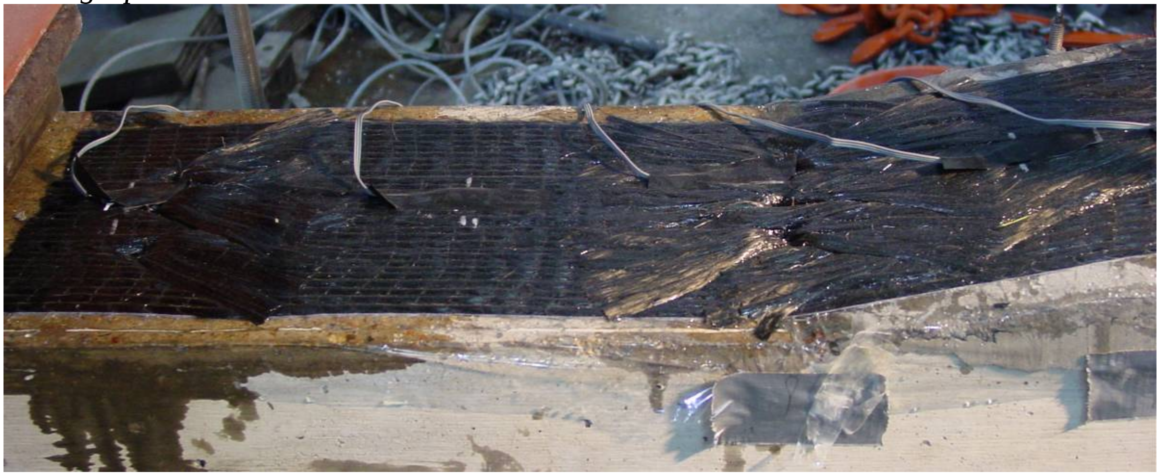

Before Testing

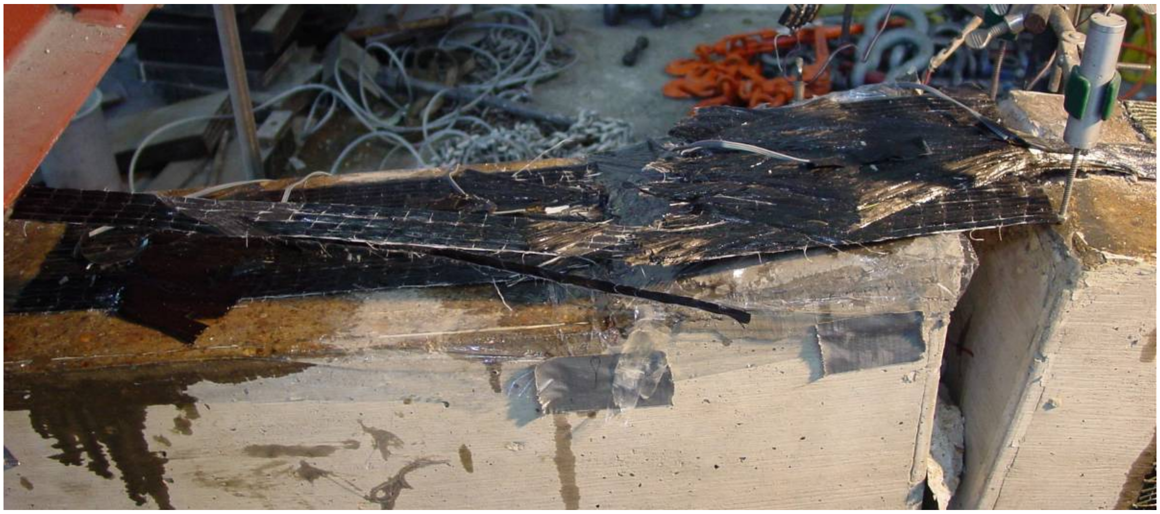

After Testing: Failure by FRP fracture

42-4s5

Test Date: April 10th, 2006
2” height transition
1 to 4 slope
2 anchors at ramp, 2 anchors at 21”, 4” width sheet, 5/8” diameter concrete hole
Sandblasting surface preparation
SCH-41 fabric

Specimen Design:

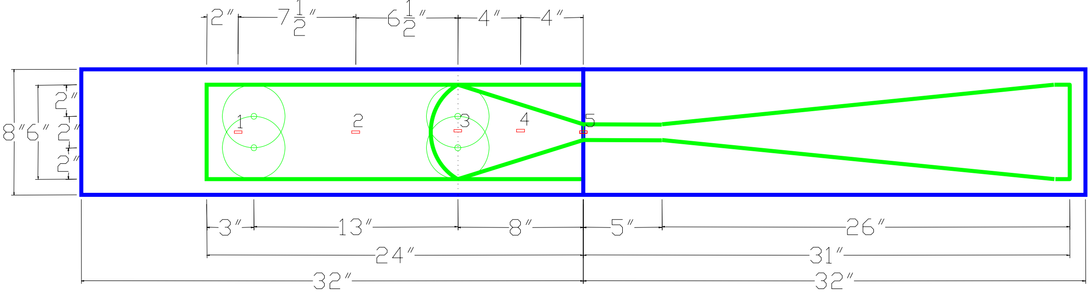

2″
7 1/2″
6 1/2″
4″
4″
8″
6″
2″
2″
2″
1
2
3
4
5
3″
13″
8″
5″
26″
24″
31″
32″
32″

Test Data:

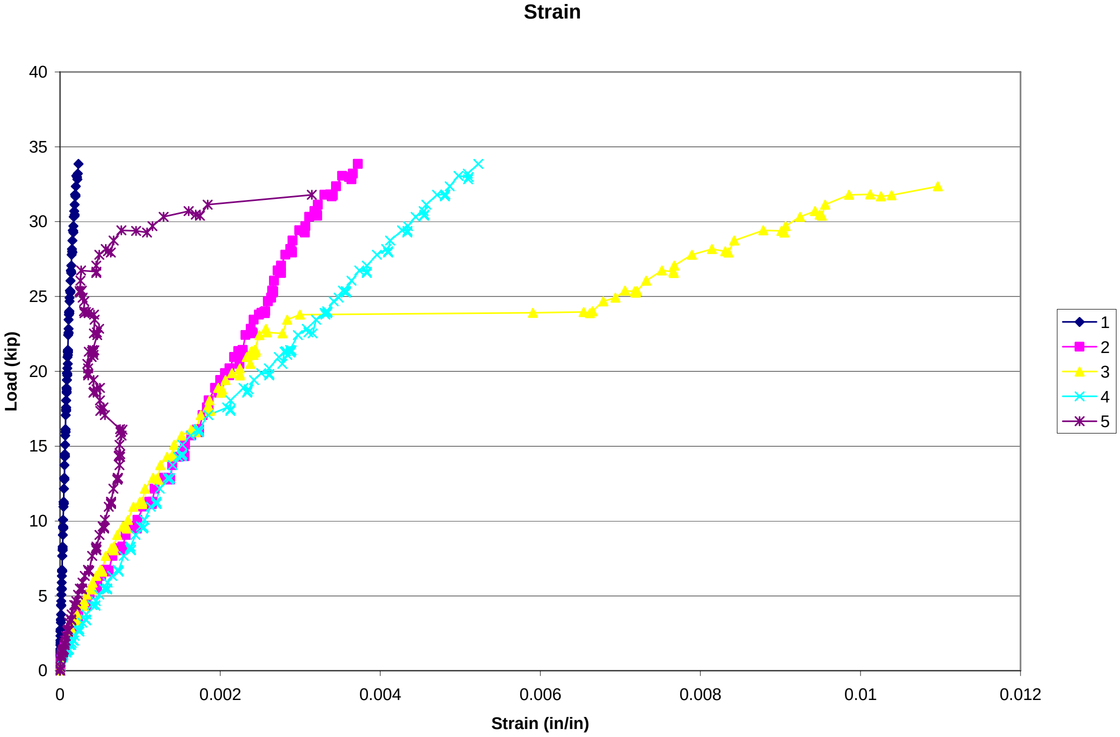

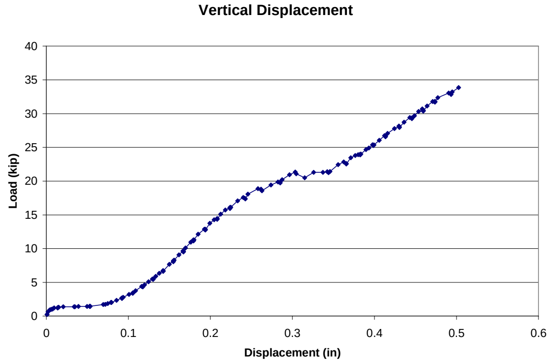

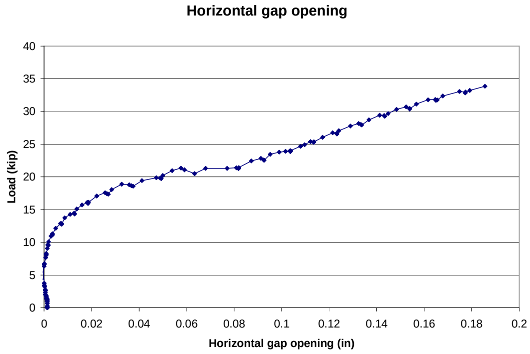

Photographs:

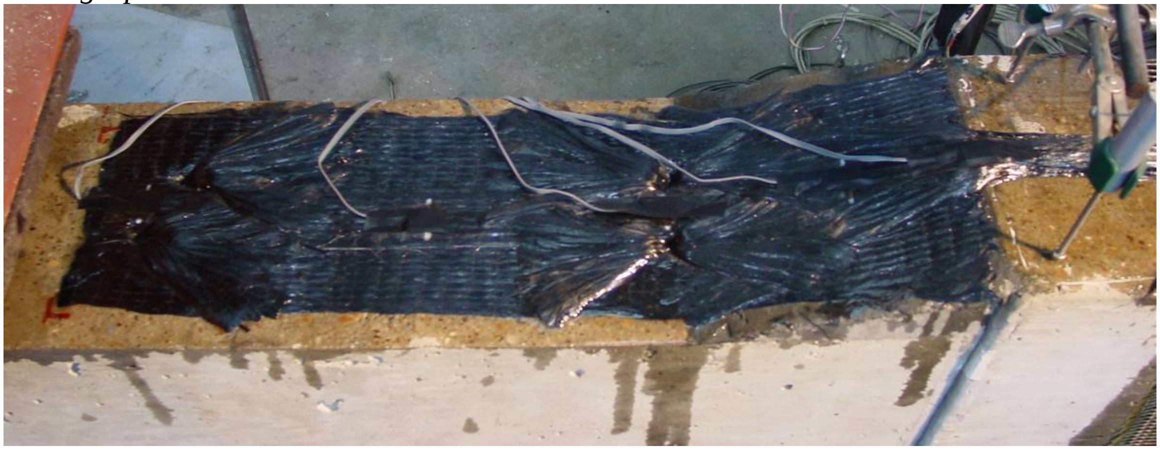

Before Testing

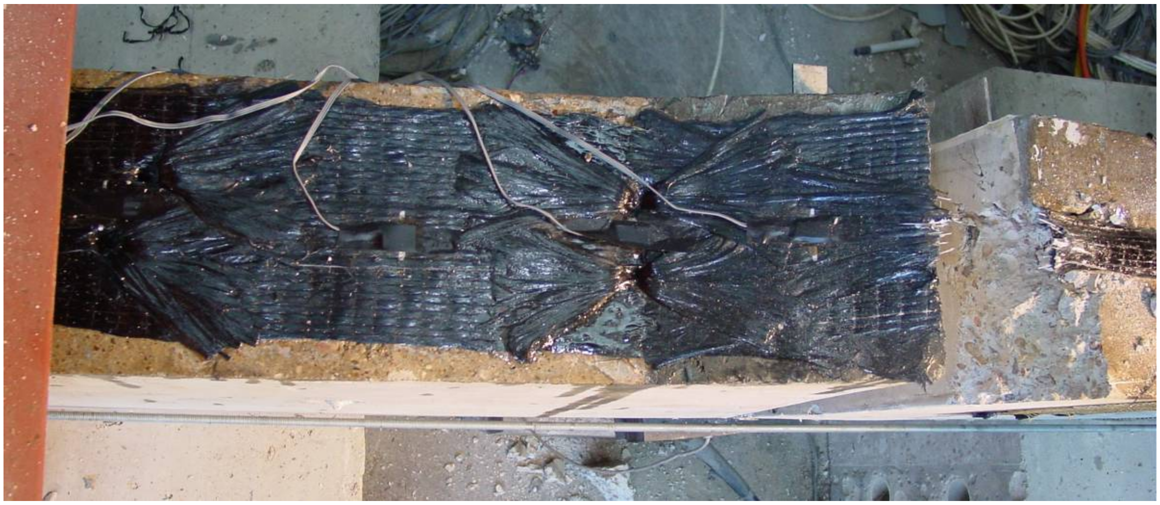

After Testing: Failure by FRP fracture

42-6s6

Test Date: April 10th, 2006
2” height transition
1 to 4 slope
3 anchors at ramp, 3 anchors at 21”, 2 2/3” width sheet, 1/2” diameter concrete hole
Sandblasting surface preparation
SCH-41 fabric

Specimen Design:

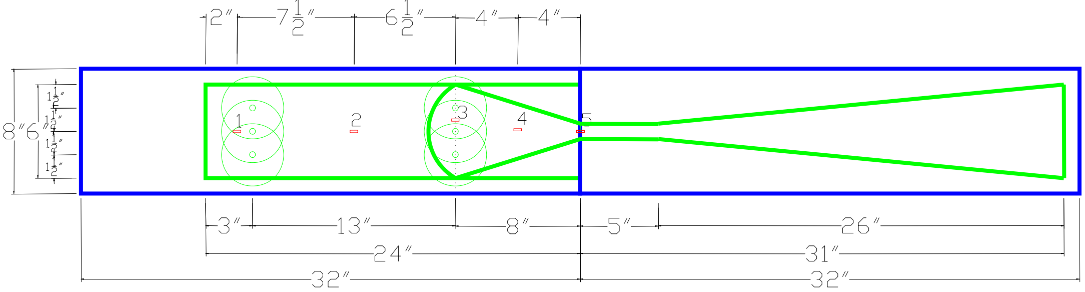
2"
7 1/2"
6 1/2"
4"
4"
8"
6"
1 1/2"
1 1/2"
1 1/2"
1 1/2"
1
2
3
4
5
3"
13"
8"
5"
26"
24"
31"
32"
32"

Test Data:

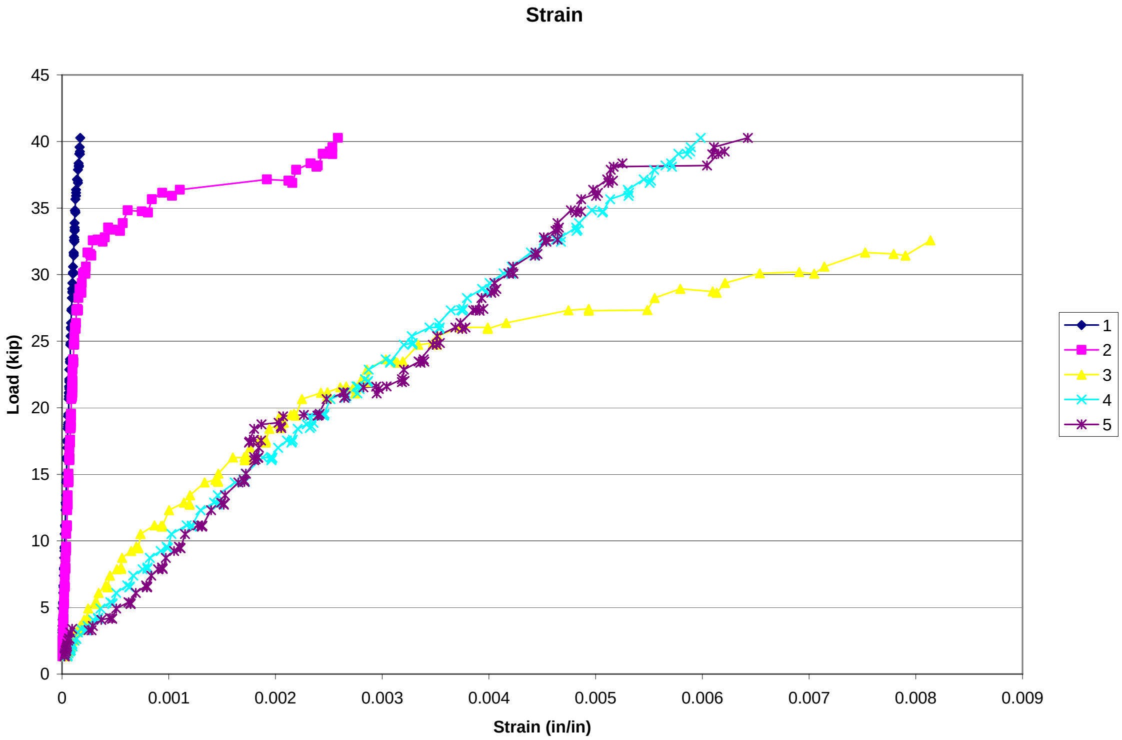

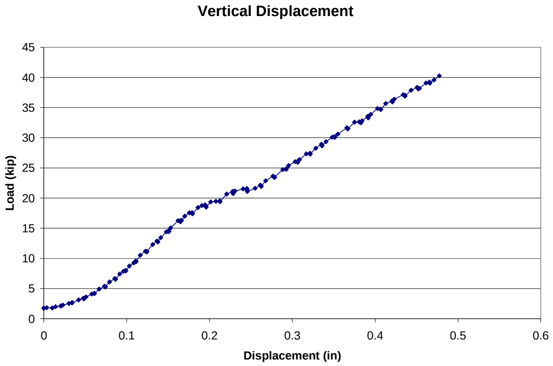
Vertical Displacement

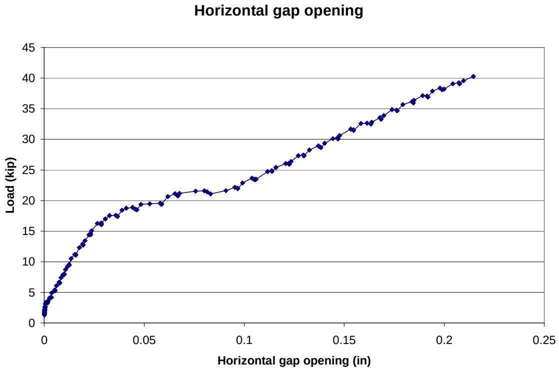
Horizontal gap opening

Photographs:

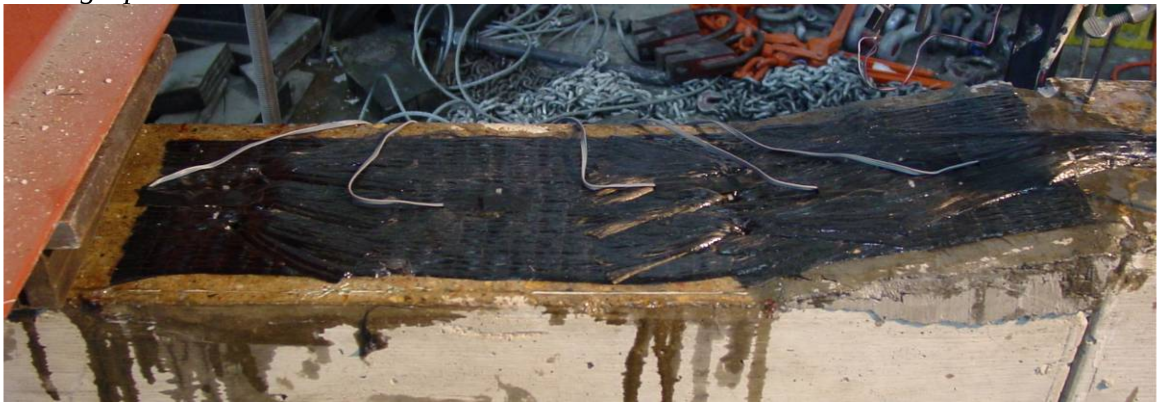
Before Testing

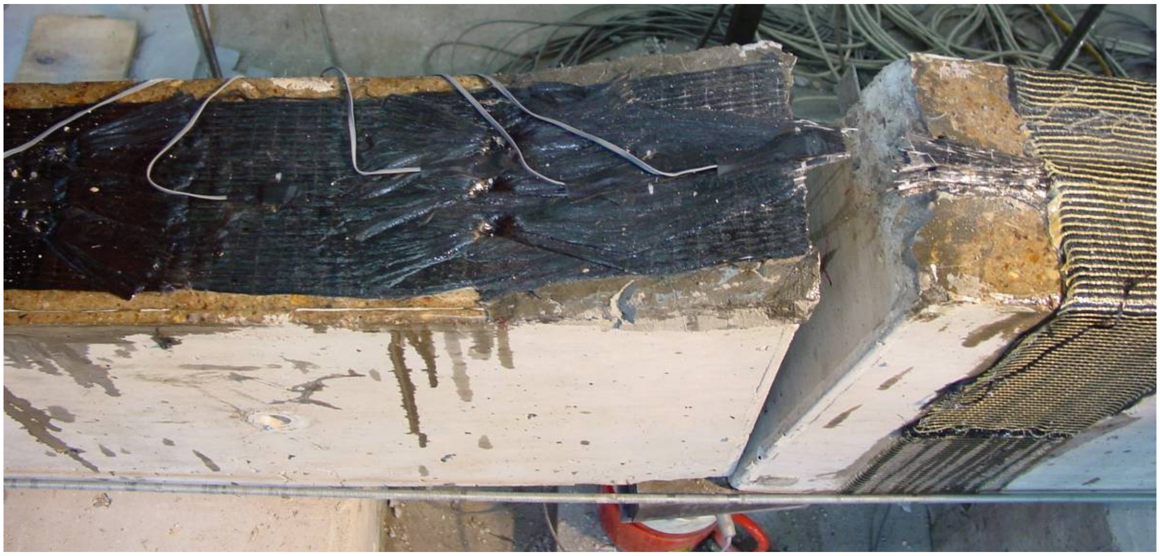
After Testing: Failure by FRP fracture

41-ns1

Test Date: March 28th, 2006
1” height transition
1 to 4 slope
No anchorage
Sandblasting surface preparation
SCH-35 fabric beam sheet, SCH-41 fabric column sheet

Specimen Design:

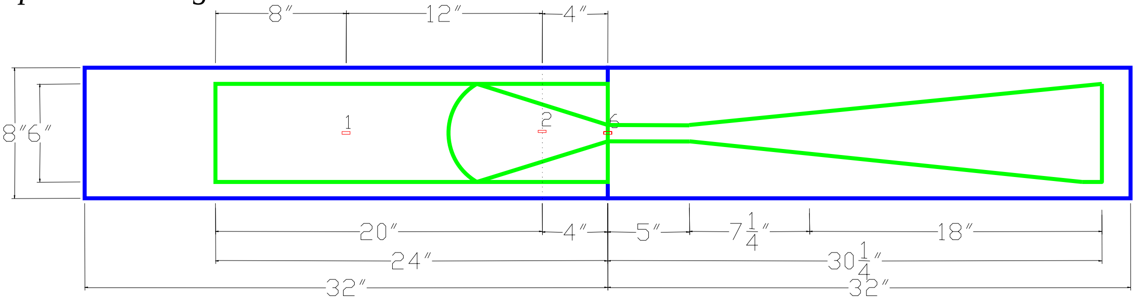

8"
12"
4"
8"
6"
1
2
6
20"
4"
5"
7 1/4"
18"
24"
30 1/4"
32"
32"

Test Data:

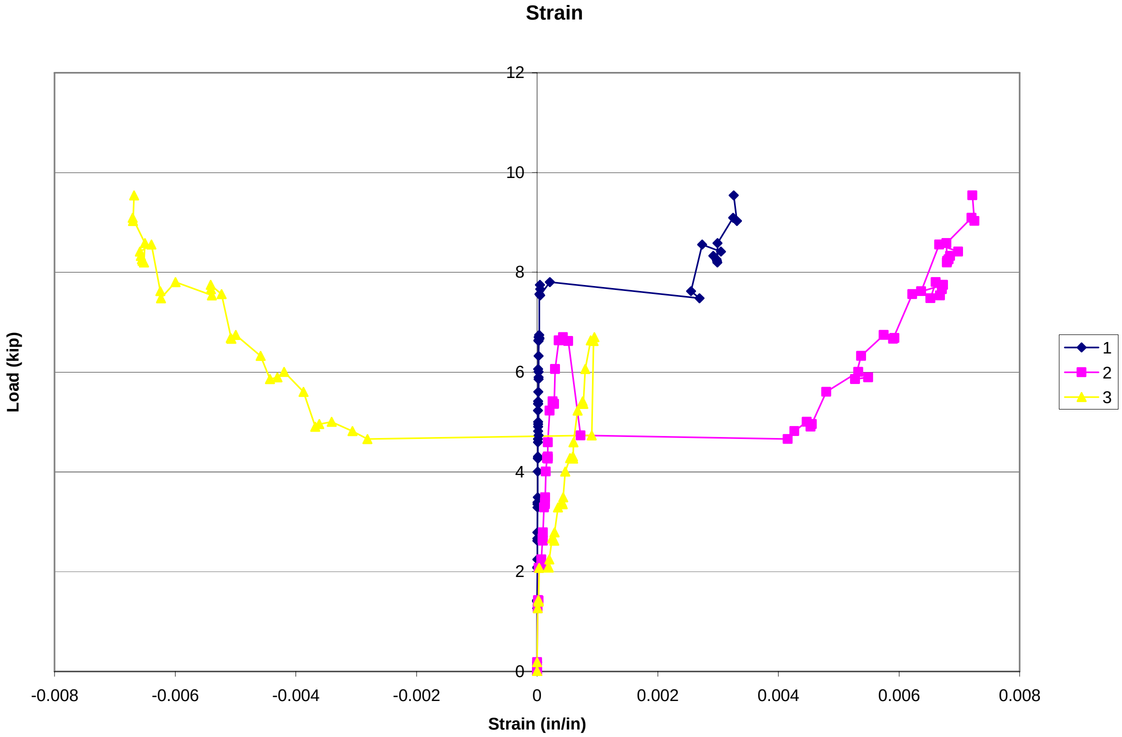

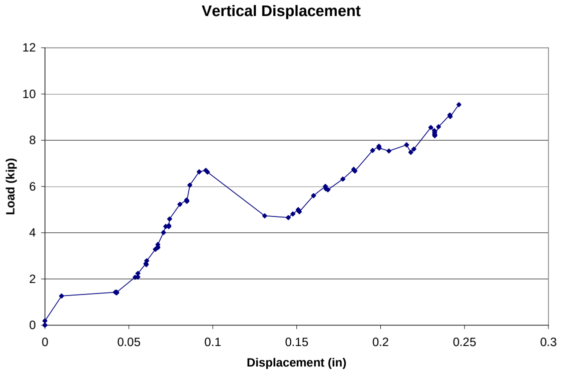
Vertical Displacement

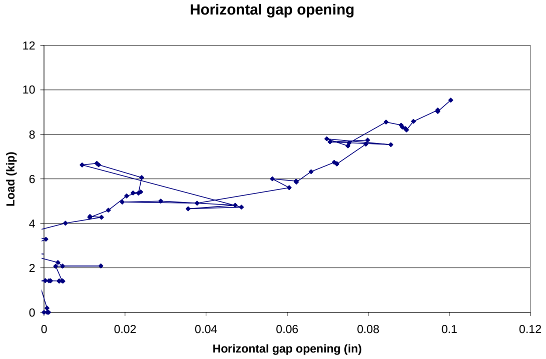
Horizontal gap opening

Photographs:

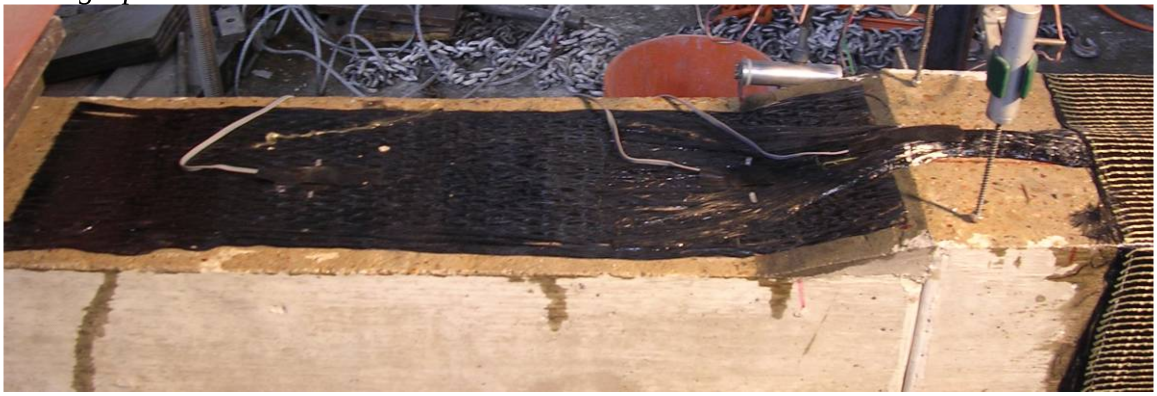

Before Testing

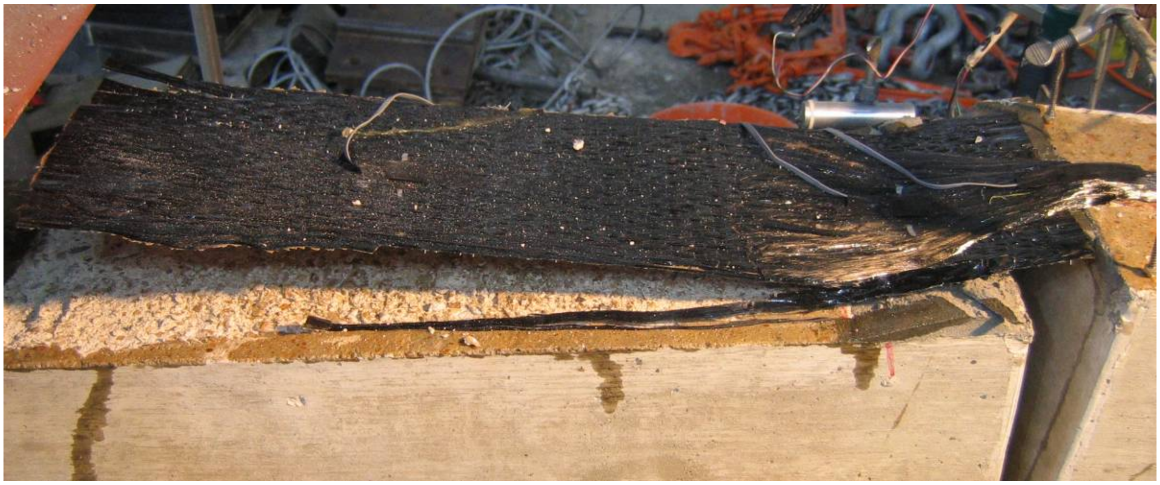

After Testing: Failure by debonding

43-ns1

Test Date: March 28th, 2006
3” height transition
1 to 4 slope
No anchorage
Sandblasting surface preparation
SCH-35 fabric beam sheet, SCH-41 fabric column sheet

Specimen Design:

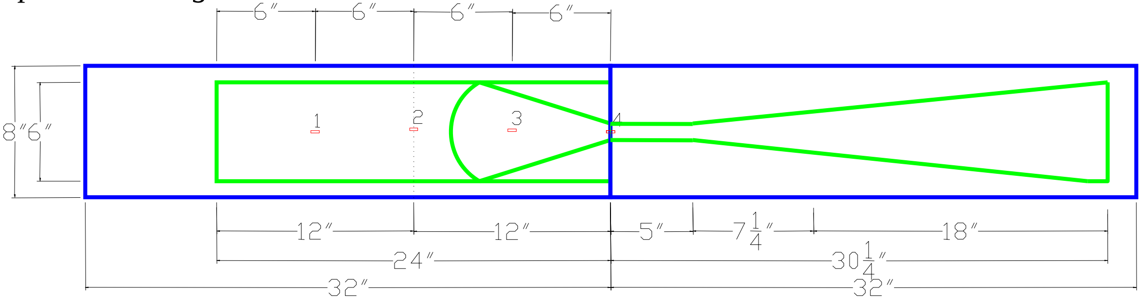

6″
6″
6″
6″
8″
6″
1
2
3
4
12″
12″
5″
7 1/4″
18″
24″
30 1/4″
32″
32″

Test Data:

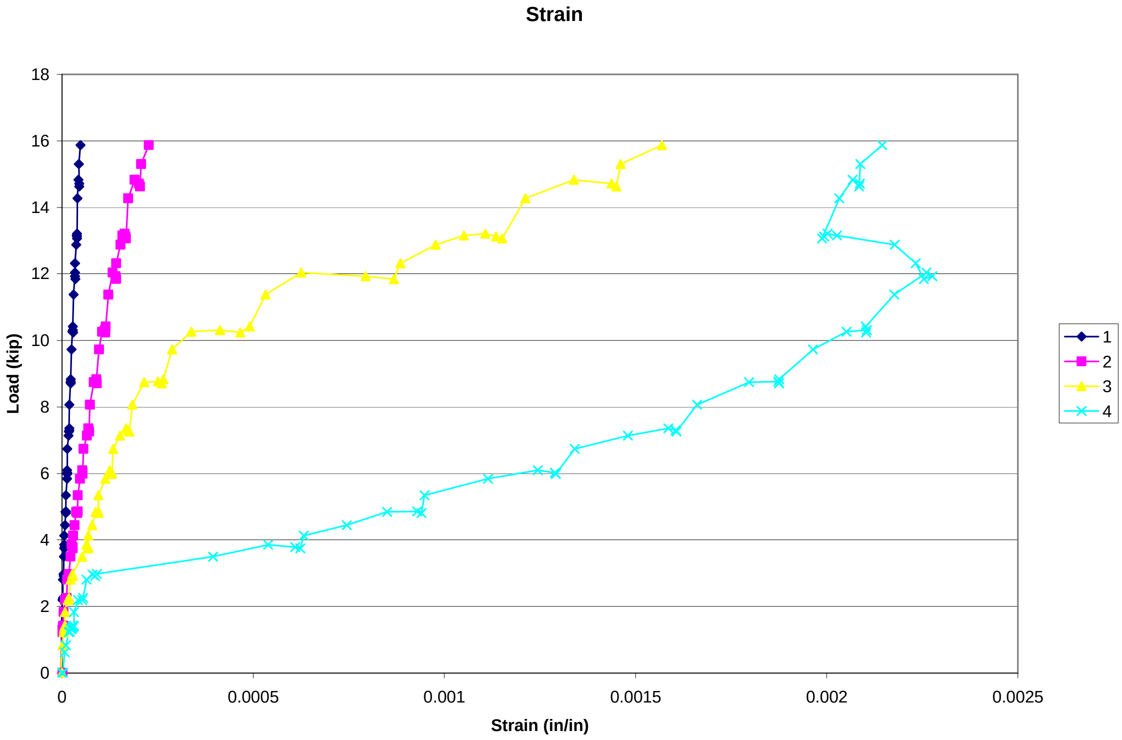

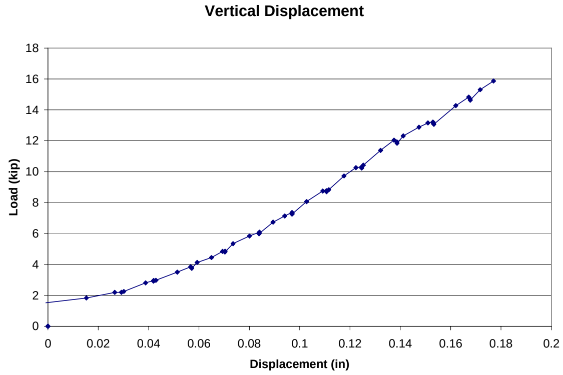

Horizontal gap opening data not available

Photographs:

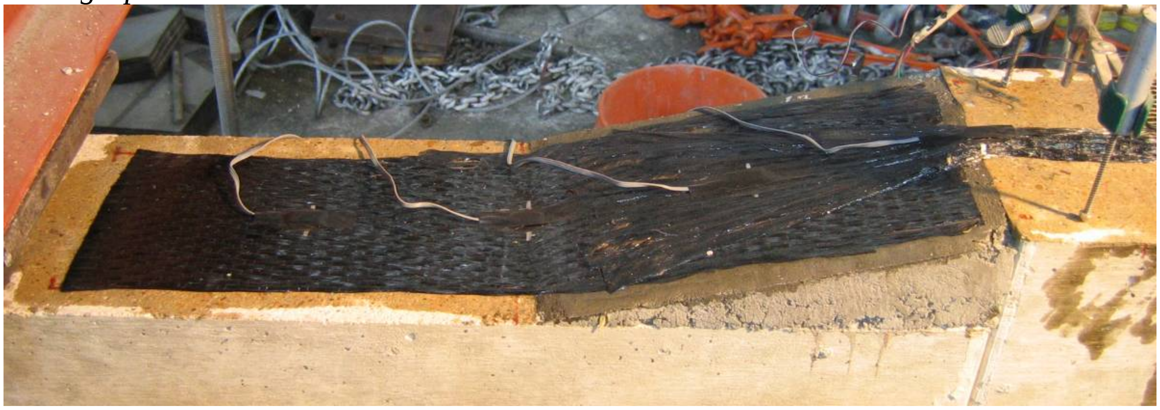

Before Testing

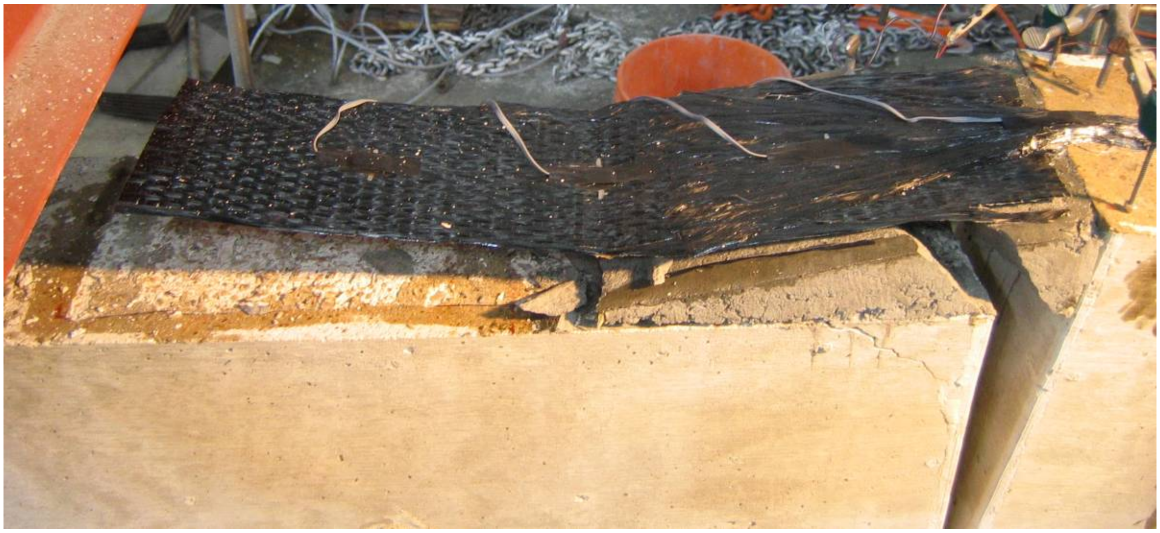

After Testing: Failure by debonding

41-6s1

Test Date: April 10th, 2006
1” height transition
1 to 4 slope
3 anchors at ramp, 3 anchors at 21”, 2 2/3” width sheet, 1/2” diameter concrete hole
Sandblasting surface preparation
SCH-35 fabric beam sheet, SCH-41 fabric anchors and column sheet

Specimen Design:

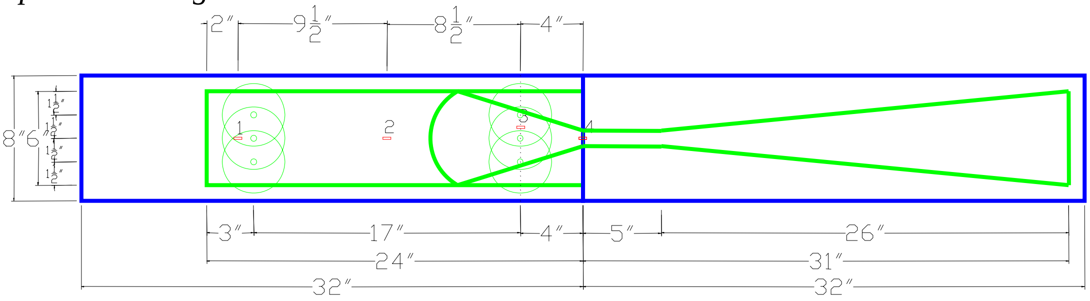
2″
9 1/2″
8 1/2″
4″
8″
6″
1 1/2″
1 1/2″
1 1/2″
1 1/2″
1
2
3
4
3″
17″
4″
5″
26″
24″
31″
32″
32″

Test Data:

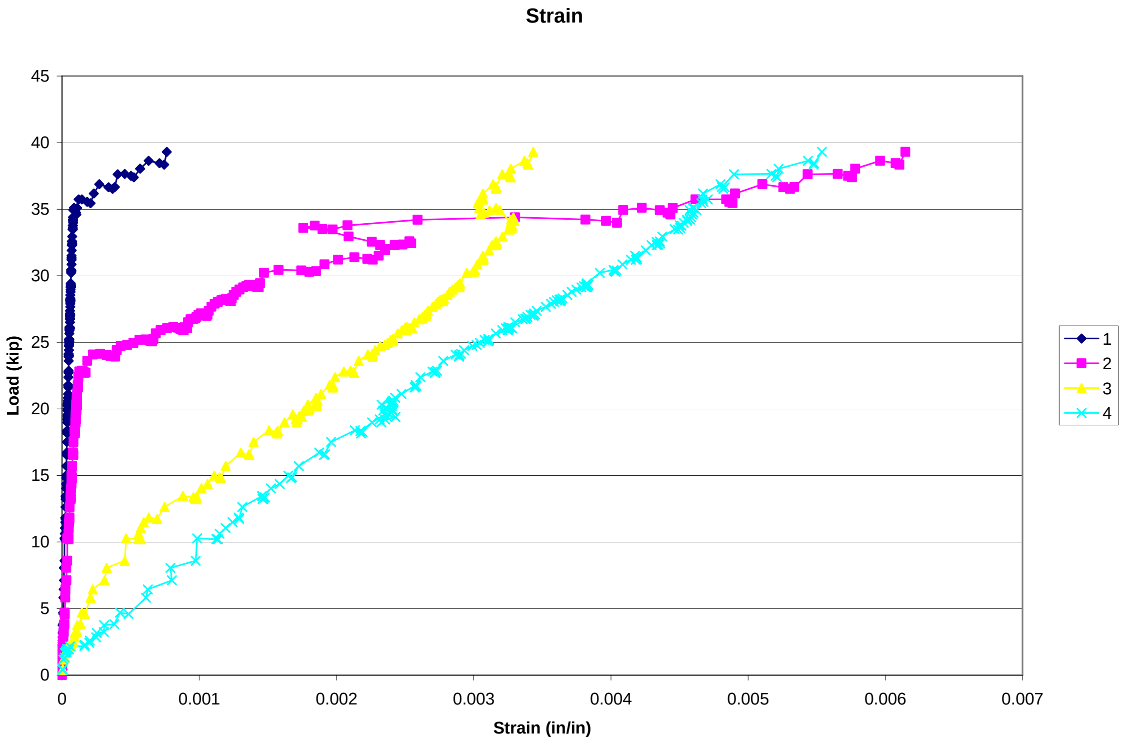

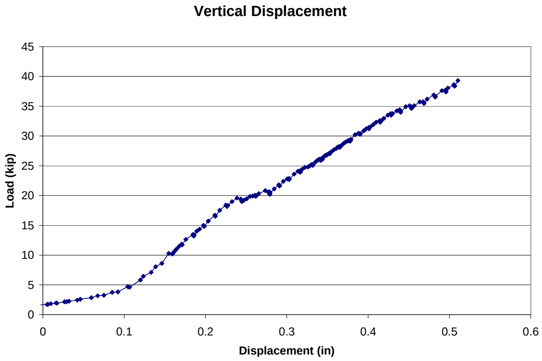
Vertical Displacement

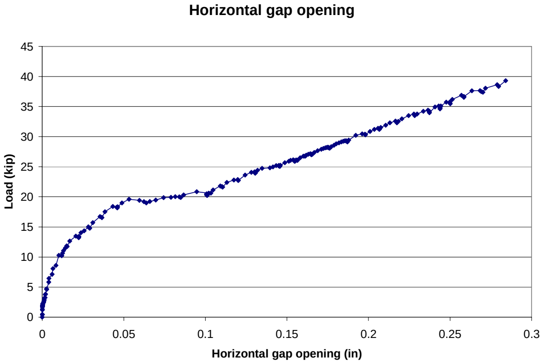
Horizontal gap opening

Photographs:

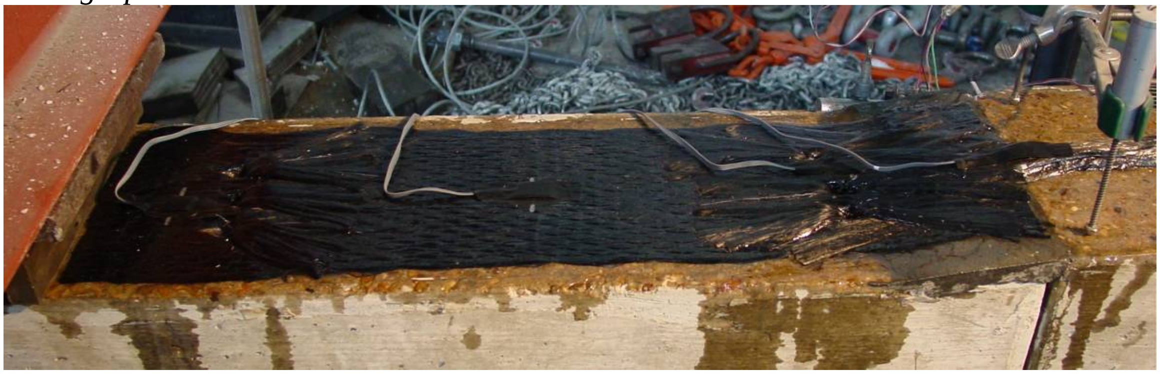

Before Testing

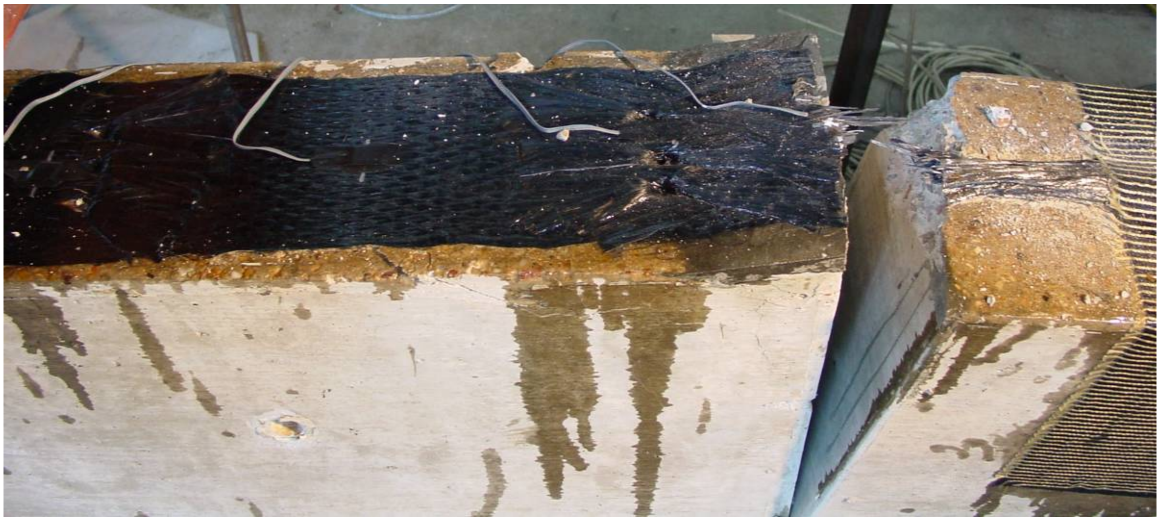

After Testing: Failure by FRP fracture

43-6s1

Test Date: April 10th, 2006
3” height transition
1 to 4 slope
3 anchors at ramp, 3 anchors at 21”, 2 2/3” width sheet, 1/2” diameter concrete hole
Sandblasting surface preparation
SCH-35 fabric beam sheet, SCH-41 fabric anchors and column sheet

Specimen Design:

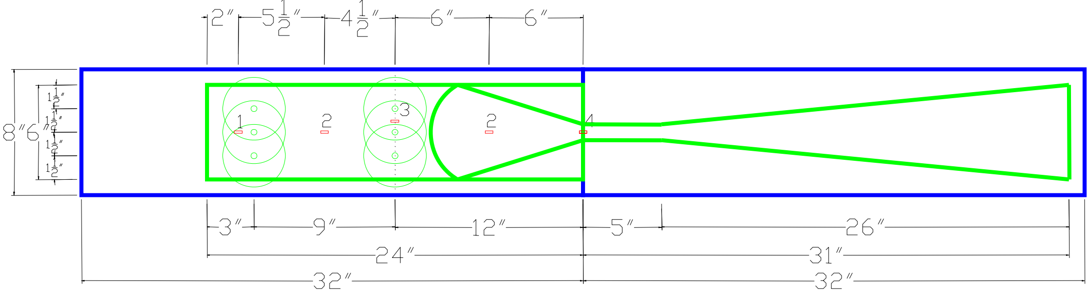
2"
5 1/2"
4 1/2"
6"
6"
8"
6"
1 1/2"
1 1/2"
1 1/2"
1 1/2"
1
2
3
2
4
3"
9"
12"
5"
26"
24"
31"
32"
32"

Test Data:

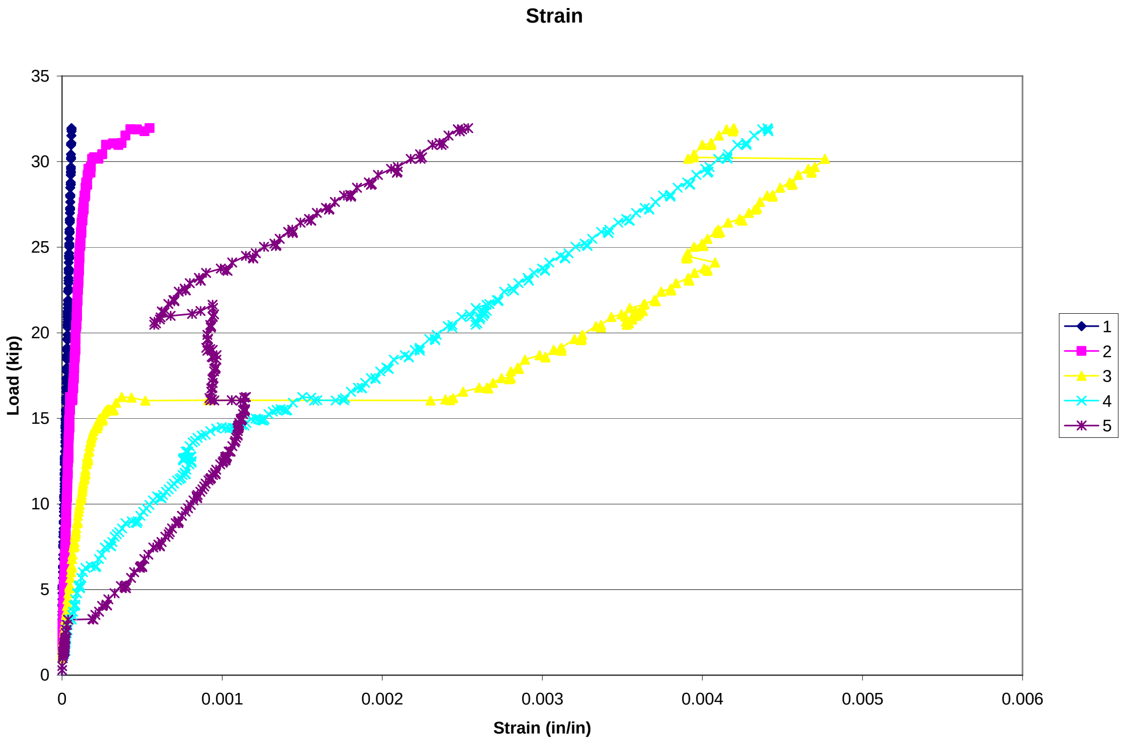

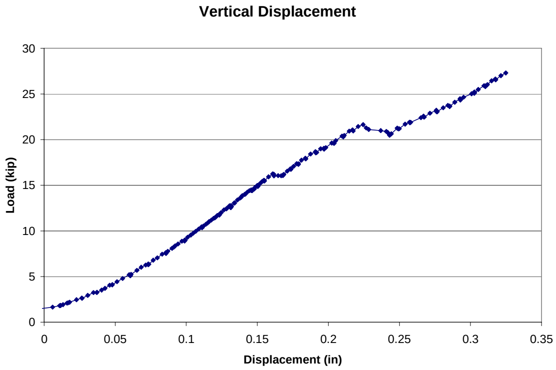

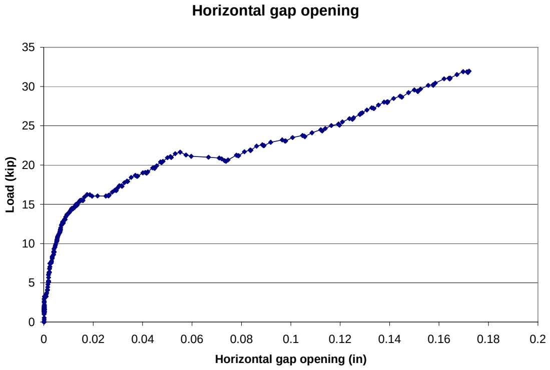

Photographs:

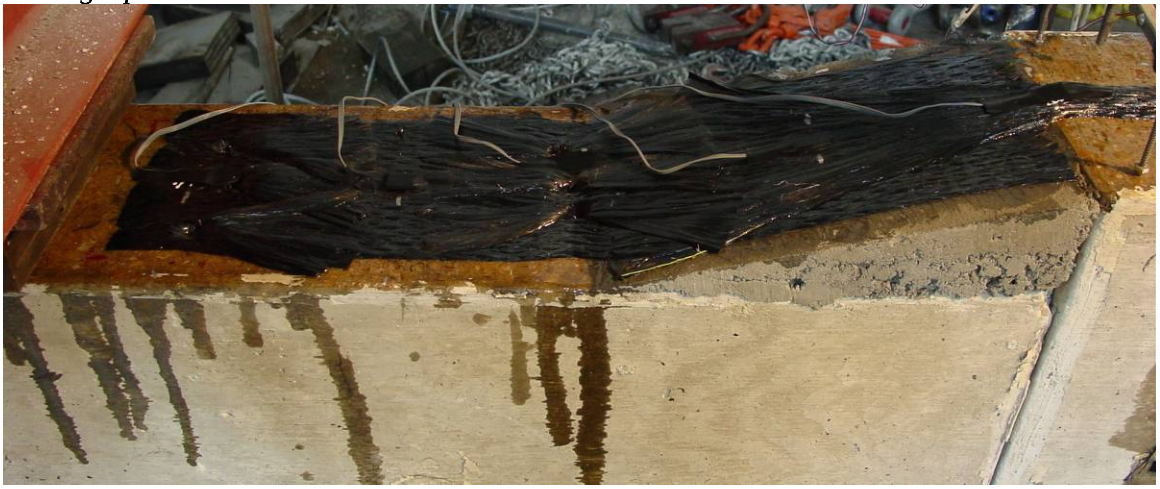

Before Testing

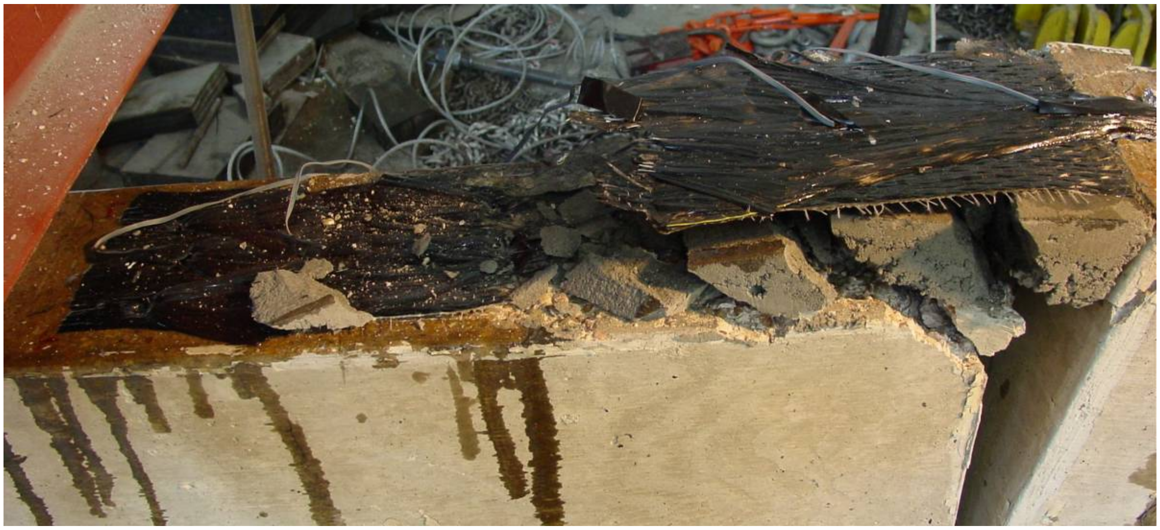

After Testing: Failure by FRP fracture

Appendix B

Design Details

Prototype Beam Design 289
CFRP Retrofit Design 291
    PM-1 Positive moment retrofit 291
    PM-2 Positive Moment Retrofit...294
    NM-1 Negative moment Retrofit..298
    NM-2 Negative Moment Retrofit 302
    FR-1 Flexural Retrofit...303
    CR-1 Continuous Reinforcement (check on rotation capacity).........309

PROTOTYPE BEAM DESIGN

span length (center to center of column) $ls := 24$ feet

Beam size height $h := 24$ inch

width $w := 12$ inch

$$d := h - 1.5 - \frac{3}{8} - \frac{1}{2}$$

Coumn size (square) $col := 18$ inch

Clear span $lc := ls - \frac{col}{12}$

Approximate Loads on Beam

Tibutary length (span length in perp. direction) $lt := 12$ feet

Dead load

beam $beam\_weight := \frac{h}{12} \cdot \frac{w \cdot .150}{12}$ $beam\_weight = 0.3$ kip per ft

slab $slab\_depth := 7$ inches

$slab\_weight := \frac{7}{12} \cdot lt \cdot .150$ $slab\_weight = 1.05$ kip per ft

$Dead\_Load := beam\_weight + slab\_weight$ $Dead\_Load = 1.35$

Live load

100 psf

$Live\_load := 0.1 \cdot lt$ $Live\_load = 1.2$

Load Factors

$fD := 1.4$ $fL := 1.7$

Total Load

$$TL := fD \cdot Dead\_Load + fL \cdot Live\_load$$

$TL = 3.93$ kip per ft

Beam Reinforcement

$fc := 4$ ksi

$fy := 60$ ksi

phi factor $p := .9$

Need negitive moment capacity $Mn := \frac{1}{11} \cdot TL \cdot lc^2$ $Mn = 180.869$ kip-ft

Need positive moment capacity $Mp := \frac{1}{16} TL \cdot lc^2$ $Mp = 124.348$ kip-ft

Based on review of typical 1970's buildings, aim for reinforcement ratio of 0.8%

So use...

Positive moment Steel	Negative moment Steel
2 #7 bars and 1 #6 bar	2 #7 bars and 1 #8 bar
$Asp := 2 \cdot A7 + A6$	$Asn := 2 \cdot A7 + 1 \cdot A8$
$Asp = 1.64$	$Asn = 1.99$
$\frac{Asp}{d \cdot w} = 6.32 \times 10^{-3}$	$\frac{Asn}{d \cdot w} = 7.669 \times 10^{-3}$
$ap := \frac{fy \cdot Asp}{.85 \cdot fc \cdot w}$ $ap = 2.412$	$an := \frac{fy \cdot Asn}{.85 \cdot fc \cdot w}$ $an = 2.926$
$Mpa := p \cdot Asp \cdot fy \cdot \frac{d - \frac{ap}{2}}{12}$	$Mna := p \cdot Asn \cdot fy \cdot \frac{d - \frac{an}{2}}{12}$
$Mpa = 150.693$	$Mna = 180.549$

capacity greater than needed, OK

For Half Scale specimen use...

Positive moment Steel	Negative moment Steel
2 #3 bars and 1 #4 bar	2 #4 bars and 1 #3 bar
Area of steel = 0.42 in^2	Area of steel = 0.51 in^2
Reinforcement ratio	Reinforcement ratio
$\frac{0.42}{6 \cdot 10.8} = 6.481 \times 10^{-3}$	$\frac{0.51}{6 \cdot 10.8} = 7.87 \times 10^{-3}$

CFRP RETROFIT DESIGN

PM-1 Positive moment retrofit

goal: Provide continuity through positive moment reinforcement
Provide sufficient CFRP strength to force hinges to form in reinforcement

Strength of Reinforced concrete section

Positive moment section: Two #3 tens, two #4 comp

$b := 6$ width of section (in)

$h := 12$ height of section (in)

$ds := 12 - .75 - \frac{2}{8} - \frac{4}{16}$ depth to tension steel (in)

$dc := 1 + \frac{5}{8}$ depth to compression steel (in)

$fy := 60$ steel yield strength (ksi)

$fc := 4$ concrete compressive strength (ksi)

$Es := 29000$ steel modulus (ksi)

$A4 := .2$ $A3 := .11$ area of #3 and #4 reinforcement (in^2)

$Ast := 2A3$ $Ast = 0.22$ area of tension steel

$Asc := 2 \cdot A4$ $Asc = 0.4$ area of compression steel

If considered compression steel....

depth to compression steel

guess $c := 2$

Given

$$Ast \cdot fy = Asc \cdot \left[Es \cdot \left(.003 \cdot \frac{c - dc}{c}\right) - .85 \cdot fc\right] + .85 \cdot .85 \cdot c \cdot fc \cdot b$$

$c := \mathrm{Find}(c)$ $c = 1.314$

$$Mc := .85 \cdot .85 \cdot c \cdot fc \cdot b \cdot \left(ds - .85 \cdot \frac{c}{2}\right) + Asc \cdot Es \cdot \left(.003 \cdot \frac{c - dc}{c}\right) \cdot (ds - dc)$$

$Mc = 157.163$ kip − in

Considering over strength of 1.25, design for capacity of

$Mc \cdot 1.25 = 196.454$

If reach moment capacity of 200 kip-in at end of CFRP retrofit (25 in from column center)
Need moment capacity of 260 kip-in at column line
Total load applied = 5 kips per loading point

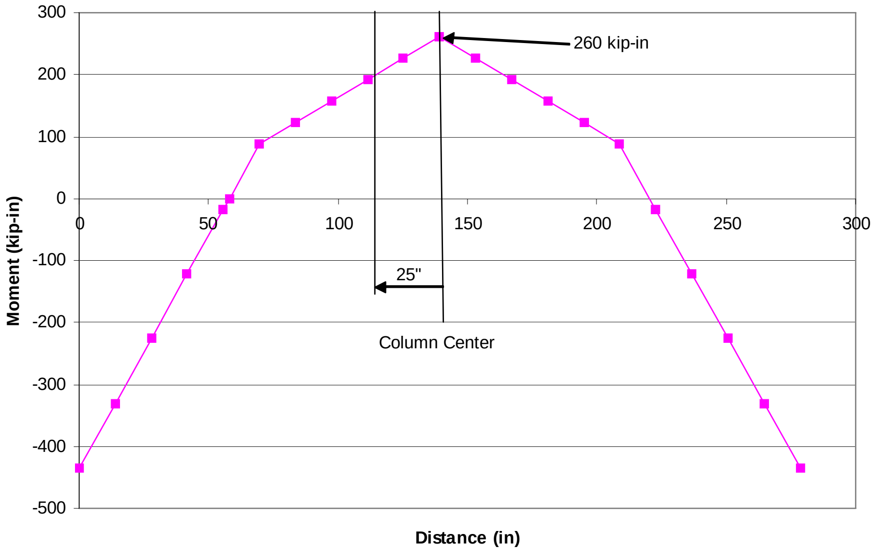

CFRP section moment capacity

CFRP for a moment capacity of 260 kip-in

$Afrp := 6 \cdot .04$ Area of CFRP (width * thickness)

$Afrp = 0.24$ (in^2)

$Efrp := 11.4 \cdot 10^3$ CFRP modulus (ksi)

$df := 12$ depth to CFRP (in)

$Ast := 0$ area of tension steel (in^2)

$Asc := 2 \cdot A4 + A3$ area of compression steel (in^2)

guess $c := 1$

Given

$$ef(c) := \left| \begin{array}{l} .003 \cdot \dfrac{df - c}{c} \ \text{ if } \left(.003 \cdot \dfrac{df - c}{c}\right) < .01 \\ .01 \ \text{ otherwise} \end{array} \right.$$ strain in CFRP

$$es(c) := \left| \begin{array}{l} .003 \cdot \dfrac{ds - c}{c} \ \text{ if } \left(.003 \cdot \dfrac{ds - c}{c}\right) < .00207 \\ .00207 \ \text{ otherwise} \end{array} \right.$$ strain in steel

$$\mathrm{Afrp}\cdot(\mathrm{ef}(c))\cdot\mathrm{Efrp} + \mathrm{Ast}\cdot\mathrm{es}(c)\cdot\mathrm{Es} = .85\cdot .85\cdot c\cdot\mathrm{fc}\cdot b + \mathrm{Asc}\cdot\left[\mathrm{Es}\cdot\left(.003\cdot\frac{c-\mathrm{dc}}{c}\right) - .85\cdot\mathrm{fc}\right]$$

$$\mathrm{caclc}(\mathrm{Afrp},c) := \mathrm{Find}(c)$$

$$c := \mathrm{caclc}(\mathrm{Afrp},c)$$

moment capacity

$$M_{cfrp} := (\mathrm{Ast})\cdot(\mathrm{es}(c))\cdot 29000\left(\mathrm{ds} - .85\cdot\frac{c}{2}\right) + \mathrm{Afrp}\cdot(\mathrm{ef}(c))\cdot\mathrm{Efrp}\cdot\left(\mathrm{df} - .85\cdot\frac{c}{2}\right)$$

$M_{cfrp} = 309.184$ kip-in > 260 kip-in

Check ultimate tensile capacity of 2 #3 bars $2\cdot A3\cdot 100 = 22$ kip

ultimate tensile capacity of CFRP $\mathrm{Afrp}\cdot 143 = 34.32$ kip

34 > 22 OK

Need CFRP width of 6"

For extra safety in actual design increase CFRP width to 7"

For column sheet increase with by 33%, use 9.3 in width

For anchors increase width by 33%, use 9.3 in width in each row

Based on size of beam maximum of 2 anchors in each row, or 4.6" width per anchor

Development length of #3 rebar

$$\mathrm{dvel} := \frac{\frac{3}{8}\cdot\mathrm{fy}\cdot 1000}{25\cdot\sqrt{\mathrm{fc}\cdot 1000}} \qquad \mathrm{dvel} = 14.23 \quad \mathrm{in}$$

ACI 12.2.2

Extend CFRP retrofit at least 14" beyond end of #3 rebars

PM-2 Positive Moment Retrofit

goal: Provide continuity through positive moment reinforcement
Provide sufficient CFRP strength to force hinges to form in reinforcement

Strength of Reinforced concrete section

Positive moment section: Two #3, one #4 tension

$b := 6$ width of section (in)

$h := 12$ height of section (in)

$ds := 12 - .75 - \frac{2}{8} - \frac{4}{16}$ depth to tension steel (in)

$dc := 1 + \frac{5}{8}$ depth to compression steel (in)

$fy := 60$ steel yield strength (ksi)

$fc := 4$ concrete compressive strength (ksi)

$Es := 29000$ steel modulus (ksi)

$A4 := .2$ $A3 := .11$ area of #3 and #4 reinforcement (in^2)

$Ast := 2A3 + A4$ $Ast = 0.42$ area of tension steel

$Asc := 0$ $Asc = 0$ area of compression steel

If considered compression steel....

depth to compression steel

guess $c := 2$

Given

$$Ast \cdot fy = Asc \cdot \left[Es \cdot \left(.003 \cdot \frac{c - dc}{c}\right) - .85 \cdot fc\right] + .85 \cdot .85 \cdot c \cdot fc \cdot b$$

$c := \text{Find}(c)$ $c = 1.453$

$$Mc := .85 \cdot .85 \cdot c \cdot fc \cdot b \cdot \left(ds - .85 \cdot \frac{c}{2}\right) + Asc \cdot Es \cdot \left(.003 \cdot \frac{c - dc}{c}\right) \cdot (ds - dc)$$

$Mc = 255.335$ kip − in

Considering over strength of 1.25, design for capacity of

$Mc \cdot 1.25 = 319.169$

If reach moment capacity of 320 kip-in at end of CFRP retrofit (4' 8" in from column center)
Need moment capacity of 510 kip-in at column line
(analysis includes hinging that limits moment to 430 kip-in and ends of beam)
Total Load applied = 6.8 kips per loading point

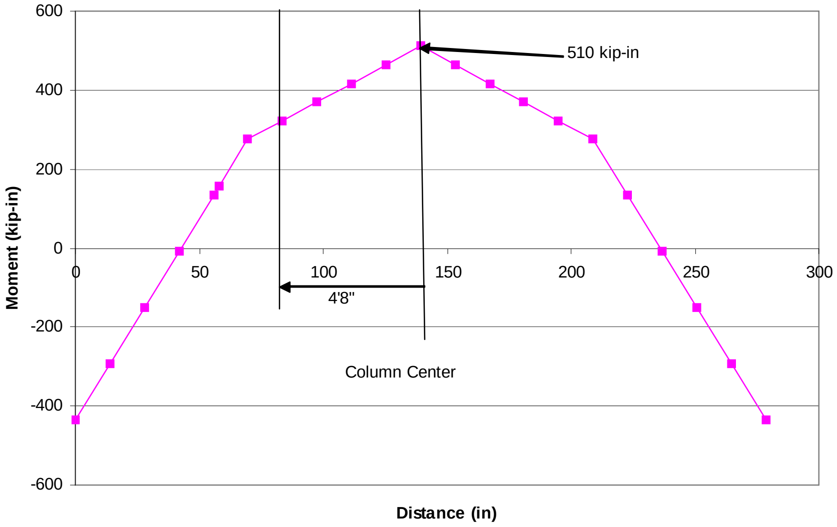

CFRP section moment capacity

CFRP for a moment capacity of 510 kip-in

$\mathrm{Afrp} := 11 \cdot .04$ Area of CFRP (width * thickness)

$\mathrm{Afrp} = 0.44$ (in^2)

$\mathrm{Efrp} := 11.4 \cdot 10^3$ CFRP modulus (ksi)

$\mathrm{df} := 12$ depth to CFRP (in)

$\mathrm{Ast} := 0$ area of tension steel (in^2)

$\mathrm{Asc} := 2 \cdot \mathrm{A4} + \mathrm{A3}$ area of compression steel (in^2)

guess $c := 1$

Given

$$\mathrm{ef}(c) := \left| \begin{array}{l} .003 \cdot \dfrac{\mathrm{df} - c}{c} \ \text{ if } \left(.003 \cdot \dfrac{\mathrm{df} - c}{c} \right) < .01 \\ .01 \ \text{ otherwise} \end{array} \right.$$

strain in CFRP

$$\mathrm{es}(c) := \left| \begin{array}{l} .003 \cdot \dfrac{\mathrm{ds} - c}{c} \ \text{ if } \left(.003 \cdot \dfrac{\mathrm{ds} - c}{c} \right) < .00207 \\ .00207 \ \text{ otherwise} \end{array} \right.$$

strain in steel

$$\mathrm{Afrp}\cdot(\mathrm{ef}(c))\cdot\mathrm{Efrp} + \mathrm{Ast}\cdot\mathrm{es}(c)\cdot\mathrm{Es} = .85\cdot.85\cdot c\cdot\mathrm{fc}\cdot b + \mathrm{Asc}\cdot\left[\mathrm{Es}\cdot\left(.003\cdot\frac{c-\mathrm{dc}}{c}\right) - .85\cdot\mathrm{fc}\right]$$

$\mathrm{caclc}(\mathrm{Afrp}, c) := \mathrm{Find}(c)$

$c := \mathrm{caclc}(\mathrm{Afrp}, c)$

moment capacity

$$M_{cfrp} := (\mathrm{Ast})\cdot(\mathrm{es}(c))\cdot 29000\left(\mathrm{ds} - .85\cdot\frac{c}{2}\right) + \mathrm{Afrp}\cdot(\mathrm{ef}(c))\cdot\mathrm{Efrp}\cdot\left(\mathrm{df} - .85\cdot\frac{c}{2}\right)$$

$M_{cfrp} = 553.579$ kip-in > 510 kip-in

Check ultimate tensile capacity of 2 #3 + 1 #4bars $(2\cdot A3 + A4)\cdot 100 = 42$ kip

ultimate tensile capacity of CFRP $\mathrm{Afrp}\cdot 143 = 62.92$ kip

62 > 42 OK

Need CFRP width of 11"

For extra safety in actual design increase CFRP width to 12"

For column sheet increase with by 33%, use 16 in width

For anchors increase width by 33%, use 16 in width in each row

Based on size of beam maximum of 2 anchors in each row, or 8" width per anchor

Development length of #4 rebar

$$\mathrm{dvel} := \frac{\frac{4}{8}\cdot\mathrm{fy}\cdot 1000}{25\cdot\sqrt{\mathrm{fc}\cdot 1000}} \qquad \mathrm{dvel} = 18.974 \text{ in}$$

ACI 12.2.2

Extend CFRP retrofit at least 19" beyond end of #4 rebar

Check rotation capacity of hinge at end of CFRP

Calculation of Ultimate Rotation Based on Mattock and Corley

Inputs

$\mathrm{Ast} := 2A3 + A4$ $\mathrm{Ast} = 0.42$ area of tension steel

$\mathrm{Asc} := 0$ $\mathrm{Asc} = 0$ area of compression steel

$ht := 10.5$ height enclosed by stirrup

$bt := 4.5$ width enclosed by stirrup

$At := .11$ Area of stirrup

$st := 5$ spacing of stirrup

$ds := 12 - .75 - \frac{3}{8} - \frac{4}{16}$ depth to tension steel (in)

$dc := .75 + \frac{3}{8} + \frac{2}{8}$ depth to compression steel (in)

$L := 136$ Length of beam (in)

$fs := 100$ ultimate tension in steel (ksi)

$Es := 31000$ Modulus of steel (ksi)

$z := 86 - 58$ distance from critical section to inflection point

$pp := \frac{At\cdot(2\cdot ht + 2\cdot bt)}{st\cdot(b\cdot ds)} + \frac{Asc}{b\cdot ds}$ $pp = 0.01$

hinge length for 2 sided

$lp := 2\cdot(.5\cdot ds + 0.05\cdot z)$ $lp = 13.425$

$ecult := 0.003 + 0.02\cdot\frac{b}{z} + \left(pp\cdot\frac{fy}{20}\right)^2$ $ecult = 8.25\times 10^{-3}$

$c := 2$ depth to neutral axis

Given

$Ast\cdot fs = ecult\cdot\left(\frac{c - dc}{c}\right)\cdot Es\cdot Asc + 0.85\cdot fc\cdot b\cdot 0.85\cdot c$

$c := \text{Find}(c)$

$c = 2.422$

$\phi ult := \frac{ecult}{c}$ $\phi ult = 3.406\times 10^{-3}$

$\phi y := .0004$

$\Theta p := (\phi ult - \phi y)\cdot lp$

$\Theta p = 0.040$

Deflection

$\Theta p\cdot 88 = 3.552$ in

Deflection < than height of beam, may not survive till catenary

NM-1 Negative moment Retrofit

goal: Provide continuity through negative moment reinforcement
Provide sufficient CFRP tensile strength to fracture 2 #4 and 1 #3 rebar

Strength of Reinforced concrete section

Negative moment section: Two #4, one #3 tension, Two #3, one #4 compression

$b := 6$ width of section (in)

$h := 12$ height of section (in)

$ds := 12 - .75 - \frac{3}{8} - \frac{4}{16}$ depth to tension steel (in)

$dc := .75 + \frac{3}{8} + \frac{2}{8}$ depth to compression steel (in)

$fy := 60$ steel yield strength (ksi)

$fc := 4$ concrete compressive strength (ksi)

$Es := 29000$ steel modulus (ksi)

$A4 := .2$ $A3 := .11$ area of #3 and #4 reinforcement (in^2)

$Ast := 2A4 + A3$ $Ast = 0.51$ area of tension steel

$Asc := 2 \cdot A3 + A4$ $Asc = 0.42$ area of compression steel

If considered compression steel....

depth to compression steel

guess $c := 2$

Given

$$Ast \cdot fy = Asc \cdot \left[Es \cdot \left(.003 \cdot \frac{c - dc}{c}\right) - .85 \cdot fc\right] + .85 \cdot .85 \cdot c \cdot fc \cdot b$$

$c := \text{Find}(c)$ $c = 1.577$

$$Mc := .85 \cdot .85 \cdot c \cdot fc \cdot b \cdot \left(ds - .85 \cdot \frac{c}{2}\right) + Asc \cdot Es \cdot \left(.003 \cdot \frac{c - dc}{c}\right) \cdot (ds - dc)$$

$Mc = 315.531$ $kip - in$

Considering over strength of 1.25, design for capacity of

$Mc \cdot 1.25 = 394.414$

If reach moment capacity of 400 kip-in at support (limit moment capacity at column line to 80 kip-in)
Need moment capacity of 270 kip-in at beginning of CFRP retrofit (25" from support)
Load when hinge forms at support = 3.5 kip

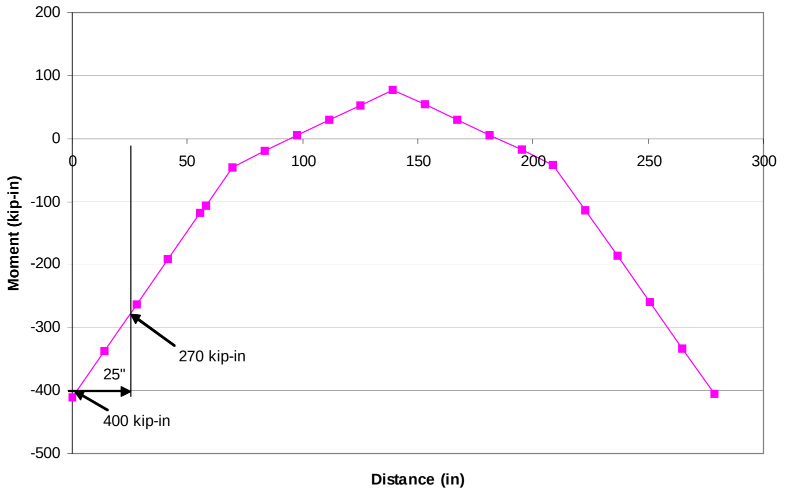

CFRP section moment capacity

CFRP for a moment capacity of 270 kip-in

$\mathrm{Afrp} := 6 \cdot .04$ Area of CFRP (width * thickness)

$\mathrm{Afrp} = 0.24$ (in^2)

$\mathrm{Efrp} := 11.4 \cdot 10^3$ CFRP modulus (ksi)

$\mathrm{df} := 12$ depth to CFRP (in)

$\mathrm{Ast} := 0$ area of tension steel (in^2)

$\mathrm{Asc} := 2 \cdot \mathrm{A3} + \mathrm{A4}$ area of compression steel (in^2)

guess $c := 1$

Given

$$\mathrm{ef}(c) := \begin{cases} .003 \cdot \dfrac{\mathrm{df} - c}{c} & \text{if } \left(.003 \cdot \dfrac{\mathrm{df} - c}{c}\right) < .01 \\ .01 & \text{otherwise} \end{cases}$$

strain in CFRP

$$\mathrm{es}(c) := \begin{cases} .003 \cdot \dfrac{\mathrm{ds} - c}{c} & \text{if } \left(.003 \cdot \dfrac{\mathrm{ds} - c}{c}\right) < .00207 \\ .00207 & \text{otherwise} \end{cases}$$

strain in steel

$$\text{Afrp}\cdot(\text{ef}(c))\cdot\text{Efrp} + \text{Ast}\cdot\text{es}(c)\cdot\text{Es} = .85\cdot.85\cdot c\cdot\text{fc}\cdot b + \text{Asc}\cdot\left[\text{Es}\cdot\left(.003\cdot\frac{c-\text{dc}}{c}\right) - .85\cdot\text{fc}\right]$$

$\text{caclc}(\text{Afrp}, c) := \text{Find}(c)$

$c := \text{caclc}(\text{Afrp}, c)$

moment capacity

$$M_{cfrp} := (\text{Ast})\cdot(\text{es}(c))\cdot 29000\left(\text{ds} - .85\cdot\frac{c}{2}\right) + \text{Afrp}\cdot(\text{ef}(c))\cdot\text{Efrp}\cdot\left(\text{df} - .85\cdot\frac{c}{2}\right)$$

$M_{cfrp} = 310.956$ kip-in > 270 kip-in

Check ultimate tensile capacity of 2 #4 bars $(2\cdot A4 + A3)\cdot 100 = 51$ kip

ultimate tensile capacity of CFRP $\text{Afrp}\cdot 143 = 34.32$ kip

increase area of CFRP to 10 in $\text{Afrp} := 10\cdot.04$

$\text{Afrp}\cdot 143 = 57.2$

57 > 51 OK

Check rotation capacity of hinge at support

Calculation of Ultimate Rotation Based on Mattock and Corley

Inputs

$\text{Ast} := 2A4 + A3$ $\text{Ast} = 0.51$ area of tension steel

$\text{Asc} := 2\cdot A3 + A4$ $\text{Asc} = 0.42$ area of compression steel

$\text{ht} := 10.5$ height enclosed by stirrup

$\text{bt} := 4.5$ width enclosed by stirrup

$\text{At} := .11$ Area of stirrup

$\text{st} := 3$ spacing of stirrup

$\text{ds} := 12 - .75 - \frac{3}{8} - \frac{4}{16}$ depth to tension steel (in)

$\text{dc} := .75 + \frac{3}{8} + \frac{2}{8}$ depth to compression steel (in)

$L := 136$ Length of beam (in)

$\text{fs} := 100$ ultimate tension in steel (ksi)

$\text{Es} := 31000$ Modulus of steel (ksi)

$z := 115$ distance from critical section to inflection point

$pp := \frac{At \cdot (2 \cdot ht + 2 \cdot bt)}{st \cdot (b \cdot ds)} + \frac{Asc}{b \cdot ds}$ $pp = 0.024$

hinge length for 2 sided

$lp := 2 \cdot (.5 \cdot ds + 0.05 \cdot z)$ $lp = 22.125$

$ecult := 0.003 + 0.02 \cdot \frac{b}{z} + \left(pp \cdot \frac{fy}{20}\right)^2$ $ecult = 9.16 \times 10^{-3}$

$c := 2$ depth to neutral axis

Given

$$Ast \cdot fs = ecult \cdot \left(\frac{c - dc}{c}\right) \cdot Es \cdot Asc + 0.85 \cdot fc \cdot b \cdot 0.85 \cdot c$$

$c := \text{Find}(c)$

$c = 1.683$

$\phi ult := \frac{ecult}{c}$ $\phi ult = 5.443 \times 10^{-3}$

$\phi y := .0003602$

$\Theta p := (\phi ult - \phi y) \cdot lp$

$\Theta p = 0.112$

Deflection

$\Theta p \cdot L = 15.294$ in

Deflection > than height of beam, may survive till catenary

Need CFRP width of 10"

For anchors increase width by 33%, use 14 in width in each row

Based on size of beam maximum of 2 anchors in each row, or 7" width per anchor

Development length of #4 rebar

$dvel := \frac{\frac{4}{8} \cdot fy \cdot 1000}{25 \cdot \sqrt{fc \cdot 1000}}$ $dvel = 18.974$ in

ACI 12.2.2

Extend CFRP retrofit at least 19" beyond end of #4 rebar

NM-2 Negative Moment Retrofit

goal: Provide continuity through negative moment reinforcement
Provide sufficient CFRP tensile strength to yield 2 #4 bars
And carry expected catenary tension load of 32 kips
And force hinge at support

Same design parameters as NM-1

Need 6" width of CFRP to force hinge at support
Expectect moment 270 kip-in, Availble moment with 6" CFRP 310 kip-in
(see NM-1 calculations)

$\mathrm{Afrp} := 6 \cdot .04$

To yield 2 #4 bars $\quad 2 \cdot \mathrm{A4} \cdot \mathrm{fy} = 24$

$\mathrm{Afrp} \cdot 143 = 34.32$

34 kip tension capacity in CFRP > yield 2 #4 bars, 24 kip
> catenary tension 32 kip

Need CFRP width of 6"

For anchors increase width by 33%, use 8 in width in each row

Based on size of beam maximum of 2 anchors in each row, or 4" width per anchor

same locations as NM-1

FR-1 Flexural Retrofit

goal: Provide flexural strengthening to reach 10 kip per loading point without catenary

Divide beam into sections and design CFRP for each section based on elastic bending moment diagram at 10 kips of load per loading point

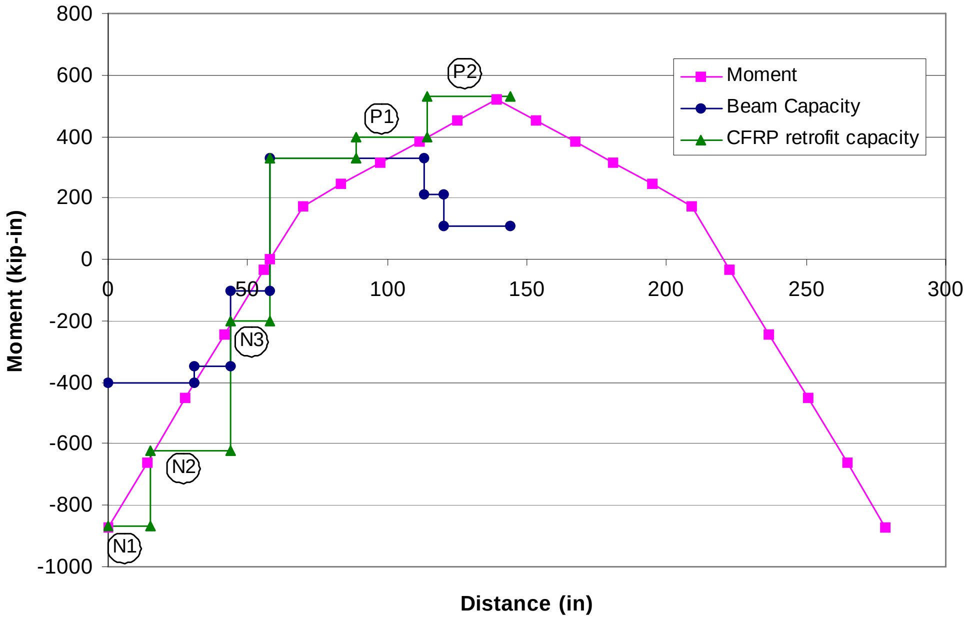

N1 = 0 to 15" from support	need 870 kip-in neg. moment capacity
N2 = 15 to 44" from support	need 620 kip-in neg. moment capacity
N3 = 44 to 58" from support	need 200 kip-in neg. moment capacity
P1 = 89 to 114" from support	need 400 kip-in pos. moment capacity
P2 = 114 to 144" from support	need 530 kip-in pos. moment capacity

CFRP section moment capacity N1

CFRP for a moment capacity of 870 kip-in

$\mathrm{Afrp} := 20 \cdot .04$ Area of CFRP (width * thickness)

$\mathrm{Afrp} = 0.8$ (in^2)

$\mathrm{Efrp} := 11.4 \cdot 10^3$ CFRP modulus (ksi)

$\mathrm{df} := 12$ depth to CFRP (in)

$\mathrm{Ast} := 2 \cdot \mathrm{A4} + \mathrm{A3}$ area of tension steel (in^2)

$\mathrm{Asc} := 2 \cdot \mathrm{A3} + \mathrm{A4}$ area of compression steel (in^2)

guess $c := 1$

Given

$$\mathrm{ef}(c) := \begin{cases} .003 \cdot \dfrac{\mathrm{df} - c}{c} & \text{if } \left(.003 \cdot \dfrac{\mathrm{df} - c}{c}\right) < .01 \\ .01 & \text{otherwise} \end{cases}$$

strain in CFRP

$$\mathrm{es}(c) := \begin{cases} .003 \cdot \dfrac{\mathrm{ds} - c}{c} & \text{if } \left(.003 \cdot \dfrac{\mathrm{ds} - c}{c}\right) < .00207 \\ .00207 & \text{otherwise} \end{cases}$$

strain in steel

$$\mathrm{Afrp} \cdot (\mathrm{ef}(c)) \cdot \mathrm{Efrp} + \mathrm{Ast} \cdot \mathrm{es}(c) \cdot \mathrm{Es} = .85 \cdot .85 \cdot c \cdot \mathrm{fc} \cdot b + \mathrm{Asc} \cdot \left[\mathrm{Es} \cdot \left(.003 \cdot \frac{c - \mathrm{dc}}{c}\right) - .85 \cdot \mathrm{fc}\right]$$

$\mathrm{caclc}(\mathrm{Afrp}, c) := \mathrm{Find}(c)$

$c := \mathrm{caclc}(\mathrm{Afrp}, c)$

moment capacity

$$M_{\mathrm{cfrp}} := (\mathrm{Ast}) \cdot (\mathrm{es}(c)) \cdot 29000 \left(\mathrm{ds} - .85 \cdot \frac{c}{2}\right) + \mathrm{Afrp} \cdot (\mathrm{ef}(c)) \cdot \mathrm{Efrp} \cdot \left(\mathrm{df} - .85 \cdot \frac{c}{2}\right)$$

$M_{\mathrm{cfrp}} = 874.179$ kip-in > 870 kip-in

Need CFRP width of 20" for N1

Use Four layers of 5" width

For anchors increase width by 33%, use 27 in width in each row

Based on size of beam maximum of 2 anchors in each row, divide each row into 2 6.5" width per anchor

CFRP section moment capacity N2

CFRP for a moment capacity of 620 kip-in

$Afrp := 8 \cdot .04$ Area of CFRP (width * thickness)

$Afrp = 0.32$ (in^2)

$Efrp := 11.4 \cdot 10^3$ CFRP modulus (ksi)

$df := 12$ depth to CFRP (in)

$Ast := 2 \cdot A4$ area of tension steel (in^2)

$Asc := 2 \cdot A3 + A4$ area of compression steel (in^2)

guess $c := 1$

Given

$$ef(c) := \begin{cases} .003 \cdot \dfrac{df - c}{c} & \text{if } \left(.003 \cdot \dfrac{df - c}{c}\right) < .01 \\ .01 & \text{otherwise} \end{cases}$$

strain in CFRP

$$es(c) := \begin{cases} .003 \cdot \dfrac{ds - c}{c} & \text{if } \left(.003 \cdot \dfrac{ds - c}{c}\right) < .00207 \\ .00207 & \text{otherwise} \end{cases}$$

strain in steel

$$Afrp \cdot (ef(c)) \cdot Efrp + Ast \cdot es(c) \cdot Es = .85 \cdot .85 \cdot c \cdot fc \cdot b + Asc \cdot \left[Es \cdot \left(.003 \cdot \frac{c - dc}{c}\right) - .85 \cdot fc\right]$$

$caclc(Afrp, c) := Find(c)$

$c := caclc(Afrp, c)$

moment capacity

$$M_{cfrp} := (Ast) \cdot (es(c)) \cdot 29000 \left(ds - .85 \cdot \frac{c}{2}\right) + Afrp \cdot (ef(c)) \cdot Efrp \cdot \left(df - .85 \cdot \frac{c}{2}\right)$$

$M_{cfrp} = 625.954$ kip-in > 620 kip-in

Need CFRP width of 8" for N2

For ease of layers continuing from N1 use 10" width, 2 layers of 5" width

For anchors increase width by 33%, use 13.5 in width in each row

Based on size of beam maximum of 2 anchors in each row, 6.75" width per anchor

CFRP section moment capacity N3

CFRP for a moment capacity of 200 kip-in

$\mathrm{Afrp} := 4 \cdot .04$ Area of CFRP (width * thickness)

$\mathrm{Afrp} = 0.16$ (in^2)

$\mathrm{Efrp} := 11.4 \cdot 10^3$ CFRP modulus (ksi)

$\mathrm{df} := 12$ depth to CFRP (in)

$\mathrm{Ast} := 0$ area of tension steel (in^2)

$\mathrm{Asc} := 2 \cdot \mathrm{A3} + \mathrm{A4}$ area of compression steel (in^2)

guess $c := 1$

Given

$$\mathrm{ef}(c) := \begin{cases} .003 \cdot \dfrac{\mathrm{df} - c}{c} & \text{if } \left(.003 \cdot \dfrac{\mathrm{df} - c}{c} \right) < .01 \\ .01 & \text{otherwise} \end{cases}$$

strain in CFRP

$$\mathrm{es}(c) := \begin{cases} .003 \cdot \dfrac{\mathrm{ds} - c}{c} & \text{if } \left(.003 \cdot \dfrac{\mathrm{ds} - c}{c} \right) < .00207 \\ .00207 & \text{otherwise} \end{cases}$$

strain in steel

$$\mathrm{Afrp} \cdot (\mathrm{ef}(c)) \cdot \mathrm{Efrp} + \mathrm{Ast} \cdot \mathrm{es}(c) \cdot \mathrm{Es} = .85 \cdot .85 \cdot c \cdot \mathrm{fc} \cdot b + \mathrm{Asc} \cdot \left[\mathrm{Es} \cdot \left(.003 \cdot \frac{c - \mathrm{dc}}{c} \right) - .85 \cdot \mathrm{fc} \right]$$

$\mathrm{caclc}(\mathrm{Afrp}, c) := \mathrm{Find}(c)$

$c := \mathrm{caclc}(\mathrm{Afrp}, c)$

moment capacity

$$M_{cfrp} := (\mathrm{Ast}) \cdot (\mathrm{es}(c)) \cdot 29000 \left(\mathrm{ds} - .85 \cdot \frac{c}{2} \right) + \mathrm{Afrp} \cdot (\mathrm{ef}(c)) \cdot \mathrm{Efrp} \cdot \left(\mathrm{df} - .85 \cdot \frac{c}{2} \right)$$

$M_{cfrp} = 208.9$ kip-in > 200 kip-in

Need CFRP width of 4" for N3

For ease of layers continuing from N1 and N2 use 5" width

For anchors increase width by 33%, use 7 in width in each row

Based on size of beam maximum of 2 anchors in each row, 3.5" width per anchor

CFRP section moment capacity P1

CFRP for a moment capacity of 400 kip-in

$Afrp := 6 \cdot .04$ Area of CFRP (width * thickness)

$Afrp = 0.24$ (in^2)

$Efrp := 11.4 \cdot 10^3$ CFRP modulus (ksi)

$df := 12$ depth to CFRP (in)

$Ast := 2 \cdot A3$ area of tension steel (in^2)

$Asc := 0$ area of compression steel (in^2)

guess $c := 1$

Given

$$ef(c) := \left| \begin{array}{l} .003 \cdot \dfrac{df - c}{c} \quad \text{if } \left(.003 \cdot \dfrac{df - c}{c} \right) < .01 \\ .01 \quad \text{otherwise} \end{array} \right.$$

strain in CFRP

$$es(c) := \left| \begin{array}{l} .003 \cdot \dfrac{ds - c}{c} \quad \text{if } \left(.003 \cdot \dfrac{ds - c}{c} \right) < .00207 \\ .00207 \quad \text{otherwise} \end{array} \right.$$

strain in steel

$$Afrp \cdot (ef(c)) \cdot Efrp + Ast \cdot es(c) \cdot Es = .85 \cdot .85 \cdot c \cdot fc \cdot b + Asc \cdot \left[Es \cdot \left(.003 \cdot \frac{c - dc}{c} \right) - .85 \cdot fc \right]$$

$caclc(Afrp, c) := Find(c)$

$c := caclc(Afrp, c)$

moment capacity

$$M_{cfrp} := (Ast) \cdot (es(c)) \cdot 29000 \left(ds - .85 \cdot \frac{c}{2} \right) + Afrp \cdot (ef(c)) \cdot Efrp \cdot \left(df - .85 \cdot \frac{c}{2} \right)$$

$M_{cfrp} = 427.4$ kip-in > 400 kip-in

Need CFRP width of 6" for P1

For ease of layers continuing from P2 use 10" width, two layers of 5" width

For anchors increase width by 33%, use 13.5 in width in each row

Based on size of beam maximum of 2 anchors in each row, 6.75" width per anchor

Last row of anchors use 4" width (don't need strength of 10" sheet so limit anchors)

CFRP section moment capacity P2

CFRP for a moment capacity of 530 kip-in

$\mathrm{Afrp} := 11 \cdot .04$ Area of CFRP (width * thickness)

$\mathrm{Afrp} = 0.44$ (in^2)

$\mathrm{Efrp} := 11.4 \cdot 10^3$ CFRP modulus (ksi)

$\mathrm{df} := 12$ depth to CFRP (in)

$\mathrm{Ast} := 0$ area of tension steel (in^2)

$\mathrm{Asc} := 2 \cdot \mathrm{A4} + \mathrm{A3}$ area of compression steel (in^2)

guess $c := 1$

Given

$$\mathrm{ef}(c) := \begin{cases} .003 \cdot \dfrac{\mathrm{df} - c}{c} & \text{if } \left(.003 \cdot \dfrac{\mathrm{df} - c}{c}\right) < .01 \\ .01 & \text{otherwise} \end{cases}$$

strain in CFRP

$$\mathrm{es}(c) := \begin{cases} .003 \cdot \dfrac{\mathrm{ds} - c}{c} & \text{if } \left(.003 \cdot \dfrac{\mathrm{ds} - c}{c}\right) < .00207 \\ .00207 & \text{otherwise} \end{cases}$$

strain in steel

$$\mathrm{Afrp} \cdot (\mathrm{ef}(c)) \cdot \mathrm{Efrp} + \mathrm{Ast} \cdot \mathrm{es}(c) \cdot \mathrm{Es} = .85 \cdot .85 \cdot c \cdot \mathrm{fc} \cdot b + \mathrm{Asc} \cdot \left[\mathrm{Es} \cdot \left(.003 \cdot \frac{c - \mathrm{dc}}{c}\right) - .85 \cdot \mathrm{fc}\right]$$

$$\mathrm{caclc}(\mathrm{Afrp}, c) := \mathrm{Find}(c)$$

$$c := \mathrm{caclc}(\mathrm{Afrp}, c)$$

moment capacity

$$M_{cfrp} := (\mathrm{Ast}) \cdot (\mathrm{es}(c)) \cdot 29000 \left(\mathrm{ds} - .85 \cdot \frac{c}{2}\right) + \mathrm{Afrp} \cdot (\mathrm{ef}(c)) \cdot \mathrm{Efrp} \cdot \left(\mathrm{df} - .85 \cdot \frac{c}{2}\right)$$

$M_{cfrp} = 557.742$ kip-in > 530 kip-in

Need CFRP width of 11" for P2

To go through column increase by 33% to 18" width

For anchors increase width by 33%, use 13.5 in width in each row

Based on size of beam maximum of 2 anchors in each row, 6.75" width per anchor

CR-1 Continuous Reinforcement (check on rotation capacity)

Calculation of Ultimate Rotation Based on Mattock and Corley

Inputs

$Ast := 2 \cdot A3$ $Ast = 0.22$ area of tension steel

$Asc := 2 \cdot A4 + A3$ $Asc = 0.51$ area of compression steel

$ht := 10.5$ height enclosed by stirrup

$bt := 4.5$ width enclosed by stirrup

$At := .11$ Area of stirrup

$st := 5$ spacing of stirrup

$ds := 12 - .75 - \frac{3}{8} - \frac{4}{16}$ depth to tension steel (in)

$dc := .75 + \frac{3}{8} + \frac{2}{8}$ depth to compression steel (in)

$L := 136$ Length of beam (in)

$fs := 100$ ultimate tension in steel (ksi)

$Es := 31000$ Modulus of steel (ksi)

$z := 81$ distance from critical section to inflection point

$pp := \frac{At \cdot (2 \cdot ht + 2 \cdot bt)}{st \cdot (b \cdot ds)} + \frac{Asc}{b \cdot ds}$ $pp = 0.018$

$lp := 2 \cdot (.5 \cdot ds + 0.05 \cdot z)$ hinge length for 2 sided $lp = 18.725$

$ecult := 0.003 + 0.02 \cdot \frac{b}{z} + \left(pp \cdot \frac{fy}{20}\right)^2$ $ecult = 7.513 \times 10^{-3}$

$c := 2$ depth to neutral axis

Given

$$Ast \cdot fs = ecult \cdot \left(\frac{c - dc}{c}\right) \cdot Es \cdot Asc + 0.85 \cdot fc \cdot b \cdot 0.85 \cdot c$$

$c := \mathrm{Find}(c)$

$c = 1.357$

$\phi ult := \frac{ecult}{c}$ $\phi ult = 5.535\times 10^{-3}$

$\phi y := .0003102$

$\Theta p := (\phi ult - \phi y)\cdot lp$

$\Theta p = 0.098$

required rotation

$\Theta r := \operatorname{atan}\left(\frac{18}{140}\right)$ $\Theta r = 0.128$

Deflection > than height of beam, may survive till catenary

Appendix C

Data From Catenary Tests

NR-1 – No retrofit..312
NR-2 – No retrofit..314
PM-1 Positive Moment Retrofit...317
PM-2 Positive Moment Retrofit...322
NM-1 Negative Moment Retrofit 326
NM-2 Negative Moment Retrofit 331
FR-1 Flexural Retrofit...335
CR-1 Continuous Reinforcement...340
Beam Construction pictures:..344

NR-1 – NO RETROFIT

Test Date: August 14th 2006
Test identified needed changes to test setup:
Compression load cell
Rotational Restraint at center column
Concrete Compressive strength: 1700psi

Beam design:

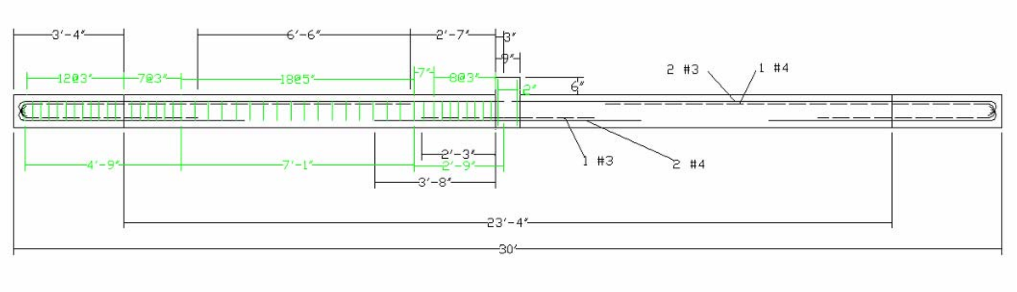
3′-4″
6′-6″
2′-7″
3″
9″
12@3″
7@3″
18@5″
7″
8@3″
2″
6″
2 #3
1 #4
4′-9″
7′-1″
2′-3″
2′-9″
3′-8″
1 #3
2 #4
23′-4″
30′

No CFRP applied

Load vs Displacement:

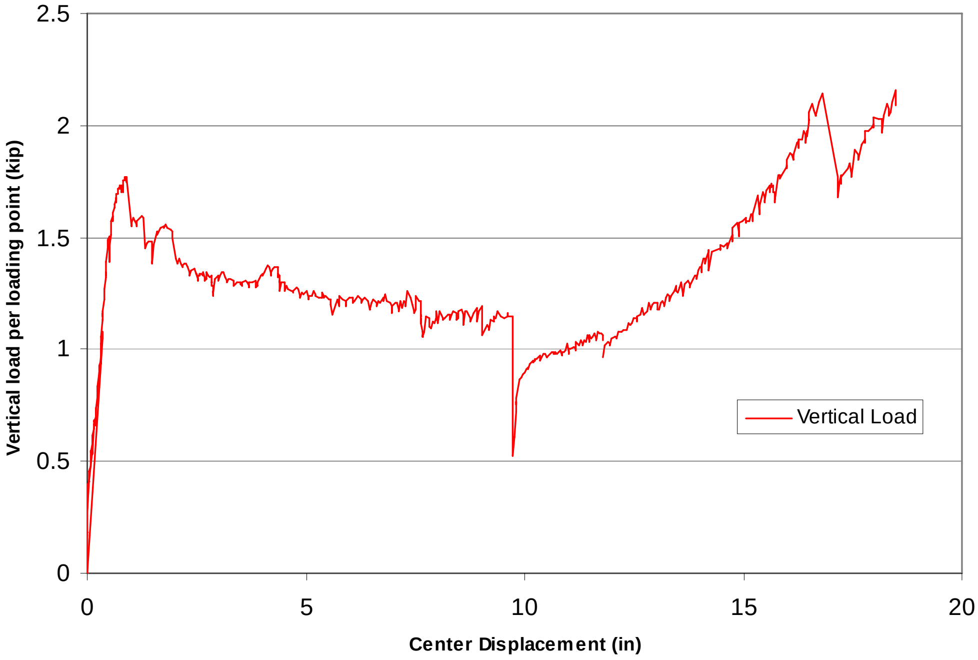

(Axial load data not available)

Pictures:

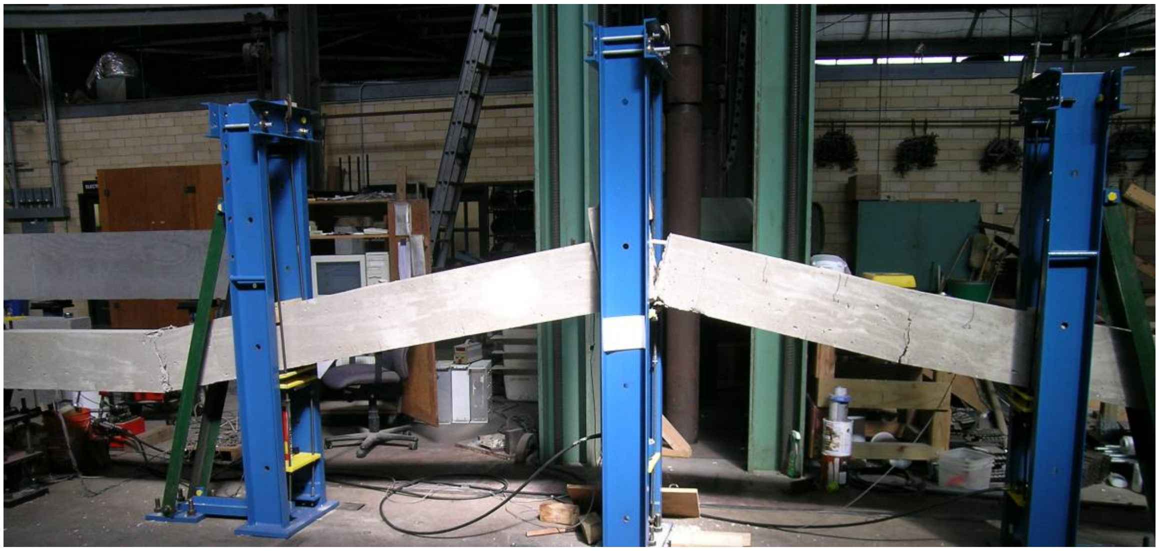

NR-2 – NO RETROFIT

Test Date: August 24th 2006
Concrete Compressive strength: 1700psi

Beam design:

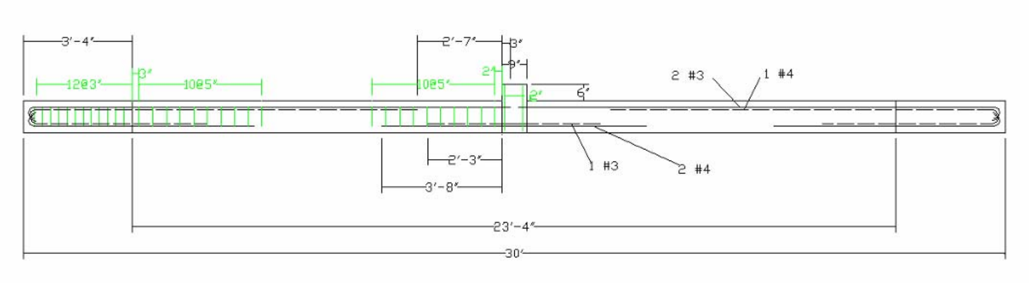
3′-4″
12@3″
3″
10@5″
2′-7″
3″
9″
2″
10@5″
2″
6″
2 #3
1 #4
2′-3″
3′-8″
1 #3
2 #4
23′-4″
30′

Strain gage locations:

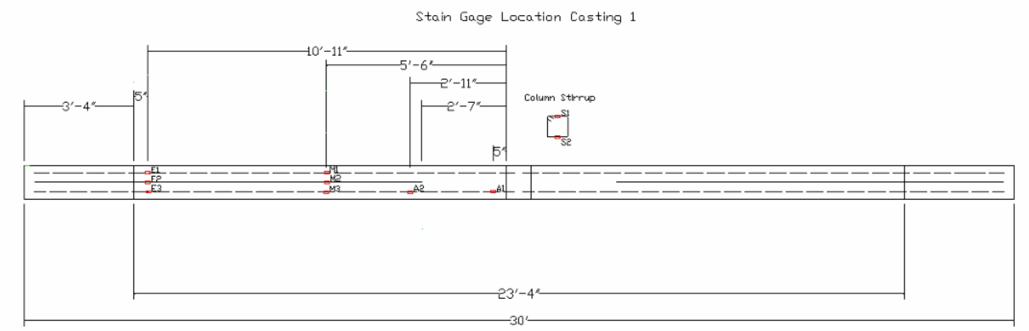
Stain Gage Location Casting 1
10′-11″
5′-6″
2′-11″
2′-7″
3′-4″
5″
Column Stirrup
S1
S2
5″
E1
E2
E3
M1
M2
M3
A2
A1
23′-4″
30′

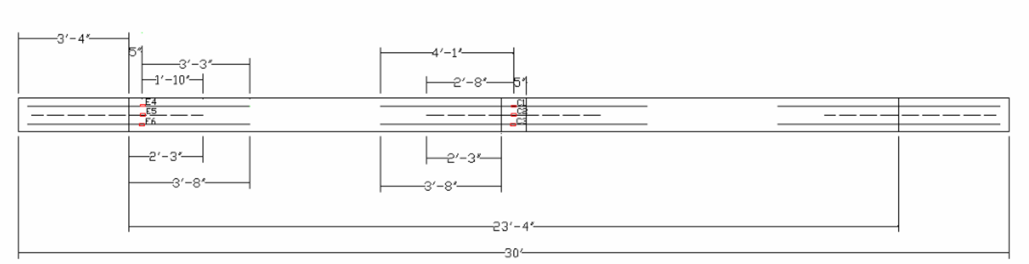
3′-4″
5″
3′-3″
1′-10″
4′-1″
2′-8″
5″
E4
E5
E6
C1
C2
C3
2′-3″
3′-8″
2′-3″
3′-8″
23′-4″
30′

No CFRP applied

Load vs Displacement:

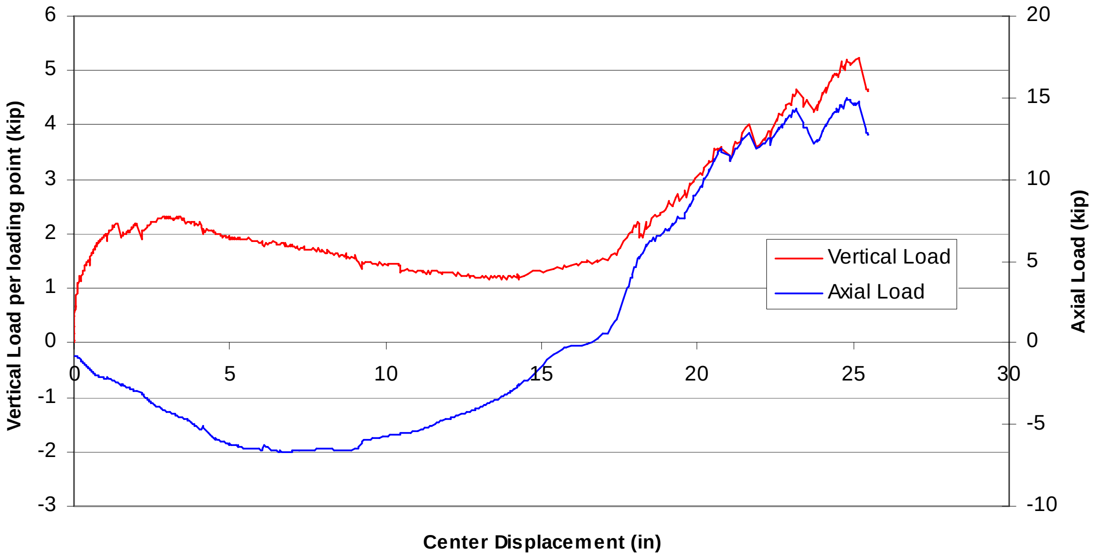

Strains:

Negative moment reinforcement

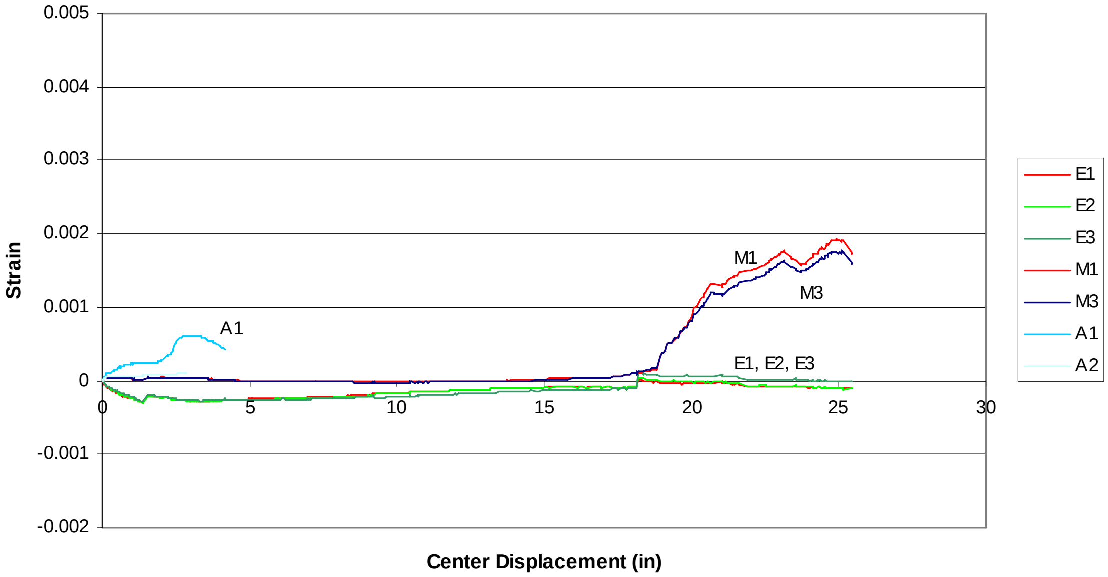

Positive moment reinforcement

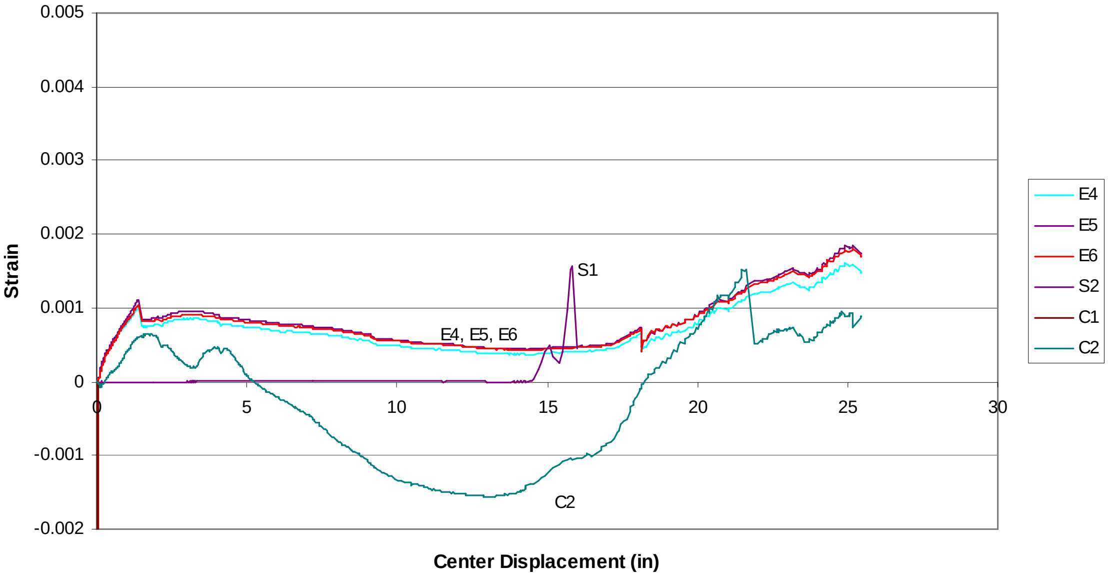

Pictures:

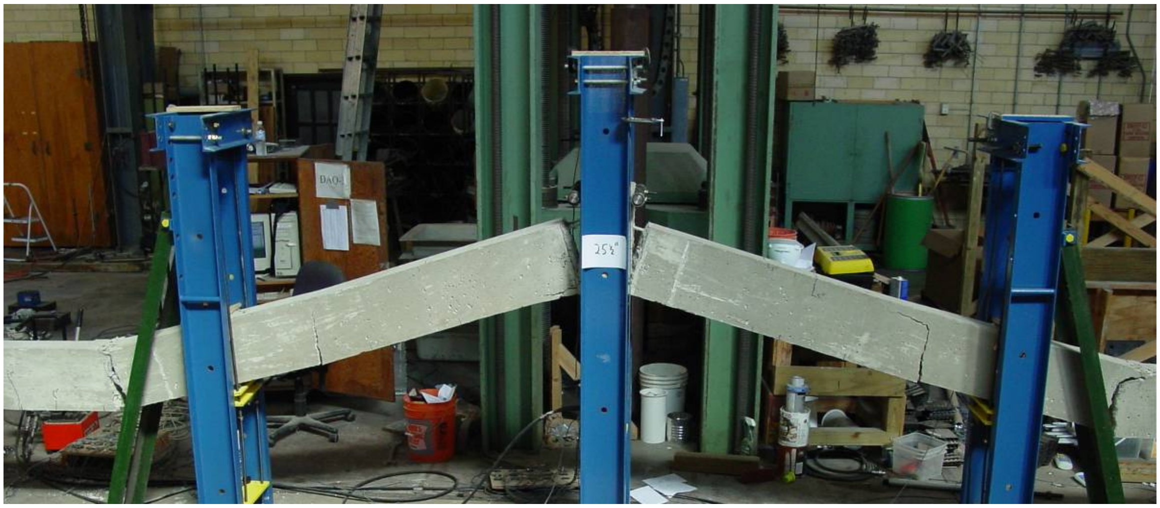

Final State

PM-1 POSITIVE MOMENT RETROFIT

Test Date: September 26th 2006
Concrete Compressive strength: 4900psi

Beam design:

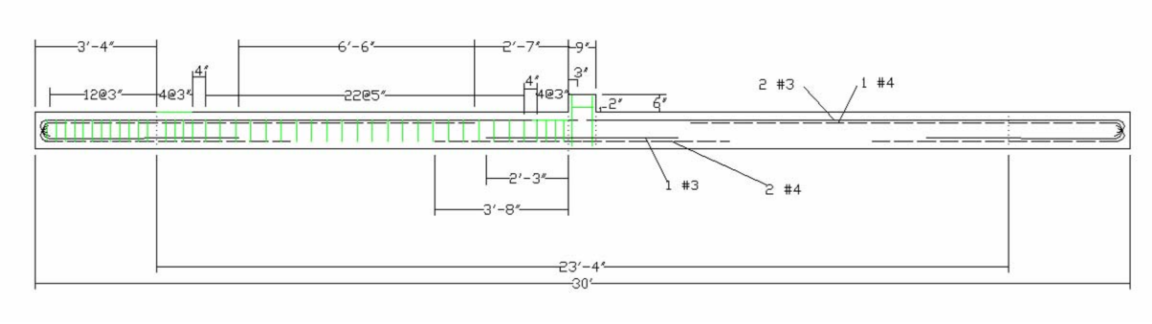
3'-4"
12@3"
4"
4@3"
6'-6"
22@5"
2'-7"
9"
4"
4@3"
3"
2"
6"
2 #3
1 #4
1 #3
2 #4
2'-3"
3'-8"
23'-4"
30'

Strain gage locations:

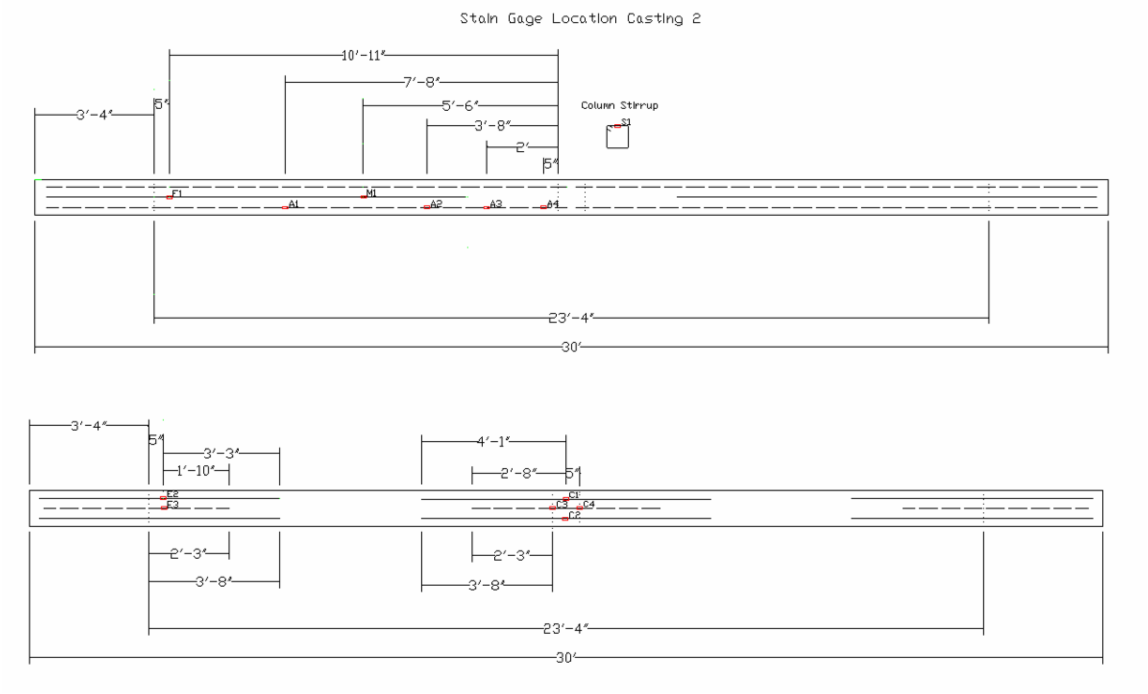
Stain Gage Location Casting 2
10'-11"
7'-8"
5'-6"
3'-8"
2"
5"
3'-4"
5"
Column Stirrup
S1
F1
M1
A1
A2
A3
A4
23'-4"
30'
3'-4"
5"
3'-3"
1'-10"
4'-1"
2'-8"
5"
E2
E3
C1
C3
C4
C2
2'-3"
3'-8"
2'-3"
3'-8"
23'-4"
30'

CFRP Design:

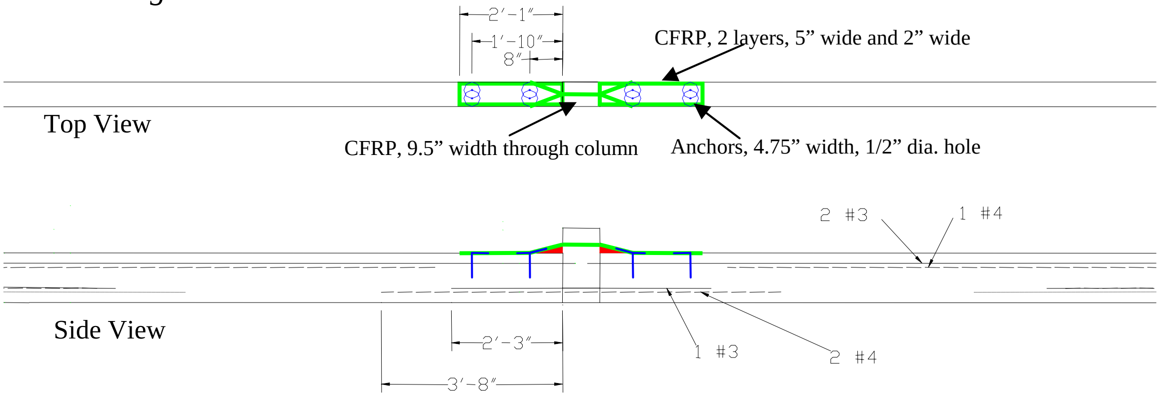
2′-1″
1′-10″
8″
CFRP, 2 layers, 5” wide and 2” wide
Top View
CFRP, 9.5” width through column
Anchors, 4.75” width, 1/2” dia. hole
2 #3
1 #4
Side View
2′-3″
3′-8″
1 #3
2 #4

CFRP strain gage locations:

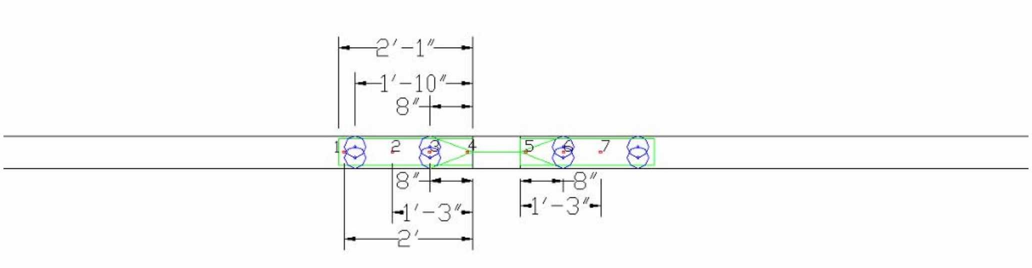
2′-1″
1′-10″
8″
1
2
3
4
5
6
7
8″
1′-3″
2′
8″
1′-3″

Load vs. Displacement:

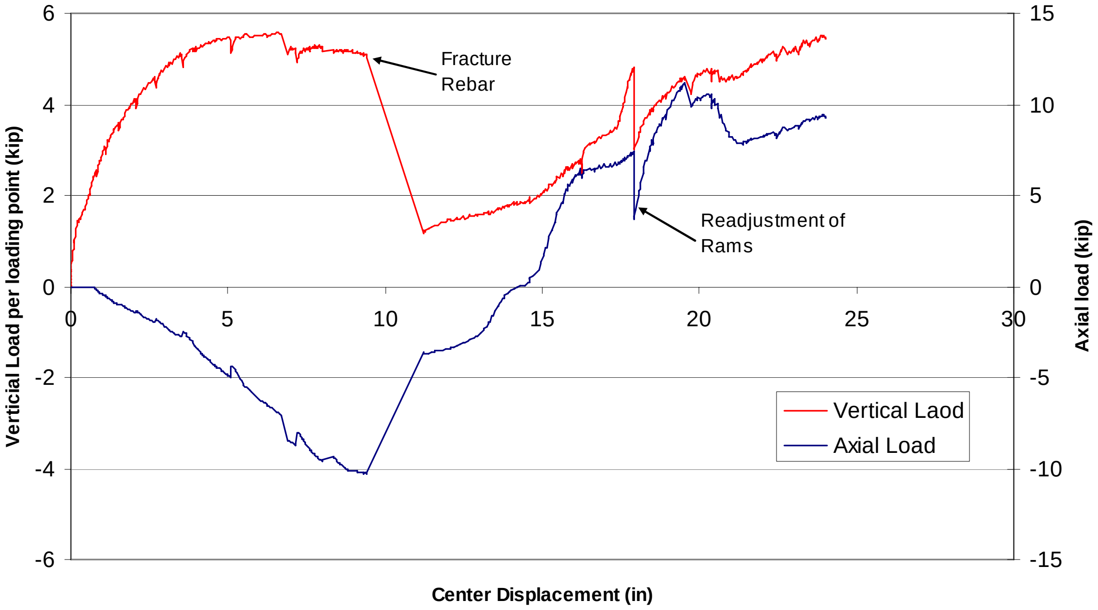

Strains:

Negative moment reinforcement

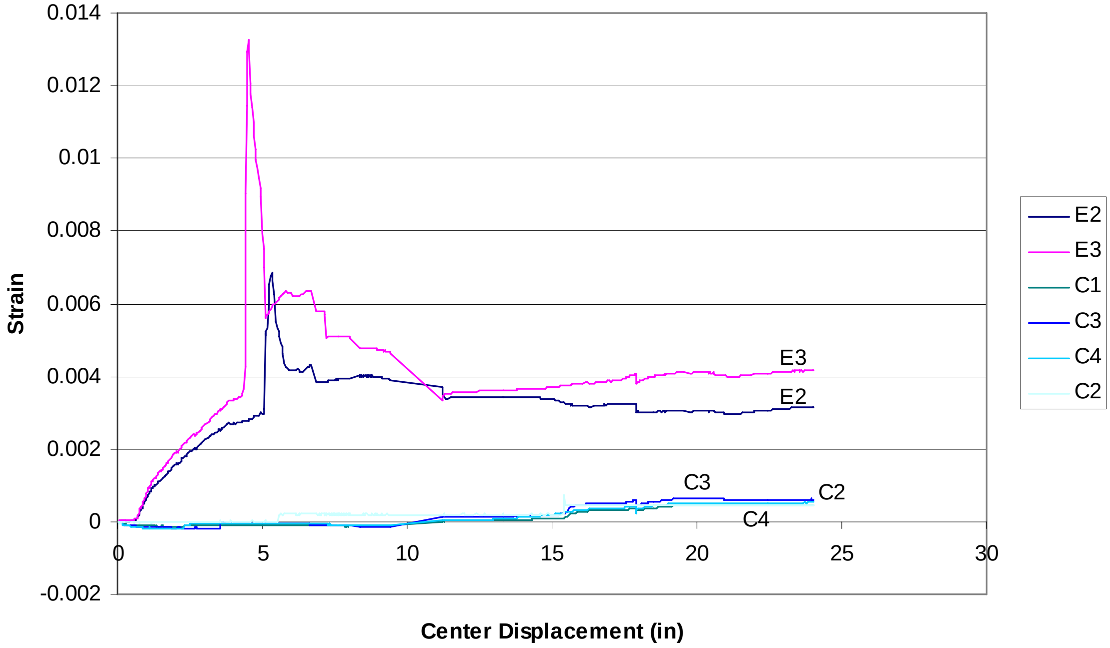

Positive moment reinforcement

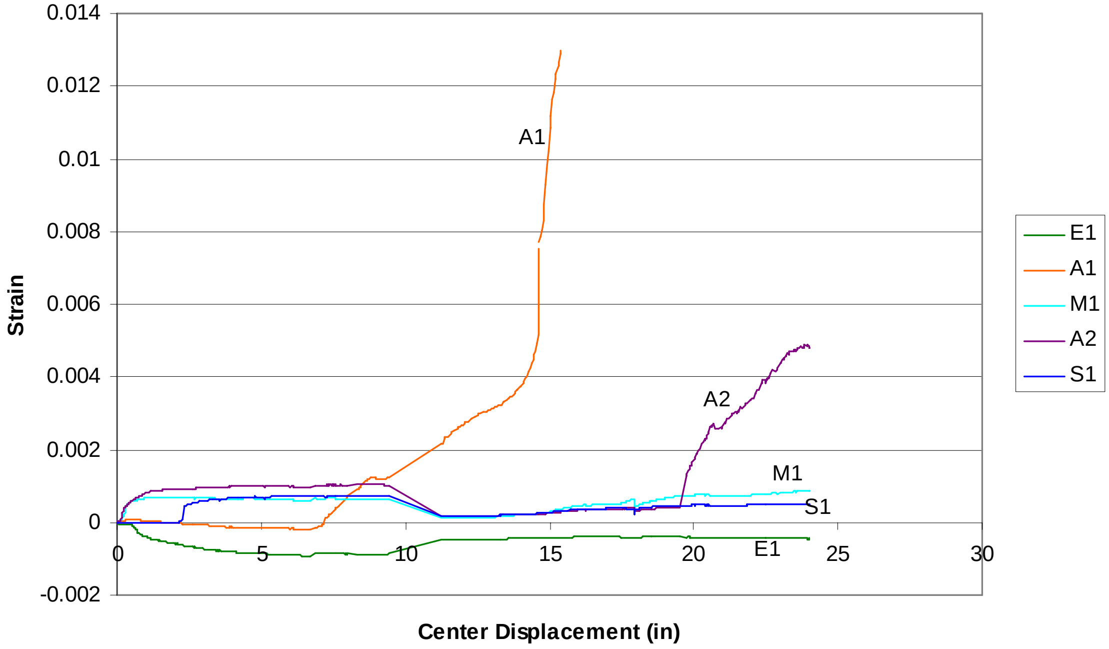

CFRP

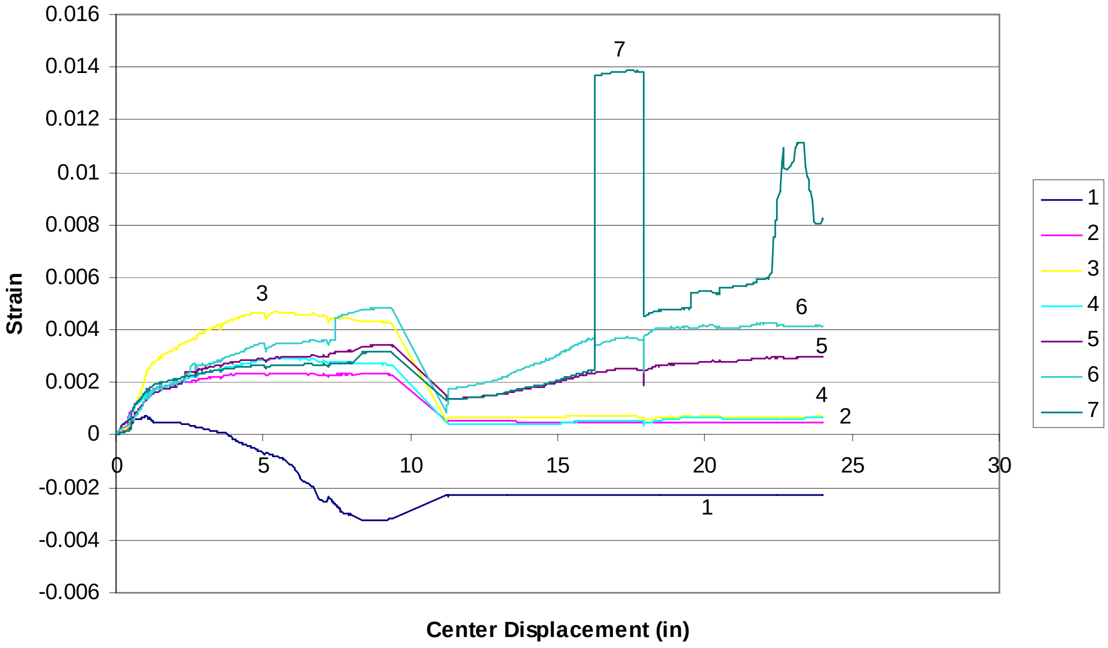

Pictures:

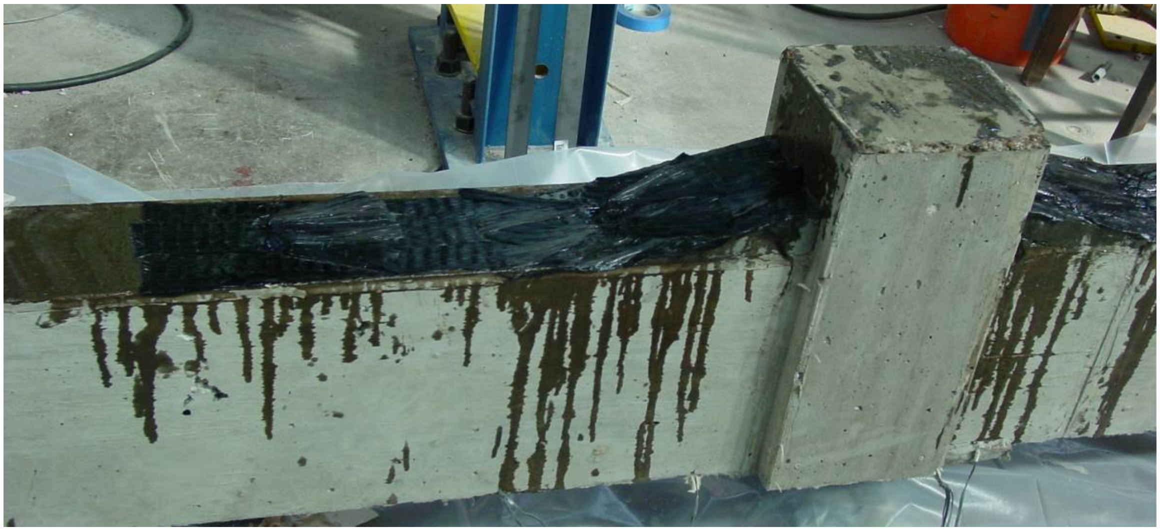

CFRP application

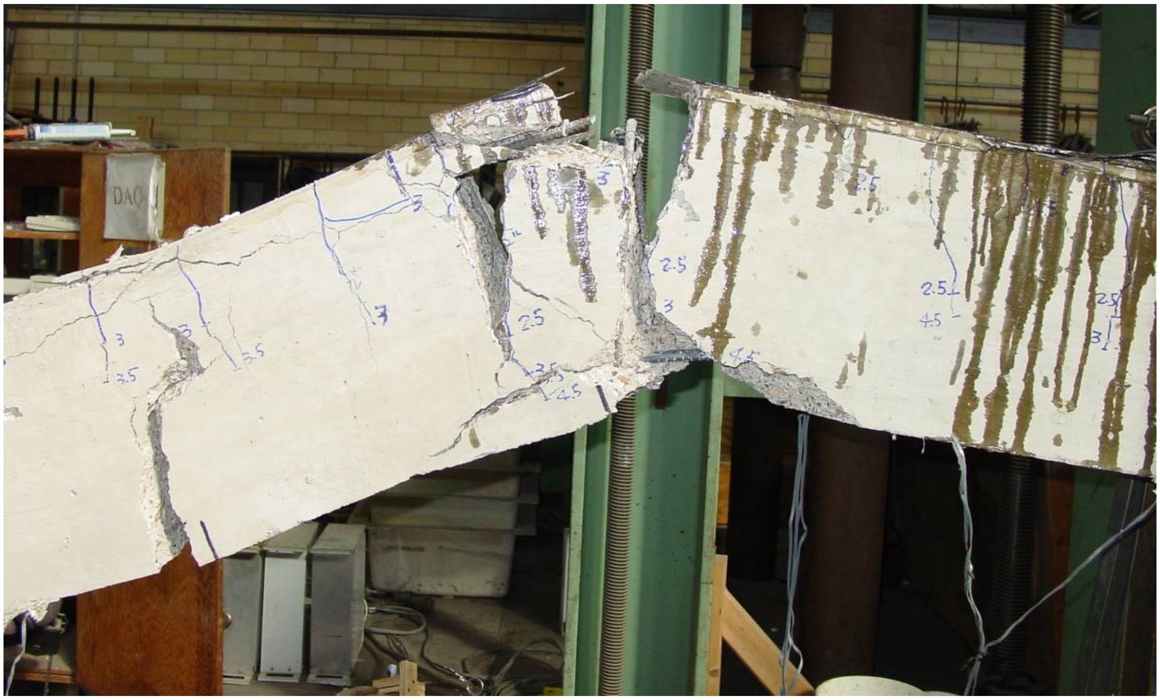
DAQ
3
3
2.5
2.5
3
2.5
4.5
3.5
4.5
3
3.5
3
2.5
4.5
2.5
3

Rebar fracture

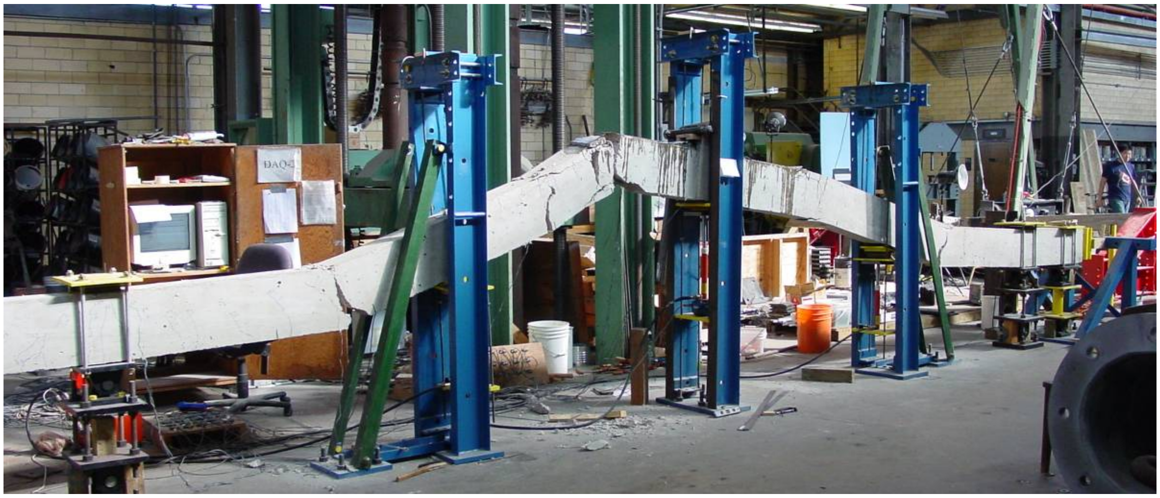

Final state

PM-2 POSITIVE MOMENT RETROFIT

Test Date: October 5th 2006
Concrete Compressive strength: 4900psi

Beam design:

Same as PM-1

Strain gage locations:

Same as PM-1

CFRP design:

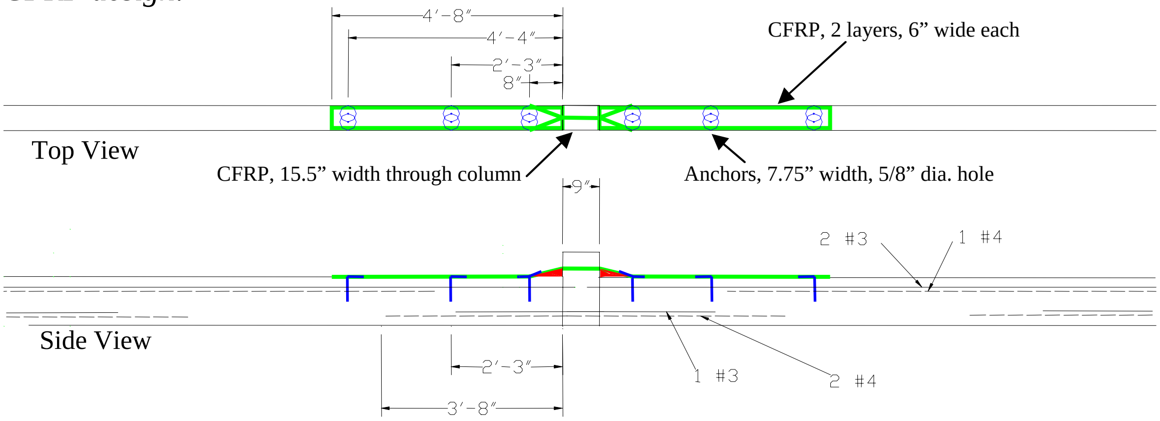
4′-8″
4′-4″
2′-3″
8″
9″
2 #3
1 #4
1 #3
2 #4
2′-3″
3′-8″

CFRP, 2 layers, 6” wide each

Top View

CFRP, 15.5” width through column

Anchors, 7.75” width, 5/8” dia. hole

Side View

CFRP strain gage locations:

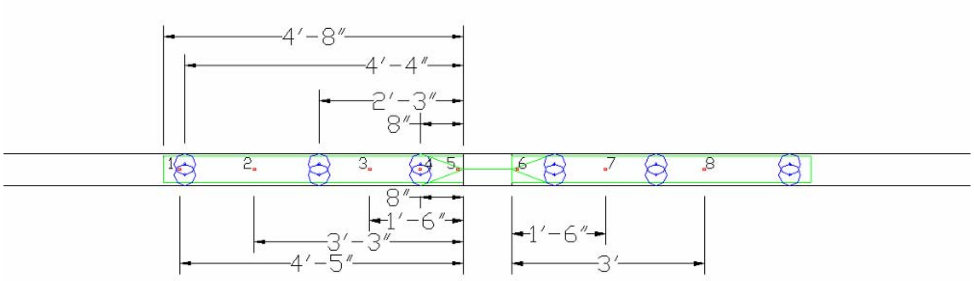
4′-8″
4′-4″
2′-3″
8″
1
2
3
4
5
6
7
8
8″
1′-6″
3′-3″
4′-5″
1′-6″
3′

Load vs. Displacement:

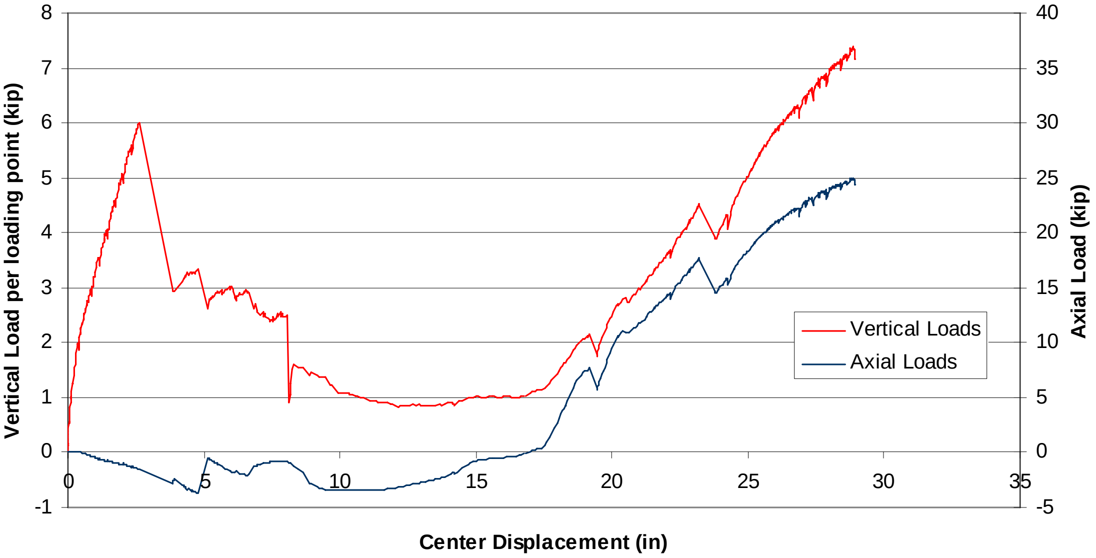

Strains:

Negative moment reinforcement

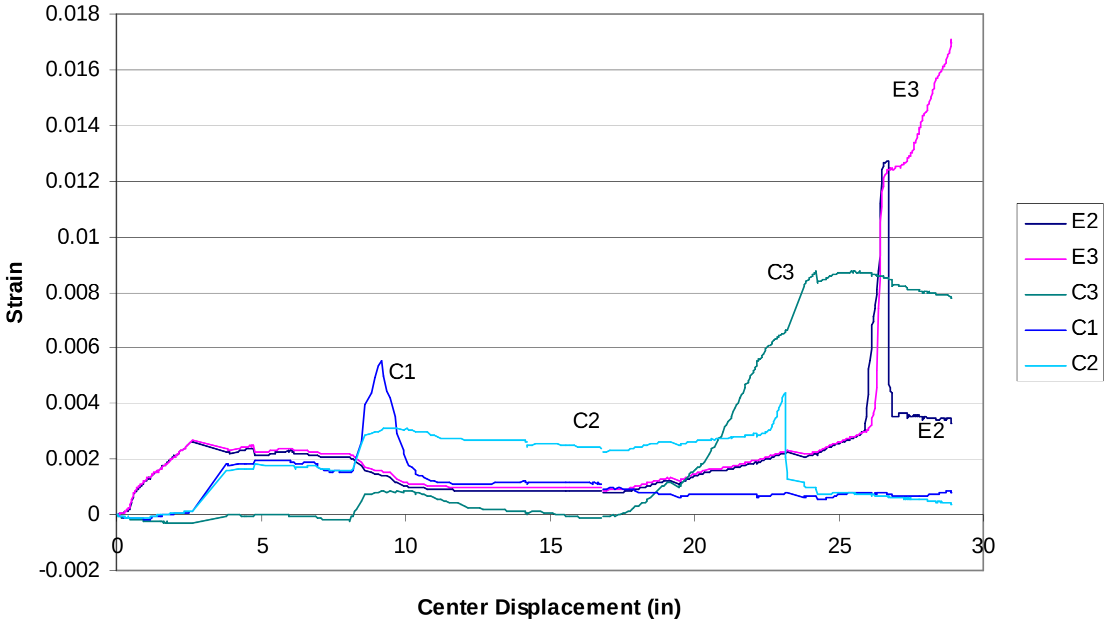

Positive moment reinforcement

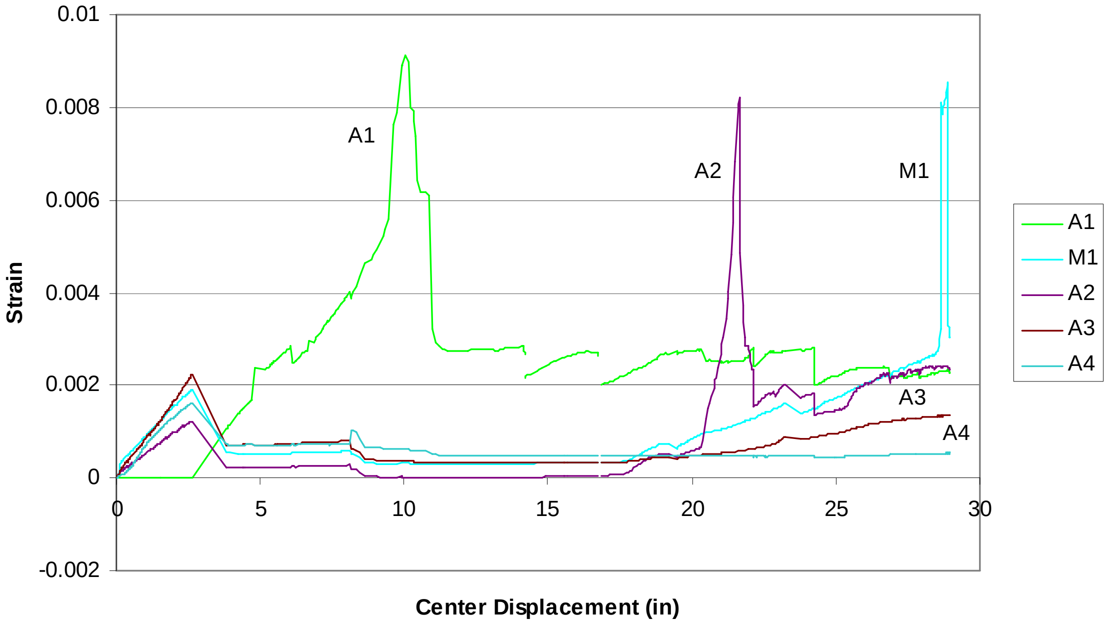

CFRP

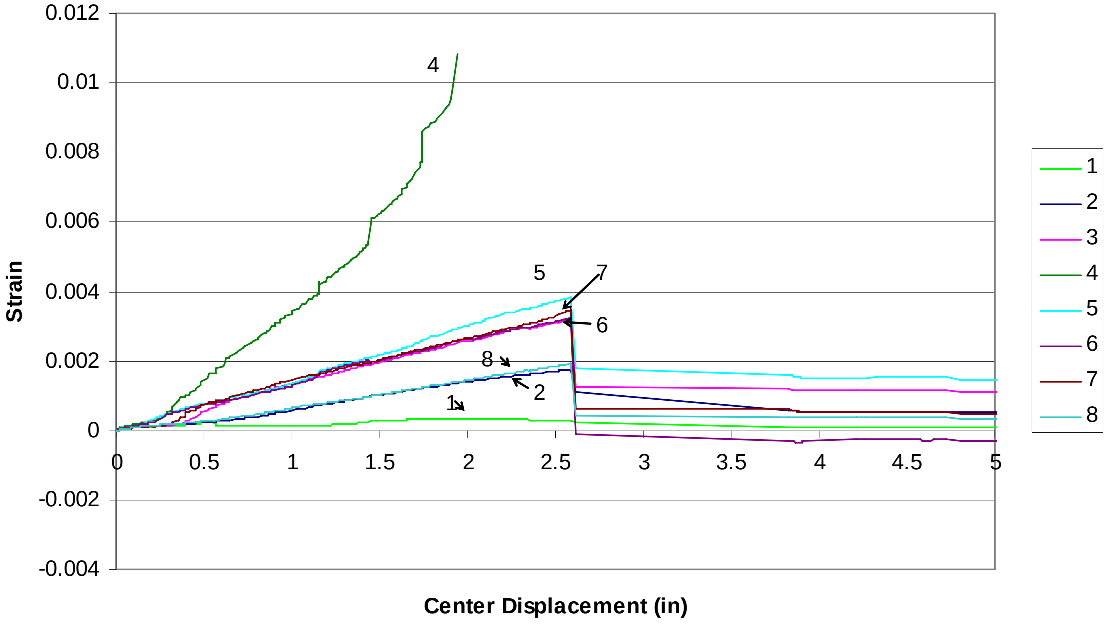

Pictures:

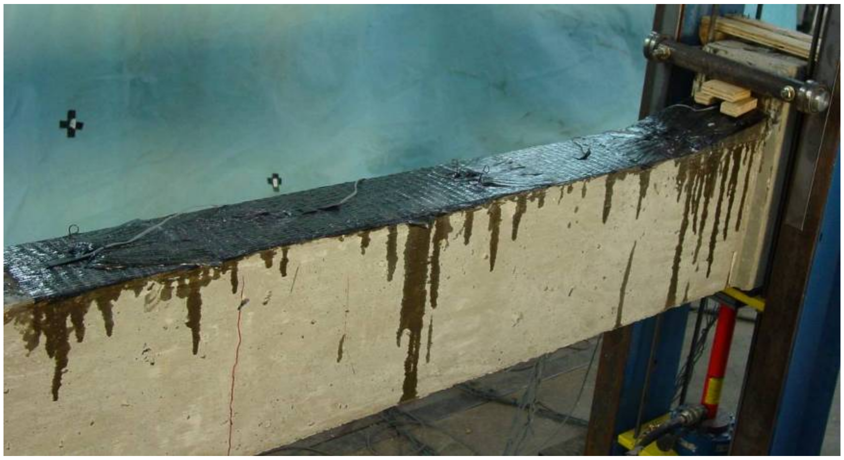

CFRP

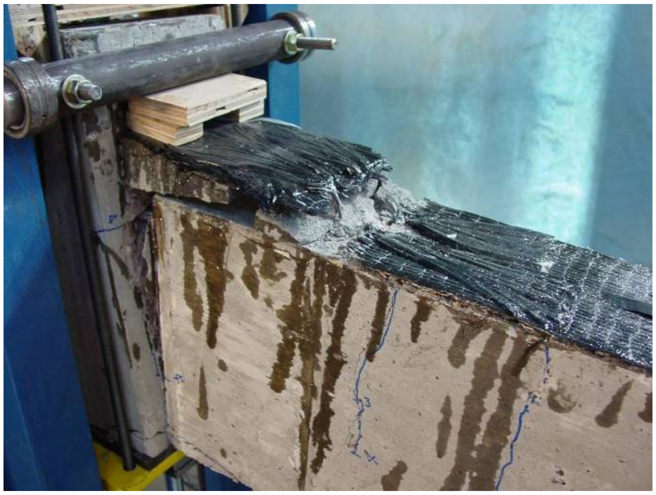

CFRP fracture

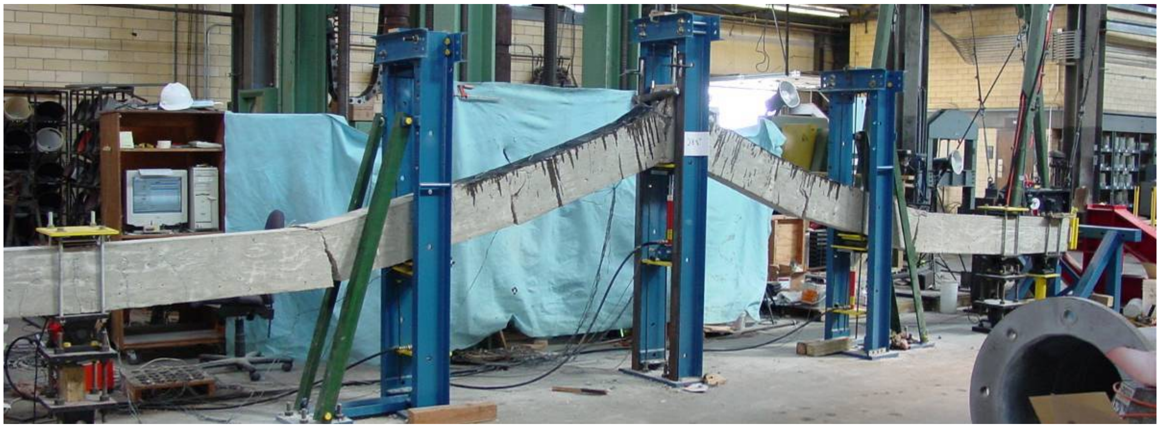

Final state

NM-1 NEGATIVE MOMENT RETROFIT

Test Date: November 3rd 2006
Concrete Compressive strength: 4900psi

Beam design: Same as PM-1

Strain gage locations: Same as PM-1

CFRP design:

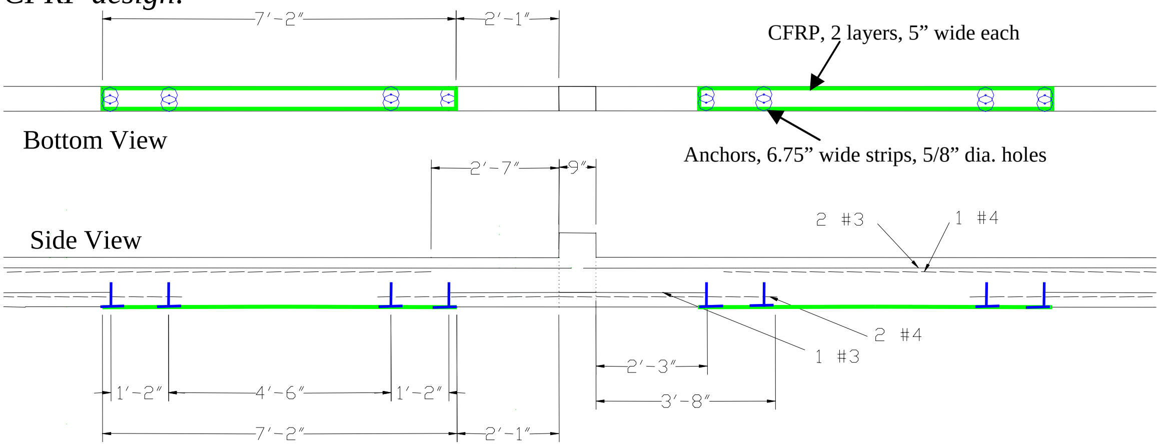

CFRP, 2 layers, 5” wide each

Anchors, 6.75” wide strips, 5/8” dia. holes

7′-2″
2′-1″
Bottom View
2′-7″
9″
Side View
2 #3
1 #4
2 #4
1 #3
2′-3″
3′-8″
1′-2″
4′-6″
1′-2″
7′-2″
2′-1″

CFRP strain gage locations:

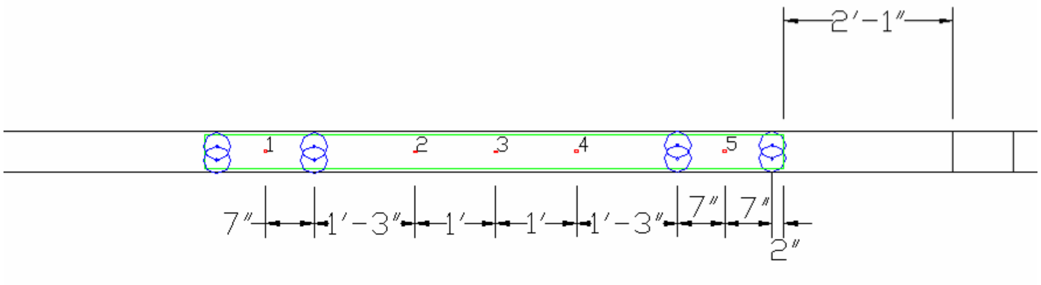

2′-1″
1
2
3
4
5
7″
1′-3″
1′
1′
1′-3″
7″
7″
2″

Load vs. Displacement:

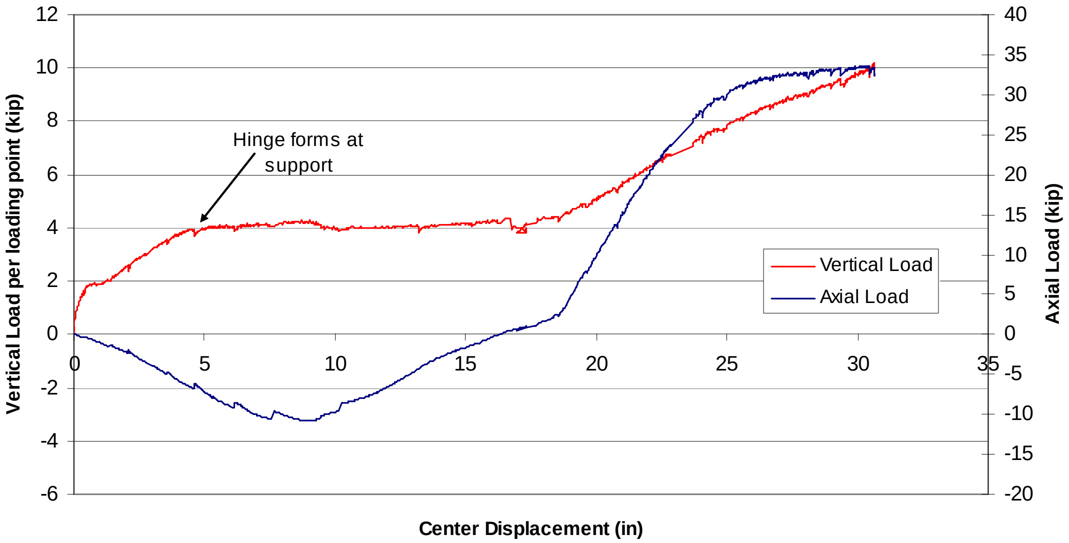

Moment at supports, calculated from measured load in tension support:

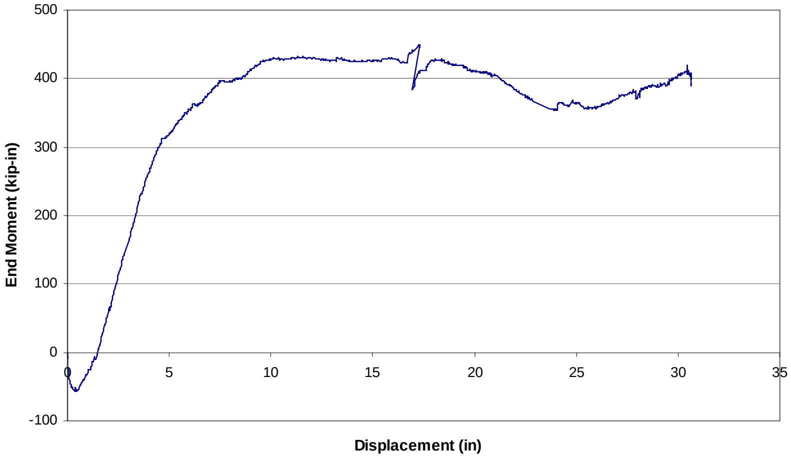

Strains:

Negative moment reinforcement

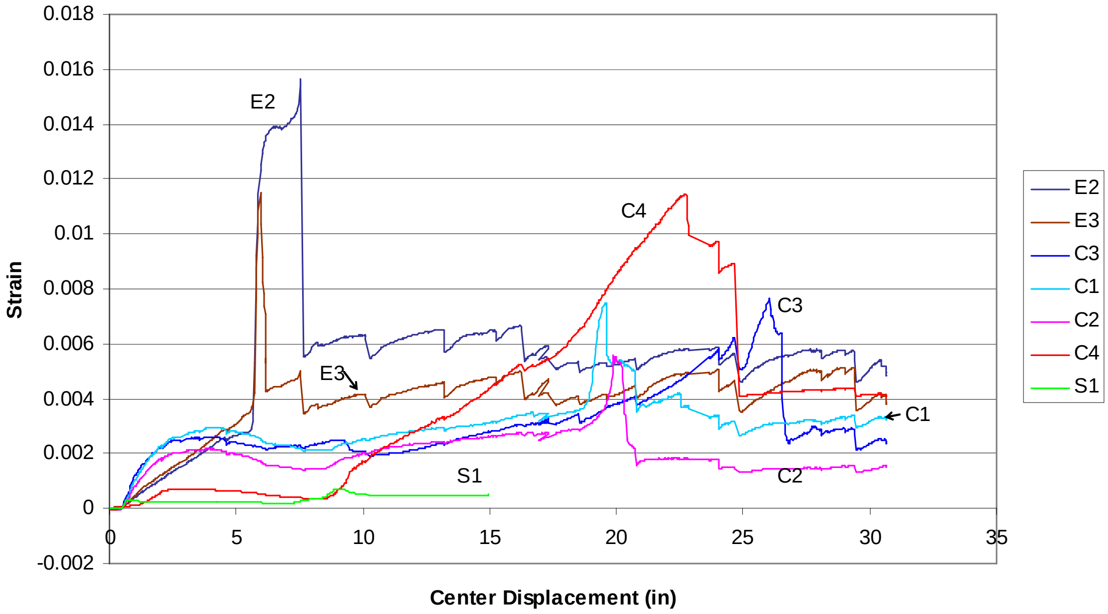

Positive moment reinforcement

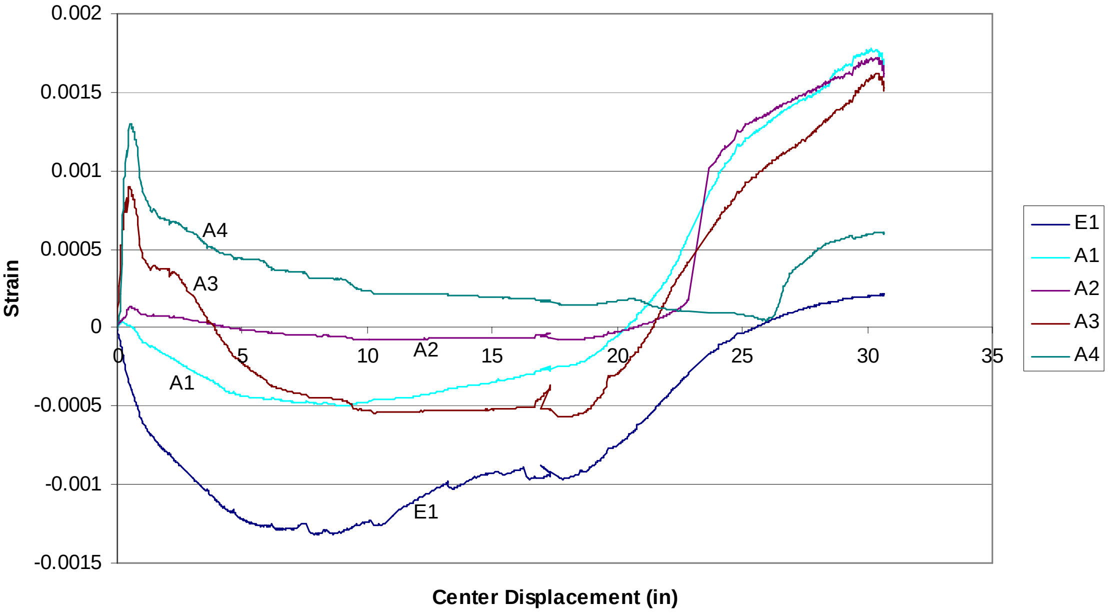

CFRP

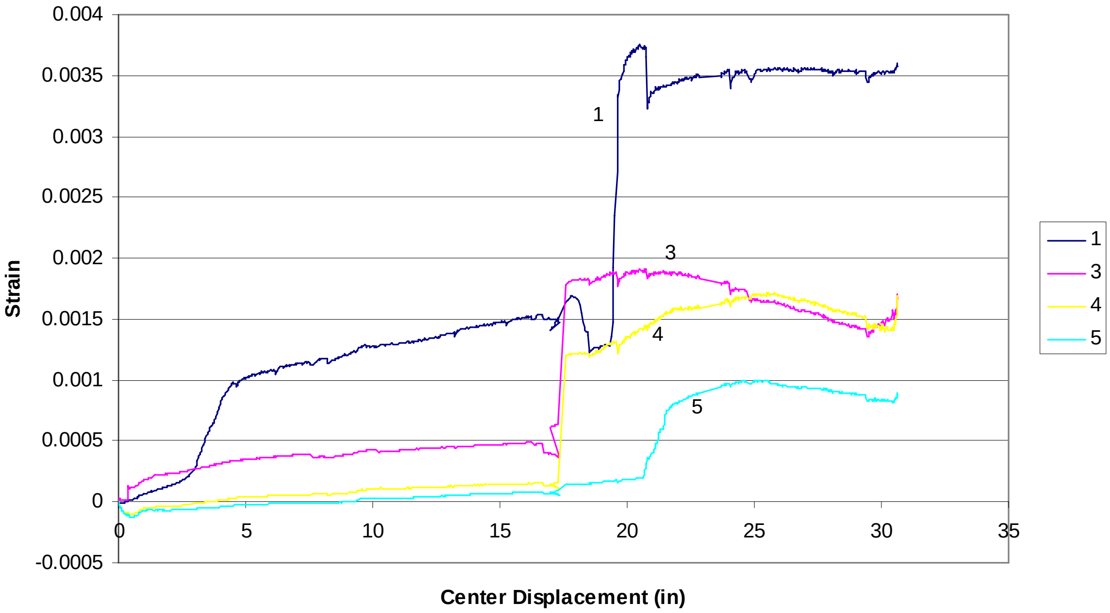

Pictures:

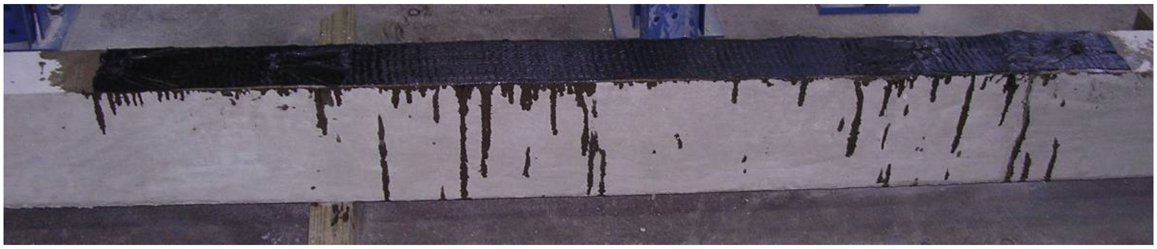

CFRP

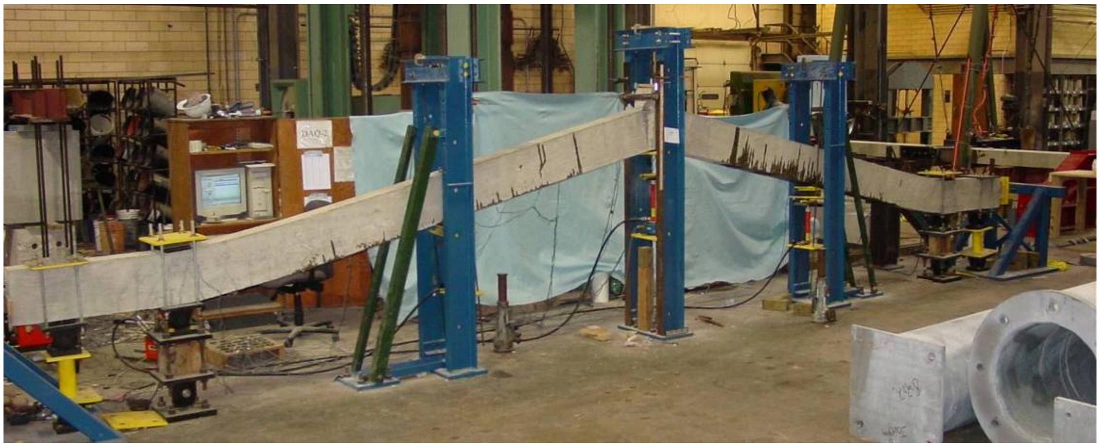

Final state

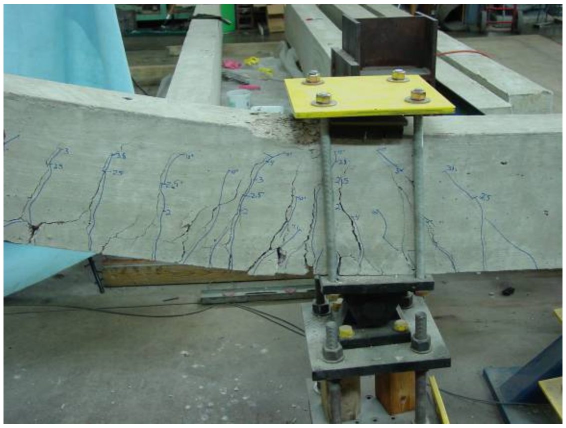

Hinge at support

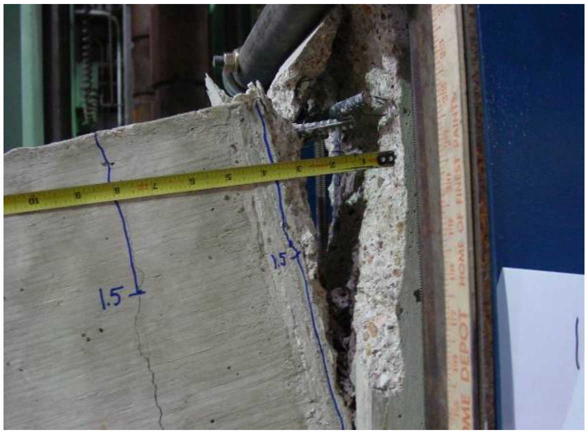

Wide crack at column

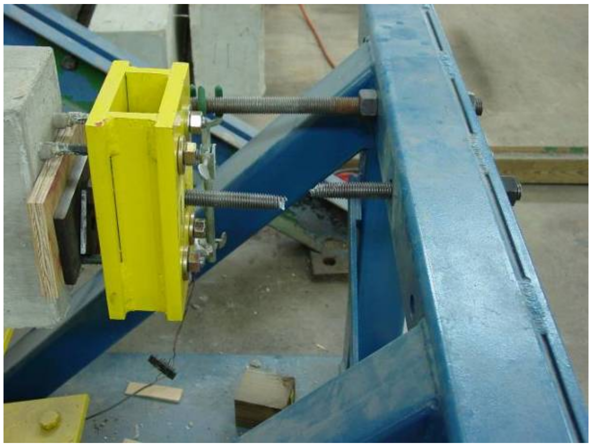

Fracture of threaded rod for axial restraint

NM-2 NEGATIVE MOMENT RETROFIT

Test Date: February 19th 2006
Concrete Compressive strength: 5300psi

Beam design: Same as PM-1

Strain gage locations:

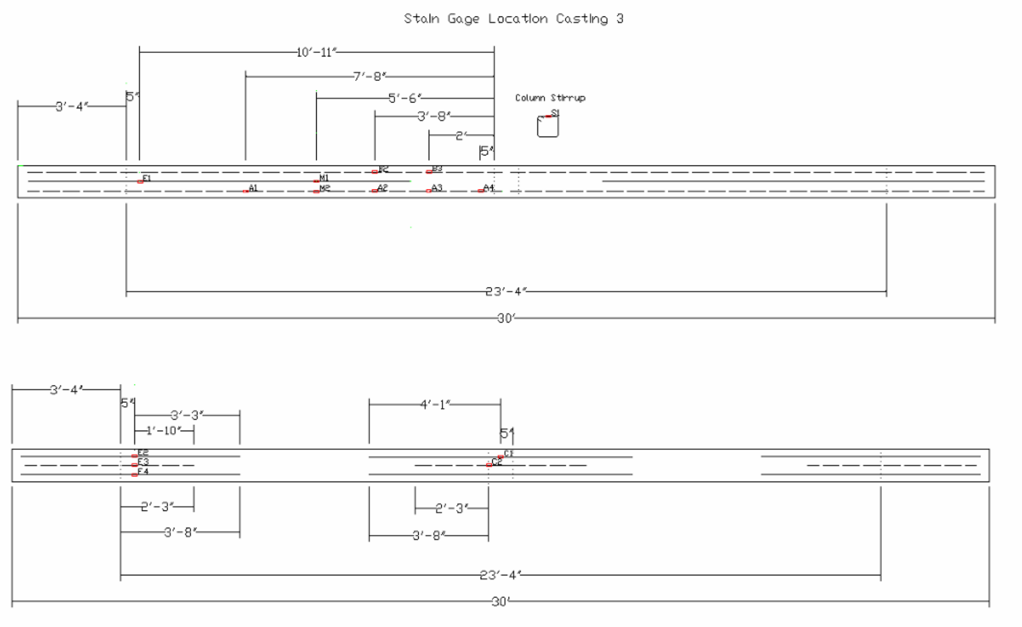
Stain Gage Location Casting 3
10′-11″
7′-8″
5′-6″
3′-8″
2′
5″
3′-4″
5″
Column Stirrup
S1
E1
M1
M2
A1
A2
A3
A4
B2
B3
23′-4″
30′
3′-4″
5″
3′-3″
1′-10″
E2
E3
E4
4′-1″
5″
C1
C2
2′-3″
3′-8″
2′-3″
3′-8″
23′-4″
30′

CFRP design:

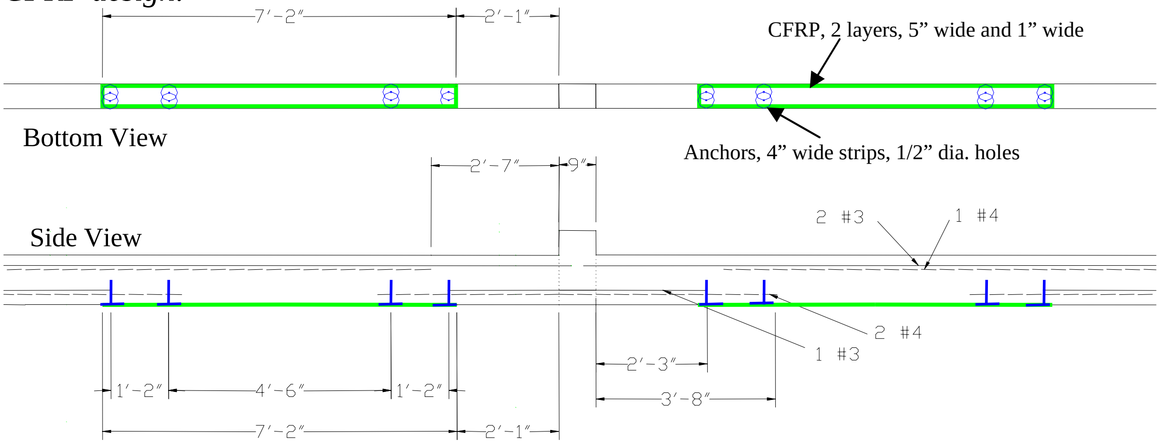
7′-2″
2′-1″
CFRP, 2 layers, 5” wide and 1” wide
Bottom View
Anchors, 4” wide strips, 1/2” dia. holes
2′-7″
9″
Side View
2 #3
1 #4
2 #4
1 #3
2′-3″
3′-8″
1′-2″
4′-6″
1′-2″
7′-2″
2′-1″

CFRP strain gage locations: Same as NM-1

Load vs. Displacement

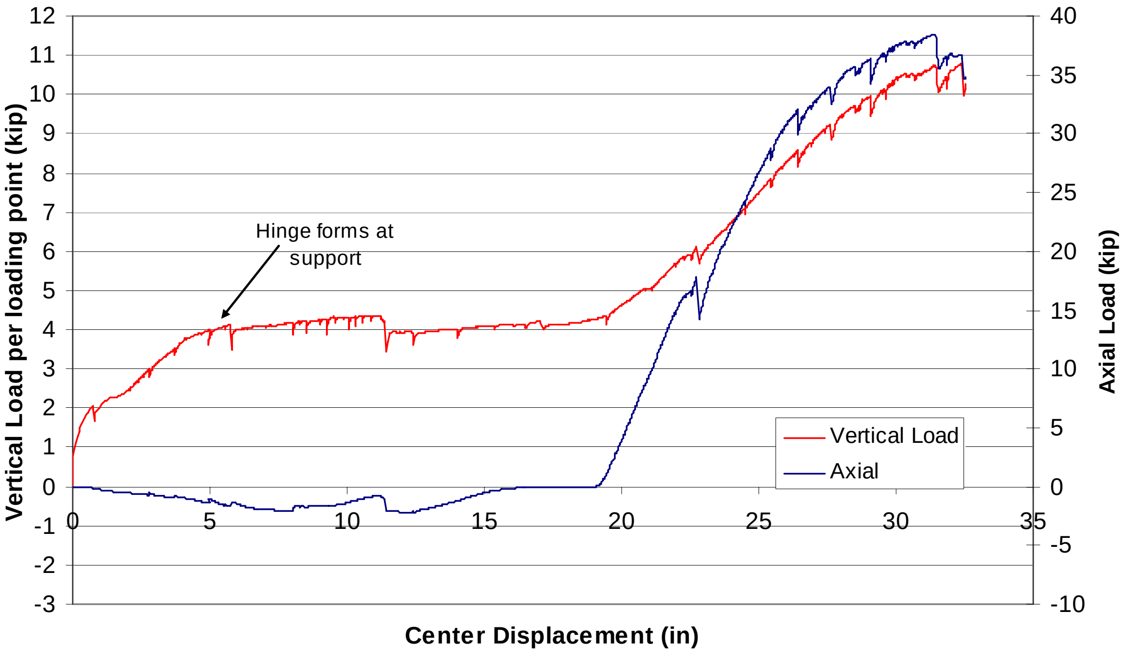

Strains:

Negative moment reinforcement

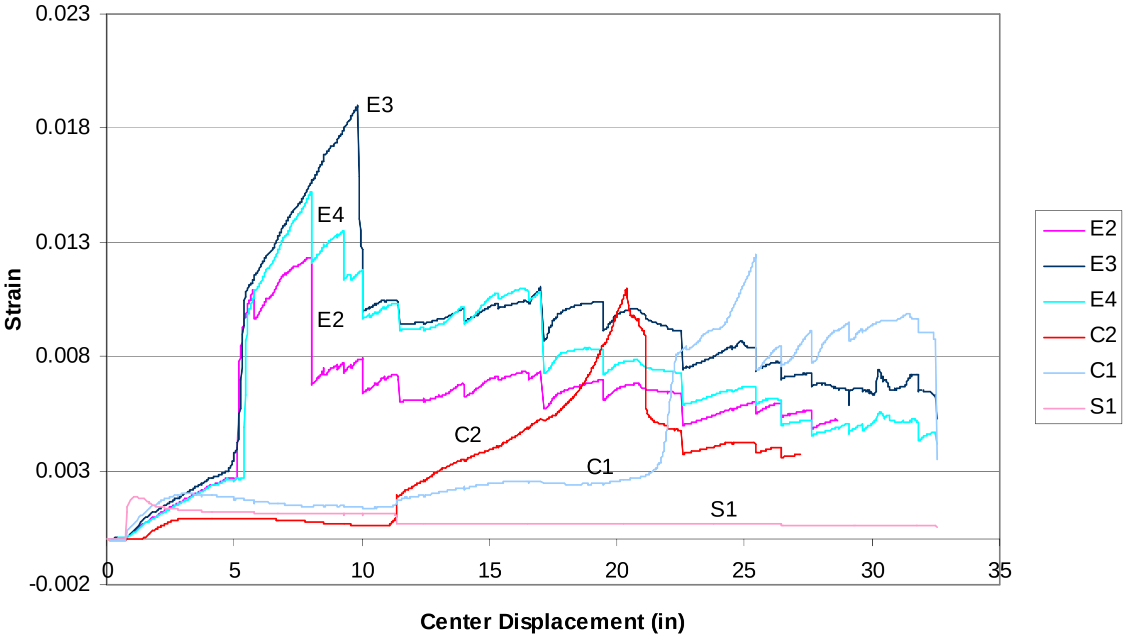

Positive moment reinforcement

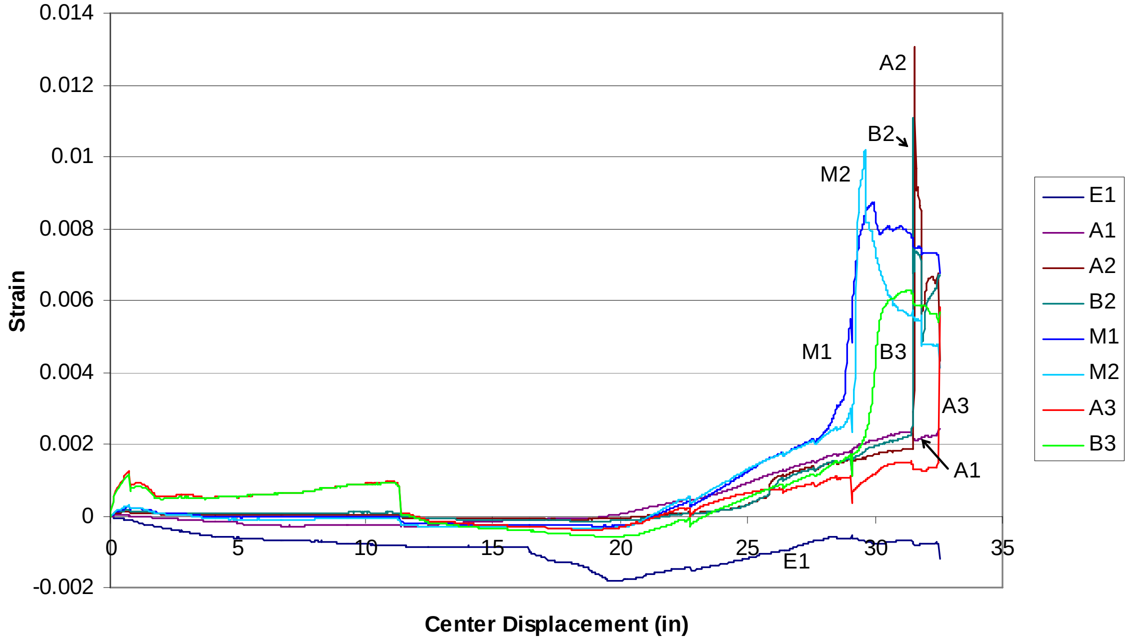

CFRP

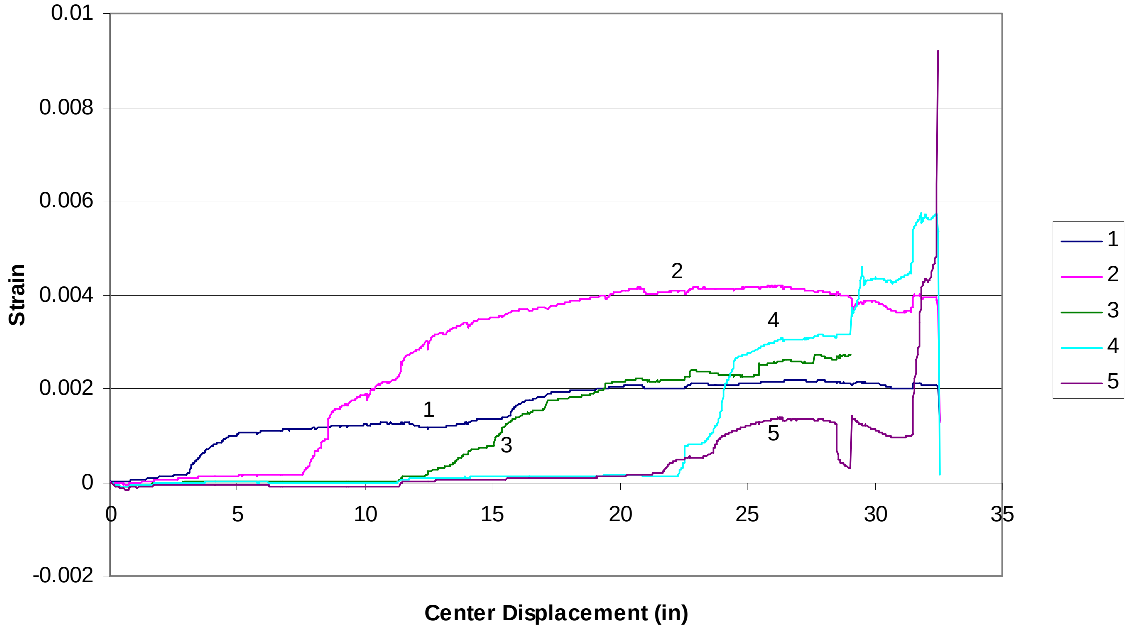

Pictures:

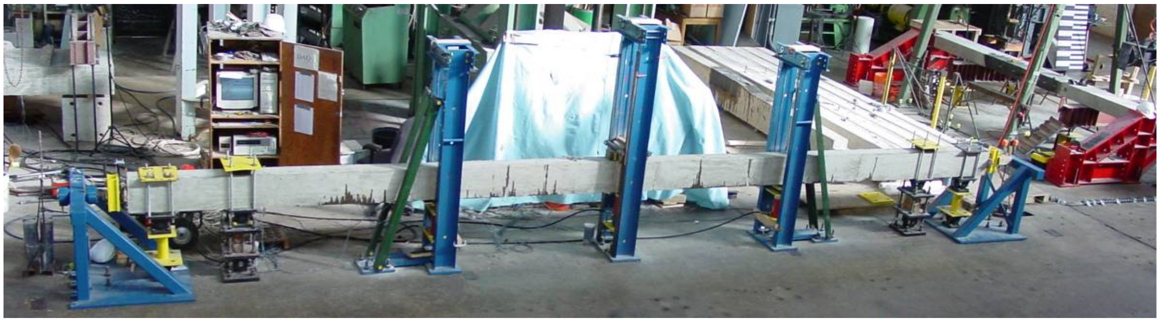

Initial State

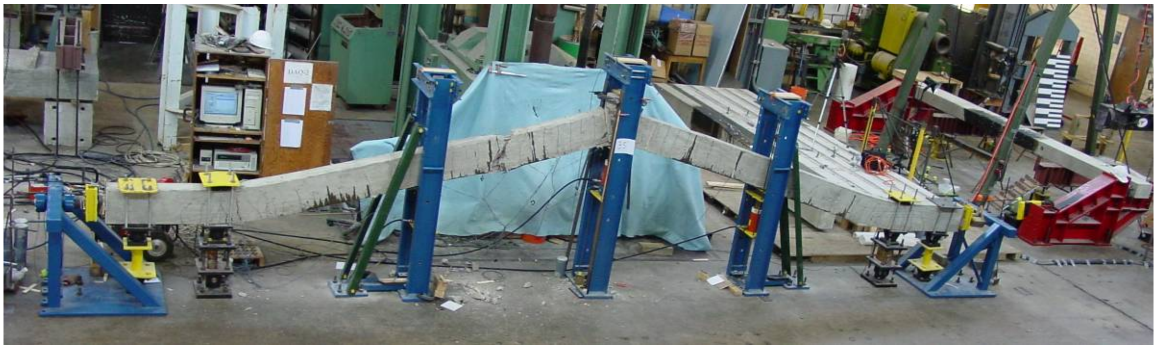

Final State

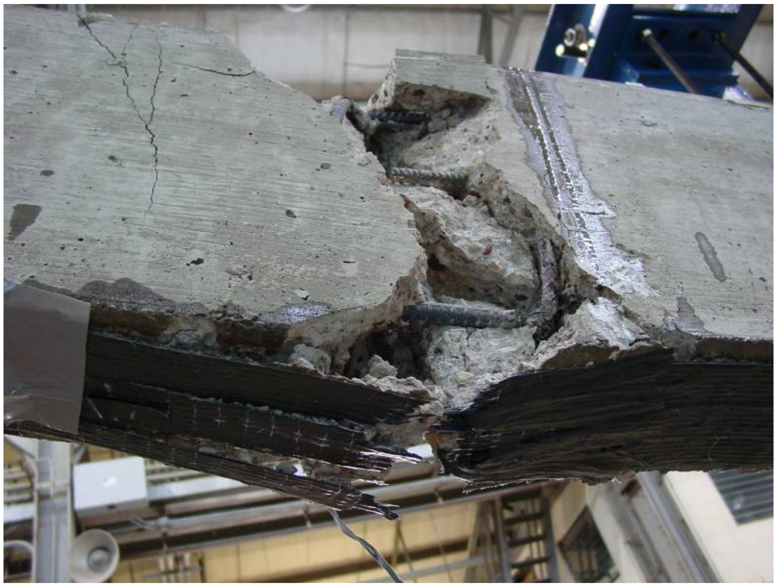

CFRP fracture

FR-1 FLEXURAL RETROFIT

Test Date: February 12th 2006
Concrete Compressive strength: 5300psi

Beam design: Same as PM-1

Strain gage locations: Same as NM-2

CFRP design:

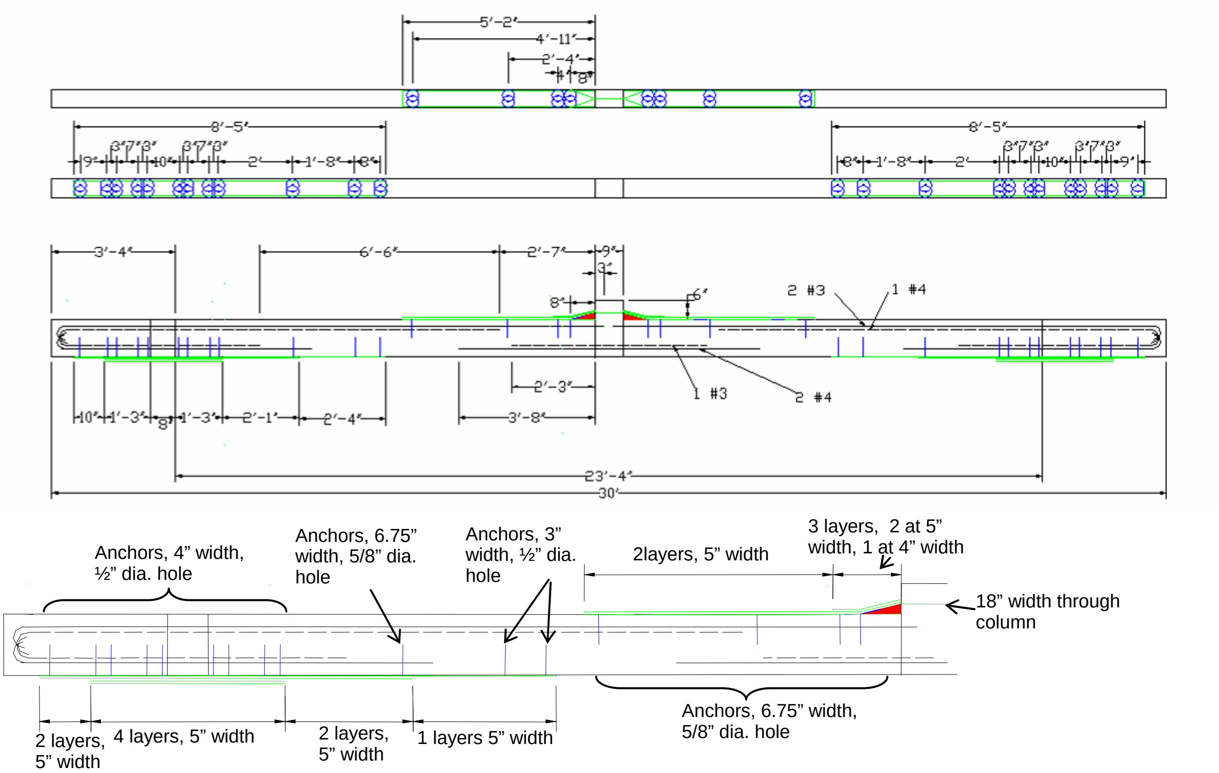

5'-2"
4'-11"
2'-4"
4"
8"
8'-5"
3"7"3"
3"7"3"
9"
10"
2'
1'-8"
8"
8'-5"
3'-4"
6'-6"
2'-7"
9"
3"
8"
6"
2 #3
1 #4
1 #3
2 #4
2'-3"
10"
1'-3"
8"
1'-3"
2'-1"
2'-4"
3'-8"
23'-4"
30'
Anchors, 4" width, ½" dia. hole
Anchors, 6.75" width, 5/8" dia. hole
Anchors, 3" width, ½" dia. hole
2layers, 5" width
3 layers, 2 at 5" width, 1 at 4" width
18" width through column
2 layers, 5" width
4 layers, 5" width
2 layers, 5" width
1 layers 5" width
Anchors, 6.75" width, 5/8" dia. hole

CFRP strain gage locations:

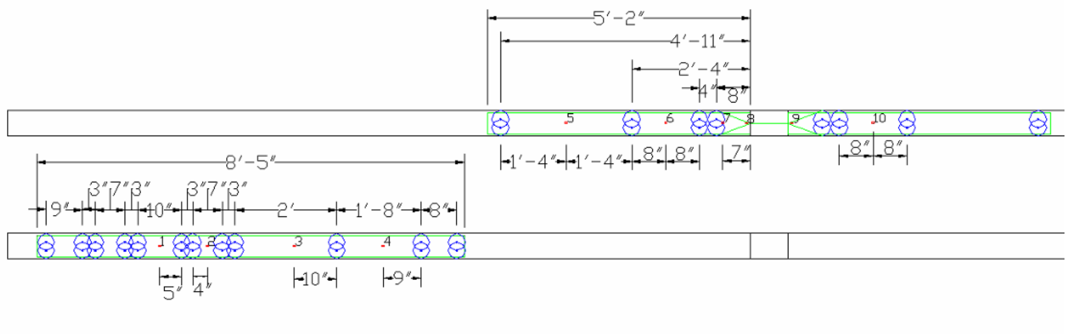

5'-2"
4'-11"
2'-4"
4"
8"
5
6
7
8
9
10
1'-4"
1'-4"
8"
8"
7"
8"
8"
8'-5"
3"7"3"
3"7"3"
9"
10"
2'
1'-8"
8"
1
2
3
4
5"
4"
10"
9"

Load vs. Displacement:

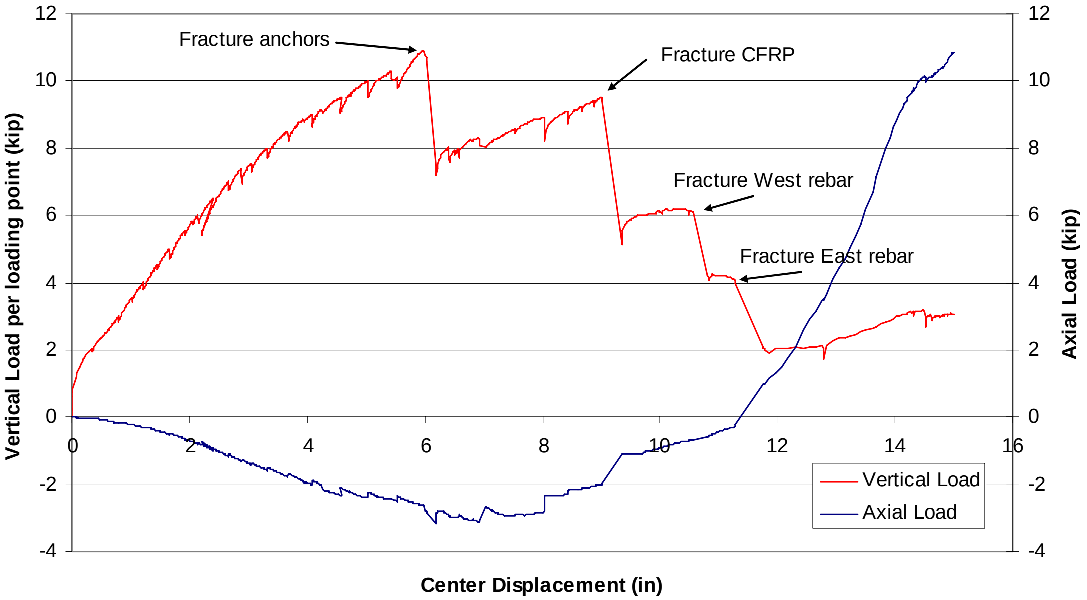

Strains:

Negative moment reinforcement

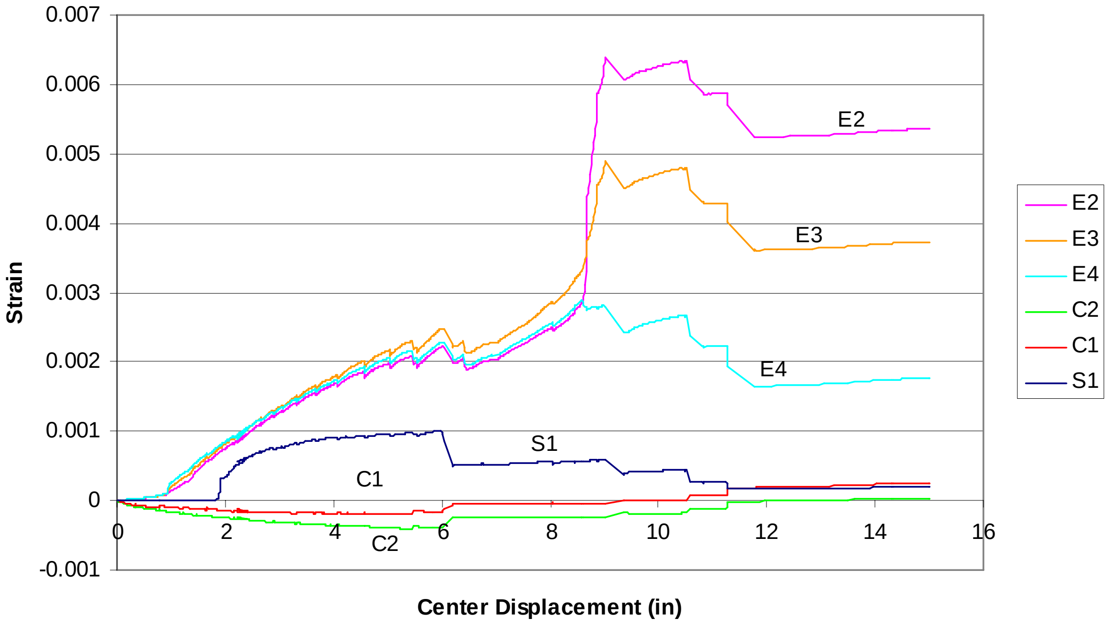

Positive moment reinforcement

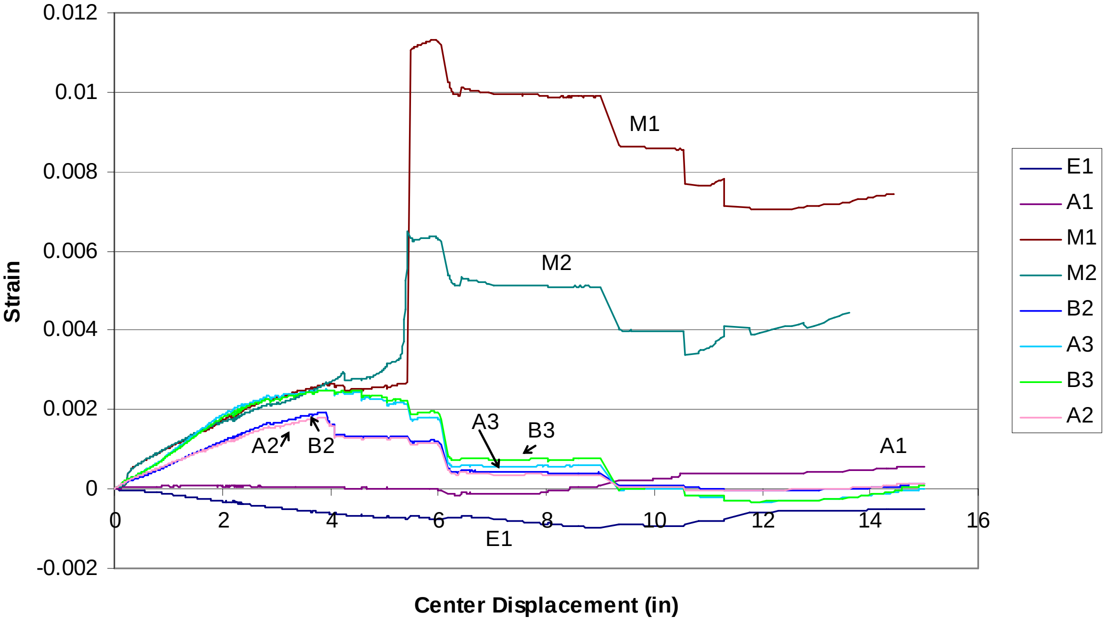

CFRP

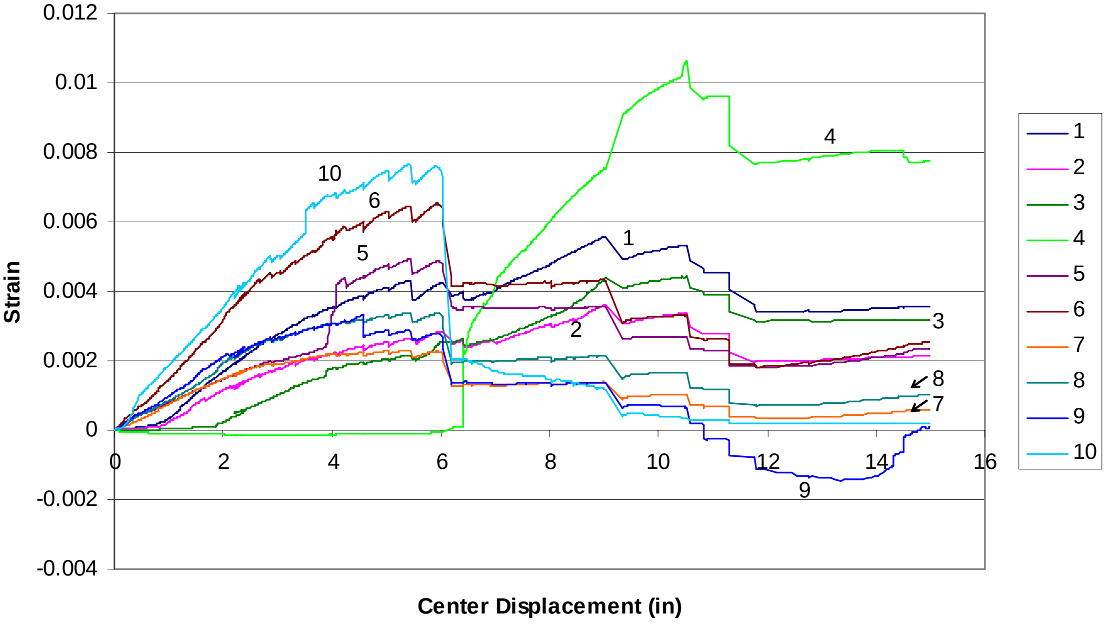

Pictures:

Negative moment CFRP

Positive moment CFRP

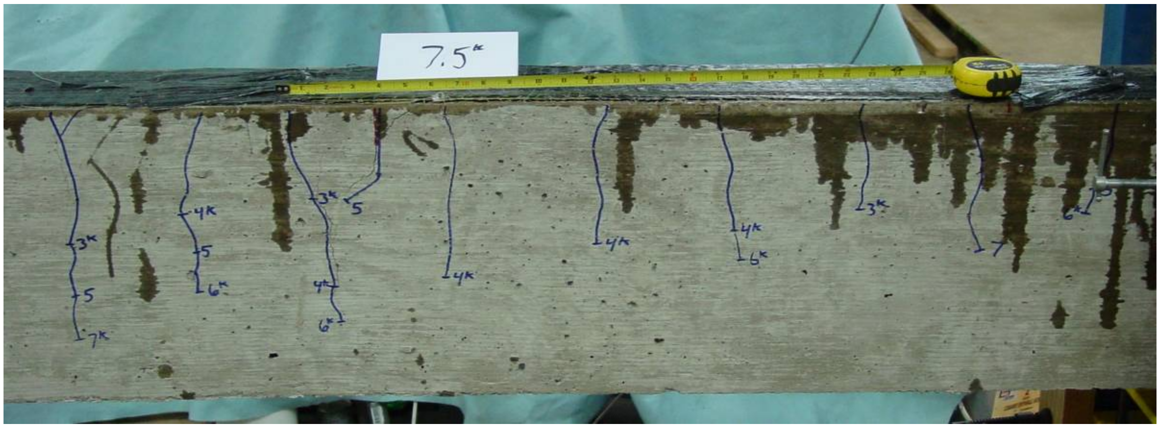
7.5k
3k
5
7k
4k
5
6k
3k
5
4k
6k
4k
4k
4k
6k
3k
7
6k

Debonding at 7.5 kip load

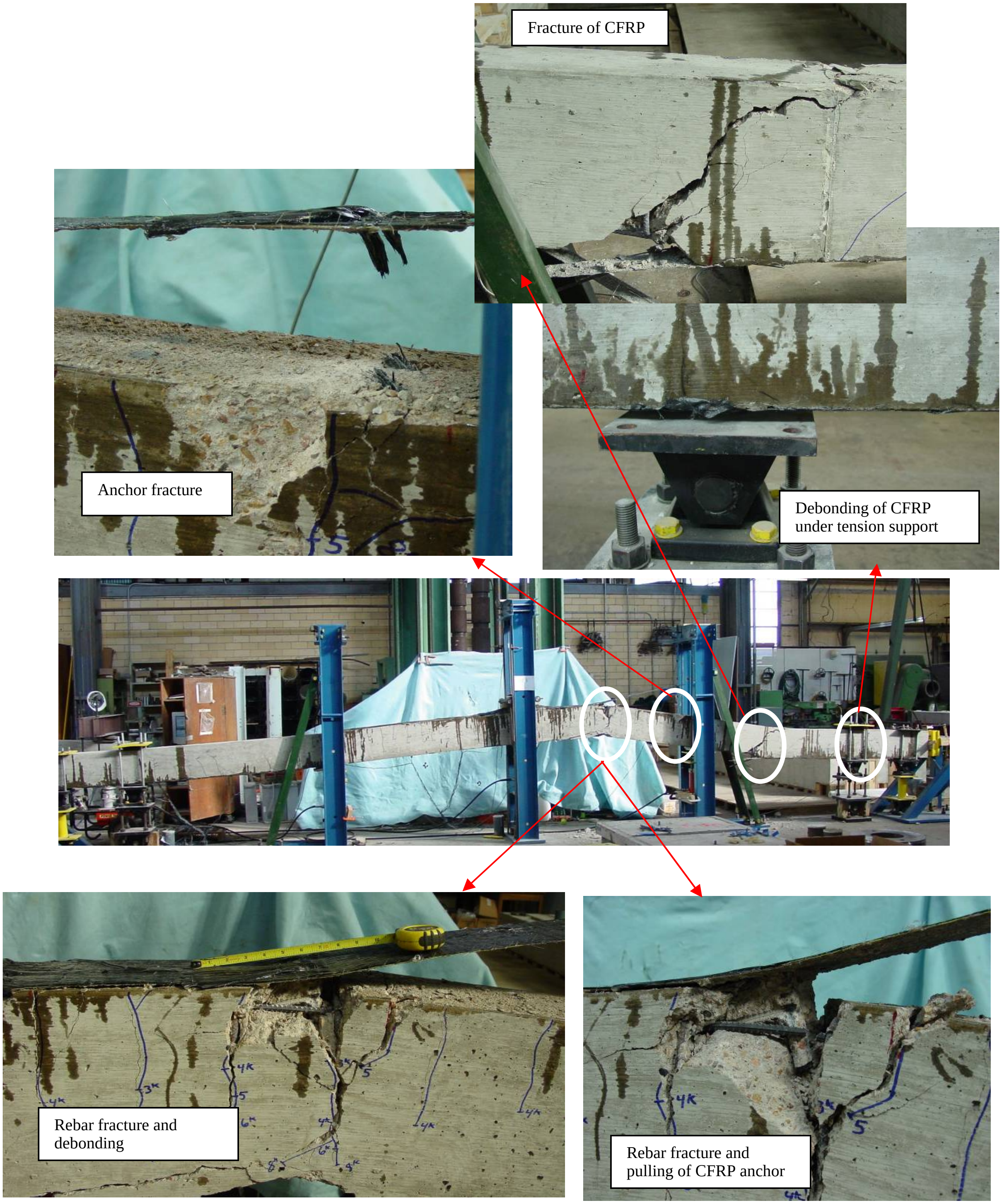
Fracture of CFRP
Anchor fracture
Debonding of CFRP under tension support
Rebar fracture and debonding
Rebar fracture and pulling of CFRP anchor

CR-1 CONTINUOUS REINFORCEMENT

Test Date: January 12th 2006
Concrete Compressive strength: 5300psi

Beam design:

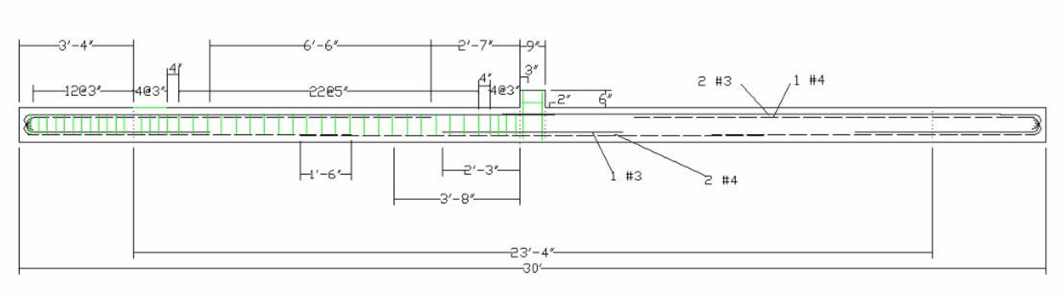
3′-4″
6′-6″
2′-7″
9″
4″
3″
12@3″
4@3″
22@5″
4″
4@3″
2″
6″
2 #3
1 #4
1′-6″
2′-3″
3′-8″
1 #3
2 #4
23′-4″
30′

Strain gage locations:

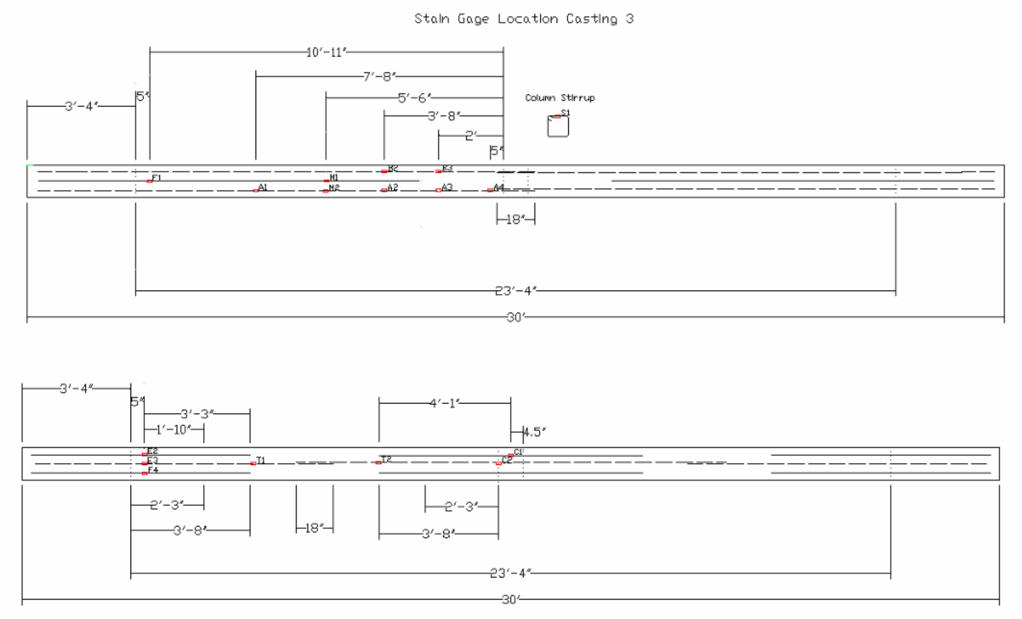
Stain Gage Location Casting 3
10′-11″
7′-8″
5′-6″
3′-8″
2′
5″
3′-4″
5″
Column Stirrup
S1
F1
A1
M1
M2
B2
A2
B3
A3
A4
18″
23′-4″
30′
3′-4″
5″
3′-3″
1′-10″
4′-1″
4.5″
E2
E3
F4
T1
T2
C1
C2
2′-3″
3′-8″
18″
2′-3″
3′-8″
23′-4″
30′

No CFRP

Load vs Displacement:

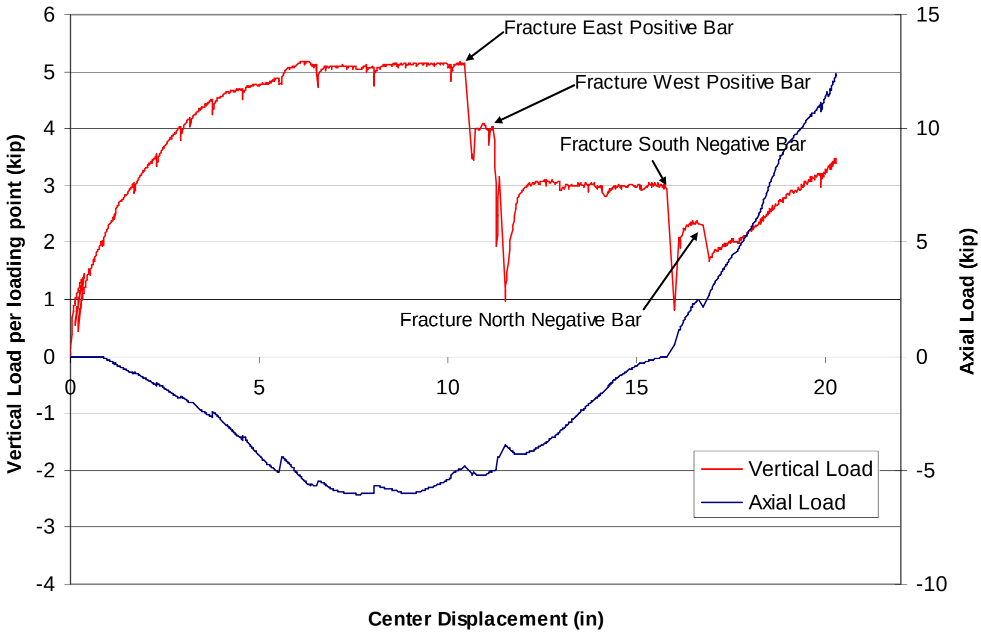

Strain:

Negative moment reinforcement

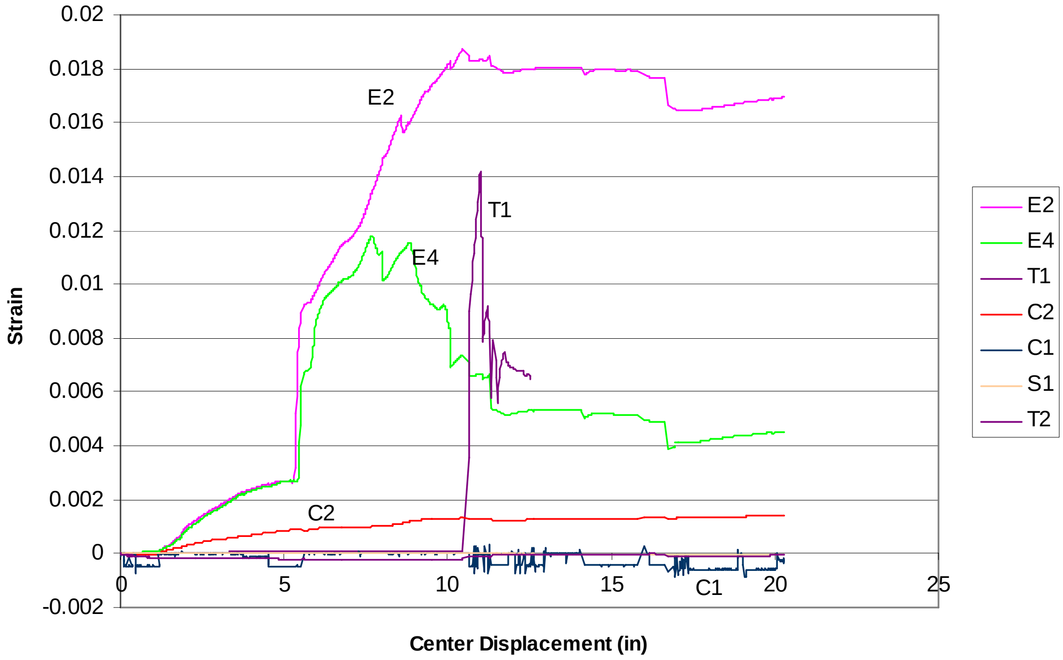

Positive moment reinforcement

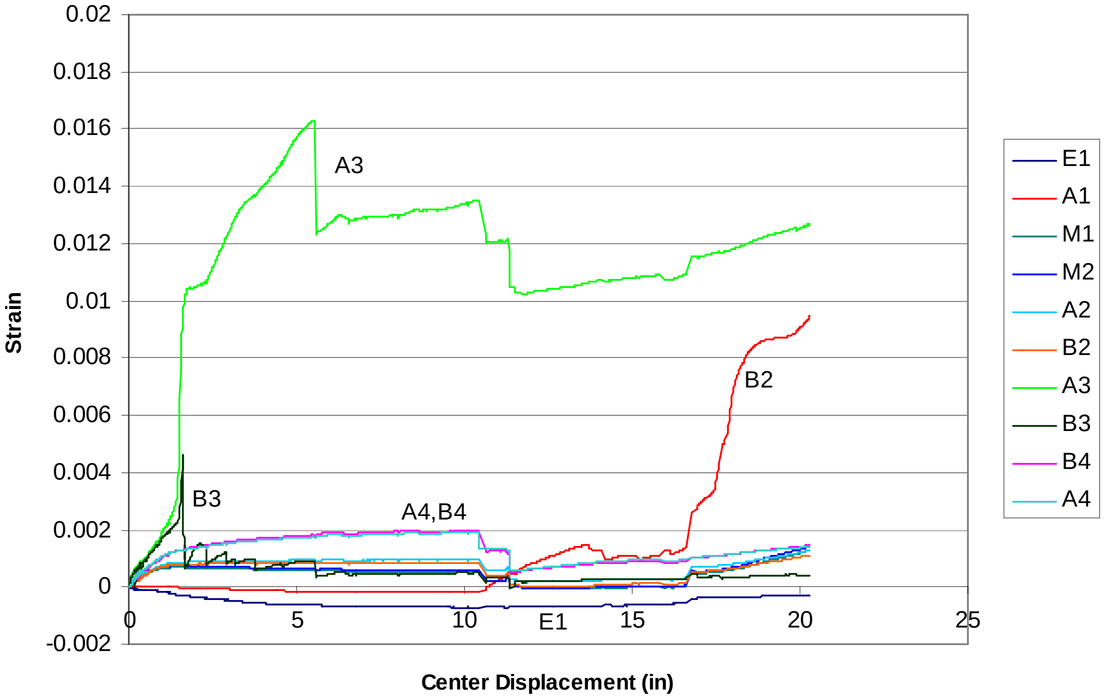

Pictures:

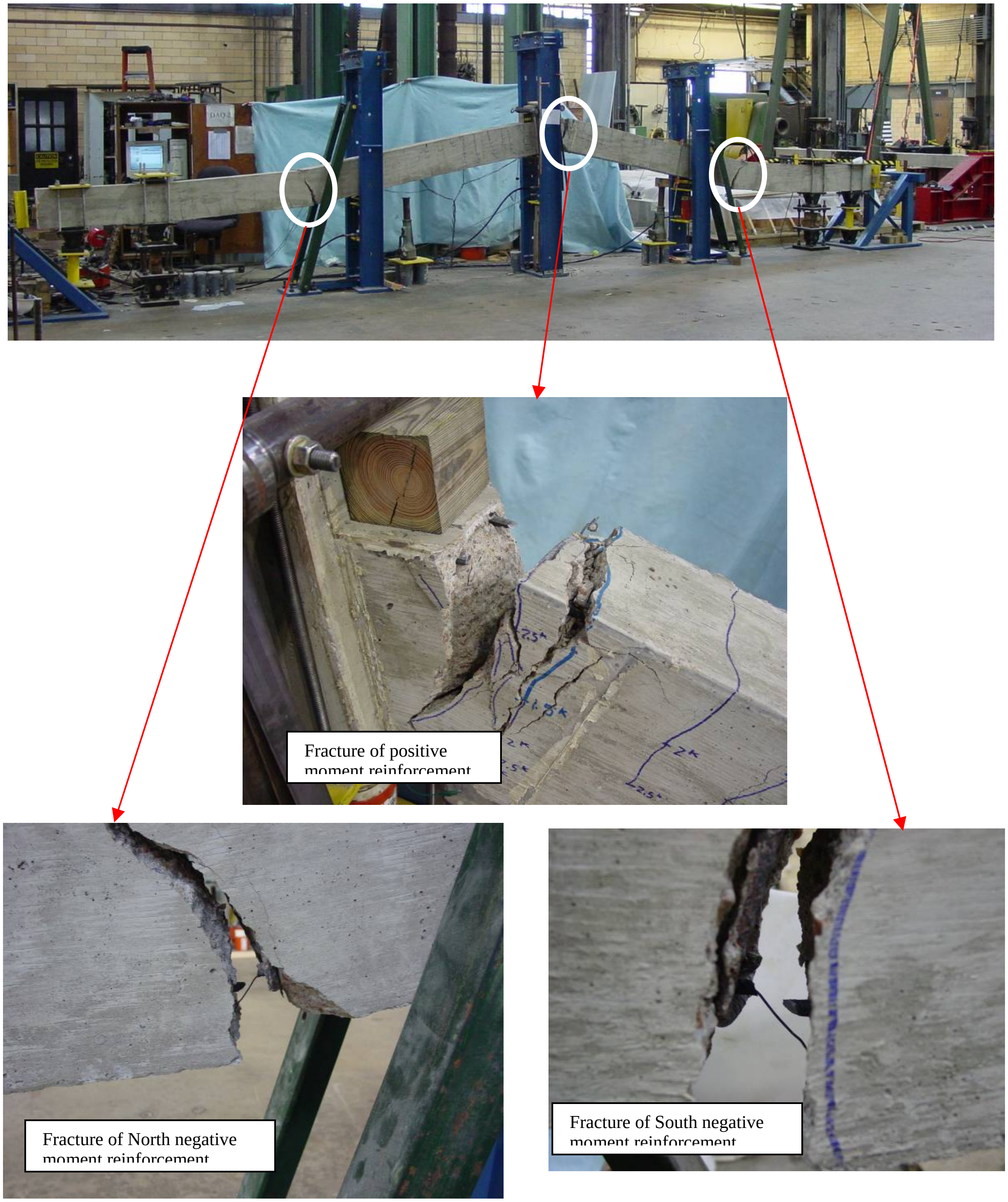
Fracture of positive moment reinforcement
Fracture of North negative moment reinforcement
Fracture of South negative moment reinforcement

BEAM CONSTRUCTION PICTURES:

Reinforcement tying

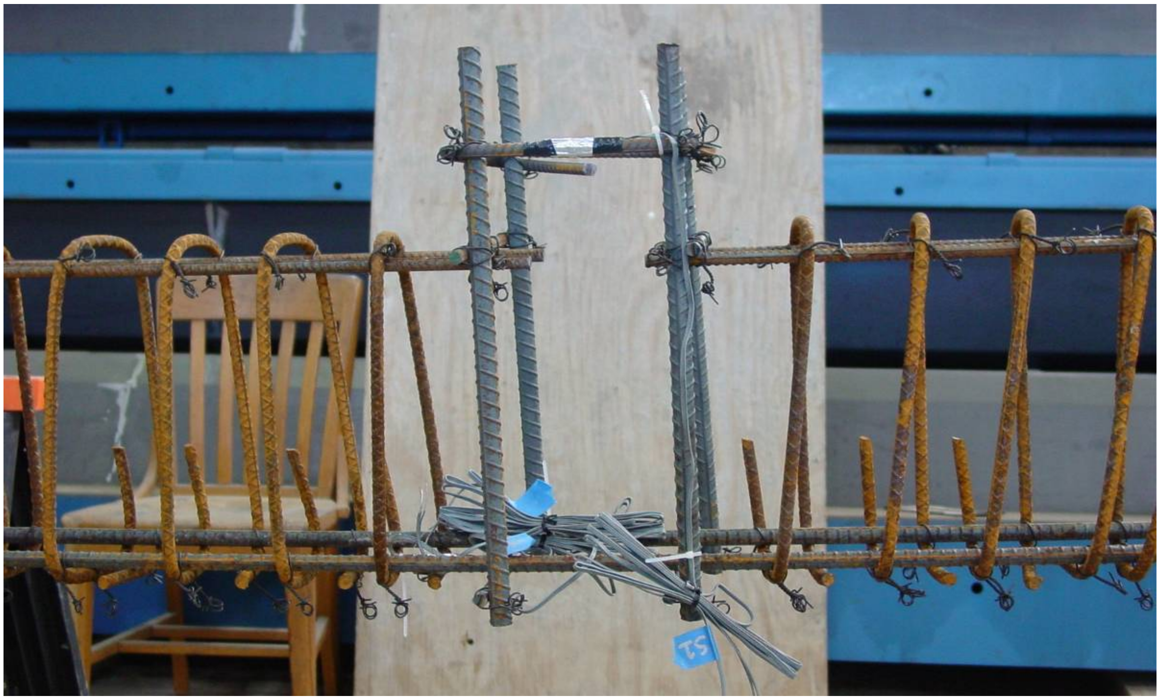

Discontinuity in positive moment reinforcement

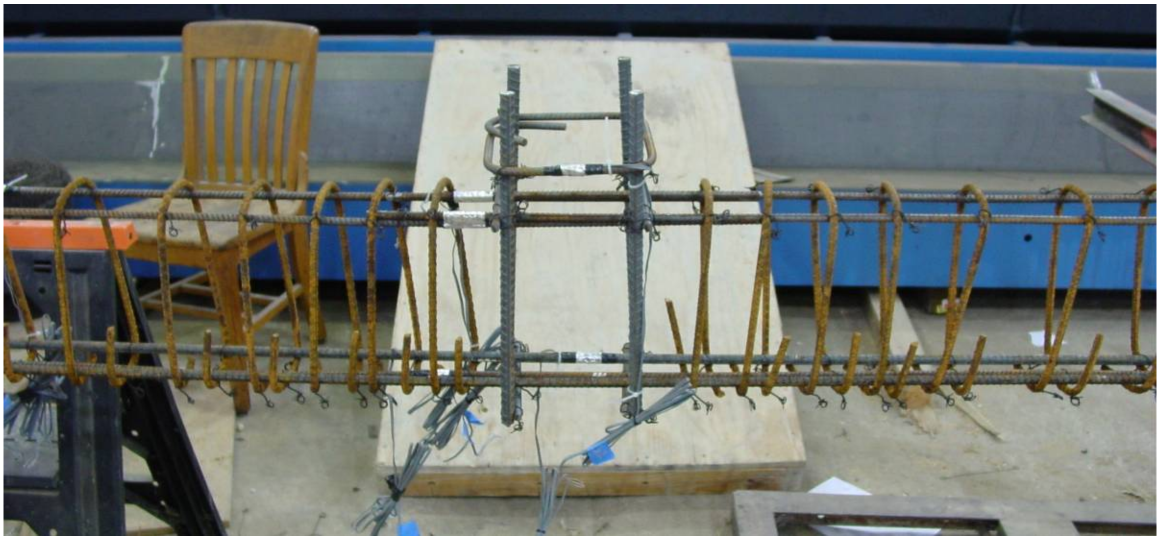

Splice in continuous reinforcement (positive moment reinforcement splice)

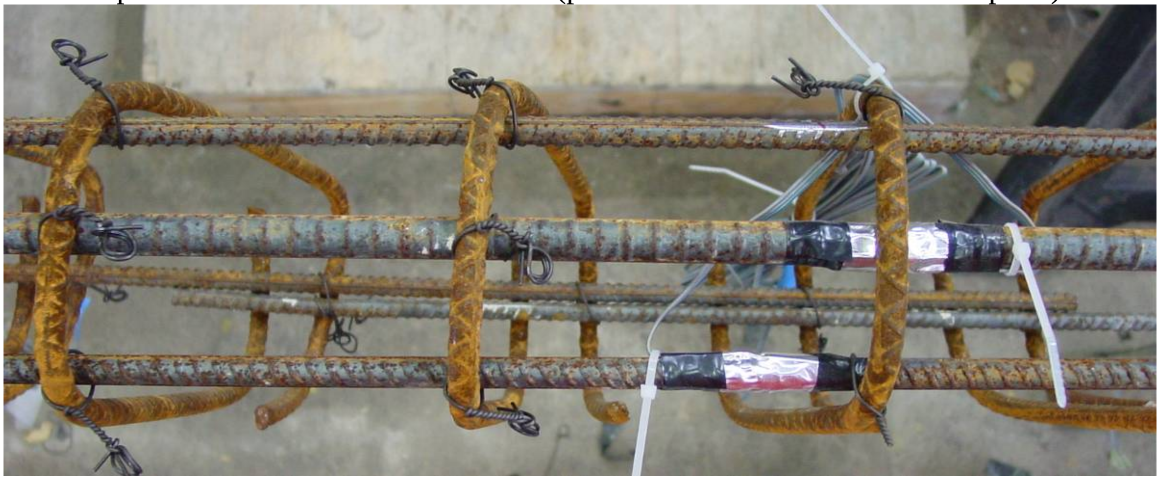

Splice in continuous reinforcement (negative moment reinforcement splice)

5 TON
Jackson

Pouring concrete

Formwork

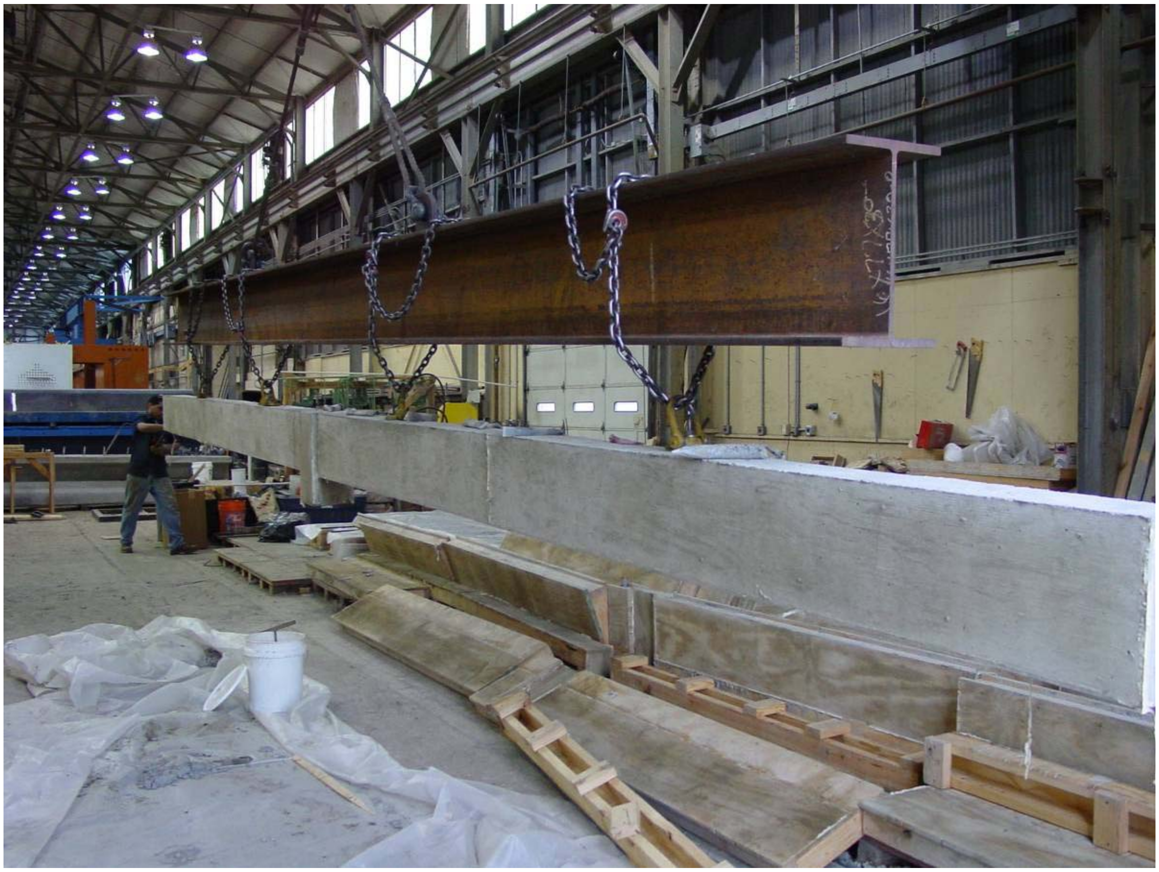

Lifting Beam

Appendix D

Catenary Analysis Models

Test Specimen Models..349
    Case 1 – Retrofitted 349
    Case 2 – Un-retrofitted..352
Prototype Models..354
    Case 1 – Retrofitted 354
    Case 2 – Un-retrofitted..357

TEST SPECIMEN MODELS

Case 1 – Retrofitted

P is the applied load
A is the axial force
M is the moment capcity of the hinge
Δ is the center displacement

Inputs:

$L := 144$	in	length of beam	$Est := 30000$	ksi	steel elastic modulus
$h := 12$	in	height of beam	$Esy := 600$	ksi	steel yield modulus
			$As := .51$	in^2	area of steel
			$fy := 60$	ksi	yield strength of steel

Inputs for beam elongation:

CFRP parameters

$Ecfrp := 14000$	ksi	modulus of CFRP
$w_{cfrp} := 6$	in	width of CFRP sheet
$t_{cfrp} := 0.04$	in	thickness of CFRP sheet
$L_{cfrp} := 80$	in	length of CFRP retrofit

Rebar Parameters

$As1 := 0.51$	in^2	Area of steel in section 1
$Ls1 := 27$	in	Length of steel in section 1
$As2 := 0.93$	in^2	Area of steel in section 2
$Ls2 := 27$	in	Length of steel in section 2

$yield := As \cdot fy \qquad yield = 30.6$

$L_y := 10$	in	Initial length of yielded rebar
$L_i := 1$	$\frac{in}{kip}$	Additional length of yielded rebar per kip axial load after yield
$E_i := 0.1$	in	Initial elongation due to rebar yielding before catenary

Parameters for steel stress vs. strain curve

$\varepsilon_{sp} := .01$

$n_s := 4$

$\sigma_{sp} := 63$

$$a_s := \frac{\varepsilon_{sp}}{\sigma_{sp}^{\,n_s}}$$

Ramberg-Osgood steel stress strain model

$$\varepsilon st(A, As) := \begin{cases} \dfrac{\frac{A}{As}}{Est} + a_s \cdot \left(\dfrac{A}{As}\right)^{n_s} & \text{if } \dfrac{A}{As} < 100 \\ .01 + \dfrac{A}{100 \cdot As} & \text{otherwise} \end{cases}$$

Moment Capacity of hinge

$M := 420 \quad \text{kip} - \text{in}$

Extensions

extension due to geometry

$$\delta e(\Delta) := h \frac{\Delta}{L \cdot \left(1 + \frac{\Delta^2}{L^2}\right)^{.5}} - L \cdot \left[1 - \left[\frac{1}{\left(1 + \frac{\Delta^2}{L^2}\right)^{.5}}\right]\right]$$

extension due to support movement

$$\delta s(A) := 0.32 + .013 \cdot A$$

extension due to beam elongation

$$\delta y(A) := \begin{cases} \dfrac{A \cdot L_{cfrp}}{Ecfrp \cdot w_{cfrp} \cdot t_{cfrp}} + \dfrac{A \cdot L_y}{Esy \cdot As} + E_i + \varepsilon st(A, As1) \cdot Ls1 + \varepsilon st(A, As2) \cdot Ls2 & \text{if } A < yield \\ \dfrac{A \cdot L_{cfrp}}{Ecfrp \cdot w_{cfrp} \cdot t_{cfrp}} + \dfrac{A \cdot \left[L_y + L_i \cdot (A - yield)\right]}{Esy \cdot As} + E_i + \varepsilon st(A, As1) \cdot Ls1 + \varepsilon st(A, As2) \cdot Ls2 & \text{otherwise} \end{cases}$$

Solution

start with displacement guess of $\Delta g := 12$

```
Solution := for  $k \in 30..2000$
                $\Delta \leftarrow 0$
                $P \leftarrow \frac{k}{100}$
                for  $i \in 1..1000$
                    $A \leftarrow \frac{P \cdot L - M}{\Delta g}$
                    $A \leftarrow 0$  if  $A < 0$
                    $\Delta \leftarrow \left|\sqrt{\left(L + \delta e(\Delta g) + \delta s(A) + \delta y(A)\right)^2 - L^2}\right|$
                    break  if  $|\Delta| - |\Delta g| < .01$
                    $\Delta g \leftarrow \Delta$
                    $i \leftarrow i + 1$
                $ans_{k,0} \leftarrow \Delta$
                $ans_{k,1} \leftarrow P$
                $ans_{k,2} \leftarrow A$
                $k \leftarrow k + 1$
            ans
```

Case 2 – Un-retrofitted

Inputs:

$L := 91.5 \ \text{in}$ Length of beam

$As := .42 \ \text{in}^2$ Area of yield steel

Inputs for beam elongation:

Rebar Parameters

$As1 := 0.42 \ \text{in}^2$ Area of steel in section 1

$Ls1 := 48 \ \text{in}$ Length of steel in section 1

$As2 := .47 \ \text{in}^2$ Area of steel in section 2

$Ls2 := 44 \ \text{in}$ Length of steel in section 2

$As3 := 0.51 \ \text{in}^2$ Area of steel in section 3

$Ls3 := 44 \ \text{in}$ Length of steel in section 3

$yield := As \cdot fy \qquad yield = 25.2$

$L_y := 20 \ \text{in}$ Initial length of yielded rebar

$L_{ib} := 1 \ \frac{\text{in}}{\text{kip}}$ Additional length of yielded rebar per kip axial load before yield

$L_{ia} := 2 \ \frac{\text{in}}{\text{kip}}$ Additional length of yielded rebar per kip axial load after yield

$E_i := 0.3 \ \text{in}$ Initial elongation due to rebar yielding before catenary

other parameters same as case 1

Moment Capacity of hinge

$M := 80$ to account for dead weight moment and cracking moment

Extensions

Extension due to geometry and support movement same as case 1

Extension due to beam elongation

$$\delta y2(A) := \begin{cases} \dfrac{\left(L_y + L_{ib} \cdot A\right) \cdot A}{Esy \cdot As} + E_i + \varepsilon st(A, As1) \cdot Ls1 + \varepsilon st(A, As2) \cdot Ls2 + \varepsilon st(A, As3) \cdot Ls3 & \text{if } A < yield \\ \dfrac{\left[\left(yield + L_y\right) + \left(L_{ia}\right) \cdot (A - yield)\right] \cdot A}{Esy \cdot As} + E_i + \left(\varepsilon st(A, As1) \cdot Ls1 + \varepsilon st(A, As2) \cdot Ls2\right) + \varepsilon st(A, As3) \cdot Ls3 & \text{otherwise} \end{cases}$$

Solution

start with displacement guess of $\Delta g := 15$

```
Solution2 :=  for  $k \in 10..250$
                  $\Delta \leftarrow 0$
                  $P \leftarrow \frac{k}{10}$
                  for  $i \in 1..1000$
                      $A \leftarrow \frac{P \cdot 69.75 - 80}{\Delta g - 10}$
                      $A \leftarrow 0$  if  $A < 0$
                      $\Delta \leftarrow \left|\sqrt{\left[\delta e(\Delta g) + L + (\delta s(A)) + \delta y2(A)\right]^2 - L^2}\right|$
                      break  if  $|\Delta| - |\Delta g| < .01$
                      $\Delta g \leftarrow \Delta$
                      $i \leftarrow i + 1$
                  $ans_{k,0} \leftarrow \Delta$
                  $ans_{k,1} \leftarrow P$
                  $ans_{k,2} \leftarrow A$
                  $k \leftarrow k + 1$
              ans
```

PROTOTYPE MODELS

Case 1 – Retrofitted

P is the applied load
A is the axial force
M is the moment capcity of the hinge
Δ is the center displacement

Inputs:

$L := 288$ in length of beam
$h := 24$ in height of beam

$Est := 30000$ ksi steel elastic modulus
$Esy := 600$ ksi steel yield modulus
$As := 2.04$ in^2 area of steel
$fy := 60$ ksi yield strength of steel

Inputs for beam elongation:

CFRP parameters

$Ecfrp := 14000$ ksi modulus of CFRP
$w_{cfrp} := 12$ in width of CFRP sheet
$t_{cfrp} := 0.08$ in thickness of CFRP sheet
$L_{cfrp} := 160$ in length of CFRP retrofit

Rebar Parameters

$As1 := 2.04$ in^2 Area of steel in section 1
$Ls1 := 54$ in Length of steel in section 1
$As2 := 3.72$ in^2 Area of steel in section 2
$Ls2 := 54$ in Length of steel in section 2

$yield := As \cdot fy$ $yield = 122.4$ $ultimate := As \cdot 100$ $ultimate = 204$

$L_y := 20$ in Initial length of yielded rebar
$L_i := 2$ $\frac{in}{kip}$ Additional length of yielded rebar per kip axial load after yield
$E_i := 0.2$ in Initial elongation due to rebar yielding before catenary

Parameters for steel stress vs. strain curve

$\varepsilon_{sp} := .01$
$n_s := 4$

$\sigma_{sp} := 63$

$$a_s := \frac{\varepsilon_{sp}}{\sigma_{sp}^{\,n_s}}$$

Ramberg-Osgood steel stress strain model

$$\varepsilon st(A, As) := \begin{cases} \dfrac{\frac{A}{As}}{Est} + a_s \cdot \left(\dfrac{A}{As}\right)^{n_s} & \text{if } \dfrac{A}{As} < 100 \\ .01 + \dfrac{A}{100 \cdot As} & \text{otherwise} \end{cases}$$

Moment Capacity of hinge

$M := 3120 \quad kip - in$

Extensions

extension due to geometry

$$\delta e(\Delta) := h \frac{\Delta}{L \cdot \left(1 + \frac{\Delta^2}{L^2}\right)^{.5}} - L \cdot \left[1 - \left[\frac{1}{\left(1 + \frac{\Delta^2}{L^2}\right)^{.5}}\right]\right]$$

extension due to support movement

$\delta s(A) := 0$

extension due to beam elongation

$$\delta y(A) := \begin{cases} \dfrac{A \cdot L_{cfrp}}{Ecfrp \cdot w_{cfrp} \cdot t_{cfrp}} + \dfrac{A \cdot L_y}{Esy \cdot As} + E_i + \varepsilon st(A, As1) \cdot Ls1 + \varepsilon st(A, As2) \cdot Ls2 & \text{if } A < yield \\ \dfrac{A \cdot L_{cfrp}}{Ecfrp \cdot w_{cfrp} \cdot t_{cfrp}} + \dfrac{A \cdot \left[L_y + L_i \cdot (A - yield)\right]}{Esy \cdot As} + E_i + \varepsilon st(A, As1) \cdot Ls1 + \varepsilon st(A, As2) \cdot Ls2 & \text{otherwise} \end{cases}$$

Max axial Load

$maxa := w_{cfrp} \cdot 125 \cdot .04 + fy \cdot As$ OR $maxa_s := 100 \cdot As$

$maxa = 182.4$ $maxa_s = 204$

Solution

start with displacement guess of $\Delta g := 24$

```
Solution := 
    for  $k \in 10..4500$
        $\Delta \leftarrow 0$
        $UL \leftarrow \frac{k}{10000}$
        for  $i \in 1..1000$
            $A \leftarrow \frac{\frac{UL \cdot L}{2} \cdot L - M}{\Delta g}$
            $A \leftarrow 0$  if  $A < 0$
            $\Delta \leftarrow \left|\sqrt{\left(L + \delta e(\Delta g) + \delta s(A) + \delta y(A)\right)^2 - L^2}\right|$
            break  if  $|\Delta| - |\Delta g| < .001$
            $\Delta g \leftarrow \Delta$
            $i \leftarrow i + 1$
        $ans_{k,0} \leftarrow \Delta$
        $ans_{k,1} \leftarrow UL$
        $ans_{k,2} \leftarrow A$
        $k \leftarrow k + 1$
    ans
```

Case 2 – Un-retrofitted

Inputs:

$L := 183$ in Length of beam

$As := 1.68$ in^2 Area of yield steel

Inputs for beam elongation:

Rebar Parameters

$As1 := 1.68$ in^2 Area of steel in section 1

$Ls1 := 156$ in Length of steel in section 1

$As2 := 3.72$ in^2 Area of steel in section 2

$Ls2 := 54$ in Length of steel in section 2

$As3 := 2.04$ in^2 Area of steel in section 3

$Ls3 := 62$ in Length of steel in section 3

$yield := As \cdot fy$ $yield = 100.8$ $As \cdot 100 = 168$

$L_y := 40$ in Initial length of yielded rebar

$L_{ib} := 2$ $\frac{in}{kip}$ Additional length of yielded rebar per kip axial load before yield

$L_{ia} := 4$ $\frac{in}{kip}$ Additional length of yielded rebar per kip axial load after yield

$E_i := 0.6$ in Initial elongation due to rebar yielding before catenary

other parameters same as case 1

Moment Capacity of hinge

$M := 590$ to account for dead weight moment and cracking moment

Extensions

Extension due to geometry and support movement same as case 1

Extension due to beam elongation

$$\delta y2(A) := \left| \begin{array}{l} \dfrac{\left(L_y + L_{ib} \cdot A\right) \cdot A}{Esy \cdot As} + E_i + \varepsilon st(A, As1) \cdot Ls1 + \varepsilon st(A, As2) \cdot Ls2 + \varepsilon st(A, As3) \cdot Ls3 \ \text{ if } \ A < yield \\ \dfrac{\left[\left(yield \cdot 2 + L_y\right) + \left(L_{ia}\right) \cdot (A - yield)\right] \cdot A}{Esy \cdot As} + E_i + \left(\varepsilon st(A, As1) \cdot Ls1 + \varepsilon st(A, As2) \cdot Ls2\right) + \varepsilon st(A, As3) \cdot Ls3 \ \text{ otherwise} \end{array} \right.$$

Solution

start with displacement guess of $\Delta g := 24$

```
Solution2 := for  k ∈ 10.. 4500
                  Δ ← 0
                  $UL \leftarrow \frac{k}{10000}$
                  for  i ∈ 1.. 1000
                      $A \leftarrow \frac{UL \cdot \frac{L^2}{2} - M}{\Delta g - 20}$
                      A ← 0  if  A < 0
                      $\Delta \leftarrow \left|\sqrt{\left[\delta e(\Delta g) + L + (\delta s(A)) + \delta y2(A)\right]^2 - L^2}\right|$
                      break  if  $|\Delta| - |\Delta g| < .01$
                      Δg ← Δ
                      i ← i + 1
                  $ans_{k,0} \leftarrow \Delta$
                  $ans_{k,1} \leftarrow UL$
                  $ans_{k,2} \leftarrow A$
                  k ← k + 1
              ans
```

References

American Concrete Institute. (1974). "Manual of Standard Practice for Detailing Concrete Structures (315-74)." Detroit, Michigan, USA.

American Concrete Institute. (1989). "Building Code Requirements for Structural Concrete (318-89)." Farmington Hills, Michigan, USA.

American Concrete Institute. (2005). "Building Code Requirements for Structural Concrete (318-05)." Farmington Hills, Michigan, USA.

American Concrete Institute. (2002). "Guide for the Design and Construction of Externally Bonded FRP Systems for Strengthening Concrete Structures (ACI 440.2R-02)." Farmington Hills, Michigan, USA.

American Society of Civil Engineers (ASCE). (2005). "Minimum Design Loads for Buildings and Other Structures (SEI/ASCE 7/05)." Reston Va., USA.

Astenah-Asl, A. (2003). "Progressive Collapse Prevention in New and Existing Buildings." *Proc. Of the 9th Arab Structural Engineering Conference, Emerging Technologies in Structural Engineering*, Abu Dhabi UAE.

Bramblett, R. M. (2000). *Strengthening of Reinforced Concrete Beams Using Carbon Fiber Reinforced Polymer Composites*, Master of Science Thesis, The University of Texas at Austin, August 2000.

Breen, J.E. (1975). "Summary Report Research Workshop on Progressive Collapse of Building Structures," Austin TX, November 18-20.

Breña, S. F. (2000). *Strengthening Reinforced Concrete Bridges Using Carbon Fiber Reinforced Polymer Composites,* Doctor of Philosophy Dissertation, The University of Texas at Austin, December 2000.

Bonacci, J. F., Maalej, F., (2001). "Behavioral Trends of RC Beams Strengthened with Externally Bonded FRP." *Journal of Composites for Construction*, May 2001, 102-113.

Burr, A. C., (2004). "Recent Development in the use of FRP Anchors and Masonry Wall Strenghening Techniques." *The Structural Engineer*, September 2004.

Catherall, J. A., (1973). *Fibre Reinforcement, M &B Monograph ME/16*, Mills & Boon Limited.

Corley, G.W., (1966). "Rotational Capacity of Reinforced Concrete Beams." *Journal of Structural Division*, ASCE, Vol. 92, ST5, October 1966, pp. 121-146.

Corley, G.W., (2003). “Applicability of Seismic Design in Mitigating Progressive Collapse” *NIST Workshop*, <www.nibs.org> (April 18, 2003).

Corley, G.W., (2004). “Lessons learned on Improving Resistance of Buildings to Terrorist Attacks.” *Journal of Performance of Constructed Facilities,* May 2004, pp 68-78.

Crawford, J.E., (2002). “Retrofit Measures to Mitigate Progressive Collapse,” *NIST/NIBS Multihazard Mitigation Council National Workshop on Prevention of Progressive Collapse,* Chicago,IL, July.

Degenkolb (1987). “The Whittier Narrows Earthquake,” Unpublished manuscript

Department of Defense (DOD). (2004). “Design of Buildings to Resist Progressive Collapse,” Unified Facilities Criteria (UFC) 4-023-03, September 2004

Estrada, J. I., (1990). *Use of Steel Elements to Strengthen a Reinforced Concrete Building,* Master of Science Thesis, The University of Texas at Austin, December 1990.

Fédération Internationale du Béton. (2001). “Externally Bonded FRP Reinforcement for RC Structures (fib-14)”, Lausanne, Switzerland.

Fitzer, E. Ed. (1985). *Carbon Fibres and Their Composites,* Springer-Verlag.

Fyfe Co. LLC. (2005a). *Quality Manual for the Tyfo Fiberwrap System,* July 2001.

Fyfe Co. LLC. (2005b). *Tyfo Systems for Beams,*< www.fyfeco.com> (June 6, 2005).

General Services Administration (GSA). (2003). “Progressive Collapse Analysis and Design Guidelines”, General Services Admistration, June 2003.

Gill, R. M. (1972). *Carbon Fibers in Composite Materials,* Butterworth & Co.

Hollaway, L. C. Ed. and Leeming M. B. (2000). *Strengthening of Reinforced Concrete Structures,* CRC Press.

Ibell, T., and A. Nanni. (2003). “The Effects of a Curved Soffit on FRP-Strengthening of Concrete Bridges” *Report Center for Infrastructure Engineering Studies UTC-R73,* Rolla, Missouri.

Izzuddin, B.A., Elghazouli, A.Y. (2004). “Failure of Lightly Reinforced Concrete Members under Fire. I: Analytical Modeling,” *Journal of Structural Engineering,* 130(1), pp. 3-17.

Japanese Society of Civil Engineers (JSCE). (1997). "Recommendations for Design and Construction of Concrete Structures using Continuous Fibre Reinforcing Materials," *Concrete Engineering Series 23, A. Machida (ed.).*

Jinno, Y, Tsukagishi, H. (1998). “Structural Properties of RC Walls Strengthened by Carbon Fiber Sheets” *Architectural Institute of Japan Annual Conference*, Fukuoka, Japan, 209-210

Khalifa, A., T. Alkhrdaji, A. Nanni, and S. Lansburg. (1999). "Anchorage of Surface Mounted FRP Reinforcement," *Concrete International: Design and Construction*, Vol. 21, No.10, pp. 49-54.

Kim, I. S. (2006). *Rehabilitation of Poorly Detailed RC Structures Using CFRP Materials*, Master of Science Thesis, The University of Texas at Austin, May 2006.

Kobayashi, K., Fujii S., Yabe Y., Tsukagoshi H., and Sugiyama T. (2001). “Advanced wrapping system with CF anchor –Stress Transfer Mechanism of CF Anchor.” *5th International Symposium on Fiber-Reinforced Polymer (FRP) Reinforcement for Concrete Structures*, Cambridge, UK, 379- 388.

Lamanna, A.J., (2002), *Flexural strengthening of reinforced concrete beams with mechanically fastened fiber reinforced polymer strips,* Doctor of Philosophy Dissertation, The University of Wisconsin at Madison, 2002.

Mallick, P. K., *Fiber-Reinforced Composites: Materials, Manufacture, and Design,* 2nd Ed., Marcel Decker, Inc., 1993.

Martin, R., and Delatte, N.J. (2000). “Another Look at the L’Ambiance Plaza Collapse,” *Journal of Performance of Constructed Facilities*,14(4), November 2000, pp. 160-165.

Masuo, K., S. Morita, Y. Jinno, and H. Watanabe. (2001). “Advanced Wrapping System with CF-anchor – Seismic Strengthening of RC Columns with Wing Walls”, *5th International Symposium on Fiber-Reinforced Polymer (FRP) Reinforcement for Concrete Structures*, Cambridge, UK. 299-308.

Mlakar, P.F., Dusenberry, D.O., Harris, J.R., Haynes G.A., Phan, L.T., and Sozen, M.A.,(2003). “The Pentagon Building Performance Report,” *American Society of Civil Engineers,* Reston Virginia.

Morphy, R.D., (1999). *Behavior of Fiber Reinforced Polymer (FRP) Stirrups as Shear Reinforcement for Concrete Structures,* Master Thesis, University of Manitoba, Winnipeg Manitoba, June 1999.

Nair, R.S. (2004). “Progressive Collapse Basics,” <http://www.aisc.org/Content /ContentGroups/Documents/ePubs_Conference_Proceedings/ProgressiveCollapse Basics.pdf> (Feb. 2, 2006).

National Institute of Standard and Technology (NIST). (2007). “Best Practices for Reducing the Ptential for Progressive Collapse in Buildings,” NISTIR 7396, February 2007.

Ozdemir, G., and U. Akyuz. (2005). “Tensile Capacities of CFRP Anchors”, *7th International Symposium on Fiber-Reinforced Polymer (FRP) Reinforcement for Concrete Structures*, Kansas City, MO.

Regan, P.E. (1975). “Catenary Action in Damaged Concrete Structures.” *Industrialization in Concrete Building Construction ACI SP-48*, pp191-225.

Ruth, P., Marchand, K.A., and Williamson, E.B. (2006). “Static Equivalency in Progressive Collapse Alternate Path Analysis: Reducing Conservatism While Retraining Structural Integrity,” *Journal of Performance of Constructed Facilities*, 20(4), pp. 349-364.

Saaticoglu, M., Serrato, F., and Foo, S. (2005). “Seismic Preformance of Masonry Infill Walls Retrofitted With CFRP Sheets.” *7th International Symposium on Fiber-Reinforced Polymer (FRP) Reinforcement for Concrete Structures,* Kansas City, MO, 341-353.

Sika. (2005). *Sika CarboDur Composite Strengthening Systems,*< www.sikausa.com> (May 6, 2005).

Sozen, M.A., Thornton C.H., Corley, W.G., and Mlakar, P.F. (1998). “The Oklahoma City Bombing: Structure and Mechanisms of the Murrah Building,” *Journal of Performance of Constructed Facilities*, 12(3), 1998, pp. 120-136.

Toutanji, H, Saxena, P, and Zhao, L. (2006). “Prediction of Bond Failure of Concrete Prisms Bonded with FRP Composiste” *Third International Conference on FRP Composites in Civil Engineering (CICE 2006)*, Miami, FL USA, pp. 63-66

Teng, J. G., Chen J.F., Smith S. T., Lam L., (2001). *FRP-Strengthened RC Structures,* John Wiley & Sons, LTD.

Wilford, J. C., and Yu, C.W. (1973) “Catenary Action in Damaged Structures” *Proceedings of the Department of Environment and CIRIA, Seminar on the Stability of Precast Concrete Structures*, London, U.K.

Wong, L.H. (2002). “Design and Detailing for Catenary Action,” <http://www.eptc.com.sg/E-Learning/Catenary_Design.pdf> (Jan 17th 2004)

Vita

Sarah Orton was born in Wichita Kansas to Thomas and Kathryn Orton in 1978. She graduated high school from Clear Lake High School in 1996. She attended the University of Texas of Austin and graduated with her BS in Civil Engineering with Highest Honors in May 2000. She then continued graduate school at the University of Illinois at Urbana Champaign and graduated with a MS in Civil Engineering in August 2002. Next, she spent time as an engineer at ABS Consulting in Houston TX. She returned to the University of Texas of Austin in 2004 and will graduate with her PhD in Civil Engineering in August 2007. She has accepted a tenure track faculty position at the University of Missouri Columbia.

Permanent address: 16422 Larkfield
Houston, TX 77059

This dissertation was typed by Sarah Orton.